Silva Gabreta 24

Scientific studies from the Bohemian Forest

NÁRODNÍ PARK BAYERISCHER WALD
NATIONAL PARK ŠUMAVA

Set of papers with results
of the Interreg V project No. 26
Silva Gabreta Monitoring – Implementation of Transboundary Monitoring of Biodiversity and Water Regime.

Financial support by the Cross-border cooperation programme
Czech Republic–Bavaria Free State ETC goal 2014–2020.

ZIEL ETZ
CÍL EÚS

Ziel ETZ | Cíl EÚS
Freistaat Bayern –
Tschechische Republik
Česká republika –
Svobodný stát Bavorsko
2014 – 2020 (INTERREG V)

Europäische Union
Evropská unie
Europäischer Fonds für
regionale Entwicklung
Evropský fond pro
regionální rozvoj

Správa
Národního parku
Šumava

NATIONALPARK
Bayerischer Wald

Vimperk 2018

Silva Gabreta	vol. 24	p. 1–20	Vimperk, 2018

The Silva Gabreta Project – transboundary cooperation in monitoring of biodiversity and water regime

Zdenka Křenová[1–3,*] **& Linda Seifert**[4]

[1]Šumava National Park, 1. máje 260, CZ-38502 Vimperk; [2]Global Change Research Centre CAS,
Bělidla 4a, CZ-60200 Brno; [3]Faculty of Science, Charles University, Benátská 2, CZ-12900 Prague,
Czech Republic
[4]Bavarian Forest National Park, Freyunger Str. 2, D-94481 Grafenau, Germany
[*] zd.krenova@gmail.com

Abstract

The Bohemian Forest represents the most extensive continuous forest landscape in central Europe. Two neighbouring national parks (NP), the Bavarian Forest NP in Germany and the Šumava NP in Czechia, protecting the most valuable part of this area have been recognized as an important site for monitoring of effect of climate change on central European biodiversity and ecosystem structure. For long time, a hydrological monitoring program in the Große Ohe headwater catchment and complex monitoring of glacial lakes recently recovering from acidification were flagships of long-term transboundary research in the Bohemian Forest. Recently published results of biodiversity research in the Bavarian Forest NP and experiences with monitoring of mires in the Šumava NP supported a necessity of multidisciplinary and transboundary research. To improve the cooperation of both national parks, optimize methodologies, and coordinate research activities in the region a new Interreg project No. 26 "Silva Gabreta Monitoring – Implementation of transboundary monitoring of biodiversity and water regime" was jointly prepared. The aims and monitoring methodologies of three main project activities are presented in this paper: (i) monitoring of forest biodiversity, (ii) monitoring of mires, and (iii) monitoring of aquatic ecosystems. In addition, we briefly present several supplementary project activities and tasks, such as modelling of mesoclimatic conditions, monitoring of effect of deicing salt, project conference and common database. As well as sampling design, methods and strategies, and brief overview of the preliminary results are mentioned.

Key words: monitoring, biodiversity, water regime, mires, transboundary cooperation, forest management

INTRODUCTION

Recent trends in ecology emphasize both the dynamics and nonequilibrium nature of ecological systems (SHIEL & BURSLEM 2003). Past decades have shown that large-scale natural disturbances, such as windthrows, fires, or insect outbreaks, can significantly moderate spatial and temporal processes in European forests, and even in central Europe (NIKLASSON et al. 2010). Increasing frequency of disturbance events have stimulated research focusing on effects of disturbance and post-disturbance forest management on biodiversity of central European mountain ecosystems.

Most recent studies have focused on the causes and consequences of natural disturbances in European temperate forests (e.g. MÜLLER et al. 2008, 2010, BÄSSLER & MÜLLER 2010, FISCHER & FISCHER 2012, SVOBODA et al. 2012) significantly contributing to our understanding of natural forest ecosystem dynamics. Numerous authors reported that traditional post-disturbance management and removal of large quantities of biological legacies (e.g. salvage cuttings) could have negative impacts on many species too (e.g. Thorn et al. 2017, Lindenmayer et al. 2017). Cavity-nesting birds and mammals, invertebrates, fungi and other taxa depending on dead wood, mosses and lichens closely associated with fallen logs are threatened with salvage logging (Hagan & Grove 1999, Martin & Eadie 1999, Nilsson et al. 2001). Research on this topic has been conducted also in the Bavarian Forest NP (BFNP) within the Biodiversity and Climate Change Project (BIOKLIM; Müller et al. 2007, 2008, 2010, Moning & Müller 2009, Bässler et al. 2010, Raabe et al. 2010).

The BIOKLIM Project was established in the BFNP in 2006 to contribute to the knowledge of expected effects of climate change on these low mountain range forest ecosystems (Bässler et al. 2008). Its fundamental objective was to quantify the dependency of various taxa on the environmental drivers affecting their local distribution. The project results confirmed that, together with the altitude, also large-scale disturbances (both windstorms and bark-beetle outbreaks) are the important drivers of biodiversity for many taxa (Bässler et al. 2010, Moning & Müller 2008, Müller et al. 2008, 2010, Raabe et al. 2010, Röder et al. 2010). The unique BIOKLIM research project focused only on biodiversity of forest ecosystems, the dominant habitat of the Bohemian Forest. The mires, however, the second most important habitat in this area, were not included notwithstanding that central European peat bogs, which originated during the Late Glacial and early Holocene, are supposed to be stable ecosystems that became hot spots of unique biological diversity, especially in mountainous areas (Spitzer & Danks 2006). Scattered distribution of these island-like habitats resulted from the changes in biota during the Pleistocene climatic oscillations (Tallis 1991). The mires as well as montane spruce forests are examples of the habitats occurring far south of their main boreal biome distributions (Dierssen & Dierssen 2001). They recently survive in the coldest, and usually the most remote, parts of central European mountains. The vulnerability of these habitat islands to climatic changes has got an increasing concern, but sensitivity of their communities to disturbances is less understood (Weltzin et al. 2000). Little is known whether mires and waterlogged forests (spruce mires) can serve as biodiversity refugia or sources of colonisers for the surrounding disturbed forest habitats. Together with mires, also catchments of mountain streams and glacial lakes were recognized as very important model ecosystems for research of the effects of natural disturbances and climate changes in central European forest ecosystems (Oulehle et al. 2013, 2018, Vrba et al. 2014, Beudert & Gietl 2015, Beudert et al. 2015, 2018, Kopáček et al. 2017). Long-term data were used as an important data source in many of these papers.

For long time, a hydrological monitoring program in the Große Ohe headwater catchment in the BFNP (Beudert & Gietl 2015) and complex monitoring of Czech and Bavarian glacial lakes recently recovering from acidification (Vrba et al. 2015, 2016) were flagships of long-term transboundary research in the Bohemian Forest (Heurich et al. 2010). Recently published valuable results of a hydrological monitoring program in the Große Ohe headwater catchment (Beudert et al. 2015, 2018) and glacial lakes research (e.g. Kopáček et al. 2017, 2018a,b, Vrba et al. 2014, 2016, Oulehle et al. 2018) have shown importance of long-term monitoring and transboundary cooperation. Results of biodiversity research in the BFNP (Bässler et al. 2015) and experiences with monitoring of mires in the Šumava National Park (ŠNP; Bufková et al. 2010) also supported a necessity of multidisciplinary and transboundary research delivering a detailed description of local biodiversity and environmental conditions in either “traditional” or “new” habitats established due to disturbance impacts. To improve the cooperation of the BFNP and ŠNP, optimize methodologies, and coordinate research activities, common Czech Republic–Bavaria Interreg project called “Silva Gabreta– monitoring of mountain ecosystems” (project No. 368) has started in January 2015 (Křenová & Seifert 2015). The outcomes of this project enabled the implementation the proposed monitoring activities within a following three-year project. The Interreg V project No. 26 "Silva Gabreta Monitoring – Implementation of transboundary monitoring of biodiversity and water regime" was jointly prepared and later successfully granted by the Cross-border cooperation programme Czech Republic–Bavaria Free State ETC goal 2014–2020. Together with BFNP, as a leading partner, also three Czech partners, the ŠNP, the Masaryk University in Brno and the Czech Agriculture University in Prague, as well as the Senckenberg Institute from Germany have been involved in this three-year project started in April 2016.

The main aim of this paper is to introduce the jointly prepared project No. 26 "Silva Gabreta Monitoring – Implementation of transboundary monitoring of biodiversity and water regime" that included three main project activities: (i) monitoring of forest biodiversity, (ii) monitoring of mires, and (iii) monitoring of aquatic ecosystems; and several supplementary activities, for example modelling of mesoclimatic conditions and monitoring of effect of deicing salt.

STUDY AREA, MONITORING DESIGN AND METHODS

The Bohemian Forest represents the most extensive continuous forest landscape in central Europe. Valuable near natural habitats of mountain old-growth forests, mires, secondary grasslands, glacial lakes, and streams in the trilateral border region of the Czech Republic, Bavaria, and Upper Austria host unique and diverse plant and animal communities. Therefore, this area is an important part of the Natura 2000 network, established to protect the most endangered habitats and species in Europe, as defined in the Habitats Directive (1992) and Birds Directive (1979). The centre of this area is protected as the Bavarian Forest National Park (BFNP, 242 km^2) and the Šumava National Park (ŠNP, 680 km^2) with the Šumava Protected Landscape Area (Šumava PLA, 1000 km^2) serving as their buffer zone (Fig. 1). Local ecosystems have been affected by acid depositions in the past decades (Vrba et al. 2003, Šantrůčková et al. 2007) as well as by ongoing climate changes. Indeed, an annual mean temperature has increased in the Bohemian Forest during the past half a century by more than 1°C (Kettle et al. 2003, Turek et al. 2014).

The forests, mainly mountain spruce and mixed forests, cover more than 85 % of this territory. Large areas of these forests have been subjected to significant natural disturbances in a few last decades (Müller et al. 2008, Fischer & Fischer 2012, Svoboda et al. 2012). As a result, the Bohemian Forest is characterized by the diverse mosaic of old-growth forests, windthrow areas, forests impacted by bark beetle, and areas influenced by traditional forestry in the past. Furthermore, the mires are the most valuable and the most sensitive habitats of the Bohemian Forest (Schreiber 1924, Spitzer & Bufková 2008). Their vegetation types range from the typical ombrotrophic dome-shaped raised bogs to minerotrophic forested or treeless fens, which are often surrounded by spruce mire or birch forest on peaty soils (Rösch 2000, Svobodová et al. 2002, Konvalinková & Prach 2002, Bastl et al. 2008, Bufková et al. 2010). More than 70% of mires and spruce mires in this transboundary region have been influenced by drainage for forest and agriculture management, and peat extraction in the past (Bufková et al. 2010). Since 1999, a comprehensive "Mire Restoration Program" improving the hydrology regime in disturbed mires has been implemented in the ŠNP (Bufková et al. 2010, Bufková 2012). Restoration measures have been implemented also in the BFNP (Jehl 1994, Strunz 1994, Englmaier 2009). In the ŠNP, selected drained and intact mires have been monitored since 2004 aiming to characterize the degradation changes induced by the hydrology disturbation and evaluate the success of restoration (Bufková et al. 2010). In the BFNP, no detail monitoring of mires has been commenced until now.

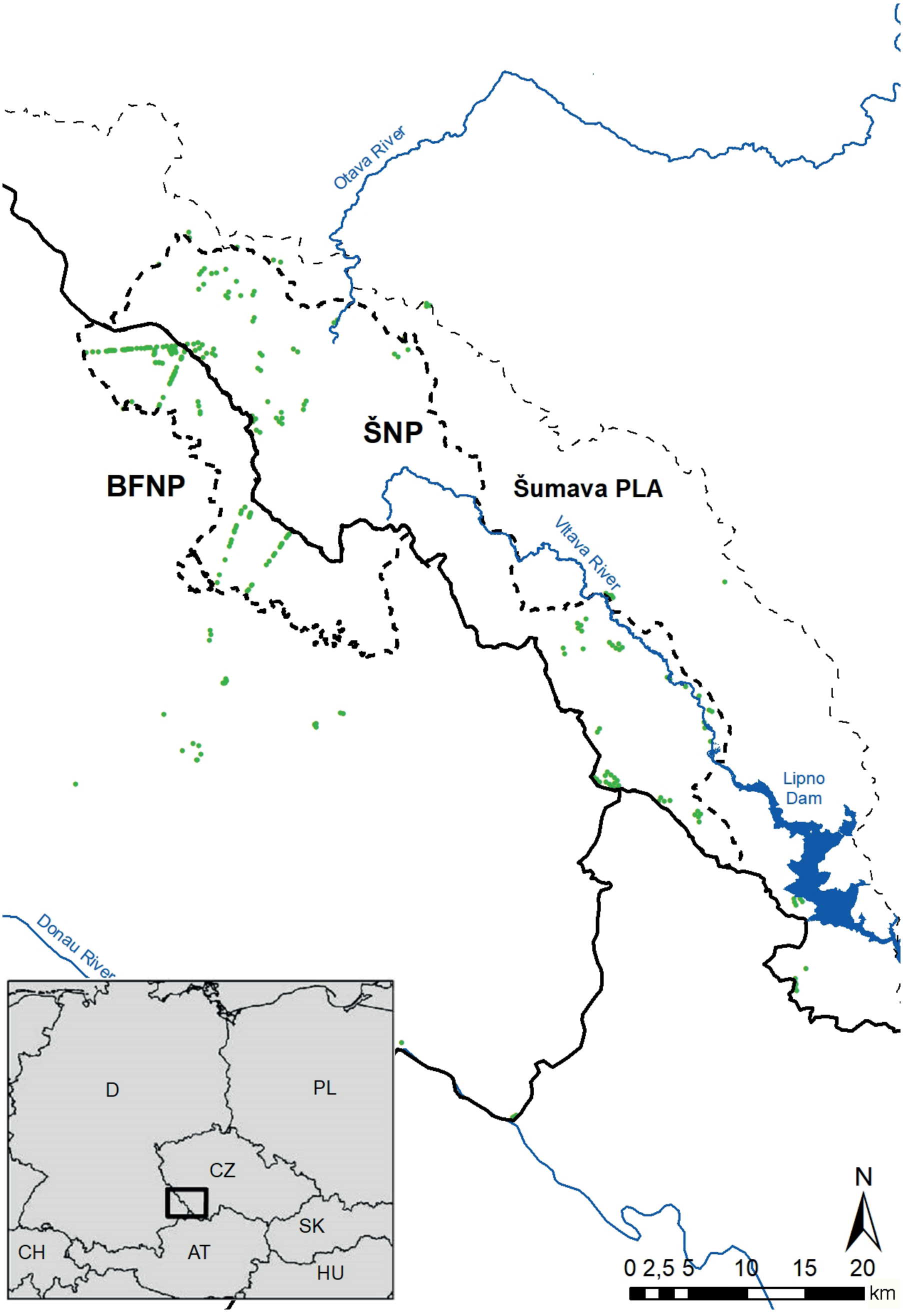

Fig. 1. Map of 157 and 120 plots (green points) in Bavaria and Czechia, respectively, where monitoring of forest biodiversity was conducted in the Interreg project No. 26 "Silva Gabreta Monitoring – Implementation of transboundary monitoring of biodiversity and water regime". Dashed lines are borders of the Bavarian Forest National Park (BFNP), Šumava National Park (ŠNP) and Šumava Protected Landscape Area (Šumava PLA).

Unlike the newly initiated monitoring of mires in the BFNP, hydrological monitoring of the Grosse Ohe catchment has a very long and successful history. The Große Ohe headwater catchment is 19.1 km² in size and its altitudinal range is from 770 m to 1453 m a.s.l. (Großer Rachel Mt.). It is 98% forested, with spruce (70%) and European beech being the dominant species (Beudert & Gietl 2015). The Große Ohe headwater catchment monitoring programme started in 1977 and the main aim of the program was to document and investigate the changes in water cycling during, and due to, the transition from commercial to near-natural forest under the strict protection and non-intervention policy (Beudert & Gietl 2015, Beudert et al. 2018). These objectives required truly long-term observation of physical-chemical parameters and of biotic components of ecosystems showing environmental changes: meteorological parameters and pollutants in ambient air (SO_2, NO_x and O_3), water and element cycles in beech and spruce stands and at the catchment level, vitality and growth of single trees, forest stands and understorey vegetation, and recovery of brown trout.

No stream catchment monitoring has been conducted in the Czech part of the region, but long-term monitoring of glacial lakes, including their catchments, has also delivered very important knowledge about ecosystem changes. The Bohemian Forest has been among the most acidified lake districts in the world (Kopáček et al. 2015, Vrba et al. 2015). Historical data (available since 1871) and regular monitoring (since 1984) on both water chemistry and aquatic biota provide a valuable background for the long-term ecological research of the catchment–lake ecosystems that currently focuses on (i) chemical reversal and biological recovery of the lakes, (ii) acidification effects on in-lake nutrient cycling, (iii) climatic effects on water chemistry, and (iv) catchment processes, including soil biogeochemistry and acidification impacts on vegetation (mountain spruce forests). Recently published papers (e.g. Vrba et al. 2014, 2016, Kopáček et al. 2015, 2017, 2018a,b, Seedre et al. 2015, Oulehle et al. 2018) well documented successful recovery of these glacial lakes ecosystems from acidification both on hydrochemical and biological levels. Long-term monitoring of glacial lakes and hydrological monitoring of the Große Ohe headwater catchment deliver unique knowledge; however, only little has been known about hydrobiology of streams and other aquatic ecosystems in the Bohemian Forest until now.

It was obvious that in the time of climatic changes, including increasing frequency of natural disturbances, more intensive and better coordinated common monitoring of biodiversity changes and water regime are crucial for responsible management of protected areas in transboundary region. More details on the monitoring of forest biodiversity, mires, and aquatic ecosystems follow bellow.

Monitoring of forest biodiversity

The Bohemian Forest provides a wide elevation gradient from ca. 300 to 1456 m a.s.l. (Grosser Arber Mt.) and a mosaic of forests of different structure and age resulted from different forestry management (managed/unmanaged) and natural disturbances (forest dieback caused by bark-beetle infestation and/or wind storms) in the past. The biodiversity data from a set of study sites distributed in different forest types (old-grown forests, windblown sites, post bark beetle sites etc.) along the elevational gradient enable us to evaluate the impacts of natural disturbances and climate changes on species and functional diversity and composition of biotic communities.

The monitoring aims to describe the biodiversity of 17 groups of flora and fauna along the gradients of elevation and forest structure using jointly developed design based on the BIOKLIM project (Bässler et al. 2015). The obtained data are fully comparable with the initial BIOKLIM data collected in the BFNP in 2006 (Friess et al. 2018) and the study area has recently been extended to the ŠNP.

Table 1. Taxonomic groups, size of their study area, and sampling methods used for monitoring of biodiversity in the Interreg project No. 26 "Silva Gabreta Monitoring – Implementation of transboundary monitoring of biodiversity and water regime".

Taxonomic group	**Study area**			**Sampling**
	0.02 ha	0.1 ha	1 ha	
Aculeata	x			Malaise trap
Arachnida	x			pitfall trap
Aves			x	grid mapping
Chiroptera		x		sound mapping
Cicadina	x			Malaise trap
Coleoptera	x			Malaise, flight interception and pitfall trap
Collembola	x			pitfall trap
Formicidae	x			pitfall and flight interception trap
Fungi		x		mapping
Heteroptera	x			Malaise, flight interception and pitfall trap
Lepidoptera		x		light traps
Lichen	x			mapping
Mammalia	x			camera traps
Mollusca	x			hand collecting
Bryophyta	x			mapping
Neuroptera	x			Malaise traps
Opiliones	x			pitfall traps
Symphyta	x			Malaise traps
Syrphidae	x			Malaise traps
Tracheophyta	x			mapping

In the BFNP, an optimized set of 157 study sites (121 in the national park and 36 in the surrounding area) were selected for the transboundary monitoring network. Thirty-six sites outside the national park were included to extend the elevation gradient to the Danube valley, i.e. from 1420 to 287 m a.s.l. (Fig. 1; for more details, see Friess et al. 2018). The study sites were distributed in elevational transects covering complete forest structural gradient including old-growth forests, areas impacted by bark beetle, and areas influenced by traditional forestry in the past.

In the Czech Republic, the forest biodiversity monitoring was conducted at 120 study sites (95 sites in the ŠNP and 25 sites in the Šumava PLA) selected from the set of the Biomonitoring project plots studied to evaluate long term changes in forest structure in non-intervention zones of the ŠNP (Čížková et al. 2011). Twenty-five sites located in nature reservations in the Šumava PLA were included to extend the elevation gradient. The study sites were grouped in two groups (Fig. 1). The first group of sites situated in the western part of the ŠNP represented the elevational gradient from the north foothill of the Bohemian Forest (the lowest elevation of 605 m a.s.l. in the Otava River valley) over the high-mountain plateau to the highest area on the border with Germany (Plesná Mt., 1332 m a.s.l.). The second group of plots was situated in the southern part of the ŠNP ranging from the Lipno reservoir (the lowest elevation of 688 m a.s.l. in the Jasánky Nature Reserve) to the main border range (Trojmezná Mt., 1340 m a.s.l.). The additional set of 30 sites was located in naturally treeless areas (mountain plains, mire meadows, *Nardus* meadows, and heathlands – all Natura 2000 habitats) in the ŠNP.

Unified protocols were used for monitoring of all taxonomic groups in both national parks. Sampling of vegetation (flowering plants, ferns, mosses and lichens), fungi, birds, snails, beetles, bugs, spiders and other insects (see Table 1 for the list of studied groups) were conducted at all study sites (for more details, also see Friess et al. 2018). Field work was conducted in seasons 2016 and 2017 and determination and data analysis continued in 2018 and 2019. The same methodology for monitoring of biodiversity in forests and natural tree-less areas in the ŠNP were used.

Four types of insect traps (Malaise, flight interception, pitfall, and light traps) were used to collect invertebrates and the following taxa from insect traps were determined: Arachnida, Opiliones, Cicadina, Collembola, Syrphidae, Heteroptera, Coleoptera, Diptera, Aculeata, Symphyta. All 157 sites in Bavaria and 150 sites in Czechia (120 forest sites and 30 tree-less sites) were equipped with flight interception and pitfall traps. Additionally, a high-informative subset of 52 sites in the BFNP or 50 forest sites in the ŠNP were selected and stratified for altitude and forest structure. The high-informative sites were continuously (from May to September) equipped with Malaise traps and once per month with light traps, which helped to record moths in night surveys. Light traps were placed at a height about 2 m, in relative open spots and used in nights without rain or strong wind.

In addition, batcorders (www.ecoobs.com) were established in these high-informative plots in the BFNP. Bat calls were recorded from May to September 2016 in all night surveys (approximately 1 hour prior sunset to 1 hour past sunrise) using automated recording devices. The batcorders were placed on wooden poles at a height of 2.5 meters above ground with the microphone facing 30° upwards in order to prevent water from accumulating at the tip of the microphone. At each site a relatively open spot was chosen for the location of the pole in order to reduce sound attenuation by dense vegetation. Survey nights with temperatures below 0°C and with a high rainfall probability were avoided as bat activity is usually reduced under these conditions (Grindal et al. 1992).

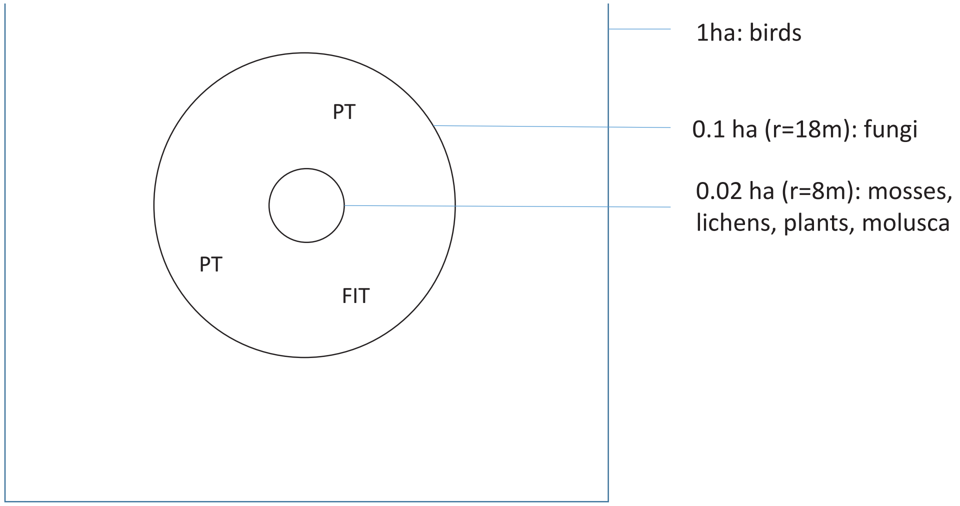

Fig. 2. Study plot diagram. Monitoring of different taxonomic groups was carried out at the plots of different size (see Table 1). One flight interception trap (FIT) and two pitfall traps (PT) were installed in all plots; Malaise traps, light traps, batcoders, and camera traps were used at a high-informative subset of 52 plots in the Bavarian Forest NP and 50 plots in the Šumava NP and PLA.

Table 2. Environmental parameters of biodiversity monitoring plots and types of their measurement.

Variables	**Definition**	**Measurement**
General information		
Geographic coordinates	coordinates according to WGS84 and ETRS	GIS model
Altitude	elevation in meters a.s.l.	
Exposition	degree	
Slope	degree	
Radiation	potential sum in the growing season (kWh/m^2)	
Climate parameters		
Temperature	annual mean temperature	GIS model
Precipitation	annual mean precipitation	
Radiation	annual mean radiation	
LiDAR data	penetration rates in different heights	airborne Laserscanner
Forest structure		
Breast height diameter	tree diameter in 1.3 m height	measurement
Tree height	in meter	measurement
Tree vitality	living or dead	estimation
Length of deadwood	in meter	measurement
Type of deadwood	standing or lying	estimation
E_{total}: total canopy cover	sample area shaded by horizontal projection of tree layer separated for occurring tree species in %	estimation
E_{3H}: high tree layer (>15 m) cover and height	% or meter	estimation
E_{3L}: lower tree layer (<15 m) cover and height	% or meter	estimation
E_2:shrub layer cover and height	% or meter	estimation
E_{1H}: herb layer cover and height	% or meter	estimation
E_{1G}: grass layer cover and height	% or meter	estimation
E_0: crypto layer cover and height	% or meter	estimation
Stone cover	%	estimation
Deadwood cover	%	estimation
Litter cover	%	estimation
Open water area cover	%	estimation
Soil		
Soil type	physical description	estimation
Moisture index	calculated	calculation
pH	for humus layer and mineral layer	lab analysis
Exchangeable nutrient elements	H, Al, Ca, Fe, K, Mg, Mn, Na	lab analysis
Cation exchange capacity		lab analysis
Base saturation		lab analysis
C/N ratio		lab analysis

Monitoring of different taxonomic groups was performed on plots of different sizes at each site (Fig. 3). Molluscs were recorded by hand collecting at suitable substrates (leaf litter, under stones, at dead wood etc.) in a single survey at 0.02-ha plots. In the field mainly macroscopic determination was conducted, partly microscopic determination was necessary with section in the lab.

All mosses, lichens (at 0.02-ha plots) and fungi (at 0.1-ha plots) species on available substrates were recorded and the available substrate types up to a height of 2 m were listed. Tree species, level of decomposition and diameter, as well as length for dead wood were measured too. If several substrates of one type were available, one per each type was recorded. If available substrates in the plot were very similar, usually three ones per each type were recorded. Partly microscopic determination was necessary with section in lab too. Vascular plants were recorded in a single survey at 0.02-ha plots in May–September. Vernal geophytes are negligible in this area due to the short growing season and the absence of rich soils. The survey was focused on the vascular understorey vegetation (including ferns) up to 1 m in height, which was estimated visually in percentage cover or on a modified scale by LONDO (1976). Species and their cover were estimated in all vegetation layers. Also the type and coverage of overlay was noted.

Birds were recorded at 1-ha plots by means of quantitative grid mapping (cf. BIBBY et al. 2000, MONING & MÜLLER 2008) at all plots. All acoustic and visual detectable breeding birds were recorded. Bird calls listening started with one minute at the edge of each plot to detect also birds that are sensitive to disturbances. Then listening went on in the plot centre for eight minutes. In the end, listening were finished with one minute at the other edge to distinguish between birds inside and outside the plot and thus to correct error detections from the centre. For each individual the specific behaviour was noted (simple detection by sighting or calling, territorial-indicating or breed-indicating young birds or food-carrying old birds). Due to phenological differences in occurrence bird mapping was repeated five times, i.e. in the end of March, in the middle of April, in the beginning and the end of Mai and in the beginning of June (MÜLLER 2005, MONING & MÜLLER 2008). Mapping was conducted from sun rise till 11 a.m. under good weather conditions, i.e. hardly wind, no rain, preferably sun (MONING & MÜLLER 2008; MÜLLER 2005). To minimize process-depended errors each plot was mapped to different hours in the morning and at least ones from each of three mapping persons. Additionally, camera traps were installed in high-informative plots to record vertebrates passing or occurring there.

Furthermore, different environmental parameters were recorded and soil samples were taken and analysed (Table 2). Forest structure was investigated at biodiversity study sites both in the BFNP (HILMERS et al. 2018) and in the ŠNP and Šumava PLA, where the methodology of the Biomonitoring project was used (ZENÁHLÍKOVÁ et al. 2015). In addition, a dendrochronology analysis was conducted to estimate the age of trees at the sites and a study of mesoclimatic conditions (ROMPORTL et al. 2018) delivered useful background for interpretation of biodiversity monitoring.

Monitoring of mires

The transboundary monitoring of mires aims to evaluate the water level balance, hydrochemistry and vegetation in drained, restored, and near-natural mires of different elevation. The study has mainly focused on the evaluation of the effects of climate changes and applied conservation measurements, particularly water regime restoration, on water regime of mires. Within the project No. 26 "Silva Gabreta – Monitoring of biodiversity and water regime", long-term monitoring of mires was optimized in the ŠNP and newly established in the BFNP. Currently, altogether 12 mires in the ŠNP and Šumava PLA and 9 mires in Bavaria (6 in the

Fig. 3. Map of mires monitoring sites (blue points) where monitoring was conducted in the Interreg project No. 26 "Silva Gabreta Monitoring – Implementation of transboundary monitoring of biodiversity and water regime". Dashed lines are borders of the Bavarian Forest National Park (BFNP), Šumava National Park (ŠNP) and Šumava Protected Landscape Area (Šumava PLA).

Table 3. Monitoring design for jointly implemented monitoring of mires in the Šumava NP. C – control intact mire, R – restored mire; Alt – altitude (m a.s.l.), Wtb – water table in boreholes, Hch – Hydrochemistry, McA – microclimate air, McS – microclimate soil, Rof – run off, Pre – precipitation, Veg – vegetation monitored on permanent plots.

Type of mire	Site	Alt (m)	Measures						
			Wtb	Hch	McA	McS	Rof	Pre	Veg
Ombrotrophic mires									
High raised bog (C)	Blatenská slať	1250	18	x				1	18
High raised bog (C)	Šárecká slať	1020	6	x	1	1		1	6
High raised bog (R)	Schachtenfiz	1140	21	x	1	1	1	1	21
High raised bog (R)	Rybárny	1020	4	x					4
High raised bog (R)	Křemelná	930	8	x			1	1	8
High raised bog (R)	Novohuťské močály	1220	11						11
High raised bog (R)	Kamerální	1210	5						5
Minerotrophic mires									
Spruce mire (C)	Tetřevská	1110		x					
Transitional mire (C)	Malý Bor	900	3	x					3
Transitional mire (C)	Roklanský les	1190	9	x					9
Meadow mire (C)	Velký Bor	870	2	x					2
Spruce mire (R)	Schachtenfilz	1140	7	x					7
Spruce mire (R)	Rybárny	1020	5	x			1		5
Spruce mire (R)	Blatenská slať	1250	2	x	1	1			2
Spruce mire (R)	Filipohuťské polesí	1120		x					
Transitional mire (R)	Křemelná	930	6						6
Meadow mire (R)	Křemelná	930	12	x					12

Table 4. Monitoring design for jointly implemented monitoring of mires in the Bavarian Forest NP. C – control intact mire, R – restored mire; Alt – altitude (m a.s.l.), Wtb – water table in boreholes, Hch – Hydrochemistry, McA – microclimate air, McS – microclimate soil, Rof – run off, Pre – precipitation, Veg – vegetation monitored on permanent plots.

Type of mire	**Site**	**Alt (m)**	**Measures**						
			Wtb	**Hch**	**McA**	**McS**	**Rof**	**Pre**	**Veg**
Ombrotrophic mires									
High raised bog (C)	Grosser Filz am Spitzberg	1320	2	x	x	x		x	6
High raised bog (C)	Zwieselter Filz	1125	2	x					6
Valley raised bog (C)	Klosterfilz	745	2	x	x	x		x	6
Valley raised bog (C)	Todten Au	720	2	x					6
Valley raised bog (C)	Dorner Au	720	1	x					3
Valley raised bog (R)	Finsterauer Filz	1045	2	x	x	x		x	6
Valley raised bog (R)	Großer Filz at Riedlhütte	745	4	x					12
Minerotrophic mires									
Spruce mire (C)	Latschenfilz	1150	2	x	x	x		x	6
Spruce mire (C)	Filzwald bei Klingenbrunn Bahnhof	750	2	x	x	x		x	6
Transitional mire (C)	Grosser Filz am Spitzberg	1320	2	x					6
Transitional mire (C)	Klosterfilz	745	1	x					3
Transitional mire (C)	Dorner Au	720	1	x					3
Spruce mire (R)	Grosser Filz at Spitzberg	1320	3	x					9
Spruce mire (R)	Zwieselter Filz	1125	2	x	x	x		x	6
Spruce mire (R)	Todten Au	720	2	x					6

BFNP and 3 in the surrounding area) together form unified set of monitoring sites (Fig. 2). All main types of mires are included: ombrotrophic alluvial and montane raised bogs, and three minerotrophic mire types, spruce mires, transitional fens, and treeless fens. The study sites are at elevations between 870 to 1250 m a.s.l.

The mire habitats under the monitoring program are ombrotrophic bogs (*Leuco-Scheuchzerion palustris*, *Oxycocco-Ericion*, *Sphagnion medii*), waterlogged and mire spruce forests (*Mastigobryo-Piceetum*, *Sphagno-Piceetum*). Both restored sites (R, where water regime restoration measures were applied) and control sites (C, i.e. intact) were included in the monitoring design (Table 3). The following environmental parameters have been recorded at all study sites: water level, hydrochemistry, runoff, air moisture and temperature (0.3 m and 1.2 m above the soil surface), soil moisture and temperature (0.01 m, 0.03 m and 1.2 m below the soil surface), precipitation, surrounding stand structure, and vegetation mapping. Three new study sites have been added recently to the already existing monitoring design in the ŠNP to cover all types of mires occurring in the region. New automatic water-level recorders have been set at study sites measured only manually so far. Monitoring was newly implemented in the BFNP (Table 4) where no detail monitoring of mires has been done until present. Additionally, several palynology studies and peat surveys were conducted in the BFNP to detect historical impact on mires.

In the ŠNP, more than one hundred permanent plots with associated water wells were monitored to characterize microtopographic, vegetation, and drainage patterns of the different mire sites. Position of water table was measured manually in all boreholes at nearly fortnight intervals. Automatic gauging (at one-hour interval) by piezometers was used in selected boreholes. Water samples from boreholes, ditches, runoff profiles from drained sites and samples from streams were taken monthly for a detailed hydrochemical analysis, including content of main cations and anions (SO_4, NO_3, NH_4, PO_4, Ca, Mg, Al, Fe), pH, conductivity and DOC. Runoff from drained sites, as well as amount of precipitation were measured continually. Vegetation, both vascular plants and mosses, was mapped at the plots of 2×2 m annually. In the BFNP, vegetation was mapped at 90 permanent plots of 2×2 m annually and six micro climate stations continuously measuring air and soil moisture, air and soil temperature, and precipitation were installed in 2016. Automatic gauging (at 1-h intervals) by piezometers was applied in 30 boreholes from which water samples for hydrochemical analysis were collected monthly from April till September 2017.

Wetland vegetation along the restored streams was studied to describe the effects of restorations. Monitoring of vegetation started in 2011 in the Hučina floodplain, i.e. three years before its restoration (Bojková et al. 2015). In order to document the vegetation prior to the stream restoration, a map of the habitat types was made. With aim to follow vegetation changes after the stream restoration, permanent plots were established along three transects laid across the stream floodplains perpendicular to the stream. Transect 1 was laid in the upper part of the studied floodplain, transect 2 in the middle, and transect 3 in the lower part. Altogether 12 plots of 4×4 m were positioned in the central open part of each floodplain and 14 plots having 10×10 m were placed in the surrounding forested parts. Boreholes were installed at a border of each plot to a depth of 1 m. Each year, vegetation relevés were recorded at all plots in early summer and the water level was measured. The first results of vegetation monitoring along the Jedlový Potok are published in this issue (Čížková & Padrtová 2018).

Monitoring of aquatic ecosystems

The monitoring consists of the following five studies focused on different aquatic ecosystems in the Bohemian Forest.

(i) A systematic long term monitoring aiming to evaluate the effects of natural disturbances and climate changes on biodiversity of streams started at seven catchments (Große Deffernik, Kolbersbach, Kleiner Regen, Große Ohe, Kleine Ohe, Sagwasser, and Reschbach) distributed throughout the BFNP. Altogether 51 sampling sites were located along the elevation gradient from 600 to 1100 m a.s.l. with sampling sections at each 100 elevational meters. From 700 to 900 m a.s.l., smaller side branches were added to sites at main streams as replicates to enable comparison of streams of similar size at all elevational steps. The results of the pilot study preceding the above-mentioned monitoring to evaluate macroinvertebrate diversity and community composition in lower sections of main streams draining the BFNP are presented in this issue (Bojková et al. 2018).

(ii) Monitoring of macroinvertebrate diversity in the core area of both national parks involved the detailed study of two model mountain catchments, upper Vydra in the ŠNP and Große Ohe in the BFNP. This monitoring aimed to explore main gradients in species data and factors governing species richness, abundance and composition of macroinvertebrate assemblages within both stream networks with a special focus on the effect of acidification. Species and environmental data were collected at 43 sites in the Vydra catchment and 49 sites in the Große Ohe catchment. Sites were distributed to cover all stream types and different forest structure within the catchments. Species and basic environmental data from the Große Ohe catchment are presented in this issue (Bojková et al. 2018).

(iii) Long-term monitoring of three restored streams, Hučina, Jedlový Potok and Žlebský Potok in the ŠNP. It was focused on the evaluation of the success of the restoration based on the data on the colonization of restored streams by benthic macroinvertebrates, development of their assemblages in relation to flow and substrate conditions, and comparison of environmental conditions and macroinvertebrate communities before and after the restoration. The results will be used for planning next stream restorations in the ŠNP in the future.

(iv) Common transboundary monitoring of bog pools was focused on the biodiversity of different aquatic invertebrates (zooplankton, benthic and free-swimming insects) and environmental drivers of their communities. Altogether 54 pools from 22 groups of pools or restored blocked ditches were investigated. Species and environmental data have been used to compare natural and artificially created bog pools, and to study relict and endangered aquatic species inhabiting raised bogs.

(v) Long term research of the glacial lakes provides crucial information on recovery of terrestrial and aquatic ecosystems from atmospheric acidification and the role of forest disturbances in water fluxes of nutrients and important elements in lake catchments. Within the Silva Gabreta project, a comparative study on pools and fluxes of major nutrients and ecologically important elements in the terrestrial and aquatic parts of both Plešné Lake and Čertovo Lake catchments has been conducted (Kopáček et al. 2018a,b). The aim of this study has been to estimate nutrient losses and leaching of toxic aluminium forms from forest soils and their effects on aquatic biota. Similar study has been commenced in Rachelsee.

Monitoring of streams (i.e. stream monitoring in the BFNP, and both in the Vydra and Große Ohe catchments) was conducted using standard methodology based on the AQEM protocol (AQEM Consortium 2002, Meier et al. 2006) to ensure compatibility of the data. Sampling of macroinvertebrates was based on a standard multi-habitat scheme designed for sampling of major mesohabitats proportionally according to their share within the sampling site (AQEM Consortium 2002). Each sample consisted of 20 plots of 0.25×0.25 m taken from all mesohabitat types with a share of at least 5% coverage at the sampling site. The 20 plots were distributed according to the share of mesohabitats. Kick-samples were sampled using a standard hand net with 0.5 mm mesh size. In the Bavarian streams, Phylib method (Schaumburg et al. 2012) was used for sampling of macrophytes, i.e. species cover was mapped. Diatoms together with other phytobenthos were sampled from the available substrate. Fish were sampled using electrofishing. Malaise traps were installed at 12 of 51 sites investigated in the BFNP in 2016 to sample adults of aquatic insects, especially Ephemeroptera, Plecoptera, and Trichoptera.

Different sampling methods were used for the monitoring of restored streams. At each sampling site, three mesohabitats, riffle, run and pool, were investigated. Macroinvertebrates were sampled semiquantitatively using a hand net with 0.25-mm mesh size. At each mesohabitat, altogether five approx. 0.25×0.25 m plots were sampled and merged into one sample characterising one mesohabitat. Prior to sampling of each plot, water depth and velocity were measured using a Flo-Mate flowmeter and water samples for chemical analysis were collected (Bojková et al. 2015). Altogether, seven sites were located in the restored parts of streams (three in Hučina, two in Žlebský Potok, and two in Jedlový Potok) and five sites were located at reference sites nearby (one site in a near-natural part of Hučina and Žlebský Potok above their restored stretches, one site in the Studená Vltava stream and in the Teplá Vltava stream, i.e. in the recipients downstream the restored stretches, and one site at the channelized Jedlový Potok above the restored stretch). For more details on the methodology of this study see Bojková et al. (2015). Pre-restoration data are available only for two streams, Jedlový Potok and Žlebský Potok.

Bog pools were investigated using several sampling methods covering various aquatic organisms. Littoral benthic macroinvertebrates were sampled semiquantitatively by a standard hand net with 0.5 mm mesh size. Sampling effort was standardized by time, i.e. macroinvertebrates were sampled by sweeping by a net for five minutes. Free-swimming aquatic insects were collected by two light traps (one trap in littoral zone and the second one in open water zone). Moreover, two activity traps were set in littoral zone. All traps were exposed for 24 hours. Microinvertebrates (Rotifera, Cladocera and Copepoda) were sampled both qualitatively and quantitatively. Qualitative samples were taken by plankton net of 40 µm mesh size from four different part of each pool to cover its heterogeneity. Eight litres of quantitative samples were taken by a 2-l vessel and concentrated through a 40-µm mesh size. Littoral vegetation coverage was estimated. Depth and size of the pool, basic physical-chemical parameters (temperature, dissolved oxygen concentration, pH, and conductivity) were measured at each pool and samples for water chemistry (total phosphorus, total nitrogen) and chlorophyll *a* concentration were analysed in the laboratory.

Long-term research of glacial lakes includes various research activities with complex methodology. Overview of research activities and references on methodology are available in Vrba et al. (2015). Comparative study on pools and fluxes of major nutrients and elements included in the Silva Gabretaproject in the catchments of Plešné and Čertovo lakes included monthly sampling of precipitation and lake water samples and annual sampling of litter of spruce and deciduous trees. The following parameters were analysed in water samples: Cl^-, SO_4^{2-}, NO_3^-, F^-, H^+, NH_4^+, Na^+, K^+, Ca^{2+}, Mg^{2+}, DOC, all forms of P, total and organic N. Aluminium and iron were analysed only in samples of lake water. Dry matter and total amount of Ca, Mg, Na, K, Al, Fe, Mn, P, C, and N were analysed in tree litter samples. More details on sampling and analytical methods are available in Kopáček et al. (2018a,b).

Project outputs

The detailed field investigation of biodiversity of different ecosystems has provided important data for both basic species inventory and evaluation of ecological changes driven by natural and anthropogenic disturbances. Our multi-taxa biodiversity monitoring delivered a large set of species records supplemented by environmental data. Field work was mainly done in the 2016 and 2017 seasons and processing of samples and species' determination and data analysis have continued until 2019. The first scientific papers have been already published (e.g. Fries et al. 2018, Hilmers et al. 2018, in press, Vondrák & Malíček, in prep.) and several others are under preparation. The common monitoring of forests offers a unique opportunity to analyse structural and biological diversity across the border and study the Bohemian Forest as a one ecosystem. The gained knowledge stimulates convergence of management of the both NPs and support preparation of common nature conservation projects.

Both newly established monitoring of mires in the BFNP and improved monitoring of mires in the ŠNP have delivered unique data sets enabling an evaluation of the restoration success. The preliminary results confirmed the importance of restoration and suggested that hydrochemical changes were more expressed in spruce mires than in raised bogs. Continuation of mire monitoring and detailed statistical analyses of data are planned to evaluate long-term trends in local temperature, precipitation, and water level fluctuation in different types of mires, which could reveal possible effects of climate changes and/or current climatic extremes on functioning of mires. Current monitoring of benthic macroinvertebrates colonising three restored streams (Bojková et al. 2017) and vegetation in their floodplains (Čížková & Padrtová 2018) in the ŠNP has delivered scientific support for planning of new restoration projects. The newly established monitoring of streams in the BFNP aims to provide unique data on an altitudinal distribution of benthic macroinvertebrates and its relation to effects of acidification and/or forest disturbances. Preliminary results are presented in this issue by Bojková et al. (2018). Continuation of this monitoring will provide sufficient data for evaluation of the altitudinal shifts in species distribution induced by climate changes, i.e. complementary data to those from terrestrial forest monitoring (e.g. Bässler et al. 2008, 2010, Fries et al. 2018).

Beudert et al. (2018) evaluated long-term hydrological for the whole Bohemian Forest that clearly suggested some positive mitigation effects of natural disturbances in the NPs, which have offset current climate changes. The study on long-term trends in precipitation and runoff in the Modravský Potok catchment (Lamačová et al. 2018) similarly confirmed that bark beetle outbreaks and changes in forest structure did not affect runoff significantly. Higher runoffs were particularly correlated with higher precipitation, whereas the lower runoffs with lack of rain and snow, and similar trends are predicted also in future (Lamačová et al. 2018). Data from the long-term monitoring of both Plešné Lake and Čertovo Lake catchments enabled to prepare the balance studies on pools and fluxes of major nutrients (Kopáček et al. 2018a,b).

New data from monitoring of effect of deicing salt to ecosystems along the roads in protected areas confirmed our assumption that Na^+ and Cl^- ions increased in the streams crossed with the roads maintained by deicing salt (Zýval et al. 2018). Increasing concentrations of Na^+ and Cl^- ions were found also in soil samples collected along the roads maintained by deicing salt, both in BFNP (Křenová et al., in press) and ŠNP.

All the above-mentioned scientific contributions have provided the basis for developing suitable management strategies to maintain and enhance biodiversity and ecosystem services.

The main project outputs planned in the project proposal included: extensive set of environmental and species data, rich material from samples of various taxa prepared for continuing determination, and results of comparative studies form useful platform for meeting the following project outputs listed in the project proposal:

1) Implementation of the common monitoring design after the standardization of methodology.

2) Preparation of common biodiversity database for forest, mire and stream monitoring

data.
3) Review of the practicability of applied monitoring designs for a long-term continuation within a monitoring program.
4) Recommendations for a common management in the both NPs.
5) Common publication of the results and collaboration of Bavarian and Czech research teams.
Part of these results are published on this issue together with several short papers delivering new information about hydrology and biodiversity, improving the Silva Gabreta Monitoring project knowledge.

CONCLUSIONS

The Interreg project No. 26 "Silva Gabreta – Monitoring of biodiversity and water regime" has offered for the first time the possibility to implement a jointly prepared transboundary monitoring design. Except for the long-term cooperation in the glacial lake research, no real common monitoring activities of the both BFNP and ŠNP had existed in the Bohemian Forest region until this Silva Gabreta Monitoring project has been implemented. The practical implementation of the common planned monitoring design with standardized methods set the starting point for a long-term, unified monitoring program in both National Parks. The collected data, results and experiences serves for the elaboration of recommendations for a common national park management. Knowledge gained from a close-to-nature reference area can substantially contribute to the enhancement of biodiversity and ecosystem services in other man-influenced biotopes and find here application.

Acknowledgments. This work and publication was granted by the Cross-border cooperation programme Czech Republic–Bavaria Free State ETC goal 2014–2020, the Interreg V project No. 26 "Silva Gabreta Monitoring – Implementation of transboundary monitoring of biodiversity and water regime" and the Ministry of Education, Youth and Sports of CR within the National Sustainability Program I (NPU I), grant number LO1415 provided the financial support for chemical analyses of soils in monitoring of effect of deicing salt in BFNP. We thank J. Bojková for many useful comments and improving our text, and V. Zýval jun. for helping with maps.

REFERENCES

AQEM CONSORTIUM, 2002: Manual for the application of the AQEM system. A comprehensive method to assess European streams using benthic macroinvertebrates, developed for the purpose of the Water Framework Directive. Version 1.0, February 2002, 202 pp.

BÄSSLER C. & MÜLLER J., 2010: Importance of natural disturbance for-time substitution as recovery of the rare polypore *Antrodiella citrinella* Niemela & Ryvarden. *Fungal Biology*, 114: 129–133.

BÄSSLER C., FÖRSTER B., MONING C. & MÜLLER J., 2008: The BIOKLIM-Project: biodiversity research between climate change and wilding in a temperate montane forest – the conceptual framework. Forest Ecology, *Landscape Research and Nature Conservation*, 7: 21–33.

BÄSSLER C., MÜLLER J. & DZIOCK F., 2010: Detection of climate-sensitive zones and identification of climate change indicators: A case study from the Bavarian Forest National Park. *Folia Geobotanica*, 45: 163–182.

BÄSSLER C., SEIFERT L. & MÜLLER, J. 2015. The BIOKLIM Project in the National Park Bavarian Forest: Lessons from a biodiversity survey. *Silva Gabreta* 21: 81–93

BASTL M., BURIAN M., KUČERA J., PRACH K., REKTORIS L. & ŠTECH, M. 2008: Central European pine bogs change along an altitudinal gradient. *Preslia*, 80: 349–363.

BEUDERT B. & GIETL G., 2015: Long-term monitoring in the Große Ohe catchment, Bavarian Forest National Park. *Silva Gabreta*, 21: 5–27.

BEUDERT B., BASSLER C., THORN S., NOSS R., SCHRÖDER B., DIEFFENBACH-FRIES H. & MÜLLER J., 2015: Bark beetles increase biodiversity while maintaining drinking water quality. *Conservation Letters*, 8: 272–281.

BEUDERT B., BERNSTEINOVÁ J., PREMIER J. & BÄSSLER C., 2018: Natural disturbance by bark beetle offsets climate change effects on streamflow in Bohemian Forest headwater catchments. *Silva Gabreta*, 24: 21–45.

Bibby C.J., Burgess N.D., Hill D.A. & Mustoe S., 2000: Bird census techniques. Second edition. Academic Press, London. 302 pp.

Bojková J., Bufková I., Rádková V., Soldán T. & Vrba J., 2017: Jak se žije v revitalizovaných potocích na Šumavě? [The life in restored streams of the Bohemian Forest.] *Živa*, 2: 74–76.

Bojková J., Čížková H., Kučerová A., Rádková V., Soldán T., Svidenský R. & Vrba J., 2015: Monitoring of the restored streams in the Vltavský Luh, Šumava National Park. *Silva Gabreta*, 21: 73–79.

Bojková J., Seifert L., Petruželová J., Šorfová V., Syrovátka V., Sroka P. & Polášková V., 2018: Species richness and composition of macroinvertebrate assemblages in the Bavarian Forest: Preliminary results of the stream monitoring. *Silva Gabreta*, 24: 171–211.

Bufková I., 2012: Program revitalizace šumavských mokřadů a rašelinišť [A restoration program for the Bohemian Forest wetlands and mires]. Ms., Správa NP a CHKO Šumava, Kašperské Hory, 33 pp. (in Czech). (library of Správa NP a CHKO Šumava, Kašperské Hory)

Bufková I., Stíbal F. & Mikulášková E., 2010: Restoration of drained mires in the Šumava National Park, Czech Republic. In: *Restoration of lakes, streams, floodplains, and bogs in Europe: principles and case studies*, Likens G. & Eiseltová M. (eds) Springer, Dordrecht: 331–354.

Čížková H. & Padrtová M., 2018: Floodplain vegetation of the restored Jedlový Potok stream in the Bohemian Forest. *Silva Gabreta*, 24: 216–221.

Čížková P., Svoboda M. & Křenová Z., 2011: Natural regeneration of acidophilous spruce mountain forests in non-intervention management areas of the Šumava National Park – the first results of the Biomonitoring project. *Silva Gabreta*, 17: 19–35.

Dierssen K. & Dierssen B., 2001: *Moore (Ekosysteme Mitteleuropas aus geobotanischer Sicht)*. Ulmer, Stuttgart, 230 pp.

Englmaier K.H., 2009: *Die Renaturierung des Seefilzes im Nationalpark Bayerischer Wald*. Berichte aus den nationalparkheft 9. Nationalparkverwaltung Bayerischer Wald, Grafenau, 28 pp.

Fischer A. & Fischer H.S., 2012: Individual-based analysis of tree establishment and forest stand development within 25 years after wind throw. *European Journal of Forest Research*, 131: 493–501.

Friess N., Bässler C., Brandl R., Hilmers T., Müller J. & Seifert L., 2018: Biodiversity along an elevational gradient of the Bavarian Forest – The BIOKLIM project. *Silva Gabreta*, 24: 149–160.

Grindal S. D., Collard T. S., Brigham R. M. & Barclay R. M. R., 1992: Influence of precipitation on reproduction by *Myotis* bats in British Columbia. *The American Midland Naturalist*, 128: 339–344.

Hagan J.M. & Grove S.L., 1999: Coarse woody debris. *Journal of Forestry*, 97: 6–11.

Heurich M., Beudert B., Rall H., & Křenová Z., 2010: National parks as model regions for interdisciplinary long-term ecological research: The Bavarian Forest and Šumava National Parks underway to transboundary ecosystem research. In: *Long-term ecological research*, Müller F., Baessler C., Schubert H. & Klotz S. (eds) Springer, Dordrecht: 327–344.

Hilmers T., Bässler C., Friess N., Müller J. & Seifert L., 2018: Changes in forest structure in the National Park Bavarian Forest. An evaluation after 10 years of the BIOKLIM-Project. *Silva Gabreta*, 24: 161–170.

Hilmers T., Friess N., Bässler C., Heurich M., Brandl R., Pretzsch H., Seidl R. & Müller J., in press: Biodiversity along temperate forest succession. *Journal of Applied Ecology*.

Jehl H., 1994: Ein moor im Wandel der Zeit. Ms., unpubl. report, Nationalparkverwaltung Bayerischer Wald, Grafenau, 26 pp. (deposited in the Nationalparkverwaltung Bayerischer Wald)

Kettle H., Kopáček J. & Hejzlar J., 2003: Modelling air temperature at Čertovo Lake back to 1781. *Silva Gabreta*, 9: 15–32.

Konvalinková P. & Prach K., 2002: Spontaneous succession of vegetation in mined peatlands: a multi-site study. *Preslia*, 82: 422–435.

Kopáček J., Cudlín P., Fluksová H., Kaňa J., Picek T., Šantrůčková H., Svoboda M. & Vaněk D., 2015: Dynamics and composition of litterfall in an unmanaged Norway spruce (*Picea abies*) forest after bark-beetle outbreak. *Boreal Environment Research,* 20: 305–323.

Kopáček J., Fluksová H., Hejzlar J., Kaňa J., Porcal P. & Turek J., 2017: Changes in surface water chemistry caused by natural forest dieback in an unmanaged mountain catchment. *Science of the Total Environment*, 584–585: 971–981.

Kopáček J., Hejzlar J., Kaňa J., Porcal P. & Turek J., 2018a: Water fluxes of ecologically important elements in Čertovo catchment–lake system from 1998–2017. *Silva Gabreta*, 24: 85–114.

Kopáček J., Hejzlar J., Kaňa J., Porcal P. & Turek J., 2018b: Water fluxes of ecologically important elements in Plešné catchment–lake system from 2000–2017. *Silva Gabreta*, 24: 115–147.

Křenová Z. & Seifert L., 2015: Silva Gabreta – monitoring of mountain ecosystems. *Silva Gabreta*, 21: 1–4.

Křenová Z., Chocholoušková Z. & Zýval V., 2012: Effects of applying deicing salt to roads in protected areas: a preliminary study in the Bavarian Forest National Park. *European Journal of Environmental Sciences*, 2: 56–61.

Křenová Z., Zýval V., Zýval V. jun & Chocholoušková Z., in press: Increasing concentration of deicing salt ions in soils of the Bavarian Forest National Park. *European Journal of Environmental Sciences*,

Lamačová A., Hruška J., Trnka M., Štěpánek P., Zahradníček P., Meitner J. & Farda A., 2018: Modelling future hydrological pattern in a Bohemian Forest headwater catchment. *Silva Gabreta*, 24: 47–67.

Lindenmayer D., Thorn S. & Banks S., 2017: Please do not disturb ecosystems further. *Nature Ecology & Evolution*, 1: 0031.

Martin K. & Eadie J.M., 1999: Nest webs: a community-wide approach to the management and conservation of cavity-nesting forest birds. *Forest Ecology and Management*, 115: 243–257.

Meier C., Haase P., Rolauffs P., Schindehütte K., Schöll F., Sundermann A., & Hering D., 2006: *Methodisches Handbuch Fließgewässerbewetung*. Universität Duisburg-Essen, 110 pp.

Moning C. & Müller J., 2008: Environmental key factors and their thresholds for the avifauna of temperate montane forests. *Forest Ecology and Management*, 256: 1198–1208.

Müller J., Bußler H., Goßner M., Rettelbach T. & Duelli P., 2008: The European spruce bark beetle *Ips typographus* (L.) in a national park – from pest to keystone species. *Biodiversity and Conservation*, 17: 2979–3001.

Müller J., Hothorn T. & Pretzsch H., 2007: Long-term effects of logging intensity on structures, birds, saproxylic beetles and wood-inhabiting fungi in stands of European beech (*Fagus sylvatica* L.). *Forest Ecology and Management*, 242: 297–305.

Müller J., Noss R.F., Bußler H. & Brandl R., 2010: Learning from a ‘‘benign neglect strategy” in a national park: response of saproxylic beetles to dead wood accumulation. *Biological Conservation*, 143: 2559–2569.

Niklasson M., Zin E. & Zielonka T., 2010: A 350-year tree-ring fire record from Białowieża Primeval Forest, Poland: implications for Central European lowland fire history. *Journal of Ecology*, 98: 1319–1329.

Nilsson S.G., Hedin J. & Niklasson M., 2001: Biodiversity and its assessment in boreal and nemoral forests. *Scandinavian Journal of Forest Research*, 3: 10–26.

Oulehle F., Chuman T., Majer V. & Hruška J., 2013: Chemical recovery of acidified Bohemian lakes between 1984 and 2012: the role of acid deposition and bark beetle induced forest disturbance. *Biogeochemistry,* 116: 83–101.

Oulehle F., Wright R.F., Svoboda M., Bače R., Matějka K., Kaňa J., Hruška J., Couture R.M. & Kopáček J., 2018: Effects of bark beetle disturbance on soil nutrient retention and lake chemistry in glacial catchment. *Ecosystems*. https://doi.org/10.1007/s10021-018-0298-1

Raabe S., Müller J., Manthey M., Duerhammer O., Teuber U., Göttlein A., Förster B., Brandl R. & Bässler C., 2010: Drivers of bryophyte diversity allow implications for forest management with a focus on climate change. *Forest Ecology and Management*, 260: 1956–1964.

Romportl D., Štěpánek D. & Janík T., 2018: Studie mezoklimatických poměrů [A study of mesoclimatic conditions]. Ms., unpubl. report, Správa NP Šumava, Vimperk, 16 pp. (library of Správa NP Šumava, Vimperk)

Röder J., Bässler C., Brandl R., Dvořák L., Floren A., Gossner M.M., Gruppe A., Jarzabek-Müller A., Vojtěch O., Wagner C. & Müller J., 2010: Arthropod species richness in the Norway spruce canopy along an elevation gradient. *Forest Ecology and Management*, 259: 1513–1521.

Rösch M., 2000: Long-term human impact as registered in an upland pollen profile from the southern Black Forest, south-western Germany. *Vegetation History and Archaeobotany*, 9: 205–218.

Šantrůčková H., Šantrůček J., Šetlík J., Svoboda M. & Kopáček J., 2007: Carbon isotopes in tree rings of Norway spruce exposed to atmospheric pollution. *Environment Science and Technology*, 41: 5778–5782.

Schaumburg J., Schranz C., Stelzer D., Vogel A. & Gutowski A., 2012: *Verfahrensanleitung für die ökologische Bewertung von Fließgewässern zur Umsetzung der EG-Wasserrahmenrichtlinie: Makrophyten und Phytobenthos. Phylib*. Bayerisches Landesamt für Umwelt, Augsburg, 191 pp.

Schreiber H., 1924: *Moore des Böhmerwaldes und des deutschen Südböhmen. IV.* Sebastianberg, 119 pp.

Seedre M., Kopáček J., Janda P., Bače R. & Svoboda M., 2015**:** Carbon pools in a montane old-growth Norway spruce ecosystem in Bohemian Forest: Effects of stand age and elevation. *Forest Ecology and Management*, 346: 106–113.

Shiel D. & Burslem F.R., 2003: Disturbing hypotheses in tropical forests. *Trends in Ecology & Evolution*, 18: 18–26.

Spitzer K. & Bufková I., 2008: *Peatlands of Šumava*. Vimperk. Správa Národního parku a Chráněné krajinné oblasti Šumava. 209 pp.

Spitzer K. & Danks H.V., 2006: Insect biodiversity of boreal peat bog. *Annual Review of Entomology*, 51: 137–161.

Strunz H., 1994: Renaturierung 1994. Ms. (deposited in Nationalparkverwaltung Bayerischer Wald).

Svoboda M., Janda P., Nagel T.A., Fraver S., Rejzek J. & Bače R., 2012: Disturbance history of an old-growth sub-alpine *Picea abies* stand in the Bohemian Forest, Czech Republic. *Journal of Vegetation Science*, 23: 86–97.

Svobodová H., Soukupová L. & Reille M., 2002: Diversified development of mountain mires, Bohemian Forest, Central Europe, in the last 13,000 years. *Quaternary International*, 91: 123–135.

Tallis J.H., 1991: *Plant Community History*. Chapman & Hall, UK, 398 pp.

Thorn S., Bässler C., Brandl R., Burton P.J., Cahall R., Campbell J.L., Castro J., Choi C.Y., Cobb T, Donato D.C., Durska E., Fontaine J.B., Gauthier S., Hebert C., Hothorn T., Hutto R.L., Lee E.J., Leverkus A.B., Lindenmayer D.B., Obrist M.K., Rost J., Seibold S., Seidl R., Thom D., Waldron K., Wermelinger B., Winter M.B., Zmihorski M., Müller J., 2017: Impacts of salvage logging on biodiversity: a meta-analysis. *Journal of Applied Ecology*, 55: 279–289.

Turek J., Fluksová H., Hejzlar J., Kopáček J. & Porcal P., 2014: Modelling air temperature in catchments of Čertovo and Plešné lakes in the Bohemian Forest back to 1781. *Silva Gabreta*, 20: 1–24.

Vondrák J. & Malíček J., in prep.: Epiphytic lichens in forests of the Šumava Mountains in the Czech Republic; abundance and frequency assessments. Submitted to *Biodiversity and Conservation*.

Vrba J., Bojková J., Chvojka P., Fott J., Kopáček J., Macek M., Nedbalová L., Papáček M., Rádková V., Sacherová V., Soldán T., & Šorf M., 2016: Constraints on the biological recovery of the Bohemian Forest lakes from acid stress. *Freshwater Biology*, 61: 376–395.

Vrba J., Kopáček J., Fott J., Kohout L., Nedbalová L., Pražáková M., Soldán T. & Schaumburg J., 2003: Long-term studies (1871–2000) on acidification and recovery of lakes in the Bohemian Forest (central Europe). *Science of the Total Environment*, 310: 73–85.

Vrba J., Kopáček J., Fott J. & Nedbalová L., 2014: Forest dieback modified plankton recovery from acidic stress. *AMBIO*, 43: 207–217.

Vrba J., Kopáček J., Tahovská K. & Šantrůčková H., 2015**:** Long-term ecological research of glacial lakes in the Bohemian Forest and their catchments. *Silva Gabreta*, 21: 53–71.

Vrba J., Bojková J., Chvojka P., Fott J., Kopáček J., Macek M., Nedbalová L., Papáček M., Rádková V., Sacherová V., Soldán T. & Šorf M., 2016: Constraints on the biological recovery of the Bohemian Forest lakes from acid stress. *Freshwater Biology*, 61: 376–395.

Weltzin J.F., Pastor J., Harth C., Bridgham S. D., Updegraff K. & Chapin C. T., 2000: Response of bog and fen plant communities to warming and water-table manipulations. *Ecology*, 81: 3464–3478.

Zenáhlíková J., Červenka J., Čížková P., Bečka P., Starý M., Marek P., Křenová Z. & Svoboda M., 2015: The Biomonitoring project – monitoring of forest ecosystems in non-intervention areas of the Šumava National Park. *Silva Gabreta*, 21: 95–104.

Zýval V, Křenová Z., Chocholoušková Z., Zýval V. jun. & Zývalová J., 2015: Effects of applying deicing salt to roads in protected areas of the Bohemian Forest region. *Silva Gabreta*, 21: 43–52.

Zýval V., Křenová Z., Raus M., Štrupl V., Zýval V. jun. & Zývalová J., 2018: Effects of deicing salt in protected areas: water quality monitoring in the river basin with the occurrence of a rare pearl mussel. *Journal of the Polish Mineral Engineering Society*, January–June 2018: 99–102.

Received: 24 July 2018
Accepted: 18 October 2018

Silva Gabreta	vol. 24	p. 21–45	Vimperk, 2018

Natural disturbance by bark beetle offsets climate change effects on streamflow in headwater catchments of the Bohemian Forest

Burkhard Beudert[1,*], **Jana Bernsteinová**[2], **Joseph Premier**[1] **& Claus Bässler**[1]

[1]*Bavarian Forest National Park, Freyungerstraße 2, D-94481 Grafenau, Germany*
[2]*Faculty of Sciences, Charles University, Prague, Albertov 6, CZ-12000, Prague, Czech Republic*
[*] Burkhard.Beudert@npv-bw.bayern.de

Abstract
In central Europe, large strictly protected areas, such as the Bavarian Forest and Šumava National Park (NP) in the Bohemian Forest, and their management have come under public pressure after adopting a "benign neglect" approach concerning natural disturbances. Here the extensive dieback of Norway spruce by bark beetle (*Ips typographus* L.) raised concern about its regional eco-hydrological effects (i.e. runoff yields) and how they interact with the effects of prevailing climate change. To address these questions, we first analysed the hydrological response of nine conterminous mostly forested catchments in the Bohemian Forest to changes in climatic factors. The catchments (39.1–333.9 km², mean elevation 800–1134 m a.s.l.) cover the Bavarian Forest NP and most parts of the Šumava NP along and across the Czech-German border. From 1978 to 2013, independent of land use changes and physiographic features, regional summer runoff decreased by 70 mm (−21% of long-term median) despite increased summer precipitation (51 mm, 8%), while winter runoff did not change (8 mm) although precipitation declined (−54 mm, −9%). This feature results from a timing effect in streamflow due to earlier snowmelt, which is driven by the regional warming in winter, especially in April, by about 3.3 K, irrespective of altitude. However, the overall decline in annual runoff yields (−59 mm, −7%), despite constant precipitation, is related to higher water vapour losses due to the increased air temperature in summer (1.5±0.3 K) while the long-term means varied between 8.9 and 13.4°C depending on altitude. A dataset consisting of three sub-catchments inside the national parks (0.7–89.7 km²) was analysed for disturbance effects (58–62% of catchment area) on precipitation runoff behaviour. The larger ones, Upper Vydra and Upper Große Ohe, strictly followed the overall trends in runoff and high flows in winter but did not show annual trends. An analysis of runoff precipitation ratio revealed a significant step change in the Bavarian Forest NP sub-catchments once cumulative disturbance exceeded 30% area (1998/1999). After this step change, catchment evapotranspiration significantly decreased by 62–120 mm and runoff increased to the same extent. The sub-catchment in the Šumava NP did not respond probably due to timing and/or scale effects. Overall, the observed declining trends in runoff yields were not caused by precipitation changes but were due to warming only. However, in small embedded catchments of the national parks, reduced evapotranspiration losses after bark beetle outbreaks and windthrow currently but temporarily compensate for climate change effects. Shifting streamflow from early summer to late winter is the common hydrological response of all catchments to warming, which in the longer term may negatively affect the water supply to vegetation and people in autumn.

Key words: streamflow, climate change, natural disturbance, protected area, national park

INTRODUCTION

Streamflow changes due to climate change are reported from most parts of the world and comprise both increases and decreases depending on the size, timing and interrelation of regionally specific climatic factors. A global analysis of streamflow revealed increased streamflow in high latitude North America and Eurasia and projected increases of 10–40% by 2050, while in Southern Europe decreased streamflow was reported with further decreases of 10–30% projected (Milly et al. 2005, Milliman et al. 2008). Stahl et al. (2010, 2012) found very similar regionally consistent trends (1964–2004) in annual streamflow, with negative signs in southern and eastern regions of Europe and positive signs in northern and western regions. Generally, streamflow trends in high latitude and western European regions are governed by increasing and/or seasonally altered precipitation, which balanced or exceeded concurrent opposing warming effects (Klein Tank et al. 2002). In eastern and southern Europe, however, streamflow responded negatively to the reduced annual precipitation yields, increased temperature (European Environment Agency 2017), and more frequent droughts (Gudmundsson & Seneviratne 2015).

Apart from precipitation issues, many studies from snow dominated or influenced regions reported changes in streamflow timing and flood peaks due to earlier snowmelt by warming in winter and early spring (McCabe & Clark 2005, Stewart et al. 2005, Wilson et al. 2010, Renner & Bernhofer 2011, Dudley et al. 2017). In addition, increasing temperature and/or radiation input during summer alone, which in energy limited central Europe correlates with evapotranspiration, should enlarge water vapour losses from catchments well supplied with water (Teuling et al. 2009).

Despite this, in the Bohemian Forest region, streamflow did not change significantly between 1965 and 2015, corresponding to unaltered annual and summer precipitation (European Environment Agency 2017). Former work on single catchment streamflow over varying periods did not report significant changes in annual runoff yields or precipitation but did reveal rising air temperatures (1953–2005, Kliment & Matoušková 2008; 1961–1998, Buchtele et al. 2006; 1962–2008, Kliment et al. 2011). More recent studies attributed changes in seasonal streamflow of two high elevation catchments to earlier snowmelt and discussed the relevance of forest cover and vegetation change on discharge dynamics (Bernsteinová et al. 2015, Langhammer et al. 2015). Klöcking et al. (2005) and Beudert et al. (2007) found altered runoff partitioning and increased precipitation related runoff following a large scale bark beetle outbreak.

Land use change (Führer et al. 2011, Tomer & Schilling 2009) and disturbance of forest ecosystems by management (Bosch & Hewlett 1982, Sahin & Hall 1995, Andreassian 2004) or by windthrow and bark beetle outbreaks (Adams et al. 2012, Bearup et al. 2014) are known to change streamflow. The magnitude of such disturbance effects might be sufficient to mask climate change effects. Moreover, post-disturbance succession of vegetation cover and its water demand proceeds continuously, which may also generate streamflow trends (Jones 2011).

In both the Bavarian Forest and Šumava national parks in the centre of the Bohemian Forest region, outbreaks of the host-specific Norway spruce bark beetle (*Ips typographus* L.) and windthrow led to extensive areas of dead spruce during the last 25 years. Concerns about the quality of drinking water and the moderation of floods could be allayed (Beudert et al. 2015, Bernsteinová et al. 2015). However, decreasing runoff yields and low flows in autumn especially, which indicate the availability of groundwater and thus drinking water, have frequently been attributed to the occurrence of disturbed or dead but unmanaged spruce stands despite public awareness of regional climate change (i.e. spring warming, changes in phenology). To provide information and scientific evidence, we analysed the hydrological response of nine conterminous mostly forested catchments in the Bohemian Forest, covering the whole (Bavarian Forest) or a major part (Šumava) of the national parks and non-conservation areas, to changes in climatic factors. Disturbance effects on streamflow in particular were examined in three sub-catchments inside the national parks, which have been heavily affected by bark beetle outbreaks and/or windthrow.

Two hypotheses about the drivers of observed eco-hydrological changes in our Bohemian Forest catchments were tested. (i) Rising air temperature has been the major driver of change in runoff yields. Increased energy input has altered the extent and timing of phase transitions of water depending on its seasonal occurrence. (ii) Extended changes in vegetation structure due to large scale bark beetle outbreaks has been decreasing evaporation losses thereby counteracting warming effects on streamflow.

The overarching goal of this study is to provide clarity and insight into man-made environmental changes, which have the potential for threatening ecosystem services.

MATERIAL AND METHODS

Catchments characteristics

We selected nine catchments and three nested sub-catchments along and across the Czech--German border, which drain north-eastern and south-western slopes of the Bohemian Forest (Fig. 1). The German streams are tributaries of the Regen and Ilz streams, which belong to the Danube River basin and thus to the Black Sea drainage system. The Czech streams belong to the Vltava/Labe (Elbe) River basin, which is a part of the North Sea drainage system (Fig. 1). The study area covers 1 156 km^2 with an elevation range of 1016 m between 440 m a.s.l. (gauging station Schönberg, Große Ohe catchment) and 1456 m a.s.l. (Großer Arber summit, Weißer Regen catchment).

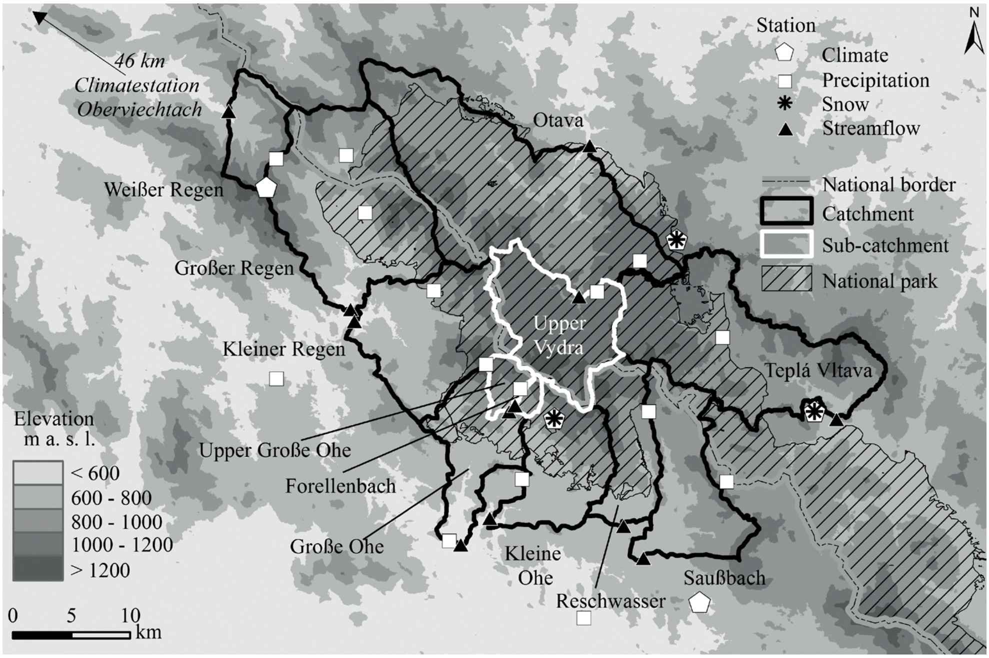

Fig. 1. Digital terrain model of the study area in the Bohemian Forest with nine catchments (black line) and three sub-catchments (white line) along and across the Czech-German border. The gauges (black triangle) and the name of the catchments are indicated. The location of regional climate and precipitation stations is shown (white symbols).

Table 1. Basic catchment characteristics and runoff data (mean ± standard deviation) for the 1978–2013 period (except for Forellenbach: 1992–2013). Code – catchment acronym; percent of disturbed area refers only to the national parks (n.a. – not applicable).

Catchment	**Code**	**Coordinates**	**Area**	**Elevation (m a.s.l.)**			**Slope**	**Forest**	**NP**	**Disturbed area** (%)		**Runoff**
			(km²)	min.	mean	max.	(°)	(%)	(%)	2003	2013	(mm.y⁻¹)
Otava	OT	N49.1406 / E13.5124	333.9	564	1083	1453	7.9	85	93	0	31	848±146
Upper Vydra	UV	N49.0252 / E13.4964	89.7	973	1134	1453	5.8	90	100	18	62	1228±232
Teplá Vltava	TV	N48.9272 / E13.7928	176.9	761	1008	1362	8.1	75	44	2	15	549±115
Regen												
Großer Regen	GR	N49.0186 / E13.2301	175.7	558	877	1336	11.1	88	43	0	11	933±182
Kleiner Regen	KR	N49.0095 / E13.2342	115.9	560	848	1453	9.5	85	34	11	26	757±161
Weißer Regen	WR	N49.1716 / E13.0912	39.1	576	918	1456	13.5	90	0	n.a.	n.a.	1011±199
Ilz												
Große Ohe	GO	N48.8370 / E13.3534	86.6	440	800	1453	8.8	79	59	11	40	798±136
Kleine Ohe	KO	N48.8567 / E13.3875	78.3	556	831	1373	8.4	73	56	18	42	799±171
Reschwasser	RW	N48.8487 / E13.5427	59.4	664	938	1373	8.7	79	63	40	60	970±180
Saußbach	SB	N48.8246 / E13.5656	89.6	645	888	1263	8.2	76	1	3	19	826±151
Upper Große Ohe	UGO	N48.9382 / E13.4124	19.1	769	999	1453	11.4	98	100	39	58	1000±201
Forellenbach	FB	N48.9427 / E13.4196	0.7	787	894	1293	8.4	98	100	39	61	1030±175

The bedrock in this part of the Bohemian massif consists of magmatic (mostly granite) and metamorphic rocks (paragneiss, migmatite, orthogneiss), which are overlain by quaternary sediments, mostly periglacial solifluction deposits and fluvial sediments (Rohrmüller et al. 2000, Šefrna 2003, Babůrek et al. 2013). Fissured rock and lower regolith form the aquifers which in the Bavarian Forest NP catchments contribute more than 50% to annual runoff (Beudert et al. 2007) and maintain the low or drought flow of streams. Predominant soils are acid cambisols with varying contents of coarse material and with differently marked signs of podsolization (kryptopodzol), rankers and initial soils. The share of mineral and organic wet soils and bogs differs between the Czech and German catchments due to topography as could be shown for the Upper Große Ohe (25%) and Upper Vydra (46%) (Bernsteinová et al. 2015).

The catchments were selected according to the length of continuous discharge records in order to cover a substantial period for the detection of long-term runoff trends – in our case 36 years (1978–2013). On the German side, Weißer Regen (WR, Lohberg), Großer Regen (GR, Zwiesel) and Kleiner Regen (KR, Lohmannmühle) in the Regen basin as well as Große Ohe (GO, Schönberg), Kleine Ohe (KO, Grafenau), Reschwasser (RW, Unterkashof), and Saußbach (SB, Linden) in the Ilz basin fulfilled this requirement. On the Czech side only Otava (OT, gauging station Rejštejn) and Teplá Vltava (TV, Lenora) offered such long-term records. However, the size of the Czech (511 km^2) and German (645 km^2) parts of the study area are comparable. It covers the whole (Bavarian Forest) or a major part (Šumava) of the national parks, as well as non-conservation areas. Additionally, the nested headwater catchments of the Upper Große Ohe (UGO, Tafelruck), Forellenbach (FB, Schachtenau), and Upper Vydra (UV, Modrava) were included for a more detailed study of precipitation runoff behaviour (Fig. 1).

The catchments vary markedly in size from 39.1 km^2 (WR) to 175.7 km^2 (GO) in the Regen system and from 0.7 km (FB) to 89.6 km (SB) in the Ilz system, while in the Czech catchments cover respectively 89.7 km^2 (UV) to 333.9 km^2 (OT) (Table 1).

The minimum elevation (gauging station) ranges between 440 m a.s.l. (GO) and 973 m a.s.l. (UV) while maximum elevation varies in a narrow range from 1263 m a.s.l. (SB) to 1456 m a.s.l. (WR). UV has the highest mean catchment elevation (1134 m a.s.l.) but also the lowest slope (5.8°) whereas, in contrast, WR has an intermediate average elevation (918 m a.s.l.) and the steepest slope (13.5°). Generally, mean slope is lower in the Czech catchments (5.8–8.1°) than in the German catchments which vary between 8.2° (SB) and 13.5° (WR).

The land cover is predominantly forest (73–98%) with the remaining vegetation made up of fens and peat bogs at higher elevations and agricultural crops and meadows in the lower parts of the larger catchments (Table 1). Norway spruce (*Picea abies* (L.) Karst.) accounts for about 70% of the forested area in the German catchments and even more in the Czech catchments. UV, UGO and FB are completely located inside the national parks and cover mostly their core zones. Excluding WR, which is completely outside the parks, the catchment areas are comprised of 1% (SB) to 93% (OT) national park.

By 2013, the areas disturbed by the host-specific spruce bark beetle (*Ips typographus* L.) and windthrow accounted for 62% (UV), 58% (UGO) and 61% (FB) of the purely national park catchments. The respective percentages in all other catchments (Table 1) ranging from 3% (SB) to 60% (RW) refer to the national park area only, as the extent of harvested or salvage-logged bark beetle or windthrown areas outside the national parks is unknown. Related to the whole catchment (Fig. 2), the respective percentage of disturbed area reduced to <1% (SB) and 38% (RW). This approach necessarily disregards disturbance effects (disruption of the water and element cycle) by regular forest or other management practices. The cumulative course of disturbed spruce stands differed between the national parks (Fig. 2). German catchments showed a bi-modal course which levelled off in the late 2000s, when Czech catchments were subject to a pronounced increase following the hurricane Kyrill in January 2007.

Mean annual runoff Q (Table 1) varied between 549 mm (TV) and 1 228 mm in the high elevation headwater catchment UV. But Q differs considerably (385 mm) between TV and GR, which are of same catchment size, but GR of lower minimum and mean elevation. This refers to the rain shadow effect that the summit region along the border creates at easterly located areas.

The meteorological divide can also be demonstrated by means of long-term (1978–2013) annual precipitation yields (P), which differ markedly between stations located west and east of the summit line (Table 2). P at Churáňov (1118 m a.s.l.) was 1 119 $mm.y^{-1}$ and thus smaller than at Waldhäuser (1 382 $mm.y^{-1}$), which is lower-lying (940 m a.s.l.) but west of the summit line. Moreover, it was equal to Grainet (1 131 $mm.y^{-1}$) which is located almost 500 m lower than Churáňov and south of it.

Annual means of air temperature (T) decreased with altitude from 5.7°C (804 m a.s.l.) to 4.8°C (1118 m a.s.l.) at Czech stations and from 7.4°C (596 m a.sl) to 3.5°C (1436 m a.s.l.) at German stations (Table 2). While the long-term variability of T is the same across all stations, mean T related to altitude is lower at Czech than at German sites as indicated by lower values at Lenora (804 m a.s.l.) than at Waldhäuser (940 m a.s.l.).

Data sources and preparation

Long-term discharge records (Table 1) and climate time series (Table 2) in daily resolution were obtained from publicly available sources: Bavarian climate and precipitation data from

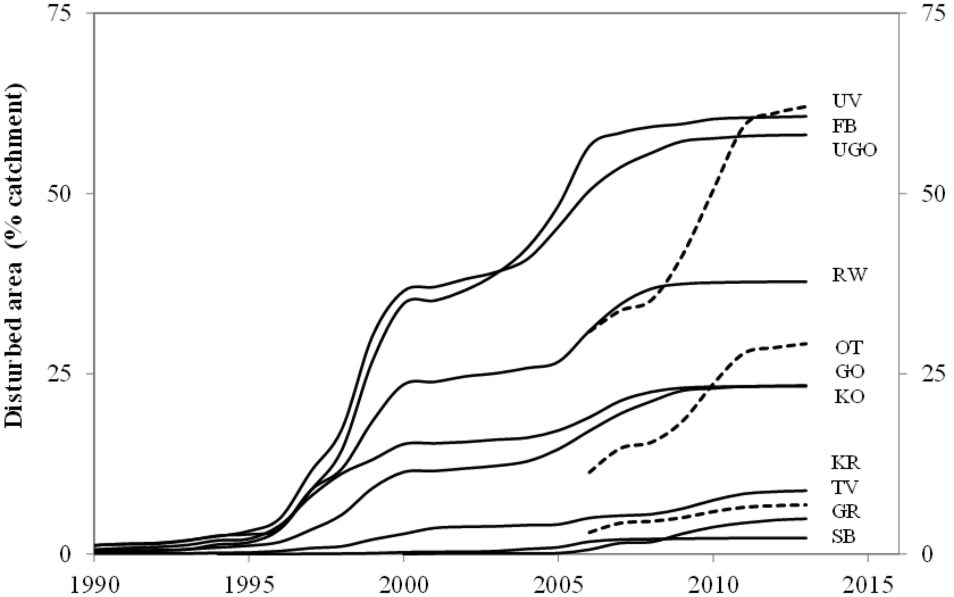

Fig. 2. Cumulative development of disturbed forests (% catchment area). Czech and German catchments are indicated by broken and solid lines, respectively: Weißer Regen (WR), Großer Regen (GR), Kleiner Regen (KR), Große Ohe (GO), Kleine Ohe (KO), Reschwasser (RW), Saußbach (SB), Otava (OT), and Teplá Vltava (TV); subcatchments: Upper Große Ohe (UGO), Forellenbach (FB), and Upper Vydra (UV).

Table 2. Regional stations used to calculate climate characteristics and to test for trend (1978–2013). Means (± standard deviation) of precipitation (P) and air temperature (T); * – snow records available; the code designates the catchment (see Table 1) for which the station data are used to calculate an area based precipitation proxy as input into the linear-mixed model.

Station	Code	Coordinates	Elevation (m a.s.l.)	P (mm.y^{-1})	T (°C)
Churáňov *	TV	N49.0673 / E13.6114	1118	1119±157	4.8±0.8
Lenora *	TV	N48.9334 / E13.7677	804	869±121	5.7±0.8
Großer Arber[1]	GR	N49.1130 / E13.1342	1436	1491±199	3.5±0.7
Waldhäuser	KO	N48.9323 / E13.4650	940	1382±200	6.0±0.7
Grainet	–	N48.7893 / E13.6291	628	1131±172	7.3±0.8
Oberviechtach	–	N49.4520 / E12.4366	596	810±134	7.4±0.8
Filipova Huť	–	N49.0284 / E13.5175	1112	1229±137	
Borová Lada	–	N48.9915 / E13.6622	892	963±149	
Železná Ruda	OT	N49.1362 / E13.2278	763	1273±201	
Kvilda	OT	N49.0515 / E13.5680	1052	1164±164	
Regen *	WR	N48.9662 / E13.1426	583	985±119	
Brennes	WR	N49.1346 / E13.1462	1040	1590±225	
Zwieslerwaldhaus	GR	N49.0923 / E13.2487	699	1360±205	
Waldschmidthaus	KR	N48.9746 / E13.3864	1350	1766±258	
Buchenau	KR	N49.0315 / E13.3272	740	1349±187	
Racheldiensthütte	GO	N48.9555 / E13.4261	875	1585±227	
Schönberg	GO	N48.8398 / E13.3401	547	1095±143	
St. Oswald	KO	N48.8859 / E13.4261	754	1095±160	
Mauth-Finsterau	RB	N48.9359 / E13.5747	1011	1286±200	
Röhrnbach	RB	N48.7789 / E13.4946	533	1060±134	
Philippsreuth	SB	N48.8807 / E13.6633	917	1306±206	
Waldkirchen	SB	N48.7237 / E13.6058	617	1142±153	

[1] 1983–2013

the German Meteorological Service, Bavarian Forest NP (station Waldhäuser), and Bavarian State Institute of Forestry (Racheldiensthütte and Waldschmidthaus stations); Bavarian discharge data from the Bavarian Hydrological Service, except for gauge Schachtenau (Forellenbach), which was provided by the Federal Environment Agency, and all Czech data from the Czech Hydrometeorological Institute.

Daily discharge data were divided by catchment area to get runoff depths (mm) of annual, seasonal (hydrological quarter and half years, beginning in November) and monthly runoff, as well as the highest and lowest daily runoff for each month. Monthly runoff data were checked for inhomogeneity using break point procedures (see below). Weak inhomogeneity was only found for KR (1992), KO (1998), and TV (1984), but regarded as transient and not substantial when mass curves were visually assessed.

Daily records of snow depth and snow melt dynamics were taken from Churáňov, Lenora, Waldhäuser, and Regen climate stations. The reference crop evapotranspiration for grass

(Doorenbois & Pruitt 1977) was calculated by using the radiation-based approach of Priestley & Taylor (1972) hereinafter used as a proxy of potential evapotranspiration and named ETP. The net radiation balance was derived according to FAO Guideline 56 (Allen et al. 1998) based on daily temperature, relative humidity (RH), actual sunshine duration records (SD) and extra-terrestrial radiation using an albedo of 0.23. A fixed factor of 1.26 on the radiation component which is valid in humid environments (Jensen 1992) was used to take the aerodynamic component into account. Due to data requirements, ETP was calculated for Churáňov and Waldhäuser station only.

Catchment precipitation of UGO (1980–2013) and FB (1992–2013) was based on P records from six monthly totalizing samplers and calculated according to Klöcking et al. (2005) including Racheldiensthütte and Waldschmidthaus (Table 2). Catchment P of UV (1980–2013) was taken from Langhammer et al. (2015). For the other catchments, the available data or model results of catchment P required for sound analyses on precipitation–runoff behaviour are lacking.

Data gaps in monthly P records for UGO (20 out of 2 448 monthly values) were filled using best fit monthly transfer functions according to Klöcking et al. (2005). This procedure was also applied to all other stations based on the complete Churáňov and Waldhäuser data sets, respectively. The time series of UV catchment P was extended to 2013 by using Filipova Huť data.

For the linear mixed-effects model only (see below), a surrogate of catchment P was generated by averaging monthly records of the two nearest high and low elevation stations (code in Table 2). Catchment P of the three nested catchments was taken as such (see above). A proxy of monthly mean catchment T was generated by applying mean monthly lapse rates between the next high and low elevation climate stations (Table 2) adjusted to mean catchment elevation.

Catchment morphological characteristics were derived from the Aster Global Digital Elevation Model provided by NASA (2009). Vegetation characteristics were extracted from the Corine Land Cover 2006 database published by European Environment Agency (2016), the Official Topographic Information System provided by the Bavarian Agency for Digitisation, High-Speed Internet and Surveying (https://www.ldbv.bayern.de/) and the spatial databases obtained from the Bavarian Forest NP and Šumava NP. Bark beetle infested and wind thrown spruce trees for both data sets were identified on annually recorded colour-infrared images (Lausch et al. 2011) and aggregated to a cumulative curve over time. The spatially distributed datasets were analysed by the Arc Editor 10.1 Spatial Analyst Tools package (ESRI).

Statistical analysis

The homogeneity of Q data was checked using ANKLIM-software package (Štěpánek 2005). All single series except UGO were proved homogeneous. Q of UGO, FB and UV, the heavily disturbed nested catchments inside the national parks were additionally tested against Q in WR, which is forested to a similar extent, under regular forest management outside the national parks and free of inhomogeneity over the period of comparison (Reeves et al. 2006).

In the second approach, the annual runoff coefficient ($Q.P^{-1}$) was calculated by expressing annual runoff (R) as a fractional percentage (%) of annual catchment precipitation (P). This approach was confined to the nested catchments for which catchment P were available (UV and UGO since 1980, FB since 1992). $Q.P^{-1}$ is an additional measure to disentangle the importance of changes in P and/or vegetation (Velpuri & Senay 2013) from changes in Q. The "segmented regression with breakpoint" procedure (SegReg, Oosterbaan 1994) was applied to detect significant changes (step changes, inflection points) in Q.P^{-1} over time. The SegReg procedure partitions an independent variable (time) into two intervals and calculates separate line segments for each interval. The breakpoint was checked using ANKLIM-software package (ŠTĚPÁNEK 2005).

For UGO and FB, the same step change was detected by using both approaches, thereby determining the before and after period (SMITH 2002). Differences in mean values of P and Q and their balance between these periods were tested by a two sample T-test and checked by the Mann-Whitney-test using the "Real Statistics Resource Pack software" (Release 4.3, www.real-statistics.com, 2016). According to the geological and geomorphological conditions (see above), extensive aquifers and deep groundwater loss are absent in this landscape. Consequently, differences in sub-surface water storage are negligible in longer term mean hydrologic budgets (HUDSON et al. 1997), which justifies the use of the catchment balance as a proxy of actual evapotranspiration (ETA).

Meteorological and hydrological data sets were tested for linear trends during the 1978 to 2013 hydrological years by using the Mann-Kendall non-parametric test. The Regional Kendall test for spatial consistency of trends was applied on P data of the Czech (n = 6) and the German side (n = 14) and the whole study area, and on German Q data (n = 7) and the whole study area (n = 9) by using the "Kendall-Family of trend tests" (HELSEL et al. 2006). For the Czech part of study area (n = 2), a mean regional Q was calculated by weighting Q with size of the two catchments to allow the application of the Mann-Kendall test. Regional T trends are presented as arithmetic means (± standard deviation) over five stations. The trend is given as the difference between the last and the first value of the regression line of any parameter emphasizing that the magnitude of any change is restricted to the period it was calculated for and improving readability. An *a priori* test for autocorrelation ("acf" package) in Q data using R 3.1.3 (www.r-project.org) resulted in a weak correlation at a lag of 7 in very few data sets only.

A linear-mixed effect model was performed to investigate the influence of catchment size, elevation, and slope, the proportion of forests and of T and P as the main drivers on log--transformed Q measures. The function "lme" (R package lme4) was applied on T, P, and Q in monthly/seasonal/annual resolution. In addition, the proportion of area inside the national park has been considered as a proxy of disturbed forests in the model, since relevant data from forests outside the national parks were not available. In the model, we accounted for repeated measurement using sub-catchment as a random effect. Furthermore, we considered a correlation structure representing first order autocorrelation. For all comparisons within and among the models, we used standardized effect sizes of the parameter estimates using an expected mean of 0 (t-values = estimates divided by the respective standard error, values ≥ 2 and ≤ -2 exceed $p<0.05$). We report conditional (variance explained by both fixed and random factors, i.e. the entire model) and marginal (variance explained by fixed factors) coefficients of determination (Pseudo-R-squared for Generalized Mixed-Effect models, function "r.squaredGLMM" from R package MuMIn). Collinearity was checked by calculating the variance inflation factor according to O'BRIEN (2007), which was <<3 between all explanatory variables and thus far below the typical thresholds of 5 or 10. For all statistical procedures, the significance level was set to $p<0.05$.

RESULTS

Our analysis of runoff yields in the Bohemian Forest catchments revealed consistent changes in Q and its seasonality but not in low and high flow measures. All are strongly related to the drastic warming trend, while precipitation was constant. In contrast, disturbance effects on

Table 3. T-values of variables in a mixed linear model explaining log-transformed runoff (monthly sum, minimum and maximum daily sum) of nine catchments and three sub-catchments. Significant values are in bold ($p<0.001$) and italics ($p<0.01$).

	Period: Winter			**Summer**		
Parameter	**Sum**	**Minimum**	**Maximum**	**Sum**	**Minimum**	**Maximum**
(Intercept)	**3.4**	1.1	0.1	*3.1*	−1.6	−0.6
T (°C)	**28.2**	**22.4**	**18.5**	**−6.2**	−1.9	**−11.9**
P (mm)	21.0	3.9	29.8	31.6	7.2	49.8
Area (km²)	−0.7	−0.5	−0.8	−0.9	−0.6	−1.2
Mean elevation (m a.s.l.)	0.7	−0.1	1.3	1.1	0.6	1.3
Forest (%)	0.9	1.6	0.1	1.1	1.4	0.5
National park (%)	−0.6	−0.8	−0.1	−0.2	−0.8	0.8
Mean slope (°)	−0.3	−0.7	−0.3	−0.3	−0.8	0.0
R^2m	0.29	0.19	0.29	0.29	0.11	0.51
R^2c	0.39	0.34	0.37	0.40	0.34	0.56

Q are only discernible in the small national park sub-catchments.

Drivers of hydrological response in the Bohemian Forest catchments

The linear mixed-model explained 34% and 56% of variation in Q measures (Table 3). Neither physical site conditions such as area size, elevation and slope, nor vegetation and land use characteristics exerted any significant influence on hydrological catchment response. Precipitation (P) is the main driver ($p<0.001$) of Q concerning both the seasonal sum and the extremes, but this is more pronounced in summer than in winter. In winter, T is a comparably strong positive driver ($p<0.001$), especially for the minimum daily sum. High T is linked to a higher portion of liquid P and to Q generation via snow melting which, on a monthly basis, frequently occurs independently from precipitation. In summer, however, T exerted a much smaller but significant negative effect on Q yields and maximum daily sum while the minimum was not affected. Generally, in summer high T is linked to stable weather conditions with less P but higher evapotranspiration losses in this region.

Model runs using seasonally and annually aggregated values of P, T and Q confirmed these results regarding both insignificant effects of catchment characteristics on Q measures and also significant effects of T.

Changes in runoff and its seasonal distribution

From 1978 to 2013, the nine non-nested catchments showed decreasing Q, ranging from −82 mm (TV) to −32 mm (OT) but a single significant change ($p<0.05$) was in RW only. Regional Q in the German and Czech part changed by −55 mm and −58 mm, respectively, and by −59 mm ($p<0.05$) for the whole study area (Fig. 3).

This is first of all the result of an overall drop in summer Q of −70 mm ($p <0.001$), or −73 mm ($p<0.001$) and −67 mm ($p >0.05$) in the German and Czech part, respectively. The change in single catchments varied between −39 mm (WR) and −122 mm (RW, $p <0.05$). This decrease originated mainly from an overall decrease in early summer (May to July) of −58 mm ($p <0.001$) and, respectively, −62 mm ($p <0.001$) and −52 mm in the German and the Czech part. More precisely, the reduction in summer Q was mainly due to the May contribution of −47 mm ($p<0.001$) for the whole study area, −48 mm ($p<0.001$) in the German and −54 mm (p<0.05) in the Czech part individually and, mostly significantly, in each single catchment ranging from −33 mm (SB) to −71 mm (RW).

Secondly, regional Q in winter changed little in both the German and Czech parts (+19 mm, −27 mm, respectively); change rates varied between −62 mm (TV) and 39 mm (GO) (Fig. 3). For the whole study area, changes were mostly negative from November to January (−24 mm) and positive from February to April (27 mm), which in all catchments developed mostly in December (−22 mm, p<0.001) and March (+24 mm, p<0.001), summing up to a zero-change (8 mm).

Changes in the maximum daily Q (not shown) generally followed the changes in Q sum. A rise in winter (1.6 mm, p<0.05) was due to an increase in March (2.3 mm, p<0.01). In summer, the maximum Q decreased by (−2.3 mm, p<0.01) due to a drop in May (−3.4 mm, p<0.01). The minimum daily Q did not change in a comparable manner across all seasons and months, with the exception of March (+0.3 mm, p<0.05) and May in which it declined in all catchments (−0.7 mm, p < 0.001).

Nested catchments showed smaller changes of annual Q, 27 mm (UGO) and −13 mm (UV), and the same changes in summer (−85 mm and −82 mm) compared to the superordinate catchments. In contrast, changes in winter Q were more pronounced (129 mm and 52 mm). Marked monthly increases (p<0.05) were observed in UGO (70 mm) in March and in UV (91 mm) in April, which contribute to the common picture of increasing Q in winter. In March, the maximum daily Q increased by 6 mm and 8 mm in UGO and UV, and in April also for UV (p<0.05), which in most other catchments showed declining daily maxima.

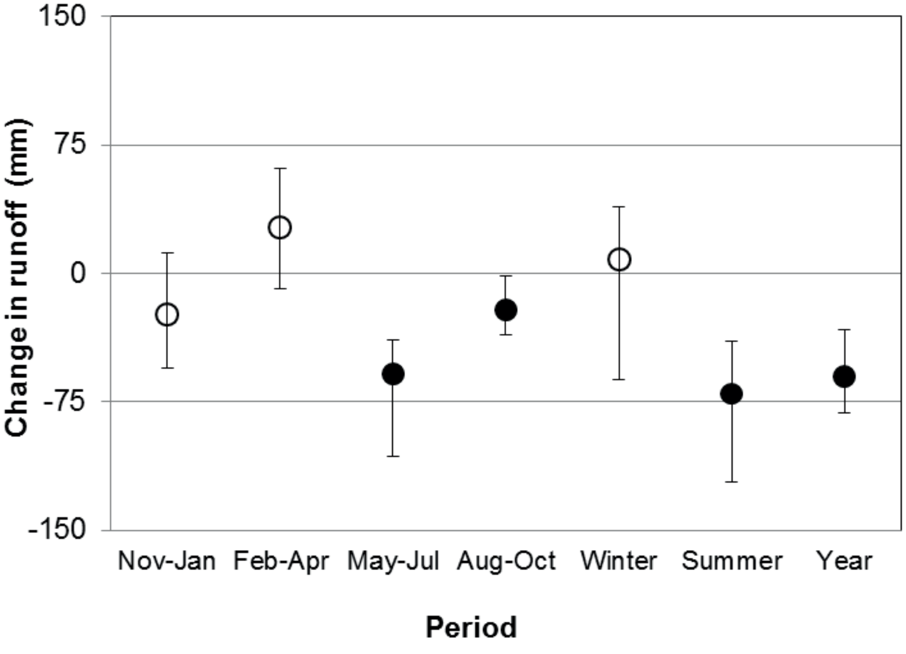

Fig. 3. Median (dots) and extreme (vertical lines) changes in runoff yield (left) of 9 catchments over seasons, hydrological half-years and years (1978–2013). Filled circles: p<0.05 according to Regional Kendall test results.

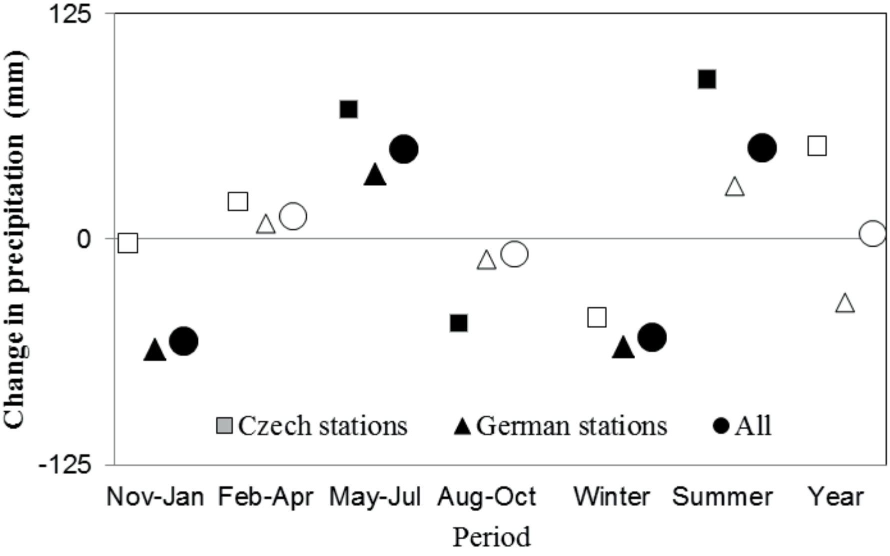

Fig. 4. Mean changes in precipitation yields at 6 Bohemian and 14 Bavarian stations and for the whole study area over seasons and years (1978–2013). Filled symbols: $p<0.05$ according to Regional Kendall test results.

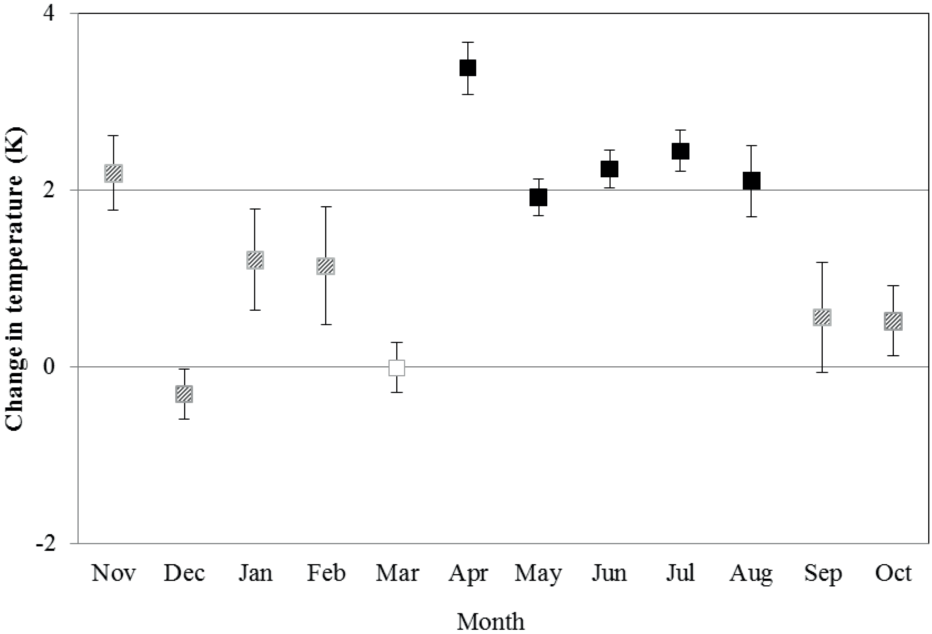

Fig. 5. Mean change and standard deviation in monthly mean air temperature at five stations (1978–2013). Filled squares indicate statistical significance at all stations of $p<0.05$, and for April ($p<0.001$). Hatched fills indicate one-directional changes at all stations, though not significant at all stations.

Changes in climatic elements and their seasonality

Mean precipitation (P) varied from 869 mm at 804 m a.s.l. to 1 766 mm at 1350 m a.s.l. There is an overall positive correlation ($p<0.05$) of P to elevation for all seasons. The lapse rate of annual P for the whole study area was 0.56 mm.m^{-1} ($p<0.01$), and that of German stations only 0.66 mm.m^{-1} ($p<0.001$). Except Železná Ruda in the north of the study area, at a given height, P was higher on the German than the Czech side underpinning the rain shadow effect the summit range exerts along the border. At all stations, changes in monthly P were mostly insignificant due to high year-to-year variability, with a few exceptions for May (increasing). The change in annual P varied between −142 mm and 134 mm and its magnitude was independent of elevation (not shown).

For the whole study area, there was an increase in summer P (51 mm, $p<0.002$) and a decrease in winter P (−54 mm, $p<0.002$) resulting in unaltered annual yields (3 mm, Fig. 4). But there were regional differences: in the Czech part, the increase in summer (89 mm, $p<0.001$) was larger than in the German part (30 mm), while the decrease in winter was smaller (−43 mm) than in the German part (−60 mm, $p<0.01$). Overall, P changes were more positive (less negative) at Czech than at German stations. Changes in winter occurred from November to January (−57 mm, $p<0.001$), but exclusively at German stations (−61 mm, $p<0.001$). Summer P increased from May to July in both the Czech (72 mm, $p<0.001$) and the German part (36 mm, $p<0.01$). This increase developed mostly in May and at all stations.

Air temperature (T) showed marked changes of similar size at all stations across the study region (Fig. 5). December was the only month with a small negative change and March was without change. For May to August, an increase of about 2 K (1978–2013) was found ($p<0.05$ at least) while the average rise in April by 3.3 K was highly significant at all stations. Thus, regional spring and summer warming occurred in a sequence of five consecutive months. In summary, T of winter and summer season increased by 1.3 K ($p<0.1$ at least) and 1.5 K ($p<0.05$ at least) respectively, resulting in a warming of 1.5 K ($p<0.01$ at least) for the whole year. The small standard deviations show that warming in spring and summer is a common transboundary feature in this region. In autumn and winter, however, larger deviations point to the site specific topographic influences.

Warming in late winter moved the date of final snow melt by six weeks from 22 April to 10 March at the lowest station (583 m a.s.l., Regen, $p<0.001$) (Fig. 6) and tended to move by three weeks from 7 May to 20 April at the highest station (1118 m a.s.l., Churáňov). At medium elevations (804–945 m a.s.l.), it moved from April/May to March/April by about four weeks ($p<0.001$). The snow cover period in autumn began nine to 32 days earlier (Regen, $p<0.01$), or remained unaltered (Lenora). Consequently, the length of the snow cover period did not change (Churáňov), or tended to decrease by 11 to 18 (Regen, Waldhäuser), or decre-

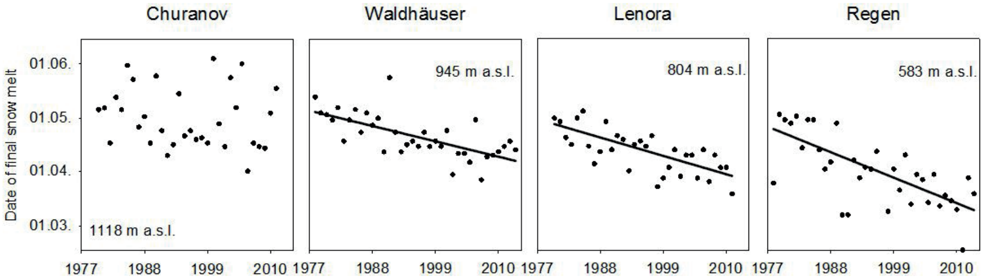

Fig. 6. Trends in final day of snow cover at German and Czech climate stations. Solid regression line indicates $p<0.05$. Note that the period for time series analysis was 1978–2013 for German stations and 1980–2011 for Czech stations.

Table 4. Absolute and relative changes in relative humidity (RH), actual vapour pressure (e_a), saturation deficit (e_s–e_a), sunshine duration (SD) and potential evapotranspiration (ETP) of the summer half-year at Churáňov (1978–2011) and Waldhäuser station (1978–2013).

Station	**Change**	**SD** (hours)	**RH** (%)	**e_a** (hPa)	**e_s–e_a** (hPa)	**ETP** (mm)
Waldhäuser	absolute	113	3,8	1.7	−0,5	44
	relative	12%	5%	17%	−15%	11%
	significance	n.s.	0.05	0.001	n.s.	0.001
Churáňov	absolute	3	5,9	1.5	0,0	23
	relative	0%	8%	16%	−1%	6%
	significance	n.s.	0.05	0.001	n.s.	0.05

ased by 36 days (Lenora, $p<0.05$). Moreover, the maximum snow depth ranging from 39±20 cm at 583 m a.s.l. up to 137±22 cm at 945 m a.s.l. did not change, indicating no change in the maximum snow water equivalent at any elevation. Annual snowfall at Regen (187±82 cm) and Waldhäuser (410±114 cm) tended to decrease by 41 cm and 112 cm. But, due to the exceptional warming in April, snowfall in this month decreased by 4 cm ($p<0.05$) and 20 cm ($p<0.01$), which equals the long-term mean at both sites.

Mean actual vapour pressure increased by about 16% at Churáňov ($p<0.001$) and 17% at Waldhäuser ($p<0.001$) in the summer half-year (Table 4), mostly generated from May to August. Saturation vapour pressure increased by about 10% at both stations due to warming (see above), the saturation deficit slightly decreased or remained constant and relative humi-

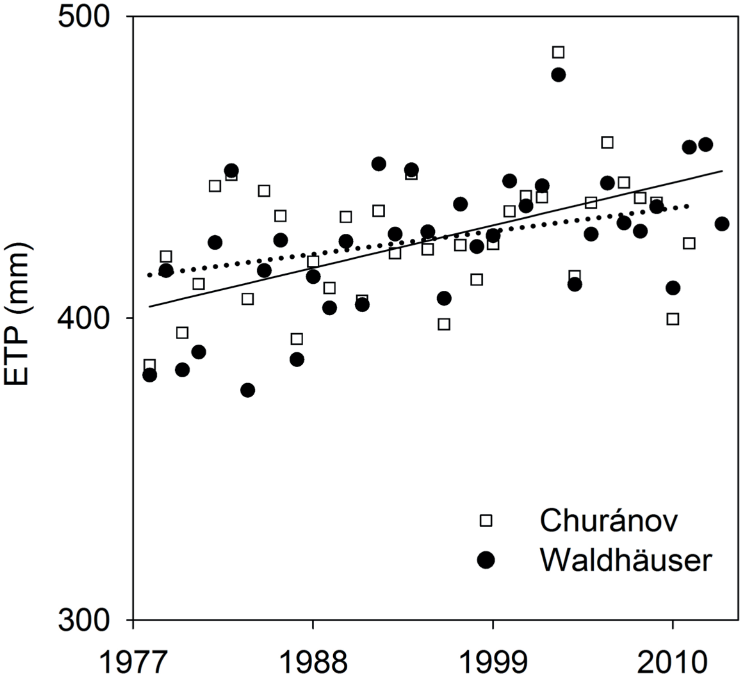

Fig. 7. Time series of summer potential evapotranspiration (ETP). Solid regression line: Waldhäuser, $p<0.001$; dotted regression line Churáňov, $p<0.05$.

dity increased ($p<0.05$). Therefore, changes in ETP which increased (Fig. 7) by 23 mm (6%, $p<0.05$) and 44 mm (11%, $p<0.001$) most probably equate to changes in ETA.

At Waldhäuser, sunshine duration increased in summer (113 hours) and even more greatly in winter (149 hours, $p<0.01$). At Churáňov, sunshine changed in winter only (51 hours). Warming in winter (see above) also led to similar changes for the whole year concerning direction and significance of changes in vapour pressure conditions. Annual ETP significantly increased by 44 mm (9%) and 65 mm (13%) at Churáňov and Waldhäuser.

Disturbance effects on catchment hydrology

In UGO and UV (1980–2013), catchment P and Q were free of trends. Moreover, the rate of change in Q was small or even positive (+27 mm, −13 mm) compared to superordinate catchments. Homogeneity tests of Q against time and WR reference data series revealed a single step change between 1998 and 1999 for both UGO ($p<0.05$) and FB. The same step change ($p<0.05$) in annual runoff coefficient $Q.P^{-1}$ was detected by the SegReg approach (Fig. 8) for both the 1980–2013 (UGO) and the 1992–2013 (UGO, FB) study period. $Q.P^{-1}$ increased from 60% to 64% (UGO, $p<0.01$) and, in the shorter period, from 59% to 64% (UGO, $p<0.01$) and from 59% to 68% (FB, $p<0.001$), respectively.

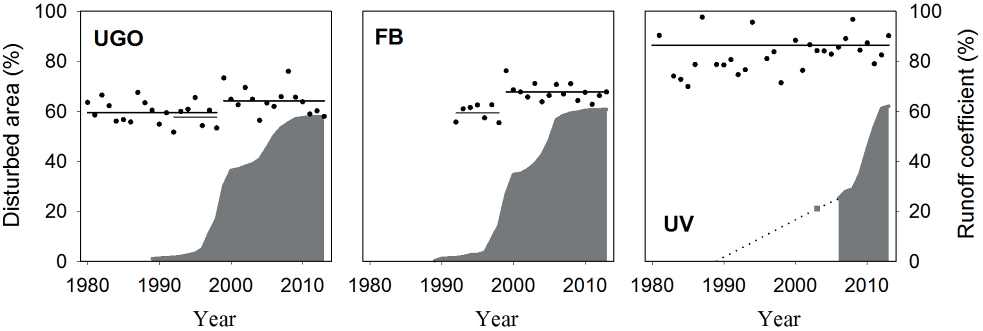

Fig. 8. Cumulative course of bark beetle and storm disturbed area (left axis, grey area) and annual runoff coefficient ($Q.P^{-1}$ – right axis, dots) in Upper Große Ohe (UGO), Forellenbach (FB), and Upper Vydra (UV) catchments. Thick black lines indicate mean $Q.P^{-1}$ in the periods before (UGO only) and after the significant step change in 1998/1999 (UGO, FB), except for UV which is free of changes over the whole study period; thin lines indicate mean $Q.P^{-1}$ for the 1992–1998 period only, to compare UGO and FB. Note that regular surveys of disturbed areas were launched in 1989 (Bavarian Forest NP) and 2003 (Šumava NP).

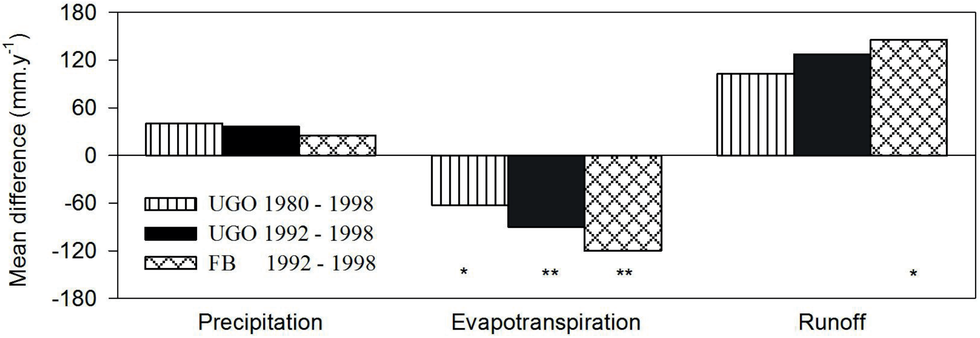

Fig. 9. Mean difference (mm.y^{-1}) of annual precipitation (P), runoff (Q) and evapotranspiration (ETA) in UGO and FB between the periods before (1980/1992–1998) and after (1999–2013) the common step change shown in Fig. 8. * $p<0.05$, ** $p<0.01$, *** $p<0.001$.

Mean P did not differ between the periods before and after the step change (25 mm and 40 mm) in both catchments (Fig. 9). However, mean Q increased by 103 and 127 mm (UGO, $p<0.08$) and 147 mm (FB, $p<0.04$) after 1998/1999. In UGO, the catchment balance as a proxy of ETA declined by 62 mm (−10%, $p<0.03$) and 90 mm (−13%, $p<0.01$) to 581±91 mm. In FB, ETA decreased even more after the step change (−120 mm, −19%, $p<0.01$) to 513±92 mm.

This common step change coincides with the occurrence of about 30% cumulative disturbed catchment area in both catchments. Linear trends in ETA (not shown) accounting for −70, −105, and −142 mm, respectively, are weakly significant at most but in general support the magnitude of change derived from the before-after approach. In contrast, UV did not present any change in $Q.P^{-1}$ or in P, R, and ETA. Compared to UGO and FB, whose dynamics of disturbed area was synchronous, UV showed an accelerated course of forest disturbance after 2007 (25% catchment area), fuelled by storm damages, when bark beetle outbreak in UGO and FB had already levelled out.

Discussion

Our analysis of runoff yields in the Bohemian Forest catchments revealed an overall decrease and an overall seasonal shift irrespective of catchment characteristics. Rising air temperature in late winter and summer was the major driver of change while precipitation did not change. Large scale bark beetle outbreaks and windthrow in heavily affected sub-catchments of the national parks reduced the forest cover and thus evapotranspiration losses, thereby counteracting warming effects on streamflow.

The significant decrease in annual streamflow in our study area does not fit the results of recent regional studies, which did not find significant changes in Q in the Bohemian Forest (Buchtele et al. 2006, Kliment & Matoušková 2008, Kliment et al. 2011, Bernsteinová et al. 2015, Langhammer et al. 2015). On the larger scale, the basin of the River Danube upstream of Vienna has shown stable runoff since 1887 (Kling et al. 2012). Moreover, Stahl et al. (2010, 2012), Milli et al. (2005), and Milliman et al. (2008) in their European and global scale analyses even revealed increasing Q in this region, like most streams in central and northwestern Europe. The most confounding factor might be the varying length and the starting date of the study period (Wilby et al. 2008), which in our study was in 1978 and thereby later than in the studies cited. It was dependent on the start of hydrological monitoring programmes in the Große Ohe catchment in 1976 (Beudert & Gietl 2015). In addition, monitoring of forest status by analysis of aerial pictures started at the end of the 1980s. So, the study period of 36 years spans the whole period before, during and after the major damages by bark beetle, which enables this study on disturbance versus climate change effects on precipitation runoff behaviour.

Climatic drivers of the change in annual streamflow

The significant decrease of annual Q in our study area did not coincide with a parallel change in annual P, which usually is the dominant driver and, for example, explains 86%, 80%, and 54% of annual runoff variability in UGO, FB, and UV, respectively. This again is contrary to the above mentioned findings, which showed concurrently unaltered P and Q in the Bohemian Forest or slightly increased P on a larger scale, although seasonal changes may have occurred (European Environment Agency 2017). There is some spatial difference in P changes in our study area, as annual yields on the Czech side (+52 mm) tend to increase, while on the German side conversely to decrease (–35 mm). However, there is also uncertainty in the relevance of these non-significant findings which would increase and decrease the respective changes in Q. The spatial coverage by P stations is quite different between the

Czech and the German part (6 vs. 14) and presumably too coarse bearing the complex terrain in mind. However, the significant and concurrent trends in both regions in winter and summer P (Fig. 4) have been proven to be consistent in the whole study area and can be used in further discussion.

The overall negative change of Q (−59 mm), which reflects an increase in the catchment balance as P was constant, is consistent with positive changes of annual ETP (44–65 mm) at two analysed climate stations (Fig. 7). The latter increase of 9–13% followed the change in vapour saturation pressure according to Clausius-Clapeyron (~7% K^{-1}) when temperature rises by 1.5 K (Fig. 5). Despite this ETP, according to Priestley & Taylor 1972, is a conservative estimate of evapotranspiration in these forested catchments, considering the mean catchment balance in UGO (614±89 mm) for example, the magnitude of change can be taken as a trend estimate in catchment evapotranspiration, which in this humid region is limited by available energy (Budyoko 1974, cit. in Zang et al. 2001). Very similar results of increasing ETA since the mid-1970s are reported from mountain watersheds in the Appalachian Mountains in the Eastern USA (Caldwell et al. 2016). Further USA LTER-catchments at sites with water surplus offered ETA even higher than expected from T increase (Jones et al. 2012). Zhang et al. (2012) derived increasing ET from satellite data in wet regions of the world like central to northern Europe. Teuling et al. (2009) as well as Matsouakas et al. (2011) stressed the close correlation between ETA and available energy, especially in central Europe, and Kaye et al. (2013) reported concurrently increasing ETP and ETA in England and Wales. Also in our study catchments, T exerted a significant negative effect on Q during summer (Table 3). Thus, there is strong support from climatological literature that increasing evapotranspiration losses due to warming could be a major driver of decreasing Q in all catchments of our study area.

Land use and gradual vegetation change as drivers

Despite this initial attribution of changes in Q to warming, other factors influencing the P–Q behaviour must be tested to avoid erroneous conclusions about climate change effects (Jones 2011): human water consumption and land-use change, and gradual vegetation change following disturbances.

In Regen and Freyung-Grafenau county, which completely enclose the German catchments, population size did not change since 1987 and may have increased by less than 3% since 1978 (Bayerisches Landesamt für Statistik 2016). In the districts of Prachatice and Klatovy which enclose the Czech catchments, it deceased by 4.6% since 1980 (Czech Statistical Office 2017). The current population density is 80 km^{-2} and less than 45 km^{-2}, respectively. Since 1987, the gross specific use per capita of drinking water in Bavaria decreased by 24% to 173 $l.d^{-1}$ (Bayerisches Landesamt für Umwelt 2017), but is less than 160 $l.d^{-1}$ in the Bavarian Forest. In the Czech Republic, gross drinking water production has dropped by 52% since 1989, and in both, the Plzeň and South Bohemian region by 18% since 2003 (Český statistický úřad 2017). In both countries, domestic use of drinking water per capita dropped to <135 $l.d^{-1}$. Moreover, drinking water in the study area generally is withdrawn and returned locally thereby not affecting the water budget at catchment outlet. In summary, changes in human water use in the study region rather have increased Q than reduced it.

Forested area increased by 1% since 1990 (European Environment Agency 2016) in the Czech districts, at the expense of cropland and pastures, and by 2% in the Bavarian Forest counties between 1980 and 2014 (Bayerisches Statistisches Landesamt 2017), by conversion of permanent grassland. Despite the fact that ETA is 10–30% larger from forests than from grassland in central European low mountain ranges (Ernstberger 1987), the freshly established forest stands are more similar to pasture than to mature stands regarding water vapour losses (Peck & Mayer 1996). In the Bavarian Forest counties (but not in the Czech districts), agricultural area decreased by 19%, in favour of settlement and transportation infrastructure. Yet less permeable or almost impermeable urban surfaces like roads and roofs reduce evaporation loss (Ramamurthy & Bou-Zeid 2014) and increase fast drainage (Boyd et al. 1993) to channels and streams. In summary, all land use changes in our catchments, if relevant, most probably decreased ETA and increased Q.

Changes in Q due to the vegetation change following disturbance are more difficult to assess as the exact spatial and temporal information on disturbances such as bark beetle outbreaks, windthrow, and forest harvest, as well as on regeneration management in areas outside the national parks, are lacking. However, the direction and strength of their influence on ETA and thus Q can be assessed approximately. In German and Czech forests, the annual harvest of timber including salvage logged timber was less than the long-term growth rate of European beech and Norway spruce (3–4%) (Thünen-Institut 2017). Therefore, forest stocks have been increasing since decades to about 260 and 400 $m^3.ha^{-1}$, respectively (Ministry of Agriculture 2017, Thünen-Institut 2017). Assuming that forest use has taken place in more or less stable rates and that Norway spruce stands, which by far dominate the study area, were on average of middle age (70–100 years) at the starting date of our study, reveals stable or slightly decreasing ETA, while the stands have been aging (Peck & Mayer 1996). The addition of broadleaves into pure Norway spruce stands has been encouraged and accelerated as a forest stabilizing measure (Möges 2007) but an increasing number of deciduous species would reduce ETA and increase Q (Kommatsu et al. 2011, Peck & Mayer 1996).

Extensive disturbances by windthrow and bark beetle started in the middle of the 1990s and were followed by the second wave in the middle of the 2000s (Fig. 2). So, the time since establishment of seedlings has been too short to increase ETA because the young spruce stands reach that of mature stands earliest at the age of about 30–50 years (Peck & Mayer 1996) or later (Wei & Zhang (2010). Moreover, the extent of natural disturbance varied from <1% to 38% (Table 1) but did not explain variation in Q (Table 3). Therefore, the effects of gradual vegetation change on Q, which decreased to a very similar extent in these non-nested catchments, are very unlikely.

Change in streamflow seasonality

Streamflow experienced a marked change in seasonal distribution. Q in summer decreased significantly despite a significant increase in P, while in winter Q remained unaltered despite a significant decrease in P. Balancing changes in summer and winter ETP with P and Q trends resulted in a Q transfer of about 80 mm from summer to winter (Table 5). It originated from the warming in January and February by about 1 K, which more often led to intermittent reduction of snowpack and, more importantly, from the exceptional warming in April and May by more than 2 K (Fig. 5) which caused an earlier final snowmelt (Fig. 6). Temperature and snowmelt altered synchronously across the whole altitudinal gradient thus accelerating water mobilization from snowpack throughout the study site. Thus, the last parts of snowmelt driven groundwater recharge and Q moved from hydrological summer into winter.

This process has affected many snow dominated or influenced catchments, mostly in mountainous regions. Ubiquitous trends to earlier snowmelt and Q metrics due to warming have been reported for the Western and Eastern USA (McCabe & Clark 2005, Maurer et al. 2007, Stewart et al. 2009, Clow 2010, Parr & Wang 2014, Dudley et al. 2017), and for northern and central Europe (Hisdal et al. 2010, Renner & Bernhofer 2011, Stahl et al. 2010, Hlavčová et al. 2015).

Table 5. Streamflow shift (Q_{shift}) from summer to winter half-year due to earlier snowmelt derived from the observed changes in water balance components (Figs. 3, 4, 7) for the whole study area. Note the small deviation from balance (bold).

Period	P	ETP	Q	Q_{shift}
Summer	51	44	−70	−77
Winter	−54	21	8	83
Year	3	65	–59	**3 / 6**

Larger effects on flooding during winter associated with earlier streamflow timing as reported in the above mentioned literature could not be found. Slightly but significantly increased maximum daily Q in winter was only due to an overall increase in March. This finding points to intermittent snowmelt due to warming and increasing precipitation in February, as precipitation decreased in March while temperature did not change. In May, by contrast, the maximum and minimum daily Q decreased significantly despite increased P, underpinning the warming effect via earlier snowmelt. Up to now, however, there is no marked decrease in summer and/or autumn low flow like in southern and east Europe (Stahl et al. 2010, Renner & Bernhofer 2011, Hlavčová et al. 2015). Obviously, the P increase in early summer was large enough to offset water losses due to earlier snowmelt with respect to groundwater recharge. Moreover, low flow in autumn is mostly sustained by slow-flowing groundwater, which in headwater catchments of the Bavarian Forest NP exhibits a mean residence time of 8–15 years (Beudert et al. 2007). Due to this buffering, several consecutive years with large P deficits, especially in winter, are needed to significantly reduce it.

Contrasting streamflow changes in severely disturbed nested catchments

The sub-catchments of the Upper Große Ohe (UGO) and Upper Vydra (UV) in the national parks did not show changes in annual Q and P. But Q and $Q.P^{-1}$ revealed a single step change ($p<0.05$) between 1998 and 1999 for UGO and the embedded FB which coincided with the steep increase in the bark beetle disturbed area by 25 percentage points to more than 30% (1998) over just 3 years (Fig. 2). This is consistent with former findings that reductions in forest cover must exceed a threshold of 20–25% (Stednick 1996, Brown et al. 2005, Beudert et al. 2007) to be detected by Q monitoring, given an annual P of more than 500 mm (Adams et al. 2012). Mean ETA in the subsequent period was by 62–90 mm (UGO) and 120 mm (FB) lower than in the period before, but does not account for the warming effects described above. This is consistent with basic physical characteristics of dead trees, which have lost most of their interception and the complete transpiration surface (Anderegg et al. 2012), thus reducing water loss from canopy. Unmanaged bark beetle disturbed areas are different to clear-cut areas (Edburg et al. 2012) in terms of remaining surface for evaporation, no damage to the living second and third layer trees, understory vegetation, and physical soil integrity. Nevertheless, the comparison with fully or partially cut catchments regarding the effects on ETA and Q may help to understand the historical changes and assess short and medium term eco-hydrological changes.

Bosch & Hewlett (1982) reported a 40-mm first-year increase in Q per 10% change in conifer forest area, while Sahin & Hall (1996) reported a mean increase in Q of 10–25 mm during the first five years after clear-cut. Overall, the Q response depends on climatological regime, physical landscape features, and dominant tree species (Stednik 1996, Brown et al. 2005). After the first bark beetle outbreak (30% area) in UGO and FB, the slope estimation by Bosch & Hewlett (1982) would fit our observed changes in evapotranspiration (net streamflow), while, after the second outbreak (~60% area), the slope of Sahin & Hall (1996) provides a better fit. The obvious persistence of decreased ETA might be the result of the sequence of two distinct bark beetle outbreaks. Firstly, dense and fast-growing stand regeneration in the stands attacked first profited from additional precipitation on soil surface and water supply (Edburg et al. 2012) and increasingly compensated for strongly reduced ETA after mature tree mortality (Brown et al. 2014). The second bark beetle outbreak, which peaked in the mid-2000s, superimposed these succession effects. Applying the concept of Wei & Zhang (2010) based on canopy height for spruce species in British Columbia, Canada, revealed that hydrological recovery due to the tree regeneration could already be 25% just 10–15 years after the first bark beetle outbreak in UGO and FB, thereby reducing its effects on Q. Moreover and in accordance with Brown et al. (2005), it gives reason to believe that Q will return to pre-disturbance levels during the next 15–25 years in these sub-catchments, notwithstanding the warming driven changes.

In UV (Šumava NP), there was no detectable trend or step change in Q and Q.P^{-1} in response to disturbances of similar magnitude (62% area) but with a very different course compared to the Bavarian Forest NP (Fig. 2). However, the mean annual ETA (178 mm) resulting from Q.P^{-1} is unrealistically low and its inter-annual variability too large (159 mm) not to raise doubts on data quality. For the embedded Rokytka stream, a Q.P^{-1} of 1 and thus zero ETA was found (Kocum et al. 2016). Irrespective of that, one may speculate that the first disturbances up to 2006 developed too slowly, allowing full compensation by natural succession while drastic disturbances (30%) caused by the Kyrill storm and bark beetle attack set in too late (2007) to generate significant hydrological changes. On the other hand, the Bavarian Forest NP sub-catchments reacted very quickly to the vegetation cover changes comparable to clear-cut catchments (Bosch & Hewlett 1982, Sahin & Hall 1996). There could be a scale effect in UV when disturbance effects on Q, which are detectable in small catchments, become invisible on a larger scale, where climate change effects may then dominate (Blöschl et al. 2007). The fact that the largest ETA and Q effects were in FB (0.7 km²), with medium effects in UGO (19.1 km²) and no effect in UV (89.7 km²), despite the areal extent of disturbance remaining the same, would support this assumption. Additional indication comes from the large RW and OT catchments with 29% and 38% disturbed area (Table 1), which did not show comparable effects on Q. On the other hand, Wei & Zhang (2010) and Zhang & Wei (2012) demonstrated that the effects of climate change and bark beetle attacks can be delineated for much larger catchments (2 860 and 1 570 km²). In UV, however, there was in fact no change at all in both Q and P, which suggests that the effects of disturbance (increasing) and climate change (decreasing) developed at a similar rate thereby offsetting each other.

Besides annual yields, strong effects on peak discharge were reported in response to extended clear-cut harvesting (Hornbeck 1973, Caissie et al. 2002, Guillemette et al. 2005) but reports about comparable responses to extended bark beetle disturbance are lacking (Slinski et al. 2016). There is a common statement that bark beetle effects on peak streamflow are weak and restricted to small events (Potts 1984, Moore & Wondzell 2005, Biederman et al. 2015). Moreover, harvesting and disturbance effects on stormflow become increasingly less important the larger the event is (Harr et al. 1975, Hornbeck et al. 1979, Caissie et al. 2002). This is in line with our findings of slightly increased peak flows. As management intervention like salvage logging did not occur in the core zones of both national parks, the splash damping properties of soil humus layers, coarse woody debris and lower vegetation were not affected by compaction, mixing or destruction by heavy machinery. This would have accelerated runoff generation by increasing surface flow, raised peak flow and forced erosion (Swanson & Dyrness 1975, Beschta et al. 1978).

Even in summer, in which reduced ETA and increased P could have exerted influence, peak flows did not change as reported by Bernsteinová et al. (2015). Low flow also did not change in summer, thereby confirming the results of Langhammer et al. (2015) and Bernsteinová et al. (2015) for a shorter period. Like in the superordinate catchments, the low summer flow is controlled by groundwater stores, which have delayed responses to altered hydrological processes in the ecosystems. So, decreased ETA and increased P on soil surfaces in regenerating stands (Bearup et al. 2014) must have increased runoff yields but not necessarily low flows.

Summary and conclusions

Nine conterminous catchments in the Bohemian Forest showed a significant decrease in annual runoff yields (1978–2013) due to significant and strong changes in air temperature. Warming acted two-fold: by hastening final snowmelt and streamflow timing in late winter and spring, and by increasing evapotranspiration mostly in summer.

Three sub-catchments in the Bavarian Forest and Šumava national parks heavily affected by bark beetle and windthrow showed differing hydrological behaviour. Streamflow seasonality and flow extremes responded identically to warming but annual runoff yields remained either unaltered or even increased. This indicates that decreased evapotranspiration due to disturbance maintained groundwater recharge and regional drinking water supply. However, during further succession towards new forests and increasing water demand as part of the natural life cycle, these benefits will level out, probably sooner the faster climate change proceeds. How persistent post-mortality hydrological changes are and whether more mixed naturally structured forests change the partitioning of evapotranspiration components in the long term – are some of the questions which future research should focus on.

There is a lot of scientific evidence in this publicly available dataset that a small change in winter flooding and the overall decrease in runoff yield are due to climate change but no evidence to relate them to natural disturbances or the national park management. Up to now, disturbance related eco-hydrological changes have been offsetting or exceeding the warming caused reduction in runoff yields.

Acknowledgements. The publication was supported by the Cross-border cooperation programme Czech Republic–Bavaria Free State ETC goal 2014–2020, the Interreg V project No. 26 “Silva Gabreta Monitoring – Implementation of Transboundary Monitoring of Biodiversity and Water Regime”.

References

Adams H.D., Luce C.H., Breshears D.D., Allen C.D., Weiler M. & Hale V.C., 2012: Ecohydrological consequences of drought- and infestation-triggered tree die-off: insights and hypotheses. *Ecohydrology*, 5: 145–159.

Anderegg W.R.L., Kane J.M. & Anderegg L.D.L., 2012: Consequences of widespread tree mortality triggered by drought and temperature stress. *Nature Climate Change*, 3: 30–36.

Andréassian V., 2004: Waters and forests: from historical controversy to scientific debate. *Journal of Hydrology*, 291: 1–27.

Babůrek J., Pertoldová J., Verner K. & Jiřička J., 2013: *Guide to the geology of Šumava Mountains*. Vimperk, 117 pp.

Bayerisches Landesamt für Statistik, 2016: Statistik kommunal 2015, Landkreise Freyung-Grafenau 09 272 und Regen 09 276 [Municipal statistics for the counties of Freyung-Grafenau and Regen]. Online https://www.statistik.bayern.de/statistikkommunal/092.pdf (accessed on 20 June 2017) (in German).

Bayerisches Landesamt für Umwelt, 2017: Trinkwasserverbrauch in Bayern [Drinking water use in Bavaria]. Online https://www.lfu.bayern.de/wasser/trinkwasserversorgung_oeffentlich/trinkwasserverbrauch/index.htm (accessed on 20 June 2017) (in German).

Bässler C., Seifert L. & Müller J., 2015: The BIOKLIM Project in the National Park Bavarian Forest: Lessons from a biodiversity survey. *Silva Gabreta*, 21: 81–93.

Bearup L.A., Maxwell R.M., Clow D.W. & McCray J.E., 2014: Hydrological effects of forest transpiration loss in bark beetle-impacted watersheds. *Nature Climate Change*, 4: 481–486.

Bernsteinová J., Bässler C., Zimmermann L., Langhammer J. & Beudert B., 2015: Changes in runoff in two neighbouring catchments in the Bohemian Forest related to climate and land cover changes. *Journal of Hydrology and Hydromechanics*, 63: 342–352.

Beschta R.L., 1978: Long-term patterns of sediment production following road construction and logging in the Oregon Coast Range. *Water Resources Research*, 14: 1011–1016.

Beudert B, Klöcking B. & Schwarze R., 2007: Grosse Ohe: impact of bark beetle infestation on the water and matter budget of a forested catchment. In: *Forest Hydrology – Results of Research in Germany and Russia*, Puhlmann H. & Schwarze R. (eds) *IHP/HWRP–Berichte*, 6: 41–62.

Beudert B. & Gietl G., 2015: Long-term monitoring in the Große Ohe catchment, Bavarian Forest National Park. *Silva Gabreta*, 21: 5–27.

Beudert B., Bässler C., Thorn S., Noss R., Schröder B., Dieffenbach-Fries H., Foullois N. & Müller J., 2015: Bark beetles increase biodiversity while maintaining drinking water quality. *Conservation Letters*, 8: 272–281.

Biederman J.A., Somor A.J., Harpold A.A., Gutmann E.D., Breshears D.D., Troch P.A., Gochis D.J., Scott R.L., Meddens, A.J.H. & Brooks P.D., 2015: Recent tree die-off has little effect on streamflow in contrast to expected increases from historical studies. *Water Resources Research*, 51: 9775–9789.

Birsan M.V., Molnar P., Burlando P. & Pfaundler M., 2005: Streamflow trends in Switzerland. *Journal of Hydrology*, 314: 312–329.

Blöschl G., Ardoin-Bardin S., Bonell M., Dorninger M. & Szolgay J., 2007: At what scales do climate variability and land cover change impact on flooding and low flows? *Hydrological Processes*, 21: 1241–1247.

Bosch J.M. & Hewlett J.D., 1982: A review of catchment experiments to determine the effect of vegetation changes on water yield and evapotranspiration. *Journal of Hydrology*, 55: 3–23.

Boyd M.J., Bufill M.C. & Knee R.M., 1993: Pervious and impervious runoff in urban catchments. *Hydrological Sciences Journal*, 38: 463–478.

Brown A.E., Zhang L., McMahon T.A., Western A.W. & Vertessy R.A., 2005: A review of paired catchment studies for determining changes in water yield resulting from alterations in vegetation. *Journal of Hydrology*, 310: 28–61.

Brown M.G., Black T.A., Nesic Z., Foord V.N., Spittlehouse D.L., Fredeen A.L. & Meyer G., 2014: Evapotranspiration and canopy characteristics of two lodgepole pine stands following mountain pine beetle attack. *Hydrological Processes*, 28: 3326–3340.

Buchtele J., Buchtelová M. & Tesař M., 2006: Role of vegetation in the variability of water regimes in the Šumava Mts forest. *Biologia*, 61: 246–250.

Caissie D., Jolicoeur S., Bouchard M. & Poncet E., 2002: Comparison of streamflow between pre and post timber harvesting in Catamaran Brook (Canada). *Journal of Hydrology*, 258: 232–248.

Caldwell P.V., Miniat C.F., Elliott K.J., Swank W.T., Brantley S.T. & Laseter S.H., 2016: Declining water yield from forested mountain watersheds in response to climate change and forest mesophication. *Global Change Biology*, 22: 2997–3012.

Clow D.W., 2010: Changes in the timing of snowmelt and streamflow in Colorado: a response to recent warming. *Journal of Climate*, 23: 2293–2306.

Český statistický úřad, 2017: Statistické ukazatele za okresy Prachatice a Klatovy [Municipal statistics for the counties of Prachatice and Klatovy]. Online https://www.czso.cz/ (accessed on 20 June 2017) (in Czech).

Delzon S. & Loustau D., 2005: Age-related decline in stand water use: sap flow and transpiration in a pine forest chronosequence. *Agricultural and Forest Meteorology*, 129: 105–119.

Doorenbos J. & Pruitt W. O., 1977: *Crop water requirement*. FAO Irrigation and Drainage Paper, 24, Rome, 154 pp.

Dudley R.W., Hodgkins G.A., McHale M.R., Kolian M.J. & Renard B., 2017: Trends in snowmelt-related streamflow timing in the conterminous United States. *Journal of Hydrology*, 547: 208–221.

Ernstberger H., 1987: *Einfluss der Landnutzung auf Verdunstung und Wasserbilanz* [*Land use effects on evapotranspiration and water balance*]. Beiträge zur Hydrologie, Kirchzarten, 189 pp. (in German).

European Environment Agency, 2016: Data and maps. Copernicus Land Monitoring Service – Corine Land Cover. Online https://www.eea.europa.eu (accessed on 10 July 2016).

European Environment Agency, 2017: Data and maps. Indicators. Online https://www.eea.europa.eu (accessed on 20 June 2017).

Gilbert R.O., 1987: *Statistical methods for environmental pollution monitoring*. Van Nostrand Reinhold, New York, 334 pp.

Gudmundsson L. & Seneviratne S.I., 2015: European drought trends. *Proceedings of the International Association of Hydrological Sciences*, 369: 75–79.

Guillemette F., Plamondon A.P., Prévost M. & Lévesque D., 2005: Rainfall generated stormflow response to clearcutting a boreal forest: peak flow comparison with 50 world-wide basin studies. *Journal of Hydrology*, 302: 137–153.

Hall J., Arheimer B., Borga M., Brázdil R., Claps P., Kiss A., Kjeldsen T.R., Kriauciuniene J., Kundzewicz Z.W., Lang M., Llasat M.C., Macdonald N., Mcintyre N., Mediero L., Merz B., Merz R., Molnar P., Montanari A., Neuhold C., Parajka J., Perdigão R.A.P., Plavcová L., Rogger M., Salinas J.L., Sauquet E., Schär C., Szolgay J., Viglione A. & Blöschl G., 2014: Understanding flood regime changes in Europe: A state of the art assessment. *Hydrology and Earth System Sciences*, 18: 2735–2772.

Harbor J.M., 1994: A practical method for estimating the impact of land-use change on surface runoff, groundwater recharge and wetland hydrology. *Journal of the American Planning Association*, 60: 95–108.

Harr R.D., Harper W.C., Krygier J.T. & Hsieh F.S., 1975: Changes in storm hydrographs after road building and clear-cutting in the Oregon Coast Range. *Water Resources Research*, 11: 436–444.

Helsel D.R., Mueller D.K. & Slack J.R., 2006: Computer program for the Kendall family of trend tests (No. 2005–5275).

Hlavčová K., Kotríková K., Kohnová S. & Valent P., 2015: Changes in the snow water equivalent in mountainous basins in Slovakia over recent decades. *Proceedings of the International Association of Hydrological Sciences*, 370: 109–116.

Hornbeck J.W., 1973: Storm flow from hardwood-forested and cleared watersheds in New Hampshire. *Water Resources Research*, 9: 346–354.

Hornbeck J.W., Martin C.W. & Eagar C., 1997: Summary of water yield experiments at Hubbard Brook experimental forest, New Hampshire. *Canadian Journal of Forest Research*, 27: 2043–2052.

Hudson J.A., Crane S.B. & Blackie J.R., 1997: The Plynlimon water balance 1969–1995: the impact of forest and moorland vegetation on evaporation and streamflow in upland catchments. *Hydrology and Earth System Sciences*, 1: 409–427.

IPCC 2013: The physical science basis. Contribution of Working Group I to the Fifth Assessment Report of the Intergovernmental Panel on Climate Change. In: *Climate Change 2013*, Stocker T.F., Qin D., Plattner G.K., Tignor M., Allen S.K., Boschung J., Nauels, A., Xia, Y., Bex, V. & Midgley P.M. (eds) Cambridge University Press, Cambridge, United Kingdom and New York, NY, USA, 1535 pp.

Jones J.A., 2011: Hydrologic responses to climate change: considering geographic context and alternative hypotheses. *Hydrological Processes*, 25: 1996–2000.

Jones J.A., Creed I.F., Hatcher K.L., Warren R.J., Adams M.B., Benson M.H., Boose E., Brown W.A., Campbell J.L., Covich A., Clow D.W., Dahm C.N, Elder K., Ford C.R., Grimm N.B., Henshaw D.L., Larson K.L., Miles E.S., Miles K.M., Sebestyen S.D., Spargo A.T., Stone A.B., Vose J.M. & Williams M.W., 2012: Ecosystem processes and human influences regulate streamflow response to climate change at long-term ecological research sites. *BioScience*, 62: 390–404.

Kay A.L., Bell V.A., Blyth E.M., Crooks S.M., Davies H.N. & Reynard N.S., 2013: A hydrological perspective on evaporation: historical trends and future projections in Britain. *Journal of Water and Climate Change*, 4: 193–208.

Klein Tank A.M.G., Wijngaard J.B., Können G.P., Böhm R., Demarée G., Gocheva A., Mileta M., Pashiardis S., Hejkrlik L., Kern-Hansen C., Heino R., Bessemoulin P., Müller-Westermeier G., Tzanakou M., Szalai S., Pálsdóttir T., Fitzgerald D., Rubin S., Capaldo M., Maugeri M., Leitass A., Bukantis A., Aberfeld R., van Engelen A. F.V., Forland E., Mietus M., Coelho F., Mares C., Razuvaev V., Nieplova E., Cegnar T., López J.A., Dahlström B., Moberg A., Kirchhofer W., Ceylan A., Pachaliuk O., Alexander L.V. & Petrovic P., 2002: Daily dataset of 20th-century surface air temperature and precipitation series for the European Climate Assessment. *International Journal of Climatology*, 22: 1441–1453.

Kliment Z. & Matoušková M., 2008: Long-term trends of rainfall and runoff regime in Upper Otava river basin. *Soil Water Reerach*, 3: 155–167.

Kliment Z., Matoušková M., Ledvinka O. & Královec V., 2011: Trend analysis of rainfall-runoff regimes in selected headwater areas of the Czech Republic. *Journal of Hydrology and Hydromechanics*, 59: 36–50.

Kling H., Fuchs M. & Paulin M., 2012: Runoff conditions in the upper Danube basin under an ensemble of climate change scenarios. *Journal of Hydrology*, 424: 264–277.

Klöcking B., Schwarze R., Beudert B., Suckow F. Lasch P., Badeck F. & Pfützner B., 2005: *Auswirkungen des Borkenkäferbefalls auf den Wasser- und Stoffhaushalt zweier Gewässereinzugsgebiete im Nationalpark Bayerischer Wald* [*Bark beetle effects on water and element budgets of two catchments in the Bavarian Forest National Park*]. Nationalparkverwaltung Bayerischer Wald, Grafenau, 184 pp. (in German).

Kocum J., Oulehle F., Janský B., Bůzek F., Hruška J. & Vlček L., 2016: Geochemical evidence for peat bog contribution to the streamflow generation process: case study of the Vltava River headwaters, Czech Republic. *Hydrological Sciences Journal*, 61: 2579–2589.

Komatsu H., Kume T. & Otsuki K., 2011: Increasing annual runoff – broadleaf or coniferous forests? *Hydrological Processes*, 25: 302–318.

Langhammer J., Su Y. & Bernsteinová J., 2015: Runoff response to climate warming and forest disturbance in a mid-mountain basin. *Water*, 7: 3320–3342.

Lausch A., Fahse L. & Heurich M., 2011: Factors affecting the spatio-temporal dispersion of *Ips typographus* (L.)

in Bavarian Forest National Park: A long-term quantitative landscape-level analysis. *Forest Ecology & Management*, 261: 233–245.

Matsoukas C., Benas N., Hatzianastassiou N., Pavlakis K.G., Kanakidou M. & Vardavas I., 2011: Potential evaporation trends over land between 1983–2008: driven by radiative or turbulent fluxes. *Atmospheric Chemistry and Physics*, 11: 7601–7616.

Maurer E.P., Stewart I.T., Bonfils C., Duffy P.B. & Cayan D., 2007: Detection, attribution, and sensitivity of trends toward earlier streamflow in the Sierra Nevada. *Journal of Geophysical Research: Atmospheres*, 112: D11118, doi:10.1029/2006JD008088.

Mayer M., 2014: Can nature-based tourism benefits compensate for the costs of national parks? A study of the Bavarian Forest National Park, Germany. *Journal of Sustainable Tourism*, 22: 561–583.

McCabe G.J. & Clark M.P., 2005: Trends and variability in snowmelt runoff in the western United States. *Journal of Hydrometeorology*, 6: 476–482.

Milliman J.D., Farnsworth K.L., Jones P.D., Xu K.H. & Smith L.C., 2008: Climatic and anthropogenic factors affecting river discharge to the global ocean, 1951–2000. *Global and Planetary Change*, 62: 187–194.

Milly P.C., Dunne K.A. & Vecchia A.V., 2005: Global pattern of trends in streamflow and water availability in a changing climate. *Nature*, 438: 347–350.

Ministry of Agriculture, 2016: Information on forests and forestry in the Czech Republic by 2015. Ministry of Agriculture of the Czech Republic, Prague, 31 pp.

Möges M., 2007: Klima-Konzept für den Staatswald. Bis 2012 beplant die Bayerische Staatsforsten alle ihre Forstbetriebsflächen nach dem Programm “Waldumbau zur Anpassung an den Klimawandel” [Climate change concept for the Bavarian state forest]. *LWF Aktuell*, 62: 42 pp. (in German).

Moore R. & Wondzell S.M., 2005: Physical hydrology and the effects of forest harvesting in the Pacific Northwest: a review. *Journal of the American Water Resources Association*, 41: 763–784.

Müller J., Bußler H., Goßner M., Rettelbach T. & Duelli P., 2008: The European spruce bark beetle *Ips typographus* in a national park: from pest to keystone species. *Biodiversity and Conservation*, 17: 2979–3001.

Murakami S., Tsuboyama Y., Shimizu T., Fujieda M. & Noguchi S., 2000: Variation of evapotranspiration with stand age and climate in a small Japanese forested catchment. *Journal of Hydrology*, 227: 114–127.

O’brien R.M., 2007: A caution regarding rules of thumb for variance inflation factors. *Quality & Quantity*, 41: 673–690.

Oosterbaan R.J., 1994: Agricultural drainage criteria. In: *Drainage Principles and Applications*, Ritzema H.P. (ed.) ILRI Publication, Wageningen, 16: 635–688.

Parr D. & Wang G., 2014: Hydrological changes in the US Northeast using the Connecticut River Basin as a case study: Part 1. Modeling and analysis of the past. *Global and Planetary Change*, 122: 208–222.

Peck A. & Mayer H., 1996: Einfluss von Bestandesparametern auf die Verdunstung von Wäldern [Influence of forest stand characteristics on evapotranspiration]. *Forstwissenschaftliches Centralblatt*, 115: 1–9 (in German).

Potts D.F., 1984: Hydrologic impacts of a large-scale mountain pine beetle (*Dendroctonus ponderosae* Hopkins) epidemic. *Journal of the American Water Resources Association*, 20: 373–377.

Priestley C.H.B. & Taylor R.J., 1972: On the assessment of surface heat flux and evaporation using large-scale parameters. *Monthly Weather Review*, 100: 81–92.

Ramamurthy P. & Bou-Zeid E., 2014: Contribution of impervious surfaces to urban evaporation. *Water Resources Research*, 50: 2889–2902.

Renner M. & Bernhofer C., 2011: Long term variability of the annual hydrological regime and sensitivity to temperature phase shifts in Saxony/Germany. *Hydrology and Earth System Sciences*, 15: 1819–1833.

Rohrmüller V.J., Gebauer D. & Mielke, H., 2000: Die Altersstellung des ostbayerischen Grundgebirges [Temporal classification of bedrock in eastern Bavaria]. *Geologica Bavarica*, 105: 73–84 (in German).

Sahin V. & Hall M. J., 1996: The effects of afforestation and deforestation on water yields. *Journal of Hydrology*, 178: 293–309.

Seibold S., Bässler C., Brandl R., Büche B., Szallies A., Thorn S., Ulyshen M.D. & Müller J., 2016: Microclimate and habitat heterogeneity as the major drivers of beetle diversity in dead wood. *Journal of Applied Ecology*, 53: 934–943.

Šerna L., 2003: Soil characteristics of the Otava River basin and relations to floods. *Acta Universitatis Carolinae*, 2: 157–172.

Slinski K.M., Hogue T.S., Porter A.T. & McCray J.E., 2016: Recent bark beetle outbreaks have little impact on streamflow in the Western United States. *Environmental Research Letters*, 11: 074010.

Smith E. P., 2002: BACI design. In: *Encyclopedia of Environmetrics*. El-Shaarawi A.H. & Piegorsch W.W. (eds), John Wiley & Sons, Chichester: 141–148.

Stahl K., Hisdal H., Hannaford J., Tallaksen L.M., van Lanen H.A.J. & Jodar J., 2010: Streamflow trends in Europe. Evidence from a dataset of near-natural catchments. *Hydrology and Earth System Sciences*, 7: 5769–5804.

Stahl K., Tallaksen L.M., Hannaford J. & Van Lanen H.A.J., 2012: Filling the white space on maps of European runoff trends: estimates from a multi-model ensemble. *Hydrology and Earth System Sciences*, 16: 2035–2047.

Stednick J.D., 1996: Monitoring the effects of timber harvest on annual water yield. *Journal of Hydrology*, 176: 79–95.

Štěpánek R., 2005: AnClim – software for time series analysis. Dept. of Geography, Faculty of Sciences, Masaryk University Brno. Online http://www.climahom.eu/software-solution/anclim (accessed on 16 June 2008).

Stewart I.T., 2009: Changes in snowpack and snowmelt runoff for key mountain regions. *Hydrological Processes*, 23: 78–94.

Stewart I.T., Cayan D.R. & Dettinger M.D., 2005: Changes toward earlier streamflow timing across western North America. *Journal of Climate*, 18: 1136–1155.

Swanson F.J. & Dyrness C.T., 1975: Impact of clear-cutting and road construction on soil erosion by landslides in the western Cascade Range, Oregon. *Geology*, 3: 393–396.

Teuling A. J., Hirschi M., Ohmura A., Wild M., Reichstein M., Ciais P., Buchmann N., Ammann C., Montagnani L., Richardson A.D., Wohlfahrt G. & Seneviratne S.I., 2009: A regional perspective on trends in continental evaporation. *Geophysical Research Letters*, 36: L02404.

Thorn S., Bässler C., Brandl R., Burton P. J., Cahall R., Campbell J. L.,Castro j., Choi C.Y., Cobb T., Donato D.C., Durska E., Fontaine J.B., Gauthier S., Hebert C., Hothorn T., Hutto R.L., Lee E.J., Leverkus A.B., Lindenmayer D.B., Obrist M.K., Rost J., Seibold S., Seidl R., Thom D., Waldron K., Wermelinger B., Winter M.A., Zmihorski M. & Müller J., 2017: Impacts of salvage logging on biodiversity – a meta-analysis. *Journal of Applied Ecology*, 55: 279–289.

Thünen-Institut, 2017: Dritte Bundeswaldinventur – Ergebnisdatenbank [The third National Forest Inventory – data base]. Online https://bwi.info (accessed on 20 June 2017) (in German).

Tomer M.D. & Schilling K.E., 2009: A simple approach to distinguish land-use and climate-change effects on watershed hydrology. *Journal of Hydrology*, 376: 24–33.

Velpuri N.M. & Senay G.B., 2013: Analysis of long-term trends (1950–2009) in precipitation, runoff and runoff coefficient in major urban watersheds in the United States. *Environmental Research Letters*, 8: 024020.

Vormoor K., Lawrence D., Schlichting L., Wilson D. & Wong W.K., 2016: Evidence for changes in the magnitude and frequency of observed rainfall vs. snowmelt driven floods in Norway. *Journal of Hydrology*, 538: 33–48.

Wei X. & Zhang M., 2010: Quantifying streamflow change caused by forest disturbance at a large spatial scale: A single watershed study. *Water Resources Research,* 46: W12525. doi:10.1029/2010WR009250

Wilby R.L., Beven K.J. & Reynard N.S., 2008: Climate change and fluvial flood risk in the UK: more of the same? *Hydrological Processes*, 22: 2511–2523.

Wilson D., Hisdal H. & Lawrence D., 2010: Has streamflow changed in the Nordic countries? – Recent trends and comparisons to hydrological projections. *Journal of Hydrology*, 394: 334–346.

Zhang L., Dawes W.R. & Walker G.R., 2001: Response of mean annual evapotranspiration to vegetation changes at catchment scale. *Water resources research*, 37: 701–708.

Zhang Y., Leuning R., Chiew F.H., Wang E., Zhang L., Liu C., Fubao S., Murray C.P. Yanjub S. & Jung M., 2012: Decadal trends in evaporation from global energy and water balances. *Journal of Hydrometeorology*, 13: 379–391.

Received: 1 September 2017
Accepted: 18 January 2018

Silva Gabreta	vol. 24	p. 47–67	Vimperk, 2018

Modelling future hydrological pattern in a Bohemian Forest headwater catchment

Anna Lamačová[1,2,*], Jakub Hruška[1,2], Miroslav Trnka[2,4], Petr Štěpánek[2,3], Pavel Zahradníček[2,3], Jan Meitner[2] & Aleš Farda[2]

[1] *Czech Geological Survey, Klárov 3, CZ-11821 Prague 1, Czech Republic*
[2] *Global Change Research Institute CAS, Bělidla 986/4a, CZ-60300 Brno, Czech Republic*
[3] *Czech Hydrometeorological Institute, Kroftova 43, CZ-61600 Brno, Czech Republic*
[4] *Institute of Agrosystems and Bioclimatology, Mendel University, Zemědělská 1, CZ-61300 Brno, Czech Republic*
[*] anna.lamacova@geology.cz

Abstract

This study focuses on estimation of the impacts of anticipated global climate change on water balance in forested headwater catchment. The investigated catchment is located in the Šumava National Park (Bohemian Forest) in the southern part of the Czech Republic. We calculated nine future water balance scenarios for periods of 2021–2050 and 2071–2100. We used data from following models: CNRM-CM5_ALADIN53, EC-EARTH_RACMO22E, EC-EARTH_RCA4, and MPI-ESM-LR_CCLM4-8-17 with 3 emission scenarios (Representative Concentration Pathways RCP2.6, 4.5, 8.5). Corrected regional climate model daily data were used in combination with hydrological model Brook90. The scenarios projected an increase of mean annual temperature of 1.1°C (RCP4.5) and 1.4°C (RCP8.5, 2021–2050) and 2.3°C (RCP4.5) and 4.2°C (RCP8.5, 2071–2100) and increase in mean annual precipitation amount of 11% (RCP 4.5) and 15% (RCP 8.5, 2021–2050) and 15% (RCP 4.5) and 20% (RCP8.5, 2071–2100). It would result in a mean annual runoff increase of 9% (RCP4.5) and 14% (RCP8.5, 2021–2050) and 12% (RCP4.5) and 16% (RCP8.5, 2071–2100). The annual runoff cycle is projected to change significantly especially in the period of 2071–2100, when a large winter runoff increase and a spring runoff maximum decrease is expected. "Pessimistic" RCP8.5 scenarios expect even no spring runoff maxima from snowmelt and project a shift of runoff maxima to December.

Key words: climate change impact, runoff, water balance, hydrological modelling, forested catchment

INTRODUCTION

Temperature increase and changes in precipitation distribution and amounts are expected to affect hydrological pattern notably (IPCC 2007, IPCC 2013). Forested landscapes are considered to be close to the natural environment in central European conditions and the Bohemian Forest represents a large forested area of high ecological importance. Forests can be affected by climate change both directly and indirectly. Increased temperature can affect vegetation cover in forests notably even regardless of precipitation changes (ADAMS et al. 2009). It can lead to tree die-off or to weakening of trees and they can become more vulnerable to tree pest (ADAMS et al. 2009, ALLEN et al. 2010, RAFFA et al. 2008). However, projected increases in drought frequency due to changes in precipitation and increases in stress from biotic agents (e.g. bark beetles) could further intensify tree mortality (ADAMS et al. 2009).

Regionally oriented studies in the Bohemian Forest documented an air temperature increase over the last century (Kliment & Matoušková 2009, Langhammer et al. 2015), however, did not detect any changes in annual or seasonal precipitation (Bernsteinová et al. 2015). Also no changes in annual runoff were found by Bernsteinová et al. (2015) and Langhammer et al. (2015), however, they noted an increase in high flows in March, which was related to significant temperature increase in late winter and early spring.

A future gradient in precipitation with an increase in the Northern Europe and decrease in the Southern Europe was projected in many studies (Forzieri et al. 2014, van Vliet et al. 2015) and runoff is expected to follow the same pattern. However, the area of central Europe lies in the transition zone, where the future precipitation changes are more ambiguous. Hanel et al. (2012) estimated changes in future hydrological pattern in area of the Czech Republic for the period of 2070–2099. According to their study runoff changes from January to May will be affected by changes in snow cover and snowmelt dynamics, with a notable shift in snowmelt from April to January–February. The summer runoff decline will be caused by summer precipitation decrease. A study from small forested headwater catchments located across the Czech Republic projected an annual runoff decrease by 15% (2021–2050) and 35% (2071–2100) (compared to the period of 1994–2011) and changes in annual cycle represented by small winter runoff increase and significant summer months decrease (Lamačová et al. 2014). It was in agreement with their previous results from two headwater catchments in the eastern part of the Czech Republic where a decrease by 10–30% was projected for the period of 2071–2100 with a significant decrease in summer months (Benčoková et al. 2011).

The aim of this paper was to analyse the changes in hydrological patterns and shifts in temperature and precipitation that might happen as a result of the projected climate change. Major objectives of the study were: (i) calibration of hydrological model Brook90 (Federer et al. 2003) to the site specific condition of the Bohemian Forest headwater catchment for the control period of 1981–2010, (ii) to simulate the effects of different climate change scenarios on future hydrological pattern in periods of 2021–2050 and 2071–2100, using the calibrated Brook90 model.

Materials and Methods

Catchment characteristics

The catchment (92.7 km^2) is situated on the northern slopes of the Bohemian Forest (Šumava in Czech) mountain range (49°02' N, 13°30' E) and entirely located in the Šumava National Park. The local climate is characterized by high precipitation with high percentage of snow (approximately 40%, according to Langhammer et al. 2015) with mean annual precipitation in the upper parts of the catchment up to 1800 mm yr^{-1} (Starostová 2012). Mean annual temperature at the Churáňov climate station located nearby (1118 m a.s.l., Fig. 1) was 4.8±0.7°C for the period of 1981–2010. Mean elevation of the catchment is 1134 m a.s.l. ranging from 973–1453 m a.s.l., mean slope is 5.8°. The investigated area is a headwater catchment of the Vydra stream and the outlet with water-level recorder operated by the Czech Hydrometeorological Institute (CHMI) is situated in the Modrava municipality downstream the junction of two major catchment streams, Modravský Potok and Roklanský Potok. We thus named the catchment according to the outlet profile as the Modrava catchment, to indicate this part of the Vydra stream that represented the investigated area. Mean annual runoff was 1151 mm (1981–2010).

The bedrock consists of magmatic rocks (granite 29%) and metamorphic rocks mostly gneiss (54%), overlain by quaternary sediments (17%). Soils are dominated by entic and

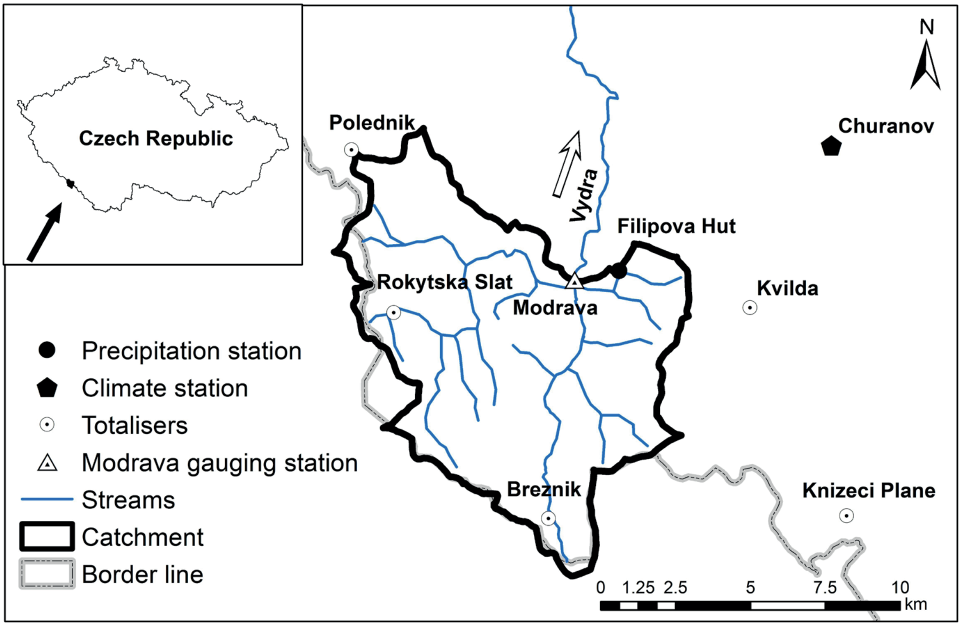

Fig. 1. A map of the study site showing the Modrava catchment and all used precipitation, climate and gauging stations.

typical podzols (47%), permanently or periodically wet soils (46%), Cambisols (3.6%), and Leptosols (3.4%) (Bernsteinová et al. 2015). The catchment is dominantly forested by Norway spruce (*Picea abies* (L.) Karst.) with different age and structure (87%). A small part of forest vegetation (about 5%) consists of mountain ash (*Sorbus aucuparia* L.). Peat bogs are covered with pines *Pinus mugo* Turra and *Pinus mugo* nothosubsp. *rotundata* (Link) Janchen & Neumayer. A small part of mountain meadows is located in the north of the catchment (6%).

Both bark beetle *(Ips typographus* L.) outbreaks and windfall affected the vegetation significantly. The first bark beetle outbreak started around the year 1994 in the southern and south-western part of the catchment along the border with the Bavarian Forest National Park in Germany. Some parts of the forest were left without any intervention, while some other areas were salvaged logged. It resulted into large clear cuts. The second outbreak started after the windstorm Kyrill in the central and eastern part in 2007. It resulted in the mosaic of logged and naturally developed spruce stands. At present, clear cuts occupied 23%, naturally developed stands with dead adult spruces 35%, and living mature stands 33% of the catchment. Wetlands (mostly peat bogs) cover 8% of the catchment (Bernsteinová et al. 2015).

The hydrological modelling

The Brook90 model is a deterministic, process-oriented, lumped parameter hydrological model that was designed to be applicable to any land surfaces at a daily time step year-round (Federer et al. 2003). Brook90 is a parameter-rich model designed primarily to study evapotranspiration and soil water movement at a point, with some provision for stream flow generation by different flow paths. Snow accumulation and melt are controlled by a degree--day method with cold content (Linsley 1949). The model uses the Shuttleworth & Wallace (1985) method for separating transpiration and soil evaporation from sparse canopies, and evaporation of interception. Actual transpiration is reduced below potential when water supply to the plant is limited.

Required inputs to the model are daily precipitation, and maximum and minimum air temperatures. Additional desirable inputs are daily solar radiation and daily mean wind speed, average vapour pressure for the day, and measured runoff (used for calculation of evaluation statistics within the program). Five parameter sets are required: canopy, location; soil (for up to 25 layers); initial and fixed parameters. In this study we did not estimate the course of future vegetation cover changes, and thus we did not modify the future canopy parameters.

The model performance was evaluated by Pearson's correlation coefficient between measured and simulated daily stream flows and by the daily and monthly Nash–Sutcliffe criterion (Nash & Sutcliffe 1970). The model was calibrated on the period of 1981–1999 and validated on the period of 2000–2010.

Meteorological and hydrological data

Meteorological data for the studied catchment (maximum and minimum daily air temperature, daily precipitation, daily mean wind speed and global radiation) were interpolated (using inverse distance weighting as an interpolation method) on the area of the catchment. For the interpolation were used the so called technical series of daily values at a particular grid point (station location) that were calculated from up to 6 neighbouring CHMI stations within a distance of 300 km, with an allowed maximum difference in altitude of 500 m. Before applying inverse distance weighting, data at the neighbour stations were standardized relatively to the altitude of the base grid point (station location). The standardization was carried out by means of linear regression and dependence of values of a particular meteorological element on altitude for each day, individually and regionally Štěpánek et al. (2011). Further details on the data processing can be found also in Štěpánek et al. (2013). The technical series were used also for validation and correction of RCM outputs (Štěpánek et al. 2016). However the mean annual precipitation amount from the technical series was too low (only 1117 mm) compared to measured data (Fig. 2). It would represent rainfall-runoff ratio of 1.05 only, therefore correction had to be used to better represent the catchment precipitation. The station network is sparse in the mountain ridge area and thus we used mean annual data from CHMI rain gauges – totalisers, located at catchment and neighbouring areas

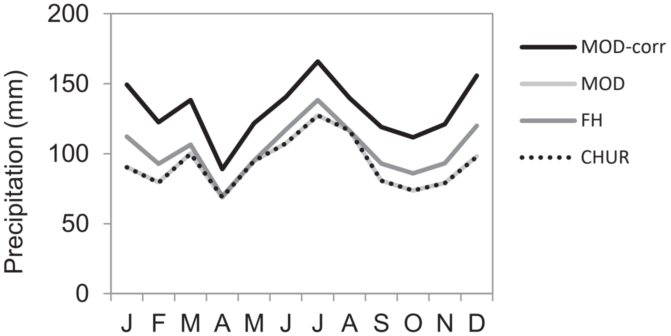

Fig. 2. Annual series of mean precipitation in the period of 1981–2010, MOD-corr – final corrected precipitation, MOD – uncorrected precipitation from "technical" data series (see section Input meteorological and hydrological data for details), FH – Filipova Huť – CHMI operated precipitation station, CHUR – CHMI operated climate station Churáňov.

(Březník, Rokytská Slať, Knížecí Pláně, Poledník, Kvilda, Filipova Huť; 1981–2010 data and details about the stations are available in Starostová, 2012). The mean annual precipitation from totalisers varied between 1165 mm (Kvilda) and 1845 mm (Březník) with an average of 1487±297 mm. We interpolated the mean annual precipitation amounts (1981–2010) from totalisers from the close vicinity of the Modrava catchment and obtained the mean annual precipitation amount of 1575 mm. The 40% difference corresponds to reports from Slovakia (Lapin et al. 1991) and Switzerland (Sevruk 1985), with the former study showing increase of precipitation totals from April to September by 35–70% when totalisers were used. Based on the comparison of annual precipitation distribution of both Modrava "technical" precipitation series and precipitation data from the CHMI Filipova Huť station (1112 m a.s.l, 49°02' N, 13°31' E) (Fig. 1), we calculated monthly correction factors and increased the precipitation to fit 1575 mm annual mean. The same monthly correction factors were used for future precipitation data.

Runoff data from the CHMI water level gauging station in Modrava (49°02' N, 13°29' E) were used without any corrections.

Future climate projections

Results from simulations performed within the European part of the global Coordinated Regional Climate Downscaling Experiment project (Euro-CORDEX, www.euro-cordex.org) with the 0.11° spatial resolution were used in this study. Experiments were forced by 3 Representative Concentration Pathway (Moss et al. 2010). These scenarios take radiative forcing (W m^{-2}) as the characteristic driving variable, instead of the concentration of the equivalent CO_2 (ppm). RCP represent a wide range of possible future emission scenarios. RCP2.6 assumes that global annual greenhouse gas emissions will peak around 2010–2020 (van Vuuren et al. 2007). RCP4.5 expects emissions to peak around 2040 and then decline (Clarke et al. 2007). RCP6 assumes that the emissions will peak around 2080 (not used in this study) and finally RCP8.5 expects emissions to rise throughout the 21st century (Riahi et al. 2007).

Four regional climate models (RCMs) with three driving global climate models (GCMs) and three different representative concentration pathway RCPs 2.6, 4.5 and 8.5 W m^{-2} scenarios were used. It represents nine plausible future scenarios in total, namely: ALADIN53 (RCM) with CNRM-CM5 driving GCM, RCP 4.5 and RCP 8.5; RACMO22E (RCM) with EC-EARTH driving GCM, RCP 4.5 and RCP 8.5; RCA4 (RCM) with EC-EARTH driving GCM, RCP 2.6, RCP 4.5 and RCP 8.5; and CCLM4-8-17 (RCM) with MPI-ESM-LR driving GCM, RCP 4.5 and 8.5. The datasets were post-processed using a correction method called distribution adjusting by percentiles developed by Štěpánek et al. (2016) that is based on the quantile mapping approach of Déqué (2007). This correction method, based on correction of individual percentiles of empirical distribution, was compared with other bias correction approaches, e.g. in Gutiérrez et al. (2018), and proved to behave very well. Compared to other quantile mapping methods it better focuses on a proper transfer function for tails of the distributions (representation of extremes).

RCM outputs were localized into positions of neighbouring CHMI climate stations and values of such series were then interpolated to obtain spatial information for the catchment. Additional monthly correction factors for precipitation were derived by comparison of technical time series and control run of a given RCM, and the appropriate corrections have been then applied for the future precipitation data. In the presented study, we decided to use two thirty-year periods from the available time series 2021–2100 and compare them to the recent period of 1981–2010. The period of 2021–2050 was chosen as a near future and the period of 2071–2100 was used to represent a more distant future.

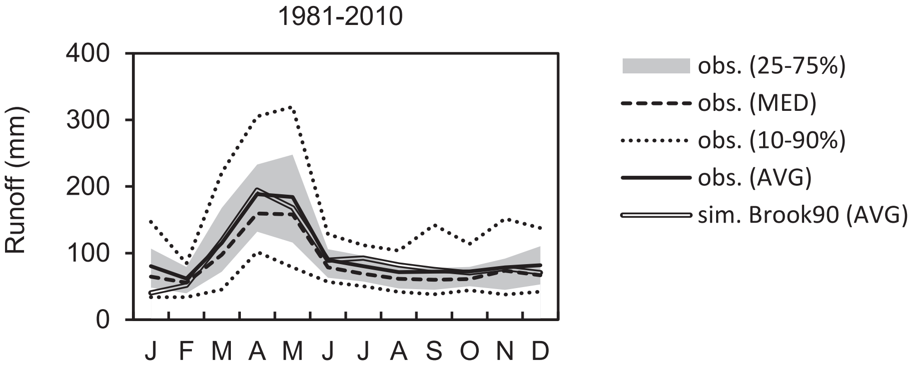

Fig. 3. Mean annual runoff cycle in the control period (1981–2010). Obs. – observed, MED – median, AVG – average, sim. Brook90 – runoff simulated by the Brook90 model, 25–75%: runoff inter-quartile range, 10–90%: runoff inter-quintile range.

Results

Performance of the Brook90 model

The corrected climatic data were used for runoff modelling using the calibrated Brook90 model in the control period 1981–2010. The mean annual runoff from the Modrava catchment calculated from observed data was 1176 mm (±236 mm) and runoff simulated by the Brook90 model was 1158 mm (±236 mm). The Brook90 model also reproduced well mean monthly runoff pattern (Fig. 3). Daily simulated and observed runoffs at the Modrava outlet in the calibration and validation period also were in relatively good agreement (Fig. 4). The Pearson's correlation coefficients were 0.72 ($r_{crit} = 0.06$, N = 6939, p = 0.05) for daily values and 0.80 ($r_{crit} = 0.14$, N = 228, p = 0.05) for monthly values in the calibration period (1981–1999). The Pearson's correlation coefficients in the validation period (2000–2010) were 0.80

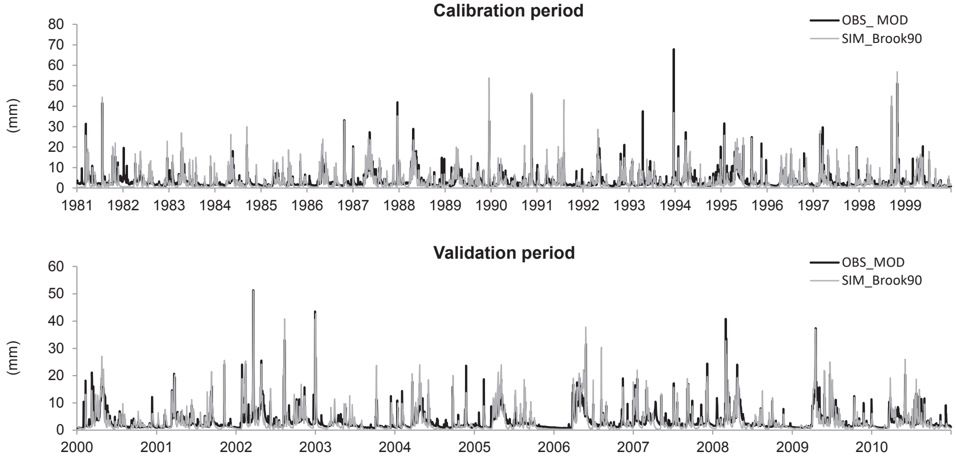

Fig. 4. Comparison of daily observed (OBS_MOD) and simulated (SIM_Brook90) runoff at Modrava outlet in the calibrated and validated period.

(r_{crit} = 0.06, N = 4018, p = 0.05) for daily values and 0.89 (r_{crit} = 0.17, N = 132, p = 0.05) for monthly values.

The Nash-Sutcliffe criterion were 0.43 for daily values and 0.58 for monthly values in the calibration period (1981–1999) and 0.59 for daily values and 0.76 for monthly values in the validation period (2000–2010).

Future temperature projections

Mean annual temperature 4.2°C was measured in the control period (1981–2010). The individual RCM models estimated an increase in mean annual temperature of 0.8–1.8°C for the period of 2021–2050 (compared to the control period of 1981–2010). The RCP 4.5 scenarios projected mean increase of 1.1°C and RCP 8.5 1.4°C (2021–2050) compared to the control period.

All scenarios (with the exception of ALADIN53, RCP 4.5) indicated an increase in November above freezing point in the period of 2071–2100. It increased from −0.3°C during control period (1981–2010) to the interval of 0.5–1.5°C (2071–2100). The summer temperatures are projected to increase notably in July by 0.8–3.1°C to 14.0–16.3°C (2071–2100) (Fig. 5). The projected increase of 1.4–4.9°C in the period of 2071–2100 would result in change of a mean annual temperature from 4.2°C (1981–2010) to 5.4–8.6°C. The RCP 4.5 scenarios projected mean increase of 2.3°C and RCP 8.5 4.2°C compared to the control period. Four of nine scenarios projected an increase of mean monthly temperatures above freezing point in all months and all scenarios expect an increase above freezing point in November and spring March. A notable increase of 1.4–6.5°C is projected for July. It represents an increase from recent 13.2°C (1981–2010) to 14.6–19.7°C (2071–2100) (Fig. 5).

Mean maximum temperatures also showed similar pattern (Fig. 5). RCM models estimated an increase of 0.7–1.7°C from 9.2°C (1981–2010) to 9.9–10.9°C (2021–2050). January mean maximum temperatures are expected to increase by 0.6–2.3°C, while maximum temperatures in July are projected to increase by 0.5–1.0°C only (Fig. 5) in the period of 2021–2050. In the period of 2071–2100, mean maximum temperatures are projected notably higher than in the control period of 1981–2010. The expected increases by 1.0–5.0°C represent temperatures from 10.2–14.2°C. January mean maximum temperatures are projected to be higher by 1.8–6.7°C. July mean maximum temperatures are projected to the increase by 1.3–4.7°C compared to the control period of 1981–2010.

Only minor differences are projected for mean monthly minimum temperatures for the period of 2021–2050 (Fig. 5). Changes of –0.3–0.6°C, compared to mean annual minimum temperature 1.5°C (1981–2010) are projected by RCM models. For the period of 2071–2100 an increase of 0.1–2.4°C in mean annual minimum temperature was projected. An increase in January is projected of 0.3–3.7°C.

Future precipitation projections

The mean annual precipitation amount for Modrava catchment was 1575 mm in the control period of 1981–2010 (Table 1). In general all models projected an increase in annual precipitation amounts. The RCP 2.6 and 4.5 scenarios estimated an increase of 4–17% and RCP 8.5 even of 7–21% for the period of 2021–2050 compared to the control period (1981–2010). Precipitation amounts are expected to increase in almost all months with the exception of March (Fig. 6). Most of the models project decrease by 15% (RCP 2.6 and 4.5) and by 18% (RCP 8.5) on average in March. Scenarios RCP 2.6 and 4.5 expect the largest increase of precipitation from November to January (23%). Scenarios RCP 8.5 expect notable increases from April to June (by 25%) and from October to January (by 25%) (Fig. 6).

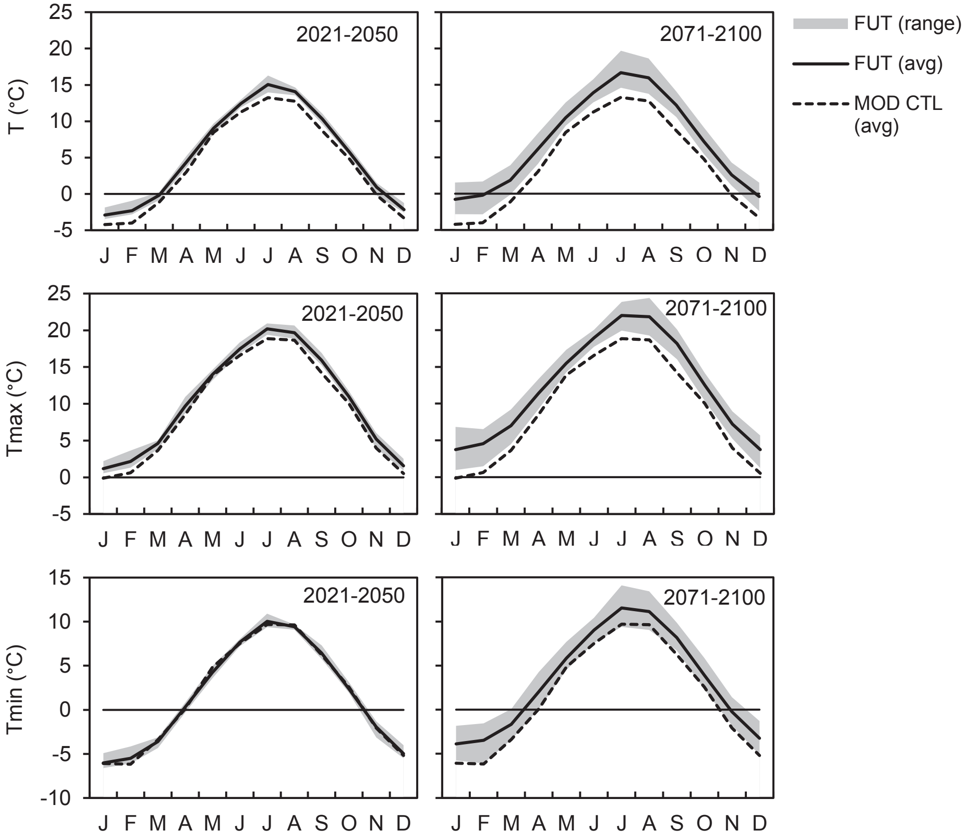

Fig. 5. Annual cycle of monthly mean, maximum and minimum air temperature. FUT – future scenarios (2021–2050 and 2071–2100), MOD ctl – control period (1981–2010). Range based on difference between maximum and minimum RCM simulations for mean temperature, minimum and maximum air temperature.

Also for the period of 2071–2100, the models projected an increase of annual precipitation amounts of 6–22% (RCP 2.6 and 4.5 scenarios) and of 13–27% (RCP 8.5 scenarios) compared to the control period (Table 1). A similar pattern of precipitation changes in the annual distribution as in the period of 2021–2050 was projected for the period 2071–2100. Precipitation amounts are mostly expected to increase with an exception of March and August. March precipitation amounts are projected to decrease by 14% (RCP 2.6 and 4.5 scenarios) and by 6% (RCP 8.5 scenarios). A decrease by 11% is projected for August (RCP 8.5 scenarios). The highest change is projected for winter months – an increase of 26% (RCP 2.6 and 4.5 scenarios) and 36% (RCP 8.5 scenarios) from November to January. A notable increase of 19% (RCP 2.6 and 4.5 scenarios) and 32% (RCP 8.5 scenarios) is also projected from April to June (Fig. 6).

Mean monthly precipitation amounts for the periods of 2021–2050 and 2071–2100 are available in Appendix 1 and 2.

Table 1. Water balance parameters at the investigated catchment for the control period (1981–2010) and two future periods (2021–2050 and 2071–2100). Means ± SD for: P – precipitation, E – evapotranspiration, and Q – runoff; P and Q was measured for control period; all E and future Q were calculated by the Brook90 model.

RCM (driving GCM)	RCP	Period	P (mm y^{-1})	E (mm y^{-1})	Q (mm y^{-1})
Modrava		1981–2010	1575±210	411±29	1176±236
ALADIN53 (CNRM-CM5)	4.5	2021–2050	1840±220	475±26	1357±215
ALADIN53 (CNRM-CM5)	8.5	2021–2050	1910±308	479±33	1431±275
RACMO22E (EC-EARTH)	4.5	2021–2050	1636±248	433±20	1197±233
RACMO22E (EC-EARTH)	8.5	2021–2050	1688±235	438±19	1249±255
RCA4 (EC-EARTH)	2.6	2021–2050	1758±264	466±25	1290±279
RCA4 (EC-EARTH)	4.5	2021–2050	1738±237	477±47	1260±221
RCA4 (EC-EARTH)	8.5	2021–2050	1828±304	479±42	1348±282
CCLM4-8-17 (MPI-ESM-LR)	4.5	2021–2050	1808±354	484±39	1322±305
CCLM4-8-17 (MPI-ESM-LR)	8.5	2021–2050	1802±275	485±28	1315±224
ALADIN53 (CNRM-CM5)	4.5	2071–2100	1919±273	504±28	1417±286
ALADIN53 (CNRM-CM5)	8.5	2071–2100	1996±286	532±30	1466±264
RACMO22E (EC-EARTH)	4.5	2071–2100	1669±233	448±23	1223±227
RACMO22E (EC-EARTH)	8.5	2071–2100	1772±241	477±25	1297±215
RCA4 (EC-EARTH)	2.6	2071–2100	1726±303	461±33	1264±261
RCA4 (EC-EARTH)	4.5	2071–2100	1852±344	568±55	1284±326
RCA4 (EC-EARTH)	8.5	2071–2100	1833±367	532±37	1302±340
CCLM4-8-17 (MPI-ESM-LR)	4.5	2071–2100	1812±328	493±38	1321±264
CCLM4-8-17 (MPI-ESM-LR)	8.5	2071–2100	1913±352	522±33	1392±311

Future evapotranspiration projections

The increase in annual evapotranspiration based on model projections was estimated to be 6 to 19% in the period of 2021–2051. It represents a change from 407 mm (1981–2010) to 433–485 mm (Table 1). Changes in seasonal distribution showed a slight increase for most of the months with absolute maximum in summer months (Fig. 7). RCMs projected an increase of mean annual evapotranspiration from 10 to 40% to 448–569 mm in the period of 2071–2100 (Table 1). The pattern of change showed increase in all of the months with absolute maximum in summer similarly to previous period, with no signs of evapotranspiration reduction due to water availability limitations (Fig. 7).

Mean monthly evapotranspiration for the periods of 2021–2050 and 2071–2100 are available in Appendix 3 and 4.

Future runoff projections

The mean annual runoff for Modrava catchment was 1176 mm in the control period of 1981–2010. The projected precipitation increase resulted in annual runoff increase in all scenarios (Table 1). The RCP 2.6 and 4.5 scenarios estimated an increase of 2–15% and RCP

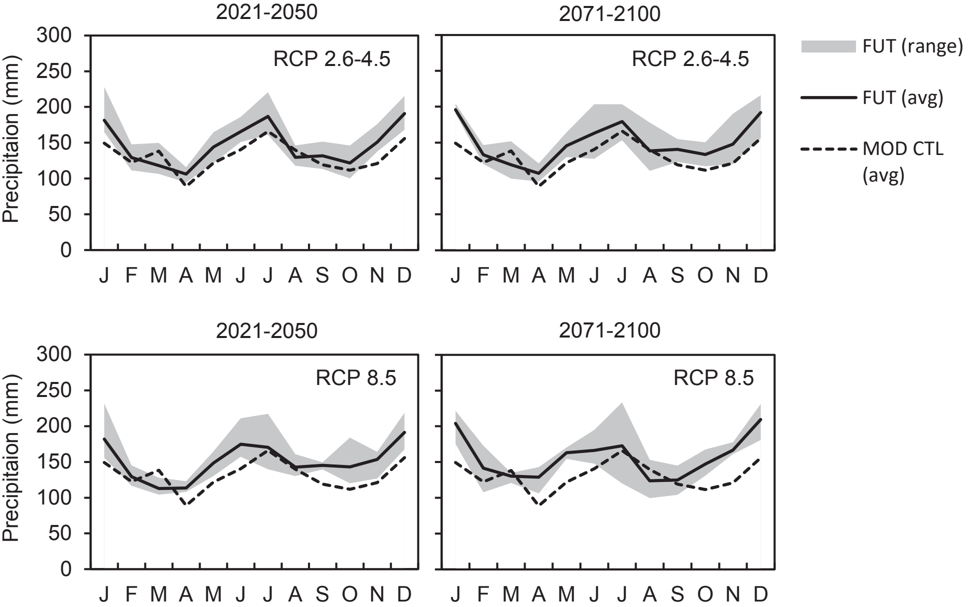

Fig. 6. Mean annual cycle of precipitation. FUT – future scenarios (2021–2050 and 2071–2100), MOD ctl – control period (1981–2010). Range based on difference between maximum and minimum RCM simulations for precipitation.

8.5 scenarios of 6–22% for the period of 2021–2050 compared to the control period (1981–2010). The future and recent monthly medians follow more or less the same pattern in case of RCP 2.6 and 4.5 scenarios however RCP 8.5 scenarios medians show a notable increase of runoff (43%) from October to December in the period of 2021–2050 (Fig. 8).

The RCP 2.6 and 4.5 scenarios projected an increase of 4–20% and RCP 8.5 scenarios of 10–25% in mean annual runoff for the period of 2071–2100 compared to the control period (1981–2010). While the flow pattern in previous period (2021–2050) was similar to control period (1981–2010), the flow pattern in the period of 2071–2100 show a significant shift in annual runoff distribution. A decrease in spring runoff (April to May) by 26% (RCP 2.6 and 4.5) and 34% (RCP 8.5) was projected. The Brook90 simulations using RCMs data showed

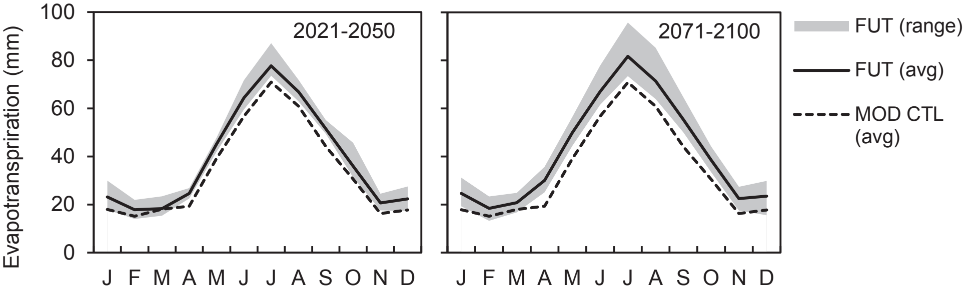

Fig. 7. Mean annual cycle of evapotranspiration. FUT – future scenarios (2021–2050 and 2071–2100), MOD CTL – control period (1981–2010). Range based on difference between maximum and minimum RCM simulations for evapotranspiration.

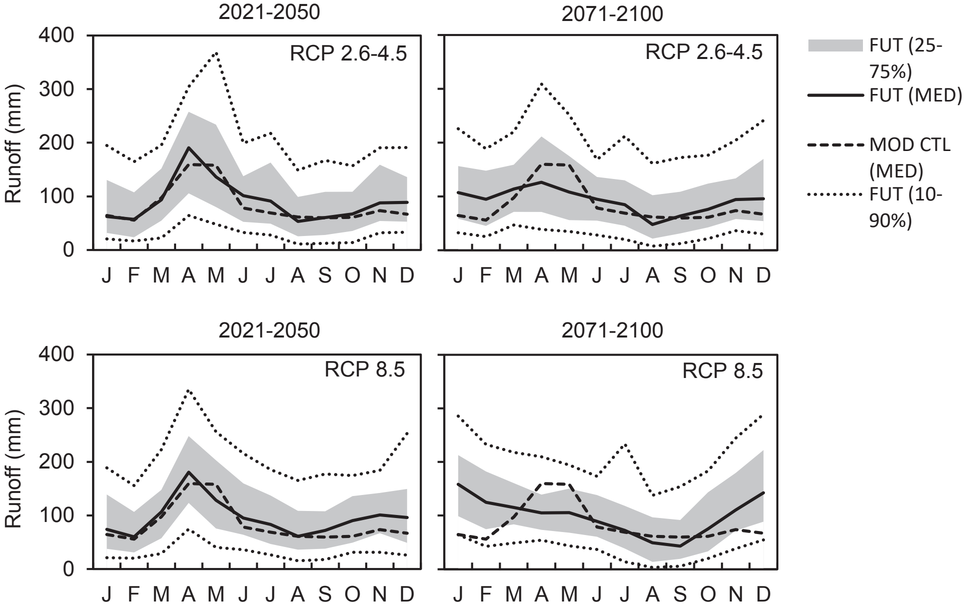

Fig. 8. Mean annual runoff cycle in the future periods (2021–2050 and 2071–2100). FUT – future, 25–75%: runoff inter-quartile range, MOD CTL (MED) – observed median from control period of 1981–2010, FUT 10–90%: future runoff inter-quintile range.

a notable decrease also in August runoff of 22% (RCP 2.6 and 4.5) and 19% (RCP 8.5) and a decrease of 28% in September (RCP 8.5). On the other hand, the winter runoff (January to February) is projected to increase a lot by 60% (RCP 2.6 and 4.5) and even 127% (RCP 8.5) (Fig. 8).

Mean monthly runoff for the periods of 2021–2050 and 2071–2100 are available in Appendix 5 and 6.

DISCUSSION

Estimation of future runoff with a hydrological model using a climate change scenarios is associated with different sources of uncertainties. We assume that in our study one of the major uncertainty is the estimated precipitation input. Precipitation represents the most important variable in hydrological modelling since it affects the runoff generation process directly. Unfortunately, the representative daily record from the catchment was not available and thus the provided data had to be adapted in order to get values that would better represent the precipitation within the catchment. Original values of "technical series" for the precipitation data interpolated from the CHMI station data for the control period of 1981–2010 were too low (mean annual runoff from the Modrava outlet exceed the precipitation amounts in some years). This may be due to the inappropriate location of surrounding rainfall stations that are not much suitable for this particular catchment area and also significant undercatch of the true rainfall reported by numerous previous studies (e.g. SEVRUK 1985, LAPIN et al. 1991), especially when compared to the totalisers. Our interpolated annual precipitation for the period of 1981–2010 (1575 mm) was slightly higher than the mean annual precipitation value from LANGHAMMER et al. (2015) who estimated mean annual value of 1378 mm for the period of 1961–2010. The difference could be also caused by the selection of different precipitation stations used for their correction. Langhammer et al. (2015) used the CHMI operated precipitation stations providing daily measurements that were not located on the mountain ridge, while we used the totalisers located in higher elevations that should provide more representative values (regarding the long-term means); however, these totalisers provided only annual data. Totaliser data after correction for evaporation were in good agreement with automated station data according to Starostová (2012). The use of totaliser data helped to reduce the bias in total amounts, however, could not be used for the seasonal distribution correction. Although we used mean monthly correction factor based on the difference in seasonal distribution between Churáňov and Filipova Huť stations (Fig. 2), this step of data processing remained highly uncertain. However, such correction was partially verified by a successful runoff simulation for the control period 1981–2010. It is also worth noting that since the Brook90 model is a lumped model, we assumed that the prevailing vegetation cover was Norway spruce and we did not change the vegetation parameters in time, although there were partial changes in vegetation cover during the control period. Bernsteinová et al. (2015) reported that the tree die-off caused by bark beetle outbreak and windfall affected 55% of the catchment by the 2011 year. This approach was chosen based on the results from studies Bernsteinová et al. (2015) and Langhammer et al. (2015) who detected only minor changes in annual runoff and the shifts in spring runoff were attributed rather to temperature increase than vegetation cover change. According to Bernsteinová et al. (2015), the vegetation cover disturbances may not have been rapid enough to generate significant trends in runoff. Regeneration of the surviving vegetation including growing forest stands and secondary structure (shrubs and herbs) can compensate the evapotranspiration losses due to partial tree die-off (Brown et al. 2014).

In respect of climatic modelling, Štěpánek et al. (2016) noted the need of RCM output correction, since the uncorrected RCM data do not capture the Czech climatic conditions well and thus are not directly useful for impact studies. RCM simulations provide outputs that can differ notably (depending e.g. on the driving GCM) and thus use of small number of scenarios for impact studies could be misleading (e.g. Hanel et al. 2012). We assume that use of nine scenarios in this study should represent a sufficiently wide range of future possible climatic conditions.

The mean annual temperature increase for Modrava is similar to the projections for the whole Czech Republic (CR) published by Štěpánek et al. (2016), who used the same RCMs and emission scenarios (plus two additional scenarios compared to our study). Štěpánek et al. (2016) reported the 1°C increase in the period of 2021–2040 and 2.0°C (RCP4.5) and 4.1°C (RCP8.5) for the end of the 21st century. Scenario projections of future precipitation in the Modrava catchment exhibit slightly higher increase compared to the area of CR, where Štěpánek et al. (2016) reported precipitation increase of 7% for the period of 2021–2040, while in our study the projected precipitation increased by 11% (RCP4.5) and 15% (RCP8.5) in the period of 2021–2050. The results by the end of the century were almost the same as for the whole area of CR – an increase of 12% compared to an increase of 13% by Štěpánek et al. (2016) for RCP4.5 and 16% compared to 6–16% for CR (RCP8.5).

A significant winter precipitation increase especially in case of RCP8.5 emission scenarios is similar to the projections for CR by Štěpánek et al. (2016). It represents a change compared to the previous ALADIN-Climate/CZ (using SRES A1B emission scenario) simulations where only a minor winter precipitation increase was projected (Štěpánek et al. 2016). Also the study of Hanel et al. (2012) that evaluated 15 different RCM experiments (using SRES A1B emission scenario) pointed out an uncertainty in winter precipitation increase and did not report any notable changes in mean annual precipitation amounts. The main change that should occur in the winter precipitation will be in the changes from snow to rain. It will be caused by the temperature increase and occurrence of warmer episodes with a temperature above freezing point. It will lead to notable spring runoff maxima decline up to shifts of runoff maxima to winter in some scenarios. Unavoidably higher winter and spring temperature imply earlier start of growing season that has been already shown across the Czech territory (e.g. Trnka et al. 2015) and in general increase of the transpiration volume in cases when plants are not limited by soil moisture content.

The studies focused on analysis of recent changes in hydrological pattern in the Bohemian Forest area mostly did not found any changes in mean annual runoff (Bernsteinová et al. 2015, Kliment & Matoušková 2009, Langhammer et al. 2015) with the exception of Beudert et al. (2018), who detected an annual runoff decline of 59 mm (for the period from 1978–2013) in the southern slope of the Bohemian Forest. Such a decrease was related to changes in evapotranspiration due to increased temperature.

The projected future mean annual runoff increase does not correspond with the results from previous regional studies that mostly assume runoff decrease as a result of climatic change across different catchment scale from small forested catchments (Benčoková et al. 2011, Lamačová et al. 2014) to mesoscale catchment (Malše River, Němečková et al. 2011). As a reason, we see the use of other RCM models than it used to be in the past. The greatest uncertainty is related to the precipitation projection. There is a big difference between individual RCM and so the difference between RCM and GCM. The projection in such a small area is definitely burdened by a higher uncertainty as it is below the resolution capability of any used RCM, and it is rather necessary to take into account the average projection of the model over a larger area. Generally, despite the bias correction, the climate models can not exactly describe spatial distribution of rainfall changes. This is also one of the reasons why we used in our analysis ensemble of the RCM, which reduces the modelling errors. However, Hanel et al. (2012) estimated a wide range of mean annual runoff changes (prevailingly decrease) across the Czech Republic. It included also estimated increase in northern part of the Czech Republic for the period of 2071–2099. However most of the future runoff changes are similar to our results such as (i) the winter runoff increase caused by shift of runoff maxima from spring snowmelt to winter and (ii) the winter precipitation increase.

CONCLUSIONS

We described the impact of nine plausible scenarios of climate change, representing a wide range of possible changes in future anthropogenic greenhouse gas emissions, on forested catchment in the Bohemian Forest in two future periods of 2021–2050 and 2071–2100. The estimated temperature and precipitation increase (especially in winter months) will significantly affect evapotranspiration and runoff. Evapotranspiration is expected to increase as a result of higher temperature and prolongation of the growing season. Mean annual runoff is projected to rise notably as a result of the precipitation increase (despite the increased evapotranspiration rate).

Changes are also modelled for the runoff annual cycle. While in the period of 2021–2050 the annual cycle will not change notably, significant shifts are projected for the period of 2071–2100. A large winter runoff increase and a spring runoff maxima decrease indicate changes in snow cover and snowmelt. Some scenarios even show no spring runoff maxima. Changes are also visible in summer, while the median runoff will not change that much the values of 10 and 25 percentiles (representing of the lowest flows) are notably lower compared to the recent period of 1981–2010.

Acknowledgements. This work was supported by the Interreg Cíl EUS (contract SOSSOD - 164/2017), by the Ministry of Education, Youth and Sports of the Czech Republic – projects LM2015075 and EF16_013/0001782 for the Czech Geological Survey, and National Sustainability Program I (NPU I, project LO1415) for the Global Change Research Institute CAS. MT, PŠ a PZ were supported by the Ministry of Agriculture of the Czech Republic (project QJ1610072: System for monitoring and forecast of impacts of agricultural drought). This research and publication were supported by the Cross-border cooperation programme Czech Republic–Bavaria Free State ETC goal 2014–2020, the Interreg V project No. 26 "Silva Gabreta Monitoring – Implementation of Transboundary Monitoring of Biodiversity and Water Regime".

REFERENCES

Adams H.D., Guardiola-Claramonte M., Barron-Gafford G.A., Villegas J.C., Breshears D.D., Zou C.B., Troch P.A. & Huxman T.E., 2009: Temperature sensitivity of drought-induced tree mortality portends increased regional die-off under global-change-type drought. *Proceedings of the National Academy of Sciences of the United States of America*, 106: 7063–7066.

Allen C.D., Macalady A.K., Chenchouni H., Bachelet D., McDowell N., Vennetier M., Kitzberger T., Rigling A., Breshears D.D., Hogg E.H. (Ted), Gonzalez P., Fensham R., Zhang Z., Castroj J., Demidova N., Lim J.H., Allard G., Running S.W., Semerci A. & Cobb N., 2010: A global overview of drought and heat-induced tree mortality reveals emerging climate change risks for forests. *Forest Ecology and Management*, 259: 660–684.

Benčoková A., Krám P. & Hruška J., 2011: Future climate and changes in flow patterns in Czech headwater catchments. *Climate Research*, 49: 1–15.

Bernsteinová J., Baessler C., Zimmermann L., Langhammer J. & Beudert B., 2015: Changes in runoff in two neighbouring catchments in the Bohemian Forest related to climate and land cover changes. *Journal of Hydrology and Hydromechanics*, 63: 342–352.

Beudert B., Bernsteinová J., Premier J. & Bässler C., 2018: Natural disturbance by bark beetle offsets climate change effects on streamflow in Bohemian Forest headwater catchments. *Silva Gabreta*, 24: xx–xx.

Brown M.G., Black T.A., Nesic Z., Foord V.N., Spittlehouse D.L., Fredeen A.L., Bowler R., Grant N.J., Burton P.J., Trofymow J.A., Lessard D. & Meyer G., 2014: Evapotranspiration and canopy characteristics of two lodgepole pine stands following mountain pine beetle attack. *Hydrological Processes*, 28: 3326–3340.

Clarke L.,Edmonds J.,Jacoby H., Pitcher H., Reilly J. & Richels R., 2007: *Scenarios of greenhouse gas emissions and atmospheric concentrations. Sub-report 2.1A of Synthesis and Assessment Product 2.1 by the US Climate Change Science Program and the Subcommittee on Global Change Research*. Office of Biological and Environmental Research, US Department of Energy, Washington, DC, 154 pp.

Déqué M., 2007: Frequency of precipitation and temperature extremes over France in an anthropogenic scenario: Model results and statistical correction according to observed values. *Global and Planetary Change*, 57: 16–26.

Federer C.A., Vorosmarty C. & Fekete B., 2003: Sensitivity of annual evaporation to soil and root properties in two models of contrasting complexity. *Journal of Hydrometeorology*, 4: 1276–1290.

Forzieri G., Feyen L., Rojas R., Floerke M., Wimmer F. & Bianchi A., 2014: Ensemble projections of future streamflow droughts in Europe. *Hydrology and Earth System Sciences*, 18: 85–108.

Gutiérrez J.M., Maraun D., Widmann M., Huth R., Hertig E., Benestad R., Roessler O., Wibig J., Wilcke R., Kotlarski S., San Martín D., Herrera S., Bedia J., Casanueva A., Manzanas R., Iturbide M., Vrac M., Dubrovsky M., Ribalaygua J., Pórtoles J., Räty O., Räisänen J., Hingray B., Raynaud D., Casado M.J., Ramos P., Zerenner T., Turco M., Bosshard T., Štěpánek P., Bartholy J., Pongracz R., Keller D.E., Fischer A.M., Cardoso R.M., Soares P.M.M., Czernecki B. & Pagé C., 2018: An intercomparison of a large ensemble of statistical downscaling methods over Europe: Results from the VALUE perfect predictor cross-validation experiment. *International Journal of Climatology*: 1–36. doi.org/10.1002/joc.5462

Hanel M., Vizina A., Máca P. & Pavlásek J., 2012: A multi-model assessment of climate change impact on hydrological regime in the Czech Republic. *Journal of Hydrology and Hydromechanics*, 60: 152–161.

IPCC, 2007: Climate Change 2007. The physical science basis. In: Solomons S., Qin D., Manning M., Chen Z, Marquis M., Averyt K.B., Tignor M. & Miller H.L. (eds): *Contribution of Working Group I to the Fourth Assessment Report of the Intergovernmental Panel on Climate Change*. Cambridge University Press, Cambridge, UK and New York, USA, 996 pp.

IPCC 2013: Climate Change 2013. The physical science basis. In: Stocker T.F., Qin D., Plattner G.K., Tignor M., Allen S.K., Boschung J. Nauels A., Xia Y., Bex V. & Midgley P.M. (eds): *Contribution of Working Group I to the Fifth Assessment Report of the Intergovernmental Panel on Climate Change*. Cambridge University Press, Campridge, UK and New York, USA, 1535 pp.

Kliment Z. & Matoušková M., 2009: Runoff changes in the Šumava Mountains (Black Forest) and the foothill regions: extent of influence by human impact and climate change. *Water Resources Management*, 23: 1813–1834.

Lamačová A., Hruška J., Krám P., Stuchlík E., Farda A., CHuman T. & Fottová D., 2014: Runoff trends analysis and future projections of hydrological patterns in small forested catchments. *Soil and Water Research*, 9: 169–181.

Langhammer J., Su Y. & Bernsteinová J., 2015: Runoff response to climate warming and forest disturbance in a mid-mountain basin. *Water*, 7: 3320–3342.

Lapin M., Faško P. & Košťálová J., 1991: Zhodnotenie zrážkových pomerov na území Slovenska po korekcii systematických chýb meraní zrážok [Evaluation of atmospheric precipitation on the area of Slovakia after correction of systematic errors in precipitation measurements]. *Vodohospodársky Časopis*, 39: 207–220 (in Slovak).

Linsley R.K., 1949: *Applied Hydrology*. McGraw-Hill, New York, 689 pp.

Moss R.H., Edmonds J.A., Hibbards K.A., Manning M.R., Rose S.K., van Vuuren D.P., Carter T.R., Emori S., Kainuma M., Kram T., Meehl G.A., Mitchell J.F.B., Nakicenovic N., Riahi K., Smith S.J., Stouffer R.J., Thomson A.M., Weyant J.P. & Wilbanks T.J., 2010: The next generation of scenarios for climate change research and assessment. *Nature*, 463: 747–756.

Nahs J.E. & Sutcliffe J.V., 1970: River flow forecasting through conceptual models. 1. A discussion of principles. *Journal of Hydrology*, 10: 282–290.

Němečková S., Slámová R. & Šípek V., 2011: Climate change impact assessment on various components of the hydrological regime of the Malše River basin. *Journal of Hydrology and Hydromechanics*, 59: 131–143.

Raffa K.F., Aukema B.H., Bentz B.J., Carroll A.L., Hicke J.A., Turner M.G. & Romme W.H., 2008: Cross-scale drivers of natural disturbances prone to anthropogenic amplification: The dynamics of bark beetle eruptions. *Bioscience*, 58: 501–517.

Riahi K., Gruebler A. & Nakicenovic N., 2007: Scenarios of long-term socio-economic and environmental development under climate stabilization. *Technological Forecasting and Social Change*, 74: 887–935.

Sevruk B., 1985: Systematischer Niederschlagsmessfehler in der Schweiz. In: *Der Niederschlag in der Schweiz*, Sevruk B. (ed.) Beitrage zur Geologie der Schweiz – Hydrologie Nr. 31, Bern: 65–75.

Shuttleworth W. & Wallace J., 1985: Evaporation from sparse crops – an energy combination theory. *Quarterly Journal of the Royal Meteorological Society*, 111: 839–855.

Starostová, M., 2012: Measuring precipitation using totalisers in Šumava. *Meteorological Bulletin*, 65: 180–183.

Štěpánek P., Zahradníček P. & Farda A., 2013: Experiences with data quality control and homogenization of daily records of various meteorological elements in the Czech Republic in the period 1961–2010. *Idojaras*, 117: 123–141.

Štěpánek P., Zahradníček P., Farda A., Skalák P., Trnka M., Meitner J. & Rajdl K., 2016: Projection of drought-inducing climate conditions in the Czech Republic according to Euro-CORDEX models. *Climate Research*, 70: 179–193.

Štěpánek P., Zahradníček P. & Huth R., 2011: Interpolation techniques used for data quality control and calculation of technical series: an example of a Central European daily time series. *Idojaras*, 115: 87–98.

Trnka M., Brázdil R., Balek J., Semerádová D., Hlavinka P., Možný M., Štěpánek P., Dobrovolný P., Zahradníček P., Dubrovský M., Eitzinger J., Fuchs B., Svoboda M., Hayes M. & Žalud Z., 2015: Drivers of soil drying in the Czech Republic between 1961 and 2012. *International Journal of Climatology*, 35: 2664–2675.

van Vliet M.T.H., Donnelly C., Stromback L., Capell R. & Ludwig F., 2015: European scale climate information services for water use sectors. *Journal of Hydrology*, 528: 503–513.

van Vuuren D.P., den Elzen M.G.J., Lucas P.L., Eickhout B., Strengers B.J., van Ruijven B., Wonink S. & van Houdt R., 2007: Stabilizing greenhouse gas concentrations at low levels: an assessment of reduction strategies and costs. *Climatic Change*, 81: 119–159.

Received: 11 July 2018
Accepted: 28 August 2018

Appendix 1. Annual and monthly precipitation (P, in mm) estimated for investigated catchment (MOD) in the control period of 1981–2010 and future simulated precipitation in the period of 2021–2050 based on different regional climate model data and climate change scenarios.

Model RCM (GCM)	MOD-corrected	ALADIN53 (CNRM-CM5)	ALADIN53 (CNRM-CM5)	RACMO22E (EC-EARTH)	RACMO22E (EC-EARTH)	RCA4 (EC--EARTH)	RCA4 (EC--EARTH)	RCA4 (EC--EARTH)	CCLM4-8-17 (MPI-ESM-LR)	CCLM4-8-17 (MPI-ESM-LR)
P		RCP 4.5	RCP 8.5	RCP 4.5	RCP 8.5	RCP 2.6	RCP 4.5	RCP 8.5	RCP 4.5	RCP 8.5
Period	1981–2010	2021–2050	2021–2050	2021–2050	2021–2050	2021–2050	2021–2050	2021–2050	2021–2050	2021–2050
Jan	149.2	171.7	177.7	165.0	155.8	228.1	172.1	231.7	170.1	162.1
Feb	122.4	136.2	130.4	111.4	145.2	120.6	130.4	116.6	147.8	125.7
Mar	138.4	118.5	108.7	107.3	110.6	107.8	106.4	104.2	149.8	128.0
Apr	89.0	115.8	109.5	96.8	108.1	112.6	94.5	113.8	110.4	123.0
May	121.8	137.6	145.2	121.4	153.2	164.6	156.4	164.5	139.6	130.2
Jun	140.6	186.2	210.9	155.0	157.2	166.4	169.7	165.2	150.9	165.2
Jul	166.0	220.6	217.1	161.1	139.7	173.1	210.8	155.5	168.8	169.4
Aug	139.7	146.2	149.6	143.6	160.8	117.9	121.1	130.2	119.4	130.2
Sep	119.1	133.9	149.4	151.6	143.2	138.1	121.2	139.5	113.3	149.3
Oct	111.6	131.6	144.2	100.2	120.1	117.6	113.6	124.3	146.2	183.9
Nov	121.0	141.4	160.6	137.5	126.7	142.9	156.9	164.0	175.9	162.9
Dec	155.9	200.3	207.1	185.2	167.5	168.0	185.1	218.5	215.3	172.5
Annual	**1575**	**1840**	**1910**	**1636**	**1688**	**1758**	**1738**	**1828**	**1808**	**1802**

Appendix 2. Annual and monthly precipitation (P, in mm) estimated for investigated catchment (MOD) in the control period of 1981–2010 and future simulated precipitation in the period of 2071–2100 based on different regional climate model data and climate change scenarios.

Model RCM (GCM)	MOD-corrected	ALADIN53 (CNRM-CM5)	ALADIN53 (CNRM-CM5)	RACMO22E (EC-EARTH)	RACMO22E (EC-EARTH)	RCA4 (EC--EARTH)	RCA4 (EC--EARTH)	RCA4 (EC--EARTH)	CCLM4-8-17 (MPI-ESM-LR)	CCLM4-8-17 (MPI-ESM-LR)
P		RCP 4.5	RCP 8.5	RCP 4.5	RCP 8.5	RCP 2.6	RCP 4.5	RCP 8.5	RCP 4.5	RCP 8.5
Period	1981–2010	2071–2100	2071–2100	2071–2100	2071–2100	2071–2100	2071–2100	2071–2100	2071–2100	2071–2100
Jan	149.2	195.4	175.2	190.5	198.5	190.0	199.2	221.6	204.2	220.9
Feb	122.4	120.1	159.7	126.5	107.7	141.1	146.6	124.8	131.0	173.0
Mar	138.4	114.4	120.8	106.5	134.9	99.8	122.3	131.1	151.9	134.3
Apr	89.0	121.0	142.9	103.2	106.1	98.2	95.7	128.6	118.2	137.1
May	121.8	148.0	170.4	129.8	169.0	144.0	164.2	154.4	142.9	159.0
Jun	140.6	203.4	194.9	151.2	160.9	154.5	178.9	160.9	127.4	147.7
Jul	166.0	200.8	233.4	177.1	165.5	162.8	203.5	172.0	153.3	120.1
Aug	139.7	177.9	153.1	138.3	130.9	142.4	123.7	112.0	110.6	99.5
Sep	119.1	154.9	127.8	144.5	122.3	140.2	122.9	104.2	139.9	145.0
Oct	111.6	150.4	148.2	125.4	130.9	116.9	145.7	142.2	127.8	167.6
Nov	121.0	143.1	161.1	120.0	164.2	153.0	132.8	163.4	190.4	177.7
Dec	155.9	189.5	208.8	156.1	180.8	183.4	216.2	217.8	214.5	231.3
Annual	**1575**	**1919**	**1996**	**1669**	**1772**	**1726**	**1852**	**1833**	**1812**	**1913**

Appendix 3. Annual and monthly evapotranspiration (E, in mm) calculated by the Brook90 model for the Modrava catchment (MOD) in the control period of 1981–2010 and future simulated evapotranspiration in the period of 2021–2050 calculated by the Brook90 model using different regional climate model data and climate change scenarios.

Model RCM (GCM)	MOD-corrected	ALADIN53 (CNRM-CM5)	ALADIN53 (CNRM-CM5)	RACMO22E (EC-EARTH)	RACMO22E (EC-EARTH)	RCA4 (EC--EARTH)	RCA4 (EC--EARTH)	RCA4 (EC--EARTH)	CCLM4-8-17 (MPI-ESM-LR)	CCLM4-8-17 (MPI-ESM-LR)
E		RCP 4.5	RCP 8.5	RCP 4.5	RCP 8.5	RCP 2.6	RCP 4.5	RCP 8.5	RCP 4.5	RCP 8.5
Period	1981–2010	2021–2050	2021–2050	2021–2050	2021–2050	2021–2050	2021–2050	2021–2050	2021–2050	2021–2050
Jan	17.9	20.6	20.5	19.0	17.8	28.8	25.5	29.9	23.0	22.7
Feb	15.1	15.7	15.9	14.0	16.5	18.0	21.9	18.5	21.4	18.9
Mar	18.0	15.3	15.9	17.3	17.0	17.8	19.3	18.4	23.4	20.4
Apr	19.4	24.7	22.6	24.7	25.5	25.6	22.5	26.8	23.0	26.3
May	39.1	44.1	46.9	43.8	43.9	46.8	44.5	47.8	41.9	45.3
Jun	56.7	71.7	70.2	59.5	60.5	60.3	63.3	62.9	66.6	64.6
Jul	70.9	86.9	87.1	74.1	74.2	75.6	78.4	73.6	75.1	74.3
Aug	60.9	71.9	71.3	62.9	65.0	67.1	65.9	65.3	65.4	66.2
Sep	44.1	49.8	50.8	49.4	49.6	51.0	52.8	50.9	53.7	55.1
Oct	30.6	34.5	35.3	31.3	33.2	33.4	36.6	36.5	37.9	45.7
Nov	16.2	18.6	20.3	17.6	18.0	20.3	21.4	22.8	24.5	22.9
Dec	17.8	21.6	22.1	19.0	17.3	21.5	24.5	25.1	27.5	22.4
Annual	**407**	**476**	**479**	**433**	**438**	**466**	**477**	**479**	**484**	**485**

Appendix 4. Annual and monthly evapotranspiration (E, in mm) calculated by the Brook90 model for the Modrava catchment (MOD) in the control period of 1981–2010 and future simulated evapotranspiration in the period of 2071–2100 calculated by the Brook90 model using different regional climate model data and climate change scenarios.

Model RCM (GCM)	MOD-corrected	ALADIN53 (CNRM-CM5)	ALADIN53 (CNRM-CM5)	RACMO22E (EC-EARTH)	RACMO22E (EC-EARTH)	RCA4 (EC--EARTH)	RCA4 (EC--EARTH)	RCA4 (EC--EARTH)	CCLM4-8-17 (MPI-ESM-LR)	CCLM4-8-17 (MPI-ESM-LR)
E		RCP 4.5	RCP 8.5	RCP 4.5	RCP 8.5	RCP 2.6	RCP 4.5	RCP 8.5	RCP 4.5	RCP 8.5
Period	1981–2010	2071–2100	2071–2100	2071–2100	2071–2100	2071–2100	2071–2100	2071–2100	2071–2100	2071–2100
Jan	17.9	22.5	20.8	20.0	19.3	25.5	28.8	31.2	27.0	26.8
Feb	15.1	15.3	16.6	15.0	13.3	20.1	21.9	20.3	19.8	23.4
Mar	18.0	16.8	18.1	18.0	21.5	17.3	22.6	24.3	24.9	23.9
Apr	19.4	26.7	33.4	27.6	32.4	25.9	31.3	35.7	25.1	32.9
May	39.1	50.1	55.0	46.7	49.4	44.4	56.5	53.1	45.1	49.5
Jun	56.7	75.7	77.8	62.5	63.6	61.5	72.4	62.9	63.2	63.7
Jul	70.9	89.6	95.7	75.5	78.1	74.6	90.2	83.9	73.4	74.4
Aug	60.9	74.4	75.8	65.1	69.4	63.9	85.2	75.7	65.8	67.6
Sep	44.1	55.2	55.4	50.7	52.1	50.0	64.6	53.7	56.3	59.8
Oct	30.6	37.5	39.6	33.5	37.1	33.7	44.2	39.5	38.2	43.3
Nov	16.2	19.4	21.8	17.5	21.2	21.3	21.7	25.3	26.9	27.4
Dec	17.8	21.1	21.8	15.6	19.1	22.6	28.5	26.6	26.9	29.9
Annual	**407**	**504**	**532**	**448**	**477**	**461**	**568**	**532**	**493**	**522**

Appendix 5. Annual and monthly runoff (Q, in mm) measured at the Modrava outlet (MOD) in the control period of 1981–2010 and future simulated runoff from the investigated catchment in the period of 2021–2050 calculated by the Brook90 model using different regional climate model data and climate change scenarios.

Model RCM (GCM)	MOD-corrected	ALADIN53 (CNRM-CM5)	ALADIN53 (CNRM-CM5)	RACMO22E (EC-EARTH)	RACMO22E (EC-EARTH)	RCA4 (EC--EARTH)	RCA4 (EC--EARTH)	RCA4 (EC--EARTH)	CCLM4-8-17 (MPI-ESM-LR)	CCLM4-8-17 (MPI-ESM-LR)
Q		RCP 4.5	RCP 8.5	RCP 4.5	RCP 8.5	RCP 2.6	RCP 4.5	RCP 8.5	RCP 4.5	RCP 8.5
Period	1981–2010	2021–2050	2021–2050	2021–2050	2021–2050	2021–2050	2021–2050	2021–2050	2021–2050	2021–2050
Jan	55.8	89.3	94.5	76.5	75.4	121.3	74.4	152.9	74.9	83.8
Feb	61.8	74.1	85.9	72.3	65.4	90.6	70.7	82.3	67.4	64.8
Mar	115.0	129.8	134.7	97.1	105.8	92.9	92.0	89.7	108.9	135.4
Apr	188.6	167.4	208.5	204.8	200.7	171.9	185.3	163.8	222.9	197.3
May	184.3	183.3	135.9	124.3	164.9	177.7	168.7	145.4	218.5	139.1
Jun	89.7	114.3	142.7	100.4	108.7	116.9	112.7	109.6	88.3	102.6
Jul	80.2	140.6	138.2	84.7	68.6	104.9	136.5	88.8	96.6	95.1
Aug	71.5	79.4	87.9	87.1	90.1	52.5	62.1	71.2	60.7	68.3
Sep	72.0	87.4	87.4	97.9	93.7	86.3	66.7	75.5	56.8	88.3
Oct	72.4	83.8	102.0	70.4	84.9	76.3	66.4	85.9	90.8	126.2
Nov	78.6	90.5	112.0	86.3	89.3	104.1	119.0	124.3	130.6	118.3
Dec	81.8	117.2	101.0	95.5	101.3	95.0	105.8	158.6	105.9	95.9
Annual	**1152**	**1357**	**1431**	**1197**	**1249**	**1290**	**1260**	**1348**	**1322**	**1315**

Appendix 6. Annual and monthly runoff (Q, in mm) measured at the Modrava outlet (MOD) in the control period of 1981–2010 and future simulated runoff from the investigated catchment in the period of 2071–2100 calculated by the Brook90 model using different regional climate model data and climate change scenarios.

Model RCM (GCM)	MOD-corrected	ALADIN53 (CNRM-CM5)	ALADIN53 (CNRM-CM5)	RACMO22E (EC-EARTH)	RACMO22E (EC-EARTH)	RCA4 (EC--EARTH)	RCA4 (EC--EARTH)	RCA4 (EC--EARTH)	CCLM4-8-17 (MPI-ESM-LR)	CCLM4-8-17 (MPI-ESM-LR)
Q		RCP 4.5	RCP 8.5	RCP 4.5	RCP 8.5	RCP 2.6	RCP 4.5	RCP 8.5	RCP 4.5	RCP 8.5
Period	1981–2010	2071–2100	2071–2100	2071–2100	2071–2100	2071–2100	2071–2100	2071–2100	2071–2100	2071–2100
Jan	55.8	109.6	147.9	119.7	149.5	96.9	137.8	184.6	116.1	181.1
Feb	61.8	90.5	151.9	109.1	109.0	105.6	113.4	112.3	95.0	153.4
Mar	115.0	125.4	128.3	114.2	128.3	129.0	132.7	120.7	118.9	131.0
Apr	188.6	172.0	121.2	136.9	115.6	141.9	101.0	99.0	219.6	134.4
May	184.3	131.9	113.4	98.2	117.1	139.1	109.9	106.5	174.0	115.6
Jun	89.7	131.2	122.6	86.8	107.7	99.2	111.3	99.2	75.0	86.8
Jul	80.2	118.4	139.9	102.4	83.2	97.2	126.2	93.5	81.5	59.8
Aug	71.5	101.0	84.4	79.6	74.3	86.1	44.3	47.4	48.1	44.0
Sep	72.0	103.0	75.6	86.4	63.5	80.8	48.0	49.6	72.0	67.5
Oct	72.4	106.1	97.0	91.4	84.7	77.4	86.2	80.7	83.9	107.8
Nov	78.6	107.6	119.8	91.6	122.5	102.3	109.0	128.0	125.1	147.2
Dec	81.8	120.1	164.3	106.6	141.1	108.7	164.0	180.9	112.1	163.5
Annual	**1152**	**1417**	**1466**	**1223**	**1297**	**1264**	**1284**	**1302**	**1321**	**1392**

Silva Gabreta	vol. 24	p. 69–84	Vimperk, 2018

Simulation of meteorological conditions in the Bohemian Forest

Beate Klöcking

Bureau of Applied Hydrology, Murnauer Str. 102a, D-81379 München, Germany
kloecking@bah-muenchen.de

Abstract
Knowledge of the meteorological conditions is essential for many applications, among those also for many research fields. Here, a reliable meteorological database for the extended area of the Bohemian Forest was developed. Meteorological data from 211 observation points were collected over a time span of 35 years. These data served as the basis for the simulation of climate conditions in the 4500 km^2 sized area with a spatial resolution of 100×100 m^2, as well as for the individual research plots of the "Silva Gabreta Monitoring" project. The simulation was performed using the geostatistical interpolation techniques included in the catchment model ArcEGMO.

Keywords: meteorological data, climate regionalisation, Bavarian Forest, Šumava

Introduction

Knowledge of the meteorological conditions at individual plots or spatially distributed over the whole area is essential for many research projects in the Bohemian Forest. Meteorological parameters have been monitored at individual sites, and by different institutions. Therefore, the quantity and quality of the different data series differ from site to site. Thus, the problem for any more sophisticated study such as the "Silva Gabreta Monitoring" projects was to get a reliable and consistent spatial distribution of the meteorological conditions over the whole study area from these station-based data. The specific topographic conditions of this low mountain lead to a huge heterogeneity, especially in air temperature and wind velocity even at the smallest scale. A further problem is the location of the Bohemian Forest at the border of three European countries, namely Austria, Germany and the Czech Republic, which implies that the concentration of meteorological observation sites is very sparse. Commercial products in the necessary spatial and temporal resolution are not available for all weather elements and the whole area until now. The German Weather Service (DWD), for example, offers regionalised daily precipitation data at a spatial resolution of 1×1 km^2 for the area of the German states only (DWD 2017). The HYRAS-dataset (Rauthe et al. 2013, Frick et al. 2014) covers Germany and the bordering river catchments, but only lasts from 1951 to 2006 and includes only gridded (5×5 km^2) datasets of air temperature and relative humidity as daily mean values besides the precipitation data.

The aim of the "Silva Gabreta Monitoring" projects is the allocation of biodiversity patterns in the Bohemian Forest. The climate database presented here will be used in combination with the collected species data (Frieß et al. 2018) to evaluate and predict ecological shifts induced by climate changes and potential consequences for the whole ecosystem.

The existing observational series of air temperature at 2 m above ground level, precipitation, global radiation, relative air humidity, and wind velocity from the different meteorological stations were collected and revised for the period 1980–2015. These station-based time series were then used as the underlying database for the calculation of the main meteorological parameters at the needed spatial and temporal resolution, namely daily values for each monitoring plot and yearly values at a spatial resolution of 100×100 m^2 for the whole study area.

MATERIALS AND METHODS

Study area

The study area covers about 4500 km^2 from the Danube River in the south to Sušice in the north with most of the Bohemian Forest (Šumava in Czech) (Fig. 1). It includes the Bavarian Forest National Park (240 km^2) in Germany and the western part of the Šumava National Park (690 km^2) in the Czech Republic. Altitudes range from 300 to 1450 m a.s.l. The mountain ridge, which extends from the Großer Osser Mt. in the north to the Dreisessel Mt. in the south, passing the Großer Arber, Großer Rachel and Lusen mounts, is nearly identical with

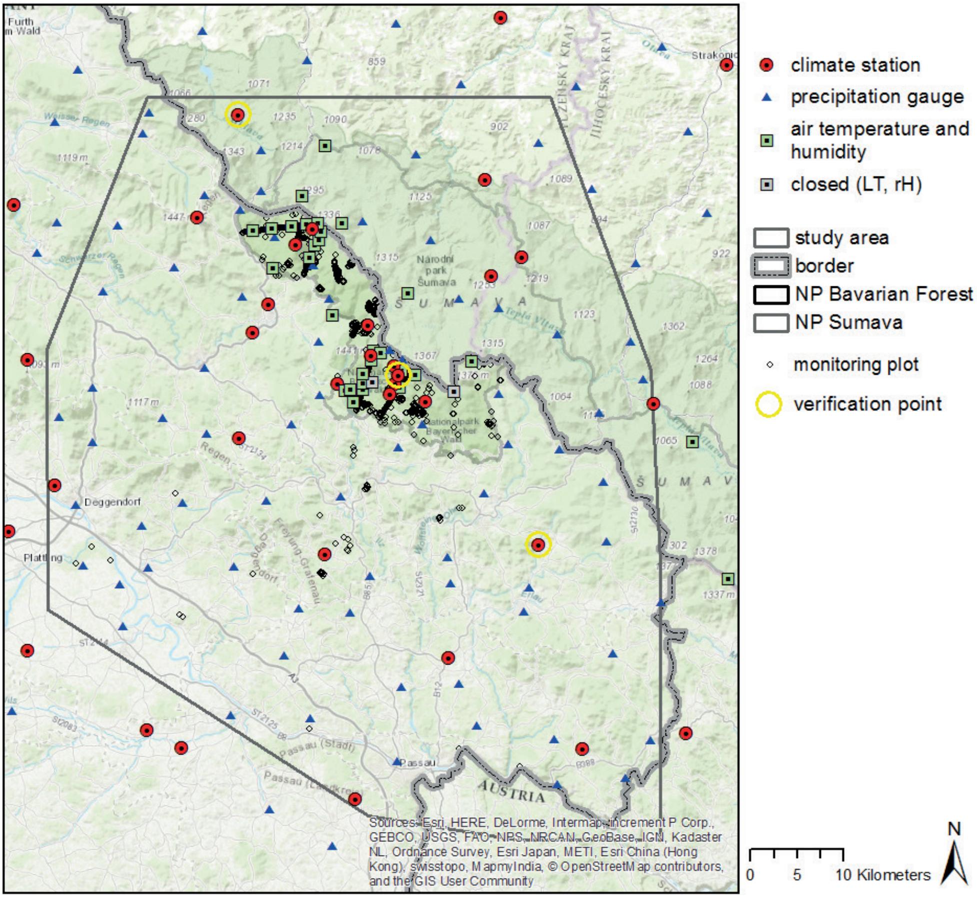

Sources: Esri, HERE, DeLorme, Intermap, increment P Corp., GEBCO, USGS, FAO, NPS, NRCAN, GeoBase, IGN, Kadaster NL, Ordnance Survey, Esri Japan, METI, Esri China (Hong Kong), swisstopo, MapmyIndia, © OpenStreetMap contributors, and the GIS User Community

Fig. 1. Study area with meteorological stations and monitoring plots.

Table 1. Used meteorological observation sites with operator and type of data (ICS – incomplete climate station, e.g. only air temperature and humidity).

Company / Institution	Country	Number of observation sites		
		Climate	Precipitation	ICS
German Meteorological Service (DWD)	Germany	12	69	
Gewässerkundlicher Dienst Bayern (GKD, LfU)	Germany		7	
Landesamt für Umwelt, Referat Grundwasser monitoring (LfU)	Germany		1	
Agrarmeteorologischer Dienst Bayern (AMD)	Germany	8		
Institut für Meteorologie und Klimaforschung – Institut für atmosphärische Umweltforschung (IMK-IFU)	Germany	1		
Administration of the Bavarian Forest NP (NPV)	Germany	5		27
Landesanstalt für Wald und Forstwirtschaft (LWF)	Germany	2	3 (+36)	
WWA Deggendorf	Germany			1
Zentralanstalt für Meteorologie und Geodynamik Österreich	Austria	1		
Czech Hydrometeorological Institute (CHMI)	Czech Republic	9	23	
Administration of the Šumava NP	Czech Republic			6
Total	**211**	**37**	**139**	**35**

the border between Germany and the Czech Republic. It forms the central European divide of the Danube and Elbe rivers and represents a climatic border.

Characteristic for this area is its boundary position within the planetary circulation belt of the prevailing westerlies and continental influences from the east. The north-south orientation of the low mountain ranges additionally strengthens this climatic border. Relief-related microclimatic features are important – these include, among others, windward/leeward effects, which affect the distribution of precipitation, and cold-air accumulation in the valleys (Noack 1979, Elling 1987). The average annual precipitation total is between 800 mm in the lowlands and 1800 mm in the higher regions. The mean annual air temperature ranges between 3.0°C at high elevations and 9.9°C at low elevations (1980–2015).

Meteorological observational data

The first step was the collection of the available meteorological data series inside and in the vicinity of the study area. Table 1gives an overview of the number of used measuring stations and their origin (see Fig. 1).

The data were retrieved from the different providers, checked, and brought into the required format for the modelling. Depending on the origin of the data, it was also necessary to aggregate temporally higher-resolution data or disaggregate temporally lower-resolution (for example totalizers) data into the required time increment of one day. These changes mainly concerned the data of the administration of the Bavarian Forest National Park (NPV), the LWF and the IMK-IFU.

Besides its five meteorological stations (Waldhäuser, Schachtenau, Waldschmidthaus, Rachel- and Schachtendiensthütte), the NPV operates some sites where air temperature and humidity are measured for different research projects (listed in the last column of Table 1). Among them are 17 BIOKLIM stations (Bässler et al. 2015) with continuous measurements since 2006, and four (until 2007 five) sites on former windthrow areas with only summer measurements since 1987/1988. The monthly precipitation sums at seven BIOKLIM stations (also only in summer) and four windthrow-stations were disaggregated by adjacent reference stations to daily values. Prerequisite for this was the existence of a quasi-continuous precipitation reference time series in daily resolution from a nearby station.

The wind speed is measured at a limited number of sites only (cf. Figs. 2, 7). These data, measured at different heights above ground level, were transformed to equivalent 2 m-values as input for the calculation of the grass reference evapotranspiration (DVWK 1996, ATV-DVWK 2002) as follows:

$$v_2 = v_z \cdot \left(\frac{2}{z}\right)^a \qquad (1)$$

where v_2 is wind speed at 2 m above ground level, v_z is wind speed at z m above ground level, and a is parameter in dependence of the surface roughness (0.13–0.7).

When evaluating the simulation results, it should be noted that, only at a few sites, there are continuous series of measurements of all required weather characteristics for the simulation period of 1 January 1980 to 31 December 2015 (see Fig. 2 for an overview of the available time series over the whole period). All measuring stations with time series of more than 180 daily values per year are counted as operational for the specific meteorological element in the year.

According to the fraction of the operational stations, the treated period can be sub-divided into three parts: 1980–1990 with a very poor meteorological database, 1991–2005 with improved coverage, and since 2006 with further continuous improvement of the database (air temperature and humidity, wind speed, and global radiation) especially by the setup of new (though mostly incomplete) climate stations in both national parks. The situation with regard to the precipitation measurements differs from this general trend, due to dismantling of many gauges by the DWD, which could only partly be compensated by the setup of new measurement sites by other providers. The particularly high fraction of precipitation gauges in the first period was caused by a measurement campaign of the summer precipitation in the research catchment Große Ohe (Thums 1993).

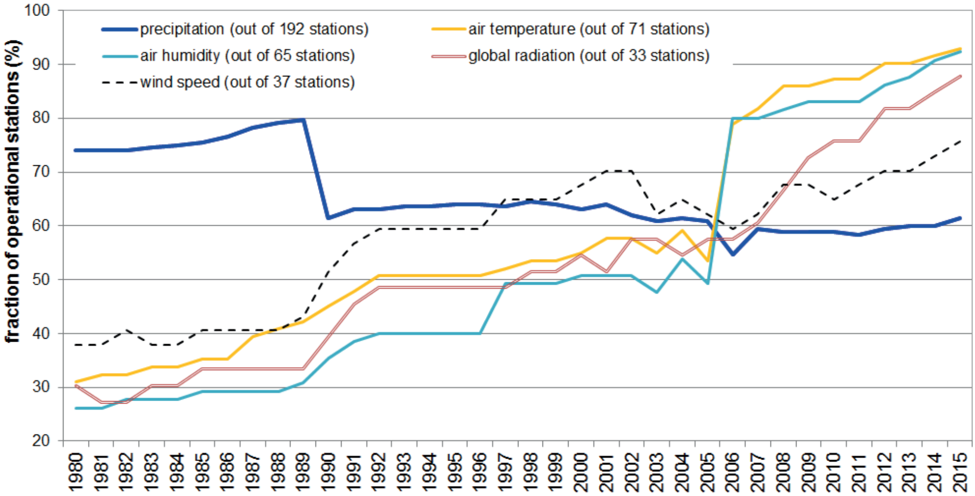

Fig. 2. Fraction of operational stations measuring precipitation (normalized to a total number of 192 stations), air temperature (normalized to 71 stations), air humidity (65 stations), global radiation (33 stations) and wind speed (37 stations).

Besides the temporal availability, the spatial distribution of the measuring stations is a crucial aspect for the regionalisation of its meteorological data. The correct position determination of the stations over the entire simulation period was difficult because of relocation, dismantling, and new setup of some observing stations. This particularly concerns the stations of the DWD. Overall, we found a high density in the central part of the Bavarian Forest National Park in the research catchment Große Ohe (Beudert et al. 2007) and around the Großer Falkenstein Mt. as a focus area of the BIOKLIM project since 2006 (Bässler et al. 2015). In the other parts of the study area, the number of measuring sites is scarce (see Figs. 4–8 for the individual meteorological elements).

Gaps in the time series were filled based on the readings of adjacent stations, employing the same technique as used for the regionalisation of the meteorological station based data (see model chapter). In doing so, the vertical and horizontal distances between the stations were taken into account, while windward/leeward effects were neglected.

GIS-model for the regionalisation of the meteorological data

In this study, two space models were built up to regionalise the station based data series, a grid-based model (100×100 m^2) for the whole study area and a point model including all monitoring plots.

An important prerequisite for the successful application of the regionalisation procedure is a good topographical characterisation of the study area. Since no high-resolution digital terrain model (DTM) was available for the Czech parts of the model area at the beginning of the project, the SRTM elevation model for Europe with a resolution of 90 m was used for these regions. This virtually free-to-air DTM was created in a joint effort by the National Aeronautics and Space Administration (NASA), The National Geospatial-Intelligence Agency (NGA), and German and Italian space agencies (Farr & Kobrick 2000). The characterisation of the German territories and all monitoring areas is based on the DTM5 of the Bavarian State Office for Digitization, Broadband and Surveying.

Model

The calculations were made with the geostatistical interpolation techniques included in the catchment model ArcEGMO (Becker et al. 2002 and Pfützner 2003). This model is a GIS-based, multi-scale modelling system for spatially simulating hydrological processes in river catchments, which has been adopted as the standard method for hydrological impact studies in the area of the Bavarian Forest National Park (Beudert et al. 2007).

The internal geostatistical interpolation techniques for regionalisation of meteorological input, the "Quadrant Method" and the "Inverse Distance Weighting Method" (nearest neighbour method), were primarily developed for application in mesoscale hydrological models. Consequently, they operate rapidly and use commonly available meteorological data (e.g. from the DWD). Although a relatively dense sampling network exists for precipitation in Germany, the other main measured values are recorded only at major meteorological stations. To allow for the effects of different spatial resolution for the individual weather values, a distinction is made between the regionalisation of data for point measurements of precipitation (total volume measured by precipitation stations and meteorological stations) and climate sampling (only meteorological stations). Series of measurements of precipitation, air temperature, wind speed, air humidity, as well as global radiation or duration of sunshine are expected for the climate sampling points.

In the "Inverse Distance Weighting Method", a variable number n of climate measurement points closest to the plot under consideration is used, independent of their direction concerning the plot. The „Quadrant Method" is based on values for the one station nearest to the

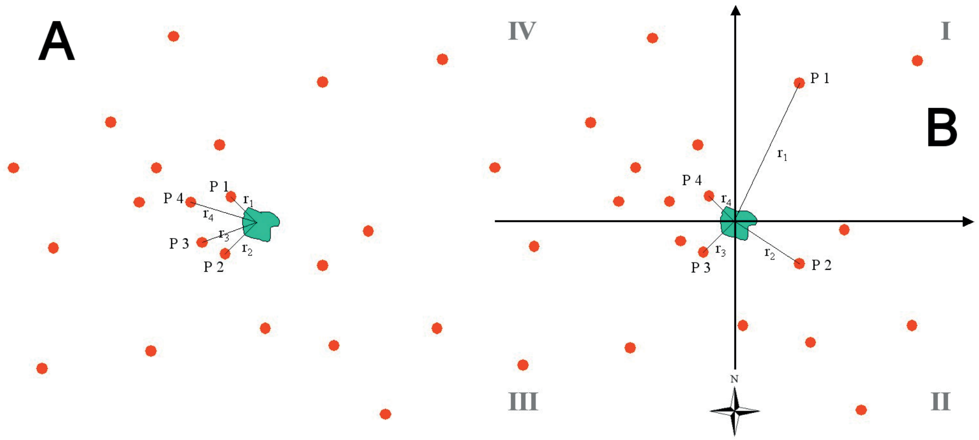

Fig. 3. Spatial distribution of selected measurement points around a sampling plot for the “Inverse Distance Weighting Method” with n = 4 (A) and the “Quadrant Method“ (B).

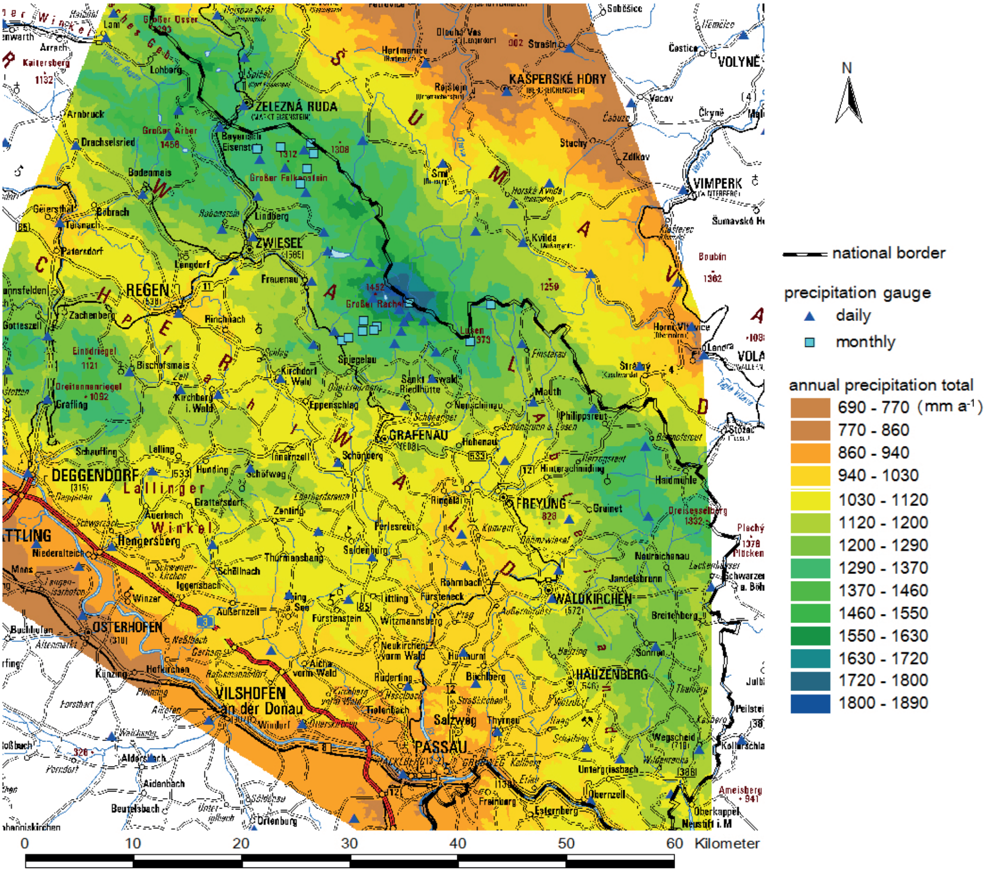

Fig. 4. Average annual precipitation total (mm) in 1980–2015.

centre in each quadrant (Fig. 3B). Thus, stations from all four directions are involved, which the "Inverse Distance Weighting Method" does not always guarantee (Fig. 3A).

Both methods employ vertical and horizontal distances between station and plot. Windward/leeward effects were neglected. The meteorological values P measured at n stations are weighted by distance according to equation 2 and allocated to the area of the plot. The sum of all weighting factors *g* is one.

$$P = \sum_{i=1}^{n} g_i P_i \qquad (2)$$

with $\sum_i g_i = 1$.

It should be emphasized that considerable problems can be caused by a low density of meteorological stations and longer gaps in the datasets. This is particularly critical in the case of extreme precipitation events. Specific analyses of this problem have been performed in the Stepenitz Basin by Lahmer et al. (2000), using different interpolation methods: the quadrant method, two Kriging methods, and several versions of the 'nearest neighbour' method. The quadrant method generally provides results which are almost as good as the more time-consuming Kriging methods.

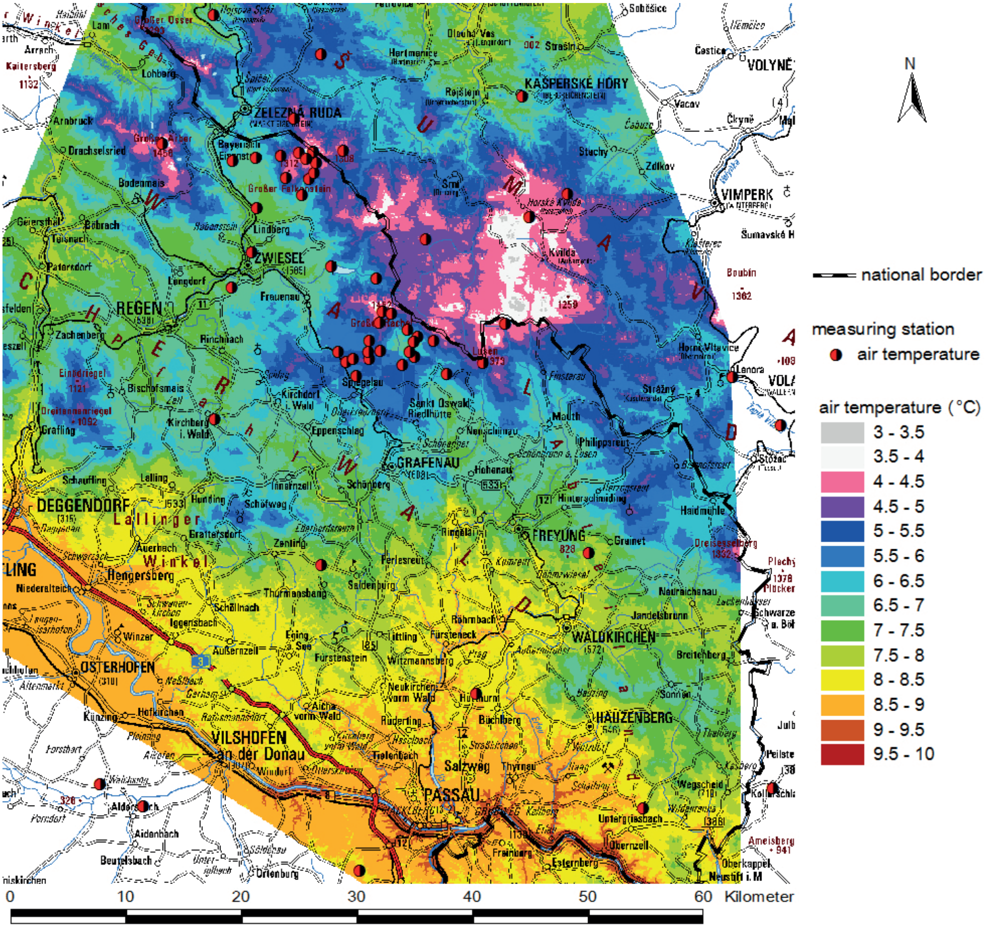

Fig. 5. Average annual air temperature (°C) in 1980–2015.

Allocation of values to the plots takes place under consideration of local topology. Therefore, the average dependence of the particular meteorological element *y* on altitude *h* is estimated by a linear regression ($y = a + b\ h$) using all daily measurements of that particular meteorological value in the simulation period. The Pearson correlation coefficient R is used as a measure of the linear correlation. It has a value between +1 and −1, where 1 is a total positive linear correlation, 0 is no linear correlation, and −1 is a total negative linear correlation.

$$R = \frac{\sum_{i=1}^{n}(h_i - \bar{h})(y_i - \bar{y})}{\sqrt{\sum_{i=1}^{n}(h_i - \bar{h})^2 \cdot \sum_{i=1}^{n}(y_i - \bar{y})^2}} \qquad (3)$$

with $\bar{h} = \frac{1}{n}\sum_{i=1}^{n} h_i$

and $\bar{y} = \frac{1}{n}\sum_{i=1}^{n} y_i$

Using this method, validated in many previous applications of ArcEGMO (e.g. Becker et al. 2002 and Pfützner 2013), we got the following average regression parameters (Table 2) for the period 1980–2015.

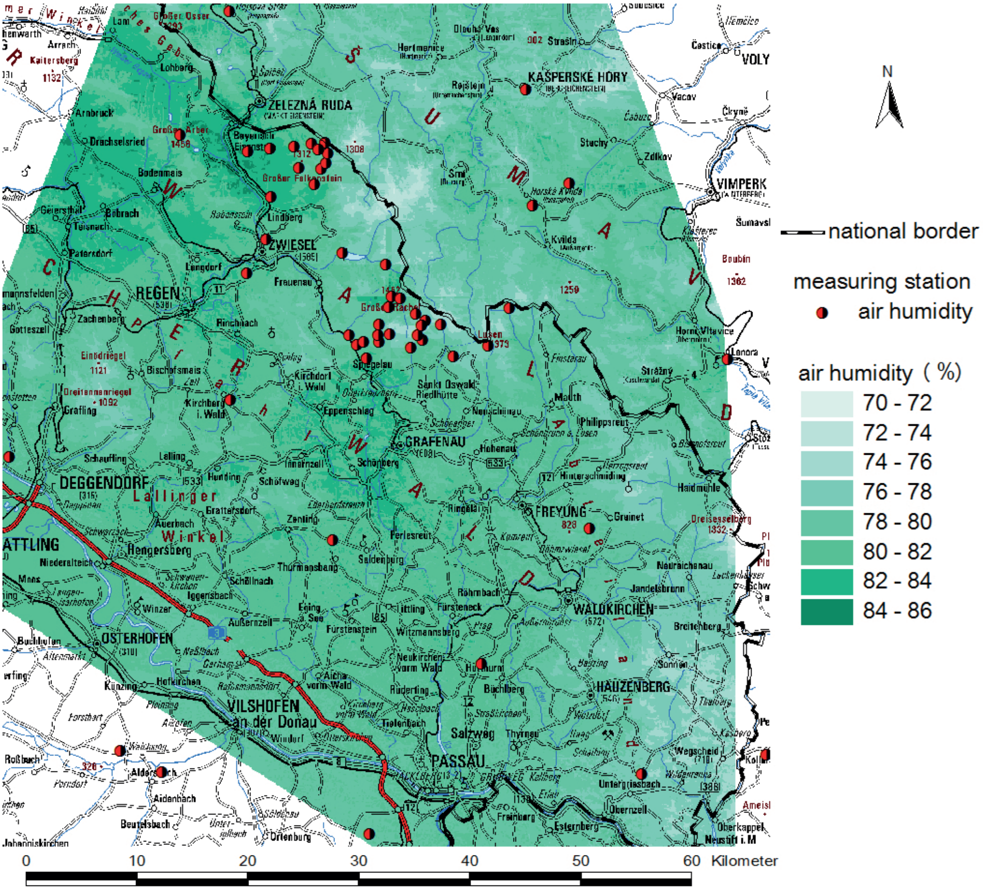

Fig. 6. Average annual air humidity (%) in 1980–2015.

Table 2. Regression and correlation coefficients for the altitude dependence of the different meteorological elements.

Attribute *y*	**elevation gradient** *a* **(m^{-1})**	**regression coeff.** *b*	**Pearson coeff. R**
precipitation	0.0021	1.62	0.77
air temperature	−0.0046	10.05	–0.93
vapour pressure	–0.0028	10.62	–0.94
wind speed	0.0012	0.83	0.45

Despite different microclimatic conditions, there is a close correlation between altitude and precipitation, temperature, and vapour pressure. An exception is the calculated elevation gradient for the wind speed which does not match the expectations (see the low Pearson coefficient in Table 2).

The topology of a specific site influences global radiation and air temperature. To take this into account, we used the equivalent slope concept (Lee 1962) for calculating the slope and aspect dependent correction for the global radiation. The slope dependent modification of the temperature is done following Schulla (1997).

Locations with only short series of measurements (for example time series from specific temporary research projects) were excluded from the final regionalisation procedure. They

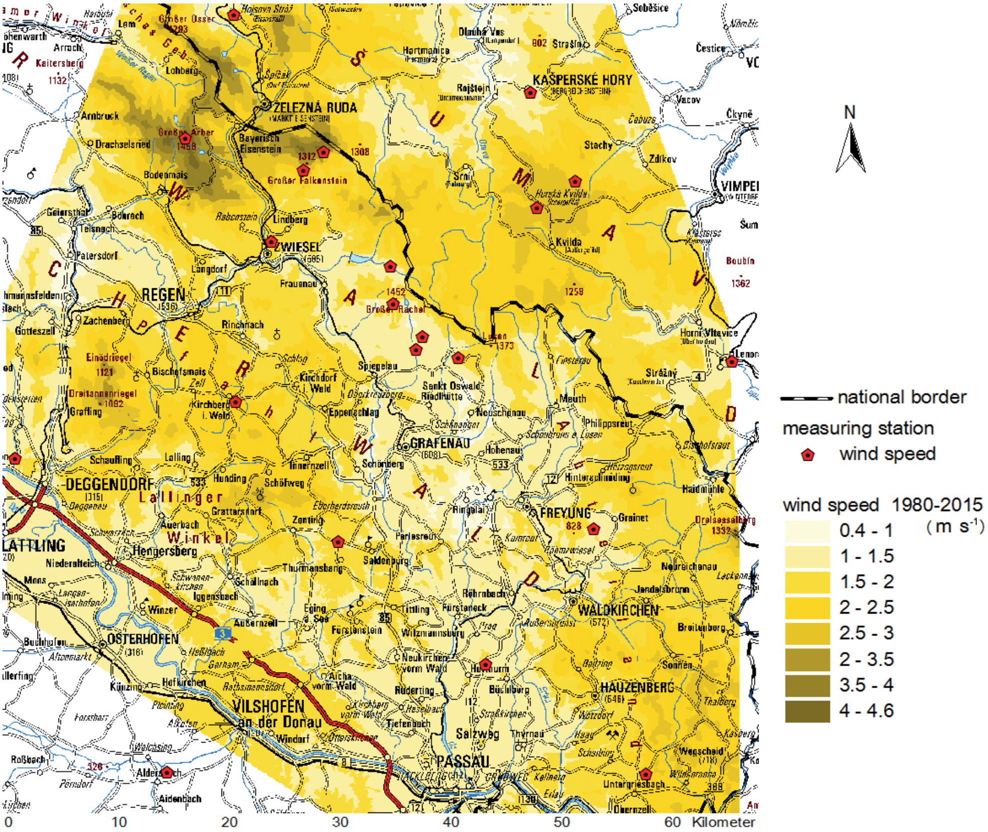

Fig. 7. Average annual wind speed 2 m above ground ($m.s^{-1}$) in 1980–2015.

were only used for gap filling and the calculation of the elevation gradients. The number of stations used as sampling points was thus reduced to 93 precipitation gauges and 71 complete and incomplete climate stations. Continuous time series of the included weather elements are thus available at all of these sampling points as truly observed or as interpolated values for 1 Jan 1980–31 Dec 2015. A correction of the precipitation (e.g. after Richter 1995) was not applied.

Results

The gridded spatial distribution of the main meteorological parameters was calculated by these 164 measuring stations using the Quadrant Method. The respecting figures show precipitation amounts (Fig. 4), air temperature (Fig. 5), air humidity (Fig. 6), wind speed (Fig. 7), and global radiation (Fig. 8) as arithmetic means of the simulated daily values for each grid in the period 1980–2015.

The specific yearly values for each of the 100×100 m^2 grid cells are available at the administration of the Bavarian Forest National Park (NPV). Data with a higher temporal resolution (day or month) can be provided for sections of the study area upon reasonable request. The meteorological parameters at the 1073 individual monitoring plots in the study area (Fig. 1) were calculated in daily, monthly and yearly resolution.

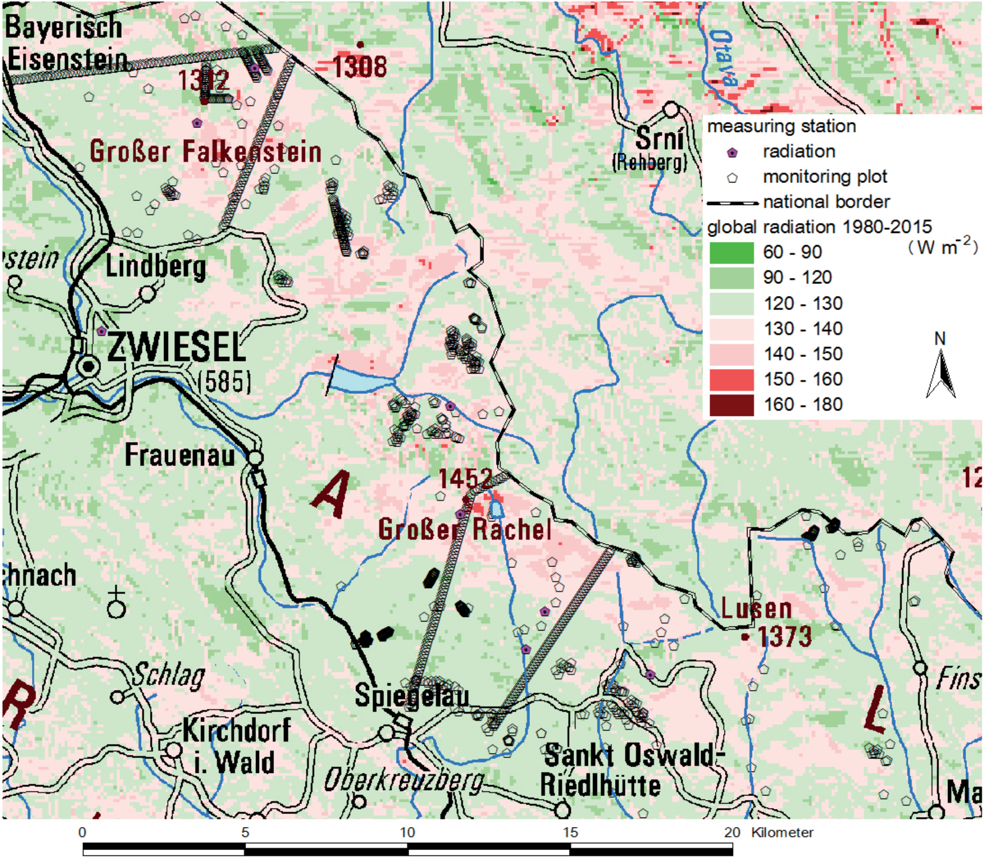

Fig. 8. Average annual global radiation (W.m^{-2}) in the central part of the Bohemian Forest (1980–2015).

Table 3. Comparison of interpolated and measured meteorological elements for three meteorological stations

Station / element	**sample size**	**average value**	**average value**	**RMSE**	**NRM-SE**	**tole-rance**	**fraction outside**
		obs.	sim.			(±)	(%)
RDH (Rachel-Diensthütte)							
precipitation (mm.d^{-1})	12536	4.34	4.17	1.85	0.42	5	2.7
air temperature (°C)	3947	7.37	7.07	0.57	0.08	2	0.3
air humidity (%)	3814	79.6	79.3	3.54	0.04	10	1.1
Grainet-Rehberg							
precipitation (mm.d^{-1})	13119	3.03	3.14	1.87	0.62	5	2.9
air temperature (°C)	13119	7.64	7.38	0.90	0.12	2	3.4
air humidity (%)	13112	80.39	81.34	5.17	0.06	10	5.8
wind speed (m.s^{-1})	8401	1.60	0.92	0.91	0.57	2	5.9
global radiation (J.cm^{-2})	3954	1045	1068	74.34	0.07	200	39.5
Hojsova Stráž							
precipitation (mm.d^{-1})	13149	3.18	3.57	2.39	0.75	5	4.6
air temperature (°C)	9861	6.67	6.21	1.02	0.15	2	8.6
air humidity (%)	9861	80.12	81.98	6.16	0.08	10	13.1
wind speed (m.s^{-1})	9861	1.46	2.37	1.12	0.77	2	12.0
global radiation (J.cm^{-2})	3255	798	866	59.68	0.07	200	31.8

The reliability of these results is determined not only by the quality of the weather measurement series and station density, but also by the topological characteristics (ground level, slope and orientation) of the individual areas. These values were determined from the DTMs as a spatial average over the individual area. Location errors especially affect the quality of the radiation and temperature calculation. The assessment must, therefore, be carried out separately for each area and the individual time periods, taking into account these boundary conditions. Overall, the spatial distribution of the simulation results seems plausible for the entire period of 1980–2015 and was also double-checked for consistency against the Czech Climatological and German Hydrological Atlas (Tolasz et al. 2007, HAD 2013). The only exception is the spatial distribution of the wind conditions (Fig. 7). The simulated wind speed at the mountain ridge between the Rachel and Lusen mounts seems to be too low. Here, the simulation is based on the measured wind data of five (seven for gap filling) stations of the NPV. The mean wind speeds at 2 m, calculated from these time series, are significantly lower than for other stations at comparable altitude. The reasons for this (possible measurement errors, lee effects, specific topographic situation in the Große Ohe catchment, or others) remains to be determined.

Besides this plausibility check of the spatial distribution, the uncertainty of the interpolated time series has been analysed for different representative sites. Three sites were selected: one grid cell in the catchment Große Ohe including the climate station Rachel-Diensthütte (RDH) at 874 m a.s.l. as an example for an area with many surrounding measuring stations, and two grid cells with a low density of surrounding climate stations, namely the grid cell icluding the CHMI-climate station Hojsova Stráž (867 m a.s.l.) and the grid cell with the DWD climate station Grainet-Rehberg (628 m a.s.l.) (marked as verification points in Fig. 1).

The daily simulation results of two different model runs were compared for these three grid cells. The first simulation was done including the specific climate station. These results are labelled as “observed”. In the second run, this station was excluded (labelled as “simulated” or “interpolated” values in the following). Only periods with existing measurements for the specific meteorological element were taken into account. Table 3 shows the sample size and the mean values for each evaluated element of the three sites. The Root Mean Square Error (*RMSE*, equation 4) and its normalised value *NRMSE* (equation 5) were used as criteria for the assessment of the reliability of the simulation results:

$$RMSE = \sqrt{\frac{\sum_{i=1}^{n}\left(y_i^{sim}-y_i^{m}\right)^2}{n}} \tag{4}$$

and $NRMSE = \frac{RMSE}{\overline{y^m}}$ (5)

with $\overline{y^m} = \frac{1}{n}\sum_{\mathrm{i}=1}^{n} y_i^m$

where y^m is the observed value, y^{sim} is the simulated value and n the sample size.

We imposed an allowed tolerance range for each meteorological element from the viewpoint of hydrological modelling, based on the sensitivity of the model against this input value. This range is marked with red lines in all y^{sim}-y^m-plots (Figs. 9–13). For the regions with a high density of stations this range corresponds to the 3-RMSE-confidence interval.

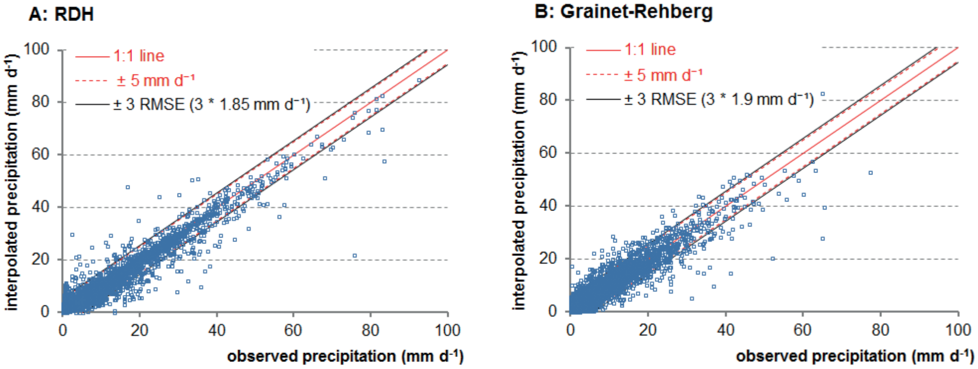

Fig. 9. Comparison of measured and interpolated values of daily precipitation sum at a site with a high station density (A: RDH) and a a site with a low station density (B: Grainet-Rehberg).

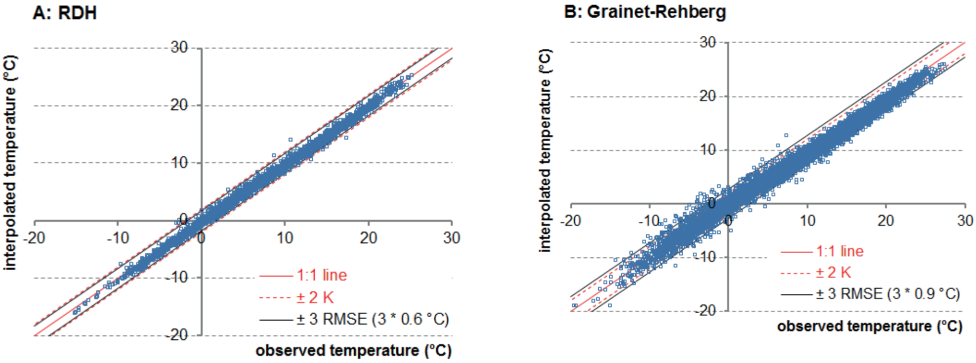

Fig. 10. Comparison of measured and interpolated values of daily air temperature at RDH (A) and Grainet--Rehberg (B).

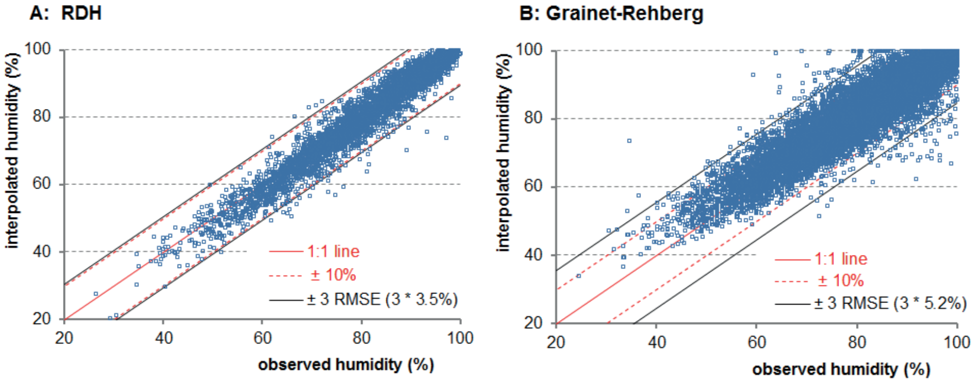

Fig. 11. Comparison of measured and interpolated values of daily air humidity at RDH (A) and Grainet--Rehberg (B).

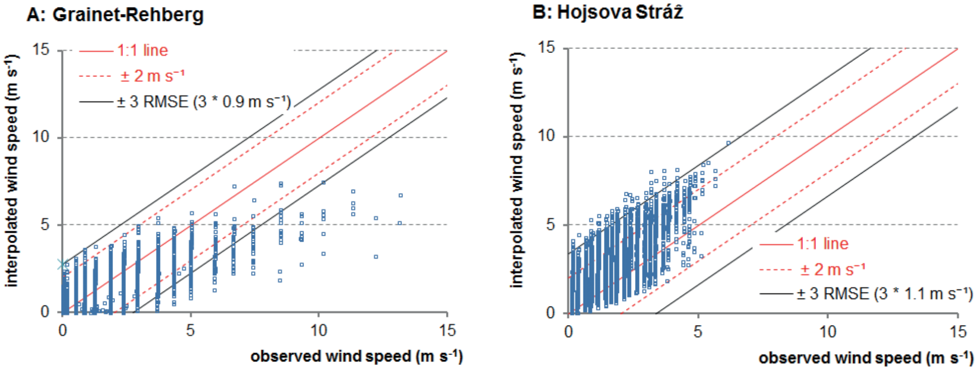

Fig. 12. Comparison of measured and interpolated values of daily wind speed at Grainet-Rehberg (A) and Hojsova Stráž (B).

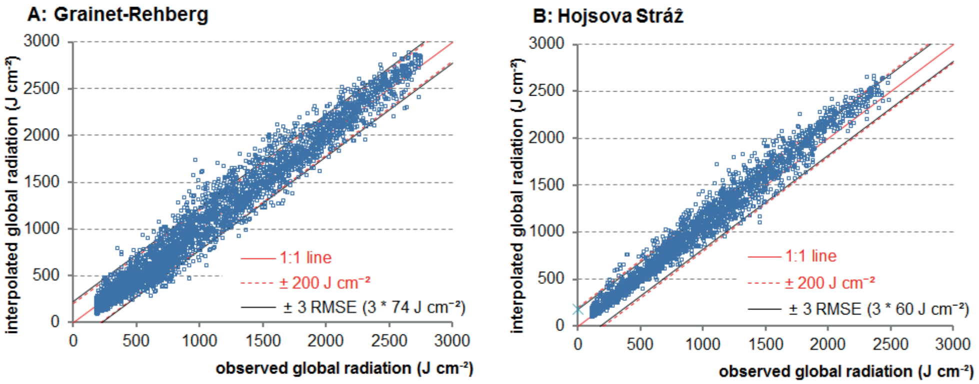

Fig. 13. Comparison of measured and interpolated values of daily global radiation at Grainet-Rehberg (A) and Hojsova Stráž (B).

The agreement between observed and interpolated values of temperature and global radiation is very good at all investigated sites. The simulated daily values fit the observed values over the whole period, as the low *NRMSE* (<0.2) show. The 3-*RMSE*-confidence intervals fall within the imposed range (Figs. 10, 13). Though the *NRMSE* for the precipitation values is significantly higher, the concordance of observation and interpolation is still acceptable. More than 95% of all interpolated daily precipitation values of the investigated sites are inside the tolerance range of ±5 mm.d^{-1} (Fig. 9, Table 3).

The positive impact of a high station density is clearly visible by direct comparison of the results for RDH and Grainet-Rehberg. The fraction of data points inside the tolerance frame is higher for RDH (Figs. 9–11), especially in case of the results for air humidity. Thougth the *NRMSE* for the humidity are very low at all sites, the interpolation results are not satisfying for Hojsova Stráž (not pictured but similar to the Grainet-Rehberg cell) and Grainet-Rehberg. The dispersion of the daily humidity values is critical (Fig. 11).

The results of the interpolation of the wind speed data are unsatisfactory too, as is shown by the high *NRMSE*-values (Table 3) and the distribution of data points (Fig. 12). The interpolated wind speed values are only reliable in the surrounding areas of the rare wind measuring stations.

As these figures demonstrate, the spatial density of surrounding stations directly determines the accuracy of the interpolation results. This translates into different reliability of the results in the three temporal intervals defined via the number of operational stations (Fig. 2). Thus, the results are less confident for the period of 1980–1990. The increasing number of measuring sites from 1991 until 2005 results in an improvement of the reliability. Since 2006, we have the maximum of operational stations, which raise the reliability further, especially for the central part of the Bavarian Forest National Park.

CONCLUSIONS

All known time series of meteorological data available in the surrounding area of the two national parks were collected, checked and, if necessary, cleaned up and put into a uniform format for the period 1980–2015. These daily time series are available for a total of 211 stations for further evaluation. These time series will be updated periodically, and extended in case of the newly set-up stations.

Based on these data, the present goal was to describe the meteorological conditions in this 4500 km^2 study area at a spatial resolution of 100×100 m^2. For this, the “Quadrant Method” was used, an internal geostatistical interpolation technique of the hydrological model ArcEGMO. The assessment of the reliability of the modelling results demonstrates its usability at large areas, with some restrictions (e.g. wind speed and air humidity). The quality of the results is very good for areas with a high station density, but decreases with a lower number of surrounding stations. Yet, the results for temperature, precipitation and radiation are still reliable for the regions with a low density of measuring stations.

This finding is consistent with the reliability estimates in previous hydrological modelling studies in the Ilz and the Große Ohe catchments (Klöcking et al. 2005, Beudert et al. 2007, Sprenger et al. 2013). The simulated stream discharges as an integrating element of the conditions in a catchment (including the meteorological characteristics) fit very well the observed values at all discharge gauges.

Despite the restrictions (e.g. wind, humidity), the results of this regionalisation method can be used for further research projects in this region, such as the allocation of biodiversity patterns in the “Silva Gabreta Monitoring” project.

If higher accuracy is required, new interpolation methods need to be developed, including small-scale weather phenomena, or windward/leeward effects. Testing and verification of these new methods can be done with the herein developed database.

Acknowledgements. This contribution was supported by the Cross-border cooperation programme Czech Republic–Bavaria Free State ETC goal 2014–2020, the Interreg V project No. 26 "Silva Gabreta Monitoring – Implementation of Transboundary Monitoring of Biodiversity and Water Regime". I am grateful to the providers (see Table 1) of the observed time series.

REFERENCES

ATV-DVWK, 2002: Verdunstung in Bezug zu Landnutzung, Bewuchs und Boden. *Merkblatt ATV-DVWK-M* 504, 144 pp.

Bässler C., Seifert L. & Müller J., 2015: The BIOKLIM Project in the National Park Bavarian Forest: Lessons from a biodiversity survey. *Silva Gabreta*, 21: 81–93.

Becker A., Klöcking B., Lahmer W. & Pfützner B., 2002: The hydrological modelling system ArcEGMO. In: *Mathematical models of large watershed hydrology*, Singh V.P. & Frevert D.K. (eds) Water Resources Publications, Littleton, Colorado: 321–384.

Beudert B., Klöcking B. & Schwarze R., 2007: Große Ohe: impact of bark beetle infestation on the water and matter budget of a forested catchment. In: *Forest Hydrology – results of research in Germany and Rusia, Part I*, Puhlmann H. & Schwarze R. (eds) IHP/HWRP-Berichte, Heft 6: 41–63.

DVWK, 1996: Ermittlung der Verdunstung von Land- und Wasserflächen. *DVWK Merkblätter zur Wasserwirtschaft* 238, 135 pp.

DWD, 2017: REGNIE (REGionalisierte NIEderschläge): Verfahrensbeschreibung und Nutzeranleitung. Ms., interner Bericht im DWD, Abteilung Hydrometeorologie, Offenbach, 9 pp.

Elling W., Bauer E., Klemm G. & Koch H., 1987: *Klima und Böden. Waldstandorte. Nationalpark Bayerischer Wald, Heft 1.* Schriftenreihe des Bayerischen Staatsministeriums für Ernährung, Landwirtschaft und Forsten, Grafenau, 255 pp.

Farr T.G. & Kobrick M., 2000: Shuttle Radar Topography Mission produces a wealth of data. *EOS Transactions of American Geophysical Union*, 81: 583–585.

Frick C., Steiner H., Mazurkiewicz A., Riediger U., Rauthe M., Reich T. & Gratzki A., 2014: Central European high-resolution gridded daily data sets (HYRAS): Mean temperature and relative humidity. *Meteorologische Zeitschrift*, 23/1: 15–32.

Friess N., Bässler C., Brandl R., Hilmers T., Müller J. & Seifert L., 2018: Biodiversity along an elevational gradient of the Bavarian Forest – The BIOKLIM project. *Silva Gabreta*, 24: 149–160.

HAD, 2013: *Hydrologischer Atlas von Deutschland*. Bundesministerium für Umwelt, Naturschutz und Reaktorsicherheit (BMU). Online http://geoportal.bafg.de/mapapps/resources/apps/HAD/index.html?lang=de

Lahmer W., Pfützner B. & Becker A., 2000: Data-related uncertainties in meso- and macroscale hydrological modelling. In: *Accuracy 2000. Proceedings of the 4th international symposium on spatial accuracy assessment in natural resources and environmental sciences.* Heuvelink, G.B.M. & Lemmens, M.J.P.M (eds). Amsterdam: 389–396.

Lee R., 1962: Theory of the "equivalent slope". *Monthly Weather Review*, 90: 165–166.

Noack E.M., 1979: *Witterung und Klima im Nationalpark Bayerischer Wald. Nationalpark Bayerischer Wald, Heft 5*. Schriftenreihe des Bayerischen Staatsministeriums für Ernährung, Landwirtschaft und Forsten, München, 132 pp.

Pfützner B. (ed.), 2003: *Modelldokumentation ArcEGMO*. Online http:\\www.arcegmo.de

Pfützner B., Klöcking B., Schumann A. & Hesse P., 2013: *Klimafolgenstudie 2012 – Wasser: Untersuchung zu den Folgen des Klimawandels in Sachsen-Anhalt*. Berichte des Landesamtes für Umweltschutz Sachsen-Anhalt, Heft 5 (Band 1), 176 pp.

Rauthe M., Steiner H., Riediger U., Mazurkiewicz A. & Gratzki A., 2013: A Central European precipitation climatology–Part I: Generation and validation of a high-resolution gridded daily data set (HYRAS). *Meteorologische Zeitschrift*, 22/3: 235–256.

Richter D., 1995: *Ergebnisse methodischer Untersuchungen zur Korrektur des systematischen Messfehlers des Hellmann-Niederschlagsmessers*. Berichte des Deutschen Wetterdienstes Nr. 194, Offenbach, 93 pp.

Schulla J., 1997: *Hydrologische Modellierung von Flussgebieten zur Abschätzung der Folgen von Klimaänderungen*. Zürcher Geographische Schriften 69, ETH Zürich, 161 pp.

Sprenger W., Blomenhofer A., Klöcking B., Neumann J. & Wendel S., 2013: *Fallstudie Ilz – Auswirkungen des Klimawandels auf den Grundwasserhaushalt und die Wasserversorgung im Bayerischen Wald*. KLIWA-

Berichte, Heft 19: 227–236.

Thums S., 1993: *Niederschlags- und Abflussauswertung der 10jährigen Messreihe 1980–1989 für das Einzugsgebiet der Großen Ohe. Wasserhaushalt und Stoffbilanzen im naturnahen Einzugsgebiet Große Ohe Bd. 5*. Nationalpark Bayerischer Wald, 196 pp.

Tolasz R. (ed.), 2007: *Climate Atlas of Czechia*. Czech Hydrometeorological Institute, Prague, 254 pp.

Received: 28 June 2018
Accepted: 4 November 2018

Silva Gabreta	vol. 24	p. 85–114	Vimperk, 2018

Fluxes of ecologically important solutes in the Čertovo catchment–lake system from 1998–2017

Jiří Kopáček*, Josef Hejzlar, Jiří Kaňa, Petr Porcal & Jan Turek

Biology Centre CAS, Institute of Hydrobiology, Na Sádkách 7, 37005 České Budějovice, Czech Republic
*jkopacek@hbu.cas.cz

Abstract
Fluxes of major ions and nutrients were measured in the catchment–lake system of atmospherically acidified Čertovo Lake between 1998 and 2017 hydrological years. Water balance was calculated from precipitation and throughfall amounts, and measured outflow from the lake. The average water outflow from the system was 1216±247 mm.yr^{-1} (i.e., 39±8 l.km^{-2}.s^{-1}), and the water residence time in the lake averaged 649±139 days. The Čertovo catchment remained an average net source of H^+ (44±13 meq.m^{-2}.yr^{-1}) despite significant reductions in sulphur and nitrogen deposition since the late 1980s. Nitrogen saturation of the catchment soils caused low retention of the deposited inorganic N (23% on average) and the terrestrial NH_4^+ removal and NO_3^- production via nitrification (50 and 25 meq.m^{-2}.yr^{-1}, respectively) were the major terrestrial H^+ sources. Net terrestrial SO_4^{2-} production (the second most important H^+ source) decreased from ~49 to ~31 meq.m^{-2}.yr^{-1} between 1998–2002 and 2013–2017, and this decrease was accompanied by decreasing production of ionic Al (Al_i) forms from ~47 to 26 meq.m^{-2}.yr^{-1}. The increasing terrestrial production of organic acid anions (A^-) compensated for the decreasing SO_4^{2-} leaching and maintained (and stabilized) low pH (4.1–4.5) in lake tributaries during the study period. Compared to precipitation, the catchment was a net source of all ions and nutrients (except for NH_4^+). The in-lake biogeochemical processes reduced the incoming H^+ by ~40% (i.e., neutralized on average 223 meq.m^{-2}.yr^{-1} H^+, on a lake-area basis). The NO_3^- and SO_4^{2-} reductions and photochemical and microbial oxidation of A^- were the most important H^+ neutralizing processes (184, 38, and 140 meq.m^{-2}.yr^{-1}, respectively), while hydrolysis of Al_i was the dominant H^+ generating process (79 meq.m^{-2}.yr^{-1}). The lake was a net sink for all nutrients, removing on average 13–38% of total (terrestrial and atmospheric) inputs of dissolved organic carbon, phosphorus, nitrogen, and silicon.

Key words: recovery from acidification, nitrogen, sulphur, organic carbon, aluminium, base cations, phosphorus, pH.

INTRODUCTION

Čertovo Lake has been the most atmospherically acidified among all eight natural lakes situated in the mountain area of the Bohemian (and Bavarian) Forest along the Czech-German border (Veselý et al. 1998, Vrba et al., 2003). The lake was acidified (pH <5.0 and with the depleted carbonate buffering system) already in the 1950s (Procházková & Blažka 1999, Oulehle et al. 2012) and its acidification further progressed until the middle 1980s, when pH ranged between 4.1 and 4.4 (Veselý et al. 1993, 1998). The lake water chemistry has been recovering from acidification since the late 1980s (Oulehle et al. 2012), exhibiting steadily decreasing concentrations of SO_4^{2-}, Cl^- and base cations (BCs = $Ca^{2+} + Mg^{2+} + Na^+ + K^+$), and increasing pH (Kopáček et al. 2016). The chemical recovery of Čertovo Lake is, however, slow and significantly delayed after the rapid decreases in emissions of S and N compounds into the atmosphere and acidic deposition in the Bohemian Forest (Kopáček & Hruška 2010). Our previous investigations of major fluxes and transformations of ions and nutrients in the Čertovo catchment–lake system showed that its terrestrial part was a significant source of acidity (due to net terrestrial production of SO_4^{2-}, NO_3^-, and H^+ in soils), while the in-lake processes (SO_4^{2-} and NO_3^- reduction and oxidation of organic acid anions) only neutralized a small part of this additional H^+ produced in the catchment (Kopáček et al. 2000a, 2001a, 2006). This terrestrial source of acidity is a legacy of long-term atmospheric acidification and N-saturation of the Čertovo catchment and was predicted to persist for decades considering the anticipated trends in atmospheric pollution (Majer et al. 2003, Oulehle et al. 2012).

The aim of this study is to evaluate how terrestrial sources of acidity and its in-lake neutralization have progressed in the Čertovo catchment–lake system during the last two decades. Relying on measured annual fluxes of major elements in precipitation, throughfall, tributaries, and output from the lake, we calculate mass balances for major ions and nutrients, quantify their sinks and sources within the catchment and the lake, and evaluate their changes during the whole 1998–2017 period. For this purpose, we review and synthesize already published studies on element fluxes in the Čertovo catchment–lake system, recalculate previous mass balances of elements (Kopáček et al. 2000a, 2001a, 2006) using new data on lake and catchment characteristics (Kopáček et al. 2016, Šobr & Janský 2016), and supplement them with unpublished data from 2006–2017.

MATERIALS AND METHODS

Site description

Čertovo Lake is situated near the Czech-German border at 13°12' E, 49°10' N, and an elevation of 1027 m a.s.l. It is a dimictic, oligotrophic lake of glacial origin, with surface area of 10.7 ha and maximum depth of 35 m. The lake volume is 1.86×10^6 m^3, of which 26%, 41%, 31%, and 2% are in the 0–5 m, 5–15 m, 15–30 m, and deeper than 30 m layers, respectively (Šobr & Janský 2016). Čertovo Lake is fishless, most crustacean zooplankton are extinct, the phytoplankton is dominated by dinoflagellates and Chrysophyceae, and filamentous microorganisms dominate the bacterioplankton (Vrba et al. 2003, 2016). Submersed littoral macrophytes are absent. The lake has seven surface tributaries (CT-I to CT-VII, Fig. 1), of which CT-II is the major tributary.

The Čertovo catchment (89 ha including the lake) is steep, with a maximum elevation gradient of 315 m. The bedrock consists of mica-schist (muscovitic gneiss), quartzite, and small amounts of pegmatite (Veselý 1994). The catchment soils are comprised of ~0.5 m deep dystric cambisol (58%), podsol (21%), and shallow (~0.2 m) leptosol (17%); wetlands and bare rocks represent ~3% and 1%, respectively. Fine soil is sandy (48–81%) with a low (1–4%) content of clay and a catchment weighted mean pool of 225 $kg.m^{-2}$ (<2 mm, dry weight soil fraction). Soil pH ($CaCl_2$ extractable) is low, with minimum values of 2.5–3.3 in A-horizons and maximum values of 3.6–4.5 in deeper mineral horizons. The mean effective cation exchange capacity of the soils is 104 $meq.kg^{-1}$ (NH_4Cl extractable Ca^{2+}, Mg^{2+}, Na^+ and K^+, and KCl extractable Al^{3+} and H^+), of which 9% is base saturation and 62% and 29% is exchangeable Al^{3+} and H^+, respectively (Kopáček et al. 2002). The Čertovo catchment has been N-saturated (resulting in elevated in-lake NO_3^- concentrations) since the ~1960s (Procházková & Blažka, 1999, Majer et al. 2003).

The catchment is forested with mature Norway spruce (*Picea abies*), with a minor admixture of European beech (*Fagus sylvatica*). The current forest was established after a severe disturbance that occurred between 1860 and 1870, and there had not been any important disturbances until windthrows in the winters of 2007 and 2008, which broke most of the trees along the south-western ridge of the catchment, mostly in the upper parts of the CT-IV

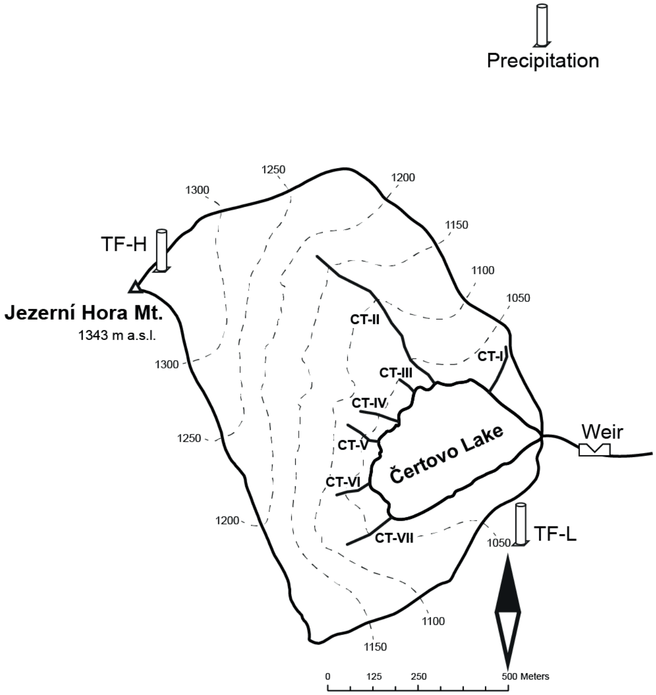

Fig. 1. Map of the Čertovo Lake catchment with the locations of sampling and measuring sites (tributaries, CT-I to CT-VII; outlet equipped with weir; precipitation in treeless area; and throughfall at low and high elevation plots, TF-L and TF-H, respectively).

to CT-VII sub-catchments (Kopáček et al. 2013b, 2016). Other relatively small patches with broken trees and a subsequent bark beetle outbreak occurred and spread throughout the whole Čertovo catchment from 2007–2011. Altogether, the total area of damaged forest (with >50% dead trees) increased from ~4 to 18% between 2000 and 2011 (Kopáček et al. 2016). Another windthrow occurred in October 2017, damaged forest close to the ridge of the catchment, but did not affect results of this study. For details on history of land use and forest composition in the Čertovo catchment see Veselý et al. (1993) and Veselý (1994). Details on the dominant understory vegetation are given by Svoboda et al. (2006).

Water sampling

Water and elements fluxes have been determined since November 1997. Atmospheric deposition was collected at three sites (Fig. 1). Precipitation was sampled in an open area without trees (2 samplers) at an elevation of 1175 m, <1 km north of the lake catchment. Throughfall was sampled at two forest plots (9 samplers at each plot) at elevations of 1045 m (TF-L) and 1330 m (TF-H). For details on the sampling plots see Kopáček et al. (2013c). At each plot, water volume was measured in each sampler, but for chemical analyses they were combined in an integrated sample. Rain was sampled in two-week intervals, and snow in four-week intervals. Samples from all seven tributaries and the outlet were taken in three-week intervals and biweekly (weekly during snowmelt period), respectively. Discharges of tributaries were estimated using a stop-watch and bucket method. These discharge values were used for calculation of volume-weighted mean composition of terrestrial export (see later). Samples were immediately filtered through a 40-µm polyamide sieve to remove coarse particles re-suspended from the streambed during sampling. The discharge from the lake was continuously monitored using a gauge-recorder (part of an MS16 automatic weather station; J. Fiedler, České Budějovice; readings in 15-minute intervals) at a weir, situated ~150 m downstream of the lake. A water column profile (5–6 depths equally distributed between the surface and bottom) was sampled at the deepest part of the lake. Data from each October were used in mass budget studies (see below).

Water chemistry analysis

Samples of precipitation, throughfall, and stream and lake water were analysed using identical methods. Samples were filtered with either membrane filters (pore size of 0.45 µm) for the determination of ions and dissolved reactive silicon, or with glass-fiber filters (pore size of 0.4 µm) for other analyses, except for samples for pH, acid neutralizing capacity (ANC, determined by Gran titration), and total concentrations of aluminium (Al_T), phosphorus (TP), organic carbon (TOC), and nitrogen (TN), which were not filtered beyond the field pre-filtration. Dissolved organic carbon (DOC) was analysed as CO_2 with several TOC analysers (Table 1), all with a detection limit of <4.0 µmol.l^{-1}. Particulate organic C (POC) in

Table 1. Methods used for the determination of individual elements and nutrient forms and their abbreviations.

Abbreviation	Explanation	Assessment
ANC	Acid neutralizing capacity	Gran titration (Tacussel in 1997–2011, then Radiometer).
H^+ (pH)	Proton concentration	pH electrode (combined, Radiometer)
NH_4^+, Ca^{2+}, Mg^{2+}, Na^+, K^+, NO_3^-, Cl^-, SO_4^{2-}, F^-	Major cations and anions	Ion chromatography (Thermo Separation Products in 1997–2000, Dionex IC25 in 2001–2011, then Dionex ICF-3000).
Si	Dissolved reactive silicon	Molybdate method (Golterman & Clymo 1969).
Al_T, Al_i, Al_o, Al_p	Total, ionic, organically bound, and particulate Al	Fractionation according to Driscoll (1984), colorimetry (Dougan & Wilson 1974) throughout 1997–2017. Al_i = dissolved Al – Al_o. Al_p = Al_T – dissolved Al.
Fe_T, Fe_i, Fe_o, Fe_p	Total, ionic, organically bound, and particulate Fe	Fractionation according to Driscoll (1984), colorimetry (Kopáček et al. 2001b) throughout 1997–2017. Fe_i = dissolved Fe – Fe_o. Fe_p = Fe_T – dissolved Fe.
DOC	Dissolved organic C	LiquiTOC analyser (Foss-Heraeus, Germany) in 1997–1999 and Shimadzu analysers TOC 5000A in 2000–2015 and then TOC-L.
POC	Particulate organic C	Analysed on glass-fiber filters (pore size of 0.4 µm) in TOC analysers (Foss-Heraeus LiquiTOC, Shimadzu TOC 5000A/SSM, and Elementar vario Micro cube in 1997–1999, 2000–2015, and 2016–2017, respectively).
TON, DON, PON	Total organic N, dissolved organic N, particulate organic N.	Kjeldahl digestion (Procházková 1960) for precipitation, CT-II and CT-VII, for throughfall in 1997–2001, otherwise TOC/TN analyzer.[1] PON = TON – DON.
TP, DP, PP	Total P, dissolved P and particulate P.	Sample pre-concentration, $HClO_4$ digestion, molybdate method (Kopáček & Hejzlar 1993). PP = TP – DP.
SRP	Soluble reactive P	Molybdate method (Murphy & Riley 1962).

[1] Concentrations of TON and DON were calculated as the differences between concentrations of total and dissolved N, respectively (determined by TOC/TN analysers Formacs (Skalar, the Netherlands) in 2002–2009 and vario TOC cube (Elementar, Germany) in 2010–2012) and inorganic N.

the lake outlet was determined on glass-fibre filters using several TOC analysers (Table 1). POC in the other samples was calculated as POC = TOC – DOC. Soluble reactive P (SRP) was determined by the molybdate method (Murphy & Riley, 1962), with the detection limit of 0.05 µmol.l^{-1}. TP and dissolved P (DP) were determined by perchloric acid digestion and the molybdate method (Kopáček & Hejzlar 1993), but samples were 3- to 4-fold concentrated by evaporation (with perchloric acid at ~100°C prior digestion) to obtain a detection limit of 0.015 µmol.l^{-1}. Particulate P (PP) was calculated as PP = TP – DP. Dissolved reactive silicon (Si) was determined by the molybdate method (Golterman & Clymo 1969). Total and dissolved organic N (TON and DON; the difference between the respective Kjeldahl N and NH_4-N) were determined by Kjeldahl digestion according to Procházková (1960), with 75 ml of samples previously evaporated to obtain a detection limit of ~2 µmol.l^{-1}. This method was used for CT-II, CT-VII, outlet and precipitation throughout the study and for throughfall from 1997–2001, otherwise concentrations of TON (DON) were the difference between total (dissolved) N, determined by the TOC/TN analysers, and inorganic N (Table 1). In this calculation, inorganic N was the sum of NO_3-N and NH_4-N, whereas NO_2-N (typically <1% of NO_3-N) was neglected. Particulate organic N (PON) was calculated as PON = TON – DON. Concentrations of NH_4^+, Ca^{2+}, Mg^{2+}, Na^+, K^+, NO_3^-, Cl^-, SO_4^{2-}, and F^- were determined by ion chromatography (Table 1). Detection limits for F^- and NH_4^+ were 0.1 and 0.4 µmol.l^{-1}, respectively. Concentrations of other ions were always higher than detection limits of the respective methods.

Fractionation of aluminium according to Driscoll (1984), i.e. Al_T, dissolved Al, and non-labile Al, were analysed in non-filtered samples, filtered samples, and cation-exchange-treated samples after their filtration, respectively, using the method by Dougan & Wilson (1974). We assumed that concentration of organically bound Al (Al_o) was equal to non-labile Al. Concentration of ionic positively charged Al species (Al_i) was the difference between dissolved Al and Al_o concentrations. Concentration of particulate Al species (Al_p) was the difference between Al_T and dissolved Al concentrations. The respective Fe fractions (Fe_T, Fe_i, Fe_o, and Fe_p) were obtained analogously to Al, and their concentrations were determined by the thiocyanate colorimetric method after sample evaporation and digestion with perchloric acid (Kopáček et al. 2001b). Equivalent concentrations (one equivalent is one mole of charge) of Al_i and Fe_i (Al_i^{n+} and Fe_i^{m+}, µeq.l^{-1}) were obtained from their molar concentrations and the average charges of Al hydroxocomplexes (n) and Fe hydroxocomplexes (m), respectively. The n and m values were estimated from the theoretical distribution of ionization fractions of aqueous Al and Fe hydroxocomplexes, respectively, at the sample pH (Stumm & Morgan 1981), neglecting F^- and SO_4^{2-} complexes (Kopáček et al. 2000b). Concentrations of organic acid anions (A^-, µeq.l^{-1}) in stream and lake water were calculated from pH and concentrations of DOC, Al_o, and Fe_o according to Kopáček et al. (2000b). Concentrations of A^- in precipitation and throughfall were calculated from the empirical relationship of A^- (µeq.l^{-1}) = 4×DOC (mg.l^{-1}) according to Mosello et al. (2008) and Kopáček et al. (2009).

The reliability of the analytical results was controlled by means of an ionic balance approach, a comparison between measured and calculated conductivities (Kopáček et al., 2000b), and a standard sample (a frozen subsample of water annually taken from CT-II tributary), which was melted and assayed with each series of samples. For example in 2009, coefficients of variation for mean concentrations of the standard sample were 1–5% for all ions (except for F^-), DOC, TP, and pH; <10% for TON and SRP; and <20% for F^- (e.g., 55±2, 36±3, 1.12±0.06, 0.84±0.08, and 1.1±0.2 µmol.l^{-1} for NO_3^-, TON, TP, SRP, and F^-, respectively, $n = 36$) (Kopáček et al. 2011). The differences between the sum of cations and the sum of all anions (including A^-) were <±10% of the total ionic content in individual precipitation and throughfall samples, and <±4% for the annual volume weighted mean concentrations.

Similarly, the differences between the sums of cations and anions (including Al_i^{n+}, Fe_i^{m+} and A^-) were <±5% of the total ionic concentration in the individual samples of stream and lake water. At higher differences, samples were re-analysed. For these ion balance controls, a half of detection limit was used when measured concentrations were lower than this limit. Positive ANC values were assumed to represent HCO_3^- concentrations and $HCO_3^- = 0$ was used for all ANC values ≤ 0 µmol.l^{-1}.

Average rates of change in chemical composition of element fluxes were based on a regression of their annual fluxes against time over the study period.

Mass balance and net terrestrial and aquatic production of water constituents

Mass balance of chemical constituents in the catchment soils and lake was calculated for individual hydrological years according to equations (1) and (2), respectively (Kopáček et al. 2016):

$$Q_{DEP}C_{DEP} + \pi_C = Q_{TE}C_{TE} + \Delta M_C \qquad (1)$$

$$Q_{TE}C_{TE} + Q_{PR}C_{PR} + \pi_L = Q_{OUT}C_{OUT} + \Delta M_L \qquad (2)$$

where π_C and π_L (both in mol.yr^{-1}) are the net mass production (when positive) or retention (when negative) of a constituent in the catchment and lake, respectively. Q_{DEP}, Q_{TE}, Q_{PR}, and Q_{OUT} (all in m^3.yr^{-1}) are water fluxes of atmospheric deposition (DEP) to the catchment soils (i.e., bulk deposition in the open area and throughfall deposition in forests), terrestrial export (TE) to the lake from the catchment (tributaries), direct atmospheric deposition to the lake surface (precipitation, PR), and total (measured) water output (OUT) from the lake, respectively. C_{DEP}, C_{TE}, C_{PR}, and C_{OUT} (all in mol.m^{-3}) are annual mean concentrations of water constituents in the atmospheric deposition to the catchment soils, in terrestrial export via tributaries, in direct atmospheric deposition to the lake surface (precipitation), and in the lake output, respectively. The concentrations were calculated as annual volume weighted means (VWM) for C_{DEP} and C_{PR} and discharge and period weighted means (DPWM) for C_{TE} and C_{OUT}. The annual DPWM value of C_{TE} was calculated using the compositions and discharges of all seven tributaries throughout the hydrological year (Likens & Bormann 1995):

$$C_{TE} = \frac{\sum C_{y,i} Q_{y,i} \tau_i}{\sum Q_{y,i} \tau_i} \qquad (3)$$

where y and i denote lake tributaries (CT-I to CT-VII, Fig. 1) and sampling period, respectively, $C_{y,i}$ is concentration of a water constituent and $Q_{y,i}$ water discharge in a tributary y during sampling i, and τ_i (days) is length of sampling period i. In this calculation, each flux was assumed to represent the whole period i given as the sum of halves of intervals between the sampling and the previous one and between the sampling and the next one. The annual DPWM value of water output from the lake (C_{OUT}) was calculated similarly by linking continuously monitored discharge data of the outlet with the corresponding weekly to biweekly concentration data.

ΔM_L (mol.yr^{-1}) in equation (2) is the change in storage of a constituent in the lake and was calculated from equation (4):

$$\Delta M_L = V\,(C_2 - C_1) \qquad (4)$$

where V (m^3) is lake volume and C_1 and C_2 (both in kg.m^{-3}) are volume weighted mean concentrations of water constituents. The C_1 and C_2 values were obtained from data on all sampled depths (usually five) between the surface and bottom at the beginning and the end of each hydrological year, respectively, by linking the volumes of sampled water layers with the corresponding concentrations. We usually used data from October sampling for this purpose. An analogous change in storage of a constituent in the catchment (ΔM_C; mol.yr^{-1}) was not measured, but was assumed to be negligible in a one-year balance compared to the total element pools in the catchment. The equation (1) was thus rearranged to

$$\pi_C{}^* = Q_{TE}C_{TE} - Q_{DEP}C_{DEP} = \pi_C - \Delta M_C,$$

where $\pi_C{}^*$ includes both the net mass production and change in storage of a constituent in the catchment.

The water balance was determined from the annual amounts (m.y^{-1}) of precipitation in the open area (H_{PR}) and throughfall (TF) at the low (L) and high (H) elevation plots ($H_{TF\text{-}L}$ and $H_{FT\text{-}H}$, respectively), Q_{OUT}, and the budget for Cl^-. The Q_{OUT} was continuously monitored using a gauge-recorder at a weir (Fig. 1). Because the total catchment area above the weir was 2.3% higher than the Čertovo catchment, the measured Q_{OUT} values were corrected accordingly to obtain water discharge from Čertovo Lake. Previously published data on element mass balances in the Čertovo catchment–lake system (Kopáček et al. 2000a, 2001a, 2006) were accordingly corrected in this study. Q_{DEP} was calculated, assuming that 10% and 90% of the catchment area (estimates based on aerial photographs) received atmospheric deposition in the form of precipitation and throughfall, respectively, and that each of sites TF-L and TF-H represented 50% of the total throughfall deposition in the study catchment:

$$\mathrm{Q_{DEP} = (A_C - A_L)\ (0.1H_{PR} + 0.9(0.5H_{TF\text{-}L} + 0.5H_{TF\text{-}H}))} \tag{5}$$

where A_C and A_L (m^2) is area of the catchment (including lake) and lake, respectively, and coefficients 0.1 and 0.9 represent portions of the catchment, receiving atmospheric deposition in the form of precipitation and throughfall, respectively.

The total water input into the lake (Q_{IN}) was the sum of Q_{TE} and Q_{PR}. $Q_{PR} = H_{PR}A_L$ and Q_{TE} was calculated from equation (2), using the measured Q_{OUT} and Q_{PR} fluxes and annual VWM concentrations of Cl^- in precipitation (Cl_{PR}), annual DPWM concentrations of Cl^- in lake tributaries (Cl_{TE}) and outlet (Cl_{OUT}), and change in storage of Cl^- in the lake (ΔCl_L, calculated form equation 4). The net removal or production of Cl^- in the lake was assumed to be negligible (e.g., Van der Perk 2006) and thus π_L of Cl^- was set to zero:

$$\mathrm{Q_{TE} = \frac{Q_{OUT}\ Cl_{OUT} - Q_{PR}Cl_{PR} + \Delta Cl_L}{Cl_{TE}}} \tag{6}$$

Annual VWM concentrations of elements deposited to the catchment soils via atmospheric deposition and canopy leaching were calculated from the amounts and VWM compositions of precipitation (C_{PR}) and throughfall at the low ($C_{TF\text{-}L}$) and high ($C_{TF\text{-}H}$) elevation plots:

$$\mathrm{C_{DEP} = \frac{0.1\ C_{PR}H_{PR} + 0.9\ (0.5\ C_{TF\text{-}L}H_{TF\text{-}L} + 0.5\ C_{TF\text{-}H}H_{TF\text{-}H})}{0.1\ H_{PR} + 0.9\ (0.5\ H_{TF\text{-}L} + 0.5\ H_{TF\text{-}H})}} \tag{7}$$

where coefficients 0.1, 0.9, 0.5 are the same as in equation (5).

Mass balance of protons in terrestrial and aquatic ecosystems

Net terrestrial and aquatic production (or consumption) of protons and the contributions of individual constituents to these processes were calculated from budgets for ions, using the equation of electroneutrality:

$$[H^+] = [SO_4^{2-}] + [NO_3^-] + [Cl^-] + [F^-] + [A^-] + [HCO_3^-] - [NH_4^+] - \\ - [Na^+] - [K^+] - [Ca^{2+}] - [Mg^{2+}] - [Al_i^{n+}] - [Fe_i^{m+}] \quad (8)$$

where brackets represent equivalent concentrations of components. According to this approach, any increase in concentration of cations and decrease in concentration of anions are H^+ consuming processes. In contrast, any decrease in concentration of cations and increase in concentration of anions are H^+ producing reactions. Changes in concentrations of ionic P and Si forms were neglected.

RESULTS

Concentrations

All tributaries were more acidic than precipitation (pH of 4.1–4.5 *vs.* 5.0) and atmospheric deposition to the catchment soils (pH of 4.8), and had higher concentrations of SO_4^{2-}, NO_3^-, H^+, and Al forms (Table 2). In contrast, deposited NH_4^+ was almost completely retained in soils and its concentration in tributaries was permanently low (<1 µmol.l^{-1}). All tributaries had lower concentrations of DOC, TP, and TON than deposition to the catchment soils, and stream water SRP was always below the detection limit of 0.05 µmol.l^{-1}. Tributaries CT-I to CT-V represented ~80% of the total terrestrial input to the lake and their chemistry was similar to that in the major tributary CT-II (Table 2), except for lower NO_3^- concentrations in CT-I, due to a small wetland in its sub-catchment. The chemistry of tributaries CT-VI and CT-VII differed from the other tributaries, being significantly less acidic (pH of 4.5 *vs.* 4.1–4.3) and having higher concentrations of BCs and Si, and lower DOC concentrations (Table 2). Such a different composition implies a higher proportion of groundwater (base flow) in these tributaries than in other sub-catchments.

The lake output had lower concentrations of H^+, NO_3^-, DOC, SO_4^{2-}, Al_i, Al_o, Fe_o, and Si, but higher concentrations of particulate forms of all nutrients (POC, PON, PP) compared to tributaries and precipitation (Table 2). Concentrations of NH_4^+ behaved differently to other ions, being higher in the lake output than in tributaries.

Details on annual average chemical composition of major fluxes in the Čertovo catchment–lake system are for individual hydrological years summarized in Appendixes 2 to 6.

Secchi disc transparency varied between 2–6 m during the study. The thermal stratification of Čertovo Lake developed characteristically for a dimictic temperate lake. The ice cover usually lasted from December to April, with the minimum, maximum, and average ice-on period of 92, 160, and 130 days, respectively, during 1998–2017. The autumn and spring overturns usually occurred in December and April, respectively, but were not always complete and bottom layers below ~25 m were not mixed in some years (e.g. in 2000; KOPÁČEK et al. 2001a). Anoxia only occurred in a thin (~1–3 m) layer above the bottom in the deepest part of the lake during the late stages of winter and summer thermal stratification (Fig. 2). At low redox potentials above the lake bottom, dissimilatory reduction processes occurred, decreasing NO_3^- and SO_4^{2-} concentrations and increasing concentrations of NH_4^+ and Fe forms, while concentrations of conservative Cl^- remained stable along the whole water column (Fig. 2). The changes in ionic composition increased the hypolimnetic pH (to ~6 from ~4.5 in the epilimnion; Fig. 2C), as well as ANC concentrations that reached positive values (the carbonate buffering system was re-established above the bottom; Fig. 2D). With the pH increase towards neutrality, ionic Al species hydrolyzed and formed Al_p (colloidal hydroxides). Concentrations of Al_i were thus lower in the anoxic zone than in the rest of water column profile, while Al_p concentrations sharply increased above the bottom (Fig. 2I,J). These high Al_p concentrations were accompanied with elevated TP concentrations

Table 2. Average (± standard deviation) values of discharge (Q, for annual data see Appendix 1) and mean composition of precipitation (C_{PR}, for annual data see Appendix 2), atmospheric deposition to the catchment soils (C_{DEP}, precipitation in treeless area and throughfall in forest, for annual data see Appendix 3), tributaries (CT-I to CT-VII), terrestrial export via tributaries (C_{TE}, for annual data see Appendix 4), total input to Čertovo Lake (C_{IN}, terrestrial export and precipitation to the lake surface, for annual data see Appendix 5), and output from the lake (C_{OUT}, for annual data see Appendix 6) during the period between November 1997 to October 2017. Units: µmol.l^{-1}, except for discharge (Q; l.s^{-1}) and pH. For location of tributaries see Fig. 1.

	C_{PR}	C_{DEP}	**CT-I**	**CT-II**	**CT-III**	**CT-IV**	**CT-V**	**CT-VI**	**CT-VII**	C_{TE}	C_{IN}	C_{OUT}
Q	*4.5±0.9	**36±5	0.7±0.3	11.2±3.8	1.6±0.6	2.1±1.0	0.8±0.3	1.7±0.8	2.0±0.9	31±6	36±7	35±7
pH	4.96±0.18	4.79±0.17	4.32±0.04	4.26±0.03	4.11±0.03	4.11±0.03	4.16±0.04	4.51±0.06	4.53±0.06	4.26±0.03	4.30±0.03	4.52±0.08
H^+	12±4	17±7	48±5	56±4	78±6	78±4	70±6	31±4	30±4	56±4	50±4	31±6
Ca^{2+}	5±2	10±2	8±3	10±2	8±2	9±1	9±2	16±2	14±1	11±2	10±2	10±2
Mg^{2+}	1.5±0.5	4.4±0.7	12±2	14±2	12±1	13±1	15±2	21±2	16±1	14±2	13±1	12±1
Na^+	7±2	12±2	34±3	31±3	29±3	28±3	30±3	40±4	39±4	32±3	29±3	27±2
K^+	3±3	24±5	8±2	8±1	6±2	8±2	9±3	10±1	11±1	8±1	8±1	8±1
NH_4^+	27±4	36±7	0.9±0.7	0.6±0.5	0.6±0.4	0.8±0.6	1.2±2.1	0.7±0.5	0.6±0.4	0.6±0.4	4±1	5±1
NO_3^-	25±4	41±6	28±15	66±16	65±18	75±27	72±37	77±26	62±13	67±16	62±14	46±7
SO_4^{2-}	10±3	16±6	40±8	35±8	41±12	40±11	43±11	43±12	35±8	37±9	34±8	36±9
Cl^-	7±2	15±2	16±2	16±2	15±3	16±3	17±5	18±2	18±2	16±2	14±2	15±1
F^-	0.5±0.5	0.9±0.5	2.4±0.6	1.9±0.6	2.0±0.6	1.9±0.7	2.0±0.7	2.1±0.7	1.6±0.4	1.9±0.5	1.7±0.5	1.8±0.5
DOC	96±17	514±66	513±159	555±171	768±208	717±204	561±135	202±42	266±67	519±158	467±139	282±35
POC	32±17	84±52	8±9	11±8	12±13	15±16	15±14	15±7	11±19	12±6	15±7	46±16
DON	11±3	25±9	13±5	20±4	20±7	19±7	19±8	13±6	14±4	19±4	18±4	15±2
PON	7±4	10±6	2.6±3.1	0.9±1.0	1.2±1.8	1.2±2.1	1.8±1.7	1.1±1.2	1.3±1.2	1.4±1.1	2±1	5±1
TP	0.54±0.26	0.87±0.21	0.14±0.04	0.13±0.05	0.15±0.07	0.14±0.06	0.10±0.03	0.07±0.02	0.10±0.04	0.12±0.05	0.17±0.05	0.14±0.02
PP	0.26±0.11	0.53±0.13	ND	0.09±0.03	ND	ND	ND	ND	0.07±0.2	0.03±0.02	ND	0.09±0.02
SRP	0.20±0.15	0.18±0.11	<0.05	<0.05	<0.05	<0.05	<0.05	<0.05	<0.05	0.03±0.01	0.05±0.02	<0.05
Si	0.3±0.1	ND	78±9	71±7	73±9	68±9	68±8	88±8	92±9	74±7	65±6	57±4
Al_T	0.4±0.4	ND	11±2	20±3	21±4	23±4	22±6	16±4	14±3	20±3	18±3	16±3
Al_i	ND	ND	6±2	13±4	14±3	15±3	15±5	13±4	10±3	14±3	12±3	12±3
Al_o	ND	ND	5±1	6±1	8±2	8±1	7±1	3±1	4±1	6±1	5±1	3±1
Fe_T	ND	ND	3.6±1.1	3.2±0.9	3.8±0.9	3.4±0.8	2.4±0.5	0.5±0.1	1.1±0.3	2.8±0.8	2.5±0.7	2.8±0.6
Fe_i	ND	ND	1.1±0.4	1.0±0.3	1.2±0.4	1.3±0.4	0.9±0.4	0.2±0.1	0.5±0.2	0.9±0.2	0.8±0.2	1.0±0.4
Fe_o	ND	ND	2.5±0.9	1.9±0.7	2.6±0.8	2.1±0.6	1.5±0.4	0.3±0.1	0.6±0.2	1.7±0.6	1.5±0.5	0.8±0.2

Explanations: *Precipitation amount deposited to the lake surface, **water amount deposited to the lake catchment with precipitation and throughfall. ND – not determined.

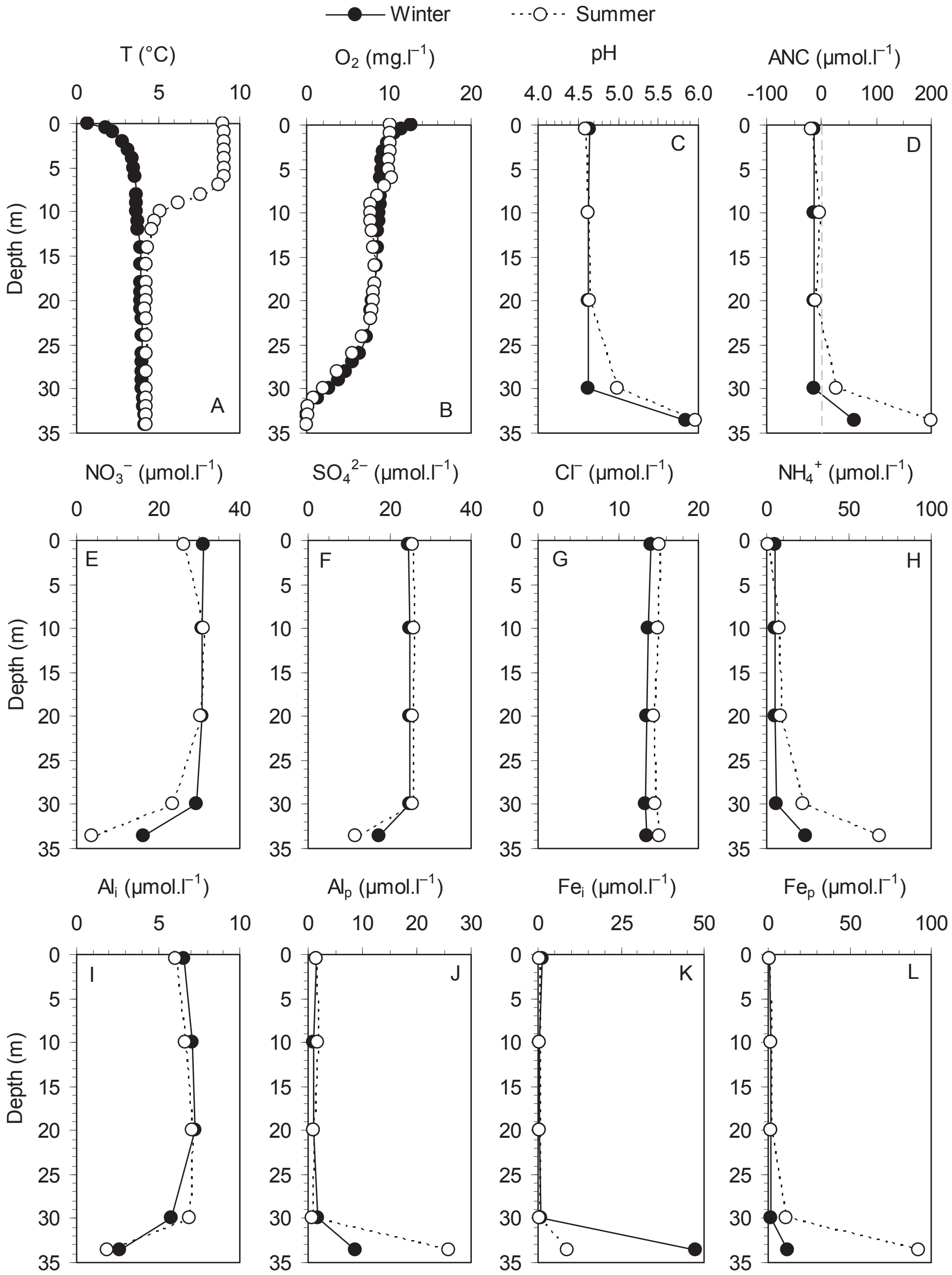

Fig. 2. Depth diagrams of temperature (T), dissolved oxygen (O_2), pH, acid neutralizing capacity (ANC), NO_3^-, SO_4^{2-}, Cl^-, NH_4^+, ionic and particulate aluminium (Al_i, Al_p) and iron (Fe_i, Fe_p) during winter (22 March 2017) and summer (23 October 2017) thermal stratification of Čertovo Lake.

Table 3. Mean (± standard deviation) element fluxes in precipitation (*PR*), deposition to the catchment soils (*DEP*), terrestrial export (*TE*), net production of water constituents in the catchment ($\pi_C{}^* = \pi_C - \Delta M_C$, calculated from equation 1), and the associated H^+ production/removal in soils of the Čertovo catchment in the 1998–2017 hydrological years.

	PR	*DEP*	*TE*	$\pi_C{}^*$	**H^+ source**†
	mmol.m^{-2}.yr^{-1}				meq.m^{-2}.yr^{-1}
H^+	16±8	25±10	69±14	44±13	
Ca^{2+}	6.6±2.6	15±3	13±4	–1±3	3±5
Mg^{2+}	1.9±0.8	6±1	18±3	12±3	–23±7
Na^+	9.4±3.9	18±3	39±7	22±6	–22±6
K^+	4.7±3.8	33±5	10±2	–23±6	23±6
$NH_4{}^+$	35±10	51±8	0.8±0.5	–50±8	50±8
$NO_3{}^-$	33±11	59±7	84±25	25±24	25±24
$SO_4{}^{2-}$	14±6	23±9	46±15	24±9	47±18
Cl^-	9±4	21±3	19±4	–2±3	–2±3
F^-	1±1	1±1	2±1	1±1	1±1
DOC (A^-)	126±36	727±94	648±209	–79±170	(–6±10)
$HCO_3{}^-$	4±4	5±6	0±0	–5±4	–5±4
TON	23±8	47±20	25±8	–21±18	
TP	0.7±0.3	1.2±0.3	0.15±0.06	–1.1±0.3	
Si	0.4±0.1	ND	92±15	91±15	
Al_T	0.5±0.4	ND	26±7	25±7	
Al_i ($Al_i{}^{n+}$)	ND	ND	17±5	17±5	(–45±14)
Fe_T	ND	ND	3.5±1.1	3.4±1.1	
Fe_i ($Fe_i{}^{m+}$)	ND	ND	1.1±0.3	1.1±0.3	(–1±0.4)

Explanations: Values are given on a catchment-area basis; ND – not determined. When deposition of an element on the catchment soils was not determined, its net production was set equal to its terrestrial export. Positive $\pi_C{}^*$ values indicate net production, while negative values indicate net removal; for their annual values see Appendix 7. † Release of cations and removal of anions are proton-consuming processes, while removal of cations and release of anions are proton-producing reactions. One meq = mmol of charge. Sum of H^+ sources and sinks gives a net production of 45 mmol.m^{-2}.yr^{-1}.

(maximum of ~1 µmol.l^{-1}) above the bottom, while its concentrations were one order of magnitude lower in the rest of water column (not shown), similarly to the lake outlet (Table 2). Despite these elevated TP concentrations, DP remained low above the lake bottom, with SRP values close to or below the detection limit.

Water fluxes

The average (± standard deviation) precipitation was 1309±273 mm.yr^{-1}, with minimum and maximum values of 780 and 2080 mm.yr^{-1} (in 2015 and 2002), respectively. The deposition to the catchment (precipitation in treeless areas plus throughfall in forest) was 1429±206 mm.yr^{-1} and ranged from 1045 to 2018 mm.yr^{-1} (Appendix 1). The average water outflow from the lake was 1216±247 mm.yr^{-1} (i.e., specific outflow of 39±8 l.km^{-2}.s^{-1}). The resulting average evapotranspiration from the catchment–lake system, based on precipitation and throughfall amounts, was 15%. This value was, however, lowered by interception. Consequently, the actual total evapotranspiration from the catchment–lake system was >15% due to the direct water evaporation from canopies. Water residence time in the lake varied between 395 and 1005 days, with an average of 649±139 days over the study period.

Element fluxes in catchment

Terrestrial part of the Čertovo catchment was a net sink for atmospherically deposited NH_4^+, but a net source of most water solutes, with exception for Cl^- (Table 3). The average fluxes of Cl^- deposition and leaching were almost equal on a long-term (Table 3), but varied in some

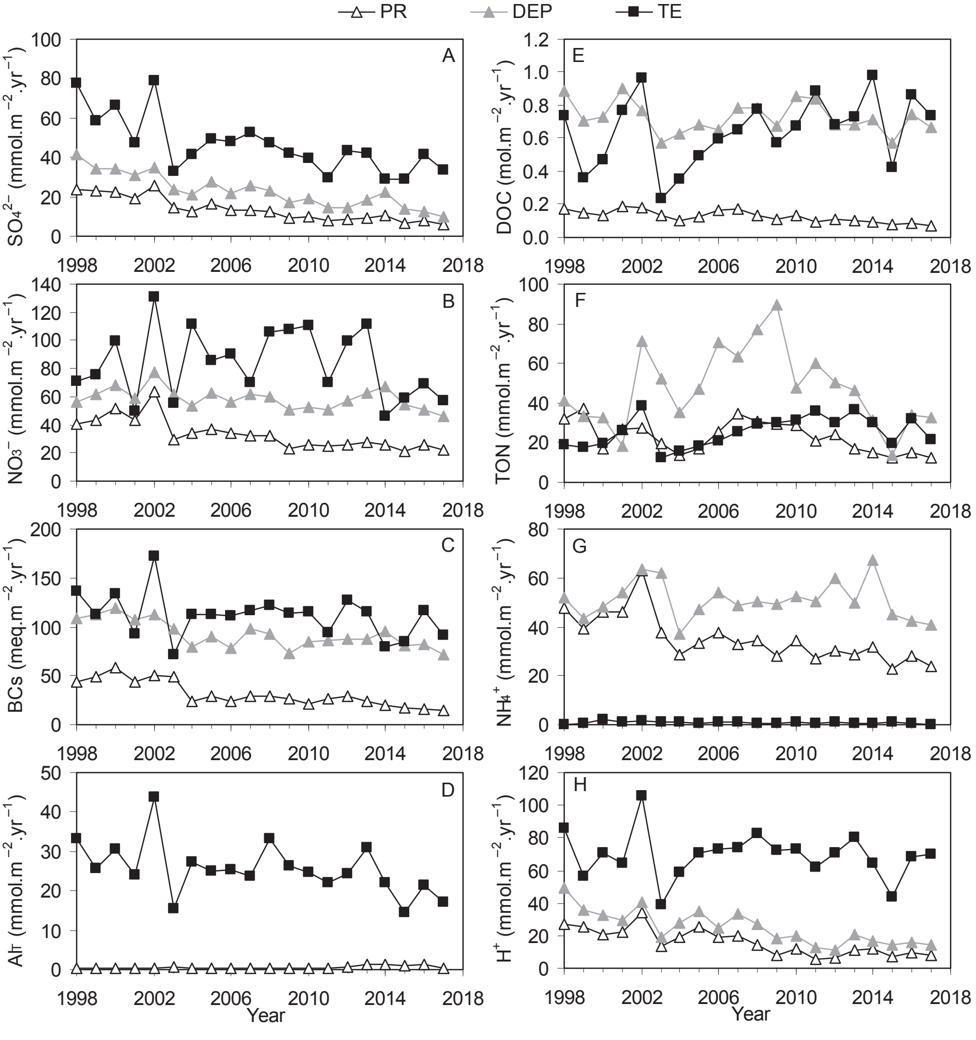

Fig. 3. Time series of annual fluxes (based on a catchment area basis) of SO_4^{2-}, NO_3^-, base cations (BCs = sum of Ca^{2+}, Mg^{2+}, Na^+ and K^+), total aluminium (Al_T), dissolved organic carbon (DOC), total organic nitrogen (TON), NH_4^+, and H^+ in precipitation (PR), deposition to the catchment soils (DEP), and terrestrial export via tributaries (TE) in the Čertovo catchment in the 1998–2017 hydrological years.

years. Terrestrial exports of NO_3^-, SO_4^{2-}, and Al_i were higher than inputs to the catchment soils by precipitation and throughfall deposition throughout the study period (Fig. 3). This change in ionic composition resulted in a significant terrestrial H^+ production of 44±13 meq. $m^{-2}.yr^{-1}$ on a catchment-area basis, and in permanently higher terrestrial exports than was the atmospheric H^+ input (Fig. 4H). This H^+ production, resulting from the H^+ mass balance (based on pH measurements) in precipitation, throughfall and tributaries, was in good concordance with H^+ production calculated from equation (8) as the sum of individual H^+ sources (terrestrial production of anions and removal of cations) and sinks (terrestrial production of cations) that averaged 45 $meq.m^{-2}.yr^{-1}$ from 1998–2017. Both estimates thus differed by

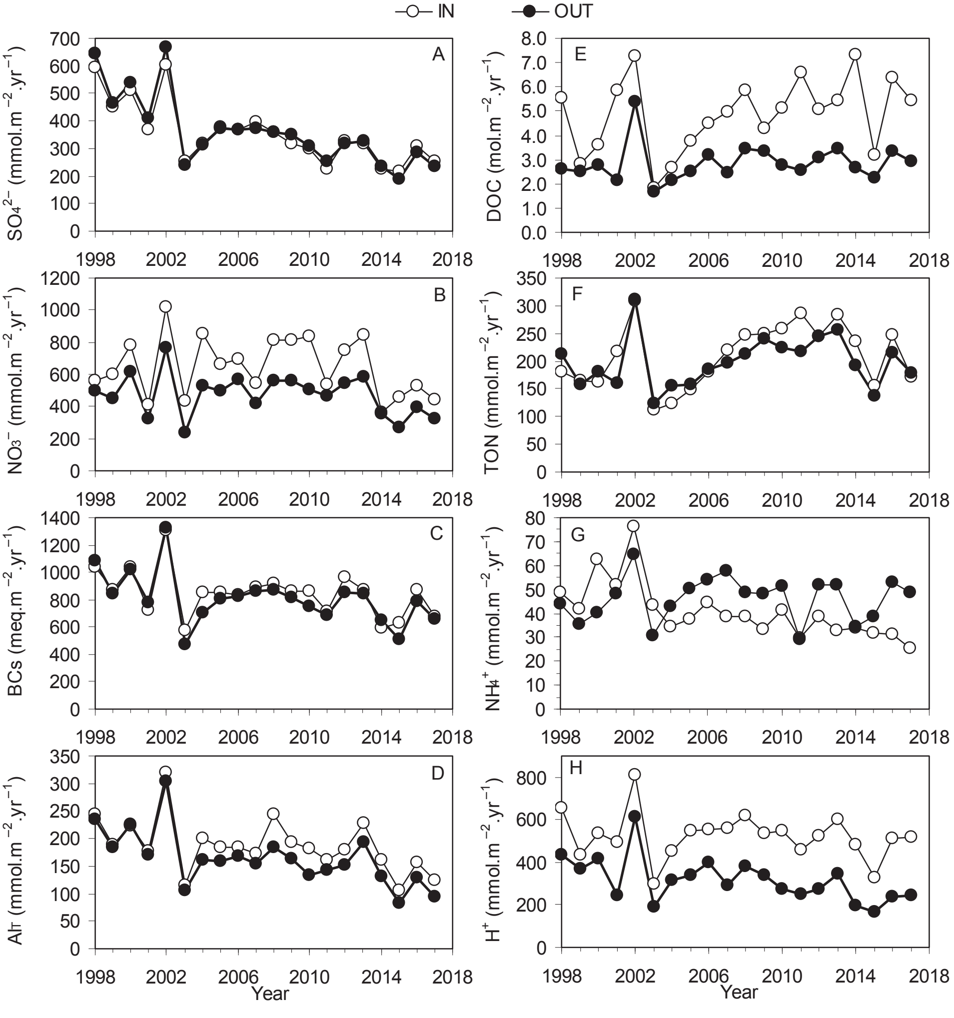

Fig. 4. Time series of annual fluxes (based on a lake area basis) of SO_4^{2-}, NO_3^-, base cations (BCs = sum of Ca^{2+}, Mg^{2+}, Na^+ and K^+), total aluminium (Al_T), dissolved organic carbon (DOC), total organic nitrogen (TON), NH_4^+, and H^+ in total input (IN, tributaries and precipitation) to and outlet (OUT) from Čertovo Lake in the 1998–2017 hydrological years.

<2% on average. The most important H^+ sources were net retention and nitrification of NH_4^+ (50 and 25 meq.m^{-2}.yr^{-1}, respectively), SO_4^{2-} production (leaching of 47 meq.m^{-2}.yr^{-1}), while terrestrial production of Al_i, Mg^{2+}, and Na^+ ions represented the most important H^+ sinks (45, 23, and 22 meq.m^{-2}.yr^{-1}, respectively).

Terrestrial exports of DOC and TON were lower than their deposition to the catchment soils (amended by contribution of canopy leaching to throughfall deposition), but were higher than their inputs via precipitation (Fig. 3). However, sources of DOC and TON in precipitation and throughfall are fundamentally different from their stream water sources. In contrast to DOC, terrestrial export of TP was even lower than its flux in precipitation, and Čertovo catchment was a net sink of deposited P, averaging 1.1 mmol.m^{-2}.yr^{-1} during this study (Table 3).

Element fluxes in lake

The in-lake processes caused reductions in NO_3^-, A^-, SO_4^{2-}, and Al_i fluxes (Table 4, Fig. 4) and a pH increase in the lake outlet compared to their inputs by tributaries and precipitation (4.5 *vs.* 4.3 on average; Table 2); i.e., the input H^+ flux decreased by ~40% from 524 to 316 meq.m^{-2}.yr^{-1} on a lake area basis (Table 4). The net in-lake H^+ removal (calculated on the basis of pH values in precipitation, tributaries and lake outlet) averaged 223 meq.m^{-2}.yr^{-1}. This value is not a simple difference between the input and output fluxes because it also includes a net change in H^+ storage in the lake (equation 2) that decreased by 15 meq.m^{-2}.yr^{-1} during the study. The pH-based estimate was similar to the H^+ removal calculated from equation (8) that averaged 234 meq.m^{-2}.yr^{-1}. Both estimates thus differed by <5% on average. The most important internal H^+ sinks were NO_3^-, A^- and SO_4^{2-} removals (184, 140, and 38 meq.m^{-2}.yr^{-1}, respectively), while Al_i transformations were the most important in-lake H^+ sources of 79 meq.m^{-2}.yr^{-1} on average (Table 4). In contrast to H^+, the lake was negligible sink for BCs (Fig. 4C), and was a net source of NH_4^+ in most years (Fig. 4G), with the long-term average production of 4 mmol.m^{-2}.yr^{-1}.

The lake was a net sink for all nutrients, removing on average 22% of TP, 36% of total N, 38% of DOC, and 13% of Si inputs (Table 4). Precipitation to the lake surface was the major SRP source, while its concentrations were <0.05 µmol.l^{-1} in tributaries (Table 2).

Discussion

Major processes affecting mass budget of protons in Čertovo catchment

Terrestrial transformations of inorganic N were the most important H^+ producing process in the Čertovo catchment (Table 3). This H^+ production due to N transformations was almost twofold higher than the maximum observed at 17 European forest sites (–5 to 46 meq.m^{-2}.yr^{-1}) by Forsius et al. (2005). The progressed stage of N-saturation of the Čertovo catchment and its low ability to retain the deposited inorganic N (on average only 23%) even after significantly reduced N deposition compared to the 1980s (Kopáček & Hruška 2010) thus contribute to the high proportion of NO_3^- in the total terrestrial export of strong acid anions (= SO_4^{2-} + NO_3^- + Cl^-) (Appendix 4), as also observed in other N-saturated areas (Rogora 2007). The terrestrial NO_3^- export usually increases after vegetation disturbances in catchments (Houlton et al. 2003, Huber et al. 2004, Huber 2005, McHale et al. 2007). The elevated NO_3^- leaching also occurred in Čertovo sub-catchments CT-IV to CT-VI that were affected by windthrows in 2007–2008 (Kopáček et al. 2016), and resulted in elevated terrestrial export of NO_3^- during 2008–2013 (Fig. 3B). This excess NO_3^- likely resulted from the mineralization of fresh dead biomass (litter and fine roots) and ceased N uptake by dead trees (Kaňa et al. 2015). Similar (and even more pronounced) ecosystem response to forest

Table 4. Mean (± standard deviation) element fluxes in total input to lake [*IN*, sum of atmospheric deposition on the lake surface (see precipitation in Table 3) and terrestrial export], output from lake (*OUT*), net in-lake production of water constituents (π_L), and the associated H^+ production/removal in Čertovo Lake in the 1998–2017 hydrological years.

	IN	**OUT**	π_L	**H^+ source**†
	mmol.m^{-2}.yr^{-1}			meq.m^{-2}.yr^{-1}
H^+	524±109	316±104	–223±58	
Ca^{2+}	103±28	101±31	–7±11	14±22
Mg^{2+}	133±26	126±27	–9±11	18±23
Na^+	298±55	275±58	–24±26	24±26
K^+	79±18	78±17	–1±6	1±6
NH_4^+	41±12	46±9	4±22	–4±22
NO_3^-	647±184	473±130	–184±57	–184±57
SO_4^{2-}	354±112	363±130	–19±26	–38±52
Cl^-	150±30	152±37	ND	
F^-	18±8	19±8	0±8	–0.8±10
HCO_3^-	3±14	0±0	–3±14	–3±14
DOC (A^-)	4875±1530	2861±766	–1875±1132	(–140±71)
TON	210±56	198±45	–140±71	
TP	1.8±0.5	1.4±0.3	–0.4±0.4	
Si	671±111	576±108	–91±67	
Al_T	187±49	164±50	–33±26	
Al_i (Al_i^{n+})	126±40	126±44	–14±23	(79±41)
Al_o	57±16	26±9	–30±14	
Al_p	4±2	12±3	11±13	
Fe_T	26±8	28±11	4±17	
Fe_i (Fe_i^{m+})	8±2	11±7	1±11	(–0.2±10)
Fe_o	16±6	8±3	–7±7	
Fe_p	2±2	9±4	10±15	

Explanations: Values are given on a lake-area basis; ND – not determined. Values of π_L were calculated from equation (2), data on the average annual change in storage of elements in the lake are not given. Positive values indicate net production, while negative values indicate net removal; for their annual values see Appendix 8. † Release of cations and removal of anions are proton-consuming processes, while removal of cations and release of anions are proton-producing reactions. One meq = mmol of charge. Sum of H^+ sources and sinks gives a net retention of 234 mmol.m^{-2}.yr^{-1}.

damage, manifested by elevated terrestrial NO_3^- exports, have occurred across the Bohemian Forest (Oulehle et al. 2013), especially in the catchment of Plešné Lake (Kopáček et al. 2017) and Rachelsee (Vrba et al. 2014), where the majority of mature Norway spruce stands were killed by bark beetle.

The release of SO_4^{2-} was two times higher than deposition to the catchment soils (46 vs. 23 mmol.m^{-2}.yr^{-1} on average) during the study (Table 3). The source of this extra SO_4^{2-} originated from S accumulated in soils during high atmospheric deposition in the 2nd half of the

20th century. The deposited SO_4^{2-} is retained in soils (i) partly by adsorption on Al and Fe hydroxides, especially as soils acidify and the positive charge of these hydroxides increases (e.g., Cosby et al. 1986, Kaňa & Kopáček 2005), and (ii) predominantly due to organic cycling of deposited SO_4^{2-} that is microbially reduced to S^0 or S^{-II} compounds and stored in soils (e.g., Novák et al. 2000, 2005). The reduced S is further used by S-oxidizing bacteria (and oxidized back to SO_4^{2-}) as an electron donor after aeration of the originally anoxic micro-sites (Clark et al. 2006). Despite the net annual terrestrial export of SO_4^{2-} decreased from ~49 to ~31 $meq.m^{-2}.yr^{-1}$ during the study period ($p < 0.001$), i.e., close to the prediction by MAGIC model (Majer et al. 2003, Oulehle et al. 2012), the H^+ fluxes remained almost stable (Fig. 3H). This disproportion resulted from the temporarilly elevated NO_3^- leaching from 2008–2013 (Fig. 3B), and importantly from the significantly ($p < 0.001$) increasing terrestrial DOC (and also A^-) export after 2003 (Fig. 3E). The decrease in terrestrial SO_4^{2-} production was mostly compensated for by significantly ($p < 0.001$) decreasing net terrestrial production of Al_i (from 47 to 26 $meq.m^{-2}.yr^{-1}$ between 1998–2002 and 2013–2017), manifested by the decreasing Al_T leaching (Fig. 3D). The water in lake tributaries thus remained strongly acidic, with pH ranging from 4.2–4.3 throughout this study (Appendix 4), despite decreasing leaching of SO_4^{2-} and Al_T (Fig. 3A,D).

The Cl^- behaved conservatively in the Čertovo catchment indicating balanced conditions in Cl^- retention and release in a long-term perspective (Tables 2 and 3). However, annual Cl^- fluxes in deposition (Apendix 3) and terrestrial export (Apendix 4) differed >10% during dry years (e.g., in 2003 and 2015), when Cl^- input exceeded its export. In contrast, higher Cl^- exports than inputs occurred in wet years. Chloride has been considered a conservative ion, with negligible retention in ecosystems, because annual Cl^- leaching from undisturbed catchments is usually similar to the total annual Cl^- input from atmospheric deposition (e.g., Peck & Hurle 1973), especially at sites where atmospheric Cl^- inputs exceed 17 $mmol.m^{-2}.yr^{-1}$ (Svensson et al. 2012). The average Cl^- deposition to the Čertovo soils of 15 $mmol.m^{-2}.yr^{-1}$ was close to this threshold (Appendix 3). On average 11% higher terrestrial export of Cl^- than its deposition also occurred from 2008–2011, i.e., in years following the partial damage of Čertovo forest in 2007 and 2008. This response was in concordance with other studies. For example, Kauffman et al. (2003) and Huber et al. (2004) have shown that a large amount of mineralisable chlorine is stored in the soil organic matter and may be leached as Cl^- from decaying litter and roots, and liberated from decomposing soil organic matter after forest damage.

Terrestrial export of Al_T decreased from ~30 to ~20 $mmol.m^{-2}.yr^{-1}$ during the study period (Fig. 3D) and was mostly associated with decreasing leaching of Al_i and its concentrations in tributaries (from 17–19 to 9 $\mu mol.l^{-1}$; Appendix 4). The decreased Al_i leaching (despite stable stream water pH; Fig. 3H) occurred due to decreasing leaching of SO_4^{2-} and represents the most important change in water recovery from acidification (Vrba et al. 2006). The Al_i leaching was the major terrestrial factor mitigating the net terrestrial H^+ production (Table 3).

Net terrestrial sources of base cations and organic acid anions

The interpretation of π_C* values for BCs (Table 3) is not very straightforward except for conservative Na^+. These values are related to BC deposition to the catchment soils that also includes canopy leaching (elements released during precipitation passing through the canopies), i.e., a part of their internal cycling between soils and vegetation. Thus calculated π_C* values suggest net Ca^{2+} and K^+ retention in soils and underestimate terrestrial Mg^{2+} production. The actual net terrestrial production of Ca^{2+}, Mg^{2+}, and K^+ (without the soil-vegetation exchange) can be estimated as the difference between their terrestrial exports and net atmospheric inputs to the catchment. Total deposition of conservative ion Na^+ was on average 1.87 fold higher than that of precipitation. The Na^+ exchange was negligible in Norway spruce canopies in the study catchment (Kopáček et al. 2009), hence, we can assume that its total (wet, dry, and horizontal) atmospheric input into the catchment was equal to the deposition to the catchment soils. Moreover, dry depositions of Ca^{2+}, Mg^{2+}, and K^+ are assumed to be similar to that of Na^+, due to the same physical size and aerodynamic properties of base cation-containing aerosols (Draaijers & Erisman 1995). Total atmospheric input of the rest of BCs can thus be roughly estimated from their precipitation fluxes, multiplied by a factor of 1.87. This provides net (without contribution of canopy exchange) atmospheric inputs of Ca^{2+}, Mg^{2+} and K^+ to the catchment of 11.2, 4.2, and 1.5 $mmol.m^{-2}.yr^{-1}$ and their 1998–2017 average terrestrial production of 0.8, 14.2, and 1.3 $mmol.m^{-2}.yr^{-1}$, respectively. The catchment was thus higher source of Mg^{2+} than Ca^{2+}, which is consistent with its almost one order of magnitude higher concentration in the Čertovo bedrock (Kopáček et al. 2002).

Similarly corrected for canopy leaching as BCs, the catchment was a net source of 18±13 $meq.m^{-2}.yr^{-1}$ A^-.

Net phosphorus retention in catchment soils

The Čertovo soils were a net sink for atmospherically deposited P. The TP fluxes averaged 0.7 and 1.2 $mmol.m^{-2}.yr^{-1}$ in precipitation and deposition to the catchment soils, respectively, while its average terrestrial export was 0.15 $mmol.m^{-2}.yr^{-1}$ (Table 3). The P pool in Čertovo soils has probably increased since their development (throughout Holocene), and the present average P concentration (catchment weighted mean for all soil horizons and soil types) is almost two fold higher than in the dominant (mica-schist) bedrock (24 *vs.* 13 $mmol.kg^{-1}$; Kopáček et al. 2002). The retained P is probably adsorbed on soil Al and Fe hydroxides that are responsible for high phosphate adsorption capacity of the Čertovo soils (11.9 $mol.m^{-2}$; Kaňa & Kopáček 2006). The present average P pool is about a half (~5.4 $mol.m^{-2}$) of the total phosphate adsorption capacity of the Čertovo soils (Kopáček et al. 2002), which suggests that soils may remain a net P sink for a long time even in future.

Major processes affecting element fluxes in Čertovo Lake

The in-lake H^+ neutralization was dominated by denitrification that reduced the input flux of NO_3^- by 28% on average (Table 4). Similar high importance of NO_3^- reduction on internal H^+ cycle was also observed in other acidified lakes with elevated NO_3^- inputs (Schindler 1986, Kelly et al. 1987). The settling (removal) velocity of NO_3^- calculated according to Kelly et al. (1987) averaged 4.4±1.7 $m.yr^{-1}$ in Čertovo Lake, and was within the range of similar data (2.8–12.7 $m.yr^{-1}$) reported for 20 European and North American lakes (Kelly et al. 1987, Kaste & Dillon 2003). The annual SO_4^{2-} retention in Čertovo Lake (5% on average) was within the range of data reported for lakes with water residence times <4 years (5–19%; Kelly et al. 1987, Thies 1997) and its mass transfer coefficient (also called "settling velocity") averaged 0.6±0.8 $m.yr^{-1}$. The SO_4^{2-} role in the internal H^+ neutralization was thus small during the study and will probably further decrease together with the decreasing in-lake SO_4^{2-} concentrations, anticipated by modelling (Majer et al. 2003, Oulehle et al. 2012). Most of the NO_3^- and SO_4^{2-} removal probably occurred in sediments, even though denitrification also could occur in the anoxic hypolimnion. The zone with depleted O_2 (<1 $mg.l^{-1}$) was, however, relatively thin in Čertovo Lake and only occurred in the deepest parts of the lake during winter and summer temperature stratification (Fig. 2; Kopáček et al. 2000a, 2001a).

The removal of A^-, the second most important in-lake H^+ neutralizing process after NO_3^- reduction (Table 4), mostly occurs in the epilimnion. This H^+ neutralizing process is associated with the partial photochemical degradation of allochthonous DOC (Kopáček et al. 2003, Porcal et al. 2010) that oxidizes DOC and produces biologically available small molecular weight compounds for bacterial growth (e.g., Wetzel et al. 1995). The DOC (and A^-) is thus photochemically and/or microbially oxidized to CO_2 and H_2O, removing one mole of H^+ per each equivalent of the oxidized A^-; e.g., for formic acid:

$$HCOO^- + H^+ + {}^1/_2O_2 = CO_2 + H_2O \qquad (9)$$

The role of A^- oxidation on in-lake H^+ neutralization will probably further increase due to almost generally increasing DOC leaching from European catchments recovering from atmospheric acidification (Monteith et al. 2007, Evans et al. 2012), which also occurs in the Bohemian and Bavarian Forest surface waters (Kopáček et al. 2013a, Beudert & Gietl 2015).

Photochemical degradation of allochthonous DOC and its increased availability for bacteria can explain the high proportion of bacteria in the total plankton biomass observed in Čertovo Lake (Vrba et al. 2003). Having a possibility to utilize the transformed allochthonous DOC, bacterial grow is not limited by availability of organic exudates from primary (algal) production, which is small in this oligotrophic lake due to low P inputs. The lower in-lake production of algal exudates than the photochemical and microbial degradation of DOC resulted in net DOC removal in Čertovo Lake (Fig. 4E). Photochemical cleaving of allochthonous organic N to NH_4^+ and NO_3^- (Porcal et al. 2014) was probably the major reason for net TON retention in the lake (Fig. 4F, Table 4).

Photochemical cleaving of DOC also significantly affects in-lake metal chemistry (Kopáček et al. 2003, Porcal et al. 2010) and was responsible for liberating ~50% of Al_o and Fe_o from their organic complexes as Al_i and Fe_i (Table 4). The Al_o and Fe_o concentrations were thus lower in the outlet than in the lake tributaries (Table 2) and the liberated metals contributed to their ionic forms, supplied by tributaries, in modifying in-lake H^+ budgets.

The higher output fluxes of NH_4^+ from Čertovo Lake than its input by tributaries and atmospheric deposition to the lake surface (Fig. 4G) resulted from internal NH_4^+ generation by dissimilatory processes in the hypolimnion (Fig. 2H). The major source of NH_4^+ for primary producers in the epilimnion is atmospheric deposition (Table 2). After its depletion, algae can utilize NO_3^- as an alternative source of reactive N (Procházková et al. 1970). The produced biomass settles and the organic matter is continuously microbially decomposed. The liberated NH_4^+ accumulates in the anoxic zone, but is usually rapidly nitrified in the oxic parts of water column in circum neutral lakes (Wetzel 2001). However, nitrification was likely suppressed in Čertovo Lake due to its strong acidification as described for North American lakes by Rudd & al. (1988). Consequently, the liberated NH_4^+ was not nitrified in Čertovo Lake, and entered its outlet after mixing to the whole water profile during spring and autumn overturns. The lake thus became the net NH_4^+ source in years when its dissimilative production in the hypolimnion exceeded its assimilation in the epilimnion and the water column was completely mixed.

Hydrolysis of Al_i (equation 10) was the most important in-lake acidity source, producing on average 79±41 meq.m^{-2}.yr^{-1} of H^+ (Table 4):

$$Al^{3+} + nH_2O = Al(OH)_n^{3-n} + nH^+ \qquad (10)$$

The hydrolysis occurs along pH gradients between the input and output water (Table 2), and between the lake surface and bottom (Fig. 2C), resulting in a decreasing positive charge of hydroxyl-Al complexes, and a net in-lake production of Al_p (mostly colloidal $Al(OH)_3$) (Kopáček et al. 2008). A part of this Al_p left the lake via outflow (11 mmol.m^{-2}.yr^{-1}), the rest (33 mmol.m^{-2}.yr^{-1}) was deposited in sediments (Table 4). A similar effect of Fe_i on the in-lake H^+ budget was negligible, due to its lower concentrations.

The formed colloidal Al hydroxides have large specific surfaces and a strong ability to bind orthophosphate from the liquid phase. Thus, orthophosphate liberated from the sedimenting organic matter by dissimilatory processes was removed from the liquid phase by adsorption on (or co-precipitation with) Al_p and transformed to PP (Kopáček et al. 2000c). This process explains low DP and SRP concentrations above the lake bottom despite elevated TP, but also HN_4^+ concentrations (Fig. 2H) from microbial decomposition of settling seston.

The annual removal of Si in Čertovo Lake averaged 91±67 $mmol.m^{-2}.yr^{-1}$. The reduction of dissolved Si in lakes is commonly associated with diatom production (Wetzel 2001). Pelagic diatoms are, however, absent in Čertovo Lake, but Chrysophyceae form an important portion of the phytoplankton biomass (Vrba et al. 2003, Nedbalová et al. 2006). The sedimentation of chrysophycean cysts and scales seems to be the most likely biological mechanism contributing to the Si depletion in the lake.

Conclusions

Despite substantial reduction of central European anthropogenic emission and the consequent deposition of S and N compounds since the late 1980s (Kopáček & Hruška, 2010), Čertovo Lake remains strongly acidic and its chemical and biological recovery from acidification is slow (Vrba et al. 2006, 2016). The H^+ production associated with N cycle (NH_4^+ assimilation and nitrification) and the excess SO_4^{2-} leaching (desorption and microbial oxidation of reduced S forms) play the most important role among the water acidifying processes in the lake catchment. The terrestrial export of SO_4^{2-} decreased by 50% during the last two decades, but this source of terrestrial acidity was partly replaced by (i) temporally elevated NO_3^- leaching from sub-catchments affected by windthrows in 2007 and 2008, (ii) continuously increasing leaching of organic acid anions as a response to decreasing SO_4^{2-} and NO_3^- deposition (Kopáček et al. 2013a), and (iii) decreased leaching of Al_i, from soils. Lake tributaries are thus strongly acidic, with pH between 4.1 and 4.5 (Table 2) and the depleted carbonate buffering system. The most important change in stream water recovery from acidification is decreasing Al_i concentration in the lake tributaries (Appendix 4) and output (Appendix 6).

The in-lake H^+ removal processes neutralize ~40% of the total (terrestrial and atmospheric) H^+ input into the lake. This internal acidity removal, however, increases lake water pH only slightly, from 4.3 to 4.5. Water leaving the whole Čertovo catchment–lake system thus remains significantly more acidic than precipitation (pH of ~5.0; Table 2). The most important in-lake neutralizing processes are NO_3^- reduction and A^- oxidation, while Al_i hydrolysis most importantly mitigates the H^+ decrease associated with the former processes. Changes in in-lake concentrations of SO_4^{2-}, BCs, and NH_4^+ only play minor roles in the internal H^+ balance (Table 4).

Results of this study suggest that chemical (and most probably also biological) recovery of Čertovo Lake will remain slow and may be even temporality reversed in future due to forest damages. The reason for such a high sensitivity of Čertovo catchment to acidification is low base saturation of soils that probably resulted from historical forest harvesting for wood, charcoal, and potash (Veselý 1994). The negative effect of acid rain thus could be strengthen by previous anthropogenic activities, highlighting the importance of cumulative stresses on ecosystems even in seemingly remote and protected areas.

Acknowledgements. We thank I. Procházka for long-term field sampling and the Šumava National Park authorities for their administrative support. This research and publication of results were supported by the

Transboundary Cooperation Program of the Czech Republic – Free State Bavaria (Target ERDF 2014–2020, Project 26 – Silva Gabreta Monitoring; data on ions) and the Czech Science Foundation (project No. P504-17-15229S; data on phosphorus and DOC).

REFERENCES

BEUDERT B. & GIETL G., 2015: Long-term monitoring in the Große Ohe catchment, Bavarian Forest National Park. *Silva Gabreta*, 21: 5–27.

CLARK J.M., CHAPMAN P.J., HEATHWAITE A.L. & ADAMSON J.K., 2006: Suppression of dissolved organic carbon by sulphate induced acidification during simulated droughts. *Environmental Science & Technology*, 40: 1776–1783.

COSBY B.J., HORNBERGER G.M., WRIGHT R.F. & GALLOWAY J.N., 1986: Modeling the effects of acid deposition: Controls of long-term sulfate dynamics by soil sulfate adsorption. *Water Resources Research*, 22: 1283–1302.

DRAAIJERS G.P.J. & ERISMAN J.W., 1995: A Canopy Budget Model to assess atmospheric deposition from throughfall measurements. *Water, Air and Soil Pollution*, 85: 2253–2258.

DOUGAN W.K. & WILSON A.L., 1974: The absorptiometric determination of aluminium in water. A comparison of some chromogenic reagents and the development of an improved method. *Analyst*, 99: 413–430.

DRISCOLL C.T., 1984: A procedure for the fractionation of aqueous aluminum in dilute acidic waters. *International Journal of Environmental Analytical Chemistry*, 16: 267–284.

EVANS C.D., JONES T.G., BURDEN A., OSTLE N., ZIELIŃSKI P., COOPER M.D.A., PEACOCK M., CLARK J.M., OULEHLE F., COOPER D. & FREEMAN C., 2012: Acidity controls on dissolved organic carbon mobility in organic soils. *Global Change Biology*, 18: 3317–3331.

FORSIUS M., KLEEMOLA S. & STARR M., 2005: Proton budgets for a monitoring network of European forested catchments: impacts of nitrogen and sulphur deposition. *Ecological Indicators*, 5: 73–83.

GOLTERMAN H.L. & CLYMO R.S., 1969: *Methods for chemical analysis of fresh waters*. Blackwell, Oxford, 172 pp.

HOULTON B.Z., DRISCOLL C.T., FAHEY T.J., LIKENS G.E., GROFFMAN P.M., BERNHARDT E.S. & BUSO D.C., 2003: Nitrogen dynamics in ice storm-damaged forest ecosystems: Implications for nitrogen limitation theory. *Ecosystems*, 6: 431–443.

HUBER C., 2005: Long lasting nitrate leaching after bark beetle attack in the highlands of the Bavarian Forest National Park. *Journal of Environmental Quality*, 34: 1772–1779.

HUBER C., BAUMGARTEN M., GÖTTLEIN A. & ROTTER V., 2004: Nitrogen turnover and nitrate leaching after bark beetle attack in mountainous spruce stands of the Bavarian Forest National Park. *Water, Air, and Soil Pollution: Focus*, 4: 391–414.

KAŇA J. & KOPÁČEK J., 2005: Sulphate sorption characteristics of the Bohemian Forest soils. *Silva Gabreta*, 11: 3–12.

KAŇA J. & KOPÁČEK J., 2006: Impact of soil sorption characteristics and bedrock composition on phosphorus concentrations in two Bohemian Forest lakes. *Water Air and Soil Pollution*, 173: 243–259.

KAŇA J., TAHOVSKÁ K., KOPÁČEK J. & ŠANTRŮČKOVÁ H., 2015: Excess of organic carbon in mountain spruce forest soils after bark beetle outbreak altered microbial N transformations and mitigated N-saturation. *PLoS ONE*, 10: e0134165.

KASTE Ø. & DILLON P.J., 2003: Inorganic nitrogen retention in acid-sensitive lakes in southern Norway and southern Ontario, Canada – a comparison of mass balance data with an empirical N retention model. *Hydrological Processes*, 17: 2393–2407.

KAUFFMAN S.J., ROYER D.L., CHANG S. & BERNER R.A., 2003: Export of chloride after clear-cutting in the Hubbard Brook sandbox experiment. *Biogeochemistry*, 63: 23–33.

KELLY C.A., RUDD J.W.M., HESSLEIN R.H, SCHINDLER D.W., DILLON P.J., DRISCOLL C.T., GHERINI S.A. & HECKY R.E., 1987: Prediction of biological acid neutralisation in acid–sensitive lakes. *Biogeochemistry*, 3: 129–140.

KOPÁČEK J. & HEJZLAR J., 1993: Semi-micro determination of total phosphorus in fresh waters with perchloric acid digestion. *International Journal of Environmental Analytical Chemistry*, 53: 173–183.

KOPÁČEK J., HEJZLAR J., PORCAL P., 2000a: Ionic fluxes in the Čertovo watershed–lake ecosystem the 1998 hydrological year. *Silva Gabreta*, 4: 117–133.

KOPÁČEK J., HEJZLAR J. & MOSELLO R., 2000b: Estimation of organic acid anion concentrations and evaluation of charge balance in atmospherically acidified colored waters. *Water Research*, 34: 3598–3606.

KOPÁČEK J., HEJZLAR J., BOROVEC J., PORCAL P. & KOTOROVÁ I., 2000c: Phosphorus inactivation by aluminum in the water column and sediments: A process lowering in-lake phosphorus availability in an acidified watershed–lake ecosystem. *Limnology and Oceanography*, 45: 212–225.

KOPÁČEK J., HEJZLAR J., KAŇA J. & PORCAL P., 2001a: Element budgets in three Bohemian Forest lakes and their watersheds in the 2000 hydrological year: I. Čertovo Lake. *Silva Gabreta*, 6: 35–52.

KOPÁČEK J., BOROVEC J., HEJZLAR J. & PORCAL P., 2001b: Parallel spectrophotometric determinations of iron, aluminum, and phosphorus in soil and sediment extracts. *Communications in Soil Science and Plant Analysis*, 32:

1431–1443.

KOPÁČEK J., KAŇA J., ŠANTRŮČKOVÁ H., PORCAL P., HEJZLAR J., PICEK T., ŠIMEK M. & VESELÝ J., 2002: Physical, chemical, and biochemical characteristics of soils in watersheds of the Bohemian Forest lakes: II. Čertovo and Černé Lakes. *Silva Gabreta*, 8: 63–63.

KOPÁČEK J., HEJZLAR J., KAŇA J., PORCAL P. & KLEMENTOVÁ S., 2003: Photochemical, chemical, and biological transformations of dissolved organic carbon and its impact on alkalinity production in acidified lakes. *Limnology and Oceanography*, 48: 106–117.

KOPÁČEK J. TUREK J., HEJZLAR J., KAŇA J. & PORCAL P., 2006. Element fluxes in watershed–lake ecosystems recovering from acidification: Čertovo Lake, the Bohemian Forest, 2001–2005. *Biologia*, 61: S413–S426.

KOPÁČEK J., HEJZLAR J. & NORTON S.A., 2008: Proton production by transformations of aluminium and iron in lakes. *Water Research*, 42: 1220–1228.

KOPÁČEK J., TUREK J., HEJZLAR J. & ŠANTRŮČKOVÁ H., 2009: Canopy leaching of nutrients and metals in a mountain spruce forest. *Atmospheric Environment*, 43: 5443–5453.

KOPÁČEK J. & HRUŠKA J., 2010: Reconstruction of acidic deposition in the catchments of Plešné and Čertovo lakes (the Bohemian Forest). *Silva Gabreta*, 16: 149–163.

KOPÁČEK J., TUREK J., HEJZLAR J. & PORCAL P., 2011: Bulk deposition and throughfall fluxes of elements in the Bohemian Forest (Central Europe) from 1998 to 2009. *Boreal Environment Research*, 16: 495–508.

KOPÁČEK J., COSBY B.J., EVANS C.D., HRUŠKA J., MOLDAN F., OULEHLE F., ŠANTRŮČKOVÁ H., TAHOVSKÁ K., WRIGHT R.F., 2013a: Nitrogen, organic carbon and sulphur cycling in terrestrial ecosystems: linking nitrogen saturation to carbon limitation of soil microbial processes. *Biogeochemistry*, 115: 33–51.

KOPÁČEK J., FLUKSOVÁ H., HEJZLAR J., KAŇA J., PORCAL P., TUREK J. & ŽALOUDÍK, J., 2013b: Chemistry of tributaries to Plešné and Čertovo lakes during 1998–2012. *Silva Gabreta*, 19: 105–137.

KOPÁČEK J., FLUKSOVÁ H., KAŇA J., PORCAL P., TUREK J. & ŽALOUDÍK J., 2013c: Chemical composition of atmospheric deposition in the catchments of Plešné and Čertovo lakes in 1998–2012. *Silva Gabreta*, 19: 1–23.

KOPÁČEK J., HEJZLAR J., KAŇA J., PORCAL P. & TUREK J., 2016: The sensitivity of water chemistry to climate in a forested, nitrogen-saturated catchment recovering from acidification. *Ecological Indicators*, 63: 196–208.

KOPÁČEK J., FLUKSOVÁ H., HEJZLAR J., KAŇA J., PORCAL P. & TUREK J., 2017: Changes in surface water chemistry caused by natural forest dieback in an unmanaged mountain catchment. *Science of the Total Environment*, 584–585: 971–981.

LIKENS G.E. & BORMANN F.H., 1995: *Biogeochemistry of a forested ecosystem, 2nd edition*. Springer-Verlag, New York, 159 pp.

MAJER V., COSBY B.J., KOPÁČEK J. & VESELÝ J., 2003: Modelling reversibility of central European mountain lakes from acidification: Part I – the Bohemian Forest. *Hydrology and Earth System Sciences*, 7: 494–509.

MCHALE M.R., BURNS D.A., LAWRENCE G.B. & MURDOCH P.S. 2007: Factors controlling soil water and stream water aluminum concentrations after a clearcut in a forested watershed with calcium-poor soils. *Biogeochemistry*, 84: 311–331.

MONTEITH D.T., STODDARD J.L., EVANS C.D., DE WIT H.A., FORSIUS M., HØGÅSEN T., WILANDER A., SKJELKVÅLE B.L., JEFFRIES D.S., VUORENMAA J., KELLER B., KOPÁČEK J. & VESELÝ J., 2007: Dissolved organic carbon trends resulting from changes in atmospheric deposition chemistry. *Nature*, 450: 537–540.

MOSELLO R., AMORIELLO T., BENHAM S., CLARKE N., DEROME J., DEROME K., GENOUW G., KOENIG N., ORRÙ A., TARTARI G., THIMONIER A., ULRICH E. & LINDROOS A.J., 2008: Validation of chemical analyses of atmospheric deposition on forested sites in Europe: 2. DOC concentration as an estimator of the organic ion charge. *Journal of Limnology*, 67: 1–14.

MURPHY J. & RILEY J. P., 1962: A modified single-solution method for the determination of phosphate in natural waters. *Analytica Chimica Acta,* 27: 31–36.

NEDBALOVÁ L., VRBA J., FOTT J., KOHOUT L., KOPÁČEK J., MACEK M. & SOLDÁN T., 2006: Biological recovery of the Bohemian Forest lakes from acidification. *Biologia*, 61: S453–S465.

NOVÁK M., KIRCHNER J.W., FOTTOVÁ D., PRECHOVÁ E., JAČKOVÁ I., KRÁM P. & HRUŠKA J., 2005: Isotopic evidence for processes of sulfur retention/release in 13 forested catchments spanning a strong pollution gradient (Czech Republic, central Europe). *Global Biogeochemical Cycles*, 19: GB4012.

NOVÁK M., KIRCHNER J.W., GROSCHEOVÁ H., HAVEL M., ČERNÝ J., KREJČÍ R. & BUZEK F., 2000: Sulfur isotope dynamics in two central European watersheds affected by high atmospheric deposition of SO_x. *Geochimica et Cosmochimica Acta*, 64: 367–383.

OULEHLE F., COSBY B.J., WRIGHT R.F., HRUŠKA J., KOPÁČEK J., KRÁM P., EVANS C.D. & MOLDAN F., 2012: Modelling soil nitrogen: The MAGIC model with nitrogen retention linked to carbon turnover using decomposer dynamics. *Environmental Pollution*, 165: 158–166.

OULEHLE F., CHUMAN T., MAJER V. & HRUŠKA J., 2013: Chemical recovery of acidified Bohemian lakes between 1984 and 2012: the role of acid deposition and bark beetle induced forest disturbance. *Biogeochemistry*, 116: 83–101.

PECK A.J. & HURLE D.H., 1973: Chloride balance of some farmed and forested catchments in southwestern Australia. *Water Resources Research*, 9: 648–657.

Porcal P., Amirbahman A., Kopáček J. & Norton S.A., 2010: Experimental photochemical release of organically bound aluminum and iron in three streams in Maine, USA. *Environmental Monitoring and Assessment*, 171: 71–81.

Porcal P., Kopáček J. & Tomková I., 2014: Seasonal photochemical transformations of nitrogen species in a forest stream and lake. *PLoS ONE*, 9: e116364.

Procházková L. & Blažka P., 1999: Chemistry and biology of the Bohemian Forest lakes in the early 1960s. *Silva Gabreta*, 3: 65–72.

Procházková L., 1960: Einfluss der Nitrate und Nitrite auf die Bestimmung des organischen Stickstoffs und Ammonimus im Wasser. *Archiv für Hydrobiologie*, 56: 179–185.

Procházková L., Blažka P. & Králová M., 1970: Chemical changes involving nitrogen metabolism in water and particulate matter during primary production experiments. *Limnology and Oceanography*, 15: 797–807.

Rogora M., 2007: Synchronous trends in N-NO_3 export from N-saturated river catchments in relation to climate. *Biogeochemistry*, 86: 251–268.

Rudd J.W.M., Kelly C.A., Schindler D.W. & Turner M.A., 1988: Disruption of the nitrogen cycle in acidified lakes. *Science*, 240: 1515–1517.

Schindler D.W., 1986: The significance of in-lake production of alkalinity. *Water Air and Soil Pollution*, 30: 931–944.

Šobr M. & Janský B., 2016: The morphometric parameters of glacial lakes in the Bohemian Forest. *Silva Gabreta*, 22: 31–61.

Stumm W. & Morgan J.J., 1981: *Aquatic Chemistry*. Willey, New York, 780 pp.

Svensson T., Lovett G.M. & Likens G.E., 2012: Is chloride a conservative ion in forest ecosystems? *Biogeochemistry*, 107:125–134

Svoboda M., Matějka K. & Kopáček J., 2006: Biomass and element pools of understory vegetation in the catchments of Čertovo Lake and Plešné Lake in the Bohemian Forest. *Biologia*, 61: S509–S521.

Thies H., 1997: A mass budget for the dystrophic Huzenbacher See (Black Forest, Germany). *Verhandlungen des Internationalen Vereinigung für Limnologie*, 26: 283–288.

Van der Perk M., 2006: *Soil and water contamination from molecular to catchment scale*, Taylor & Francis, London, 402 pp.

Veselý J., 1994: Investigation of the nature of the Šumava lakes: a review. *Časopis Národního Muzea, Praha, Řada Přírodovědná*, 163: 103–120.

Veselý J., Almquist-Jacobson H., Miller L.M., Norton S.A., Appleby P., Dixit A.S. & Smol J.P., 1993: The history and impact of air pollution at Čertovo Lake, southwestern Czech Republic. *Journal of Paleolimnology*, 8: 211–231.

Veselý J., Hruška J., Norton S.A. & Johnson C.E., 1998: Trends in water chemistry of acidified Bohemian lakes from 1984 to 1995: I. Major solutes. *Water Air and Soil Pollution*, 108: 107–127.

Vrba J., Kopáček J., Fott J., Kohout L., Nedbalová L., Pražáková M., Soldán T. & Schaumburg J., 2003: Long-term studies (1871–2000) on acidification and recovery of lakes in the Bohemian Forest (Central Europe). *Science of the Total Environment*, 310: 73–85.

Vrba J., Kopáček J., Bittl T., Nedoma J., Štrojsová A., Nedbalová L., Kohout L. & Fott J., 2006: A key role of aluminium in phosphorus availability, food web structure, and plankton dynamics in strongly acidified lakes. *Biologia*, 61: S441–S451.

Vrba J., Kopáček J., Fott J. & Nedbalová L., 2014: Forest die-back modified plankton recovery from acidic stress. *Ambio*, 43: 207–217.

Vrba J., Bojková J., Chvojka P., Fott J., Kopáček J., Macek M., Nedbalová L., Papáček M., Rádková V., Sacherová V., Soldán T. & Šorf M., 2016: Constraints on the biological recovery of the Bohemian Forest lakes from acid stress. *Freshwater Biology*, 61: 376–395.

Wetzel R.G., Hatcher P.G. & Bianchi T.S., 1995: Natural photolysis by ultraviolet irradiance of recalcitrant dissolved organic matter to simple substrates for rapid bacterial metabolism. *Limnology and Oceanography*, 40: 1369–1380.

Wetzel R.G., 2001: *Limnology. Lake and river ecosystems*. Academic Press, New York, 1006 pp.

Received: 23 May 2018
Accepted: 20 July 2018

Appendix 1. Water balance in Čertovo Lake and its catchment in hydrological years (from November 1997 to October 2017). Precipitation amount (H_{PR}, mm.yr^{-1}), deposition to the catchment soils (Q_{DEP}, mm.yr^{-1}; precipitation in the open area and throughfall in the forest), terrestrial export from catchment via all lake tributaries (Q_{TE}, mm.yr^{-1}), water output from lake (Q_{OUT}, mm.yr^{-1}), specific runoff from catchment–lake system (SR, l.km^{-2}.s^{-1}), and water residence time in lake (WRT, day).

	1998	**1999**	**2000**	**2001**	**2002**	**2003**	**2004**	**2005**	**2006**	**2007**	**2008**	**2009**	**2010**	**2011**	**2012**	**2013**	**2014**	**2015**	**2016**	**2017**
H_{PR}	1580	1359	1625	1464	2080	1057	1167	1368	1413	1401	1410	1253	1289	1108	1268	1220	1085	780	1298	962
Q_{DEP}	1418	1406	1564	1527	2018	1156	1150	1375	1424	1599	1564	1481	1362	1350	1447	1505	1335	1045	1594	1257
Q_{TE}	1347	1050	1321	1108	1926	763	1057	1238	1334	1358	1422	1374	1236	1150	1401	1446	1051	909	1329	1144
Q_{OUT}	1364	1071	1319	1100	1920	755	1078	1217	1301	1334	1376	1329	1200	1094	1351	1386	1024	802	1262	1085
SR	43.2	34.0	41.8	34.9	60.9	24.0	34.2	38.6	41.3	42.3	43.6	42.1	38.0	34.7	42.8	43.9	32.5	25.4	40.0	34.4
WRT	557	708	575	690	395	1005	704	623	583	569	552	571	633	694	562	548	741	946	601	699

Appendix 2. Precipitation amount (H_{PR}) and volume weighted mean composition of precipitation (C_{PR}) in the catchment of Čertovo Lake in hydrological years between November 1997 and October 2017. Units: µmol.l^{-1}, except for H_{PR} (m^3.m^{-2}.yr^{-1}) and pH. ND – not determined.

	1998	**1999**	**2000**	**2001**	**2002**	**2003**	**2004**	**2005**	**2006**	**2007**	**2008**	**2009**	**2010**	**2011**	**2012**	**2013**	**2014**	**2015**	**2016**	**2017**
H_{PR}	1.58	1.36	1.63	1.46	2.08	1.06	1.14	1.37	1.41	1.40	1.41	1.25	1.29	1.11	1.27	1.22	1.09	0.78	1.30	0.96
pH	4.77	4.74	4.89	4.82	4.78	4.90	4.78	4.73	4.86	4.85	5.00	5.21	5.05	5.28	5.29	5.04	4.97	5.06	5.11	5.08
H^+	17.1	18.4	12.9	15.3	16.6	12.6	16.7	18.8	13.7	14.0	9.9	6.2	9.0	5.2	5.1	9.2	10.8	8.8	7.7	8.3
Ca^{2+}	4.2	5.4	7.1	6.1	5.8	10.3	4.5	4.7	3.6	3.7	4.2	5.8	4.2	7.3	5.3	4.6	3.7	4.6	2.9	3.2
Mg^{2+}	1.6	2.3	1.8	2.1	1.4	2.3	1.3	1.2	1.0	2.2	1.3	1.0	1.0	1.1	1.2	1.5	1.4	1.7	0.8	1.0
Na^+	8.6	10.5	11.4	8.9	6.9	11.7	7.6	6.9	5.4	6.3	7.4	5.2	4.5	4.9	8.3	5.4	5.9	7.1	3.4	4.7
K^+	7.4	10.5	6.5	4.3	2.6	9.6	2.0	2.4	2.3	2.8	2.3	2.4	1.8	2.2	1.8	2.0	2.1	2.4	1.1	1.3
NH_4^+	30.2	28.8	28.3	31.6	30.2	35.3	25.1	24.5	26.6	23.4	24.5	22.3	26.9	24.6	23.8	23.5	29.1	29.5	21.6	25.0
NO_3^-	25.5	32.0	31.6	29.5	30.5	28.3	29.7	26.9	24.3	22.9	23.1	18.2	20.1	22.4	20.4	22.8	24.1	26.6	19.5	22.8
SO_4^{2-}	15.2	17.0	13.9	13.0	12.3	13.6	10.7	11.9	9.2	9.4	9.0	7.4	7.9	7.1	6.6	7.6	9.9	8.1	5.9	6.2
Cl^-	9.1	8.9	9.3	8.5	6.3	11.9	7.7	6.4	5.3	6.6	6.9	4.7	4.1	4.6	9.2	5.5	5.9	6.7	3.5	4.0
F^-	ND	ND	0.2	0.2	1.8	0.6	0.3	1.0	0.5	0.2	0.3	0.3	0.2	0.2	0.3	1.5	0.5	0.6	0.2	0.4
HCO_3^-	0.0	0.0	1.2	1.7	1.0	17.0	0.1	1.7	2.1	4.1	2.1	6.8	6.8	7.6	4.5	2.7	3.1	5.0	2.8	3.4
DOC	108	108	80	126	87	124	90	90	115	124	97	90	106	82	84	82	83	99	65	75
POC	ND	ND	ND	ND	ND	81.5	22.4	25.9	38.0	29.7	56.5	40.9	20.7	32.3	20.5	24.4	24.5	17.7	20.5	17.0
DON	14.2	8.6	7.3	12.7	8.4	7.2	7.4	10.1	12.6	14.5	14.4	16.8	14.7	8.8	13.4	8.1	7.3	9.6	7.5	8.0
PON	6.3	19.0	3.2	5.6	4.8	11.1	4.9	2.5	5.4	10.1	7.5	6.6	7.5	10.0	5.5	5.9	6.3	6.5	4.0	4.7
TP	0.43	0.53	0.48	0.90	0.39	1.18	0.34	0.49	0.94	0.56	0.65	0.87	0.58	0.47	0.27	0.34	0.27	0.75	0.23	0.23
PP	0.27	0.39	0.26	0.33	0.23	0.56	0.20	0.19	0.44	0.27	0.18	0.36	0.23	0.34	0.14	0.17	0.21	0.22	0.14	0.16
SRP	0.08	0.11	0.20	0.43	0.07	0.56	0.08	0.24	0.32	0.23	0.35	0.39	0.07	0.09	0.09	0.13	0.03	0.34	0.06	0.04
Si	ND	ND	0.36	0.49	0.27	0.29	0.29	0.29	0.29	0.29	0.29	0.29	0.29	0.29	0.29	0.29	0.29	0.29	0.29	0.29
Al_T	0.2	0.3	0.3	0.2	0.1	0.5	0.3	0.2	0.2	0.2	0.2	0.3	0.2	0.2	0.6	1.1	1.3	1.1	1.0	0.2

Appendix 3. Deposition amount (Q_{DEP}) and volume weighted mean composition of atmospheric deposition to the catchment soils (C_{DEP}; precipitation in the open area and throughfall in the forest; calculated from equation 7) in the catchment of Čertovo Lake in hydrological years between November 1997 and October 2017. Units: µmol.l^{-1}, except for Q_{DEP} (m^3.m^{-2}.yr^{-1}) and pH. ND – not determined.

	1998	**1999**	**2000**	**2001**	**2002**	**2003**	**2004**	**2005**	**2006**	**2007**	**2008**	**2009**	**2010**	**2011**	**2012**	**2013**	**2014**	**2015**	**2016**	**2017**
Q_{DEP}	1.42	1.41	1.56	1.53	2.02	1.16	1.13	1.38	1.42	1.60	1.56	1.48	1.36	1.35	1.45	1.51	1.34	1045	1594	1257
pH	4.46	4.59	4.68	4.72	4.69	4.78	4.61	4.60	4.77	4.68	4.76	4.91	4.84	5.02	5.12	4.87	4.91	4.87	5.00	4.93
H^+	34.9	25.7	20.8	19.2	20.2	16.6	24.4	25.4	17.0	20.8	17.4	12.4	14.5	9.6	7.6	13.5	12.3	13.5	9.9	11.7
Ca^{2+}	12.9	12.4	12.7	10.8	9.6	14.4	11.9	11.0	8.5	9.3	10.1	8.6	10.4	8.8	10.1	10.0	9.5	10.8	6.9	7.7
Mg^{2+}	4.6	7.0	4.8	4.4	4.6	4.8	4.6	4.3	3.2	4.7	3.9	2.9	3.8	3.8	4.0	4.2	5.0	5.3	3.2	3.9
Na^+	14.1	13.9	16.7	12.5	10.6	13.5	13.3	12.3	11.0	13.8	13.5	9.6	10.5	10.6	11.8	9.6	13.7	15.4	9.1	11.6
K^+	27.1	27.0	24.6	27.2	16.7	32.3	23.8	22.7	20.8	19.7	18.1	16.3	23.2	28.0	20.1	20.2	28.9	29.4	22.3	21.8
NH_4^+	36.5	30.8	30.7	35.3	31.4	53.5	32.8	34.3	37.9	30.5	32.2	33.1	38.4	37.2	41.3	33.1	50.4	43.1	26.6	32.2
NO_3^-	39.4	44.1	43.8	38.7	38.2	53.4	47.4	45.2	39.4	38.8	38.5	34.3	38.6	37.4	39.2	41.7	50.2	52.0	32.0	36.7
SO_4^{2-}	29.1	24.2	21.7	20.3	17.4	20.6	18.5	20.0	15.2	15.9	14.5	11.6	13.9	10.7	10.0	12.3	17.0	13.2	7.8	7.7
Cl^-	17.1	15.2	15.8	13.3	12.7	17.7	18.0	14.8	12.6	15.9	15.6	11.8	12.8	13.6	16.6	11.7	16.6	19.5	11.5	14.5
F^-	ND	ND	0.5	0.5	1.9	0.7	0.8	0.9	1.0	1.0	0.7	0.5	0.3	0.4	1.3	1.8	1.2	1.5	0.7	1.2
HCO_3^-	0.0	0.0	0.8	1.2	1.4	20	0.4	0.3	3.3	0.7	1.0	2.9	4.2	9.5	7.8	1.5	5.8	6.8	5.7	4.5
DOC	624	503	467	590	379	498	557	494	459	491	503	456	627	623	474	453	534	550	469	533
POC	ND	ND	ND	ND	ND	169	110	103	108	186	97	108	75	61	11	23	21	25	75	92
DON	29.0	23.6	20.8	12.2	23.2	21.4	19.8	24.7	28.8	27.2	39.1	49.0	26.6	35.9	27.6	27.2	21.5	10.5	15.1	19.1
PON	ND	ND	ND	ND	11.9	23.8	11.4	9.6	20.7	12.4	10.1	11.5	8.4	8.5	7.4	3.5	2.2	2.5	6.0	6.9
TP	0.63	0.85	0.91	0.85	0.51	1.38	0.71	0.63	1.06	0.86	0.99	1.05	0.77	1.22	0.70	0.61	0.83	0.87	0.95	0.92
PP	0.31	0.52	0.54	0.60	0.38	0.45	0.50	0.43	0.62	0.60	0.48	0.60	0.50	0.94	0.42	0.39	0.62	0.61	0.60	0.51
SRP	0.19	0.12	0.23	0.10	0.03	0.47	0.09	0.09	0.32	0.12	0.30	0.30	0.10	0.12	0.15	0.10	0.07	0.14	0.22	0.30

Appendix 4. Mean annual discharge (Q_{TE}) and discharge and period weighted mean concentrations of water constituents (C_{TE}) of terrestrial export via all tributaries to Čertovo Lake (calculated from equation 3) in hydrological years between November 1997 and October 2017. Units: µmol.l^{-1}, except for Q_{TE} (m^3.m^{-2}.yr^{-1}, given on a catchment-area basis) and pH. ND – not determined.

	1998	**1999**	**2000**	**2001**	**2002**	**2003**	**2004**	**2005**	**2006**	**2007**	**2008**	**2009**	**2010**	**2011**	**2012**	**2013**	**2014**	**2015**	**2016**	**2017**
Q_{TE}	1.35	1.05	1.32	1.11	1.93	0.76	1.04	1.24	1.33	1.36	1.42	1.37	1.24	1.15	1.40	1.45	1.05	0.91	1.33	1.14
pH	4.20	4.27	4.27	4.24	4.26	4.29	4.24	4.24	4.26	4.26	4.24	4.28	4.23	4.27	4.29	4.25	4.21	4.32	4.29	4.22
H^+	63.6	53.7	53.5	58.1	55.0	51.0	56.9	57.3	54.6	54.6	58.2	52.4	59.1	53.9	50.7	55.6	61.3	48.4	51.5	60.9
Ca^{2+}	12.3	15.2	13.2	10.3	12.3	11.4	13.5	10.9	10.8	9.2	10.0	9.7	10.7	8.7	10.2	9.0	8.0	9.8	8.6	7.9
Mg^{2+}	16.4	15.3	15.6	12.4	13.4	14.8	17.9	14.7	12.8	14.0	13.5	13.6	16.1	13.5	15.1	13.3	12.2	15.5	14.2	13.1
Na^+	35.9	36.9	35.2	31.6	29.4	32.3	34.6	32.1	28.4	33.3	30.1	29.0	29.8	29.7	32.6	26.1	28.9	34.6	34.8	30.7
K^+	7.8	9.6	8.9	6.6	8.5	9.8	11.1	7.7	7.7	6.4	8.2	7.7	9.3	8.1	8.1	9.0	5.9	7.4	7.6	6.9
NH_4^+	0.1	0.3	1.7	0.7	0.9	1.1	0.8	0.4	0.7	0.6	0.4	0.5	0.8	0.3	0.8	0.4	0.3	1.3	0.3	0.1
NO_3^-	52.5	71.9	75.2	44.8	67.7	72.2	107	69.3	67.9	51.3	74.8	78.3	89.7	61.0	71.0	77.1	44.2	65.3	51.9	50.1
SO_4^{2-}	57.8	55.6	50.4	43.0	41.0	42.9	40.0	40.1	36.2	38.5	33.1	30.5	31.8	25.6	30.9	29.3	27.7	31.8	31.0	29.3
Cl^-	18.4	16.0	16.1	15.9	13.3	15.0	20.3	16.8	13.3	16.9	17.6	13.0	14.5	15.4	16.1	14.0	14.6	14.0	15.0	14.8
F^-	2.4	1.6	1.2	2.2	3.1	1.8	2.5	2.5	2.1	1.9	2.2	1.1	1.2	1.7	1.6	2.6	1.6	2.0	1.7	1.6
DOC	545	347	358	697	502	304	338	402	445	481	548	417	548	772	486	506	937	465	647	641
POC	ND	ND	ND	ND	ND	17	1.7	19	6	3	17	23	8	16	10	8	20	14	13	11
DON	13.9	16.6	14.9	23.6	17.4	16.4	15.0	13.0	15.2	17.5	19.9	20.3	24.4	29.5	20.5	22.4	24.0	21.1	22.6	17.8
PON	ND	ND	ND	ND	2.48	0.31	0.00	1.60	0.58	1.09	0.95	1.62	1.06	1.96	0.91	2.73	4.65	0.31	1.29	1.22
TP	0.16	0.08	0.09	0.18	0.11	0.08	0.08	0.08	0.10	0.10	0.12	0.09	0.12	0.22	0.11	0.13	0.27	0.08	0.13	0.10
PP	0.05	0.00	0.04	0.04	0.03	0.00	0.02	0.02	0.04	0.02	0.03	0.03	0.04	0.06	0.01	0.02	0.09	0.00	0.02	0.01
SRP	0.02	0.02	0.02	0.03	0.01	0.01	0.03	0.02	0.03	0.03	0.03	0.02	0.03	0.04	0.03	0.03	0.04	0.02	0.04	0.04
Si	79.5	74.5	69.7	76.3	66.1	77.7	80.3	75.0	69.3	75.6	67.3	67.2	70.7	74.5	76.6	62.0	65.6	87.3	82.9	84.2
Al_T	24.6	24.5	23.1	21.7	22.6	20.4	26.3	20.2	18.9	17.4	23.4	19.2	20.0	19.2	17.5	21.4	20.8	15.9	16.0	14.8
Al_i	17.6	19.5	17.5	12.9	16.2	15.8	19.7	13.1	12.4	10.9	15.7	14.3	13.8	11.6	12.6	13.8	10.5	9.9	9.1	9.0
Al_o	6.5	4.5	5.6	8.5	6.1	4.3	6.2	6.6	6.1	6.2	7.1	4.4	5.6	6.4	4.2	7.7	9.6	5.7	6.7	5.5
Fe_T	2.9	2.0	2.0	3.9	2.6	1.9	1.8	2.7	2.2	2.8	2.7	2.3	2.8	4.7	2.8	2.6	4.5	2.5	3.5	3.3
Fe_i	0.8	0.8	1.0	1.2	0.6	0.7	0.6	0.5	0.5	0.9	0.9	1.1	1.2	1.2	1.0	0.9	0.9	0.9	1.0	0.9
Fe_o	1.8	0.9	1.0	2.5	1.7	1.2	1.1	1.7	1.6	1.8	1.6	1.1	1.5	2.8	1.5	1.6	3.1	1.4	2.3	2.1

Appendix 5. Total water input (Q_{IN}) and mean annual composition of water input (terrestrial export and precipitation to the lake surface) to Čertovo Lake in hydrological years between November 1997 and October 2017. Units: µmol.l^{-1}, except for Q_{IN} (m^3.m^{-2}.yr^{-1}, given on a lake-area basis) and pH. ND – not determined.

	1998	1999	2000	2001	2002	2003	2004	2005	2006	2007	2008	2009	2010	2011	2012	2013	2014	2015	2016	2017
Q_{IN}	11.4	9.0	11.3	9.6	16.2	6.6	8.7	10.4	11.2	11.3	11.8	11.3	10.3	9.5	11.5	11.8	8.8	7.4	11.0	9.3
pH	4.24	4.32	4.32	4.29	4.30	4.35	4.29	4.28	4.31	4.31	4.28	4.33	4.28	4.32	4.34	4.29	4.26	4.35	4.33	4.26
H^+	57.2	48.4	47.7	51.6	50.0	44.8	51.7	52.3	49.4	49.5	52.4	47.3	52.9	48.2	45.7	50.8	55.0	44.2	46.4	55.5
Ca^{2+}	11.2	13.7	12.3	9.6	11.5	11.2	12.4	10.1	9.9	8.6	9.3	9.3	9.9	8.5	9.6	8.6	7.4	9.2	7.9	7.4
Mg^{2+}	14.4	13.3	13.6	10.8	11.9	12.8	15.7	12.9	11.3	12.5	12.1	12.2	14.2	12.0	13.6	12.1	10.9	14.1	12.6	11.9
Na^+	32.1	32.9	31.8	28.1	26.5	29.1	31.0	28.8	25.5	30.0	27.4	26.4	26.6	26.8	29.9	23.9	26.0	31.7	31.1	28.0
K^+	7.7	9.8	8.5	6.3	7.8	9.7	9.9	7.0	7.0	6.0	7.5	7.1	8.4	7.5	7.5	8.3	5.4	6.9	6.8	6.3
NH_4^+	4.2	4.6	5.5	5.4	4.7	6.6	4.0	3.6	4.0	3.4	3.3	2.9	4.0	3.1	3.3	2.8	3.9	4.3	2.8	2.7
NO_3^-	48.8	65.9	68.9	42.5	62.9	65.2	97.1	63.8	62.4	47.8	68.6	71.6	81.0	56.5	65.4	71.5	41.7	61.3	48.1	47.3
SO_4^{2-}	51.9	49.8	45.1	38.4	37.3	38.2	36.1	36.4	32.8	34.9	30.2	27.9	28.8	23.5	28.2	27.1	25.5	29.3	28.1	26.9
Cl^-	17.1	14.9	15.1	14.8	12.4	14.5	18.7	15.4	12.3	15.6	16.4	12.1	13.2	14.1	15.4	13.1	13.5	13.3	13.7	13.7
F^-	2.1	1.4	1.0	1.8	2.9	1.6	2.2	2.3	1.9	1.7	2.0	1.0	1.1	1.6	1.4	2.5	1.4	1.8	1.5	1.4
DOC	484	311	318	610	449	275	306	361	404	437	494	381	493	692	442	462	831	427	579	583
POC	ND	ND	ND	ND	ND	27	4	20	10	6	22	25	10	17	11	10	21	14	14	12
DON	14.0	15.4	13.8	21.9	16.3	14.9	14.0	12.6	14.9	17.1	19.2	19.9	23.2	27.1	19.7	20.9	21.9	19.9	20.8	16.8
PON	1.90	6.91	0.46	0.86	2.78	2.03	0.21	1.72	1.20	2.20	1.74	2.17	1.87	2.89	1.42	3.06	4.86	0.96	1.60	1.57
TP	0.15	0.15	0.15	0.29	0.14	0.26	0.11	0.14	0.21	0.16	0.18	0.18	0.18	0.25	0.13	0.15	0.27	0.15	0.14	0.11
PP	0.04	0.06	0.07	0.09	0.05	0.09	0.05	0.04	0.09	0.05	0.05	0.06	0.06	0.09	0.02	0.04	0.11	0.02	0.04	0.03
SRP	0.03	0.03	0.04	0.09	0.02	0.10	0.03	0.05	0.07	0.06	0.07	0.06	0.04	0.05	0.04	0.04	0.04	0.06	0.05	0.04
Si	68.5	63.3	59.7	64.7	57.6	65.4	69.8	65.2	60.6	66.3	59.4	59.8	61.9	65.8	68.2	55.6	57.5	78.1	73.2	75.6
Al_T	21.3	20.9	19.8	18.4	19.8	17.3	22.9	17.6	16.5	15.3	20.6	17.1	17.5	17.0	15.6	19.3	18.4	14.3	14.3	13.3
Al_i	15.2	16.6	15.0	11.0	14.2	13.3	17.1	11.4	10.8	9.6	13.8	12.7	12.1	10.3	11.2	12.4	9.2	8.9	8.0	8.0
Al_o	5.6	3.8	4.8	7.2	5.3	3.6	5.4	5.8	5.4	5.4	6.3	3.9	4.9	5.6	3.8	6.9	8.4	5.1	5.9	5.0
Fe_T	2.6	1.7	1.7	3.3	2.2	1.6	1.5	2.3	1.9	2.4	2.4	2.0	2.5	4.1	2.5	2.3	4.0	2.2	3.1	2.9
Fe_i	0.7	0.7	0.8	1.0	0.6	0.6	0.6	0.4	0.4	0.8	0.8	1.0	1.0	1.1	0.9	0.8	0.8	0.8	0.9	0.8
Fe_o	1.5	0.7	0.8	2.2	1.5	1.0	0.9	1.5	1.4	1.6	1.4	1.0	1.3	2.4	1.3	1.4	2.8	1.3	2.0	1.9

Appendix 6. Water output (Q_{OUT}) and mean annual composition of water output from Čertovo Lake (C_{OUT}) in hydrological years between November 1997 and October 2017 Units: µmol.l^{-1}, except for Q_{OUT} (m^3.m^{-2}.yr^{-1}, given on a lake-area basis) and pH. ND – not determined.

	1998	1999	2000	2001	2002	2003	2004	2005	2006	2007	2008	2009	2010	2011	2012	2013	2014	2015	2016	2017
Q_{OUT}	11.4	8.9	11.0	9.2	16.0	6.3	8.6	10.1	10.8	11.1	11.5	11.1	10.0	9.1	11.2	11.5	8.5	6.7	10.5	9.0
pH	4.42	4.39	4.42	4.58	4.41	4.51	4.44	4.47	4.43	4.58	4.47	4.52	4.56	4.57	4.61	4.53	4.64	4.60	4.65	4.56
H^+	38.2	41.1	38.1	26.5	38.5	30.7	36.3	33.7	37.0	26.4	33.5	30.5	27.5	27.2	24.4	29.8	23.1	25.2	22.6	27.3
Ca^{2+}	12.6	12.9	12.2	11.5	12.0	10.1	10.4	10.2	10.9	9.7	9.8	8.7	8.8	8.7	8.6	8.3	8.6	7.4	8.3	7.6
Mg^{2+}	14.8	14.5	13.5	12.5	12.6	11.3	13.1	12.3	11.2	12.2	11.5	11.5	12.4	12.4	12.5	12.2	12.4	13.0	12.1	11.8
Na^+	30.9	30.4	32.7	29.7	26.4	25.2	26.5	26.7	24.5	26.4	26.0	25.9	25.6	26.1	26.5	25.2	27.1	27.9	27.0	27.1
K^+	9.5	9.1	9.2	7.2	7.6	7.9	8.7	7.7	7.8	7.0	7.3	7.4	7.4	7.6	7.4	7.3	7.4	7.5	7.3	6.9
NH_4^+	3.9	4.0	3.7	5.3	4.1	4.9	5.0	5.0	5.0	5.2	4.3	4.4	5.2	3.2	4.6	4.5	4.0	5.8	5.0	5.4
NO_3^-	43.7	50.2	55.9	35.0	48.1	38.2	61.0	49.2	52.8	37.4	48.9	50.7	51.0	51.4	48.2	50.7	41.6	39.8	37.3	35.7
SO_4^{2-}	56.9	52.0	49.2	45.0	41.6	38.3	36.4	36.8	34.0	33.7	31.6	31.5	31.1	27.6	28.2	28.3	27.6	28.1	27.0	26.2
Cl^-	18.3	16.1	16.3	15.4	15.8	13.4	17.5	16.3	13.7	15.2	15.4	13.9	13.7	13.8	14.8	13.2	14.4	14.4	14.3	14.1
F^-	2.4	1.9	1.3	2.1	2.7	1.3	2.0	2.3	1.8	1.9	1.9	1.1	1.1	1.4	1.1	2.2	1.9	2.7	1.7	1.6
DOC	232	280	254	231	337	268	246	250	296	223	301	302	275	282	272	299	311	335	317	324
POC	ND	ND	ND	ND	ND	64	48	48	50	48	54	79	49	37	22	20	18	53	52	46
DON	14.2	12.7	12.9	13.3	12.7	12.9	13.2	11.3	12.7	13.1	13.1	17.0	18.3	19.6	17.4	17.3	16.0	16.8	16.1	15.9
PON	4.5	4.9	3.6	4.1	6.9	6.7	4.8	4.2	4.4	4.7	5.4	4.8	4.0	4.3	4.3	4.9	6.5	3.8	4.5	3.8
TP	0.14	0.15	0.11	0.16	0.16	0.20	0.13	0.14	0.14	0.13	0.15	0.16	0.13	0.15	0.12	0.13	0.16	0.15	0.13	0.12
PP	0.08	0.08	0.06	0.12	0.10	0.14	0.09	0.09	0.09	0.09	0.09	0.12	0.07	0.09	0.08	0.09	0.11	0.10	0.09	0.09
SRP	0.01	0.01	0.01	0.01	0.01	0.02	0.02	0.04	0.03	0.03	0.03	0.02	0.03	0.04	0.03	0.03	0.03	0.03	0.02	0.01
Si	59.2	58.2	56.7	58.2	55.1	53.8	56.6	55.5	50.3	56.3	54.6	53.0	55.7	59.7	57.2	53.7	57.3	63.4	61.1	65.9
Al_T	20.7	20.6	20.5	18.5	19.0	16.9	18.6	15.8	15.5	13.8	16.1	14.9	13.5	15.6	13.6	16.8	15.5	12.4	12.4	10.4
Al_i	17.4	17.7	17.0	14.7	14.6	12.5	14.1	11.9	11.0	10.7	12.4	11.6	10.6	12.2	11.0	12.3	11.1	8.0	7.6	7.0
Al_o	2.6	2.4	2.7	2.3	3.4	2.7	3.3	2.6	3.2	2.1	2.5	2.2	1.6	1.7	1.3	2.9	3.0	3.2	2.9	2.0
Fe_T	3.2	2.6	2.2	3.3	4.5	3.4	2.9	2.5	2.0	2.7	2.6	2.8	2.5	2.5	2.7	2.2	2.2	3.1	2.7	2.4
Fe_i	1.6	0.8	0.9	1.7	2.1	0.4	1.4	1.0	1.0	1.2	1.0	1.0	1.0	0.9	0.9	0.5	0.7	0.8	0.6	0.5
Fe_o	0.6	0.9	0.8	0.7	1.3	0.4	0.8	0.9	0.8	0.7	1.0	1.0	0.8	0.8	0.8	0.8	0.5	1.1	0.8	0.8

Appendix 7. Net production of water constituents in the catchment of Čertovo Lake (π_C* calculated from equation 1) in hydrological years between November 1997 and October 2017. Units: µmol.l⁻¹. Positive values indicate net production, while negative values indicate net removal. ND – not determined.

	1998	**1999**	**2000**	**2001**	**2002**	**2003**	**2004**	**2005**	**2006**	**2007**	**2008**	**2009**	**2010**	**2011**	**2012**	**2013**	**2014**	**2015**	**2016**	**2017**
H^+	27	19	29	32	34	26	30	29	36	30	39	39	43	43	43	42	46	33	40	48
Ca^{2+}	–1.3	–1.4	–1.8	–4.6	2.3	–11	0.6	–1.3	1.7	–1.7	–1.1	0.4	–0.7	–1.7	–0.3	–1.4	–4.2	–2.7	0.3	–0.6
Mg^{2+}	12	6	10	6	9	7	13	10	9	8	9	10	12	9	11	9	6	9	10	9
Na^+	21	18	15	14	18	12	20	18	17	17	15	19	18	17	20	16	11	17	24	18
K^+	–21	–27	–20	–31	–9	–39	–15	–17	–15	–17	–12	–10	–16	–25	–13	–12	–31	–26	–19	–17
NH_4^+	–38	–41	–35	–48	–32	–80	–35	–38	–40	–35	–35	–35	–42	–43	–42	–34	–64	–48	–32	–35
NO_3^-	11	13	23	–8	28	–9	56	19	26	6	32	41	47	17	31	34	–20	6	13	10
SO_4^{2-}	27	23	25	15	23	12	20	18	20	20	17	18	16	13	21	17	6	17	22	21
Cl^-	0.5	–4.3	–2.7	–2.4	0.0	–12	0.7	0.4	–0.2	–1.8	0.5	0.3	0.4	–0.5	–1.0	1.8	–6.5	–8.4	1.2	–1.1
F^-	1.5	1.6	0.6	2.2	1.1	0.7	1.7	1.4	1.0	0.8	1.4	0.6	0.8	1.3	0.2	0.7	0.0	0.3	0.8	0.2
DOC	–113	–326	–195	–116	104	–451	–268	–146	–44	–97	–5	–75	–143	40	–4	34	258	–167	85	56
POC	ND	ND	ND	ND	–1	–239	–118	–95	–110	–217	–89	–94	–75	–55	–1	–16	–7	–16	–77	–90
DON	–17	–15	–10	–1	–7	–16	–7	–14	–16	–15	–23	–33	–5	–13	–8	–6	–3	9	5	–3
PON	ND	ND	ND	ND	–10	–36	–13	–9	–22	–13	–10	–11	–8	–8	–7	–1	2	–3	–6	–6
TP	–0.5	–1.1	–1.0	–1.0	–0.4	–2.0	–0.7	–0.6	–1.0	–0.9	–1.0	–1.0	–0.7	–1.2	–0.6	–0.5	–0.8	–0.9	–1.0	–0.9
PP	–0.3	–0.7	–0.6	–0.8	–0.4	–0.7	–0.5	–0.5	–0.6	–0.7	–0.5	–0.6	–0.5	–1.0	–0.4	–0.4	–0.7	–0.7	–0.7	–0.6
Si	79	75	68	76	66	78	80	75	69	76	67	67	71	74	76	62	66	87	83	84
Al_T	24	24	23	22	23	20	26	20	19	17	23	19	20	19	17	21	21	16	16	15
Al_i	18	20	17	13	16	16	20	13	12	11	16	14	14	12	13	14	10	10	9	9
Al_o	6.5	4.5	5.6	8.5	6.1	4.3	6.2	6.6	6.1	6.2	7.1	4.4	5.6	6.4	4.2	7.7	9.6	5.7	6.7	5.5
Fe_T	2.0	2.0	2.0	3.9	2.6	1.9	1.8	2.7	2.2	2.8	2.7	2.3	2.8	4.7	2.8	2.6	4.5	2.5	3.5	3.3
Fe_i	0.8	0.8	1.0	1.2	0.6	0.7	0.6	0.5	0.5	0.9	0.9	1.1	1.2	1.2	1.0	0.9	0.9	0.9	1.0	0.9
Fe_o	1.2	0.9	1.0	2.5	1.7	1.2	1.1	1.7	1.6	1.8	1.6	1.1	1.5	2.8	1.5	1.6	3.1	1.4	2.3	2.1

Appendix 8. Net production of water constituents in Čertovo Lake (π_L, calculated from equation 2) in hydrological years between November 1997 and October 2017. Units: µmol.l^{-1}. Positive values indicate net production, while negative values indicate net removal. ND – not determined.

	1998	**1999**	**2000**	**2001**	**2002**	**2003**	**2004**	**2005**	**2006**	**2007**	**2008**	**2009**	**2010**	**2011**	**2012**	**2013**	**2014**	**2015**	**2016**	**2017**
H^+	–22	–20	–17	–35	–9	–34	–13	–17	–19	–25	–18	–20	–22	–34	–19	–23	–39	–24	–22	–27
Ca^{2+}	–0.4	–0.8	1.0	–0.4	–2.2	–0.4	–1.5	–1.3	0.7	–0.2	–0.6	0.6	–2.3	–0.7	–0.3	–0.3	0.8	–2.8	–0.4	–2.2
Mg^{2+}	0.1	0.0	–1.0	0.1	–2.0	–0.7	0.1	–1.9	–0.9	0.0	–2.6	–0.6	–1.4	–0.6	–0.6	–0.6	1.3	–4.0	–1.6	–0.4
Na^+	0.2	–3.7	0.3	0.3	–4.1	–3.8	–3.3	–3.3	–2.2	–3.6	–2.8	–5.0	0.3	–2.4	–2.6	–0.7	2.5	–5.9	–8.0	0.9
K^+	3.3	–5.0	4.4	–1.6	–0.6	–1.2	–0.4	–0.9	0.9	0.0	–0.1	–0.7	–0.8	–0.1	–0.2	0.0	0.9	–0.3	–0.8	–0.3
NH_4^+	1.1	–1.7	–1.2	0.0	–3.4	2.0	–0.3	1.3	0.4	2.8	0.9	–0.3	1.1	–3.3	3.7	0.0	3.6	–0.5	1.8	1.6
NO_3^-	–10	–20	–17	–13	–16	–28	–27	–17	–18	–11	–21	–23	–21	–12	–13	–24	–9	–38	–18	–20
SO_4^{2-}	–0.6	–2.2	1.7	–6.3	–6.3	–2.9	0.0	–3.6	–1.5	–2.4	–2.3	0.1	0.4	–2.9	0.1	–0.6	0.4	–3.5	–3.2	–1.3
Cl^-	ND	ND	ND	ND	ND	ND	ND	ND	ND	ND	ND	ND	ND	ND	ND	ND	ND	ND	ND	ND
F^-	0.3	0.5	0.3	0.2	–1.1	1.7	0.5	0.1	–1.1	0.8	–0.4	–1.4	0.0	1.2	0.1	0.1	–0.2	0.2	–0.6	0.6
DOC	–103	–187	–82	–333	–54	–107	–154	–83	–76	–229	–231	–41	–297	–420	–148	–97	–537	–305	–246	–198
POC	ND	ND	ND	ND	ND	88	39.7	–25	80	54	109	–15	–63	41	17	–17	32	23	89	57
DON	5.7	–3.1	–2.2	–6.2	–4.9	–11	–5.1	5.5	–6.5	–5.0	–2.8	1.1	–3.2	–10	7.4	–17	–9.0	2.9	–11.1	8.2
PON	4.0	–3.6	3.6	0.5	0.4	11	1.7	–1.2	9.6	3.0	–2.2	6.3	0.9	3.5	–2.6	7.4	4.7	–4.0	3.0	1.4
TP	–0.04	–0.12	–0.04	–0.07	–0.03	–0.09	0.02	–0.05	0.01	–0.06	–0.05	0.01	–0.11	–0.11	0.01	–0.03	–0.08	–0.06	–0.01	0.01
PP	0.02	–0.03	0.00	0.04	0.04	0.05	0.00	0.04	0.08	–0.02	–0.01	0.07	0.00	0.05	0.05	–0.01	0.10	0.03	0.06	0.07
SRP	–0.07	–0.02	0.00	–0.06	–0.03	–0.09	0.03	–0.03	–0.03	–0.05	–0.05	–0.02	0.00	–0.03	–0.02	0.00	–0.03	–0.05	–0.04	–0.05
Si	–9.9	–6.1	–6.1	–11	–4.8	–11	–14	–13	–15	–11	–5.4	–18	6.9	–11	–17	–1.4	1.5	–25.2	–5.4	–9.4
Al_T	–1.2	–2.4	–1.6	–3.3	–2.8	–1.3	–6.7	–2.8	–3.8	0.0	–9.2	–4.4	–3.8	0.6	–0.1	–4.4	–4.7	–7.8	–2.2	–5.8
Al_i	–1.3	0.3	0.7	–3.0	–1.4	–2.0	–7.1	0.3	–1.9	2.3	–5.1	–2.8	0.0	3.6	–2.1	–1.4	–0.5	–2.0	–2.3	–2.4
Al_o	–0.5	–2.9	–2.2	–4.2	–1.8	–2.1	–2.0	–3.2	–3.2	–2.7	–4.8	–2.4	–3.9	–5.5	–0.2	–3.1	–6.0	–2.3	–2.7	–4.2
Fe_T	1.7	–1.4	3.0	0.5	1.3	5.6	–1.3	0.3	1.6	–1.9	0.8	0.8	–2.1	0.1	–1.0	2.0	–2.3	–1.5	0.7	0.5
Fe_i	–0.3	–0.5	2.4	–1.9	1.5	0.5	–0.1	0.1	1.5	0.2	–0.6	0.7	–0.4	0.5	–0.9	–0.2	0.5	–1.6	0.5	–1.2
Fe_o	–0.3	–0.4	0.0	–1.2	0.1	–0.2	–0.9	–0.5	0.0	–1.1	–0.4	–0.6	–0.5	–1.8	–0.6	–0.6	–2.9	0.9	–1.1	–1.8

Silva Gabreta	vol. 24	p. 115–147	Vimperk, 2018

Fluxes of ecologically important solutes in the Plešné catchment–lake system from 2000–2017

Jiří Kopáček*, Josef Hejzlar, Jiří Kaňa, Petr Porcal & Jan Turek

Biology Centre CAS, Institute of Hydrobiology, Na Sádkách 7, 37005 České Budějovice, Czech Republic
* jkopacek@hbu.cas.cz

Abstract
Fluxes of major ions and nutrients were measured in the catchment–lake system of atmospherically acidified Plešné Lake between 2000 and 2017 hydrological years. The system has been recovering from acidification since the late 1980s. Bark beetle killed ~90% of mature Norway spruce trees in the catchment from 2004–2008 and all dead biomass was left in the catchment. The average water outflow from the system was 1087±232 mm.yr^{-1} (i.e., 34±7 l.km^{-2}.s^{-1}) and the water residence time in the lake averaged 338±70 days during 2000–2017. The Plešné catchment was an average net source of H$^+$ (35±18 meq.m^{-2}.yr^{-1}) throughout the study. The most important H$^+$ sources were net release of NO$_3^-$ and SO$_4^{2-}$ (76 and 37 meq.m^{-2}.yr^{-1}, respectively) and retention of NH$_4^+$ in soils (41 meq.m^{-2}.yr^{-1}), while terrestrial production of Al$_i$ and base cations represented the most important H$^+$ sinks (53 and 78 meq.m^{-2}.yr^{-1}, respectively). The maximum terrestrial H$^+$ production of 58 meq.m^{-2}.yr^{-1} occurred after the tree dieback (an average for 2006–2010). The in-lake biogeochemical processes reduced the incoming H$^+$ by ~65% (i.e., neutralized on average 267 meq.m^{-2}.yr^{-1} H$^+$ on a lake-area basis), and reached maximum values of 359 meq.m^{-2}.yr^{-1} on average from 2006–2010. The NO$_3^-$ and SO$_4^{2-}$ reductions and photochemical and microbial oxidation of organic acid anions (A$^-$) were the most important H$^+$ neutralizing processes (395, 25, and 151 meq.m^{-2}.yr^{-1}, respectively), while hydrolysis of Al$_i$ was the dominant H$^+$ generating process (243 meq.m^{-2}.yr^{-1}). The H$^+$ concentrations in the lake have started to decrease since 2009, because inputs of NO$_3^-$ and A$^-$ have remained high enough to neutralize H$^+$ by NO$_3^-$ reduction and A$^-$ oxidation, while H$^+$ production by Al$_i$ hydrolysis has decreased due to decreasing terrestrial Al$_i$ export. The changes in composition of tributaries after the tree dieback thus caused rapid pH increase to >5 and a reestablishment of the carbonate buffering system in Plešné Lake.

Key words: recovery from acidification, nitrogen, sulphur, organic carbon, aluminium, base cations, phosphorus, pH

INTRODUCTION

Plešné Lake is the most productive among the glacial lakes in the Bohemian Forest (VRBA et al., 2003, 2016). After sparse historical studies from the end of the 19th century (FRIČ 1874) and the early 1960s (PROCHÁZKOVÁ & BLAŽKA 1999), the limnology of Plešné Lake has become the subject of regular monitoring since 1984 (VESELÝ et al. 1998a, b). The historical data on chemical and biological research of Plešné Lake were summarized by VESELÝ (1994) and HEJZLAR et al. (1998). The lake was atmospherically acidified already in the early 1960s (pH <5.4) and acidification progressed until the middle 1980s, when pH ranged between 4.4 and 4.7 (VESELÝ et al. 1998a). The lake has been recovering from acidification since the late 1980s (MAJER et al. 2003). HEJZLAR et al. (1998) performed the first complex limnological study of Plešné Lake including water and sediment chemistry and biota. Since 2000, regular research on the lake has been further intensified, focusing on fluxes of major ions within the whole catchment–lake system, including water-sediment and soil-water interactions, and in-lake nutrients cycles (e.g., KOPÁČEK et al. 2001a, 2004, 2006, KAŇA et al. 2013, 2015).

Scientific interest in Plešné Lake further increased in the middle 2000s, when bark beetle killed most of mature spruce trees in its catchment. Since the tree dieback, element leaching from soils and lake water chemistry have started to change (Oulehle et al. 2012, Kopáček et al. 2017). The aim of this paper is to (i) evaluate major sources and sinks of acidity in the terrestrial and aquatic parts of the Plešné catchment–lake system in the 2000–2017 period using mass budget study on major ions and nutrients, (ii) evaluate their changes after the onset of tree dieback in 2004, and (iii) compare how major fluxes of elements differ from those in Čertovo catchment–lake system (Kopáček et al. 2018b), a similar acidified ecosystem in the same mountain area, but with predominately healthy forest and lower terrestrial phosphorus export. For this purpose, we review and synthesize already published studies on element fluxes in the Plešné catchment–lake system, recalculate previous mass balances of elements (Kopáček et al. 2001a, 2006) using new data on lake and catchment characteristics (Šobr & Janský 2016, Kopáček et al. 2017), and supplement them with unpublished data.

MATERIALS AND METHODS

Site description

Plešné Lake is situated near the Czech-Austrian border at 13°52' E, 48°47' N, and an elevation of 1087 m a.s.l. It is a dimictic, oligotrophic lake of glacial origin, with surface area of 7.2 ha and maximum depth of 17.7 m. The lake volume is 553×10^3 m^3, of which 48%, 33%, 18%, and 1% are in the 0–5 m, 5–10 m, 10–15 m, and deeper than 15 m layers, respectively (Šobr & Janský 2016). Plešné Lake is fishless at present, with recovering plankton and littoral communities. Acid-tolerant species of green algae, dinoflagellates, and filamentous cyanobacteria dominate in phytoplankton biomass, while two abundant copepods and scarce pelagic rotifers form the current zooplankton (Vrba et al. 2003, 2016). Littoral and submerged macrophytes (*Carex rostrata, Isoëtes echinospora*) were sparse 1–2 decades ago, but their area rapidly increased during the last decade and reached ~0.28 ha in 2016 (Čtvrtlíková et al. 2016). Anoxia occurs regularly in the PL hypolimnion during both winter and summer stratification periods (Kopáček et al. 2004). Plešné Lake has two surface tributaries (PL-I and PL-II) and one known subsurface inlet (PL-IV) (Fig. 1). The PL-III tributary was subsurface until 2001, when the PL water level was decreased by ~0.5 m after a reconstruction of its outlet and a short inlet into the lake has appeared.

The Plešné catchment (67 ha including the lake) is steep, with a maximum elevation gradient of 288 m. The bedrock consists of granite (Veselý, 1994). The catchment is covered with ~0.2 m deep leptosol (38%), and ~0.45 m deep podsol (29%) or dystric cambisol (27%); the rest is bare rocks (5%) and wetlands (~1%). Fine soil is rich in sand (~75%) and low in clay (~2%), and its catchment-weighted-mean pool is 92 $kg.m^{-2}$ (<2 mm, dry weight soil fraction). Soil pH ($CaCl_2$ extractable) is low, with minimum values of 2.5–3.1 in A-horizons and maximum (3.2–4.4) in the deepest mineral horizons. The mean effective cation exchange capacity of the soils was 129 $meq.kg^{-1}$ (NH_4Cl and KCl extractable) in 2000, of which 15% was base saturated and the remaining was dominated by exchangeable Al^{3+} (57%) and protons (28%) (Kopáček et al. 2002).

In 2000, mature Norway spruce forest (*Picea abies*) covered ~90% of the Plešné catchment, was dominated by healthy trees, and dead trees (~7% of all adult trees) occupied <3% of the forest area in small patches distributed over the whole catchment (Kopáček et al. 2013a, 2017). The rest of vegetation cover (in steep slopes) was dominated by grass (*Calamagrostis villosa*) and fern (*Athyrium distentifolium*). Blueberry (*Vaccinium myrtillus*) and fern formed the dominant understory vegetation in forest in 2004 (Svoboda et al. 2006). Forest in Plešné catchment has been damaged by a bark beetle (*Ips typographus*) outbreak since the

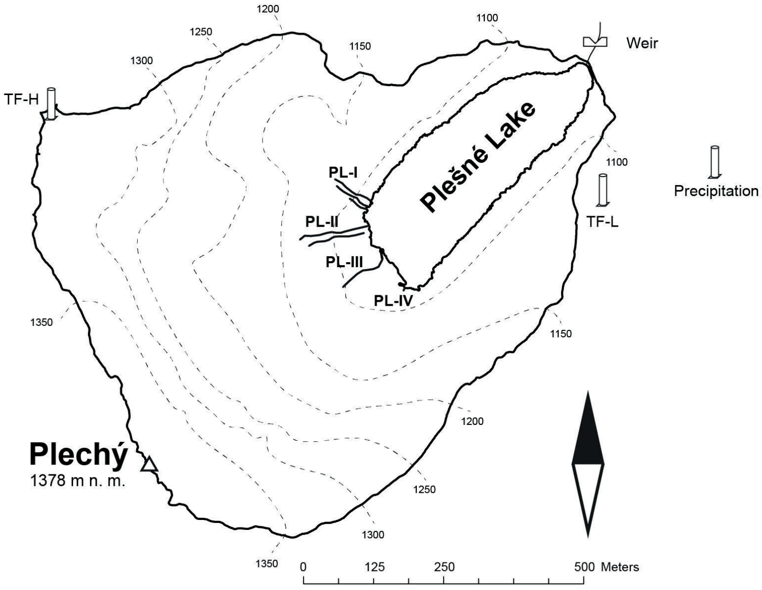

Fig. 1. Map of the Plešné Lake catchment with the locations of sampling and measuring sites (tributaries, PL-I to PL-IV; outlet equipped with weir; precipitation in treeless area; and throughfall at low and high elevation plots, TF-L and TF-H, respectively).

summer of 2004 (northwest part with the PL-I and PL-II sub-catchments; Fig. 1) and around 2006 (the rest of the catchment). Most of trees died within 2–3 years after the onset of infestation in the individual catchment parts. The trees lost most needles during first several months after the infestation. Then, they have been continuously losing twigs, bark, and branches until the end of this study, and were continuously broken (but not uprooted) by winds. Most of the trees died by 2009. In 2013, 88% of the original ~17,700 adult spruce trees in the PL catchment were dead, 66% were broken, and 93% of the Plešné forest area lost more than 80% of its original healthy trees. All dead biomass was left in the catchment (Kopáček et al. 2013a, 2017).

Water sampling and analyses

Precipitation was sampled in a treeless area (2 samplers; 13.871 E, 48.776 N) at an elevation of 1087 m, close to the lake catchment (Fig. 1). Throughfall was sampled at two forest plots (9 samplers each) at low elevation of 1122 m (TF-L; 13.868 E, 48.775 N; situated close to the lake) and high elevation of 1334 m (TF-H; 13.855 E, 48.777 N; situated close to the summit). Both throughfall plots were located in flat areas in mature Norway spruce forests (>150 years old). The TF-H and TF-L plots have been affected by a bark beetle outbreak since the summers of 2004 and 2006, respectively, and all trees above the collectors died within 2–3 years of infestation. By 2015, all the original adult trees were already broken by winds at both plots. Rain was regularly sampled in two-week intervals (May to October). Snow was sampled in two to four-week intervals (November to April). Samples were pre-filtered through a 200 µm polyethylene sieve to remove coarse particles, either during collecting (rain collectors were equipped with a sieve) or immediately after melting the snow from the winter collectors. Then, samples were stored in the dark at 4°C and subsamples for analysis of nitrogen and phosphorus forms were frozen (–20°C). Samples were analysed within <3 weeks after sampling. For more details see Kopáček et al. (2013b).

Samples from lake tributaries were taken in approximately three-week intervals (more frequently during the snowmelt period) from November 1999 to October 2017, except for the PL-IV tributary that was sampled from January 2000. Samples were taken near the inlets to the lakes, except for subsurface tributaries that were sampled in a shallow artificial well (PL-IV) and in a small natural cave (PL-III during 1998–2001). The water discharge of surface tributaries was estimated by means of a stop-watch and calibrated bucket at small natural waterfalls or rapids. In sub-catchments containing several tributaries in close proximity (PL-I and PL-II), an integrated sample was taken with sample volumes proportional to the discharge of the individual streams. Samples were immediately filtered through a 40-µm polyamide sieve to remove coarse particles re-suspended from the streambed during sampling. For more details see Kopáček et al. (2013a).

Samples from lake outlet were taken biweekly (weekly during the snowmelt period) and immediately filtered through a 200-µm polyamide sieve to remove zooplankton and coarse particles. The discharge from the lake was continuously monitored using a gauge-recorder (part of an MS16 automatic weather station; J. Fiedler, České Budějovice; readings in 15-minute intervals) at a weir situated ~20 m downstream of the lake (Fig. 1). A water column profile (5 depths equally distributed between the surface and bottom) was sampled at the deepest part of the lake each October.

Methods for water analyses were identical to those used for water samples in the Čertovo catchment–lake system (Kopáček et al. 2018b). For abbreviations of individual water constituents and other methodological details see Table 1. Equivalent concentrations (one equivalent is one mole of charge) of ionic Al (Al_i) and Fe (Fe_i), i.e, Al_i^{n+} and Fe_i^{m+} (µeq.l^{-1}) were obtained from their molar concentrations and the average charges of Al hydroxocomplexes (n) and Fe hydroxocomplexes (m), respectively. The n and m values were estimated from the theoretical distribution of ionization fractions of aqueous Al and Fe hydroxocomplexes, respectively, at the sample pH (Stumm & Morgan 1981), neglecting F^- and SO_4^{2-} complexes (Kopáček et al. 2000a). Concentrations of organic acid anions (A^-, µeq.l^{-1}) in stream and lake water were calculated from pH and concentrations of DOC and organic Al and Fe forms (Al_o and Fe_o) according to Kopáček et al. (2000a). Concentrations of A^- in precipitation and throughfall were calculated from the empirical relationship of A^- (µeq.l^{-1}) = 4×DOC (mg.l^{-1}) according to Mosello et al. (2008) and Kopáček et al. (2009). The reliability of the analytical results was controlled by means of an ionic balance approach, a comparison between measured and calculated conductivities (Kopáček et al., 2000a), and a standard sample, which was melted and assayed with each series of samples. The differences between the sum of cations and the sum of all anions (including A^-) were <±10% of the total ionic content in individual precipitation and throughfall samples, and <±4% for the annual volume weighted mean concentrations. Similarly, the differences between the sums of cations and anions (including Al_i^{n+}, Fe_i^{m+} and A^-) were <±5% of the total ionic concentration in the individual samples of stream and lake water. At higher differences, samples were re-analysed. For these ion balance controls, a half of detection limit was used when measured concentrations were lower than this limit (Table 1).

Mass balance and net terrestrial and aquatic production of water constituents

Mass balance of chemical constituents in the Plešné catchment and lake was based on previous studies (Kopáček et al. 2001a, 2004, 2006) and was calculated for individual hydrological years from November 1 to October 31 according to equations (1) and (2), respectively:

$$Q_{DEP}C_{DEP} + \pi_C = Q_{TE}C_{TE} + \Delta M_C \qquad (1)$$

Table 1. Methods used for the determination of individual elements and nutrient forms and their abbreviations.

Abbreviation	Explanation	Assessment
ANC, HCO_3^-	Acid neutralizing capacity, bicarbonate	Gran titration (Tacussel in 1997–2011, then Radiometer). ANC = HCO_3^- for ANC >0 µmol.l^{-1}; HCO_3^- = 0 for ANC ≤ 0 µmol.l^{-1}.
H^+ (pH)	Proton concentration	pH electrode (combined, Radiometer)
NH_4^+, Ca^{2+}, Mg^{2+}, Na^+, K^+, NO_3^-, Cl^-, SO_4^{2-}, F^-	Major cations and anions	Ion chromatography (Thermo Separation Products in 1997–2000, Dionex IC25 in 2001–2011, then Dionex ICF-3000). Detection limits for ions were 0.1–0.4 µmol.l^{-1}.
Si	Dissolved reactive silicon	Molybdate method (Golterman & Clymo 1969).
Al_T, Al_i, Al_o, Al_p	Total, ionic, organically bound, and particulate Al	Fractionation according to Driscoll (1984), colorimetry (Dougan & Wilson 1974) throughout 1997–2017; detection limit of 0.1 µmol.l^{-1}. Al_i = dissolved Al – Al_o. Al_p = Al_T – dissolved Al. Dissolved Al = Al_i + Al_o.
Fe_T, Fe_i, Fe_o, Fe_p	Total, ionic, organically bound, and particulate Fe	Fractionation according to Driscoll (1984), colorimetry (Kopáček et al. 2001b) throughout 1997–2017; detection limit of 0.3 µmol.l^{-1}. Fe_i = dissolved Fe – Fe_o. Fe_p = Fe_T – dissolved Fe. Dissolved Fe = Fe_i + Fe_o.
DOC	Dissolved organic C	LiquiTOC analyser (Foss-Heraeus, Germany) in 1997–1999 and Shimadzu analysers TOC 5000A in 2000–2015 and then TOC-L; detection limit of <4.0 µmol.l^{-1}.
POC	Particulate organic C	Analysed on glass-fiber filters (pore size of 0.4 µm) in TOC analysers (Foss-Heraeus LiquiTOC, Shimadzu TOC 5000A/SSM, and Elementar vario Micro cube in 1997–1999, 2000–2015, and 2016–2017, respectively).
TON, DON, PON	Total organic N, dissolved organic N, particulate organic N.	Kjeldahl digestion (Procházková 1960) for precipitation, CT-II and CT-VII, for throughfall in 1997–2001, otherwise TOC/TN analyzer[1]; detection limit of ~2 µmol.l^{-1}. PON = TON – DON.
TP, DP, PP	Total P, dissolved P and particulate P.	Sample pre-concentration, $HClO_4$ digestion, molybdate method (Kopáček & Hejzlar 1993); detection limit of 0.015 µmol.l^{-1}. PP = TP – DP.
SRP	Soluble reactive P	Molybdate method (Murphy & Riley 1962), detection limit of 0.05 µmol.l^{-1}.

[1] Concentrations of TON and DON were calculated as the differences between concentrations of total and dissolved N, respectively (determined by TOC/TN analysers Formacs (Skalar, the Netherlands) in 2002–2009 and vario TOC cube (Elementar, Germany) in 2010–2012) and inorganic N.

$$Q_{TE}C_{TE} + Q_{PR}C_{PR} + \pi_L = Q_{OUT}C_{OUT} + \Delta M_L \qquad (2)$$

In these equations, π_C and π_L (both in mol.yr^{-1}) are the net mass production (when positive) or removal (when negative) of a constituent in the catchment and lake, respectively. ΔM_C and ΔM_L (both in mol.yr^{-1}) are annual changes in storage of a constituent in the catchment and lake, respectively. Q_{DEP}, Q_{TE}, Q_{PR}, and Q_{OUT} (all in m^3.yr^{-1}) are water fluxes of atmospheric deposition (DEP) to the catchment soils (i.e., precipitation in the treeless area and throughfall deposition in forests), terrestrial export (TE) to the lake from the catchment (tributaries), direct atmospheric deposition to the lake surface (precipitation, PR), and total (measured) water output (OUT) from the lake, respectively. C_{DEP}, C_{TE}, C_{PR}, and C_{OUT} (all in mol.m^{-3}) are annual mean concentrations of water constituents in the atmospheric deposition to the catchment soils, in tributaries, in direct atmospheric deposition to the lake surface (precipitation), and in the lake output, respectively.

The water balance was determined from the annual amounts (H, m.y^{-1}) of precipitation in the treeless area (H_{PR}) and throughfall at plots $H_{TF\text{-}L}$ and $H_{TF\text{-}H}$, continuously monitored Q_{OUT}, and the budget for Cl$^-$. Q_{DEP} was calculated from equation (3):

$$Q_{DEP} = (A_C - A_L)\,(0.2H_{PR} + 0.8(0.5H_{TF\text{-}L} + 0.5\mathrm{H}_{TF\text{-}H})) \tag{3}$$

where A_C and A_L is area of the catchment (including lake) and lake, respectively, and coefficients 0.2 and 0.8 represent portions of the catchment, receiving atmospheric deposition in the form of precipitation (treeless area and thin forest) and throughfall (dense forest), respectively. These estimates were based on aerial photographs. In this calculation we assumed that each of plots TF-L and TF-H represented 50% of the total throughfall deposition in the study catchment (coefficients of 0.5).

The total water input into the lake (Q_{IN}, m^3.yr^{-1}) was the sum of Q_{TE} and Q_{PR}. $Q_{PR} = H_{PR}{\cdot}A_L$ and Q_{TE} was calculated from equation (2), using the measured Q_{OUT} and Q_{PR} fluxes and annual volume weighted mean concentrations of Cl$^-$ in precipitation (Cl_{PR}), annual average concentrations of Cl$^-$ in lake tributaries ($Cl_{TE}{}^*$) and outlet (Cl_{OUT}), and change in storage of Cl$^-$ in the lake (ΔCl_L). The $Cl_{TE}{}^*$ values were calculated as arithmetical mean for all tributaries, because Cl$^-$ concentrations in tributaries were similar. The net removal or production of Cl$^-$ in the lake was assumed to be negligible (e.g., Van der Perk 2006) and thus π_L of Cl$^-$ was set to zero in equation (2) that was rearranged to:

$$\mathrm{Q_{TE}} = \frac{\mathrm{Q_{OUT}Cl_{OUT} - Q_{PR}Cl_{PR} + \Delta Cl_L}}{\mathrm{Cl_{TE}}^*} \tag{4}$$

The ΔM_L (mol.yr^{-1}) in equation (2), as well as ΔCl_L in equation (4), is the change in storage of a constituent in the lake and was calculated from equation (5):

$$\Delta M_L = V\,(C_2 - C_1) \tag{5}$$

where V (m^3) is lake volume and C_1 and C_2 (both in mol.m^{-3}) are volume weighted mean concentrations of water constituents. The C_1 and C_2 values were obtained from data on samples taken from five depths between the surface and bottom in the deepest part of the lake at the beginning and the end of each hydrological year, respectively, by linking volumes of the sampled water layers with the corresponding concentrations. We usually used data from October sampling for this purpose. An analogous change in storage of a constituent in the catchment (ΔM_C; mol.yr^{-1}) was not regularly measured. The equation (1) was thus rearranged to:

$$\pi_C{}^* = Q_{TE}C_{TE} - Q_{DEP}C_{DEP} = \pi_C - \Delta M_C,$$

where $\pi_C{}^*$ includes both the net mass production and change in storage of a constituent in the catchment.

The annual average compositions of precipitation and throughfall were calculated as volume weighted means (VWM) for C_{PR} and throughfall at the low ($C_{TF\text{-}L}$) and high ($C_{TF\text{-}H}$) elevation plots. When the SRP and F$^-$ concentrations were below their detection limits of 0.05 and 0.1 µmol.l^{-1} (~2% and ~25% of all samples; Kopáček et al. 2011), respectively, a half of these values were used in subsequent data evaluation.

Annual average composition of deposition to catchment soils (C_{DEP}) by both precipitation and throughfall (i.e., via atmospheric deposition and canopy leaching) were calculated from the respective precipitation and throughfall amounts and VWM compositions:

$$\mathrm{C_{DEP}} = \frac{0.2\ \mathrm{C_{PR}H_{PR}} + 0.8\ (0.5\ \mathrm{C_{TF\text{-}L}H_{TF\text{-}L}} + 0.5\ \mathrm{C_{TF\text{-}H}H_{TF\text{-}H}})}{0.2\ \mathrm{H_{PR}} + 0.8\ (0.5\ \mathrm{H_{TF\text{-}L}} + 0.5\ \mathrm{H_{TF\text{-}H}})} \tag{6}$$

where coefficients 0.2, 0.8, and 0.5 are the same as in equation (3).

Annual average compositions of surface tributaries (PL-I and PL-II during the whole study and PL-III from 2002) were calculated for individual hydrological years as discharge and period-weighted mean (DPWM) concentrations (Likens & Bormann 1995):

$$\mathrm{C} = \frac{\sum \mathrm{C_i Q_i} \tau_\mathrm{i}}{\sum \mathrm{Q_i} \tau_\mathrm{i}} \tag{7}$$

where Q_i is water discharge and C_i is concentration of a water constituent during the sampling *i* (the annual number of samplings was 17–19), and τ_i (days) is the length of sampling period *i*. In this calculation, each flux was assumed to represent the whole period *i* given as the sum of halves of intervals between the sampling and the previous one and between the sampling and the next one.

For subsurface tributaries, with no data on discharge (PL-IV during the whole study and PL-III prior to 2002), annual average concentrations were calculated as period-weighted means.

Annual average compositions of terrestrial export to the lake from the catchment via tributaries (C_{TE}) was calculated as follows: Because discharge of subsurface tributaries was unknown, annual average values of C_{TE} (representing a mixture of surface and subsurface tributaries) were calculated from annual average composition of subsurface (C_{SUBSUR}) and surface (C_{SUR}) tributaries and their relative proportions (*r* and *1 – r*, respectively) to the total terrestrial water export. The *r* value was estimated from the balance for Ca^{2+} ions, because Ca^{2+} concentrations were about twofold higher in subsurface than in surface PL tributaries and could be used as a tracer (Kopáček et al. 2001a, 2017):

$$rQ_{TE}C_{SUBSUR} + (1 - r)Q_{TE}C_{SUR} + Q_{PR}C_{PR} + \pi_L = Q_{OUT}C_{OUT} + \Delta M_L \tag{8}$$

The π_L value (–503 mol.yr^{-1}) was estimated from a net Ca accumulation in the lake sediments. This value was based on the average mass accumulation rate in the Plešné sediments (85 g.m^{-2}.yr^{-1}), the average concentration of Ca in the uppermost sediment layer (78 µmol.g^{-1} dry weight), and lake area. The average mass accumulation rate was calculated from the average accumulation rate of sediment (5.3 mm.yr^{-1}) and the water content of the uppermost sediment layer (98.4%) in the Plešné sediments (Schmidt et al. 1993). For more details see (Kopáček et al. 2001a). The ΔM_L values were calculated from equation (5). The computed *r* values were 0.3–0.4 during the study, suggesting that ~30–40% of the Q_{TE} entered the lake via the subsurface tributaries. Then, the C_{TE} values of all water constituents (except for Cl^-) were computed as:

$$\mathrm{C_{TE}} = \frac{\mathrm{rQ_{TE}C_{SUBSUR}} + (1 - \mathrm{r})\mathrm{Q_{TE}C_{SUR}}}{\mathrm{Q_{TE}}} \tag{9}$$

The annual average C_{SUBSUR} values were arithmetical means of annual concentrations of water constituents in the PL-III and PL-IV tributaries. The annual average C_{SUR} values were calculated using compositions and discharges of PL-I and PL-II as:

$$C_{SUR} = \frac{\sum C_{y,i} Q_{y,i} \tau_i}{\sum Q_{y,i} \tau_i} \tag{10}$$

where y and i denote lake tributary and sampling period, respectively, $C_{y,i}$ is concentration of a water constituent, and $Q_{y,i}$ is water discharge in a tributary y during sampling i.

Annual average compositions of the total water input into the lake (C_{IN}) was calculated from the total input of water constituents into the lake, i.e. the sum of their fluxes by tributaries ($Q_{TE}C_{TE}$) and atmospheric deposition ($Q_{PR}C_{PR}$) according to equation (11):

$$C_{IN} = \frac{Q_{TE}C_{TE} + Q_{PR}C_{PR}}{Q_{TE} + Q_{PR}} \tag{11}$$

Annual average composition of lake output (C_{OUT}) was calculated from equation (7) by linking continuously monitored discharge data of the outlet (average discharges for τ_i periods) with the corresponding weekly to biweekly concentration data.

Mass balance of protons in terrestrial and aquatic ecosystems

Net terrestrial and aquatic production (or consumption) of protons and the contributions of individual constituents to these processes were estimated from budgets for ions, using the equation of electroneutrality:

$$\begin{aligned}[\mathrm{H}^+] = {} & [\mathrm{SO_4}^{2-}] + [\mathrm{NO_3}^-] + [\mathrm{Cl}^-] + [\mathrm{F}^-] + [\mathrm{A}^-] + [\mathrm{HCO_3}^-] - [\mathrm{NH_4}^+] - \\ & - [\mathrm{Na}^+] - [\mathrm{K}^+] - [\mathrm{Ca}^{2+}] - [\mathrm{Mg}^{2+}] - [\mathrm{Al_i}^{n+}] - [\mathrm{Fe_i}^{m+}]\end{aligned} \tag{12}$$

where brackets represent equivalent concentrations of components. According to this approach, any increase in concentration of cations and decrease in concentration of anions are H^+ consuming processes. In contrast, any decrease in concentration of cations and increase in concentration of anions are H^+ producing reactions. Changes in concentrations of ionic P and Si forms were neglected.

In-lake nitrate and sulphate removal

The lake ability to remove NO_3^- and SO_4^{2-} was assessed using the following two coefficients (e.g. for NO_3^-): (i) R_{NO3} = the NO_3^- removal coefficient (the ratio of net in-lake NO_3^- removal to the total NO_3^- input, and (ii) S_{NO3} = the mass transfer coefficient for NO_3^- (also called "settling velocity"; m.yr^{-1}). The relationship between S_{NO3} and R_{NO3} values is given by equation (13) (Kelly et al. 1987):

$$S_{NO3} = R_{NO3} \frac{q_s}{1 - R_{NO3}} \tag{13}$$

where q_s (m.yr^{-1}) is the areal water load per unit area of the lake. The q_s value was calculated as $q_s = Q_{TE}/A_L$ (Kaste & Dillon 2003).

RESULTS

Concentrations

The average chemical composition of Plešné tributaries differed from atmospheric deposition to the catchment soils in higher concentrations of H^+, SO_4^{2-}, NO_3^-, metals, DOC, TON, TP and Si, and in one order-of-magnitude lower NH_4^+ concentrations (Table 2). The composition of surface inlets differed from the subsurface inlets predominantly in lower concentrations of Ca^{2+}, Mg^{2+}, NO_3^- and SO_4^{2-}, and higher concentrations of TP, SRP, DOC, DON, Al_o and Fe_o (Table 2). The TP pool was dominated by SRP (on average ~80%).

Annual average chemical composition of tributaries exhibited pronounced changes during the study period (Appendix 4). Concentrations of NO_3^-, K^+, Ca^{2+}, Mg^{2+}, H^+, and Al_i started to increase immediately after the tree dieback (after 2004), reached their maxima in 2009–2011, and then decreased almost to their pre-disturbance levels by 2017. In contrast, concentrations of DOC and P forms started to increase more slowly, and their increase continued until the end of this study (Appendix 4). Concentrations of SO_4^{2-}, Na^+, and Si were not affected by the tree dieback.

Compared to the chemistry of surface and subsurface tributaries and total water input to the lake (including precipitation), composition of the lake output had lower concentrations of H^+, NO_3^-, Al forms, DOC, DON, TP, SRP and Si, but higher concentrations of NH_4^+, HCO_3^-, POC, PON and PP (Table 2). Changes in in-lake concentrations of SO_4^{2-}, Cl^-, F^-, base cations (BCs = $Ca^{2+} + Mg^{2+} + Na^+ + K^+$), and Fe forms were almost negligible.

The thermal stratification of Plešné Lake developed characteristically for a dimictic temperate lake. The ice cover usually lasted from December to April, with the minimum, maximum, and average ice-on period of 100, 170, and 135 days, respectively, during 2000–2017. Secchi disc transparency varied between 0.8–1.5 m during the study and the thermocline depth between 3–5 m. The autumn and spring overturns usually occurred in December and April, respectively. Dissolved O_2 was depleted above the lake bottom within a month after the development of thermal stratification and the anoxic layer increased up to 12 m depth before the overturns (Fig. 2B). At low redox potentials above the lake bottom, dissimilatory reduction processes occurred, decreasing NO_3^- and SO_4^{2-} concentrations and increasing concentrations of NH_4^+ and Fe forms, while concentrations of conservative Cl^- remained stable along the whole water column (Fig. 2). Concentrations of NO_3^- also rapidly decreased in the epilimnion due to assimilation by algae, and the NO_3^- maxima (persisting from spring overturn) usually were in the middle of the water column during its summer thermal stratification (Fig. 2E).

The changes in ionic composition were accompanied by changes in water ANC and pH. The carbonate buffering system was depleted in the most of water column after spring overturns until 2013, then it has re-established and ANC concentrations have become positive throughout the year, with elevated values in the hypolimnion (Fig. 2D). The hypolimnetic pH increased toward ~6 during both winter and summer stratification (Fig. 2C). During winter stratification, the lowest pH values were below the ice, because water from surface tributaries (with temperature close to freezing point) had lower density than the rest of water column and flew through the surface layer. During summer stratification, water from tributaries was colder and denser than that in the epilimnion and mixed with the deeper water layers. In addition, pH increased in the epilimnion due to assimilative processes (NO_3^- removal, see later) in summer. Consequently, the lowest pH values were in the middle of the water column in summer (Fig. 2C). With the pH increase towards neutrality, ionic Al species hydrolyzed and formed Al_p (colloidal hydroxides). Hence, Al_p concentrations were higher in summer than in winter and in the hypolimnion than in the epilimnion (Fig. 2J). In contrast, concentrations of Al_i were higher in winter than in summer (Fig. 2I). The high Al_p concentrations were accompanied with elevated TP concentrations (maximum of ~3.3 $\mu mol.l^{-1}$), while concentrations of dissolved P forms (DP and SRP) were an order of magnitude lower above the bottom (not shown).

Table 2. Average (± standard deviation) values of discharge (*Q*, for annual data see Appendix 1) and mean composition of precipitation (C_{PR}, for annual data see Appendix 2), atmospheric deposition to the catchment soils (C_{DEP}, precipitation in treeless area and throughfall in forest, for annual data see Appendix 3), tributaries (PL-I to PL-IV), terrestrial export via tributaries (C_{TE}, for annual data see Appendix 4), total input to Plešné Lake (C_{IN}, terrestrial export and precipitation to the lake surface, for annual data see Appendix 5), and output from the lake (C_{OUT}, for annual data see Appendix 6) during the period between November 1999 to October 2017. Units: µmol.l^{-1}, except for discharge (*Q*; l.s^{-1}) and pH. For location of tributaries see Fig. 1.

	C_{PR}	C_{DEP}	PL-I	PL-II	PL-III	PL-IV	C_{TE}	C_{IN}	C_{OUT}
Q	[*] 3.3±0.6	[**] 27±5	1.7±0.9	1.3±0.7	3.4±1.8	ND	19.4±4	22.6±5	21.9±5
pH	5.07±0.17	4.95±0.23	4.21±0.09	4.27±0.09	4.49±0.09	4.74±0.04	4.33±0.08	4.38±0.08	4.88±0.21
H^+	9±3	13±7	63±14	55±11	33±6	18±2	48±9	42±8	15±6
Ca^{2+}	4.0±0.8	8.2±3.3	20±4	21±5	27±4	41±6	25±4	22±4	22±4
Mg^{2+}	1.2±0.3	3.2±1.3	7.4±1.8	7.6±2.1	10±2	15±3	9±2	8±2	9±2
Na^+	6.7±1.3	10±3	42±6	43±7	43±5	52±3	45±5	39±4	38±2
K^+	2.3±0.9	14±10	22±11	20±11	16±6	16±4	19±8	17±7	16±7
NH_4^+	27±5	31±6	0.8±0.6	0.9±0.8	0.8±0.6	0.6±0.6	0.6±0.6	4±1	5±1
NO_3^-	23±2	34±10	95±51	106±54	117±40	143±51	110±43	98±38	58±31
SO_4^{2-}	8.1±1.8	12±5	28±7	28±6	33±9	44±11	32±7	28±6	29±7
Cl^-	6.3±1.3	11±4	13±3	13±3	13±2	14±2	13±3	12±2	13±2
F^-	0.6±0.5	0.8±0.4	3.5±1.0	3.4±0.9	5.0±1.3	7.0±1.3	4.4±1.0	3.8±0.9	4.1±0.8
HCO_3^-	4.5±4.0	5.3±4.3	0	0	0	0	0	0.6±0.6	3.3±5.2
DOC	93±18	367±190	1165±280	841±177	432±102	153±22	766±159	669±142	408±104
POC	33±30	109±211	11±23	24±20	20±25	24±23	21±16	21±16	197±73
DON	12±4	18±6	35±8	28±8	20±7	10±2	27±6	25±68	20±5
PON	6±2	8±6	2±2	2±2	1±2	1±1	1±1	2±1	18±6
TP	0.44±0.16	0.66±0.22	1.39±0.42	1.18±0.26	0.63±0.15	0.18±0.04	0.98±0.23	0.91±0.20	0.46±0.10
PP	0.24±0.09	0.42±0.18	0.07±0.05	0.04±0.03	0.05±0.06	0.03±0.04	0.06±0.02	0.09±0.02	0.37±0.09
SRP	0.15±0.11	0.13±0.07	1.10±0.37	0.99±0.23	0.51±0.14	0.11±0.02	0.78±0.21	0.70±0.18	0.04±0.02
Si	0.5±0.3	ND	138±24	131±25	129±17	142±9	134±18	115±15	101±9
Al_T	0.4±0.3	ND	31±4	30±5	29±5	30±7	31±4	26±4	20±3
Al_i	ND	ND	17±5	18±6	22±6	26±7	20±5	17±5	10±3
Al_o	ND	ND	14±3	11±2	6±1	2±1	10±1	8±1	5±2
Fe_T	ND	ND	2.7±0.6	1.9±0.3	0.9±0.1	0.2±0.1	1.7±0.3	1.5±0.2	1.6±0.3
Fe_i	ND	ND	0.6±0.2	0.5±0.2	0.3±0.1	0.0±0.0	0.4±0.2	0.4±0.1	0.3±0.1
Fe_o	ND	ND	1.9±0.6	1.3±0.3	0.6±0.1	0.2±0.1	1.2±0.3	1.0±0.2	0.7±0.2

Explanations: [*] Precipitation amount deposited to the lake surface, [**] water amount deposited to the lake catchment with precipitation and throughfall.

Water fluxes

The average (± standard deviation) precipitation was 1346±241 mm.yr^{-1} and varied between 1020 and 1953 mm.yr^{-1} in 2015 and 2002, respectively. The deposition to the catchment soils (precipitation in treeless areas plus throughfall in forest) was 1338±223 mm.yr^{-1} and ranged

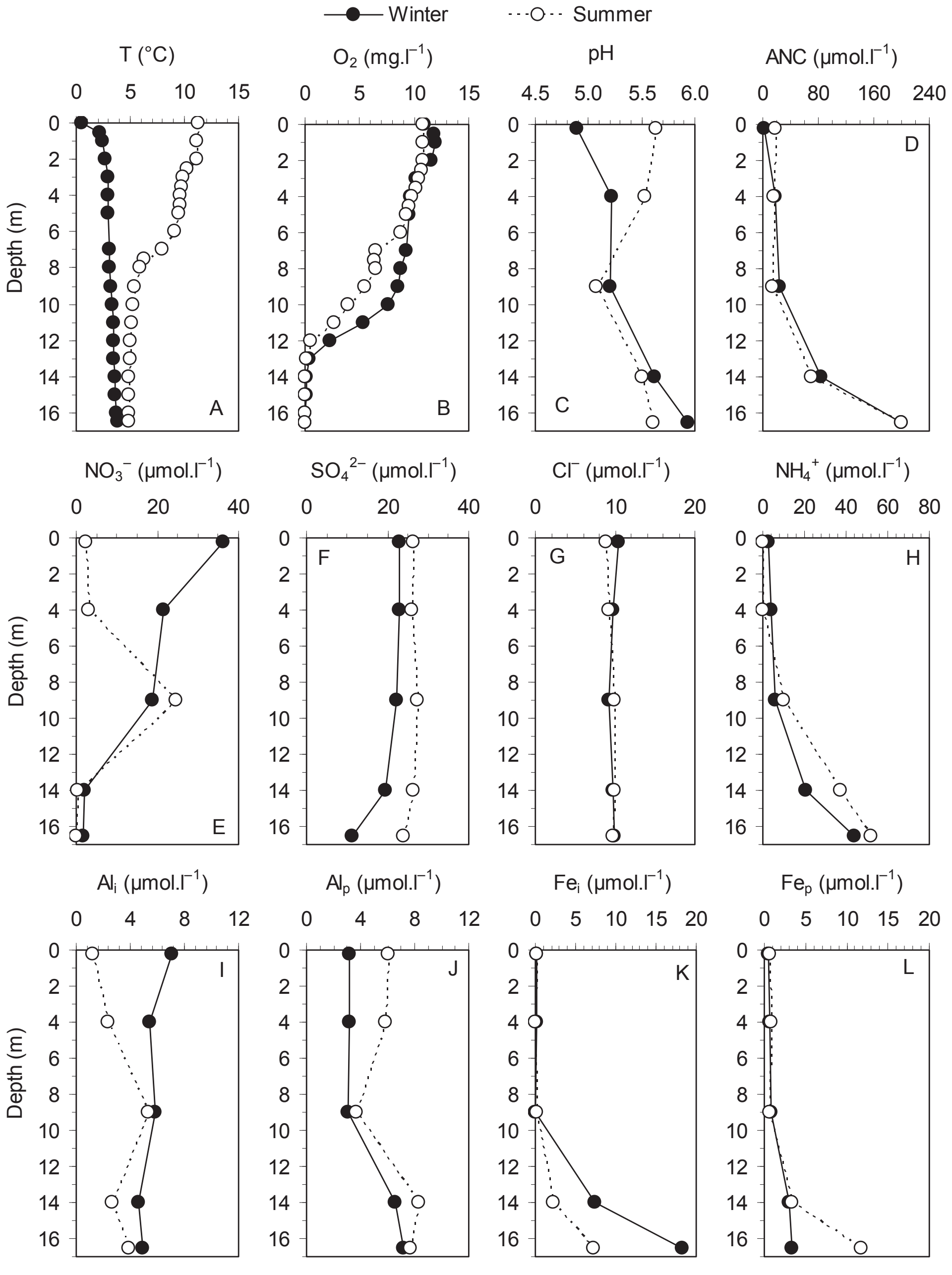

Fig. 2. Depth diagrams of temperature (T), dissolved oxygen (O_2), pH, acid neutralizing capacity (ANC), NO_3^-, SO_4^{2-}, Cl^-, NH_4^+, ionic and particulate aluminium (Al_i, Al_p) and iron (Fe_i, Fe_p) during winter (17 March 2017) and summer (2 October 2017) thermal stratification of Plešné Lake.

between 1019 and 1969 mm.yr^{-1} (Appendix 1). The average water outflow from the lake was 1087±232 mm.yr^{-1} (i.e., specific outflow of 34±7 l.km^{-2}.s^{-1}). The resulting average evapotranspiration from the catchment–lake system, based on precipitation and throughfall amounts, was 19±8 % during 2000–2017. This value was, however, lowered by interception in the period of healthy forest. Consequently, the actual average evapotranspiration from the Plešné catchment–lake system was >19% due to the direct water evaporation from canopies during the study period.

The tree dieback only had small effect (increase) on water outflow from Plešné catchment–lake system relatively to the atmospheric water input. The ratio between water outflow and water input to the catchment soils increased from 0.72 to 0.84 (averages for 2000–2004 and 2005–2017 periods, respectively, Appendix 1). In contrast, evapotranspiration from the catchment decreased due to ceased transpiration of dead trees, while soil wetness increased (for more details see Kopáček et al. 2017). The increased runoff was similar to other catchments in the Bohemian and Bavarian Forest where disturbance exceeded 30% of forest areas (Beudert et al. 2018).

Water residence time in Plešné Lake varied between 211 and 481 days, and averaged 338±70 days during the study period.

Element fluxes in catchment

Terrestrial exports of NO_3^-, SO_4^{2-}, BCs (except for Na^+), and Al_T were higher than their inputs to the catchment by precipitation and throughfall throughout the study period, and further increased after the tree dieback (Fig. 3). Terrestrial exports of DOC and TON were lower than their deposition to the catchment soils prior to 2009, but then higher (Fig. 3E,F). Terrestrial exports of TP and SRP (not shown) behaved similarly to DOC and increased until the end of this study. The Plešné catchment was a net P source, averaging 0.19±0.51 mmol.m^{-2}.yr^{-1} during this study (Table 3).

On a long-term basis, the Plešné catchment was a net sink for atmospherically deposited NH_4^+ (Table 3) both prior to and after tree dieback (Fig. 3). The average Cl^- deposition and leaching were almost equal on a long-term (Table 3), but differed on the annual basis. The Plešné catchment usually accumulated Cl^- prior to the tree dieback, but became a net Cl^- source from 2008 to 2017, when both fluxes equalled (Fig. 4A). Terrestrial export of Na^+ was stable (except for elevated flux in 2002), permanently higher than its atmospheric input, and was not affected by the tree dieback (Fig. 4B). The elevated Na^+ export in 2002 resulted (as in the case of other water constituents; Figs. 3 and 4B) from extremely high discharge (Appendix 1), associated with a summer heavy rain event. Patterns in terrestrial export of Si were similar to Na^+ and their concentrations in tributaries were closely correlated (Kopáček et al. 2017).

Terrestrial transformations of ionic fluxes resulted in a net terrestrial H^+ production of 35±18 meq.m^{-2}.yr^{-1} on a catchment-area basis during 2000–2017 (Table 3), with maximum production of 58 meq.m^{-2}.yr^{-1} from 2006–2010. The average pH of tributaries was thus permanently lower than pH of precipitation and deposition to the catchment soils (Table 2). The average H^+ production, based on pH values in precipitation, throughfall and tributaries, was in good concordance with H^+ production calculated from equation (12) as the sum of individual H^+ sources (terrestrial production of anions and removal of cations) and sinks (terrestrial production of cations) that averaged 36.5 meq.m^{-2}.yr^{-1} during 2000–2017. Both estimates thus differed by <4% on average. The net terrestrial H^+ production (the difference between annual terrestrial export and deposition to the catchment soils; see Fig. 3H) was highest after the tree dieback (56 meq.m^{-2}.yr^{-1} on average during 2006–2010). The most important H^+ sources were net release of NO_3^-, SO_4^{2-}, and A^- (76, 37, and 15 meq.m^{-2}.yr^{-1},

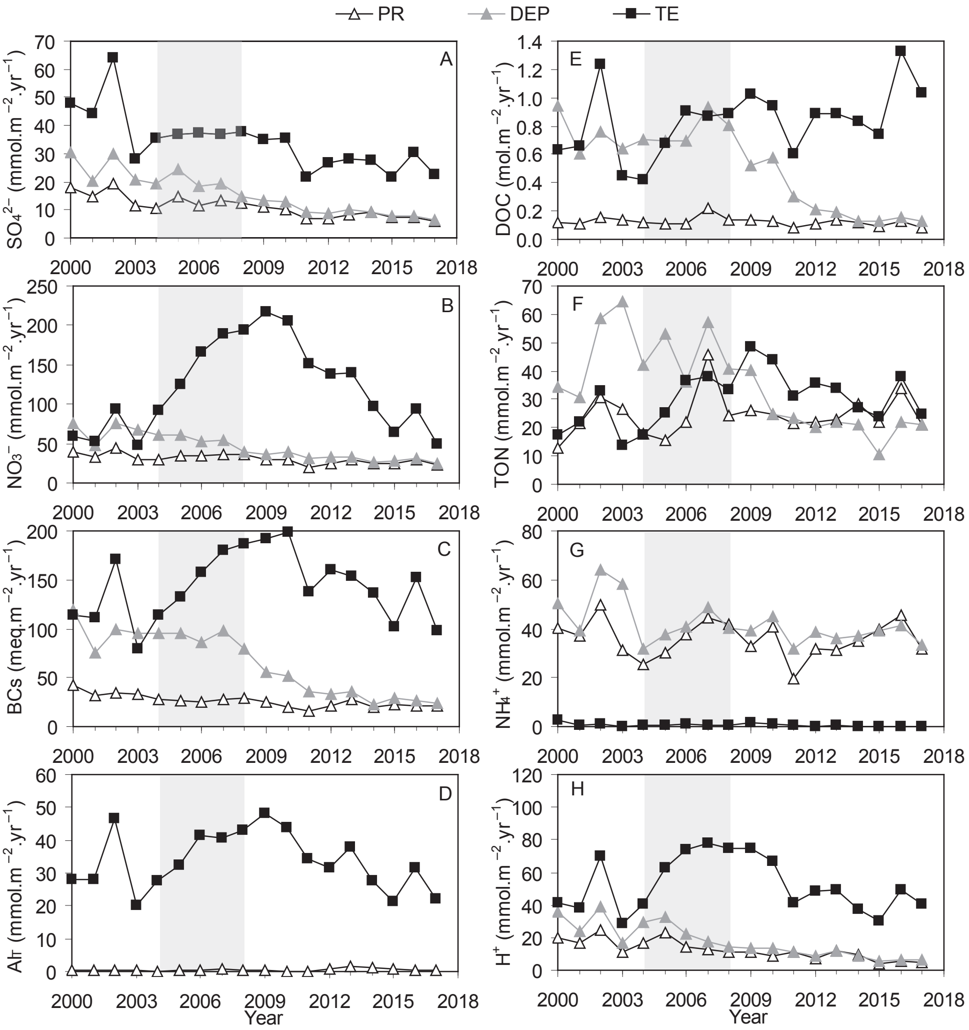

Fig. 3. Time series of annual fluxes (based on a catchment area basis) of SO_4^{2-}, NO_3^-, base cations (BCs = sum of Ca^{2+}, Mg^{2+}, Na^+ and K^+), total aluminium (Al_T), dissolved organic carbon (DOC), total organic nitrogen (TON), NH_4^+, and H^+ in precipitation (PR), deposition to the catchment soils (DEP), and terrestrial export via tributaries (TE) in the Plešné catchment in the 2000–2017 hydrological years. Grey area indicates the period of bark beetle outbreak in the Plešné catchment.

respectively) and retention of NH_4^+ in soils (41 $meq.m^{-2}.yr^{-1}$), while terrestrial production of Al_i and BCs represented the most important H^+ sinks (53 and 78 $meq.m^{-2}.yr^{-1}$, respectively). The contribution of NO_3^-, BCs, and Al to modifying terrestrial H^+ export reached maximum values during 2005–2011 (Fig. 3), while that of A^- in 2016–2017 (see high terrestrial export of DOC in Appendix 4).

Table 3. Mean (± standard deviation) element fluxes in precipitation (*PR*), deposition to the catchment soils (*DEP*), terrestrial export (*TE*), net production of water constituents in the catchment ($\pi_C^* = \pi_C - \Delta M_C$, calculated from equation 1), and the associated H^+ production/removal in soils of the Plešné catchment in the 2000–2017 hydrological years.

	PR	***DEP***	***TE***	π_C^*	**H^+ source†**
	mmol.m^{-2}.yr^{-1}				meq.m^{-2}.yr^{-1}
H^+	12±6	18±11	53±17	35±18	
Ca^{2+}	5.4±1.2	11±5	27±7	16±9	–32±19
Mg^{2+}	1.6±0.5	4.4±2.0	10.1±3	5.7±3.4	–11±7
Na^+	9.0±2.6	13±5	48±9	34±9	–34±9
K^+	3.2±1.4	20±14	21±10	1.1±20	–1±20
NH_4^+	36±8	42±9	0.7±0.6	–41±9	41±9
NO_3^-	31±6	45±17	121±57	76±63	76±63
SO_4^{2-}	11±4	16±8	34±11	19±6	37±12
Cl^-	9±3	14±6	15±4	0.3±5.3	0±5
F^-	0.8±0.6	1.0±0.6	5±2	5±1	5±1
DOC (A^-)	124±30	507±291	834±241	326±426	(15±24)
HCO_3^-	6±4	6±4	0±0	–6±4	–6±4
TON	24±7	35±16	30±9	–3±20	
TP	0.6±0.2	0.9±0.4	1.1±0.3	0.19±0.51	
Si	0.7±0.3	ND	144±23	143±24	
Al_T	0.5±0.4	ND	34±9	33±9	
Al_i (Al_i^{n+})	ND	ND	22±8	22±8	(–53±20)
Fe_T	ND	ND	1.8±0.5	1.4±0.5	
Fe_i (Fe_i^{m+})	ND	ND	0.5±0.2	0.5±0.2	(–0.5±0.2)

Explanations: Values are given on a catchment-area basis; ND – not determined. When deposition of an element on the catchment soils was not determined, its net production was set equal to its terrestrial export. Positive π_C^* values indicate net production, while negative values indicate net removal; for their annual values see Appendix 7. † Release of cations and removal of anions are proton-consuming processes, while removal of cations and release of anions are proton-producing reactions. One meq = mmol of charge. Sum of H^+ sources and sinks gives a net production of 36.5 mmol.m^{-2}.yr^{-1}.

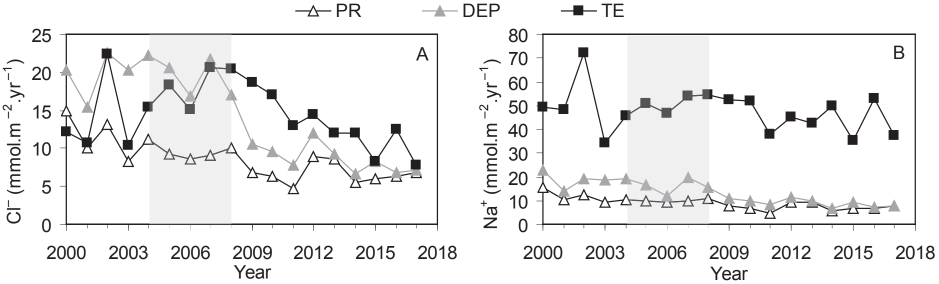

Fig. 4. Time series of annual fluxes (based on a catchment area basis) of Cl^- and Na^+ in precipitation (PR), deposition to the catchment soils (DEP), and terrestrial export via tributaries (TE) in the Plešné catchment in the 2000–2017 hydrological years. Grey area indicates the period of bark beetle outbreak in the Plešné catchment.

Element fluxes in lake

The internal processes caused reductions in NO_3^-, A^-, SO_4^{2-}, and Al_i fluxes (Table 4, Fig. 5) and increased pH in the lake outlet compared to their values in the lake input by tributaries and precipitation. The average input flux of H^+ decreased by ~65% from 403 to 136 meq.$m^{-2}.yr^{-1}$ on a lake area basis (Table 4). The net in-lake H^+ removal (calculated on the basis of pH values in precipitation, tributaries and lake outlet) averaged 267 meq.$m^{-2}.yr^{-1}$ during the

Table 4. Mean (± standard deviation) element fluxes in total input to lake (*IN*, sum of atmospheric deposition on the lake surface, see precipitation in Table 2, and terrestrial export), output from lake (*OUT*), net in-lake production of water constituents (π_L), and the associated H^+ production/removal in Plešné Lake in the 2000–2017 hydrological years.

	IN	***OUT***	π_L	**H^+ source†**
	mmol.$m^{-2}.yr^{-1}$			meq.$m^{-2}.yr^{-1}$
H^+	398±125	136±70	–266±71	
Ca^{2+}	205±53	201±51	–6±21	13±41
Mg^{2+}	76±22	78±21	3±10	–6±20
Na^+	361±66	343±73	–21±36	21±35
K^+	157±75	145±64	–10±19	10±19
NH_4^+	41±10	45±19	3±32	–3±32
NO_3^-	920±419	531±320	–395±129	–395±123
SO_4^{2-}	263±81	364±94	–12±17	–25±34
Cl^-	115±33	117±36	ND	
F^-	36±11	37±12	1±10	1±9
HCO_3^-	5±4	27±42	33±52	33±52
DOC (A^-)	6251±1778	3673±1170	–2400±673	(–151±65)
TON	246±73	339±98	93±70	
TP	8.5±2.4	4.1±1.2	–4.3±1.3	
Si	1056±172	907±171	–136±85	
Al_T	248±65	186±52	–62±33	
Al_i (Al_i^{n+})	163±57	91±43	–74±33	(243±81)
Al_o	78±19	47±19	–29±14	
Al_p	7±3	48±16	41±22	
Fe_T	14±4	14±4	1±4	
Fe_i (Fe_i^{m+})	3±2	3±1	–1±2	(1±2)
Fe_o	10±3	6±2	–3±2	
Fe_p	1±0.4	5±2	5±3	

Explanations: Values are given on a lake-area basis; ND – not determined. Values of π_L were calculated from equation (2), data on the average annual change in storage of elements in the lake are not given. Positive values indicate net production, while negative values indicate net removal; for their annual values see Appendix 8. † Release of cations and removal of anions are proton-consuming processes, while removal of cations and release of anions are proton-producing reactions. One meq = mmol of charge. Sum of H^+ sources and sinks gives a net retention of 258 mmol.$m^{-2}.yr^{-1}$.

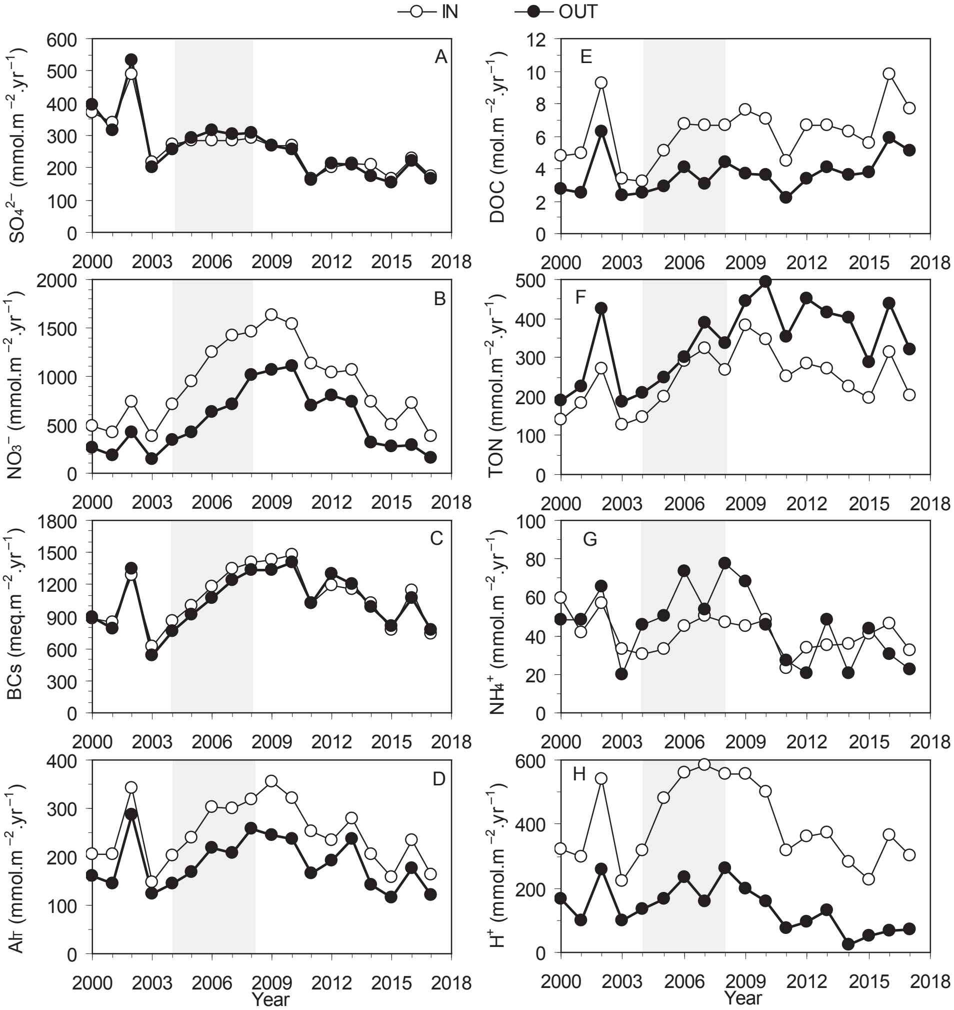

Fig. 5. Time series of annual fluxes (based on a lake area basis) of SO_4^{2-}, NO_3^-, base cations (BCs = sum of Ca^{2+}, Mg^{2+}, Na^+ and K^+), total aluminium (Al_T), dissolved organic carbon (DOC), total organic nitrogen (TON), NH_4^+, and H^+ in total input (IN, tributaries and precipitation) to and outlet (OUT) from Plešné Lake in the 2000–2017 hydrological years. Grey area indicates the period of bark beetle outbreak in the Plešné catchment.

whole study, and reached maximum values of 359 meq.m^{-2}.yr^{-1} on average during 2006–2010. This value is not a simple difference between the input and output fluxes because it also includes a net change in H^+ storage in the lake (equation 2) that decreased by 4 meq.m^{-2}.yr^{-1} during the study (lake water pH during autumn overturns increased from 5.0 in 1999 to 5.4 in 2017). The pH-based estimate was similar to the H^+ removal calculated from equation (12) that averaged 257 meq.m^{-2}.yr^{-1}. Thus, both estimates differed by ~4% on average.

The most important internal H^+ sinks were NO_3^-, A^- and SO_4^{2-} removals (395, 151, and 25 meq.m^{-2}.yr^{-1}, respectively), while Al_i transformations were the most important in-lake H^+ sources of 243 meq.m^{-2}.yr^{-1} on average (Table 4). In contrast to H^+, the lake was negligible sink for BCs (Fig. 5C) and was a net source of NH_4^+ in most years (especially in 2004–2009; Fig. 5G), with the long-term average production of 3 mmol.m^{-2}.yr^{-1}.

The lake was a net sink for all nutrients, removing on average 51% of TP, 25% of total N, 38% of DOC, and 13% of Si inputs (Table 4). Terrestrial export via tributaries was the major SRP source for the lake (6.3 meq.m^{-2}.yr^{-1}) and represented ~74% of TP input to the lake. Organic dissolved P and PP from soils formed together 20% of the TP input, while atmospheric inputs of all P forms only represented 6% of the total TP input to Plešné Lake during the study.

DISCUSSION

Major processes affecting mass budget of protons in Plešné catchment

Terrestrial transformations of inorganic N (IN = NO_3-N + NH_4-N) were the most important H^+ producing process in the Plešné catchment, with the 2000–2017 average of 117 meq.m^{-2}.yr^{-1} (Table 3). This value was 2.5 times higher than the maximum observed at 17 European forest sites (–5 to 46 meq.m^{-2}.yr^{-1}) by Forsius et al. (2005), and even higher than in strongly N-saturated Čertovo catchment in the same mountain area (Fig. 6). The IN-related production of H^+ in the Plešné catchment was significantly affected by tree dieback, with averages of 51 and 142 meq.m^{-2}.yr^{-1} in 2000–2004 and 2005–2017, respectively, and the maximum of 219 meq.m^{-2}.yr^{-1} in 2009. The ability of the N-saturated Plešné catchment to retain the deposited IN was thus low already prior to the tree dieback, averaging 38% during 2000–2004. After the tree dieback, however, the catchment became a significant net source of NO_3^- and its terrestrial export exceeded IN deposition to the catchment soils by 85% on average during 2005–2017, with the maximum of 189% in 2009 (Fig. 3B). Similar steep increase in NO_3^- leaching after vegetation disturbances in catchments usually results from the mineralization of abundant dead biomass (litter and fine roots) and diminished N uptake by dead trees (Houlton et al. 2003, Huber 2005, McHale et al. 2007, Kaňa et al. 2015).

The release of SO_4^{2-} was more than twice higher as deposition to the catchment soils (34

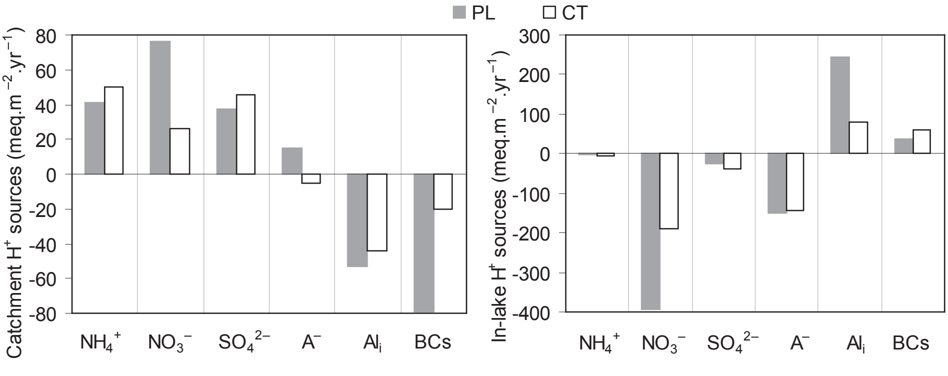

Fig. 6. Comparison of mean sources (when positive) and removal (when negative) of H^+ in Plešné (PL) and Čertovo (CT) lakes and their catchments, associated with fluxes of NH_4^+, NO_3^-, SO_4^{2-}, organic acid anions (A^-), ionic Al forms (Al_i) and base cations (BCs) in the 2000–2017 hydrological years. Data for CT were derived from database given by Kopáček et al. (2018b).

vs. 16 $mmol.m^{-2}.yr^{-1}$ on average) during the study (Table 3). The most likely source of this extra SO_4^{2-} was S accumulated in soils from high atmospheric deposition during the preceding decades as in the case of Čertovo Lake (Fig. 6). The net annual terrestrial exports of SO_4^{2-} decreased by ~50% during the study (as predicted by MAGIC modelling on the basis of development of its atmospheric deposition and S retention in soils; Majer et al. 2003, Oulehle et al. 2018) and were not affected by the tree dieback (Fig. 3A).

On a long-term, the Cl^- behaved conservatively in the Plešné catchment, only with negligible average production during 2000–2017 (Table 3). However, the terrestrial Cl^- export exceeded its atmospheric input after the tree dieback (Fig. 4A), similarly as observed in other disturbed forests (e.g., Kauffman et al. 2003, Huber et al. 2004). This elevated Cl^- leaching originates from mineralization of organically bound chlorine, stored in the soil organic matter (Lovett et al. 2005, Bastviken et al. 2007, Öberg & Bastviken 2012).

Leaching of A^- started to contribute to the terrestrial H^+ production with ~5 year delay after the tree dieback, when leaching of DOC increased (Fig. 3). The increase in DOC occurred as concentrations of NO_3^-, H^+, and polyvalent cations started to decrease in soil water, suggesting that disturbance-induced changes in N cycling strongly influenced DOC leaching via both chemical and biological mechanisms (Kopáček et al. 2018a). Elevated DOC leaching after tree dieback was also observed elsewhere and was mostly attributed to increasing soil wetness due to disrupted or diminished transpiration by dead trees (e.g., Nieminen 2004, Mikkelson et al. 2013, Bearup et al. 2014).

The leaching of BCs and Al_i peaked in 2009–2010, and then started to decrease to their pre-disturbance levels (Fig. 3). Their fluxes were affected by the tree dieback similarly to NO_3^- (Fig. 3) that became the dominant strong acid anion in water, and cations accompanied predominantly its leaching as counter-ions. Consequently, the decreasing terrestrial export of SO_4^{2-} from the Plešné catchment was not accompanied by decreasing Al_i, as observed in the Čertovo catchment during the same period (Kopáček et al. 2018b).

Net terrestrial sources of base cations

The interpretation of π_C* values for BCs (Table 3) is not very straightforward because they were related to deposition of BCs to the catchment soils that also included canopy leaching (elements released during precipitation passing through the canopies) prior to the tree dieback. Later, BCs were also released from decaying dead biomass. The calculated π_C* values thus underestimated net terrestrial production of Ca^{2+}, Mg^{2+}, and K^+ in soils until 2004 and then overestimated this production for all BCs after the tree dieback. The actual net terrestrial production of BCs can be roughly estimated as the difference between their terrestrial exports and net atmospheric inputs to the catchment during 2000–2004, when the net accumulation of BCs in mature trees was low. This period also preceded effects of tree dieback on throughfall composition and terrestrial export of BCs (Fig. 3C). Deposition of Na^+ to the catchment soils was on average 1.6 fold higher than that of precipitation during 2000–2004. Because the Na^+ exchange is negligible in Norway spruce canopies in the study catchment (Kopáček et al. 2009), we can assume that its total (wet, dry, and horizontal) atmospheric input into the catchment was equal to its deposition to the catchment soils. Moreover, dry depositions of Ca^{2+}, Mg^{2+}, and K^+ are assumed to be similar to that of Na^+, due to the same physical size and aerodynamic properties of base cation-containing aerosols (Draaijers & Erisman 1995). Total atmospheric inputs of BCs to the Plešné catchment can thus be roughly estimated from their precipitation fluxes, multiplied by a factor of 1.6. This provides net atmospheric inputs of Ca^{2+}, Mg^{2+}, Na^+, and K^+ to the catchment of 10.2, 3.3, 18.8, and 8.2 $mmol.m^{-2}.yr^{-1}$, and their 2000–2004 average terrestrial production of 11.2, 4.4, 31.2, and 1.5 $mmol.m^{-2}.yr^{-1}$, respectively. The higher net terrestrial source of Ca^{2+} than Mg^{2+} is consistent with its almost twofold higher concentration in the Plešné granitic bedrock (Kopáček et al. 2002). Thus estimated net terrestrial production of BCs is similar to their weathering rate assessed by modelling (64 *vs.* 75 meq.m^{-2}.yr^{-1}; Oulehle et al. 2018).

After the tree dieback, terrestrial export of BCs increased, while their atmospheric deposition to the catchment soils continually decreased (Fig. 3C) due to thinning of dead canopies, and consequently, decreasing horizontal deposition and ceasing their canopy exchange (Kopáček et al. 2013b, 2017). The average ratio of Na^+ fluxes in total deposition *vs.* precipitation decreased to 1.4 on average for the 2005–2017 period. The net terrestrial productions of Ca^{2+}, Mg^{2+}, Na^+, and K^+ during 2005–2017 (corrected using the Na-related factor of 1.4) were respectively 22.4, 8.9, 35.9, and 21.8 mmol.m^{-2}.yr^{-1}, and were thus higher by 11.2, 4.5, 4.7 and 20.3 mmol.m^{-2}.yr^{-1} than prior to the tree dieback. This excess leaching of BCs can be considered as their average annual loss from the decaying dead biomass to receiving waters during the last 13 years. The tree dieback and release from dead biomass are important sources of BCs for soil solutions (e.g., Berg & McClaugherty 2008, Palviainen et al. 2004). The increased availability of BCs in the Plešné soils caused their rapid recovery from acidification. The released BCs replaced a part of H^+ and Al_i from the soil sorption complex and significantly increased soil base saturation in the upper soils (from 39–65% and from 21–38% in the O and A horizons, respectively) between 2000 and 2015 (Kaňa et al. 2013, unpublished data).

Net phosphorus release from catchment soils

The forest soils of the Plešné catchment are an important source of P for the lake (Table 3), and the terrestrial P export closely correlates with DOC leaching (Kopáček et al. 2017). This terrestrial P flux, dominated by SRP, is ~5-times higher than that to the Čertovo Lake (Kopáček et al. 2018b), and is the major reason for Plešné Lake having the highest productivity of the Bohemian Forest lakes (Vrba et al. 2003, 2016). The most probable reasons for the high terrestrial P export from the Plešné catchment are (i) higher P release from the granitic bedrock (while mica schist dominates in the rest of the Bohemian Forest lake district), (ii) a lower overall phosphate sorption capacity of the Plešné soils (due to the lower concentrations of Fe hydroxides and lower pools of podsol and dystric cambisol, and a higher proportion of less-adsorbing leptosol), and (iii) high microbial P transformations and enzymatic P hydrolysis (Šantrůčková et al. 2004, Kaňa & Kopáček 2006, Tahovská et al. 2018).

Major processes affecting element fluxes in Plešné Lake

The in-lake H^+ neutralization was dominated by NO_3^- removal (Table 4, Fig. 6). The process removed on average 395±132 meq.m^{-2}.yr^{-1} NO_3^- (and H^+), i.e., 43% of the total NO_3^- input to the lake by inlets and atmospheric deposition. This internal acid neutralizing process is typical for acidified lakes with elevated NO_3^- inputs (Kelly et al. 1987, Schindler 1986). Contribution of denitrification and assimilation in the total NO_3^- removal was approximately 1/3 and 2/3, respectively, in Plešné Lake (Kopáček et al. 2006). Acidified lakes with elevated NO_3^- inputs usually receive low P inputs, their primary production is P-limited, the algal uptake of N is low, and their NO_3^- removal is dominated by denitrification in the sediments (Schindler 1986, Molot & Dillon 1993, Kaste & Dillon, 2003). While Čertovo Lake (Kopáček et al. 2018b) represents such a typical acidified oligotrophic lake, Plešné Lake receives both high NO_3^- and P inputs (Table 2). Due to high primary production in Plešné Lake (Kopáček et al. 2004), N assimilation was higher than the NH_4^+ input (the primary N source for freshwater phytoplankton) and NO_3^- assimilation became an alternative N source for the plankton. Consequently, NO_3^- assimilation prevailed in the NO_3^- removal in Plešné Lake, while denitrification was the major NO_3^- sink in Čertovo Lake (Kopáček et al. 2018b). The average S_{NO3} values were two-fold higher in Plešné than in Čertovo Lake (9.4 vs. 4.4 m.yr^{-1}), but both values were within the range of similar data (2.8–12.7; on average 6.4 m.yr^{-1}) reported for 20 European and North American lakes by Kelly et al. (1987) and Kaste & Dillon (2003).

The annual SO_4^{2-} retention in Plešné Lake (5% on average, the mass transfer coefficient of 0.5±0.7 m.yr^{-1}) was similar to Čertovo Lake, as well as lakes with short (<4 years) water residence times (Kelly et al. 1987). The SO_4^{2-} role in the internal H^+ neutralization was thus small during the study (Fig. 6) and will further decrease together with the decreasing in-lake SO_4^{2-} concentrations, anticipated by modelling (Majer et al. 2003, Oulehle et al. 2018).

The in-lake removal of A^- (151 meq.m^{-2}.yr^{-1}) was the second most effective H^+ neutralizing process. This H^+ neutralizing process is associated with the partial photochemical degradation of allochthonous DOC (Kopáček et al. 2003, Porcal et al. 2004, 2010) that oxidizes DOC and produces biologically available small molecular weight compounds for bacterial growth (e.g., Wetzel et al. 1995). The DOC (and A^-) is thus photochemically and/or microbially oxidized to CO_2 and H_2O, removing one mole of H^+ per each equivalent of the oxidized A^-; e.g. for formic acid:

$$HCOO^- + H^+ + {}^1/_2O_2 = CO_2 + H_2O \quad (14)$$

The photochemical and microbial decomposition removed 38% of DOC supplied by surface inlets and decreased DOC concentrations in the outlet (Fig. 5E). This acid neutralizing process will likely remain important in all the Bohemian and Bavarian Forest lakes due to the continuing increase in DOC leaching to surface waters in this area (Beudert & Gietl 2015, Kopáček et al. 2018a).

The photochemical cleaving of DOC liberated 30–40% of Al_o and Fe_o from their organic complexes as Al_i and Fe_i (Table 4) and thus the Al_o and Fe_o concentrations were lower in the outlet than in the lake tributaries (Table 2). This proportion of liberated metals was lower than in Čertovo Lake (~50%; Kopáček et al. 2018b) due probably to the lower water transparency, higher pH, and shorter water residence time. The liberated metals contributed to their ionic forms, supplied by tributaries, in modifying in-lake H^+ budgets.

Hydrolysis of Al_i (equation 15) was the most important in-lake source of acidity, producing on average 243±81 meq.m^{-2}.yr^{-1} of H^+ (Table 4, Fig. 6):

$$Al^{3+} + nH_2O = Al(OH)_n^{3-n} + nH^+ \quad (15)$$

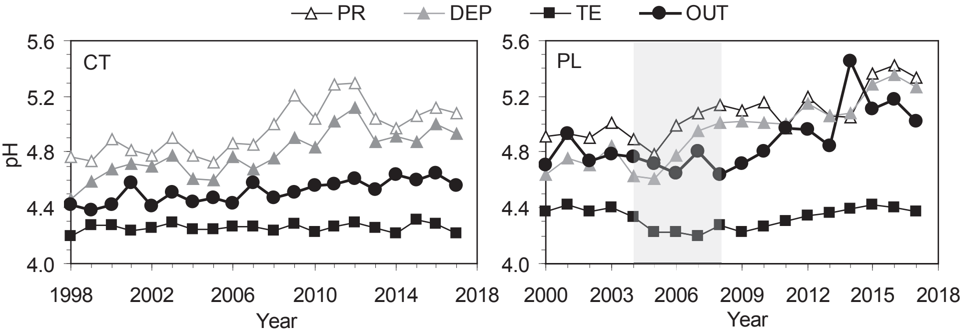

Fig. 7. Time series of annual average pH of precipitation (PR), deposition to the catchment soils (DEP), and terrestrial export via tributaries (TE), and output (OUT) from lake in the Čertovo (CT; data from Kopáček et al. 2018b) and Plešné (PL) catchment–lake systems in the 1998–2017 hydrological years. Grey area indicates the period of bark beetle outbreak in the Plešné catchment.

The hydrolysis occurs along pH gradients between the input and output water (Table 2), and between the lake surface and bottom (Fig. 2C,J), resulting in a decreasing positive charge of hydroxyl-Al complexes and a net in-lake production of Al_p (mostly colloidal $Al(OH)_3$)(Kopáček et al. 2008). A part of this particulate Al left the lake via outflow (41 $mmol.m^{-2}.yr^{-1}$), the rest (62 $mmol.m^{-2}.yr^{-1}$) was deposited in the sediments (Table 4). The H^+ production associated with the Al_i hydrolysis was three times higher in Plešné than in Čertovo Lake (Kopáček et al. 2018b), due to higher terrestrial Al_i exports after the tree dieback and higher water pH, and consequently, higher proportion of Al_i transformed to Al_p.

Similarly to Al_i, the Fe_i partly hydrolyzed in the lake along pH gradients, but its effect on the in-lake H^+ budget was negligible, due to lower concentrations. The lake was a small net source of Fe_T (Table 4), similarly to Čertovo Lake (Kopáček et al. 2018b). This suggests that both lakes receive some unmeasured Fe_p source, e.g., deposition of needles from shoreline trees (Psenner 1984) or overland flow.

The net internal H^+ neutralization was more pronounced in Plešné than Čertovo Lake throughout the study period, and has further accelerated since 2009 (Fig. 7) together with decreasing leaching of Al_i (Fig. 3). The H^+ concentrations in the lake have started to decrease since 2009 (Fig. 5H), because terrestrial exports of NO_3^-, A^- (DOC), and TP have remained high enough to neutralize H^+ by NO_3^- reduction and A^- oxidation, while H^+ production by Al_i hydrolysis has decreased. The changes in composition of tributaries thus caused the rapid pH increase in Plešné Lake (while its values only slightly increased in Čertovo Lake; Fig. 7), and a reestablishment of the carbonate buffering system (see annual average HCO_3^- concentrations in the lake outlet; Appendix 6).

Plešné Lake was a net sink for all nutrients (Table 4, Fig. 5). The in-lake retention of total N (297±142 $mmol.m^{-2}.yr^{1}$) was caused by high NO_3^- removal, while the lake was a net source of TON and also NH_4^+(as in Čertovo Lake; Kopáček et al. 2018b). The net NH_4^+ production shows that the internal NH_4^+ source can exceed its sinks in acidified lakes, which have ceased nitrification (Rudd & al. 1988) and have significant assimilation of NO_3^-. This pattern was for Plešné Lake discussed in detail elsewhere (Kopáček et al. 2004, 2006).

The lake was an average sink of 4.3 and 6.2 $mmol.m^{-2}.yr^{-1}$ of TP and SRP, respectively, during the whole study. The percent retention of P was twice as high in Plešné as in Čertovo Lake (51% *vs.* 22%) despite a ~50% shorter water residence time. The disproportion could be partly caused by higher abiotic PP production in Plešné Lake. Dissolved P can be converted to PP by both biomass production and abiotic P immobilization by colloidal Al_p in acidified lakes with elevated Al inputs (Kopáček et al. 2000a, 2004). The Al_p production was three times higher in Plešné than in Čertovo Lake.

The average Si removal of 136±85 $mmol.m^{-2}.yr^{-1}$ was probably too high to be explained by sedimentation of diatoms, which are absent in the plankton of Plešné Lake (Vrba et al. 2003, Nedbalová et al. 2006, 2016). Similarly, as in Čertovo Lake (Kopáček et al. 2018b), we assume that some abiotic processes could contribute to the internal Si sink in Plešné Lake, besides the sedimentation of biogenic Si.

Conclusions

Recovery of Plešné Lake from atmospheric acidification was disrupted by bark beetle outbreak in its catchment that killed ~90% of mature Norway spruce trees during 2004–2008. All dead biomass was left in the catchment. NO_3^- became the dominant anion, with maximum concentrations within 5–7 years after the tree dieback, and then started to decrease. Terrestrial exports of Al_i, K^+, H^+, Mg^{2+}, and Ca^{2+} accompanied NO_3^- leaching. Elevated losses of TP, SRP, and DOC continued until the end of the study. These changes affected H^+

balance in both terrestrial and aquatic ecosystems.

The terrestrial H^+ production was dominated by NH_4^+ removal and the excess leaching of SO_4^{2-} from soils (desorption and microbial oxidation of reduced S forms) during 2000–2004, i.e., prior to the tree dieback. Then, net terrestrial NO_3^- production became the dominant H^+ producing process for 10 following years (Fig. 3). Since 2008, the relative importance of A^- in the terrestrial H^+ production has steadily increased, and has become the dominant process in 2017. The future trend in terrestrial H^+ production will be probably governed by A^- leaching, NH_4^+ retention, and also (despite its continuous decrease) by net SO_4^{2-} release, while the importance of NO_3^- will further decrease due to increasing N consumption by regenerating forest. The elevated A^- leaching will probably last until the decrease of elevated soil wetness back to their pre-disturbance levels (Kopáček et al. 2018a) and termination of the enhanced production of DOC from dead biomass that can continue (albeit with decreasing intensity) for up to three decades after a mortality event, as observed elsewhere (Hyvönen et al. 2000, Shorohova & Kapitsa 2016).

In the lake, microbial processes significantly decreased concentrations of NO_3^-, A^-, H^+, and Al_i. Their net effect was ~65% reduction of the total (terrestrial and atmospheric) H^+ input into the lake. The in-lake acidity removal neutralized almost all H^+ production in the catchment, and consequently, the water leaving the whole Plešné catchment–lake system had pH similar to that in precipitation (Fig. 7). The most important in-lake neutralizing processes were NO_3^- reduction and A^- oxidation, while Al_i hydrolysis most importantly mitigated the H^+ decrease associated with the former processes. Despite the decreasing NO_3^- leaching, its input to the lake remains higher than its present in-lake biological demand. The present terrestrial export of NO_3^- (together with TP) thus results in a still high H^+ neutralization due to NO_3^- assimilation. Moreover, H^+ neutralization by photochemical and microbial oxidation of A^- remains high due to still elevated leaching of DOC (Fig. 3E). In contrast, Al_i leaching and its in-lake hydrolysis decrease, resulting in lower H^+ production. The net result of these processes is that lake water pH increases and the carbonate buffering system has established in the lake after more than a half of century (Oulehle et al. 2018). These favourite conditions for biological recovery of Plešné Lake from acidification will probably persist until the terrestrial exports of NO_3^-, TP, and DOC will decrease back to their pre-disturbance levels.

Further research of Plešné Lake should include more detailed studies on the development of in-lake food web structure and sediment diagenesis. It is probable that (i) the role of sulphur controls on the fate of geochemical elements in the lake sediment will decrease with decreasing terrestrial export of SO_4^{2-} (Couture et al. 2016), and (ii) the settling particulate organic carbon will become more available for microbial decomposition due to decreasing load of Al and decreasing formation of organic-Al complexes that are substantially stabilized against microbial decay (Mulder et al. 2001, Scheel et al. 2007).

Acknowledgements. We thank L. Švejda for long-term field sampling and the Šumava National Park authorities for their administrative support. This research and publication of results were supported by the Transboundary Cooperation Program of the Czech Republic – Free State Bavaria (Target ERDF 2014-2020, Project 26 – Silva Gabreta Monitoring) and the Czech Science Foundation (project No. P504-17-15229S).

REFERENCES

Bastviken D., Thomsen F., Svensson T., Karlsson S., Sandé P., Shaw G., Matucha M. & Öberg G., 2007: Chloride retention in forest soil by microbial uptake and by natural chlorination of organic matter. *Geochimica et Cosmochimica Acta*, 71: 3182–3192.

Bearup L.A., Maxwell R.M., Clow D.W. & McCray J.E., 2014: Hydrological effects of forest transpiration loss in bark beetle-impacted watersheds. *Nature Climate Change*, 4: 481–486.

Berg B. & McClaugherty C., 2008: *Plant litter. Decomposition. Humus formation. Carbon sequestration,* 2nd edition, Springer, New York, 338 pp.

Beudert B. & Gietl G., 2015: Long-term monitoring in the Große Ohe catchment, Bavarian Forest National Park. *Silva Gabreta*, 21: 5–27.

Beudert B., Bernsteinová J., Premier J. & Bässler C., 2018: Natural disturbance by bark beetle offsets climate change effects on streamflow in headwater catchments of the Bohemian Forest. *Silva Gabreta*, 24: 21–45.

Couture R.M., Fischer R., Van Cappellen P. & Gobeil C., 2016: Non-steady state diagenesis of organic and inorganic sulfur in lake sediments. *Geochimica et Cosmochimica Acta*, 194: 15–33.

Čtvrtlíková M., Hejzlar J., Vrba J., Kopáček J., Nedoma J., Hekera P., Wade A.J. & Roy S., 2016: Lake water acidification and temperature have a lagged effect on the population dynamics of *Isoëtes echinospora* via offspring recruitment. *Ecological Indicators*, 70: 420–430.

Draaijers G.P.J., Erisman J.W., 1995: A Canopy Budget Model to assess atmospheric deposition from throughfall measurements. *Water, Air and Soil Pollution*, 85: 2253–2258.

Dougan W.K. & Wilson A.L., 1974: The absorptiometric determination of aluminium in water. A comparison of some chromogenic reagents and the development of an improved method. *Analyst*, 99: 413–430.

Driscoll C.T., 1984: A procedure for the fractionation of aqueous aluminum in dilute acidic waters. *International Journal of Environmental Analytical Chemistry*, 16: 267–284.

Forsius M., Kleemola S. & Starr M., 2005: Proton budgets for a monitoring network of European forested catchments: impacts of nitrogen and sulphur deposition. Ecological Indicators, 5: 73–83.

Frič A., 1874: Über weitere Untersuchungen der Böhmerwaldseen. *Sitzungsberichte der königlichen böhmischen Gesellschaft der Wissenschaften in Prag, Jahrgang 1873*, 3: 103–109.

Golterman H.L. & Clymo R.S., 1969: *Methods for chemical analysis of fresh waters.* Blackwell, Oxford, 172 pp.

Houlton B.Z., Driscoll C.T., Fahey T.J., Likens G.E., Groffman P.M., Bernhardt E.S. & Buso D.C., 2003: Nitrogen dynamics in ice storm-damaged forest ecosystems: Implications for nitrogen limitation theory. *Ecosystems* 6: 431–443.

Huber C., Baumgarten M., Göttlein A. & Rotter V., 2004: Nitrogen turnover and nitrate leaching after bark beetle attack in mountainous spruce stands of the Bavarian Forest National Park. *Water, Air, and Soil Pollution: Focus,* 4: 391–414.

Huber C., 2005: Long lasting nitrate leaching after bark beetle attack in the highlands of the Bavarian Forest National Park. *Journal of Environmental Quality*, 34: 1772–1779.

Hyvönen R., Olsson B.A., Lundkvist H. & Staaf H., 2000: Decomposition and nutrient release from *Picea abies (L.) Karst.* and *Pinus sylvestris L.* logging residues. *Forest Ecology and Management*, 126: 97–112.

Hejzlar J., Kopáček J., Vrba J., Čížková R., Komárková J. & Šimek K., 1998: Limnological study of Plešné Lake in 1994–1995. *Silva Gabreta*, 2: 155–174.

Kaňa J. & Kopáček J., 2006: Impact of soil sorption characteristics and bedrock composition on phosphorus concentrations in two Bohemian Forest lakes. *Water Air and Soil Pollution*, 173: 243–259.

Kaňa J., Tahovská K. & Kopáček J., 2013: Response of soil chemistry to forest dieback after bark beetle infestation. *Biogeochemistry*, 113: 369–383.

Kaňa J., Tahovská K., Kopáček J. & Šantrůčková H., 2015: Excess of organic carbon in mountain spruce forest soils after bark beetle outbreak altered microbial N transformations and mitigated N-saturation. *PLoS ONE*, 10: e0134165.

Kaste Ø. & Dillon P.J., 2003: Inorganic nitrogen retention in acid-sensitive lakes in southern Norway and southern Ontario, Canada – a comparison of mass balance data with an empirical N retention model. *Hydrological Processes*, 17: 2393–2407.

Kauffman S.J., Royer D.L., Chang S. & Berner R.A., 2003: Export of chloride after clear-cutting in the Hubbard Brook sandbox experiment. *Biogeochemistry*, 63: 23–33.

Kelly C.A., Rudd J.W.M., Hesslein R.H, Schindler D.W., Dillon P.J., Driscoll C.T., Gherini S.A. & Hecky R.E., 1987: Prediction of biological acid neutralisation in acid-sensitive lakes. *Biogeochemistry*, 3: 129–140.

Kopáček J. & Hejzlar J., 1993: Semi-micro determination of total phosphorus in fresh waters with perchloric acid digestion. *International Journal of Environmental Analytical Chemistry*, 53: 173–183.

Kopáček J., Hejzlar J. & Mosello R., 2000a: Estimation of organic acid anion concentrations and evaluation of charge balance in atmospherically acidified colored waters. *Water Research,* 34: 3598–3606.

Kopáček J., Hejzlar J., Borovec J., Porcal P. & Kotorová I., 2000b: Phosphorus inactivation by aluminum in the water column and sediments: A process lowering in-lake phosphorus availability in an acidified watershed–lake ecosystem. *Limnology and Oceanography*, 45: 212–225.

Kopáček J., Hejzlar J., Kaňa J. & Porcal P., 2001a: Element budgets in three Bohemian Forest lakes and their watersheds in the 2000 hydrological year: III. Plešné Lake. *Silva Gabreta*, 6: 73–86.

Kopáček J., Borovec J., Hejzlar J. & Porcal P., 2001b: Parallel spectrophotometric determinations of iron, aluminum, and phosphorus in soil and sediment extracts. *Communications in Soil Science and Plant Analysis*, 32:

1431–1443.

Kopáček J., Kaňa J., Šantrůčková H., Porcal P., Hejzlar J., Picek T. & Veselý J., 2002: Physical, chemical, and biochemical characteristics of soils in watersheds of the Bohemian Forest lakes: I. Plešné Lake. *Silva Gabreta*, 8: 43–62.

Kopáček J., Hejzlar J., Kaňa J., Porcal P. & Klementová S., 2003: Photochemical, chemical, and biological transformations of dissolved organic carbon and its impact on alkalinity production in acidified lakes. *Limnology and Oceanography*, 48: 106–117.

Kopáček J., Brzáková M., Hejzlar J., Nedoma J., Porcal P. & Vrba J., 2004: Nutrient cycling in a strongly acidified mesotrophic lake. *Limnology and Oceanography*, 49: 1202–1213.

Kopáček J. Turek J., Hejzlar J., Kaňa J. & Porcal P., 2006. Element fluxes in watershed-lake ecosystems recovering from acidification: Čertovo Lake, the Bohemian Forest, 2001–2005. *Biologia*, 61: S427–S440.

Kopáček J., Turek J., Hejzlar J. & Šantrůčková H., 2009: Canopy leaching of nutrients and metals in a mountain spruce forest. *Atmospheric Environment*, 43: 5443–5453.

Kopáček J., Turek J., Hejzlar J. & Porcal P., 2011: Bulk deposition and throughfall fluxes of elements in the Bohemian Forest (Central Europe) from 1998 to 2009. *Boreal Environment Research*, 16: 495–508.

Kopáček J., Fluksová H., Hejzlar J., Kaňa J., Porcal P., Turek J. & Žaloudík, J., 2013a: Chemistry of tributaries to Plešné and Čertovo lakes during 1998–2012. *Silva Gabreta*, 19: 105–137.

Kopáček J., Fluksová H., Kaňa J., Porcal P., Turek J. & Žaloudík J., 2013b: Chemical composition of atmospheric deposition in the catchments of Plešné and Čertovo lakes in 1998–2012. *Silva Gabreta*, 19: 1–23.

Kopáček J., Fluksová H., Hejzlar J., Kaňa J., Porcal P. & Turek J., 2017: Changes in surface water chemistry caused by natural forest dieback in an unmanaged mountain catchment. *Science of the Total Environment*, 584–585: 971–981.

Kopáček J., Evans C.D., Hejzlar J., Kaňa J., Porcal P. & Šantrůčková H., 2018a: Factors affecting leaching of dissolved organic carbon after tree dieback in an unmanaged European mountain forest. *Environmental Science and Technology*, 52: 6291−6299.

Kopáček J., Hejzlar J., Kaňa J., Porcal P. & Turek J., 2018b: Water fluxes of ecologically important elements in Plešné catchment–lake system from 2000–2017. *Silva Gabreta*, 24: 115–148.

Likens G.E. & Bormann F.H., 1995: *Biogeochemistry of a forested ecosystem*, *2nd edition*. Springer-Verlag, New York, 159 pp.

Lovett G.M., Likens G.E., Buso D.C., Driscoll C.T. & Bailey S.W., 2005: The biogeochemistry of chlorine at Hubbard Brook, New Hampshire, USA. *Biogeochemistry*, 72: 191–232.

Majer V., Cosby B.J., Kopáček J. & Veselý J., 2003: Modelling reversibility of central European mountain lakes from acidification: Part I – the Bohemian Forest. *Hydrology and Earth System Sciences*, 7: 494–509.

McHale M.R., Burns D.A., Lawrence G.B. & Murdoch P.S. 2007: Factors controlling soil water and stream water aluminum concentrations after a clearcut in a forested watershed with calcium-poor soils. *Biogeochemistry*, 84: 311–331.

Mikkelson K.M., Bearup L.A., Maxwell R.M., Stednick J.D., McCray J.E. & Sharp J.O., 2013: Bark beetle infestation impacts on nutrient cycling, water quality and interdependent hydrological effects. *Biogeochemistry*, 2013, 115: 1–21.

Mosello R., Amoriello T., Benham S., Clarke N., Derome J., Derome K., Genouw G., Koenig N., Orrù A., Tartari G., Thimonier A., Ulrich E. & Lindroos A.J., 2008: Validation of chemical analyses of atmospheric deposition on forested sites in Europe: 2. DOC concentration as an estimator of the organic ion charge. *Journal of Limnology*, 67: 1–14.

Molot L.A. & Dillon P.J., 1993: Nitrogen mass balances and denitrification rates in central Ontario Lakes. *Biogeochemistry*, 20: 195–212.

Mulder J., De Wit H.A., Boonen H.W.J. & Bakken L.R., 2001: Increased levels of aluminium in forest soils: Effects on the stores of soil organic carbon. *Water Air and Soil Pollution*, 130: 989–994.

Murphy J. & Riley J. P., 1962: A modified single-solution method for the determination of phosphate in natural waters. *Analytica Chimica Acta*, 27: 31–36.

Nedbalová L., Vrba J., Fott J., Kohout L., Kopáček J., Macek M. & Soldán T., 2006: Biological recovery of the Bohemian Forest lakes from acidification. *Biologia*, 61(Suppl. 20): S453–S465.

Nieminen M., 2004: Export of dissolved organic carbon, nitrogen and phosphorus following clear-cutting of three Norway spruce forests growing on drained peatlands in southern Finland. *Silva Fennica*, 38: 123–132.

Öberg G. & Bastviken D., 2012: Transformation of chloride to organic chlorine in terrestrial environments: variability, extent, and implications. *Critical Reviews in Environmental Science and Technology*, 42: 2526–2545.

Oulehle F., Chuman T., Majer V. & Hruška J., 2013: Chemical recovery of acidified Bohemian lakes between 1984 and 2012: the role of acid deposition and bark beetle induced forest disturbance. *Biogeochemistry*, 116: 83–101.

Oulehle F., Wright R.F., Svoboda M., Bače R., Matějka K., Kaňa J., Hruška J., Couture R.M. & Kopáček J., 2018: Effects of bark beetle disturbance on soil nutrient retention and lake chemistry in glacial catchment. *Ecosystems*, doi.org/10.1007/s10021-018-0298-1.

Palviainen M., Finér L., Kurka A.M., Mannerkoski H., Piirainen S. & Starr M., 2004: Release of potassium, calcium, iron and aluminium from Norway spruce, Scots pine and silver birch logging residues. *Plant Soil*, 259: 123–136.

Porcal P., Hejzlar J. & Kopáček J., 2004: Seasonal and photochemical changes of DOM in an acidified forest lake and its tributaries. *Aquatic Sciences*, 66: 211–222.

Porcal P., Amirbahman A., Kopáček J. & Norton S.A., 2010: Experimental photochemical release of organically bound aluminum and iron in three streams in Maine, USA. *Environmental Monitoring and Assessment*, 171: 71–81.

Procházková L., 1960: Einfluss der Nitrate und Nitrite auf die Bestimmung des organischen Stickstoffs und Ammonimus im Wasser. *Archiv für Hydrobiologie,* 56: 179–185.

Procházková L. & Blažka P., 1999: Chemistry and biology of the Bohemian Forest lakes in the early 1960s. *Silva Gabreta*, 3: 65–72.

Psenner R., 1984: The proportion of empneuston and total atmospheric inputs of carbon, nitrogen, and phosphorus in the nutrient budget of small mesotrophic lake (Piburger See, Austria). *Internationale Revue der gesamten Hydrobiologie*, 69: 23–39.

Rudd J.W.M., Kelly C.A., Schindler D.W. & Turner M.A., 1988: Disruption of the nitrogen cycle in acidified lakes. *Science*, 240: 1515–1517.

Šantrůčková H., Vrba J., Picek T. & Kopáček J., 2004: Soil biochemical activity and phosphorus transformations and losses from acidified forest soils. *Soil Biology & Biochemistry*, 36: 1569–1576.

Scheel T., Dörfler C. & Kalbitz K., 2007: Precipitation of dissolved organic matter by aluminum stabilizes carbon in acidic forest soils. *Soil Science Society of America Journal*, 71: 64–74.

Schindler D.W., 1986: The significance of in-lake production of alkalinity. *Water Air and Soil Pollution*, 30: 931–944.

Schmidt R., Arzet K., Facher E., Fott J., Irlweck K., Řeháková Z., Rose N., Straškrabová V. & Veselý J., 1993: Acidification of Bohemian lakes. Recent trends and historical development. Ms., unpubl. report, Ost-West Program, Rep. GZ 45.168/1-276(b), Mondsee, 156 pp.

Shorohova E. & Kapitsa E., 2016: The decomposition rate of non-stem components of coarse woody debris (CWD) in European boreal forests mainly depends on site moisture and tree species. *European Journal of Forest Research*, 135: 593–606.

Stumm W. & Morgan J.J., 1981: *Aquatic Chemistry*. Willey, New York, 780 pp.

Svoboda M., Matějka K. & Kopáček J., 2006: Biomass and element pools of understory vegetation in the catchments of Čertovo Lake and Plešné Lake in the Bohemian Forest. *Biologia*, 61: S509–S521.

Tahovská K., Čapek P., Šantrůčková H. & Kopáček J., 2018: In-situ phosphorus dynamics in soil: long-term ion-exchange resin study. *Biogeochemistry*, doi.org/10.1007/s10533-018-0470-x.

Van der Perk M., 2006: *Soil and water contamination from molecular to catchment scale*, Taylor & Francis, London, 402 pp.

Veselý J., 1994: Investigation of the nature of the Šumava lakes: a review. *Časopis Národního Muzea, Praha, Řada Přírodovědná*, 163: 103–120.

Veselý J., Hruška J., Norton S.A. & Johnson C.E., 1998a: Trends in water chemistry of acidified Bohemian lakes from 1984 to 1995: I. Major solutes. *Water Air and Soil Pollution*, 108: 107–127.

Veselý J., Hruška J. & Norton S.A., 1998b: Trends in water chemistry of acidified Bohemian lakes from 1984 to 1995: II. Trace elements and aluminum. *Water Air and Soil Pollution*, 108: 425–443.

Vrba J., Kopáček J., Fott J., Kohout L., Nedbalová L., Pražáková M., Soldán T. & Schaumburg J., 2003: Long-term studies (1871–2000) on acidification and recovery of lakes in the Bohemian Forest (Central Europe). *Science of the Total Environment*, 310: 73–85.

Vrba J., Bojková J., Chvojka P., Fott J., Kopáček J., Macek M., Nedbalová L., Papáček M., Rádková V., Sacherová V., Soldán T. & Šorf M., 2016: Constraints on the biological recovery of the Bohemian Forest lakes from acid stress. *Freshwater Biology*, 61: 376–395.

Wetzel R.G., Hatcher P.G. & Bianchi T.S., 1995: Natural photolysis by ultraviolet irradiance of recalcitrant dissolved organic matter to simple substrates for rapid bacterial metabolism. *Limnology and Oceanography*, 40: 1369–1380.

Received: 23 May 2018
Accepted: 20 July 2018

Appendix 1. Water balance in Plešné Lake and its catchment in hydrological years (from November 1999 to October 2017). Precipitation amount (H_{PR}, mm.yr^{-1}), deposition to the catchment soils (Q_{DEP}, mm.yr^{-1}; precipitation in the open area and throughfall in the forest), terrestrial export from catchment via all lake tributaries (Q_{TE}, mm.yr^{-1}), water output from lake (Q_{OUT}, mm.yr^{-1}), specific runoff from catchment–lake system (*SR*, l.km^{-2}.s^{-1}), and water residence time in lake (*WRT*, day).

	2000	**2001**	**2002**	**2003**	**2004**	**2005**	**2006**	**2007**	**2008**	**2009**	**2010**	**2011**	**2012**	**2013**	**2014**	**2015**	**2016**	**2017**
H_{PR}	1655	1408	1953	1146	1315	1406	1425	1516	1513	1418	1293	1050	1186	1351	1068	1020	1465	1041
Q_{DEP}	1549	1349	1969	1160	1265	1337	1356	1553	1453	1403	1366	1090	1209	1335	1093	1019	1459	1115
Q_{TE}	971	1017	1655	723	886	1060	1236	1218	1386	1252	1230	838	1069	1126	906	799	1248	947
Q_{OUT}	1011	1018	1667	730	921	1060	1229	1216	1371	1227	1196	835	1052	1113	860	803	1243	923
SR	32.0	32.3	52.9	23.2	29.2	33.6	39.0	38.6	43.5	38.9	37.9	26.5	33.4	35.3	27.3	25.5	39.4	29.3
WRT	348	345	211	481	382	332	286	289	256	286	294	421	334	316	409	438	283	381

Appendix 2. Precipitation amount (H_{PR}) and volume weighted mean composition of precipitation (C_{PR}) in the catchment of Plešné Lake in hydrological years between November 1999 and October 2017. Units: µmol.l^{-1}, except for H_{PR} (m^3.m^{-2}.yr^{-1}) and pH. ND – not determined.

	2000	**2001**	**2002**	**2003**	**2004**	**2005**	**2006**	**2007**	**2008**	**2009**	**2010**	**2011**	**2012**	**2013**	**2014**	**2015**	**2016**	**2017**
H_{PR}	1.66	1.41	1.95	1.15	1.32	1.41	1.43	1.52	1.51	1.42	1.29	1.05	1.19	1.35	1.07	1.02	1.47	1.04
pH	4.91	4.94	4.91	5.01	4.89	4.79	4.99	5.08	5.14	5.10	5.16	4.97	5.20	5.07	5.05	5.37	5.42	5.34
H^+	12.2	11.6	12.4	9.8	12.9	16.3	10.3	8.4	7.3	8.0	6.9	10.6	6.3	8.6	8.9	4.3	3.8	4.6
Ca^{2+}	4.6	4.3	3.4	6.2	3.4	4.3	3.6	3.0	3.9	4.4	3.6	3.4	2.9	4.7	4.3	5.1	3.4	4.2
Mg^{2+}	1.2	1.5	1.2	1.8	1.4	1.0	1.0	1.9	1.2	1.1	0.9	1.0	1.0	1.2	1.2	1.6	0.8	1.0
Na^+	9.6	7.4	6.4	8.2	7.9	6.9	6.5	6.5	7.2	5.5	5.0	4.3	7.8	6.8	5.4	6.7	4.7	7.4
K^+	4.5	3.1	2.1	4.3	3.5	1.8	2.2	2.2	1.8	1.8	1.6	2.0	1.7	2.0	2.1	2.3	1.3	1.9
NH_4^+	24.4	26.2	25.4	27.3	19.3	21.3	26.5	29.4	27.8	23.0	31.4	18.5	26.7	23.0	32.6	39.2	31.1	30.7
NO_3^-	24.2	23.3	22.5	25.6	22.5	24.4	24.2	23.8	23.6	20.8	22.9	19.4	20.9	21.4	23.8	24.6	20.3	22.9
SO_4^{2-}	11.0	10.5	9.9	10.0	8.0	10.5	8.0	8.7	8.4	7.7	7.9	6.7	5.9	6.2	8.6	7.3	5.1	5.6
Cl^-	9.0	7.2	6.7	7.2	8.5	6.6	6.0	6.0	6.6	4.8	4.8	4.4	7.5	6.4	5.2	5.9	4.4	6.6
F^-	0.2	0.2	0.6	0.3	0.4	0.4	0.5	0.4	0.4	0.2	0.0	0.4	1.4	2.0	1.3	0.7	0.5	0.7
HCO_3^-	0.7	2.1	0.9	4.9	1.1	0.3	3.9	1.6	3.1	3.6	5.2	2.0	3.8	5.9	7.0	15.5	9.9	9.6
DOC	70	77	79	123	94	81	78	142	89	94	97	78	92	104	111	92	85	80
POC	ND	ND	ND	109	15	40	31	82	45	52	7	10	6	24	15	4	24	39
DON	5.5	8.2	10.4	11.2	10.1	7.1	10.7	21.9	9.2	11.3	13.7	13.3	12.5	12.6	17.9	14.7	15.2	13.7
PON	2.3	6.9	5.4	12.1	3.6	4.0	4.7	8.2	6.7	7.1	5.6	7.2	6.2	4.3	8.8	7.0	7.7	6.5
TP	0.37	0.65	0.29	0.71	0.48	0.30	0.33	0.68	0.37	0.32	0.41	0.73	0.23	0.33	0.46	0.61	0.30	0.42
PP	0.23	0.21	0.15	0.44	0.25	0.24	0.22	0.27	0.22	0.19	0.21	0.45	0.14	0.16	0.23	0.24	0.13	0.28
SRP	0.10	0.40	0.10	0.15	0.23	0.04	0.05	0.42	0.10	0.07	0.07	0.20	0.05	0.13	0.16	0.19	0.14	0.10
Si	0.07	0.07	0.22	0.38	0.38	0.38	0.38	0.38	0.68	0.67	1.04	0.86	0.86	0.86	0.46	0.68	0.68	0.68
Al_T	0.2	0.2	0.2	0.3	0.1	0.2	0.2	0.4	0.2	0.4	0.1	0.1	0.6	1.1	1.2	0.8	0.3	0.2

Appendix 3. Deposition amount (Q_{DEP}) and volume weighted mean composition of atmospheric deposition to the catchment soils (C_{DEP}; precipitation in the open area and throughfall in the forest; calculated from equation 6) in the catchment of Plešné Lake in hydrological years between November 1999 and October 2017. Units: µmol.l^{-1}, except for Q_{DEP} (m^3.m^{-2}.yr^{-1}) and pH. ND – not determined.

	2000	**2001**	**2002**	**2003**	**2004**	**2005**	**2006**	**2007**	**2008**	**2009**	**2010**	**2011**	**2012**	**2013**	**2014**	**2015**	**2016**	**2017**
Q_{DEP}	1.55	1.35	1.97	1.16	1.27	1.34	1.36	1.55	1.45	1.40	1.37	1.09	1.21	1.34	1.09	1.02	1.46	1.12
pH	4.64	4.76	4.71	4.85	4.63	4.61	4.78	4.95	5.01	5.02	5.02	5.00	5.15	5.06	5.08	5.29	5.35	5.26
H^+	22.9	17.4	19.7	14.2	23.5	24.5	16.6	11.2	9.8	9.6	9.6	10.0	7.1	8.7	8.3	5.1	4.5	5.5
Ca^{2+}	13.4	9.8	9.1	14.1	12.0	12.0	10.3	9.0	8.0	7.3	7.2	6.3	4.9	5.8	4.0	5.5	3.8	4.5
Mg^{2+}	4.7	3.5	3.5	4.9	5.0	4.4	3.8	4.7	3.8	2.9	3.2	2.7	2.2	1.8	1.5	2.0	1.3	1.5
Na^+	14.9	10.2	9.9	16.0	15.0	12.5	8.6	12.8	10.7	7.9	7.3	7.7	9.6	7.3	6.1	9.3	5.0	6.9
K^+	26.3	19.2	15.1	28.6	26.2	25.5	26.1	22.8	20.5	11.0	9.2	7.2	3.7	3.8	3.2	3.7	2.8	2.9
NH_4^+	32.5	29.2	32.6	50.1	25.2	28.2	30.0	31.4	27.8	28.1	33.0	29.1	31.8	27.1	33.7	38.6	28.2	29.7
NO_3^-	49.3	35.6	38.7	58.1	47.6	44.9	38.3	35.1	27.3	26.1	28.7	28.8	27.1	24.7	24.8	26.8	20.9	22.3
SO_4^{2-}	19.5	15.2	15.2	17.9	15.2	18.1	13.6	12.3	10.0	9.4	9.5	8.4	7.2	7.6	8.6	7.7	5.3	5.9
Cl^-	13.1	11.4	11.4	17.5	17.6	15.4	12.5	14.0	11.8	7.5	7.0	7.2	9.9	6.9	6.1	8.1	4.7	6.5
F^-	0.5	0.6	1.0	0.6	0.4	0.8	1.5	0.9	0.6	0.4	0.0	0.6	0.8	1.7	0.9	1.2	0.5	0.8
HCO_3^-	1.1	1.0	0.3	7.5	1.1	0.4	4.5	1.4	5.8	5.8	4.0	4.8	4.8	6.4	8.2	16.7	9.8	10.8
DOC	607	451	386	553	558	518	512	603	555	371	419	276	173	146	117	130	109	117
POC	ND	ND	ND	158	136	914	147	154	166	119	56	9	7	11	8	18	22	32
DON	22.1	22.6	23.0	33.6	19.2	25.9	17.1	22.9	13.4	19.1	9.9	15.1	13.1	14.5	13.0	8.5	11.6	14.8
PON	0.0	0.0	6.8	22.0	14.0	13.6	9.6	13.8	14.7	9.6	8.1	6.5	3.6	2.1	6.1	1.8	3.3	4.2
TP	0.82	0.65	0.49	0.84	0.76	0.82	0.81	1.07	0.89	0.72	0.71	0.73	0.31	0.51	0.63	0.43	0.28	0.33
PP	0.61	0.41	0.36	0.63	0.56	0.59	0.55	0.67	0.61	0.48	0.44	0.48	0.18	0.23	0.25	0.23	0.13	0.23
SRP	0.12	0.14	0.05	0.08	0.10	0.13	0.10	0.26	0.11	0.10	0.08	0.15	0.06	0.21	0.30	0.11	0.11	0.05

Appendix 4. Mean annual discharge (Q_{TE}) and period weighted mean concentrations of water constituents (C_{TE}) of terrestrial export via all tributaries to Plešné Lake (calculated from equation 9) in hydrological years between November 1999 and October 2017. Units: µmol.l^{-1}, except for Q_{TE} (m^3.m^{-2}.yr^{-1}, given on a catchment-area basis) and pH. ND – not determined.

	2000	**2001**	**2002**	**2003**	**2004**	**2005**	**2006**	**2007**	**2008**	**2009**	**2010**	**2011**	**2012**	**2013**	**2014**	**2015**	**2016**	**2017**
Q_{TE}	0.97	1.02	1.66	0.72	0.89	1.06	1.24	1.22	1.39	1.25	1.23	0.84	1.07	1.13	0.91	0.80	1.25	0.95
pH	4.37	4.43	4.37	4.40	4.34	4.23	4.22	4.19	4.27	4.23	4.27	4.31	4.34	4.36	4.39	4.42	4.41	4.37
H^+	42.2	37.5	42.3	39.8	46.1	59.0	60.0	64.0	53.7	59.4	54.3	49.5	45.3	43.7	40.8	38.1	39.3	42.5
Ca^{2+}	21	21	18	20	24	23	26	28	27	30	31	31	30	27	27	24	23	19
Mg^{2+}	7.5	6.5	7.3	6.9	8.8	8.8	8.8	11.1	9.4	10.8	12.3	12.3	11.2	10.7	10.4	9.1	7.9	6.6
Na^+	51	48	44	47	51	48	38	44	39	42	42	45	42	38	55	44	42	40
K^+	9.0	8.2	8.6	9.8	11.4	14.4	19.6	24.8	23.8	30.4	33.1	32.1	24.7	22.8	20.0	18.3	17.9	13.2
NH_4^+	2.7	0.7	0.6	0.3	0.8	0.4	0.8	0.6	0.5	1.3	0.9	0.6	0.2	0.5	0.1	0.2	0.1	0.1
NO_3^-	62	51	57	66	105	118	134	155	140	174	167	180	130	125	107	81	76	52
SO_4^{2-}	49	44	39	39	40	35	30	30	27	28	29	26	25	25	30	27	24	24
Cl^-	13	11	14	14	17	17	12	17	15	15	14	15	13	11	13	10	10	8
F^-	2.7	4.8	4.6	4.2	5.4	5.2	4.4	5.2	4.9	2.9	2.9	5.1	3.9	6.4	4.9	4.0	3.8	3.3
DOC	653	644	748	615	472	638	732	717	641	816	764	716	832	790	923	929	1059	1094
POC	ND	26	ND	13	10	0.1	9	71	24	23	11	25	16	17	22	34	9	19
DON	18.1	20.7	19.9	18.4	18.8	23.5	29.1	30.4	22.2	37.3	33.8	36.1	33.0	30.1	28.8	27.3	29.1	25.7
PON	ND	0.82	ND	0.86	0.83	0.06	0.48	0.63	1.88	1.33	1.78	1.24	0.48	0.23	0.87	2.36	1.47	0.53
TP	0.75	0.72	0.75	0.66	0.59	0.71	1.00	0.98	0.95	1.23	1.21	1.17	1.18	1.33	1.09	1.18	1.17	1.00
PP	0.03	0.03	0.05	0.04	0.06	0.03	0.10	0.08	0.05	0.08	0.09	0.09	0.09	0.06	0.04	0.06	0.05	0.03
SRP	0.59	0.59	0.56	0.48	0.42	0.57	0.73	0.77	0.75	1.03	1.02	1.02	0.99	1.11	0.87	0.87	0.93	0.83
Si	141	142	125	149	149	133	111	133	112	121	121	148	127	106	183	138	135	148
Al_T	28.7	27.4	28.2	27.7	31.2	30.7	33.4	33.4	31.2	38.4	35.5	41.1	29.7	33.6	30.5	26.6	25.4	23.5
Al_i	17.8	16.3	16.7	17.6	20.7	19.5	22.1	23.0	22.7	29.5	26.9	31.6	20.5	22.4	18.2	13.7	13.7	11.7
Al_o	10.6	10.5	10.6	9.1	9.7	10.8	10.7	9.7	7.6	8.6	7.5	8.0	7.9	10.1	11.3	12.3	11.3	11.3
Fe_T	1.7	1.7	1.7	1.2	1.3	1.6	1.5	1.6	1.5	1.6	1.7	1.6	1.8	1.6	2.1	2.0	2.1	2.3
Fe_i	0.6	0.5	0.4	0.2	0.2	0.2	0.3	0.4	0.5	0.7	0.7	0.5	0.5	0.3	0.4	0.3	0.3	0.5
Fe_o	1.0	1.2	1.3	0.9	1.0	1.3	1.2	1.1	1.0	0.8	0.8	1.0	1.2	1.2	1.5	1.6	1.7	1.7

Appendix 5. Total water input (Q_{IN}) and mean annual composition of water input (terrestrial export and precipitation to the lake surface) to Plešné Lake in hydrological years between November 1999 and October 2017. Units: µmol.l^{-1}, except for Q_{IN} (m^3.m^{-2}.yr^{-1}, given on a lake-area basis) and pH. ND – not determined.

	2000	**2001**	**2002**	**2003**	**2004**	**2005**	**2006**	**2007**	**2008**	**2009**	**2010**	**2011**	**2012**	**2013**	**2014**	**2015**	**2016**	**2017**
Q_{IN}	8.79	8.88	14.1	6.46	7.83	9.19	10.5	10.5	11.7	10.6	10.3	7.21	9.04	9.62	7.73	6.89	10.6	8.00
pH	4.44	4.48	4.42	4.46	4.39	4.28	4.27	4.25	4.32	4.28	4.32	4.36	4.40	4.41	4.44	4.48	4.46	4.42
H^+	36.6	33.4	38.2	34.5	40.5	52.4	53.2	56.0	47.7	52.6	48.4	43.9	40.2	38.8	36.4	33.1	34.4	37.6
Ca^{2+}	18	18	16	17	21	20	23	24	24	26	28	27	26	24	24	21	20	17
Mg^{2+}	6.3	5.7	6.5	6.0	7.6	7.6	7.8	9.8	8.3	9.5	10.8	10.7	9.9	9.3	9.1	7.9	6.9	5.9
Na^+	43	41	38	40	44	42	34	39	35	37	37	39	38	34	48	39	37	35
K^+	8.2	7.4	7.7	8.8	10.1	12.5	17.3	21.5	20.9	26.5	29.2	27.7	21.7	19.9	17.5	15.9	15.6	11.7
NH_4^+	6.8	4.7	4.0	5.1	3.9	3.6	4.3	4.8	4.0	4.2	4.7	3.2	3.7	3.6	4.6	6.0	4.3	4.1
NO_3^-	55	47	52	59	91	103	119	136	125	153	149	156	116	110	96	73	68	48
SO_4^{2-}	42	38	35	34	35	31	27	27	25	25	26	23	22	22	27	24	22	22
Cl^-	12	10	13	13	16	16	11	15	14	14	13	14	13	10	12	10	9	8
F^-	2.3	4.0	4.1	3.5	4.6	4.4	3.9	4.5	4.3	2.6	2.5	4.4	3.6	5.8	4.4	3.6	3.4	3.0
DOC	543	554	655	528	408	553	643	634	570	720	680	623	735	694	811	805	925	962
POC	ND	28	10	30	11	6	12	72	27	27	11	23	15	18	21	29	11	21
DON	15.7	18.7	18.6	17.1	17.3	21.0	26.6	29.2	20.5	33.8	31.3	32.8	30.3	27.7	27.3	25.4	27.2	24.2
PON	0.44	1.79	0.74	2.84	1.30	0.66	1.05	1.73	2.50	2.11	2.26	2.10	1.23	0.41	1.96	3.04	2.33	1.30
TP	0.68	0.71	0.68	0.67	0.57	0.65	0.91	0.93	0.87	1.11	1.11	1.11	1.06	1.19	1.01	1.10	1.05	0.92
PP	0.06	0.06	0.07	0.11	0.09	0.06	0.12	0.11	0.07	0.09	0.11	0.14	0.10	0.08	0.07	0.09	0.06	0.06
SRP	0.50	0.56	0.50	0.42	0.39	0.49	0.63	0.72	0.66	0.90	0.90	0.90	0.86	0.97	0.78	0.77	0.82	0.74
Si	114	120	107	122	124	113	96	114	98	105	106	127	110	91	158	117	117	128
Al_T	23.4	23.0	24.3	22.9	26.0	26.0	28.9	28.6	27.2	33.3	31.1	35.1	25.8	29.1	26.5	22.8	22.0	20.5
Al_i	14.5	13.7	14.4	14.5	17.2	16.5	19.1	19.7	19.8	25.5	23.5	27.0	17.8	19.2	15.6	11.6	11.8	10.2
Al_o	8.6	8.8	9.2	7.5	8.1	9.2	9.2	8.3	6.6	7.5	6.6	6.8	6.8	8.7	9.7	10.4	9.7	9.8
Fe_T	1.4	1.5	1.5	1.1	1.1	1.4	1.4	1.4	1.4	1.5	1.5	1.4	1.6	1.4	1.9	1.7	1.9	2.0
Fe_i	0.5	0.4	0.3	0.2	0.2	0.2	0.2	0.3	0.4	0.6	0.6	0.4	0.4	0.3	0.4	0.2	0.3	0.5
Fe_o	0.9	1.0	1.1	0.8	0.8	1.1	1.0	1.0	0.8	0.7	0.7	0.8	1.1	1.1	1.3	1.3	1.5	1.5

Appendix 6. Water output (Q_{OUT}) and mean annual composition of water output from Plešné Lake (C_{OUT}) in hydrological years between November 1999 and October 2017 Units: µmol.l^{-1}, except for Q_{OUT} (m^3.m^{-2}.yr^{-1}, given on a lake-area basis) and pH. ND – not determined.

	2000	2001	2002	2003	2004	2005	2006	2007	2008	2009	2010	2011	2012	2013	2014	2015	2016	2017
Q_{OUT}	8.44	8,50	13.9	6.10	7.69	8.85	10.3	10.2	11.4	10.2	9.99	6.97	8.79	9.29	7.18	6.70	10.4	7.70
pH	4.70	4.93	4.73	4.79	4.76	4.72	4.64	4.81	4.64	4.71	4.80	4.97	4.97	4.85	5.44	5.11	5.18	5.02
H^+	19.9	11.7	18.6	16.3	17.3	19.1	22.7	15.5	22.8	19.3	15.8	10.8	10.8	14.2	3.6	7.8	6.6	9.5
Ca^{2+}	21	18	18	17	19	20	21	24	22	25	28	29	29	25	27	22	19	17
Mg^{2+}	7.4	6.1	7.2	6.0	7.4	7.5	7.2	9.6	8.6	9.8	10.8	11.6	11.7	10.0	10.6	8.8	7.6	7.2
Na^+	41	37	38	34	38	39	36	40	37	38	37	40	41	35	41	39	35	36
K^+	8.8	8.1	7.7	8.2	9.0	9.3	11.9	15.1	17.5	21.7	26.4	26.1	25.6	24.1	21.6	19.3	15.8	14.9
NH_4^+	5.7	5.7	4.7	3.3	5.9	5.7	7.2	5.3	6.8	6.7	4.6	3.9	2.3	5.2	2.8	6.5	2.9	2.9
NO_3^-	31	22	30	23	44	48	61	70	88	104	110	100	91	80	45	40	27	21
SO_4^{2-}	47	37	38	33	34	33	31	30	27	26	26	23	24	23	24	23	21	21
Cl^-	13	10	14	11	15	15	13	15	15	14	14	14	14	12	12	11	11	9
F^-	3.4	3.7	5.1	3.3	3.7	4.3	3.7	4.6	4.6	2.7	3.0	5.1	3.5	5.7	4.9	4.4	3.8	3.4
HCO_3^-	0.0	0.0	0.1	0.3	0.2	0.0	0.0	0.1	0.3	0.4	0.1	2.4	2.5	3.4	14.9	12.2	12.2	10.9
DOC	328	295	453	386	326	325	396	305	386	362	364	312	380	435	497	562	565	664
POC	0	223	264	165	158	152	157	202	158	252	213	260	156	151	350	207	235	249
DON	14.2	12.9	15.5	14.4	13.1	12.2	16.0	19.6	18.9	24.5	26.2	24.5	27.3	23.0	24.2	23.1	21.8	22.6
PON	8.3	13.8	15.0	15.9	13.9	16.0	13.4	18.6	10.6	19.0	23.3	25.9	24.0	21.5	31.6	19.7	20.2	19.1
TP	0.34	0.34	0.40	0.39	0.31	0.36	0.41	0.37	0.42	0.55	0.52	0.48	0.53	0.66	0.61	0.51	0.49	0.54
PP	0.27	0.26	0.29	0.30	0.24	0.30	0.30	0.30	0.33	0.39	0.46	0.39	0.45	0.54	0.53	0.42	0.41	0.43
SRP	0.01	0.03	0.03	0.02	0.03	0.04	0.06	0.04	0.04	0.07	0.03	0.05	0.04	0.06	0.03	0.03	0.04	0.05
Si	89	87	95	100	104	100	90	104	96	100	99	116	115	94	110	110	102	111
Al_T	19.2	16.9	20.6	20.2	18.8	18.9	21.3	20.5	22.5	24.0	23.7	23.7	21.8	25.5	19.7	17.1	17.0	15.6
Al_i	10.4	8.5	10.2	10.2	9.9	9.3	11.5	11.3	13.9	15.7	15.2	10.8	9.5	11.2	3.8	5.3	5.3	4.2
Al_o	4.6	3.8	6.3	5.3	5.0	5.1	6.1	4.0	4.4	3.3	3.1	2.4	3.2	6.8	6.7	8.2	7.9	7.0
Fe_T	1.5	1.5	1.9	2.0	1.8	1.5	1.5	1.2	1.4	1.4	1.4	1.2	1.3	1.5	1.8	1.8	1.9	2.0
Fe_i	0.4	0.4	0.2	0.3	0.4	0.3	0.4	0.3	0.3	0.4	0.4	0.3	0.4	0.3	0.1	0.3	0.3	0.2
Fe_o	0.6	0.5	0.9	1.0	0.7	0.7	0.7	0.6	0.7	0.4	0.4	0.3	0.4	0.5	0.6	0.9	0.9	1.0

Appendix 7. Net production of water constituents in the catchment of Plešné Lake (π_C* calculated from equation 1) in hydrological years between November 1999 and October 2017. Units: µmol.l^{-1}. Positive values indicate net production, while negative values indicate net removal. ND – not determined.

	2000	**2001**	**2002**	**2003**	**2004**	**2005**	**2006**	**2007**	**2008**	**2009**	**2010**	**2011**	**2012**	**2013**	**2014**	**2015**	**2016**	**2017**
H^+	5.6	14.4	18.9	17.1	12.6	28.1	41.7	49.8	43.4	48.7	43.6	36.6	37.2	33.3	30.8	31.6	34.1	36.0
Ca^{2+}	–0.2	7.5	7.3	–2.8	6.8	7.4	14.7	16.6	18.1	21.3	23.1	23.0	24.4	20.5	22.3	16.9	18.8	13.6
Mg^{2+}	–0.1	1.8	3.2	–0.9	1.7	3.2	4.7	5.1	5.4	7.5	8.7	8.7	8.8	8.5	8.6	6.5	6.4	4.8
Na^+	27.2	34.1	31.9	21.4	30.0	32.1	28.4	28.1	28.0	33.1	33.9	35.5	31.5	29.3	48.0	32.3	36.4	31.5
K^+	–32.9	–17.2	–9.4	–36.1	–26.1	–17.8	–9.1	–4.3	2.3	18.0	22.8	22.7	20.6	18.3	16.2	13.5	14.6	9.8
NH_4^+	–49.2	–38.1	–38.1	–79.9	–35.2	–35.2	–32.1	–39.4	–28.6	–30.1	–35.7	–37.3	–35.7	–31.6	–40.5	–49.0	–32.9	–34.9
NO_3^-	–16.8	3.9	10.7	–27.1	36.5	60.8	92.2	110.6	111.8	144.6	135.0	142.3	99.2	95.3	77.5	47.1	51.1	25.9
SO_4^{2-}	18.2	23.4	20.7	10.1	18.3	11.8	15.4	14.5	16.9	17.3	18.1	14.9	16.8	15.9	20.0	17.3	18.0	17.0
Cl^-	–8.3	–4.6	0.0	–13.7	–7.8	–2.1	–1.5	–0.9	2.4	6.5	6.1	6.1	2.2	2.4	5.8	0.1	4.6	0.6
F^-	1.9	4.0	3.5	3.2	4.9	4.1	2.8	4.1	4.3	2.5	2.9	4.4	3.0	4.4	3.9	2.5	3.2	2.4
DOC	–315	46	288	–271	–326	–15	170	–51	60	400	298	357	636	617	782	763	932	957
POC	ND	ND	ND	–241	–184	ND	–152	–126	–150	–111	–51	13	7	4	12	10	–16	–19
DON	–17.2	–9.3	–7.5	–35.5	–8.7	–9.2	10.4	1.3	8.2	16.0	22.8	16.4	18.2	12.9	13.2	16.4	15.5	8.3
PON	ND	27	–8	–34	–19	–17	–10	–17	–14	–9	–7	–7	–4	–3	–7	0	–2	–4
TP	–0.56	–0.14	0.16	–0.68	–0.50	–0.33	0.10	–0.39	0.02	0.43	0.42	0.23	0.83	0.73	0.34	0.63	0.85	0.61
PP	–0.95	–0.50	–0.38	–0.97	–0.74	–0.71	–0.51	–0.78	–0.59	–0.47	–0.39	–0.53	–0.12	–0.21	–0.26	–0.23	–0.10	–0.24
SRP	0.40	0.41	0.50	0.36	0.28	0.41	0.62	0.44	0.63	0.92	0.93	0.82	0.91	0.86	0.51	0.74	0.80	0.77
Si	138	142	124	148	148	133	111	132	111	120	120	147	126	105	182	138	135	147
Al_T	28.0	27.3	28.0	27.2	31.0	30.5	33.1	32.8	31.0	38.0	35.4	40.9	29.0	32.4	30.2	25.6	25.3	23.5
Al_i	17.8	16.3	16.7	17.6	20.7	19.5	22.1	23.0	22.7	29.5	26.9	31.6	20.5	22.4	18.2	13.7	13.7	11.7
Al_o	10.6	10.5	10.6	9.1	9.7	10.8	10.7	9.7	7.6	8.6	7.5	8.0	7.9	10.1	11.3	12.3	11.3	11.3
Fe_T	1.7	1.3	1.2	0.6	0.7	1.1	1.1	1.0	0.9	0.9	1.2	1.3	1.6	1.4	1.4	1.8	2.0	2.2
Fe_i	0.6	0.5	0.4	0.2	0.2	0.2	0.3	0.4	0.5	0.7	0.7	0.5	0.5	0.3	0.4	0.3	0.3	0.5
Fe_o	1.0	1.2	1.3	0.9	1.0	1.3	1.2	1.1	1.0	0.8	0.8	1.0	1.2	1.2	1.5	1.6	1.7	1.7

Appendix 8. Net production of water constituents in Plešné Lake (π_L, calculated from equation 2) in hydrological years between November 1999 and October 2017. Units: µmol.l^{-1}. Positive values indicate net production, while negative values indicate net removal. ND – not determined.

	2000	2001	2002	2003	2004	2005	2006	2007	2008	2009	2010	2011	2012	2013	2014	2015	2016	2017
H^+	–22	–25	–18	–25	–22	–34	–34	–40	–27	–34	–36	–36	–33	–27	–35	–28	–27	–29
Ca^{2+}	1.7	–0.7	–0.8	0.1	0.1	–1.4	–0.3	0.7	–0.9	0.3	0.5	–0.8	1.8	–1.9	–0.3	–1.5	–7.8	–0.1
Mg^{2+}	1.1	0.9	–0.5	0.6	1.1	–0.8	–0.4	1.1	–0.4	1.5	0.2	0.2	1.7	–1.1	2.0	0.8	–2.0	2.1
Na^+	–7.5	–10.3	–1.1	–2.0	–5.6	–3.9	–0.8	3.1	–0.9	1.6	–2.6	–1.6	6.1	–3.4	–4.8	–4.5	–6.9	2.7
K^+	–0.1	0.1	–0.4	0.2	–1.2	–3.1	–3.5	–4.0	–2.3	–2.2	–0.3	–2.6	2.7	0.4	2.0	0.1	–3.2	1.5
NH_4^+	1.0	1.6	–1.5	1.5	0.3	3.9	4.0	–0.4	4.2	0.4	2.2	–9.4	4.4	2.1	–3.8	0.6	–3.3	–6.4
NO_3^-	–31	–28	–21	–31	–39	–58	–54	–51	–38	–33	–45	–82	–31	–54	–78	–49	–47	–33
SO_4^{2-}	–3.2	–4.2	–1.5	–2.6	–2.5	0.2	1.4	–0.9	0.5	0.6	–1.7	–5.0	2.7	–1.2	–3.3	–2.3	–3.0	–0.7
Cl^-	ND	ND	ND	ND	ND	ND	ND	ND	ND	ND	ND	ND	ND	ND	ND	ND	ND	ND
F^-	1.0	–1.3	0.7	0.3	–0.9	0.5	–1.4	2.0	0.1	–1.5	0.4	1.8	0.3	–0.1	1.4	–1.1	–0.6	1.0
HCO_3^-	9.1	3.2	–4.9	3.3	–0.5	1.3	1.6	–0.7	1.6	–4.2	6.6	5.7	3.3	9.4	21.8	15.1	3.3	4.0
DOC	–209	–237	–139	–362	–168	–211	–276	–279	–232	–362	–336	–393	–348	–168	–267	–331	–309	–265
POC	ND	194	263	243	55	234	133	159	85	272	28	343	106	141	343	169	277	288
DON	–0.1	–5.2	–3.9	–6.5	–7.7	–9.5	–10.4	–13.6	1.1	–8.3	2.7	–14.0	–9.9	–8.3	1.8	–9.3	–7.4	–2.6
PON	5.9	12.5	16.3	16.5	8.0	21.0	3.2	21.1	2.9	23.1	16.8	31.4	25.2	17.6	26.1	13.9	19.7	19.9
TP	–0.29	–0.41	–0.26	–0.29	–0.38	–0.34	–0.45	–0.59	–0.55	–0.45	–0.51	–0.81	–0.48	–0.62	–0.46	–0.71	–0.54	–0.43
PP	0.25	0.18	0.27	0.20	0.08	0.20	0.21	0.19	0.14	0.47	0.49	0.09	0.42	0.39	0.50	0.24	0.38	0.37
SRP	–0.51	–0.57	–0.48	–0.42	–0.36	–0.47	–0.59	–0.71	–0.64	–0.85	–0.91	–0.86	–0.86	–0.92	–0.85	–0.74	–0.81	–0.72
Si	–22	–32	–14	–24	–21	–19	–15	–7	–6	–12	–2	2	–14	–4	–42	–35	–7	–17
Al_T	–3.7	–6.6	–2.9	–5.6	–10.4	–6.2	–9.7	–5.2	–9.5	–6.5	–4.8	–20.8	–0.7	–5.2	–10.5	–11.2	–2.5	–8.1
Al_i	–5.8	–4.1	–3.4	–11.3	–8.2	–7.0	–8.1	–7.8	–7.5	–6.9	–8.4	–26.9	–7.0	–8.2	–14.6	–8.5	–6.3	–6.3
Al_o	–2.1	–4.2	–2.6	–4.1	–5.0	–3.1	–4.8	–3.2	–3.4	–4.9	–3.5	–6.3	–1.7	–0.5	–0.2	–4.2	–1.0	–4.7
Fe_T	0.66	0.12	0.58	1.32	–0.25	–0.01	0.07	–0.44	0.12	–0.52	0.19	–0.72	0.00	0.43	–0.21	0.27	0.19	–0.38
Fe_i	–0.02	–0.04	–0.05	–0.23	0.25	–0.13	0.27	–0.15	0.01	–0.10	–0.20	–0.49	0.05	0.06	–0.36	–0.24	0.06	–0.33
Fe_o	–0.03	–0.27	–0.11	–0.03	–0.47	–0.27	–0.40	–0.43	–0.25	–0.58	–0.26	–0.74	–0.56	–0.53	–0.44	–0.32	–0.56	–0.64

Silva Gabreta	vol. 24	p. 149–160	Vimperk, 2018

Biodiversity along an elevational gradient of the Bohemian Forest – the BIOKLIM project

Nicolas Friess[1,*], **Claus Bässler**[2], **Roland Brandl**[1], **Torben Hilmers**[3],
Jörg Müller[2,4] **& Linda Seifert**[2]

[1]Faculty of Biology, Philipps-Universität Marburg, Karl-von-Frisch Str. 8, DE-35032 Marburg, Germany
[2]Bavarian Forest National Park, Freyunger Str. 2, DE-94481 Grafenau, Germany
[3]Technical University of Munich, Hans-Carl-Von-Carlowitz-Platz 2, DE-85354 Freising, Germany
[4]Field Station Fabrikschleichach, Biocenter, University of Würzburg, Glashüttenstraße 5,
DE-96181 Rauhenebrach, Germany
[*] nico.friess@posteo.de

Abstract

To monitor the response of forest biodiversity to environmental changes, the BIOKLIM project collected data on species occurrences along transects covering the elevational gradient within the Bavarian Forest National Park and adjacent areas. The monitoring program was launched in 2006 and repeated in 2016 as a part of the Silva Gabreta Monitoring project. Here we show the potential of such regional monitoring programs for characterizing alpha, beta and gamma biodiversity of 15 groups of organisms along the elevational gradient in forests mainly dominated by European beech and Norway spruce. Overall, we recorded 4,179 species of which 1,918 are common (based on Shannon diversity) and 1,222 dominant (based on Simpson diversity). Asymptotic extrapolation suggested that between 5,340 and 6,100 species might occur in the terrestrial ecosystems of the Bohemian Forest. Most groups showed significant responses in alpha diversity to elevation. However, the relationships varied strongly in strength and shape. Changes in species composition along the elevational gradient were mostly due to turnover and contributed strongly to the overall diversity of the study region. These first analyses show that monitoring schemes as implemented in the Silva Gabreta Monitoring offer the opportunity to study biodiversity along environmental gradients. In the long run resampling of the plots established in 2006 allows characterizing the responses of the communities to changes in forest structure and/or climate.

Key words: biodiversity monitoring, ecology, protected areas, European beech, Norway spruce, Silver fir, Bavarian Forest National Park

Introduction

Following a set-aside strategy, national parks aim at conserving ecosystems in a state as natural as possible and at protecting ecological processes that structure these systems (McNeely & Miller 1983). Nevertheless, national parks are not isolated and therefore biodiversity of the communities occurring within the protected area will change with time, e.g. due to changes in the climate or disturbances (Hannah 2008). One important aim of national parks is therefore also to document such changes and to launch research to understand the processes that underpin fluctuations and trends of biodiversity (Heurich et al. 2010).

Founded in the year 1970, the Bavarian Forest National Park is the oldest national park in Germany. After its expansion in 1997 the national park covers an area of over 24,000 hectares and is part of the Bohemian Forest – the largest contiguous forest area in central Europe. After several consecutive disturbances, mostly due to wind throws and bark beetle outbreaks, the administration of the national park decided to implement a benign-neglect strategy and not to interfere (e.g. by salvage logging) with the natural processes (Müller et al. 2010). Thereby, deadwood availability and structural heterogeneity increased in large areas of the historically managed forest within the park (Lehnert et al. 2013). To monitor environmental changes within the park as well as the response of forest biodiversity to such natural disturbances, the BIOKLIM project was initiated in the year 2006 (Bässler et al. 2009). This project collected data on relevant environmental variables, as well as data on the occurrence and abundance of species of plants, fungi and animals along the elevational gradient of the national park. These groups represent a large proportion of the diversity of central European forests. Such standardized surveys offer baseline data on the biodiversity that are necessary to assess the response of communities to changing environmental conditions and processes that structure these communities. Furthermore, using a space-for-time approach the elevational gradient allowed first insights how the communities will change with global warming (Bässler et al. 2010). As the Bavarian Forest National Park represents only a rather small proportion of the contiguous forest covering the Bohemian Forest, the BIOKLIM survey is now integrated in an interregional monitoring scheme conducted by the Bavarian Forest and Šumava National Parks as part of the Silva Gabreta Monitoring project (Křenová & Seifert 2015, 2018). As part of this monitoring scheme, the survey of the biodiversity inhabiting the forests along the elevational gradient was repeated in the year 2016 (Bässler et al. 2015) and additionally this monitoring was expanded to streams (Bojková et al. 2018).

To show the potential of repeated surveys as implemented here, we present data on the diversity of 15 groups of organisms based on the two surveys conducted in the years 2006 and 2016. The aim of this study is to give a general overview of the biodiversity found in the Bavarian Forest National Park and adjacent areas (gamma diversity) and how biodiversity in terms of alpha and beta diversity is structured along the elevational gradient in the terrestrial ecosystems of the Bohemian Forest. Here, our analyses are based on a harmonized dataset from the two surveys in 2006 and 2016 generated with similar sampling methods conducted on the same study plots.

Material and methods

Sampling area

The surveys were conducted in 2006 and repeated in 2016 in the German part of the Bohemian Forest covering an elevational gradient from 287 to 1420 m a.s.l. Details of these two surveys are described in Bässler et al. (2009, 2015). The original design of 331 study plots was optimized for resampling in 2016 in order to cover the structural gradient across the whole elevational gradient and to maximize the number of plots covered by both surveys (Bässler et al. 2015). The final set of plots with harmonized data of both surveys used in this study consisted of 133 plots ranging from plots at low elevations in the Danube valley to high elevation plots on the mountain ranges of the Bavarian Forest National Park (Fig 1).

Species sampling

Species sampling of both surveys followed the same methods for each taxonomic group on the 133 study plots. Overall 15 groups of plants, fungi, and animals were included in this study (Table 1). The taxonomic rank differed considerably (Table 1). Species were sampled using standard methods suitable for an appropriate sampling of the respective taxon. Higher plants, fungi, and birds were recorded on all 133 plots. Insect samples from flight-interception and pitfall traps of one plot were unfortunately lost in 2016. The other taxa were sam-

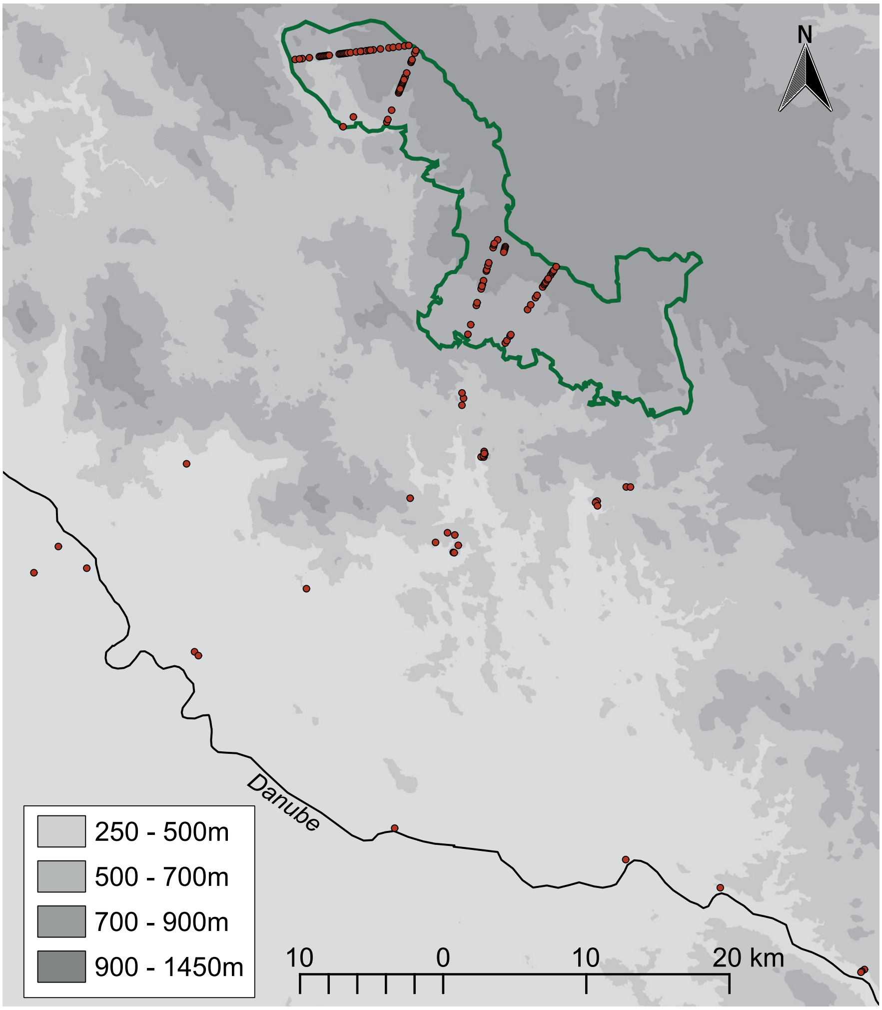

Fig. 1. An overview map of the 133 sampling plots (red points) across the elevational gradient. Main sampling transects are located within the Bavarian Forest National Park (green line). Additional lowland plots (<650 m a.s.l.) outside the NP extended the elevation gradient down to the Danube River representing the gradient from 287–1420 m a.s.l. Some sampling points are not visible (overlaid) due to scaling.

pled on subsets of the study plots due to the constraints imposed by labor-intensive collection methods. We applied hand collections (gastropods, number of the study plots surveyed: n = 108), field mapping (lichens, wood mosses and soil mosses, n = 109), flight-interception traps (beetles, true bugs, spiders and harvestmen, n = 132), pitfall traps (beetles, springtails, spiders and harvestmen, n = 132), malaise traps (bees and wasps, cicadas, hoverflies and true bugs, n = 52), and light traps (moths, n = 33; Table 1). For details of the sampling methods used for different taxa, see Bässler et al. (2009, 2015). All specimens were determined to species by specialists for the respective taxon. For the present communication, the occurrence data of both surveys were aggregated in presence-absence matrices. Thus the results of the present analysis do not distinguish between the two sampling events.

Table 1. Sampling methods for the groups sampled during the BIOKLIM project. FC – field collection, PT – pitfall traps, FIT – flight-interception trap, MT – malaise trap, LT – light trap. Number of species refers to the overall number of species found on the plots during both surveys. Number of plots refers to the number of plots with harmonized data for both survey years.

Group	Taxon	FC	PT	FIT	MT	LT	Number of species	Number of plots
Plants	Spermatophyta	x					297	133
Soil mosses	Bryophyta	x					84	109
Wood mosses	Bryophyta	x					149	109
Lichens	Fungi	x					125	109
Fungi	Fungi	x					562	133
Snails and Slugs	Gastropoda	x					103	133
Birds	Aves	x					51	133
Bees and wasps	Aculeata				x		308	52
Beetles	Coleoptera		x	x			1305	132
Cicadas	Cicadoidea				x		215	52
Hoverflies	Syrphidae				x		185	52
Moths	Lepidoptera					x	272	33
Spiders	Arachnida		x	x			292	132
Springtails	Collembola		x				51	132
True bugs	Heteroptera			x	x		180	52
Sum							4179	

Analysis

All statistical analyses were conducted in the software environment *R* (v. 3.4.3; R Core Team 2017). To estimate metrics of species richness, we used the rarefaction-extrapolation framework suggested by Chao et al. (2014) using the aggregated matrices. We calculated Hill numbers for the aggregated matrices to analyze the diversity of common and dominant species within one framework. Hill numbers represent a family of diversity indices expressed in effective numbers of species that differ among themselves by the exponent q (Hill 1973, Chao et al. 2014). The value of q determines the sensitivity of the diversity measure to rare or common species. Here, Hill numbers with $q = 0$ are equivalent to the species richness of the assemblage which counts species without regard to their prevalence. Hill numbers of orders lower than 1 are sensitive to rare species, while orders higher than 1 are sensitive to the most common or dominant species (Jost 2007). Hill numbers with $q = 1$ conform to the exponential of the frequently used Shannon index and represent the effective number of common species. Hill numbers with $q = 2$ are termed Simpson diversity and discount all but the most common or dominant species (Hsieh et al. 2016). In order to get comparable estimates based on sampling effort we rarified respectively extrapolated the diversity estimates for all groups to 99 sites, which leads to an extrapolation by an factor of three for the group sampled on the fewest number of sites (moths sampled on 33 sites; Hsieh et al. 2016). Additionally, we calculated estimates of the asymptotic richness (i.e. the number of species after extrapolation to the point where an increase in sampling units does not further increase the number of species) for each group separately as an estimate of the lower bound of total species richness, as well as the number of common and dominant species (Chao, 1987). We used

999 replicated bootstraps to calculate confidence intervals around the species-accumulation curves. These methods are implemented in the iNEXT package (Hsieh et al. 2016).

In order to investigate the response of each of the 15 taxa to the elevational gradient on alpha diversity, we modeled the number of observed species for each site using generalized linear models with a Poisson error distribution with elevation above sea level as linear and quadratic predictor. For the analysis of beta diversity, we calculated pairwise Sørensen dissimilarity indices across the assemblages of all 15 groups, based on species-site matrices with varying dimensions depending on the respective group. Beta diversity was partitioned into its additive components of turnover (i.e. dissimilarity due to replacement of species) and nestedness (i.e. dissimilarity due to species loss; Baselga 2010). Subsequently, we calculated generalized dissimilarity models (GDM) on distance matrices for both the turnover and nestedness component including elevation above sea level as predictor variable, while controlling for spatial distance by including the spatial position of the site into the model (i.e. GPS coordinates). GDMs allow the analysis of spatial patterns of community composition under consideration of non-linear relationships between dissimilarity in community composition along environmental gradients (Ferrier et al. 2007). All GDMs were calculated using

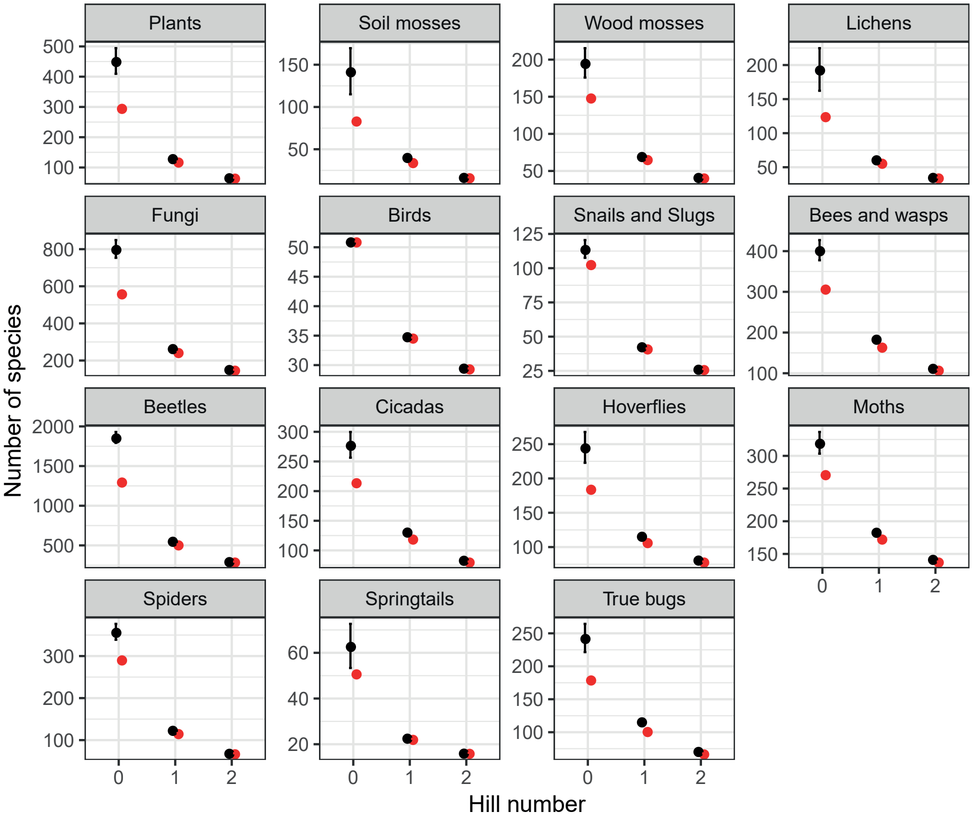

Fig. 2. Observed as well as asymptotic estimates of the number of species of 15 important taxonomic groups. Calculations are based on Hill numbers of the orders 0 (i.e. species richness), 1 (i.e. Shannon diversity representing 'common' species), and 2 (i.e. Simpson diversity representing 'dominant' species). Black circles indicate asymptotic estimations with standard errors. Red circles indicate observed values.

Table 2. Results of the generalized linear models of the number of species of the 15 studied groups. Elevation was included as a linear and quadratic predictor to account for nonlinear relationships. Tables show *z*-values of the predictor together with its statistical significance and the explained deviance of the model. Groups with significant effects of elevation on the number of species are given in bold.

Group	Elevation (z-value)	P-value	Elevation^2 (z-value)	P-value	Explained deviance
Plants	**−6.55**	**<0.001**	**5.53**	**<0.001**	**0.08**
Soil mosses	1.58	0.114	−1.90	0.057	0.03
Wood mosses	**3.51**	**<0.001**	**−3.54**	**<0.001**	**0.04**
Lichens	1.52	0.133	0.17	0.866	0.28
Fungi	3.05	<0.050	−4.62	<0.001	0.20
Birds	0.10	0.918	−0.68	0.494	0.12
Snails and Slugs	**−4.67**	**<0.001**	**1.96**	**<0.050**	**0.43**
Bees and wasps	**−8.10**	**<0.001**	**3.11**	**<0.050**	**0.58**
Beetles	**−9.65**	**<0.001**	**8.28**	**<0.001**	**0.15**
Cicadas	**−7.77**	**<0.001**	**6.56**	**<0.001**	**0.27**
Hoverflies	−0.09	0.928	−0.23	0.817	0.01
Moths	**2.12**	**<0.050**	**−2.61**	**<0.05**	**0.13**
Spiders	**−6.99**	**<0.001**	**7.93**	**<0.001**	**0.29**
Springtails	−0.44	0.661	0.78	0.437	0.07
True bugs	**−5.15**	**<0.001**	**4.49**	**<0.001**	**0.21**

the default of three I-splines. The calculated coefficient for each of the three I-splines represents the rate of change along a third of the gradient of the environmental predictor when keeping all other predictors constant (i.e. high values of the first I-spline indicate a high rate of change along the first third of the gradient). To quantify the contribution of alpha and beta diversity among plots and among elevational zones to the overall gamma diversity in our study system, we used additive diversity partitioning as implemented in the R package vegan, version 2.4-6 (Oksanen et al. 2018). For this analysis, we divided the elevational gradient into five equally spaced zones (1: 287–514 m a.s.l., n = 22; 2: 514–740 m, n = 33; 3: 740–967 m, n = 32; 4: 967–1193 m, n = 37; 5: 1193–1420 m, n = 33). The levels of the sampling hierarchy thus included the alpha diversity at the plot level, beta diversity among plots, beta diversity among elevational zones, and the overall gamma diversity.

RESULTS AND DISCUSSION

Based on the data from both surveys, we recorded 4,179 species of which 1,918 are common (Shannon diversity) and 1,222 dominant (Simpson diversity). The mean number of species per site and across all sampled taxa was 417±21 species (mean ± standard error). Overall, the sampling effort of our surveys was sufficient to cover most of the common and dominant species of the study system and an increase in sampling effort would only increase the number of rare species for some groups as indicated by the differences between estimated and observed number of species, for the three orders of Hill numbers (Fig. 2). For order 0, which includes also rare species the difference is rather large compared to the other two orders. Beetles and fungi account for more than a quarter of all species and contribute considerably to the overall (gamma) biodiversity (Fig. 3). After asymptotic extrapolation, the expected species richness ranges from 5,340 to 6,100 species for the terrestrial ecosystem of the national park. However, our methods were not able to generate reliable data for the species living in the canopy (especially phytophagous insects), soil or deadwood dwelling species. Thus, the estimate of 6,100 species is only a lower bound for the total terrestrial biodiversity. Furthermore, this study ignored aquatic ecosystems like rivers or bogs, which also host species rich communities and have been the subject of an additional survey as part of the Silva Gabreta Monitoring project (Křenová & Seifert 2015, Bojková et al. 2015, 2018).

Our results show that the elevational gradient forms one of the major gradients of environmental change for biotic communities in the Bohemian Forest. Besides changes in macroclimatic conditions, the elevational gradient is accompanied by several changes in forest types and structures. Our lower sites in the Danube valley range from riparian forests at the most western sites in the river delta of the Isar and the Danube River to a xerothermic forest at the steep southern slope of the Jochensteiner Hänge near Passau. As typical for low mountain ranges in Europe, the higher sites are covered by mountain mixed forests with European beech (*Fagus sylvatica*) as the dominant species at mid elevations and Norway spruce (*Picea abies*) at high elevations (Heurich & Neufanger 2005, Barbati et al. 2014, Hilmers et al. 2018). Thus, it is not surprising that the observed number of species also change with elevation as found for nearly all taxa in our study. However, patterns of these changes vary strongly in strength and shape ranging from more or less linear declines to more complex U- and hump-shaped relationships (Fig. 4, Table 2).

In general, changes in community composition along the elevational gradient are mostly due to species turnover among sites. Nestedness showed no obvious pattern with elevation,

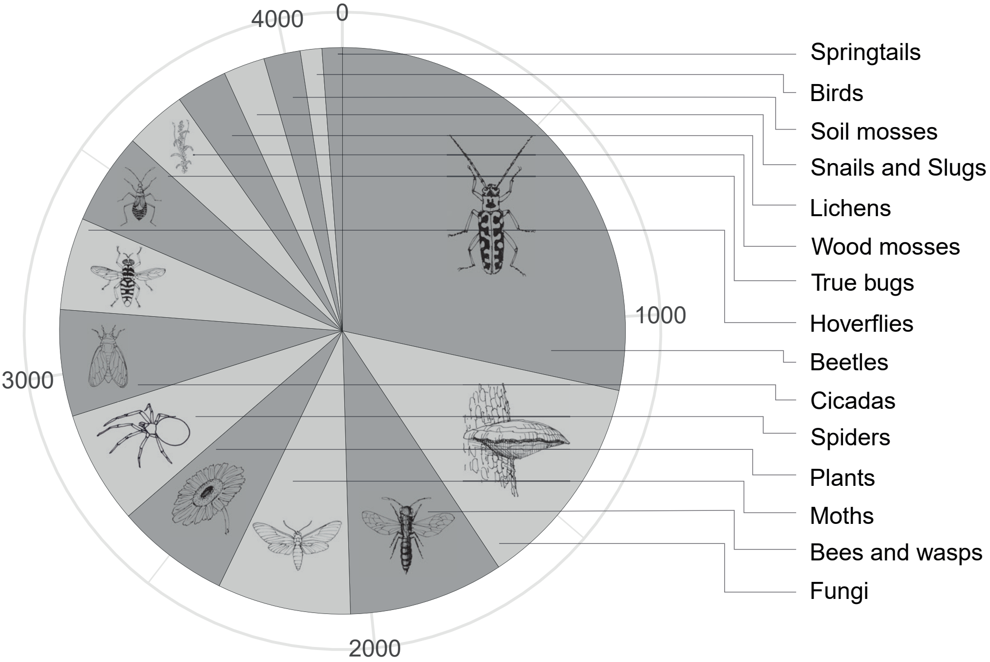

Fig. 3. Relative proportions of the species richness of the 15 groups under study after rarefaction/interpolation on three times the sampling units of the taxonomic group with the lowest number of sampling sites (i.e. 3×33 sites = 99 sites). Segment sizes conform to the number of species of the organism group with an overall estimated number of 4,135 species.

i.e. nestedness of the communities does not increase with elevation (Fig. 5, Table 3). Thus, we do not observe increased rates of species loss as we would expect if environmental conditions get harsher or too harsh for most species at higher elevations. The constant turnover of species along the elevational gradient contributes strongly to the observed gamma diversity of the Bohemian Forest. Additive partitioning showed that for most taxa beta diversity among elevational zones contributed most to the overall observed species pool, exceeding the contributions of local alpha diversity and beta diversity among plots within elevational zones (Fig. 6).

CONCLUSIONS

The implementation of the monitoring scheme generated reliable data for all taxonomic groups under study. This enables upcoming studies to investigate changes in species richness and community composition, as well as changes in the elevational distribution of species in response to a changing climate and changes in forest structure (BODIN et al. 2012). Here, a first study of HILMERS et al. (2018) revealed differential responses of taxonomic and

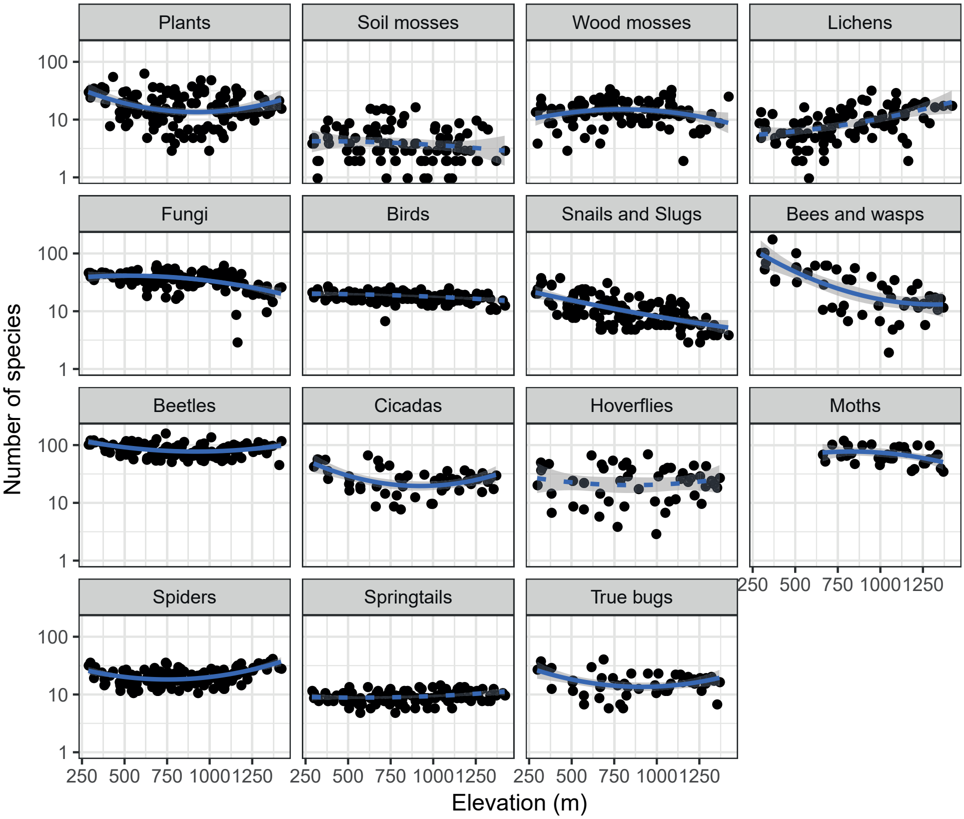

Fig. 4. Relationships of the number of species with elevation above sea level for the 15 groups of sampled organisms. Each point represents the number of species observed at a study site during the two surveys. Blue lines are based on generalized linear models with elevation as linear and quadratic predictor. Shaded areas indicate 95 % confidence intervals. Dashed lines indicate no significant effect of elevation on the number of species.

trophic groups to the stages of forest succession in the study region, which offers a dynamic baseline for assessing the effects of external drivers, such as changes in the temperature regime (Bodin et al. 2012, Thom et al. 2017). To overcome the shortcomings of a space-for-time approach it is necessary to resample the elevational gradient in regular intervals (Bässler et al. 2015). Although urgently needed, long-term regional biodiversity surveys along environmental gradients accompanied by a monitoring of changes in environmental conditions and habitat variables are still rare in ecological research (Lepetz et al. 2009; but see Greenland et al. 2003). Several studies revealed that species might respond to ongoing environmental change by adapting their distributions, including elevational upward shifts due to increasing temperatures (Bässler et al. 2013, Rumpf et al. 2018). Here, species' responses might vary strongly in strength and even direction (Lenoir et al. 2010, Bässler et al. 2013, Alexander et al. 2017). Despite their static nature, protected areas have the potential to buffer negative impacts of climate change on species by improving habitat quality and quantity (Thomas & Gillingham 2015, Betts et al. 2017). Thus, for the successful implemen-

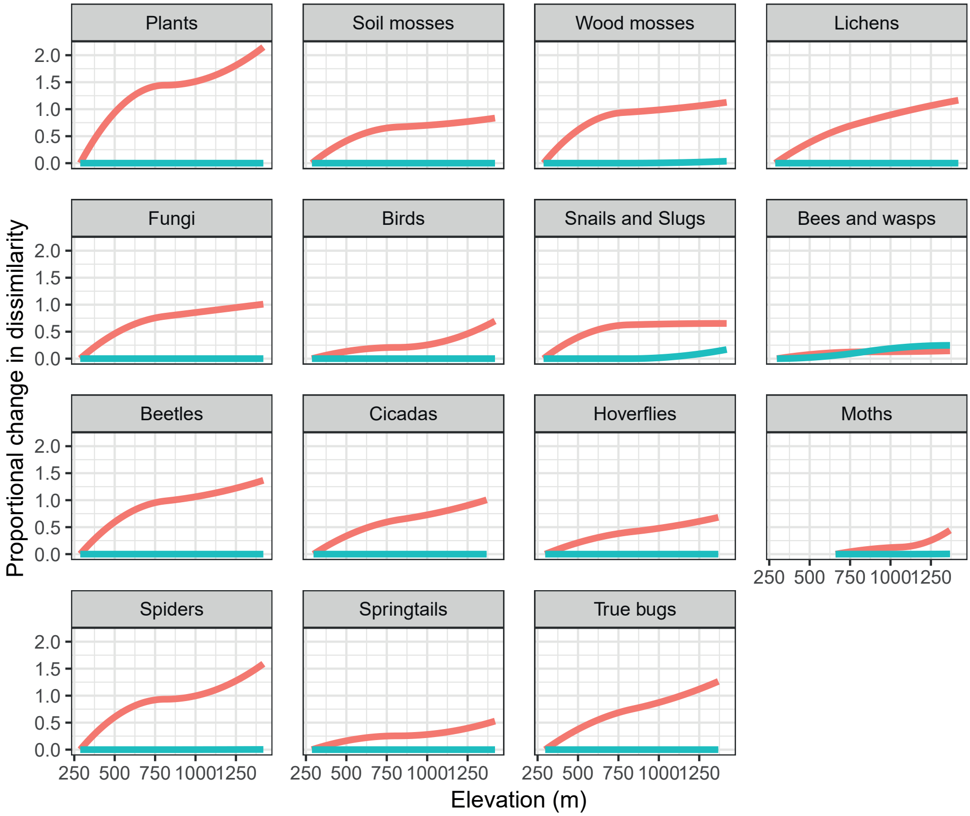

Fig. 5. I-Splines of generalized dissimilarity models after beta diversity partitioning into its turnover and nestedness components. For each group two models were calculated with dissimilarities among sites partitioned in turnover and nestedness as response matrices and dissimilarity among sites in geographic space (i.e. latitude and longitude) and elevation a.s.l. as predictor matrices. Red lines indicate the rate of change in dissimilarity due to turnover along the elevational gradient. Blue lines indicate the rate of change in dissimilarity due to nestedness along the elevational gradient.

Table 3. Percent of explained deviance of the generalized dissimilarity models by dissimilarity in elevation a.s.l. as a predictor for community dissimilarity in terms of turnover or nestedness.

Group	**Explained deviance**	
	Turnover	**Nestedness**
Plants	35.8	0
Soil mosses	5.5	0
Wood mosses	24.7	0.3
Lichens	12.5	0
Fungi	20.7	0
Birds	35.8	0
Snails and Slugs	21.9	4.2
Bees and wasps	1.7	5.6
Beetles	46.6	0
Cicadas	41.1	0
Hoverflies	15.1	0
Moths	25.6	0
Spiders	33.3	0
Springtails	13.6	0
True bugs	26.3	0

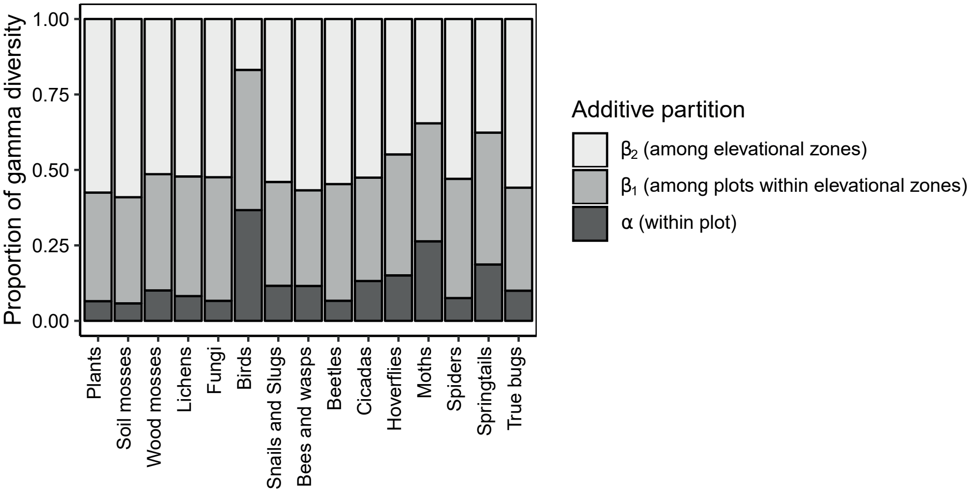

Fig. 6. Results of additive partitioning with three levels of sampling hierarchy including plot-level diversity (i.e. α-diversity), β-diversity among plots within five equally spaced elevational zones, as well as β-diversity among elevational zones. The height of the stacked bar indicates the relative contribution of the respective level of sampling hierarchy to the overall observed diversity (i.e. gamma diversity).

tation of conservation measures, it is crucial to understand how species will respond to changing environmental conditions and which species are most threatened. The BIOKLIM project and its continuation as part of the Silva Gabreta Monitoring will make an important contribution in the endeavor to understand species' responses to global change.

Acknowledgements. This research was supported by the Bavarian State Forestry and the Bavarian State Ministry of the Environment, Public Health, and Consumer Protection. Monitoring activities from 2016 to 2018 and publishing was granted by the transboundary cooperation program Bavaria Free State–Czech Republic–ETC goal 2014–2020, the Interreg V project No. 26 "SILVA GABRETA Monitoring: Realization of a transboundary Monitoring of Biodiversity and Water Balance". Additionally, TH and NF received scholarships from the Rudolf and Helene Glaser Foundation organized in the "Stifterverband für die deutsche Wissenschaft". We thank two anonymous referees for valuable comments on the initial submission.

References

Alexander J., Chalmandries L., Lenoir J., Burgess T., Essl F., Haider S., Kueffer C., McDougall K., Milbau A., Nuñez M., Pauchard A., Rabitsch W., Rew L., Sanders N. & Pellissier L., 2017: Lags in the response of mountain plant communities to climate change. *Global Change Biology*, 24: 563–579.

Barbati A., Marchetti M., Chirici G. & Corona P., 2014: European forest types and forest Europe SFM indicators: tools for monitoring progress on forest biodiversity conservation. *Forest Ecology and Management*, 321: 145–157.

Baselga A., 2010: Partitioning the turnover and nestedness components of beta diversity. *Global Ecology and Biogeography,* 19: 134–143.

Bässler C., Förster B., Moning C. & Müller J., 2009: The BIOKLIM-Project: biodiversity research between climate change and wilding in a temperate montane forest – the conceptual framework. *Waldökologie, Landschaftsforschung und Naturschutz*, 7: 21–33.

Bässler C., Müller J., Hothorn T., Kneib T., Badeck F. & Dziock F., 2010: Estimation of the extinction risk for high-montane species as a consequence of global warming and assessment of their suitability as cross-taxon indicators. *Ecological Indicators*, 10: 341–352.

Bässler C. Hothorn T., Brandl R. & Müller J., 2013: Insects overshoot the expected upslope shift caused by climate warming. *PLoS ONE*, 8: e65842.

Bässler C., Seifert L. & Müller J., 2015: The BIOKLIM Project in the National Park Bavarian Forest: Lessons from a biodiversity survey. *Silva Gabreta*, 21: 81–93.

Betts M. Phalan B., Frey S., Rousseau J. & Yang Z., 2018: Old-growth forests buffer climate-sensitive bird populations from warming. *Diversity and Distributions*, 24: 439–447.

Bodin J., Beadeu V., Bruno E., Cluzeau C., Moisselin J.M., Walther G.R. & Dupouey J.L., 2012: Shifts of forest species along an elevational gradient in Southeast France: climate change or stand maturation? *Journal of Vegetation Science*, 24: 269–283.

Bojková J., Čížková H., Kučerová A., Rádková V., Soldán T., Svidenský R. & Vrba J., 2015: Monitoring of the restored streams in the Vltavský Luh (Šumava National Park). *Silva Gabreta*, 21: 73–79.

Bojková J., Seifert L., Petruželová J., Šorfová V., Syrovátka V., Sroka P., Polášková V., 2018: Species richness and composition of macroinvertebrate assemblages in the Bavarian Forest: Preliminary results of the stream monitoring. *Silva Gabreta*, 24: 171–211.

Chao A., 1987: Estimating the population size for capture-recapture data with unequal catchability. *Biometrics*, 43: 783–791.

Chao A., Gotelli N., Hsieh T.C., Sander E., Ma K.H., Colwell R.K. & Ellison A.M., 2014: Rarefaction and extrapolation with Hill numbers: a framework for sampling and estimation in species diversity studies. *Ecological Monographs*, 84: 45–67.

Ferrier S., Manion G., Elith J. & Richardson K., 2007: Using generalized dissimilarity modelling to analyse and predict patterns of beta diversity in regional biodiversity assessment. *Diversity and Distributions*, 13: 252–264.

Greenland D. & Goodin D.G., 2003: Climate variability and ecosystem response at selected LTER sites at multiple timescales. In: *Climate variability and ecosystem response in long-term ecological research sites*, Greenland D., Goodin D.G. & Smith R.C (eds) Oxford University Press, Oxford, New York: 391–393.

Hannah L., 2008: Protected areas and climate change. *Annals of the New York Academy of Sciences*, 1134: 201–212.

Heurich M. & Neufanger M., 2005: Die Wälder des Nationalparks Bayerischer Wald. Ergebnisse der Waldinventur 2002/2003 im geschichtlichen und waldökologischen Kontext. *Wissenschaftliche Schriftenreihe der Nationalparkverwaltung Bayerischer Wald.* Nationalparkverwaltung Bayerischer Wald, Grafenau, 178 pp.

Heurich M., Beudert B., Rall H., & Křenová Z., 2010: National parks as model regions for interdisciplinary long-term ecological research: The Bavarian Forest and Šumava National Parks underway to transboundary ecosystem research. In: *Long-term ecological research*, Müller F., Baessler C., Schubert H. & Klotz S. (eds) Springer, Dordrecht: 327–344.

Hill M.O., 1973: Diversity and evenness: A unifying notation and its consequences. *Ecology*, 54: 427–432.

Hilmers T., Friess N., Bässler C., Heurich M., Brandl R., Pretzsch H., Seidl R. & Müller J., 2018: Biodiversity along temperate forest succession. *Journal of Applied Ecology*, https://doi.org/10.1111/1365-2664.13238

Hilmers T., Bässler C., Friess N., Heurich M., Müller J. & Seifert L., 2018: Changes in forest structure in the National Park Bavarian Forest. An evaluation after 10 years of the BIOKLIM-Project. *Silva Gabreta*, 24: 161–170.

Hsieh T.C., Ma K.H. & Chao A., 2016: iNEXT: an R package for rarefaction and extrapolation of species diversity (Hill numbers). *Methods in Ecology and Evolution*, 7: 1451–1456.

Jost, L. 2007. Partitioning Diversity into Independent Alpha and Beta Components. *Ecology*, 88: 2427–2439.

Křenová Z. & Seifert L., 2015: SILVA GABRETA – monitoring of mountain ecosystems. *Silva Gabreta*, 21: 1–4

Křenová Z. & Seifert L., 2018: The Silva Gabreta Project – transboundary cooperation in monitoring of biodiversity and water regime. *Silva Gabreta*, 24: 1–20.

Lehnert L. W., Bässler C., Brandl R., Burton P. J. & Müller J., 2013: Conservation value of forests attacked by bark beetles: Highest number of indicator species is found in early successional stages. *Journal for Nature Conservation*, 21: 97–104.

Lenoir J., Gégout J., Guisan A., Vittoz P., Wohlgemuth T., Zimmermann N., Dullinger S., Pauli H., Willner W. & Svenning J.-C., 2010: Going against the flow: potential mechanisms for unexpected downslope range shifts in a warming climate. *Ecography*, 33: 295–303.

Lepetz V., Massot M., Schmeller D. S. & Clobert J., 2009: Biodiversity monitoring: some proposals to adequately study species' responses to climate change. *Biodiversity and Conservation*, 18: 3185.

McNeely J.A., & Miller K.R., 1983: IUCN, national parks, and protected areas: Priorities for action. *Environmental Conservation*, 10: 13–21.

Müller J., Noss R. F., Bussler H. & Brandl R., 2010: Learning from a "benign neglect strategy" in a national park: Response of saproxylic beetles to dead wood accumulation. *Biological Conservation*, 143: 2559–2569.

Oksanen J., Blanchet F. G., Friendly M., Kindt R., Legendre P., McGlinn D., Minchin P. R., O'Hara R. B., Simpson G. L., Solymos P., Stevens M.H.H., Szoecs E. & Wagner H., 2018: vegan: Community Ecology Package. R package version 2.4-6. http://CRAN.R-project.org/package=vegan.

R Core Team, 2017: R: A language and environment for statistical computing. R Foundation for Statistical Computing, Vienna.

Rumpf S., Hülber K., Klonner G., Moser D., Schütz M., Wessely J., Willner W., Zimmermann N. & Dullinger S., 2018: Range dynamics of mountain plants decrease with elevation. *Proceedings of the National Academy of Sciences*, 115: 1848–1853.

Thom D., Rammer W., Dirnböck T., Müller J., Kobler J., Katzensteiner K., Helm N. & Seidl R., 2017: The impacts of climate change and disturbance on spatio-temporal trajectories of biodiversity in a temperate forest landscape. *Journal of Applied Ecology*, 54: 28–38.

Thomas C. & Gillingham P., 2015: The performance of protected areas for biodiversity under climate change. *Biological Journal of the Linnean Society*, 115: 718–730.

Received: 4 July 2018
Accepted: 17 September 2018

Silva Gabreta	vol. 24	p. 161–170	Vimperk, 2018

Changes in forest structure in the Bavarian Forest National Park – an evaluation after 10 years of the BIOKLIM-Project

Torben Hilmers[1,*], Claus Bässler[2], Nicolas Friess[3], Marco Heurich[2], Jörg Müller[2,4] & Linda Seifert[2]

[1]*Technical University of Munich, Hans-Carl-Von-Carlowitz-Platz 2, D-85354 Freising, Germany*
[2]*Bavarian Forest National Park, Freyunger Str. 2, D-94481 Grafenau, Germany*
[3]*Faculty of Biology, Philipps-Universität Marburg, Karl-von-Frisch Str. 8, D-35032 Marburg, Germany*
[4]*University of Würzburg, Glashüttenstr. 5, D-96181 Rauhenebrach, Germany*
[*] torben.hilmers@tum.de

Abstract

Biodiversity is diminishing globally at an unprecedented rate in times of intensive land use and ongoing climate change. Since biodiversity is related to important ecosystem functions and services it is nowadays the goal by law to maintain and improve biodiversity. In this perspective, the BIOKLIM-Project carried out two large forest structure and biodiversity surveys within the Bavarian Forest National Park in 2006 and 2016 to provide a broad range of data to assess the effects of a changing forest structure and climate on species and communities across different taxonomic groups. In this paper, we present the changes in forest structure between the two surveys. Results showed that study plots which were formerly affected from disruptive events such as storms and bark beetle infestations made progress in succession and thus occupy higher classes of forest succession. Furthermore, the results showed that disruptive events again caused disturbances, especially at the high elevations of the Bavarian Forest National Park. Hence, disturbances mainly affected spruce. Anyway, since the forest systems, with the exception of disturbances that might occur, are inert systems, the forest structure changed only slightly on the study plots between the two years of investigation.

Key words: Bavarian Forest National Park, Bohemian Forest, climate change, forest structure, forest succession, biodiversity

INTRODUCTION

Human activity affects biodiversity in terms of habitat transformation and degradation, habitat fragmentation, climate change, harvesting and pollution (TITTENSOR et al. 2014). Thus, global assessments show that the extinction risk of the species increases on average, while the population size decreases (PIMM et al. 2014). Over the last 20 years, remarkable progress has been made to understand how biodiversity loss affects the environment, the functioning of ecosystems and thus society (CARDINALE et al. 2012). For instance, species extinction has serious impact on important key processes for the productivity and sustainability of the Earth's ecosystems (ISBELL et al. 2011).

Since 1970, when the Bavarian Forest National Park was founded, the vast forests along the park have been allowed to develop without any human interference (HEURICH et al. 2011).

This ensures the expression of natural environmental forces and the undisturbed dynamics of the area's natural communities. The major disturbances in mature spruce stands by bark beetles (mainly *Ips typographus*, >5000 ha; see Lehnert et al. 2013) in the 1990s could not be related to any species reaction due to a lack of data (but see Beudert et al. 2015). Apart from such structural changes due to a benign neglect strategy, the analysis of long-term climate data showed that the Bavarian Forest National Park experienced significant higher temperatures especially during the growing season (Bässler et al. 2008). Both, changes in forest structure and climate change can have a major impact on biodiversity (Hilmers et al. 2018, Schall et al. 2017).

Understanding the inherent changes in species diversity as forests develop provides an important baseline for assessing the effects of external drivers such as climate change (Thom et al. 2017). In the absence of such a dynamic baseline, observed changes in biodiversity that are simply the effect of forest dynamics could be easily misattributed to effects of climate change.

Within the framework of the BIOKLIM-Project of the Bavarian Forest National Park, long-term experimental plots have been established for regular monitoring of the state of forest structure and biodiversity. The first survey of forest structure and biodiversity took place in 2006 (Bässler et al. 2008). Repeat recordings in 2016 were carried out on the designated BIOKLIM plots (Bässler et al. 2015). In the course of the repeated survey the changes in forest structure between the two recording years 2006 and 2016 were analyzed comparatively.

During the last hundred years, spruce and fir show a general increasing level of radial growth which is interrupted by a growth decline mainly during the 1960s and 1970s. Due to the species-specific differences in growth, different growth relations occurred between spruce and fir in that period. In the time of high rates of sulphur dioxide emissions, spruce outranges fir while, particularly during the last 30 years, the growth relation inverts (Uhl et al. 2013). Results of studies of mixed mountain forests in Europe show that the growth of spruce is declining in the last decades while the growth of fir is increasing. The volume increment of fir even exceeded on average that of spruce in the last 20 years. Growth of beech has so far remained largely unaffected of climate change in mountain mixed forests (Hilmers et al., unpubl. results). Based on these results, it can be expected that spruce will be pushed back into its realized niche (before human intervention in the National Park and emission load) by the re-strengthening of fir.

The aim of this study was to analyze changes in forest structure between the two surveys (2006 and 2016) in order to investigate whether possible changes in biodiversity can be attributed to changes in forest structure or to climate change. In this contribution we summarized the changes in forest structure on the BIOKLIM-Project plots between the two surveys in 2006 and 2016.

Material and methods

Study area

We used data from two surveys of forest structure in the Bavarian Forest National Park in south-eastern Germany in 2006 and 2016 (Bässler et al. 2008, Bässler et al. 2015). The study area covers ~5,000 km² and comprises a wide range of stages of forest succession that resulted from considerable variation in disturbance history and stand age (Fig. 1). The area is characterized by a homogenous geology (Bohemian Massif, granitic and gneissic bedrock) and predominantly acidic soils. Cultivation and management in this area became important only around 1850 and small areas of old-growth forests still exist (Röder et al. 2010).

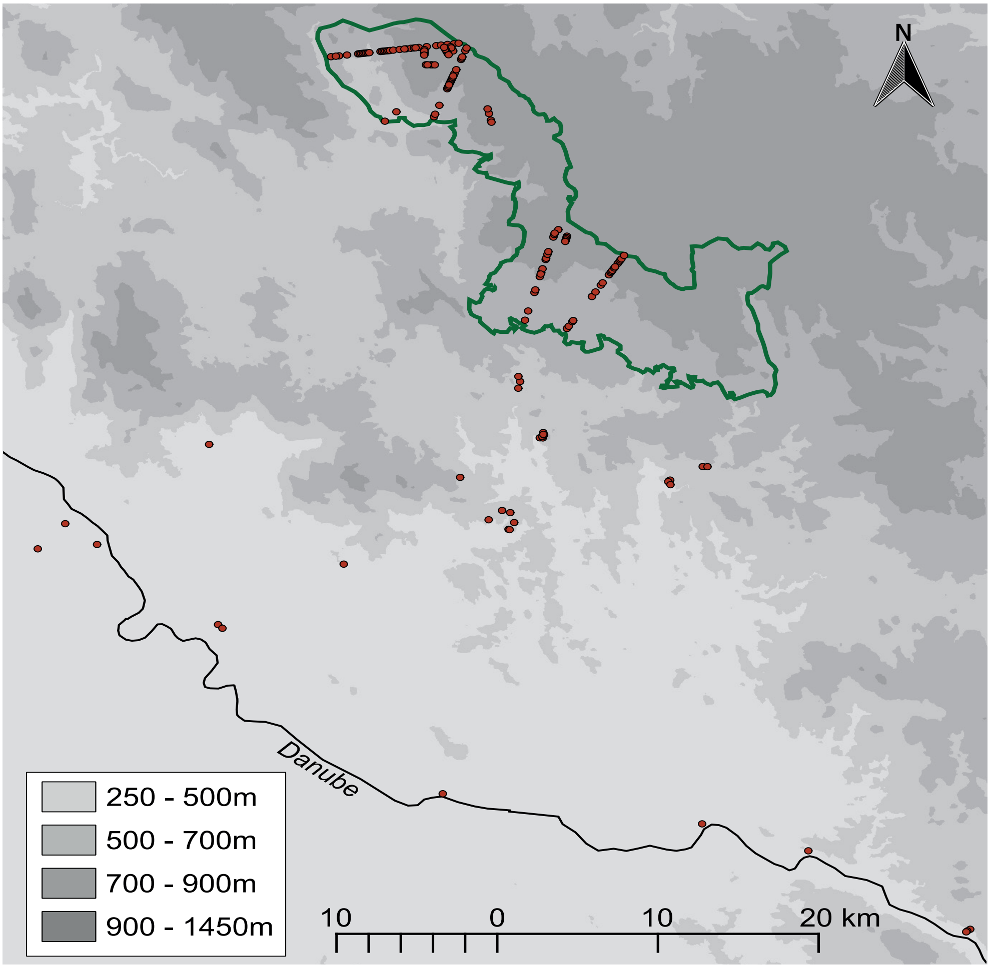

Fig. 1. An overview map of the 133 sampling plots (red points) across the elevational gradient. Main sampling transects are located within the Bavarian Forest National Park (green line). Additional lowland plots (<650m) outside the NP extended the elevation gradient down to the Danube River represent the gradient from 287–1420 m a.s.l. Some sampling points are not visible (overlayed) due to scaling.

The proportion of spruce at all elevations increased during the last century owing to forest management (Röder et al. 2010). The total annual precipitation is between 900 and 1800 mm and increases with elevation (Fig. 2), which ranges from 300 to 1450 m a.s.l. Annual mean air temperature varies between 3.4°C at high elevations and 9.7°C at low elevations (Fig. 2). The study plots are dominated by mixed mountain forests of European beech (*Fagus sylvatica;* ~50%), Norway spruce (*Picea abies* (L.) Karst.; ~30%) and silver fir (*Abies alba* Mill.; ~10%), however admixed with oak (*Quercus* sp.; ~7%) at the lowest elevations. Above 1200 m a.s.l., Norway spruce (~ 85 %) becomes dominant with a lower proportion of beech (~12 %).

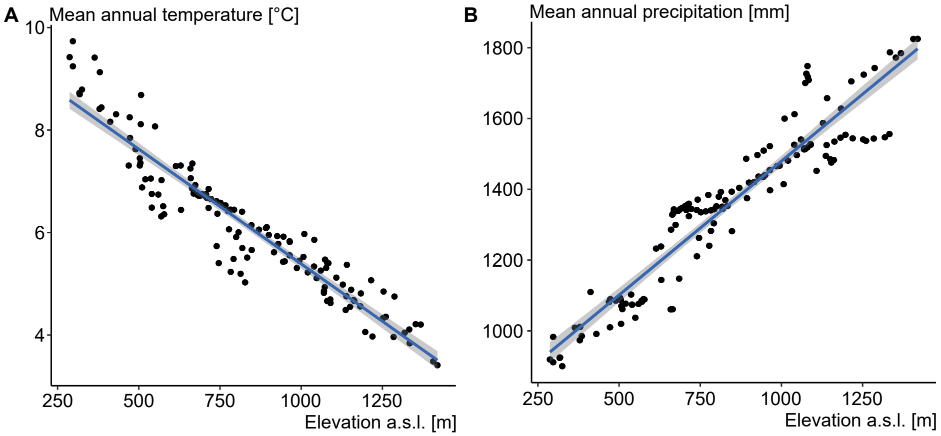

Fig. 2. Climate of the study region based on interpolated data from 1980 to 2006. A – mean annual temperature (°C) in relation to elevation (m a.s.l.) of all 133 study plots; the blue regression line is based on a linear model; the grey area depicts the 95% confidence interval ($R^2 = 0.89$, $p < 0.001$). B – mean annual precipitation (mm) in relation to elevation (m a.s.l.) of all 133 study plots; the blue regression line is based on a linear model, with the grey area depicting the 95% confidence interval ($R^2 = 0.89$, $p < 0.001$).

Data

Forest structure was characterized on two different scales (1 ha and 500 m²). On the 1-ha scale forest structure was characterized visually on 133 plots in the field (Fig. 1). The 133 study plots were selected by optimizing the design from Bässler et al. (2009). Optimization was done by categorization of all plots in respect to their available taxonomical information. Out of the most informative sampling plots we selected those best covering the structural gradient (canopy cover) across the elevation gradient (for final selection, see Fig. 1). For representation of the elevation gradient, we created a set of 100 plots out of the original 331 plots, including 62 highly informative plots and all 38 lowland plots (<650m). As special additions, we added the 33 old-growth forest and meadow plots due to their great importance for the area.

Canopy cover of the upper- (>2/3 of dominant height), middle- (1/3–2/3 of dominant height) and under layer (<10m) was determined by the sample area shaded by horizontal projection of tree layer separated for the occurring tree species (leaves, branches, trunks) in percent. Gaps were measured by the sample area covered by horizontal projection in percent. Height of the under layer was addressed visually in meter. Furthermore, we visually described the immediate surroundings around the plot center. It was addressed whether the center of the plot is in a gap, at the edge of a gap or in a closed forest. Standing and downed woody debris were recorded in the field on a 1000 m² circular plot (see Bässler et al. (2008) for a detailed description).

Forest structure recordings in the BIOKLIM project were extended by more detailed recordings when they were taken in 2016. During the last recording, every tree >7cm DBH was recorded in the field on plots with a circular area of 500 m². Since this detailed information are not available for the 2006 survey, required data were obtained from airborne light detection and ranging (LiDAR). Full-waveform LiDAR data were collected across our plots using a Riegl LMS-Q560 under leaf-on conditions (nominal sensor altitude: 400 m, average point density: 25 points m^{-2}) in the year 2006. Single trees in an area of 500 m² around the center of each plot were detected using 3D segmentation (Yao et al. 2012). On both surveys (2006 and 2016) the vegetation in the herbaceous layer (up to 1 m height), shrub layer (up to 5 m height), tree layer 1 (>5 to 15 m height) and tree layer 2 (>15 m) were estimated on 200 m² circular plots in the field. As there is a lack of LiDAR data for the plots outside the Bavarian Forest National Park these analyses contain only 99 plots within the National Park which both surveys have in common. Standing and downed woody debris were again recorded in the field on a 1000 m² circular plot.

Stages of forest succession

In our study, the 99 plots which both surveys have in common were classified to successional stages by combining the decision trees of Zenner et al. (2016) and Tabaku (2000). The decision trees incorporate information on canopy projection area, maximum diameter at breast height (DBH), proportion of dead wood, normalized quartile of the DBH, and the cover and height of the regeneration layer. The combination of these two protocols was necessary as Zenner et al. (2016) only considered trees with DBH >7 cm, and Tabaku (2000) explicitly also included regeneration and establishment stages. The combined decision tree was used to identify nine successional stages on 99 plots in the Bavarian Forest National Park, i.e., gap, regeneration, establishment, early-optimum, mid-optimum, late-optimum, planter (mixture of trees of different ages, sizes and heights), terminal and decay stages.

Results and discussion

The results show that the canopy cover of the upper layer has increased at medium elevations, compared to the first survey in 2006 (Fig. 3B) and there are less percentages of gaps on the study plots (Fig. 3F). During the last 10 years, the plots which had been exposed due to storms and bark beetle infestations in the first survey have grown over again. At higher elevations, the canopy cover of the upper layer decreased due to renewed disturbances by storms and bark beetle infestations, especially in the Northern part of the Bavarian Forest National Park (Fig. 3B). At the same time, the volume of deadwood at higher elevations (Fig. 3A) and the percentages of gaps (Fig. 3F) have increased. The middle and under layer remained unchanged (Fig. 3C-E). The evaluations of the position of the plot center within the 1 ha plot and the percentage of gaps on the plots also reflected the renewed disturbances of storms and bark beetles in the Bavarian Forest National Park. Above all, a change in the position of the plot center within the 1 ha plot in the direction of the open area could be observed. In particular, the plots which had been already disturbed at the first survey in 2006 (at the edge of the gap) were again affected by disturbances. The gaps have widened to such an extent that the centers of the plots were on the open area at the last survey in 2016 (Fig. 3G).

Considering tree species-specific changes in the canopy covers, revealed that the abovementioned disturbances in the higher elevations affected spruce particularly (Fig. 4). Compared to the first survey, some areas were affected by disturbances and the spruce was removed completely on some plots. Looking at the middle layer, it is striking that beech is the dominant tree species there. In the under layer, there is a balanced ratio between beech and spruce, except for the high elevations. There are only few study plots with beech at elevations above 1200 m a.s.l. However, it should be emphasized that despite the disturbances in the upper layers, a new generation of spruce trees is already present on some plots (Fig. 4F). Due to the benign neglect strategy of the Bavarian Forest National Park coarse woody debris will remain in the forest. Given the importance of deadwood for forest regeneration and recovery from disturbance, this will favor the future natural regeneration in the disturbed stands especially spruce regeneration (Svoboda et al. 2010).

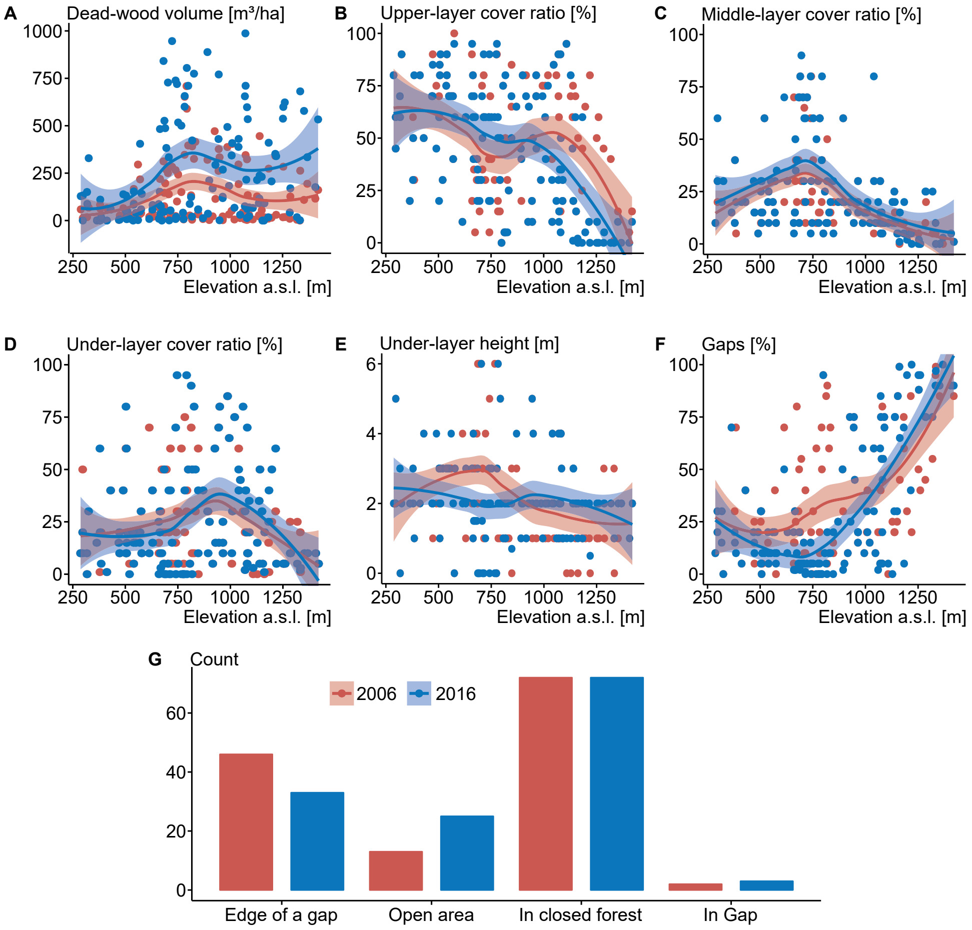

Fig. 3. Comparative representation of forest structure parameters of the BIOKLIM-Project surveys from 2006 (red) and 2016 (blue). Data are based on 133 plots which both surveys have in common: A – volume of dead-wood on the study plots; B – canopy cover of the upper layer in percent; C – canopy cover of the middle layer in percent; D – canopy cover of the under layer in percent; E – height of the under layer; F – the percentage of gaps on the study plots; G – position of the plot center within the 1 ha rectangle around the plot. Lines were generated by fitting a loess curve.

The situation of fir along the elevational gradient remains largely unchanged. Although the biological possibility exists to colonize higher elevations, no changes are visible after 10 years. This is consistent with the findings of Máliš et al. (2016). In their study about tree range shifts in the Western Carpathians they also did not find any elevation shifts for fir and beech in the last decades. Other authors, e.g. Janík et al. (2014), have also shown that fir has a disadvantage in rejuvenation compared to beech. This is primarily due to the increased shade tolerance of beech in advanced regeneration.

If forest structure parameters are combined into forest successional stages, the results are similar to those already described (Fig. 5). It becomes clear that many of the formerly disturbed plots from 2006 have made progress in succession and occupy higher stages of suc-

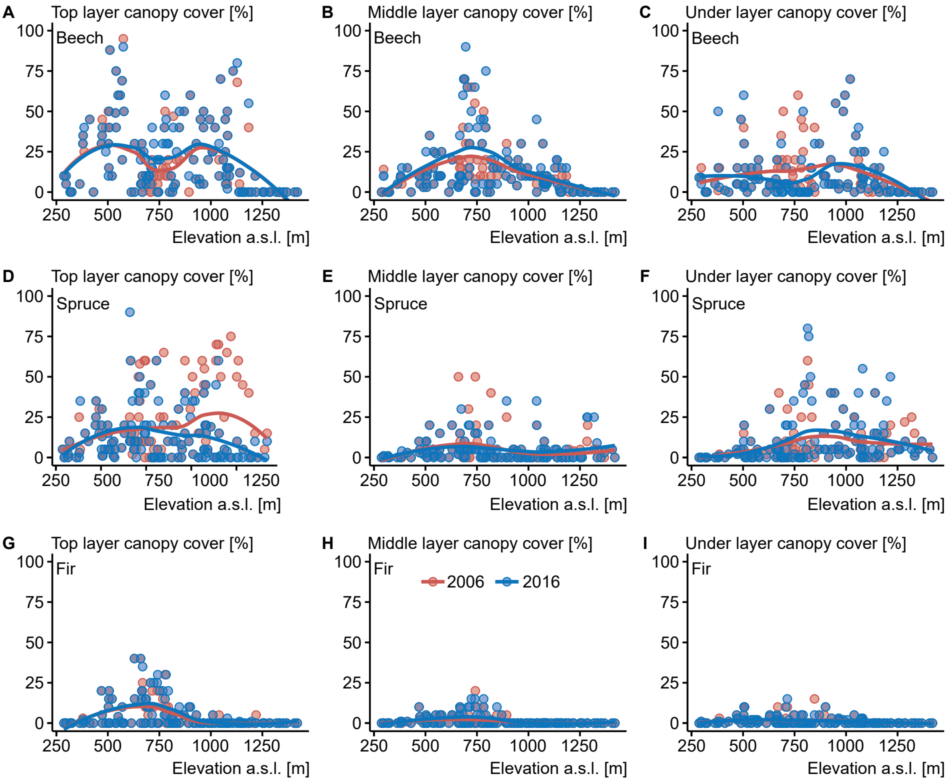

Fig. 4. Comparative representation of the canopy cover of beech (A, B, C), spruce (D, E, F) and fir (G, H, I) of the BIOKLIM-Project surveys from 2006 (red) and 2016 (blue). Data are based on 133 plots which both surveys have in common: A, D, G – canopy cover of the upper layer in percent; B, E, H – canopy cover of the middle layer in percent; C, F, I – canopy cover of the under layer in percent. Lines were generated by fitting a loess curve.

cession. In comparison between the two recording years there are 7% less study plots situated in the gap stage and 13% more study plots situated in the regeneration or establishment stage (Fig. 5).

The recurring disturbances at higher elevations mainly affect the optimal and terminal stages. There are fewer plots in the optimal and terminal stages (−17%) and more plots in the decay stage (+11%). On the one hand, plots have changed from the terminal stage to the decay stage, but some plots have also changed from the optimum stages to the decay stage (Fig. 5). These are primarily the plots at high elevations of the northern part of the Bavarian Forest National Park, which have been affected by disturbances. This makes it clear that forest succession does not always strictly follow the sequence shown, but can change into the gap, regeneration or decay stage at any time due to disturbances (Fig. 5).

Since forest systems, with the exception of disturbances that might occur, are inert systems, the forest structure in relation to the values described above changed only slightly on the study plots between the two years of investigation (2006 and 2016).

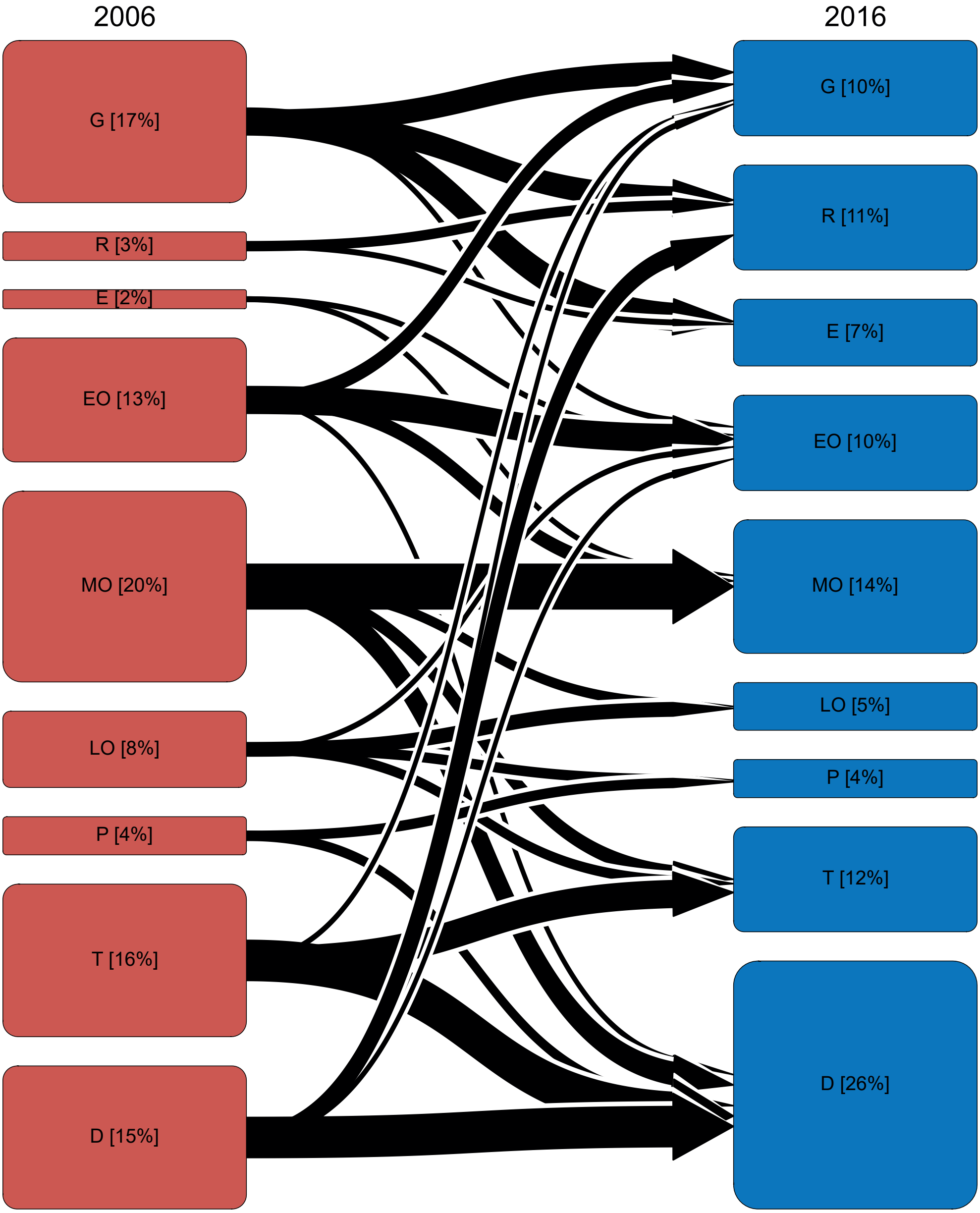

Fig. 5. Comparison of the percentages of plots in every forest successional stage in our study between the two surveys in 2006 (red) and 2016 (blue) and their transition between the two surveys. The successional stages considered here follow Tabaku (2000) and Zenner et al. (2016). Data are based on 99 plots in the Bavarian Forest National Park. Stages of forest succession: G – gap; R – regeneration; E – establishment; EO – early optimum; MO – mid optimum; LO – late optimum; P – plenter; T – terminal; D – decay. Note that it was not possible to determine forest successional stages for the plots outside the national park in the year 2006 due to missing LiDAR data.

CONCLUSION

Forest systems, with the exception of occurring disturbances, are inert systems. Therefore, no major changes in the described variables were expected during the first BIOKLIM-Project repeat recording, since no major disturbances occurred either. However, at mid elevations, we found a recovery from disturbances and at higher elevations we found renewed minor disturbances due to bark beetle infestation. Especially spruce is affected by these new disturbances. Anyway, we found that plots formally disturbed in the 2006 survey have made progress and occupy higher stages of forest succession nowadays. As conclusions about the response of multiple taxa to climate change can only be drawn with the information about changes in forest structure (Schall et al. 2017, Hilmers et al. 2018) it is crucial to continue the monitoring of forest structure in future BIOKLIM surveys. Information on changes in forest structure provides the basis for characterizing responses of biodiversity caused by climate change. In the absence of such a dynamic baseline, observed changes in biodiversity that are simply the effect of forest dynamics could be easily misattributed to effects of climate change. LiDAR provides an excellent tool to describe changes in forest structure to a sufficient scale for forest structure and biodiversity analyses in the future. In addition, a merger with data of long term experimental plots following the same approach in the Šumava National Park is in preparation and allows us to expand our analyses on the influence of climate change and forest structure on biodiversity.

Acknowledgements. This research was mainly supported by the Bavarian State Forestry and the Bavarian State Ministry of the Environment, Public Health, and Consumer Protection. The survey 2016 and publishing was granted by the Cross-border cooperation program Czech Republic − Bavaria Free State ETC goal 2014−2020, the Interreg V Project No. 26 “SILVA GABRETA Monitoring of Biodiversity and Water Regime”. TH and NF received additional scholarships from the Rudolf and Helene Glaser Foundation organized in the “Stifterverband für die deutsche Wissenschaft”.

REFERENCES

Bässler C., Förster B., Moning C. & Müller J., 2008: The BIOKLIM-Project: biodiversity research between climate change and wilding in a temperate montane forest–the conceptual framework. *Waldökologie, Landschaftsforschung und Naturschutz*, 7: 21–33.

Bässler C., Seifert L. & Müller J., 2015: The BIOKLIM Project in the National Park Bavarian Forest: Lessons from a biodiversity survey. *Silva Gabreta*, 21: 81–93.

Beudert B., Bässler C., Thorn S., Noss R., Schröder B., Dieffenbach-Fries H., Foullois N. & Müller J., 2015: Bark beetles increase biodiversity while maintaining drinking water quality. *Conservation Letters*, 8: 272–281.

Cardinale B.J., Duffy J.E., Gonzalez A., Hooper D.U., Perrings C., Venail P., Narwani A., Mace G.M., Tilman D., Wardle D.A., Kinzig A.P., Daily G.C., Loreau M., Grace J.B., Larigauderie A., Srivastava D.S. & Naeem S., 2012: Biodiversity loss and its impact on humanity. *Nature*, 486: 59–67.

Heurich M., Baierl F., Günther S. & Sinner K.F., 2011: Management and conservation of large mammals in the Bavarian Forest National Park. *Silva Gabreta*, 17: 1–18.

Hilmers T., Friess N., Bässler C., Heurich M., Brandl R., Pretzsch H., Seidl R. & Müller J., 2018: Biodiversity along temperate forest succession. *Journal of Applied Ecology*, 55: 2756-2766.

Isbell F., Calcagno V., Hector A., Connolly J., Harpole W.S., Reich P.B., Scherer-Lorenzen M., Schmid B., Tilman D., van Ruijven J., Weigelt A., Wilsey B.J., Zavaleta E.S. & Loreau M., 2011: High plant diversity is needed to maintain ecosystem services. *Nature*, 477: 199–202.

Janík D., Adam D., Hort L., Král K., Šamonil P., Unar P. & Vrška T., 2014: Tree spatial patterns of *Abies alba* and *Fagus sylvatica* in the Western Carpathians over 30 years. *European Journal of Forest Research*, 133: 1015–1028.

Lehnert L.W., Bässler C., Brandl R., Burton P.J. & Müller J., 2013: Conservation value of forests attacked by bark beetles: Highest number of indicator species is found in early successional stages. *Journal for Nature Conservation*, 21: 97–104.

Máliš F., Kopecký M., Petřík P., Vladovič J., Merganič J. & Vida T., 2016: Life stage, not climate change, explains observed tree range shifts. *Global Change Biology*, 22: 1904–1914.

Pimm S.L., Jenkins C.N., Abell R., Brooks T.M., Gittleman J.L., Joppa L.N., Raven P.H., Roberts C.M. & Sexton J.O., 2014: The biodiversity of species and their rates of extinction, distribution, and protection. *Science*, 344: 1246752.

Röder J., Bässler C., Brandl R., Dvořák L., Floren A., Goßner M.M., Gruppe A., Jarzabek-Müller A., Vojtěch O., Wagner C. & Müller J., 2010: Arthropod species richness in the Norway Spruce (*Picea abies* (L.) Karst.) canopy along an elevation gradient. *Forest Ecology and Management*, 259: 1513–1521.

Schall P., Gossner M.M., Heinrichs S., Fischer M., Boch S., Prati D., Jung K., Baumgartner V., Blaser S., Böhm S., Buscot F., Daniel R., Goldmann K., Kaiser K., Kahl T., Lange M., Müller J., Overmann J., Renner S.C., Schulze E.D., Sikorski J., Tschapka M., Türke M., Weisser W.W., Wemheuer B., Wubet T. & Ammer C., 2017: The impact of even-aged and uneven-aged forest management on regional biodiversity of multiple taxa in European beech forests. *Journal of Applied Ecology*, 55: 267–278.

Svoboda M., Fraver S., Janda P., Bače R. & Zenáhlíková J., 2010: Natural development and regeneration of a Central European montane spruce forest. *Forest Ecology and Management*, 260: 707–714.

Tabaku V., 2000: Struktur von Buchen-Urwäldern in Albanien im Vergleich mit deutschen Buchen-Naturwaldreservaten und Wirtschaftswäldern [Structure of beech primeval forests in Albania in comparison with German beech natural forest reserves and commercial forests]. Ph.D. thesis, Universität Göttingen, Cuvillier Verlag, Göttingen, 206 pp. (in German).

Thom D., Rammer W., Dirnböck T., Müller J., Kobler J., Katzensteiner K., Helm N. & Seidl R., 2017: The impacts of climate change and disturbance on spatio-temporal trajectories of biodiversity in a temperate forest landscape. *Journal of Applied Ecology*, 54: 28–38.

Tittensor D.P., Walpole M., Hill S.L.L., Boyce D.G., Britten G.L., Burgess N.D., Butchart S.H.M., Leadley P.W., Regan E.C., Alkemade R., Baumung R., Bellard C., Bouwman L., Bowles-Newark N.J., Chenery A.M., Cheung W.W.L., Christensen V., Cooper H.D., Crowther A.R., Dixon M.J.R., Galli A., Gaveau V., Gregory R.D., Gutierrez N.L., Hirsch T.L., Höft R., Januchowski-Hartley S.R., Karmann M., Krug C.B., Leverington F.J., Loh J., Lojenga R.K., Malsch K., Marques A., Morgan D.H.W., Mumby P.J., Newbold T., Noonan-Mooney K., Pagad S.N., Parks B.C., Pereira H.M., Robertson T., Rondinini C., Santini L., Scharlemann J.P.W., Schindler S., Sumaila U.R., Teh L.S.L., Kolck J. van, Visconti P. & Ye Y., 2014: A mid-term analysis of progress toward international biodiversity targets. *Science*, 346: 241–244.

Uhl E., Ammer C., Spellmann H., Schölch M. & Pretzsch H., 2013: Zuwachstrend und Stressresilienz von Tanne und Fichte im Vergleich [Growth trend and stress-resilience of fir and spruce in comparison]. *Allgemeine Forst und Jagdzeitung*, 11–12: 278–292 (in German).

Yao W., Krzystek P. & Heurich M., 2012: Tree species classification and estimation of stem volume and DBH based on single tree extraction by exploiting airborne full-waveform LiDAR data. *Remote Sensing of Environment*, 123: 368–380.

Zenner E.K., Peck J.E., Hobi M.L. & Commarmot B., 2016: Validation of a classification protocol: meeting the prospect requirement and ensuring distinctiveness when assigning forest development phases. *Applied Vegetation Science*, 19: 541–552.

Received: 28 June 2018
Accepted: 30 August 2018

Silva Gabreta	vol. 24	p. 171–211	Vimperk, 2018

Species richness and composition of macroinvertebrate assemblages in the Bavarian Forest National Park: Preliminary results of the stream monitoring

Jindřiška Bojková[1,*], Linda Seifert[2], Jana Petruželová[1], Vanda Šorfová[1], Vít Syrovátka[1], Pavel Sroka[3] & Vendula Polášková[1]

[1]*Department of Botany and Zoology, Masaryk University, Kotlářská 2, CZ-61137 Brno, Czech Republic*
[2]*Bavarian Forest National Park, Freyungerstraße 2, D-94481 Grafenau, Germany*
[3]*Institute of Entomology, Biology Centre CAS, Branišovská 31, CZ-37005 České Budějovice, Czech Republic*
[*] bojkova@centrum.cz

Abstract

Ongoing monitoring of streams in the Bavarian Forest National Park (BFNP) is focused on the effects of climate changes and natural disturbances on the community composition and diversity of benthic macroinvertebrates in the Bohemian Forest. This study provides the data on macroinvertebrate assemblages of ten streams draining the area of the BFNP (BF streams), which are included in the monitoring survey, and 48 sites distributed evenly in the Große Ohe stream network (GO catchment). The GO catchment serves as a model stream network to study environmental and spatial structuring of macroinvertebrate assemblages on the local scale. We aim to evaluate species richness, abundance and species composition of macroinvertebrates along the main environmental gradients and to consider the possible impact of acidification. Species recorded at all studied sites are compared with available literature data from the BFNP. Altogether 40,682 individuals of 184 species were recorded in our study, 130 and 168 species in the BF streams and GO catchment, respectively. Macroinvertebrate assemblages of the BF streams are significantly influenced by substrate roughness and water quality. Within the GO catchment, stream size and acidity are the main ecological gradients forming the assemblages, with a significant influence of local habitat properties (such as amount of coarse particulate organic matter (CPOM), concentration of ionic aluminium (Al_i), depth of water, and water chemistry). Species richness of macroinvertebrates is positively related to stream size and negatively to CPOM, whereas their abundance is significantly affected by acidity and Al_i, being strongly limited in Al_i>53 µg.l^{-1}. More species of Ephemeroptera, Coleoptera and Diptera, including several acid sensitive species, were found in the GO catchment in comparison with earlier data from the period of strong acidification, which indicates ongoing recovery of streams from acidification. Streams are recently inhabited by numerous moderately acid sensitive species, which is mirrored by their favourable acid status (prevailing acid class 2, predominantly neutral to episodically weakly acidic conditions) assessed based on scoring of acid sensitive species. Acid status based on the overall composition of assemblages shows prevailing acid class 3 (periodically critically acidic conditions) with considerable number of streams of acid classes 4 and 5 indicating strong acid stress. Overall, acid status of streams is not aligned with the altitude, stream size or any habitat property within the model GO catchment suggesting that the stream network is a mosaic of various local conditions determining water chemistry. Thus, macroinvertebrates can find suitable conditions or refugia in some parts of the catchment.

Key words: biodiversity, macroinvertebrates, acidification, acid status assessment, Bohemian Forest, Große Ohe

INTRODUCTION

Springs and streams of the Bavarian Forest National Park (BFNP, German part of the Bohemian Forest) have kept the natural character despite historical local modifications of channels to facilitate timber transportation. Dense stream network is dominated by cold headwater (crenal and epirhitral) streams with relatively heterogeneous catchments, thus offering diverse environment for aquatic biota. In-stream environment is significantly influenced by dead wood in different stadium of decomposition. Dead wood of different size, from branches to large logs forming large cascades and pools or, in extreme cases, completely covering stream channels, is abundant particularly in streams flowing in unmanaged forests. Characteristic phenomenon is the interference of the effects of anthropogenic atmospheric acidification and natural disturbances on the stream water chemistry. Strong atmospheric acidification of headwater streams occurred from the 1960s to 1980s, peaked in the mid-1980s, and was followed by gradual recovery since the 1990s (ALEWELL et al. 2001, SCHAUMBURG et al. 2010, BEUDERT & GIETL 2015) caused by significant reduction in sulphur dioxide, nitrogen oxides and ammonia emissions in central Europe (KOPÁČEK et al. 2002, KOPÁČEK & VESELÝ 2005). Concurrently, rapid dieback of large forest area due to wind storms and/or bark beetle outbreaks peaking in 1997 caused changes in the chemistry of all water fluxes, mainly leaching of nitrate, dissolved organic carbon (DOC) and aluminium to streams draining affected areas and also to lakes (VRBA et al. 2014, BEUDERT et al. 2015, BEUDERT & GIETL 2015, KOPÁČEK et al. 2017). Consequent water quality deterioration in streams and increase of episodic acid runoff temporarily slowed down the recovery of streams from acidification (SCHAUMBURG et al. 2010, HOFFMANN et al. 2011). Nevertheless, mechanism of episodic acidification of stream water has changed, as it is no longer driven by sulphate, but by DOC, which has to be considered as a natural process (BEUDERT & GIETL 2015).

Regular monitoring activities in the BFNP encompass the long-term acidification monitoring and hydrological monitoring of the model catchment with near-natural forest without management intervention. The hydrological monitoring commencing in 1977 has been focused on the water cycle in the Große Ohe catchment and runoff changes caused by the transition from commercial to near-natural forest in this catchment (BEUDERT & GIETL 2015). The long-term acidification monitoring commenced in 1986 and has been focused on the assessment of recovery from acidification based on water chemistry, macroinvertebrates and diatoms in Seebach, Hinterer Schachtenbach, Vorderer Schachtenbach, Große Ohe, and Rachelsee (LFW 1999, KIFINGER et al. 2004, SCHAUMBURG et al. 2008, 2010, HOFFMANN et al. 2011, SCHEEL et al. 2014, LFU 2015). These sites are a part of the network of the ICP Waters, the International Cooperative Programme for assessment and monitoring of the effects of air pollution on rivers and lakes (SKJELKVÅLE & DE WIT 2011). In 2016, a systematic monitoring aiming to evaluate the effects of natural disturbances and climate changes on biodiversity of streams (focusing mainly on macroinvertebrates) started at seven streams distributed throughout the BFNP (Große Deffernik, Kolbersbach, Kleiner Regen, Große Ohe, Kleine Ohe, Sagwasser, and Reschbach). The conceptual framework of the monitoring is analogous to the terrestrial biodiversity survey BIOKLIM (for more details see BÄSSLER et al. 2015). Sampling sites are distributed in seven streams following the altitudinal gradient every 100 altitudinal meters from 600 to 1100 m a.s.l. This monitoring is designed as a long-term study with proposed regular repetition of sampling in the future.

Information on stream macroinvertebrates are, however, incomplete, and generally missing from the pre-acidification period (but see THIEM 1906). Several studies are published in grey literature and, thus, inaccessible for a wider scientific audience (e.g. EISENREICH 1974, KUHN 1984, SCHÖLL 1987). Some individual records of species are available in faunistic studies (e.g. Hebauer 1975, 1980, Seitz 1988, 1992, Weinzierl 1999, Soldán et al. 2012). Probably the first complex faunistic study of stream biodiversity by Schöll (1987, 1989) was focused on the southern (old) part of the current BFNP where catchments of Flanitz, Schwarzach, Große Ohe, Kleine Ohe, and Sagwasser were investigated. Based on the field study conducted in 1984 and 1985, Schöll (1989) reported 182 species (or higher taxa) and pointed out the role of pH in the distribution of species calling for immediate reduction of emissions of acidifying compounds. Another complex faunistic study on four aquatic insect orders (Ephemeroptera, Plecoptera, Coleoptera, and Trichoptera) covered entire Niederbayern and reported 289 species for the Bavarian Forest (Schulte & Weinzierl 1990). The study area, however, included the whole Bavarian Forest, thus, also species found at lower altitudes out of the BFNP were included. The same is true for Pitsch (1994) who studied four aquatic invertebrate groups (Trichoptera, Odonata, Amphipoda, Isopoda) reporting 121 species in the Bavarian Forest, and provided the distribution of individual species in the longitudinal profile of six studied stream systems. Data gathered during the long-term acidification monitoring of streams are unpublished, partially available in the project reports (e.g. Kifinger et al. 2004, Schaumburg et al. 2010). They document gradual increase of species richness in recovering streams which was slowed down or interrupted by increased effects of episodic acid runoffs after the forest dieback (Schaumburg et al. 2010, Hoffmann et al. 2011).

In this study, we provide new data on macroinvertebrates inhabiting streams in the BFNP based on the two separate surveys conducted in 2015. Both surveys are the part of the broader transboundary study focusing on the stream biodiversity in the Bohemian Forest. The first survey explores patterns in diversity and assemblage structuring of macroinvertebrates in two neighbouring montane catchments in the non-interventional part of the Bohemian Forest (Šumava in Czech), upper Große Ohe catchment in the BFNP and upper Vydra catchment in the Šumava National Park. The second survey, already mentioned above, investigates stream biota and environmental conditions along the gradient of altitude in order to evaluate the effects of natural disturbances and climate changes on biodiversity of streams in the BFNP. Both surveys have started recently and full data are not available yet. This study presents the preliminary results with a special focus on insufficiently known macroinvertebrate diversity of the Bavarian Forest streams. The main aims of the study are to describe species richness and composition of macroinvertebrate assemblages inhabiting main streams draining the BFNP and the model Große Ohe catchment, which tohether cover all stream types in the studied area. We aim to explore main gradients in species data and factors governing species richness, abundance and composition of macroinvertebrate assemblages. We consider the possible effect of acidification on macroinvertebrates. Last but not least, we aim to provide a species list of the macroinvertebrates found at the studied sites and compare them with available literature data.

MATERIAL AND METHODS

Study sites and data

Two sets of species and environmental data were evaluated. The first one included species data from 48 sites distributed in the upper Große Ohe catchment (Fig. 1), which were supplemented by detailed environmental data. The second dataset included species data from 10 main rivers draining the area of the BFNP (Fig. 2).

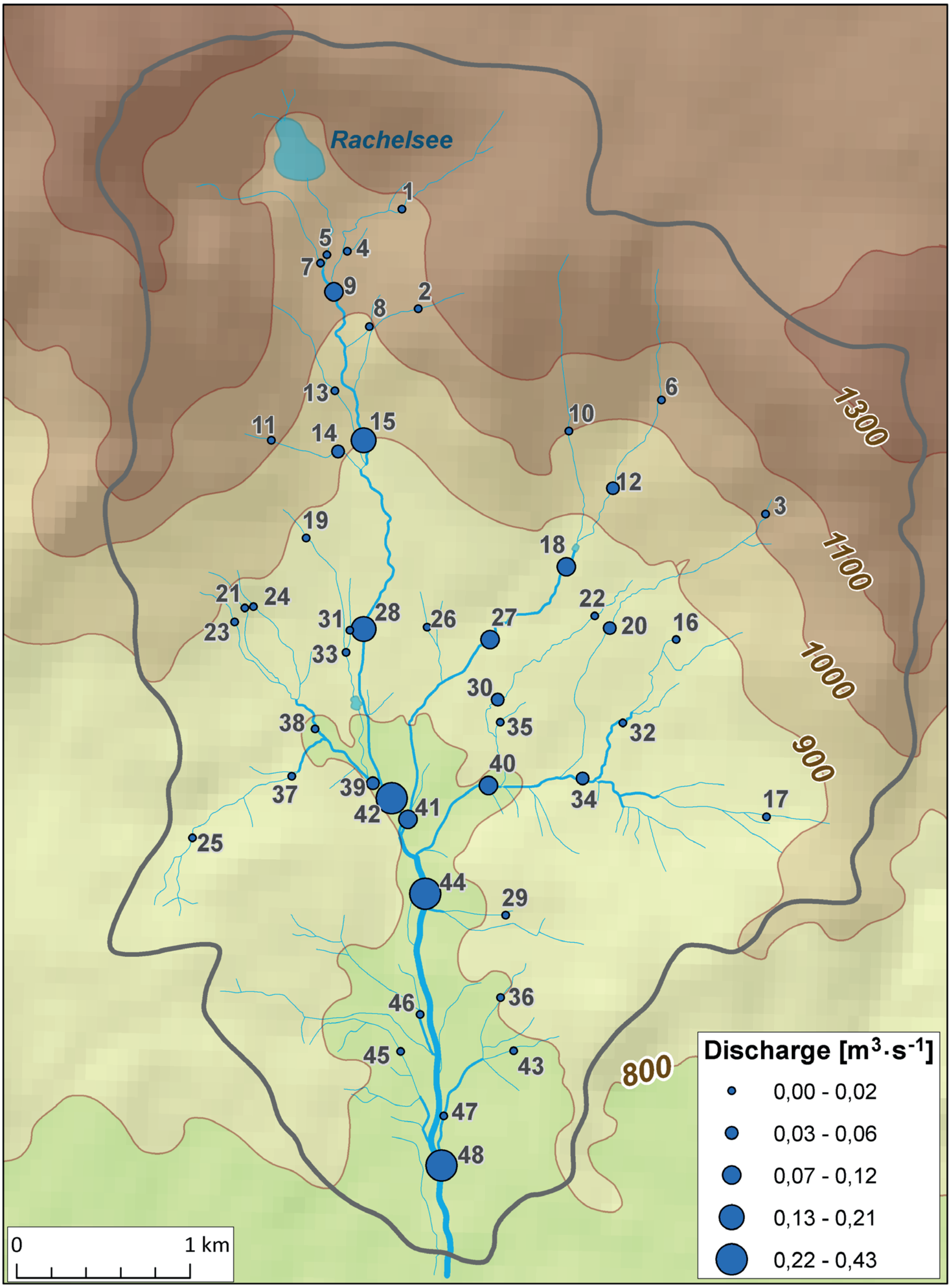

Fig. 1. Map of the GO catchment with the investigated sites (numbers of sites are available in Table 1). Size of symbols indicates discharge of streams.

Große Ohe catchment (GO catchment)

The upper Große Ohe catchment, hereinafter referred as GO, is 19.1 km² large, with the altitudinal gradient from 760 to 1300 m a.s.l. The catchment is 98% forested, with Norway spruce (*Picea abies* (L.)) and European beech (*Fagus sylvatica* L.) being the dominant species (Beudert & Gietl 2015). Since 1992, bark beetle (*Ips typographus* L.) damaged spruce forests on 58% of the catchment area and converted them into varying succession stages with rapidly growing young spruce (Beudert et al. 2015). Fortyeight sites (Fig. 1, Table 1) were selected based on four rules: sites to be distributed as much evenly as possible; the proportion of Strahler's stream orders to reflect their real proportion within the catchment; sites not to be too far from roads or footpath to avoid disturbing protected landscape; and finally, the number of sites not to exceed 50. The same approach was applied in the upper Vydra catchment in the Šumava National Park where 43 sites were selected. In contrast to the Große Ohe, the network of Vydra is less dense and streams are rather low-sloping, flow-

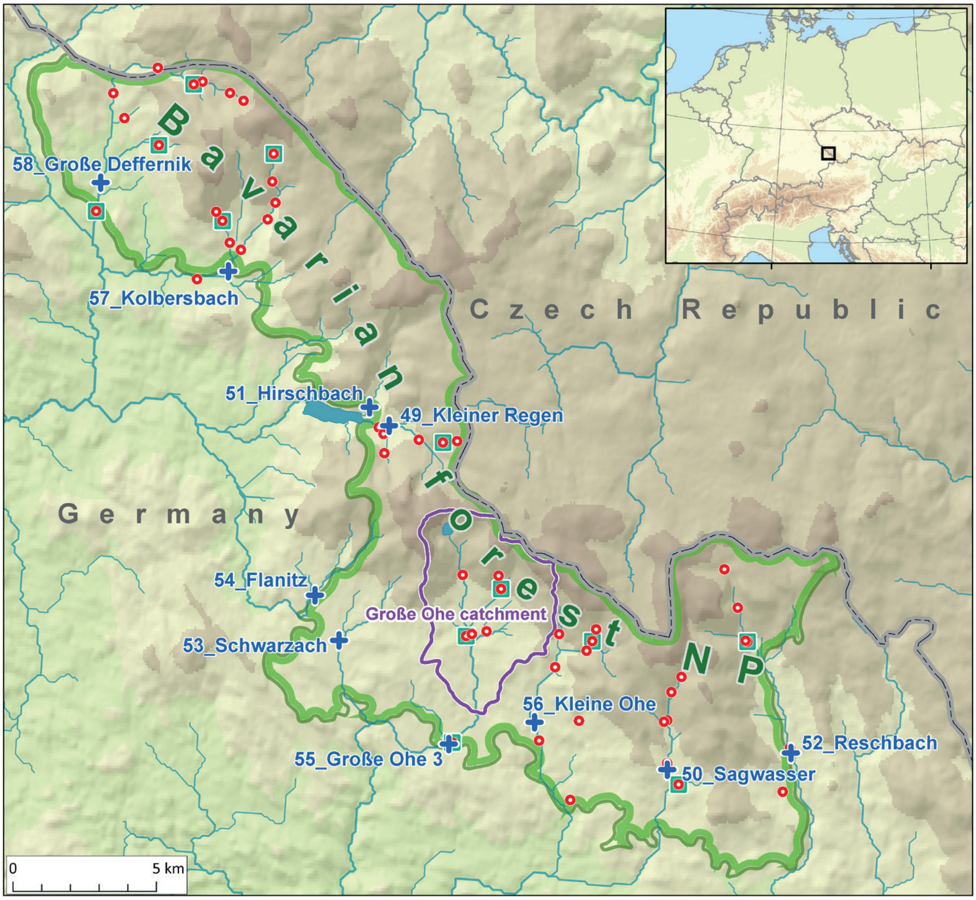

Fig. 2. Map of the BF streams investigated, with seven altitudinal transects and sites studied within them in the monitoring of stream biodiversity. Legend of symbols: blue cross – sites on the BF streams studied in this study (with the name of the sites, see Table 1), red circles – sites on altitudinal transects, green square – sites with additional sampling of insects by Malaise traps.

Table 1. List of sites with coordinates and main environmental characteristics. Nr. – number of site used in Table 3 and Figs. 1, 2, 9; ASW – average stream width, AV – average velocity, TP – total phosphorus, phi – substrate roughness.

Site	Nr.	Abbrev.	N coord.	E coord.	Altitude (m a.s.l.)	ASW (m)	Discharge ($m^3.s^{-1}$)	AV ($m.s^{-1}$)	Conduct. ($\mu S.cm^{-1}$)	TP ($\mu g.l^{-1}$)	phi
GO catchment											
LT of Seebach 1	1	LTSEE1	48.97222	13.41062	1095	1	0.0048	0.27	13	3.0	−8.19
LT of Seebach 3	2	LTSEE3	48.96700	13.41208	1087	0.7	0.0004	0.02	14	3.0	−5.84
Tiefe Seige 1	3	TISE1	48.95693	13.44055	1052	2	0.0028	0.49	18	1.1	−7.98
LT of brook 12	4	LTBR12	48.97000	13.40632	1036	0.3	0.0020	0.34	12	2.4	−7.18
Seebach 1	5	SEEB1	48.96967	13.40492	1030	2	0.0145	0.25	12	1.8	−9.21
Markungsgraben 1	6	MARK1	48.96273	13.43177	1026	0.5	0.0044	0.24	17	0.8	−8.28
Rachelbach	7	RACHEL	48.96933	13.40423	1022	1	0.0031	0.22	19	1.8	−8.92
LT of Seebach 2	8	LTSEE2	48.96618	13.40773	1014	1	0.0001	0.08	14	1.9	−7.61
Seebach 2	9	SEEB2	48.96787	13.40520	1009	4	0.0881	0.45	14	1.8	−9.45
Kaltenbrunnenseige	10	KALTEN	48.96103	13.42452	1004	2.5	0.0131	0.37	13	1.3	−8.38
Rachelschachtenbach 1	11	RACHSCH1	48.96055	13.40088	988	0.5	0.0007	0.27	16	2.0	−5.88
Markungsgraben 2	12	MARK2	48.95797	13.42805	942	2	0.0406	0.63	16	2.3	−9.3
RT of Seebach 1	13	RTSEE1	48.96240	13.40490	942	1.5	0.0205	0.46	14	1.4	−9.16
Rachelschachtenbach 2	14	RACHSCH2	48.95942	13.40588	906	1	0.0364	0.55	14	1.9	−7.95
Seebach 3	15	SEEB3	48.96017	13.40773	899	4	0.1613	0.85	13	1.8	−9.49
Weitauseige 1	16	WEIT1	48.95085	13.43293	886	1	0.0032	0.41	15	4.1	−7.84
Vorderer Schachtenbach 1	17	VOSCH1	48.94147	13.44028	877	1	0.0012	0.14	18	14.9	−7.62
Hinterer Schachtenbach 1	18	HISCH1	48.95372	13.42438	874	2	0.0782	0.60	15	2.7	−8.98
brook with impoundment 1	19	BRIM1	48.95490	13.40315	869	0.4	0.0017	0.25	17	3.9	−5.26
Tiefe Seige 2	20	TISE2	48.95063	13.42785	865	1.5	0.0424	0.68	18	2.9	−8.1
sources of „Dreibach“ 2	21	SODRE2	48.95198	13.39987	864	0.75	0.0005	0.17	23	2.5	−5.27
Forellenbach 1	22	FORE1	48.95132	13.42645	859	0.8	0.0105	0.37	21	13.4	−6.63

Table 1. Continued.

Site	Nr.	Abbrev.	N coord.	E coord.	Altitude (m a.s.l.)	ASW (m)	Discharge ($m^3.s^{-1}$)	AV ($m.s^{-1}$)	Conduct. ($\mu S.cm^{-1}$)	TP ($\mu g.l^{-1}$)	phi
sources of „Dreibach“ 3	23	SODRE3	48.95123	13.39910	855	1	0.0017	0.21	22	5.4	−8.13
sources of „Dreibach“ 1	24	SODRE1	48.95205	13.40055	851	0.5	0.0026	0.24	21	1.9	−7.08
Hüttenbach 1	25	HUTT1	48.93938	13.39472	834	0.5	0.0051	0.36	29	12.3	−3.5
RT of Hinterer Schachtenbach	26	RTHISCH	48.95060	13.41313	824	0.4	0.0046	0.12	15	6.1	−3.22
Hinterer Schachtenbach 2	27	HISCH2	48.94990	13.41845	823	2	0.0711	0.54	15	3.4	−7.17
Seebach 4	28	SEEB4	48.95040	13.40800	819	5	0.2121	0.62	14	3.2	−8.29
LT of Große Ohe	29	LTGO	48.93568	13.41990	817	1	0.0014	0.21	28	10.1	−5.31
Forellenbach 2	30	FORE2	48.94663	13.41888	817	0.75	0.0257	0.35	19	11.1	−9.01
LT of brook with impoundment	31	LTBRIM	48.95023	13.40668	817	0.4	0.0054	0.16	15	6.7	−6.29
Weitauseige 2	32	WEIT2	48.94580	13.42883	815	2	0.0213	0.35	20	9.2	−5.68
brook with impoundment 2	33	BRIM2	48.94908	13.40642	814	0.6	0.0067	0.12	18	7.9	−4.63
Vorderer Schachtenbach 2	34	VOSCH2	48.94275	13.42572	813	2.5	0.0448	0.32	19	10.5	−7.58
LT of Forellenbach	35	LTFO	48.94552	13.41913	812	0.75	0.0043	0.31	36	18.2	−5.26
RT of Guglödgraben	36	RTGU	48.93148	13.41965	802	0.75	0.0010	0.13	22	5.6	−5.31
Hüttenbach 2	37	HUTT2	48.94267	13.40310	800	0.8	0.0105	0.22	27	19.1	−7.08
„Dreibach“ 1	38	DREI1	48.94497	13.40417	795	2	0.0175	0.24	23	9.4	−5.96
RT of Seebach 2	39	RTSEE2	48.94230	13.40928	793	2	0.0561	0.50	24	13.2	−5.44
Vorderer Schachtenbach 3	40	VOSCH3	48.94233	13.41832	792	3	0.1189	0.52	21	9.4	−8.55
Hinterer Schachtenbach 3	41	HISCH3	48.94043	13.41230	790	2	0.0943	0.42	17	5.4	−2.72
Seebach 5	42	SEEB5	48.94132	13.41002	788	5	0.3408	0.65	17	5.1	−7.79
Guglödgraben 1	43	GUGL1	48.92865	13.42077	784	0.4	0.0006	0.19	18	5.0	−5.26
Große Ohe 1	44	GROH1	48.93670	13.41317	782	5	0.4315	0.67	17	6.2	−7.83
RT of Große Ohe 2	45	RTGO2	48.92838	13.41122	774	1	0.0052	0.28	21	5.2	−2.55

Table 1. Continued.

Site	Nr.	Abbrev.	N coord.	E coord.	Altitude (m a.s.l.)	ASW (m)	Discharge ($m^3.s^{-1}$)	AV ($m.s^{-1}$)	Conduct. ($\mu S.cm^{-1}$)	TP ($\mu g.l^{-1}$)	phi
RT of Große Ohe 1	46	RTGO1	48.93055	13.41300	773	0.75	0.0046	0.22	20	4.6	−5.68
Guglödgraben 2	47	GUGL2	48.92530	13.41513	769	0.5	0.0064	0.12	29	11.7	−4.07
Große Ohe 2	48	GROH2	48.92287	13.414	761	6	0.4124	0.56	17	5.7	−6.54
BF streams											
Kleiner Regen	49	KLRE	49.00728	13.37093	877	6	0.4150	0.80	17	–	−9.31
Sagwasser	50	SAGW	48.90118	13.50667	838	4	0.1381	0.31	19	–	−9.19
Hirschbach	51	HIRSCH	49.01293	13.36142	828	6	0.1988	0.90	22	–	−9.17
Reschbach	52	RESCH	48.90717	13.56527	826	8	0.7060	0.55	21	–	−8.7
Schwarzach	53	SCHWAR	48.93960	13.34927	799	2.5	0.0985	0.55	29	–	−7.55
Flanitz	54	FLAN	48.95363	13.33738	793	4	0.2033	0.88	19	–	−8.05
Große Ohe 3	55	GROH3	48.90785	13.40252	745	6	0.5690	0.65	22	–	−4.7
Kleine Ohe	56	KLOH	48.91522	13.44308	745	5	0.2511	0.56	35	–	−8.86
Kolbersbach	57	KOLBER	49.05460	13.29272	725	10	0.3139	0.95	26	–	−8.78
Große Deffernik	58	GRDE	49.08152	13.23087	678	6	0.3718	0.53	35	–	−8.18

ing on a montane plain covered by spruce forests in different succession stages and large area of raised bogs with dense growth of *Pinus* × *pseudopumilio* (Willk.) Beck.

Main streams draining the Bavarian Forest NP (BF streams)

Stream network in the BFNP is dominated by rapid headwater streams with coarse to very coarse bed substratum, flowing on heterogeneous and steep terrain. The largest streams draining the area are only between four- and six-meter wide. Ten streams along the NW to SE border of the BFNP were investigated (Fig. 2, Table 1) in order to bring the data on macroinvertebrate variability to help to establish the design of the systematic monitoring of

Fig. 3. Photos of different stream habitats investigated. A – 33_brook with impoundment 2, B – 11_Rachelschachtenbach 1, C – 3_Tiefe Seige 1, D – 42_Seebach 5, E – 55_Große Ohe 3, F – 52_Reschbach (see Table 1 for more information on these sites).

streams along the altitudinal gradient. Altitude and type of streams were similar, i.e. epi- to metarhitral streams (average stream width 6 m) with coarse, stones and boulders dominating, bed substrate and altitude about 785 m a.s.l. (Fig. 3, Table 2). Some of the streams were rich on aquatic mosses. Water had near neutral pH; current velocity was relatively high (average velocity 0.67 m.s^{-1}), with turbulent flow in all streams.

Literature data

Comparison of our data collected in 2015 with studies covering the entire Bavarian Forest (Pitsch 1994) and Niederbayern (Schulte & Weinzierl 1990) is complicated as the studies include only the total list of species for the entire area of the Bavarian Forest, i.e. including low altitude streams outside the National Park and in the Danube valley. Therefore, only species recorded by our study and both above-mentioned faunistic studies were included in Table 3. Direct comparison is possible only with Schöll (1987) and Kifinger et al. (2004) that studied the GO catchment (Tables 3, 4). Schöll (1987) studied macroinvertebrates at 14 streams in the GO catchment (included also in our study) in 1984–1985, i.e. in the period of strong acidification. Kifinger et al. (2004) included data from acidification monitoring of four streams in the Große Ohe catchment (Seebach, Vorderer Schachtenbach, Hinterer Schachtenbach, Große Ohe) in 2001–2002, i.e. period after the forest dieback. Both studies concerned with all macroinvertebrates except for Chironomidae, which were not determined. Later reports of the acidification monitoring (Schaumburg et al. 2010, Hoffmann et al. 2011, LfU 2015) did not include the list of recorded species and data on macroinvertebrates were presented only as acid classes for individual rivers or periods based on species data.

Sampling methods and processing of samples

One-shot sampling of macroinvertebrates was conducted in May 2015 at all investigated sites. Sampling was based on a standard multi-habitat scheme designed for sampling major in-stream habitats proportionally according to their share within the sampling section (AQEM Consortium 2002). Each sample consisted of 20 plots 0.25×0.25 m (1.25 m^2) taken from all habitat types with a share of at least 5% coverage at the sampling site. Samples were taken by a standard hydrobiological hand net with 0.5 mm mesh size. Sampling protocol was based on standard AQEM protocol. The cover of different particle sizes on the stream bed was visually estimated and substrate roughness was described by phi (Gordon et al. 1992). Slope was measured using optical level (South NL20) and water velocity was measured by Flo-Mate device (Model 2000; Marsch-McBirney, Frederick, MD, USA). Discharge was calculated from water velocity and depth measured in a cross transect at each site. Samples of macroinvertebrates were fixed with formaldehyde and hand-sorted under the dissecting microscope in the laboratory. Sorted individuals were identified by specialists to as low determination level as possible. Two thirds of the taxa in the final datasets are species (121 species) and the remaining taxa are on higher levels, including 27 groups of species, 33 genera and 3 subfamilies or families. As the majority of taxa was identified to the species level, we use the term "species" for all the taxa throughout the text. Identified individuals were preserved in 70% ethanol or mounted dry and deposited at the Department of Botany and Zoology, Masaryk University in Brno. Only oligochaetes, which were not abundant, were not determined and are not included in the dataset. Semiquantitative sampling was supplemented by collecting of Plecoptera and Trichoptera adults by sweeping of riparian vegetation.

Samples of water for hydrochemical analyses were taken along with the sampling of macroinvertebrates in the Große Ohe catchment (and also in the Vydra catchment), not in the BF streams. Only one-shot sampling of water completed within ten days after the snowmelt-

Table 2. Environmental characteristics of the 48 sites in the Große Ohe catchment and 10 main rivers draining the Bohemian Forest NP.

Variables	GO catchment			BF streams		
	mean	**min.**	**max.**	**mean**	**min.**	**max.**
Altitude (m a.s.l.)	876	760	1095	785	678	877
Discharge ($m^3.s^{-1}$)	0.05077	0.00004	0.43153	0.31655	0.03806	0.70597
Average width (m)	1.7	0.3	6.0	5.8	2.5	10.0
Slope (%)	8.8	0.4	25.6	2.8	0.8	5.2
Max. velocity ($m^3.s^{-1}$)	0.74	0.20	1.53	1.26	0.78	1.67
Average velocity ($m^3.s^{-1}$)	0.35	0.02	0.85	0.67	0.31	0.95
Max. depth (m)	0.45	0.08	1.50	0.68	0.25	1.50
Average depth (m)	0.18	0.03	0.50	0.30	0.15	0.4
Pools (%)	32	0	90	15	5	60
pH	5.6	4.5	6.4	6.4	5.7	7.1
Conductivity ($\mu S.cm^{-1}$)	18	12	36	24	17	35
ANC ($\mu mol.l^{-1}$)	31	−21	206	–	–	–
Al_i ($\mu g/l^{-1}$)	40	0	201	–	–	–
DOC ($mg.l^{-1}$)	7.9	0.5	34.2	–	–	–
TN ($mg.l^{-1}$)	0.5	0.2	1.1	–	–	–
TP ($\mu g/l^{-1}$)	5.9	0.8	19.1	–	–	–
Cl^- ($mg.l^{-1}$)	0.4	0.2	2.4	–	–	–
SO_4^{2-} ($mg.l^{-1}$)	2.1	0.4	4.8	–	–	–
Na^+ ($mg.l^{-1}$)	1.0	0.4	2.1	–	–	–
K^+ ($mg.l^{-1}$)	0.3	0.1	0.7	–	–	–
Ca^{2+} ($mg.l^{-1}$)	1.1	0.4	2.9	–	–	–
Mg^{2+} ($mg.l^{-1}$)	0.4	0.2	0.8	–	–	–
O_2 ($mg.l^{-1}$)	10.6	9.5	11.5	8.3	7	11
Oxygen saturation (%)	101	86	106	104	103	106
Temperature (°C)	8.5	6.0	12.0	11.2	10.4	11.4
phi	−6.8	−2.5	−9.5	−8.3	−4.7	−9.3
Macrophytes (%)	6	0	30	9	5	20
Dead wood (%)	8	5	30	0	0	0
CPOM (%)	14	5	40	6	5	10
FPOM (%)	8	5	20	10	10	10

water outflow is available due to restricted entrance to the area, which is situated in the core zone of both national parks. The area, with abundant fallen trees, windthrows and dead wood, is not safely accessible before the snowmelt in spring and the entrance is strictly restricted due to nesting of capercaillie (*Tetrao urogallus*) until the end of July. Shortly after the sampling, water samples were filtered through 0.4-µm pore size glass-fibre filters (MN-GF5) for the analyses of dissolved compounds. Dissolved organic carbon (DOC) was analysed in the filtrate with a LiquiTOC analyser (Foss/Heraeus). Dissolved phosphate (P_d) was determined by the molybdate method after perchloric acid digestion and acid neutralising capacity (ANC) by Gran titration. Fractionation of Al was analysed in filtered samples. Ionic Al (Al_i) was obtained as the difference between dissolved and organically-bound Al. Concentrations of major ions were analysed by ion chromatography. All concentrations used in this study were above the detection limits and accuracy of the analyses was checked using ion balance control including ionic Al forms and organic acid anions for each sample according to Kopáček et al. (2000). More details on the analytical methods, their accuracy, and precision are given in Kopáček et al. (2004).

Data evaluation

Differences in the species richness and abundance at sites of GO catchment and BF streams were tested by non-parametric Mann-Whitney U test. Rarefaction curves were performed to evaluate the possible impact of different number of individuals on species richness in the datasets. For each sampling site, acid class scored by species was calculated. Species with unknown affiliation to acid classes based on Braukmann & Biss (2004) were excluded from the analysis. Two approaches of acid class assessment were used: (i) Based on maximum sensitivity of bioindicators – species are cumulatively added from acid sensitive to acid very resistant till the threshold is reached. Calculation is based on abundance classes of species (according to Alf et al. 1992), when threshold is 4, or based on dominance of species, when threshold is 10% (Braukmann 2001, Braukmann & Biss 2004). (ii) Based on the composition of all classified species when the acid class expresses mean value of acid classes scored by all species included in the analysis. The value is weighted average of acid class based on species abundances.

Multidimensional statistic methods were used to describe the variability in species data from the GO catchment and BF streams. Non-Metric Multidimensional Scaling (NMDS) was used to project sites in 2-dimensional ordination space. NMDS was calculated on Bray-Curtis dissimilarity matrix obtained from ln(x+1) transformed species data. We applied NMDS via a wrapper function metaMDS of the vegan package (Oksanen et al. 2017), which performs several random starts and rotates the final projection so that the variance is maximized on the first dimension. Once the NMDS ordination was finalized, we searched for environmental variables that would enable the interpretation of general gradients represented by NMDS dimensions using visualisation techniques and by fitting smooth surfaces onto the ordination via Generalized Additive Models (GAM). We also searched for species that best followed these gradients with the same methods, but with expected Poisson distributed errors. Environmental variables for constrained ordinations were selected based on Spearman correlations. Variables with R>0.65 were excluded from the analyses. Forward selection was performed to select variables explaining the highest percent of variability for db-RDA (via ordiR2step function of the vegan package, Oksanen et al. 2017).

All statistical analyses were carried out in R (R Core Team 2017) using the following packages: “vegan” (Oksanen et al. 2017), “ggplot2” (Wickham 2009), “Hmisc” (Harrell 2017), “RColorBrewer” (Neuwirth 2014) and “goeveg” (Goral & Schellenberg 2017).

RESULTS

GO catchment and BF streams: species richness and abundance

In total, 40,682 individuals and 184 species were recorded in the BF streams and GO catchment (Table 3, 5); 114 species were common, 16 and 54 species were found only in the BF streams and GO catchment, respectively. Eight endangered (2 – stark gefährdet) or vulnerable (3 – gefährdet) species based on the Bavarian/German Red list (Binot et al. 1998, Anonymus 2005) were found: *Ameletus inopinatus* (3/2), *Rhithrogena hercynia* (–/2), *Perla marginata* (3/3), and *Leuctra alpina* (3/3), *Brachycentrus montanus* (3/–), *Hydropsyche silfvenii* (3/2), *Drusus chrysotus* (3/3), and *Chaetopteryx major* (3/3). The total number of species was higher in the GO catchment (168 species) than in the BF streams (130 species). However, higher species richness per site (i.e. alpha diversity) was found in the BF streams (Mann-Whitney U test, $p<0.001$, Fig. 4) which indicates higher habitat heterogeneity there. The total abundance per a site was also higher in the BF streams (Mann-Whitney U test, $p = 0.006$, Fig. 4). Higher number of species found in the GO catchment was influenced more by higher beta diversity within the catchment than higher number of individuals found, as the rarefaction curves reach their asymptotes (Fig. 5). The most species-rich groups were Chironomidae and Trichoptera (Table 5). Less species of Chironomidae, Coleoptera, and Plecoptera were found in the BF streams than in the GO catchment.

Abundance of macroinvertebrates in the GO catchment was significantly correlated with three mutually related variables, positively with pH and ANC, and negatively with Al_i concentration (Table 6). Abundance increased with increasing pH being variable above 5.5 at sites with different ANC, while it was variable in Al_i from 0 to 53 $\mu g.l^{-1}$ and steeply decreased in its higher concentrations (Fig. 6). Species richness was, however, not correlated with acidity and was slightly positively related to discharge and negatively to coarse particulate organic matter (CPOM) in the substrate (Table 6). Relations of species richness and abundance were not evaluated in the BF streams because of low number of sites.

Composition of macroinvertebrate assemblages and its relation to environmental variables

GO catchment

Stream network of the GO catchment included relatively wide range of stream sizes, from small streamlets 0.3 m wide with discharge 4.10^{-5} $m^3.s^{-1}$ to a 6-m-wide stream with dis-

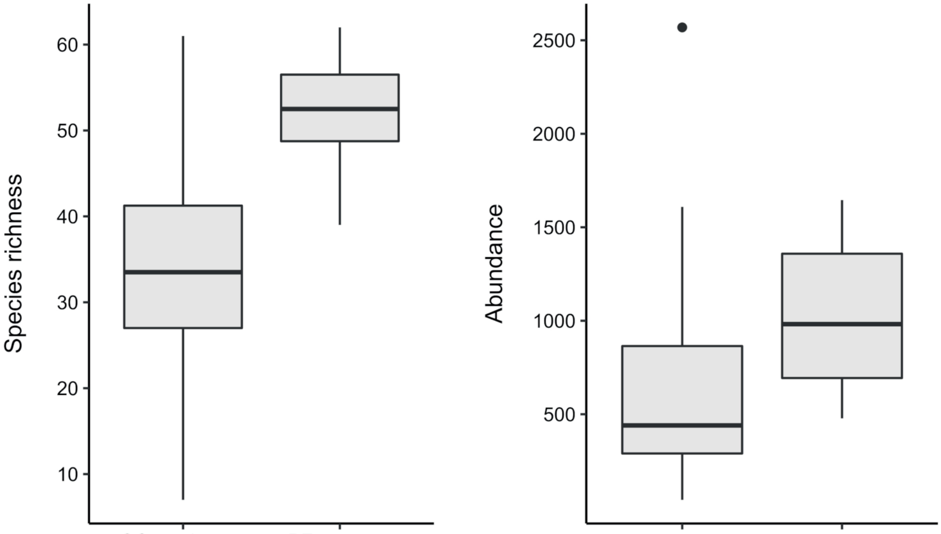

Fig. 4. Comparison of species richness and abundance between the GO catchment and BF streams.

Table 3. List of species found in the GO catchment and BF streams. Frequency/mean abundance and list of sites (see site numbers in Table 1) where each species was found, are shown. Species/taxa are sorted according to their frequency in the GO catchment. The following literature data are shown: records from the GO catchment (Sch = Schöll 1987, Kif = Kifinger et. al. 2004) and from the area of Bavarian Forest National park and surrounding area (BFNP: S&W = Schulte & Weinzierl 1990, Pit = Pitsch 1994). "+" = species was found, "-" = species was not found, "n.i." = group is not included/determined in the study. Acid class values according to Braukmann & Biss (2004) are shown in the last column. Explanatory notes for acid classes: species occurring in 1 – continuously neutral (not acidic) waters, 2 – predominantly neutral to episodically weakly acidic, 3 – periodically critically acidic, 4 – periodically very acidic, and 5 – permanently very acidic.

Group / species	Frequency / mean abund.		Sites	GO catchm.		BFNP		Acid class
	GO catchm.	BF streams		Sch	Kif	S&W	Pit	
Ephemeroptera								
Baetis alpinus (Pictet, 1843)	28 / 35	10 / 91,5	4, 9, 10, 11, 12, 14, 15, 16, 17, 18, 19, 20, 22, 23, 27, 28, 29, 30, 32, 33, 34, 35, 38, 39, 40, 42, 44, 48, 49, 50, 51, 52, 53, 54, 55, 56, 57, 58	+	+	+	n.i.	2
Ameletus inopinatus Eaton, 1887	25 / 7,4	3 / 3,3	3, 6, 9, 10, 11, 12, 13, 14, 15, 16, 17, 20, 25, 26, 27, 28, 30, 32, 33, 34, 37, 39, 40, 42, 44, 49, 50, 52	+	+	+	n.i.	3
Baetis rhodani (Pictet, 1843)	17 / 36,6	8 / 17,9	4, 18, 22, 27, 30, 32, 33, 34, 35, 38, 39, 40, 42, 44, 45, 46, 48, 50, 52, 53, 54, 55, 56, 57, 58	–	–	+	n.i.	3
Rhithrogena semicolorata (Curtis, 1834)	14 / 13,6	9 / 15	4, 18, 22, 27, 28, 30, 32, 33, 36, 39, 40, 42, 44, 48, 49, 50, 51, 52, 53, 55, 56, 57, 58	+	–	+	n.i.	2
Habrophlebia lauta Eaton, 1884	13 / 4,8	2 / 2	4, 18, 20, 27, 30, 33, 34, 38, 40, 42, 45, 46, 48, 54, 56	–	–	–	n.i.	2
Rhithrogena iridina (Kolenati, 1839) / *R. picteti* Sowa, 1971	10 / 16,4	3 / 3,7	14, 22, 23, 30, 32, 33, 34, 35, 38, 40, 53, 55, 56	–	–	–	n.i.	2 / 2
Ecdyonurus picteti (Meyer-Dür, 1864)	8 / 4,3	3 / 2,7	12, 22, 30, 34, 35, 38, 39, 40, 49, 51, 54	–	–	–	n.i.	–
Nigrobaetis niger (Linnaeus, 1761)	7 / 4	2 / 5,5	27, 34, 35, 39, 45, 47, 48, 55, 56	–	–	+	n.i.	2
Ecdyonurus venosus (Fabricius, 1775)	5 / 5,4	6 / 3,5	27, 30, 42, 44, 48, 50, 52, 53, 54, 56, 58	–	–	+	n.i.	2

Table 3. Continued

Group / species	Frequency / mean abund.		Sites	GO catchm.		BFNP		Acid class
	GO catchm.	BF streams		Sch	Kif	S&W	Pit	
Epeorus assimilis Eaton, 1885	5 / 10,8	7 / 3,7	4, 30, 42, 44, 48, 50, 51, 52, 53, 54, 56, 57	–	–	–	n.i.	2
Ephemerella mucronata (Bengtsson, 1909)	1 / 1	2 / 19	4, 50, 56	–	–	+	n.i.	1
Habroleptoides confusa Sartori & Jacob, 1986	1 / 2	2 / 2,5	4, 54, 58	–	–	+	n.i.	1
Habrophlebia fusca (Curtis, 1834)	1 / 4	1 / 2	17, 58	–	–	+	n.i.	–
Nigrobaetis muticus (Linnaeus, 1758)	1 / 115	4 / 12,8	4, 51, 56, 57, 58	–	–	–	n.i.	2
Rhithrogena hercynia Landa, 1969	1 / 10	3 / 2,7	10, 49, 51, 58	–	–	–	n.i.	–
Rhithrogena loyolaea Navás, 1922	1 / 18	0 / 0	10	–	–	+	n.i.	2
Plecoptera								
Protonemura auberti Illies, 1954	43 / 39,7	0 / 0	1, 2, 4, 5, 6, 7, 8, 9, 10, 11, 12, 13, 14, 15, 16, 17, 18, 19, 20, 21, 22, 23, 24, 25, 26, 27, 28, 29, 30, 31, 32, 33, 34, 35, 36, 37, 38, 39, 41, 42, 45, 46, 47	–	+	+	n.i.	5
Leuctra aurita Navás, 1919 / *L. pseudocingulata* Mendl, 1968	32 / 9,2	9 / 18,2	1, 4, 5, 6, 7, 8, 9, 10, 11, 12, 13, 14, 15, 16, 17, 18, 20, 22, 24, 26, 27, 28, 32, 34, 35, 37, 39, 40, 41, 42, 44, 46, 49, 50, 51, 52, 53, 54, 55, 56, 57	+	+	+	n.i.	2 / 4
Siphonoperla torrentium (Pictet, 1841)	28 / 11,5	7 / 4,6	4, 5, 7, 8, 9, 10, 13, 16, 17, 18, 20, 22, 24, 26, 27, 28, 29, 30, 32, 34, 37, 38, 39, 40, 41, 42, 44, 48, 50, 51, 52, 53, 54, 55, 56	+	+	+	n.i.	3
Leuctra braueri Kempny, 1898	27 / 24,7	3 / 3,3	10, 11, 14, 16, 17, 18, 19, 20, 21, 22, 23, 26, 29, 30, 31, 32, 33, 34, 35, 36, 38, 40, 43, 45, 46, 47, 48, 49, 52, 57	–	+	+	n.i.	3
Leuctra inermis group	25 / 33,3	10 / 63,9	7, 9, 10, 12, 14, 15, 18, 19, 20, 22, 23, 27, 28, 30, 33, 34, 35, 36, 38, 39, 40, 41, 42, 44, 48, 49, 50, 51, 52, 53, 54, 55, 56, 57, 58	+	+	+	n.i.	4

Table 3. Continued

Group / species	Frequency / mean abund.		Sites	GO catchm.		BFNP		Acid class
	GO catchm.	BF streams		Sch	Kif	S&W	Pit	
Isoperla oxylepis (Despax, 1936)	24 / 7,4	9 / 29,8	10, 11, 15, 16, 17, 18, 19, 22, 24, 26, 27, 28, 30, 31, 32, 34, 35, 36, 39, 42, 44, 45, 46, 48, 50, 51, 52, 53, 54, 55, 56, 57, 58	–	–	+	n.i.	3
Leuctra nigra (Olivier, 1811)	22 / 5	0 / 0	2, 6, 7, 8, 10, 11, 16, 17, 22, 24, 25, 26, 27, 32, 34, 36, 38, 42, 43, 45, 47, 48	+	+	+	n.i.	5
Amphinemura sulcicollis (Stephens, 1836)	20 / 19,9	8 / 21,3	5, 7, 9, 12, 14, 15, 16, 18, 20, 27, 28, 30, 34, 38, 39, 40, 41, 42, 44, 48, 49, 50, 51, 52, 53, 54, 56, 57	+	+	+	n.i.	3
Brachyptera seticornis (Klapálek, 1902)	20 / 8,6	6 / 21,3	1, 4, 9, 10, 11, 12, 15, 18, 20, 22, 26, 28, 30, 34, 37, 39, 40, 42, 44, 48, 49, 50, 51, 52, 56, 58	+	+	+	n.i.	5
Isoperla goertzi Illies, 1952 / *I. rivulorum* (Pictet, 1841) / *I. silesica* Illies, 1952	20 / 12,1	3 / 12,7	9, 10, 11, 12, 13, 14, 18, 20, 27, 28, 30, 31, 32, 33, 34, 38, 39, 40, 41, 44, 49, 50, 57	+	+	+	n.i.	2 / 2
Leuctra spp. juv.	18 / 24,1	3 / 20,7	4, 5, 6, 8, 9, 10, 11, 13, 14, 15, 16, 18, 19, 23, 30, 33, 37, 46, 49, 50, 51	+	+	+	n.i.	–
Leuctra alpina Kühtreiber, 1934	15 / 23,4	0 / 0	1, 3, 4, 6, 7, 8, 9, 10, 11, 13, 19, 21, 25, 29, 37	–	+	+	n.i.	2
Diura bicaudata (Linnaeus, 1758)	14 / 2,6	1 / 2	1, 4, 6, 7, 8, 9, 11, 13, 17, 25, 39, 42, 45, 46, 53	+	+	+	n.i.	5
Nemoura cinerea (Retzius, 1783)	12 / 19,9	0 / 0	1, 2, 4, 7, 8, 17, 25, 26, 29, 31, 43, 47	+	+	+	n.i.	5
Protonemura austriaca Theischinger, 1976 / *P. intricata* (Ris, 1902)	11 / 55	10 / 71,5	15, 18, 27, 28, 30, 34, 40, 41, 42, 44, 48, 49, 50, 51, 52, 53, 54, 55, 56, 57, 58	+	+	+	n.i.	4 / –
Nemurella pictetii Klapálek, 1900	9 / 8,7	0 / 0	1, 7, 8, 10, 25, 35, 43, 46, 47	+	+	+	n.i.	5
Leuctra hippopus Kempny, 1899	4 / 2	2 / 2,5	27, 36, 40, 42, 55, 56	+	+	+	n.i.	5
Leuctra prima group	4 / 5,5	0 / 0	6, 22, 31, 35	–	+	+	n.i.	–

Table 3. Continued

Group / species	Frequency / mean abund.		Sites	GO catchm.		BFNP		Acid class
	GO catchm.	BF streams		Sch	Kif	S&W	Pit	
Perlodes cf. *microcephalus* (Pictet, 1833)	4 / 2,5	3 / 2,7	28, 40, 42, 44, 52, 53, 55	+	+	+	n.i.	2
Nemoura marginata group	2 / 2,5	0 / 0	21, 26	–	–	+	n.i.	5
Chloroperla tripunctata (Scopoli, 1763)	1 / 1	1 / 4	44, 51	–	–	+	n.i.	–
Protonemura meyeri (Pictet, 1841)	1 / 2	1 / 3	48, 56	+	+	+	n.i.	4
Perla marginata (Panzer, 1799)	0 / 0	2 / 5	57, 58	–	–	+	n.i.	2
Protonemura praecox (Morton, 1894)	0 / 0	1 / 10	50	–	–	+	n.i.	4
Trichoptera								
Limnephilidae g . sp. juv.	42 / 20,3	10 / 26,1	1, 4, 5, 6, 7, 8, 9, 10, 11, 12, 13, 14, 15, 16, 17, 18, 20, 22, 23, 24, 25, 26, 27, 29, 30, 31, 32, 33, 34, 35, 37, 38, 39, 40, 41, 42, 43, 44, 45, 46, 47, 48, 49, 50, 51, 52, 53, 54, 55, 56, 57, 58	+	+	+	+	–
Plectrocnemia conspersa (Curtis, 1834)	28 / 5	3 / 1,3	1, 2, 3, 6, 7, 8, 9, 10, 11, 13, 17, 22, 24, 25, 26, 28, 29, 30, 31, 34, 35, 36, 37, 38, 39, 40, 43, 46, 49, 50, 51	+	+	+	+	5
Sericostoma personatum (Spence, 1826)	28 / 5,4	10 / 4,6	10, 11, 12, 14, 15, 17, 18, 19, 20, 21, 22, 23, 24, 26, 27, 29, 31, 33, 35, 36, 38, 39, 41, 43, 44, 45, 46, 48, 49, 50, 51, 52, 53, 54, 55, 56, 57, 58	+	+	+	+	3
Rhyacophila praemorsa McLachlan, 1879	21 / 4,5	3 / 4,7	1, 4, 5, 11, 13, 14, 15, 16, 17, 18, 19, 22, 30, 31, 33, 34, 35, 37, 38, 39, 40, 49, 50, 52	+	+	+	+	4
Chaetopteryx major McLachlan, 1876	19 / 7,8	0 / 0	11, 16, 19, 20, 21, 22, 23, 25, 26, 31, 32, 35, 36, 37, 38, 39, 45, 46, 47	–	–	–	+	4
Odontocerum albicorne (Scopoli, 1763)	19 / 5,5	8 / 10,5	14, 16, 18, 20, 22, 26, 27, 28, 30, 31, 33, 34, 39, 40, 41, 42, 44, 45, 48, 49, 52, 53, 54, 55, 56, 57, 58	+	+	+	+	4

Table 3. Continued

Group / species	Frequency / mean abund.		Sites	GO catchm.		BFNP		Acid class
	GO catchm.	BF streams		Sch	Kif	S&W	Pit	
Philopotamus ludificatus (McLachlan, 1878)	19 / 14,8	9 / 23,2	6, 11, 12, 14, 18, 19, 20, 22, 26, 28, 30, 34, 36, 38, 39, 40, 42, 44, 46, 49, 50, 51, 52, 53, 54, 56, 57, 58	+	+	+	+	2
Rhyacophila tristis Pictet, 1834	14 / 5,3	6 / 3,8	10, 12, 14, 16, 18, 20, 30, 32, 34, 37, 38, 39, 41, 44, 49, 51, 52, 54, 56, 58	+	+	+	+	2
Potamophylax latipennis (Curtis, 1834) / *P. luctuosus* (Piller & Mitterpacher, 1783)	13 / 3,1	4 / 2,8	1, 8, 10, 11, 20, 21, 29, 34, 38, 40, 41, 44, 48, 49, 54, 55, 56	+	+	+	+	3 / 4
Rhyacophila fasciata Hagen, 1859 / *R. vulgaris* Pictet, 1834 / *R. obliterata* McLachlan, 1863	13 / 2,3	8 / 4,9	4, 8, 9, 20, 22, 27, 28, 33, 37, 38, 39, 40, 48, 50, 51, 52, 53, 54, 56, 57, 58	+	+	+	+	4 / 4 / 4
Hydropsyche tenuis Navás, 1932	12 / 6,9	9 / 20,9	14, 15, 18, 20, 27, 28, 34, 37, 39, 40, 42, 44, 49, 50, 51, 52, 53, 54, 56, 57, 58	–	+	+	+	2
Chaetopteryx villosa (Fabricius, 1798)	11 / 7,3	7 / 7,7	11, 14, 16, 18, 22, 26, 27, 28, 32, 37, 45, 50, 51, 52, 53, 56, 57	+	–	+	+	5
Lithax niger (Hagen, 1859)	11 / 2,4	1 / 2	12, 18, 21, 22, 30, 31, 33, 34, 35, 39, 41, 53	+	+	+	+	2
Potamophylax cingulatus cf. (Stephens, 1837)	11 / 3	6 / 5,7	17, 18, 22, 24, 34, 35, 38, 40, 46, 47, 48, 49, 50, 52, 53, 55, 56, 57	–	–	+	+	4
Ptilocolepus granulatus (Pictet, 1834)	10 / 2,5	1 / 2	4, 6, 7, 9, 12, 13, 15, 18, 28, 34, 53	+	–	+	+	3
Allogamus uncatus (Brauer, 1857)	9 / 3,6	2 / 1,5	8, 10, 22, 24, 25, 35, 37, 38, 46, 51, 53	+	–	+	+	4
Chaetopterygopsis maclachlani Stein, 1874	8 / 3,8	2 / 14	7, 10, 12, 20, 27, 28, 34, 48, 53, 58	+	–	+	+	5
Drusus annulatus (Stephens, 1837)	7 / 3,3	1 / 4	8, 12, 17, 22, 25, 32, 33, 50	+	+	+	+	5
Drusus discolor (Rambur, 1842)	7 / 6	2 / 3,5	9, 10, 12, 13, 18, 28, 44, 49, 51	+	+	+	+	4
Ecclisopteryx madida (McLachlan, 1867)	7 / 4,1	3 / 1,7	20, 22, 30, 32, 33, 34, 35, 49, 50, 51	+	+	+	+	3

Table 3. Continued

Group / species	Frequency / mean abund.		Sites	GO catchm.		BFNP		Acid class
	GO catchm.	BF streams		Sch	Kif	S&W	Pit	
Apatania fimbriata (Pictet, 1834)	6 / 6,8	1 / 4	9, 22, 29, 33, 35, 37, 50	+	+	+	+	4
Glossosoma conformis Neboiss, 1963	6 / 2,8	7 / 10,4	18, 27, 30, 34, 44, 48, 49, 50, 51, 52, 53, 54, 56	–	–	+	+	1
Plectrocnemia geniculata McLachlan, 1871	6 / 4,7	0 / 0	4, 5, 7, 12, 13, 31	+	+	+	+	5
Rhyacophila evoluta McLachlan, 1879	5 / 2	4 / 4,8	9, 14, 28, 38, 42, 49, 51, 57, 58	–	+	+	+	3
Rhyacophila glareosa McLachlan, 1867	5 / 4,8	3 / 2	9, 10, 12, 15, 18, 49, 50, 51	–	–	+	+	4
Crunoecia cf. *irrorata* (Curtis, 1834)	4 / 1,3	0 / 0	11, 13, 17, 18	+	+	+	+	–
Wormaldia occipitalis (Pictet, 1834)	4 / 2,8	0 / 0	6, 16, 24, 36	–	–	+	+	3
Agapetus fuscipes Curtis, 1834	3 / 74,7	2 / 21	21, 24, 29, 57, 58	–	–	+	+	1
Drusus chrysotus (Rambur, 1842)	3 / 2,3	0 / 0	11, 24, 29	–	–	+	+	3
Halesus digitatus (Schrank, 1781) / *H. tesselatus* (Rambur, 1842)	3 / 2,7	4 / 1,5	39, 41, 48, 51, 53, 54, 58	–	–	+	+	2 / –
Anomalopterygella chauviniana (Stein, 1874)	2 / 3	3 / 2,7	44, 48, 52, 55, 58	–	–	+	+	2
Allogamus auricollis (Pictet, 1834)	1 / 2	2 / 1	40, 52, 56	+	+	+	+	1
Halesus radiatus (Curtis, 1834)	1 / 2	1 / 2	33, 58	–	–	+	+	–
Hydatophylax infumatus (McLachlan, 1865)	1 / 1	0 / 0	27	–	+	+	+	–
Micrasema longulum McLachlan, 1876	1 / 2	1 / 1	44, 51	+	+	+	+	3
Micrasema minimum McLachlan, 1876	1 / 2	5 / 10,6	40, 51, 52, 54, 56, 58	–	–	+	+	3
Micropterna lateralis (Stephens, 1837)	1 / 2	0 / 0	2	–	–	–	–	4
Agapetus ochripes Curtis, 1834	0 / 0	3 / 2	54, 56, 58	–	–	+	+	1
Brachycentrus montanus Klapálek, 1892	0 / 0	1 / 12	58	–	–	+	+	–
Hydropsyche dinarica Marinković-Gospodnetić, 1979	0 / 0	2 / 15	54, 58	–	–	+	–	–
Hydropsyche silfvenii Ulmer, 1906	0 / 0	1 / 5	55	–	–	+	+	2
Hydroptila spp.	0 / 0	1 / 1	54	–	–	+	–	–
Rhyacophila dorsalis (Curtis, 1834)	0 / 0	2 / 2	52, 56	+	–	+	+	4
Silo pallipes (Fabricius, 1781)	0 / 0	2 / 1,5	49, 58	+	+	+	+	3
Tinodes cf. *rostocki* McLachlan, 1878	0 / 0	3 / 1,7	50, 56, 57	–	–	+	+	1

Table 3. Continued

Group / species	Frequency / mean abund.		Sites	GO catchm.		BFNP		Acid class
	GO catchm.	BF streams		Sch	Kif	S&W	Pit	
Coleoptera								
Limnius perrisi (Dufour 1843)	38 / 100,6	10 / 150,3	6, 9, 10, 11, 12, 14, 15, 16, 17, 18, 19, 20, 22, 23, 24, 25, 26, 27, 28, 30, 31, 32, 33, 34, 35, 36, 37, 38, 39, 40, 41, 42, 43, 44, 45, 46, 47, 48, 49, 50, 51, 52, 53, 54, 55, 56, 57, 58	+	+	+	n.i.	4
Elmis latreillei Bedel, 1878	27 / 16,8	3 / 3,7	1, 4, 8, 9, 10, 11, 12, 13, 14, 16, 17, 19, 20, 21, 22, 23, 24, 25, 26, 29, 32, 35, 36, 37, 38, 43, 46, 49, 50, 51	–	–	+	n.i.	4
Elmis aenea (P.W.J. Müller, 1806)	17 / 16,8	9 / 14,1	4, 9, 11, 15, 18, 27, 28, 30, 33, 34, 37, 39, 40, 41, 42, 44, 48, 49, 50, 51, 52, 53, 54, 56, 57, 58	–	–	+	n.i.	3
Odeles marginata cf. (Fabricius, 1798)	16 / 3,4	0 / 0	11, 12, 14, 15, 16, 17, 18, 19, 23, 26, 27, 29, 30, 36, 37, 44	–	–	–	n.i.	–
Esolus angustatus (P.W.J. Müller, 1821)	14 / 17	10 / 14,7	9, 18, 22, 27, 28, 30, 32, 34, 38, 39, 40, 41, 44, 48, 49, 50, 51, 52, 53, 54, 55, 56, 57, 58	+	+	+	n.i.	3
Elmis rioloides (Kuwert, 1890)	7 / 19	8 / 18	27, 34, 39, 40, 42, 44, 48, 51, 52, 53, 54, 55, 56, 57, 58	–	–	+	n.i.	–
Hydraena dentipes Germar, 1842	7 / 2,1	0 / 0	11, 27, 28, 30, 34, 39, 40	–	–	+	n.i.	2
Hydraena gracilis Germar, 1824	7 / 3,9	5 / 6	18, 22, 30, 32, 34, 44, 48, 50, 52, 55, 56, 58	–	+	+	n.i.	2
Hydraena saga Orchymont, 1930	6 / 2,3	0 / 0	16, 18, 22, 29, 32, 35	+	–	+	n.i.	–
Oreodytes sanmarki (Sahlberg, 1826)	6 / 2,8	5 / 3,6	27, 34, 40, 41, 42, 48, 49, 50, 52, 56, 58	+	+	+	n.i.	3
Anacaena globulus (Paykull, 1798)	5 / 2,2	0 / 0	2, 25, 26, 37, 43	–	+	+	n.i.	4
Agabus guttatus (Paykull, 1798)	4 / 4,3	0 / 0	7, 8, 25, 43	+	+	+	n.i.	4
Elodes sp.	2 / 3	0 / 0	21, 35	–	+	–	n.i.	3
Elmis maugetii Latreille, 1798	1 / 18	8 / 6,4	48, 51, 52, 53, 54, 55, 56, 57, 58	–	+	+	n.i.	3
Limnebius truncatellus (Thunberg, 1794)	1 / 1	0 / 0	8	–	–	+	n.i.	–

Table 3. Continued

Group / species	Frequency / mean abund.		Sites	GO catchm.		BFNP		Acid class
	GO catchm.	BF streams		Sch	Kif	S&W	Pit	
Limnius volckmari (Panzer, 1793)	0 / 0	1 / 1	55	–	–	+	n.i.	–
Diptera, Chironomidae								
Tvetenia bavarica group	36 / 14,5	10 / 33,7	2, 4, 5, 6, 8, 9, 10, 11, 12, 13, 14, 16, 17, 18, 19, 20, 22, 23, 26, 27, 29, 30, 31, 32, 33, 34, 35, 36, 38, 39, 40, 42, 44, 45, 46, 48, 49, 50, 51, 52, 53, 54, 55, 56, 57, 58	n.i.	n.i.	n.i.	n.i.	–
Trissopelopia sp.	32 / 5	6 / 4,7	2, 4, 5, 6, 7, 8, 9, 10, 11, 12, 13, 17, 18, 20, 22, 25, 26, 27, 28, 30, 31, 32, 33, 37, 39, 41, 42, 43, 45, 46, 47, 48, 49, 50, 51, 54, 55, 57	n.i.	n.i.	n.i.	n.i.	–
Macropelopia sp.	22 / 8,1	1 / 2	2, 5, 8, 10, 11, 17, 19, 21, 22, 23, 24, 25, 27, 29, 31, 33, 35, 36, 43, 45, 46, 47, 55	n.i.	n.i.	n.i.	n.i.	–
Micropsectra spp.	19 / 4	3 / 5,3	2, 5, 6, 7, 8, 9, 11, 14, 15, 18, 22, 24, 25, 27, 32, 34, 36, 40, 44, 49, 53, 54	n.i.	n.i.	n.i.	n.i.	–
Thienemanniella partita Schlee, 1968	19 / 3,1	4 / 2,5	8, 10, 12, 13, 14, 15, 16, 17, 18, 20, 22, 27, 28, 31, 34, 37, 39, 44, 48, 49, 53, 54, 56	n.i.	n.i.	n.i.	n.i.	–
Heterotrissocladius marcidus (Walker, 1856)	18 / 4,7	3 / 9,3	2, 5, 7, 10, 22, 24, 25, 26, 27, 31, 32, 34, 38, 41, 43, 46, 47, 48, 49, 53, 55	n.i.	n.i.	n.i.	n.i.	4
Brillia bifida (Kieffer, 1909)	17 / 2,2	4 / 1,8	2, 4, 6, 8, 11, 13, 15, 16, 19, 24, 36, 37, 38, 39, 45, 46, 48, 49, 51, 52, 58	n.i.	n.i.	n.i.	n.i.	4
Zavrelimyia sp.	13 / 10,5	0 / 0	1, 4, 5, 7, 8, 10, 13, 17, 22, 32, 36, 43, 47	n.i.	n.i.	n.i.	n.i.	–
Eukiefferiella minor (Edwards, 1929) / *E. fittkaui* Lehmann, 1972	12 / 6,8	8 / 10,6	2, 12, 18, 20, 22, 27, 30, 34, 40, 42, 44, 48, 49, 50, 51, 52, 53, 54, 56, 58	n.i.	n.i.	n.i.	n.i.	–
Parametriocnemus stylatus (Kieffer, 1924)	12 / 5,4	0 / 0	2, 10, 11, 16, 17, 19, 22, 23, 29, 36, 45, 46	n.i.	n.i.	n.i.	n.i.	–

Table 3. Continued

Group / species	Frequency / mean abund.		Sites	GO catchm.		BFNP		Acid class
	GO catchm.	BF streams		Sch	Kif	S&W	Pit	
Cricotopus annulator group	11 / 13,8	3 / 8,7	10, 12, 14, 16, 27, 30, 34, 38, 40, 41, 48, 49, 50, 51	n.i.	n.i.	n.i.	n.i.	–
Stempellinella brevis (Edwards, 1929) / *S. flavidula* (Edwards, 1929)	11 / 3,4	4 / 2,5	5, 8, 12, 20, 22, 23, 25, 26, 27, 29, 36, 50, 54, 55, 58	n.i.	n.i.	n.i.	n.i.	–
Diamesa dampfi (Kieffer, 1924) / *D. permacra* (Walker, 1856)	10 / 11,4	1 / 22	10, 12, 16, 18, 20, 22, 30, 31, 34, 40, 58	n.i.	n.i.	n.i.	n.i.	–
Heterotanytarsus apicalis (Kieffer, 1921)	10 / 2,3	0 / 0	5, 7, 8, 11, 13, 17, 22, 25, 31, 35	n.i.	n.i.	n.i.	n.i.	–
Conchapelopia sp.	8 / 13,1	9 / 3,6	5, 9, 38, 39, 42, 44, 47, 48, 49, 50, 52, 53, 54, 55, 56, 57, 58	n.i.	n.i.	n.i.	n.i.	–
Cricotopus tremulus (Linnaeus, 1758)	8 / 10,1	2 / 2,5	12, 16, 18, 22, 30, 33, 34, 40, 51, 58	n.i.	n.i.	n.i.	n.i.	–
Diamesa cinerella group	8 / 46,8	6 / 5,5	12, 16, 17, 18, 22, 30, 34, 40, 49, 50, 51, 52, 53, 58	n.i.	n.i.	n.i.	n.i.	–
Paratrichocladius rufiventris (Meigen, 1830)	8 / 35,1	6 / 5,5	27, 29, 30, 34, 38, 40, 44, 48, 49, 50, 53, 54, 55, 56	n.i.	n.i.	n.i.	n.i.	–
Corynoneura lobata Edwards, 1924	7 / 1,7	0 / 0	2, 6, 7, 8, 17, 25, 33	n.i.	n.i.	n.i.	n.i.	–
Eukiefferiella brevicalcar (Kieffer, 1911)	7 / 2,1	2 / 1,5	1, 7, 9, 12, 18, 20, 24, 50, 52	n.i.	n.i.	n.i.	n.i.	–
Eukiefferiella devonica group	7 / 4,6	0 / 0	9, 12, 18, 20, 27, 34, 37	n.i.	n.i.	n.i.	n.i.	–
Polypedilum scalaenum (Schrank, 1803)	7 / 4,3	1 / 2	19, 23, 35, 41, 45, 46, 48, 55	n.i.	n.i.	n.i.	n.i.	–
Cricotopus cf. *albiforceps*	6 / 4,8	0 / 0	1, 4, 7, 8, 9, 12	n.i.	n.i.	n.i.	n.i.	–
Krenopelopia sp.	6 / 3,3	0 / 0	2, 10, 11, 14, 36, 43	n.i.	n.i.	n.i.	n.i.	–
Orthocladius lignicola (Kieffer, 1914)	6 / 1,8	0 / 0	4, 5, 8, 12, 14, 45	n.i.	n.i.	n.i.	n.i.	–
Pseudorthocladius sp.	6 / 2	0 / 0	3, 19, 24, 31, 35, 46	n.i.	n.i.	n.i.	n.i.	–
Orthocladius rubicundus group	5 / 18,8	4 / 5	27, 30, 34, 40, 48, 51, 53, 54, 58	n.i.	n.i.	n.i.	n.i.	–
Apsectrotanypus trifascipennis (Zettersted-t,1838)	4 / 3,5	1 / 1	27, 41, 47, 48, 55	n.i.	n.i.	n.i.	n.i.	–
Eukiefferiella claripennis (Lundbeck, 1898)	4 / 4,8	2 / 5	4, 12, 18, 23, 49, 50	n.i.	n.i.	n.i.	n.i.	–
Metriocnemus fuscipes group	4 / 1,5	0 / 0	17, 22, 25, 46	n.i.	n.i.	n.i.	n.i.	–
Potthastia longimanus Kieffer, 1922	4 / 2	4 / 2,3	15, 17, 24, 38, 51, 55, 56, 58	n.i.	n.i.	n.i.	n.i.	–

Table 3. Continued

Group / species	Frequency / mean abund.		Sites	GO catchm.		BFNP		Acid class
	GO catchm.	BF streams		Sch	Kif	S&W	Pit	
Prodiamesa olivacea (Meigen, 1818)	4 / 3,8	1 / 16	45, 46, 47, 48, 55	n.i.	n.i.	n.i.	n.i.	–
Rheocricotopus fuscipes (Kieffer, 1909)	4 / 2,8	0 / 0	17, 33, 45, 46	n.i.	n.i.	n.i.	n.i.	–
Rheotanytarsus sp.	4 / 3,5	3 / 11,3	34, 40, 44, 48, 54, 56, 58	n.i.	n.i.	n.i.	n.i.	–
Synorthocladius semivirens (Kieffer, 1909)	4 / 6,5	2 / 1	29, 34, 40, 48, 49, 54	n.i.	n.i.	n.i.	n.i.	–
Thienemannimyia sp.	4 / 3,5	2 / 1	18, 27, 32, 42, 51, 56	n.i.	n.i.	n.i.	n.i.	–
Heleniella ornaticollis (Edwards, 1929)	3 / 2,3	0 / 0	11, 14, 29	n.i.	n.i.	n.i.	n.i.	–
Limnophyes sp.	3 / 1,7	0 / 0	8, 14, 24	n.i.	n.i.	n.i.	n.i.	–
Natarsia sp.	3 / 1,7	1 / 8	2, 38, 47, 55	n.i.	n.i.	n.i.	n.i.	–
Orthocladius obumbratus group	3 / 19	0 / 0	1, 34, 40	n.i.	n.i.	n.i.	n.i.	–
Paracladopelma sp.	3 / 5,3	0 / 0	23, 29, 33	n.i.	n.i.	n.i.	n.i.	–
Polypedilum pedestre (Meigen, 1830)	3 / 2,3	1 / 2	11, 36, 48, 55	n.i.	n.i.	n.i.	n.i.	–
Rheocricotopus effusus (Walker, 1856)	3 / 5,7	0 / 0	2, 8, 18	n.i.	n.i.	n.i.	n.i.	–
Cricotopus reversus Hirvenoja, 1973 / *C. intersectus* (Stæger, 1839)	2 / 20	0 / 0	20, 31	n.i.	n.i.	n.i.	n.i.	–
Orthocladius rivicola group	2 / 1	0 / 0	22, 30	n.i.	n.i.	n.i.	n.i.	–
Polypedilum convictum (Walker, 1856)	2 / 2	0 / 0	8, 32	n.i.	n.i.	n.i.	n.i.	–
Tanytarsus spp.	2 / 1,5	0 / 0	11, 36	n.i.	n.i.	n.i.	n.i.	–
Krenosmittia sp.	1 / 1	0 / 0	17	n.i.	n.i.	n.i.	n.i.	–
Neozavrelia sp.	1 / 8	0 / 0	18	n.i.	n.i.	n.i.	n.i.	–
Odontomesa fulva (Kieffer, 1919)	1 / 1	1 / 4	47, 55	n.i.	n.i.	n.i.	n.i.	–
Orthocladius frigidus (Zetterstedt, 1838)	1 / 4	1 / 1	44, 49	n.i.	n.i.	n.i.	n.i.	4
Paraphaenocladius pseudirritus Strenzke, 1950	1 / 8	0 / 0	31	n.i.	n.i.	n.i.	n.i.	–
Polypedilum uncinatum (Goetghebuer, 1921)	1 / 1	1 / 1	22, 49	n.i.	n.i.	n.i.	n.i.	–
Psectrocladius limbatellus (Holmgren, 1869) / *P. sordidellus* (Zetterstedt, 1838)	1 / 1	0 / 0	7	n.i.	n.i.	n.i.	n.i.	–
Tvetenia discoloripes group	1 / 2	4 / 8,5	44, 51, 54, 56, 58	n.i.	n.i.	n.i.	n.i.	–
Diptera, other families								

Table 3. Continued

Group / species	Frequency / mean abund.		Sites	GO catchm.		BFNP		Acid class
	GO catchm.	BF streams		Sch	Kif	S&W	Pit	
Dicranota sp.	47 / 7,2	10 / 15,3	1, 2, 3, 4, 5, 6, 7, 8, 9, 10, 11, 12, 13, 14, 15, 16, 17, 18, 19, 20, 22, 23, 24, 25, 26, 27, 28, 29, 30, 31, 32, 33, 34, 35, 36, 37, 38, 39, 40, 41, 42, 43, 44, 45, 46, 47, 48, 49, 50, 51, 52, 53, 54, 55, 56, 57, 58	+	+	n.i.	n.i.	4
Simuliidae g. sp.	42 / 36,4	9 / 58,6	1, 2, 4, 5, 6, 7, 8, 9, 10, 12, 13, 14, 15, 16, 17, 18, 19, 20, 22, 23, 24, 25, 26, 27, 28, 30, 31, 32, 33, 34, 36, 37, 38, 39, 40, 41, 42, 43, 44, 45, 46, 47, 49, 50, 51, 52, 53, 54, 56, 57, 58	+	+	n.i.	n.i.	–
Eloeophila sp.	23 / 3,6	7 / 2,4	8, 9, 13, 16, 19, 20, 21, 22, 25, 26, 27, 28, 30, 31, 32, 33, 35, 38, 39, 42, 43, 45, 47, 49, 51, 53, 54, 55, 56, 57	–	–	n.i.	n.i.	5
Pedicia sp.	17 / 2	2 / 1,5	1, 2, 6, 8, 11, 13, 22, 23, 24, 26, 29, 31, 32, 35, 43, 45, 46, 52, 56	–	+	n.i.	n.i.	4
Chelifera sp.	16 / 3,9	5 / 1,4	2, 5, 9, 10, 11, 12, 13, 14, 20, 22, 23, 29, 34, 38, 44, 48, 49, 51, 55, 56, 57	–	–	n.i.	n.i.	–
Wiedemannia sp.	6 / 1,8	4 / 1,3	3, 5, 18, 20, 30, 34, 50, 51, 52, 54	–	–	n.i.	n.i.	–
Ceratopogoninae g. sp.	5 / 2	5 / 1	9, 19, 20, 29, 34, 50, 52, 54, 55, 56	–	–	n.i.	n.i.	–
Ibisia marginata (Fabricius, 1781)	2 / 2	5 / 30	23, 38, 49, 52, 54, 57, 58	–	–	n.i.	n.i.	2
Molophilus sp.	2 / 2	1 / 1	39, 45, 55	–	–	n.i.	n.i.	3
Neolimnomyia cf. *filata* (Walker, 1856)	2 / 1,5	0 / 0	33, 47	–	–	n.i.	n.i.	–
Scleroprocta sp.	2 / 1,5	0 / 0	22, 39	–	–	n.i.	n.i.	–
Dolichopeza albipes (Ström, 1768)	1 / 1	0 / 0	7	–	–	n.i.	n.i.	–
Hemerodromia sp.	1 / 4	1 / 1	21, 56	–	–	n.i.	n.i.	–

Table 3. Continued

Group / species	Frequency / mean abund.		Sites	GO catchm.		BFNP		Acid class
	GO catchm.	BF streams		Sch	Kif	S&W	Pit	
Chrysopilus sp. juv.	1 / 2	0 / 0	2	–	–	n.i.	n.i.	–
Ptychoptera sp.	1 / 2	0 / 0	38	–	–	n.i.	n.i.	–
Tipula cf. *variicornis* Schummel, 1833	1 / 2	0 / 0	36	–	–	n.i.	n.i.	–
Antocha sp.	0 / 0	1 / 6	58	–	–	n.i.	n.i.	–
Berdeniella sp.	0 / 0	2 / 4	51, 58	–	–	n.i.	n.i.	–
Hexatoma sp.	0 / 0	1 / 1	55	–	–	n.i.	n.i.	–
Chrysops sp.	0 / 0	1 / 4	55	–	–	n.i.	n.i.	–
Megaloptera								
Sialis fuliginosa Pictet, 1836	13 / 2,4	4 / 2,8	4, 5, 7, 8, 22, 26, 27, 31, 38, 40, 45, 47, 48, 50, 55, 56, 58	+	+	n.i.	n.i.	–
Crustacea								
Gammarus fossarum Koch, 1836	31 / 244,1	5 / 232,6	12, 13, 14, 16, 18, 19, 20, 21, 22, 23, 24, 26, 29, 30, 31, 32, 33, 34, 35, 36, 38, 39, 40, 41, 42, 43, 44, 45, 46, 47, 48, 50, 51, 52, 56, 57	+	–	n.i.	+	2
Asellus aquaticus (Linnaeus, 1758)	2 / 2	0 / 0	12, 29	–	–	n.i.	+	1
Mollusca								
Pisidium casertanum (Poli, 1791)	25 / 9	2 / 6,5	5, 8, 10, 11, 13, 15, 17, 19, 21, 22, 26, 29, 30, 32, 33, 35, 36, 37, 39, 41, 43, 45, 46, 47, 48, 55, 58	–	–	n.i.	n.i.	–
Ancylus fluviatilis Müller, 1773	0 / 0	2 / 12	56, 58	–	–	n.i.	n.i.	1
Tricladida								
Polycelis sp.	12 / 12,8	7 / 58,4	12, 14, 18, 20, 22, 32, 34, 35, 38, 40, 44, 48, 49, 51, 53, 54, 56, 57, 58	+	+	n.i.	n.i.	–
Dugesia sp.	4 / 26,8	2 / 4,5	3, 16, 29, 35, 52, 58	–	–	n.i.	n.i.	–
Crenobia alpina (Dana, 1766)	1 / 4	0 / 0	24	+	–	n.i.	n.i.	–

charge 0.4 $m^3.s^{-1}$ (Fig. 3, Table 2). The sites covered wide altitudinal gradient, from 760 to 1095 m a.s.l., and various slope of terrain (0.4–25.6%). Water chemistry in the GO catchment was influenced by acidification and changes caused by the forest dieback and following development of forest within the area. The variability in ANC (range: −21 to 206 µmol.l^{-1}) was partly associated with altitude (Spearman correlation R = −0.53) and slightly also with the concentration of ionic Al_i (0–201 µg.l^{-1}, R = 0.37). The sites were relatively variable in the concentration of total phosphorus (TP, 0.8–19.1 µg.l^{-1}) and, particularly, DOC (0.5–34.2 mg.l^{-1}), both were negatively correlated with altitude (−0.69 in TP and −0.57 in DOC).

Main gradients in species data were associated with stream size (average stream width, depth, and flow velocity) and acidic conditions (ANC, pH, and Al_i) linked with altitude (Fig. 7). Water conductivity and substrate (phi and CPOM) were partly independent on them as

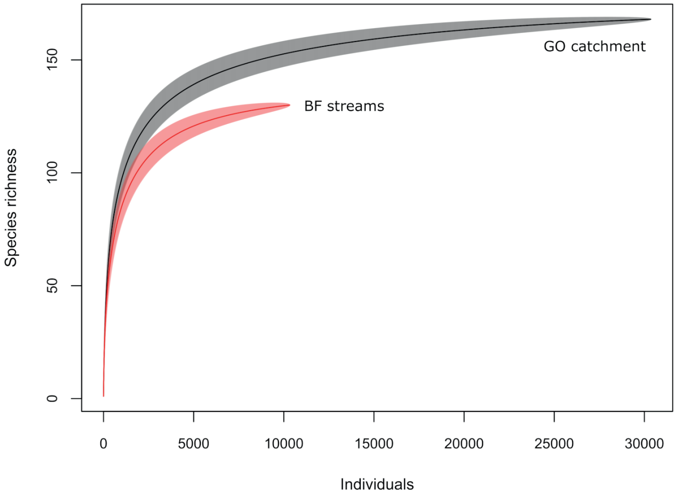

Fig. 5. Species richness of the GO catchment and BF streams modelled by rarefaction curves. The transparent area around a curve represents 95% confidence interval.

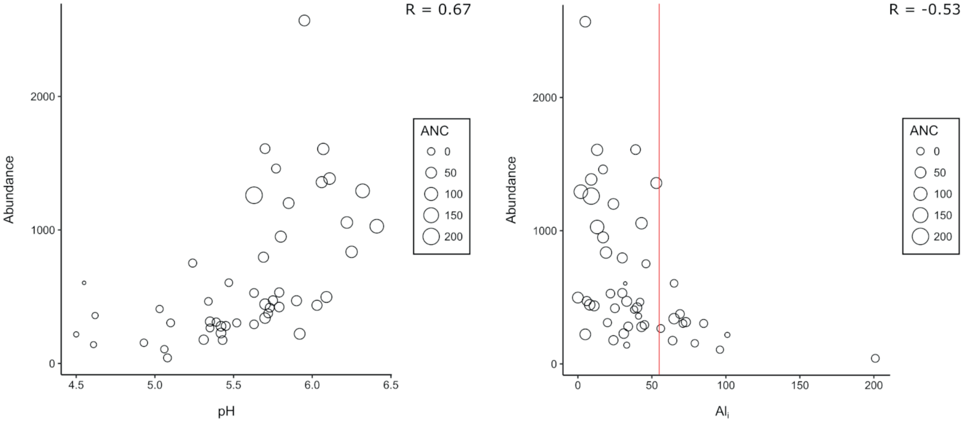

Fig. 6. Relation of species abundance, and pH and Al_i at the GO catchment. Different size of circles shows ANC.

they can differ in streams of similar size and acid conditions (Fig. 7). Conductivity represented mainly the concentrations of cations (Ca, Na, K, and less Mg), Cl, and TP, because it was strongly (R>0.60) correlated with them. Average velocity (significantly correlated (R>0.65) with stream width and discharge), pH (correlated with ANC, R = 0.87), and slope (correlated with altitude, R = 0.81) explained 25.2% of variability in species data (Table 7).

Fig. 7. The NMDS ordination diagrams showing variables significantly fitted into the ordination of samples of the GO catchment. The size and colour of the symbols are proportional to the measured values of the variables, while the contour lines indicate their fit into the ordination. Phi value decreases with increasing roughness of bed substrate.

Table 4. List of species reported by Schöll (1987) and Kifinger et al. (2004) from the GO catchment not found in our study.

Group / species	Schöll 1987	Kifinger et al. 2004	acid class
Crustacea			
Niphargus sp.		+	4
Ephemeroptera			
Ephemerella ignita Poda, 1761	+		1
Leptophlebia marginata (Linnaeus, 1767)		+	3
Leptophlebia vespertina (Linnaeus, 1758)	+		3
Odonata			
Aeshna cyanea (Müller, 1764)		+	
Pyrrhosoma nymphula (Sulzer, 1776)	+		
Plecoptera			
Amphinemura standfussi (Ris, 1902)	+		4
Capnia vidua Klapálek, 1904	+	+	3
Leuctra autumnalis Aubert, 1948	+		4
Leuctra digitata Kempny, 1899	+		3
Leuctra handlirschi Kempny, 1898		+	
Leuctra pseudosignifera Aubert, 1954	+	+	
Leuctra rauscheri Aubert, 1957		+	4
Nemoura cambrica Stephens, 1836	+	+	5
Nemoura mortoni Ris, 1902	+		
Protonemura montana Kimmins, 1941	+		2
Protonemura nitida (Pictet, 1935)	+		3
Protonemura risi (Jacobson & Bianchi, 1905)	+		
Siphonoperla montana (Pictet, 1841)	+		
Heteroptera			
Gerris sp.		+	
Trichoptera			
Acrophylax zerberus Brauer, 1867	+		
Adicella reducta (McLachlan, 1865)		+	3
Beraea pullata (Curtis, 1834)	+		3
Ecclisopteryx guttulata (Pictet, 1834)		+	3
Glossosoma intermedium (Klapálek, 1892)		+	2
Limnephilus centralis Curtis, 1834	+		
Lype phaeopa (Stephens, 1836)	+		
Notidobia ciliaris (Linnaeus, 1761)	+		
Parachiona picicornis (Pictet, 1834)	+		4
Philopotomus montanus (Donovan, 1813)	+		3
Polycentropus flavomaculatus (Pictet, 1834)	+		
Pseudopsilopteryx zimmeri (McLachlan, 1876)	+	+	4
Psilopteryx psorosa (Kolenati, 1860)	+		2
Wormaldia triangulifera McLachlan, 1878	+		
Coleoptera			
Deronectes platynotus (Germar, 1834)	+	+	3
Elmis rietscheli Steffan, 1958	+		
Hydroporus nigrita (Fabricius, 1792)		+	
Oulimnius tuberculatus (P. W. J. Müller, 1806)	+		
Platambus maculatus (Linnaeus, 1758)		+	
Diptera			
Atherix ibis (Fabricus, 1798)	+		3

Table 5. Number of species found in different macroinvertebrate groups in the GO catchment and BF streams. Rarefied number of species for the GO catchment is in the brackets.

Group	GO catchment	BF streams	Total
Ephemeroptera	16	15	16
Plecoptera	22	17	24
Trichoptera	37	38	45
Coleoptera	15	9	16
Chironomidae	55	31	55
Diptera (except Chironomidae)	16	14	20
Megaloptera	1	1	1
Crustacea	2	1	2
Mollusca	1	2	2
Tricladida	3	2	3
Species	**168 (153.2±1.8)**	**130**	**184**
Individuals	**30,354**	**10,328**	**40,682**

Other significant factors, i.e. CPOM, conductivity, Al_i, and average depth explained up to 2% of variability in species data (Table 7).

The diagram of species best fitted to NMDS ordination (Fig. 8) emphasized mainly species of mid-altitude and near neutral conditions of larger streams. They included mainly common rhithral species, the stoneflies *Amphinemura sulcicollis*, *Leuctra inermis* Gr., and *Protonemura austriaca/intricata*, and running water beetles *Elmis rioloides* and *Limnius perrisi*. Small brooks had usually lower species richness (Table 6) and their assemblages are likely a subset of those at more species-rich sites. Only few species were characteristic for small streams with low pH and higher Al_i (Fig. 8): *Nemoura cinerea*, *Agabus guttatus*, and

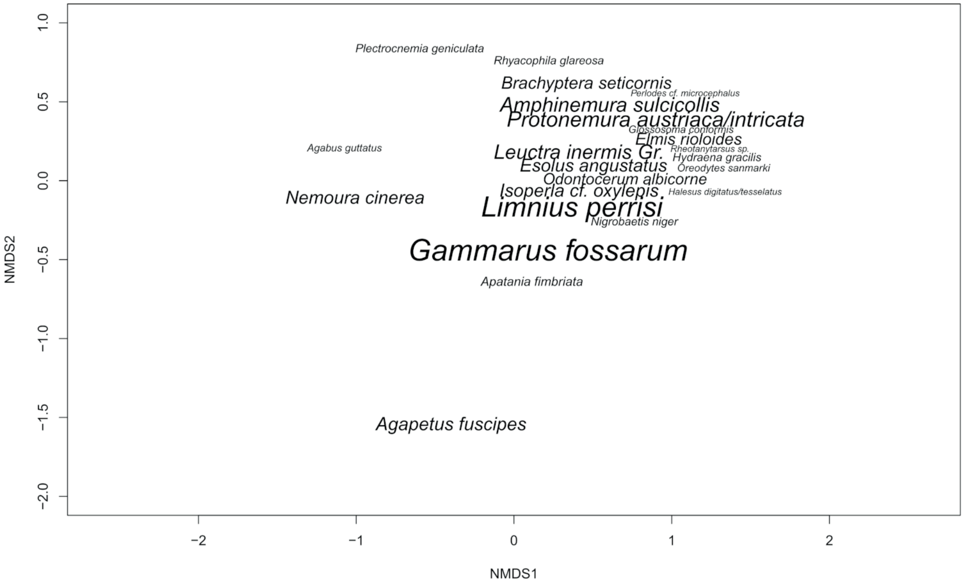

Fig. 8. Ordination diagram of species in the GO catchment. Only species with frequency. >2 and fit >0.4 are displayed and the font size is proportional to the square root of their total abundance.

Table 6. Spearman correlations of species richness, abundance and acid class of the GO sites with environmental variables. Significant correlations are in bold ($p<0.001$)

Variables	**Species richness**	**Total abundance**	**Acid class – abundance**	**Acid class – dominance**	**Acid class – weighted average**
Altitude	−0.29	−0.30	0.36	0.23	0.29
Slope	−0.34	−0.21	0.27	0.13	0.09
pH	0.34	**0.67**	**−0.53**	**−0.63**	**−0.72**
Conductivity	0.05	0.27	−0.22	−0.20	−0.39
Temperature	0.23	0.19	−0.01	−0.01	−0.10
O_2	0.14	0.06	−0.11	−0.24	−0.07
O_2 saturation	0.11	−0.06	0.08	0.00	0.20
DOC	0.15	0.01	0.14	0.31	0.18
TN	−0.11	−0.01	−0.24	−0.04	−0.08
TP	0.33	0.42	−0.22	−0.12	−0.24
ANC	0.33	**0.61**	−0.46	**−0.56**	**−0.68**
Cl^-	−0.07	0.14	−0.28	−0.22	−0.44
SO_4^{2-}	0.17	0.12	−0.01	−0.17	−0.18
Na^+	0.26	0.42	−0.36	−0.29	**−0.48**
K^+	−0.09	0.20	−0.21	−0.20	−0.44
Ca^{2+}	0.21	0.35	−0.28	−0.25	−0.43
Mg^{2+}	0.06	0.20	−0.21	−0.08	−0.18
Al_i	−0.26	**−0.53**	0.44	**0.49**	**0.52**
Discharge	**0.50**	0.25	−0.33	−0.20	0.02
Pools proportion	−0.25	−0.10	0.20	0.19	0.12
Max. velocity	0.36	0.16	−0.14	−0.09	0.08
Average velocity	0.42	0.24	−0.33	−0.26	0.00
Max. depth	0.29	0.12	−0.11	0.00	0.21
Average depth	0.28	0.12	−0.11	0.06	0.22
Average width	0.41	0.24	−0.11	−0.12	0.12
Phi	−0.15	0.06	−0.10	−0.04	−0.20
Macrophytes	−0.11	−0.14	0.09	0.13	0.13
Wood	−0.15	−0.24	0.11	0.05	0.17
CPOM	−0.52	−0.18	0.21	0.02	−0.13
FPOM	0.10	−0.01	0.16	0.16	0.02
Species richness	–	**0.61**	−0.40	**−0.47**	−0.21
Total abundance	**0.61**	–	−0.50	**−0.57**	**−0.55**

Plectrocnemia geniculata were classified as tolerant species adapted to strong acidity (Table 3). Small, but less acidic streams were inhabited by crenobiont *Agapetus fuscipes* sensitive to acidity. *Gammarus fossarum* was abundant at slightly acidic sites with high proportion of CPOM in the bed substrate (cf. Figs. 7, 8).

Based on maximum sensitivity of bioindicators, most of sites belonged to acid class 2, predominantly neutral to episodically weakly acidic streams, however, with almost two times more streams of acid classes 3 and 4 in assessment based on dominance than abundance classes (Fig. 9). Based on all classified species (weighted average), most streams were classified as periodically critically acidic (acid class 3). However, considerable number of

Table 7. Results of the db-RDA with forward selection on GO catchment and BF streams. Cumulative value of adjusted R-squared, percentage of explained variability, F-ratio, and p-value are shown for each significant variable.

Variables	R^2_{adj}	**Explained variability (%)**	**F-ratio**	**p-value**
GO catchment				
Average velocity	0.10360	10.36	6.4322	0.002
pH	0.19916	9.556	6.4886	0.002
Slope	0.25170	5.254	4.1594	0.002
Conductivity	0.27212	2.042	2.2349	0.004
CPOM	0.29163	1.951	2.1839	0.002
Al_i	0.31388	2.225	2.3620	0.004
Average depth	0.32879	1.491	1.9111	0.008
<All variables>	0.34795			
BF streams				
Phi	0.18121	18.12	2.9918	0.006
Conductivity	0.27181	9.06	1.9954	0.020
<All variables>	0.50624			

sites fell into periodically strongly acidic and permanently very acidic (acid classes 4 and 5) (Fig. 9) indicating strong biotic changes caused by acidification. Relation of acid class with water acidity measured at the sites was very weak in the acid class based on abundance classes (Table 6), showing very wide extent of pH and mainly ANC at the sites of acid class 2 (Fig. 10). The strongest relation was found in the acid class based on weighted average which significantly correlated with water pH and ANC ($R = -0.72$), and Al_i ($R = 0.52$) (Table 6, Fig. 10). Acid class of sites were not correlated with stream size or any habitat property, and, importantly, neither with altitude nor slope (Table 6).

BF streams

Main gradients in species data were associated with altitude, terrain topography (slope) closely linked with substrate roughness (phi) and share of pools, and water pH (Fig. 11). The composition of macroinvertebrate assemblages significantly changed from steep sites with boulder-stony substrate and dominating riffles to low-slope sites with finer substratum and equal share of riffles and pools (samples arranged from right to left in the diagrams, Fig. 11). Most influential variable in db-RDA was phi (strongly negativelly correlated with slope and macrophytes cover, $R<-0.65$) which explained 18.1% variability in species data. Water conductivity (significantly correlated with pH and altitude, $R = 0.67$ and -0.72) explained 9.1% variability in species data (Table 7).

The diagram with the species best fitted to this ordination (Fig. 12) showed a numerous group of species associated with the middle part of the gradient (moderately-slope streams with stony substrate) including mainly common and abundant rhithral species (*Elmis rioloides*, *Esolus angustatus*, *Protonemura austriaca*/*intricata*, *Amphinemura sulcicollis*, *Polycelis* sp., etc.) and some species with narrower habitat requirements being sensitive to organic pollution and higher temperatures (*Hydropsyche tenuis*, *Rhyacophila tristis*, *Rhithrogena hercynia*). Low-slope gravel streams were preferred by *Nigrobaetis muticus*, *Anomalopterygella chauviniana*, *Orthocladius rubicundus* Gr., and *Elmis maugetii*. The second gradient showed the variability associated with the altitude and water pH. Sites at higher altitudes had lower pH, although its range was not wide (from 5.9 to 7.1). Species as-

Site	Nr.	Acid class - abundance	Acid class - dominance	Acid class - weighted aver.	pH	ANC	Al$_i$
GO catchment							
Rachelbach	**7**	3	3	5	4.5	-17	101
Hüttenbach 1	**25**	2	3	4	4.6	-21	32
Guglödgraben 2	**47**	3	3	4	4.6	-12	33
Hüttenbach 2	**37**	2	3	4	4.6	-11	41
Markungsgraben 1	**6**	2	2	3	4.9	0	79
LT of Seebach 2	**8**	3	3	5	5.0	-2	38
LT of Seebach 1	**1**	4	3	5	5.1	-1	96
Seebach 2	**9**	2	3	4	5.1	4	71
Seebach 1	**5**	3	3	4	5.1	4	56
Tiefe Seige 1	**3**	4	3	5	5.1	5	201
LT of brook 12	**4**	2	2	3	5.2	7	46
Markungsgraben 2	**12**	2	2	4	5.3	2	65
RT of Seebach 1	**13**	2	2	3	5.3	2	42
LT of Seebach 3	**2**	4	4	5	5.3	9	20
Tiefe Seige 2	**20**	2	2	4	5.3	14	45
Weitauseige 1	**16**	2	3	4	5.3	16	69
RT of Grosse Ohe 1	**46**	2	3	4	5.3	24	24
RT of Hinterer Schachtenbach	**26**	2	2	3	5.4	14	64
Seebach 4	**28**	2	2	4	5.4	18	34
Vorderer Schachtenbach 1	**17**	3	3	4	5.4	22	73
RT of Grosse Ohe 2	**45**	2	2	3	5.4	30	43
LT of brook with impoundment	**31**	2	3	4	5.4	30	31
Seebach 3	**15**	2	3	4	5.5	7	85
Rachelschachtenbach 2	**14**	2	2	3	5.6	15	22
LT of Forellenbach	**35**	2	2	3	5.6	26	9
Rachelschachtenbach 1	**11**	2	2	3	5.7	17	25
Grosse Ohe 1	**44**	2	2	3	5.7	31	39
Grosse Ohe 2	**48**	2	2	4	5.7	37	30
Guglödgraben 1	**43**	3	3	4	5.7	44	65
RT of Seebach 2	**39**	2	2	3	5.7	46	8
Hinterer Schachtenbach 1	**18**	2	2	3	5.8	18	17
Hinterer Schachtenbach 2	**27**	2	2	3	5.8	22	30
Kaltenbrunnenseige	**10**	2	2	4	5.8	23	6
Seebach 5	**42**	2	2	3	5.8	28	40
"Dreibach"1	**38**	2	2	3	5.8	55	17
Hinterer Schachtenbach 3	**41**	2	3	4	5.9	36	33
brook with impoundment 2	**33**	2	2	3	5.9	49	24
sources of "Dreibach" 1	**24**	2	2	2	5.9	50	5
brook with impoundment 1	**19**	2	2	3	6.0	37	11
Vorderer Schachtenbach 2	**34**	2	2	3	6.0	49	5
sources of "Dreibach" 3	**23**	2	2	2	6.1	52	0
Forellenbach 2	**30**	2	2	2	6.1	55	53
Vorderer Schachtenbach 3	**40**	2	2	3	6.1	60	13
Weitauseige 2	**32**	2	2	2	6.1	65	9
Forellenbach 1	**22**	2	2	3	6.2	65	43
sources of "Dreibach" 2	**21**	2	2	2	6.3	63	19
LT of Grosse Ohe	**29**	1	1	2	6.3	118	2
RT of Guglödgraben	**36**	2	2	2	6.4	116	13
BF streams							
Grosse Ohe 3	**55**	2	2	4	5.7	39	49
Reschbach	**52**	2	2	3	5.7	-	-
Sagwasser	**50**	1	2	3	6.1	-	-
Kleiner Regen	**49**	2	2	3	6.2	-	-
Flanitz	**54**	1	2	3	6.4	-	-
Schwarzach	**53**	2	2	3	6.6	-	-
Kleine Ohe	**56**	1	2	3	6.7	-	-
Hirschbach	**51**	2	2	3	6.8	-	-
Kolbersbach	**57**	1	2	3	6.8	-	-
Grosse Deffernik	**58**	1	2	3	7.1	-	-

Fig. 9. Acid classes of the sites in the GO catchment calculated by three different methods. Sites are sorted by pH and ANC. Acid classes: 2 – predominantly neutral to episodically weakly acidic streams, 3 – periodically critically acidic streams, 4 – periodically strongly acidic streams, and 5 – permanently very acidic streams.

sociated with higher altitude included species able to inhabit periodically acidic waters, such as *Rhyacophila praemorsa*, *R. glareosa*, *Ameletus inopinatus, Heterotrissocladius marcidus* (Table 3). All of them are pollution sensitive, with very low saprobic index (Moog 2002, Graf et al. 2008, Zahrádková et al. 2009).

Acid classes of sites calculated by three different methods showed fairly different results. The acid classes based on abundance classes showed half and half streams belonging to acid class 1 and acid class 2, whereas the acid classes based on dominance classified all sites as acid class 2 (Fig. 10). The strictest method, based on weighted average, classified all sites as acid class 3, except for Große Ohe 3 belonging to acid class 4 (Fig. 10).

Discussion

The two sets of data included in this study cover the variability in stream types and their environmental attributes, as well as main patterns in macroinvertebrate diversity in the BFNP. The BF streams contain "the largest" streams in the area with sampling sites located near the border of the BFNP, i.e. at the lower altitude of the monitored stream biodiversity (Fig. 2). The main outcome of this study is to provide the data on the array of species relevant for future systematic monitoring focusing on altitudinal shifts in species distribution and variability in the assemblages relevant for planning of the monitoring design. The GO catchment represents a typical example of stream network common at the area, i.e. steep, richly branching network with diverse forest in the catchment (Figs. 1, 2), being a model system for stream biodiversity monitoring in the Bohemian Forest. Sampling sites were located evenly within the catchment and their Strahler's orders proportionally correspond to real distribution of Strahler's orders within the catchment (cf. Fig. 1). Thus, data on key ecological gradients and diversity patterns found in the GO catchment are aimed to provide a detailed insight into the structuring of macroinvertebrate assemblages on the local scale.

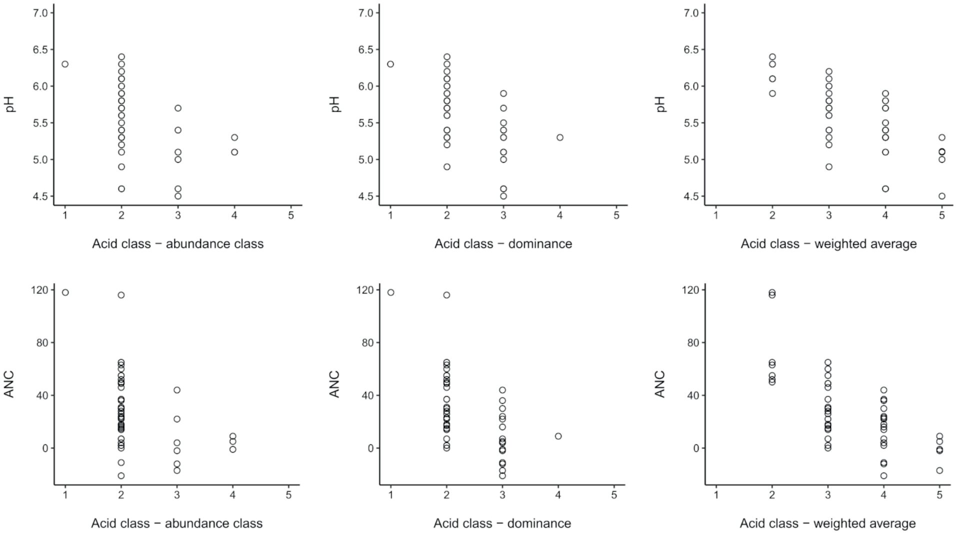

Fig. 10. Relation of acid classes of the sites in the GO catchment calculated by three different methods with pH and ANC.

Species richness and abundance of macroinvertebrates and their relation to acidification

The BF streams provide heterogeneous environment for variety of rhitral species resulting in higher alpha diversity and abundance of macroinvertebrates than in the GO catchment (Fig. 4), where alpha diversity is positively related to the stream size (i.e. significantly correlates with water discharge, average velocity, and stream width). Higher gamma diversity found in the GO catchment (168 species compared to 130 species in the BF streams) is attributable not only to three times more individuals examined, but mainly to higher environmental variability among sites resulting in higher beta diversity. Rarefied species richness is 153.2±1.8 species found for 10,328 individuals examined in the GO catchment comparing to 130 species in the BF streams (Fig. 5). Within the GO catchment, species richness (and total abundance) is not related to altitude, but rather to stream type and amount of CPOM (Table 6). Likewise, main gradient in species composition of assemblages is related to stream type – stream size and flow velocity (Fig. 7). It emphasizes the necessity to include sufficient number of replicates of same stream types in the altitudinal transects studied in the monitoring of stream biodiversity. Sampling sites added on side branches from 700 to 900 m a.s.l. (see Fig. 2) differing from a stream type of a main stream in each transect, are well-supported.

Species richness of macroinvertebrates is significantly related to water pH and toxic Al concentrations in acidic streams (e.g. Guerold et al. 2000, Baldigo et al. 2009, Traister et al. 2013), although the relation cannot be apparent in naturally acidic streams (Dangles et al. 2004). In the GO catchment, species richness is, surprisingly, not influenced by stream acidity (pH, ANC or Al_i) or altitude which is aligned with the effects of acidification in the region. The GO catchment has been without any doubts affected by the acidification since the mid-1980s (Schöll 1987, LfW 1999, Alewell et al. 2001, Kifinger et al. 2004, Schaum-

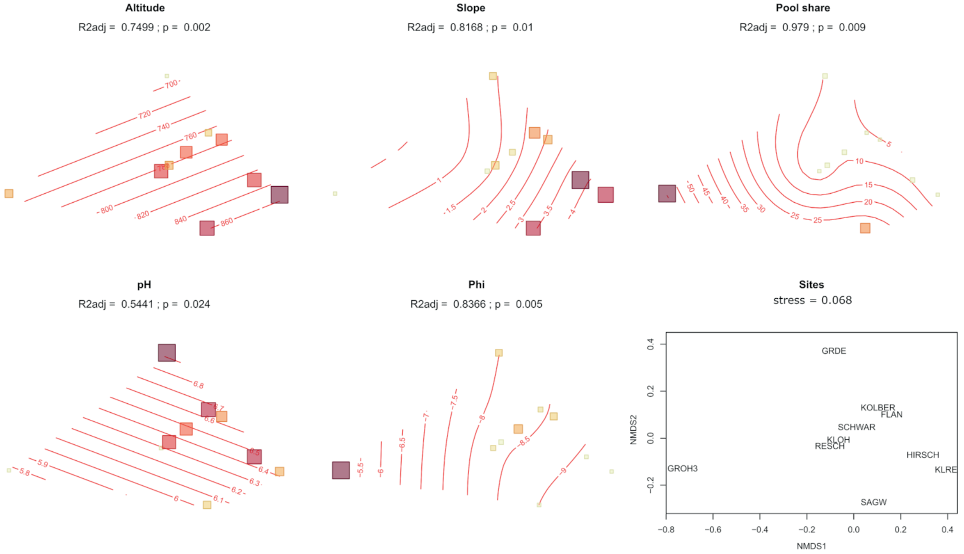

Fig. 11. The NMDS ordination diagrams showing variables significantly fitted into the ordination of BF streams species data. The size and colour of the symbols are proportional to the measured values of the variables, while the contour lines indicate their fit into the ordination. Phi value decreases with increasing roughness of bed substrate.

burg et al. 2010). Acid sensitive fish and macroinvertebrates (particularly mayflies and *Gammarus fossarum*) died out locally and their absence and/or low abundance and species-richness were documented especially at higher altitudes of the BFNP (Schöll 1987, 1989). The long-term acidification monitoring documented gradual increase of species richness along with increasing pH and decreasing difference between minimal and maximal annual pH in Große Ohe and Vorderer Schachtenbach (Schaumburg et al. 2010). In contrast, this gradual recovery leading to relatively advanced phase of recovery in the late-1990 was followed by pronounced deterioration of water chemistry due to forest dieback in the catchments of Seebach and Hinterer Schachtenbach (Schaumburg et al. 2010). It caused temporary decrease of macroinvertebrate species richness in Seebach and Hinterer Schachtenbach (Schaumburg et al. 2010). Nevertheless, last data available to us (after 2005) indicate overall positive trends (LfU 2015) and we can assume that macroinvertebrates studied by our study refer to much more developed phase of recovery. Therefore, acidity seems to be recently not so strong environmental filter to structure species richness within environmentally heterogeneous stream network of Große Ohe.

Total abundance of macroinvertebrates, unlike their species richness, is significantly related to ANC, pH and Al_i (Fig. 6). The relation is non-linear, abundance is low up to pH about 5.5 and then steeply increases being highest at sites with high ANC. Likewise, abundance is variable, related to ANC, in Al_i concentration from 0 to 53 µg.l^{-1}, and dramatically decreases in Al_i>53. It clearly demonstrates persisting effect of Al toxicity on macroinvertebrates. The highest Al_i concentration, extremal within our dataset, is 201 µg.l^{-1} in “Tiefe Seige 1” (TISE1, nr. 3) which has the lowest macroinvertebrate abundance (42). It is comparable with strongly acidified streams with extreme hydrochemistry (pH 4–4.7 and Al_i between 0.2 and 2.0 mg.l^{-1}) in the Czech Republic (Horecký et al. 2006, 2013), which are inhabited only by extremely acid-tolerant species (*Leuctra nigra*, *Nemurella pictetii*, *Plectrocnemia conspersa*, and *Corynoneura* spp.) (Horecký et al. 2006).

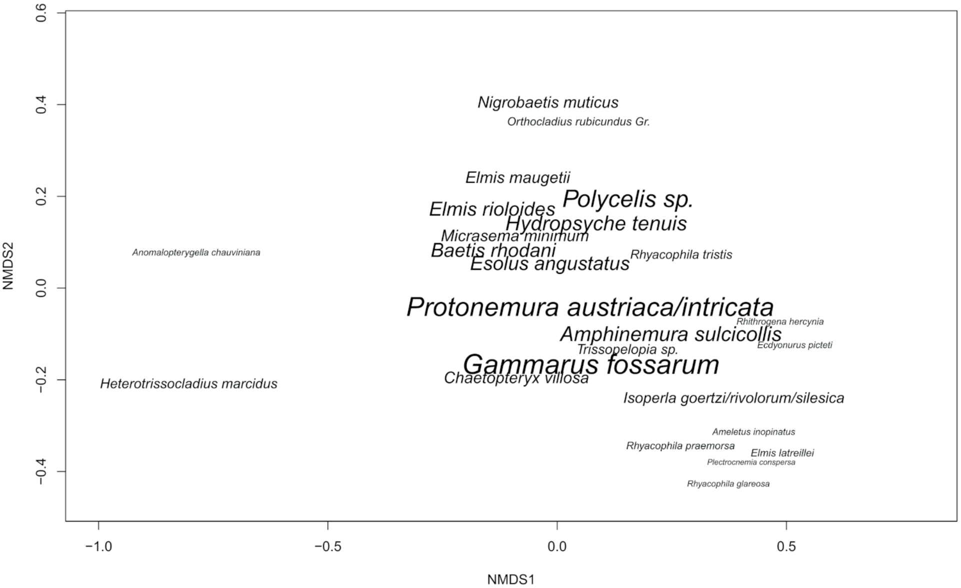

Fig. 12. Ordination diagram of species in the BF streams. Only species with frequency >2 and fit >0.6 are displayed and the font size is proportional to the square root of their total abundance.

Community composition of macroinvertebrates: important gradients and acid status of streams

The main compositional gradient in species data in the BF streams, which are environmentally relatively similar each other, is aligned with substrate roughness (Fig. 11). Composition of macroinvertebrate assemblages differs from sloping Kleiner Regen and Hirschbach above Frauenau drinkwater reservoir and Sagwasser (streams with large stones dominating in bed substrate) to low-sloping Große Ohe near Riedlhütte (fine gravel-dominated substrate) (Fig. 11). Substrate roughness explains 18% of variability in species data. Water conductivity, second significant factor explaining 9% of variability in species data, likely express the difference in water quality among catchments resulting from different bedrock and land cover. Composition of macroinvertebrate assemblages is, naturally, more complex in the GO catchment. Most important factors shaping macroinvertebrate assemblages are average flow velocity and water pH which represent two main independent gradients in species data (Fig. 7). The remaining five significant factors (slope, water conductivity, CPOM, Al_i, and average stream depth) determine local environmental conditions in different parts of the network. Macroinvertebrates are influenced by local catchment properties, such as local terrain topography determining morphology of streams, forest structure influencing the amount of CPOM in streams, and also water chemistry. The significant effect of water conductivity can be interpreted as possible influence of nutrients, cations, and Cl, because these are significantly correlated with conductivity. Detailed insight to the role of local influences, catchment properties as well as spatial structuring on the macroinvertebrate assemblages within the GO network require further study.

Composition of macroinvertebrate assemblages in the Bohemian Forest streams have been studied mainly to describe and assess the effect of acidification (Růžičková 1998, Alewell et al. 2001, Fricová et al. 2007, Svobodová et al. 2012, LfU 2015). Acidification monitoring, which gathered extensive species data since the early 1980s, has been concentrated primarily on evaluation of species richness and acid status of streams, and their temporal changes (e.g. Schaumburg et al. 2010, LfU 2015). Acid status assessment is based on maximum sensitivity of bioindicators, i.e. species are cumulatively added from acid sensitive to acid very resistant till the threshold is reached (Braukmann & Biss 2004). In the 1980s, acid status of streams in the Bavarian Forest ranged from permanently very acidic (acid class 5 – Rachelsee inlets) and periodically strongly acidic (acid class 4 – Markungsgraben, Seebach, Große Ohe, and Sagwasser) to periodically critically acidic streams (acid class 3 – Vorderer Schachtenbach, Hinterer Schachtenbach, Hirschbach, and Kleiner Regen) (LfU 2015). Recently (2005–2013), acid status of most streams reached class 2 (predominantly neutral to episodically weakly acidic) or even class 1 (continuously neutral streams) in the case of Hirschbach and Sagwasser (LfU 2015). Only Rachelsee inlets remained under strong acid stress (acid class 4).

Evaluation of our data using the same method (i.e. scoring of species with maximal sensitivity, when threshold based on sum of abundance classes of scoring species is 4) shows same results in the above-mentioned streams (Fig. 9). Of all GO and BF streams, six streams reach even the status of continuously non-acidic streams and most streams belong to acid class 2 (Fig. 9), including streams of various acidity (from pH 4.6 and negative ANC to pH 6.8 and positive ANC). Thus, the acid class of streams is not related to pH and ANC measured directly in the field (Table 6, Fig. 10), which suggests that this assessment overestimates acid sensitive species. It is caused by quite permissive threshold, which can be reached by two species of acid class 2 with abundance class 2 (from 2 to 20 individuals according to Alf et al. 1992), it means in fact by four specimens, irrespective of the rest of specimens in the sample. Thus, we calculated the acid class based on two other methods, scoring of species with maximal sensitivity with threshold based on species dominance (recommended method by Braukmann & Biss 2004) and by average acid class based on all scoring species in the sample (weighted average). The results are much better related to pH and ANC (Table 6, Fig. 10) and show the relation of the assemblage to the acidity from different perspectives.

Acid class assessment based on the dominance emphasizes the contribution of moderately acid sensitive species scoring many streams to acid class 2, the rest being acid class 3 (with 2 exceptions). However, 31 of 43 streams classified as acid class 2 were scored by the only species, i.e. the remaining scoring species together do not reach the threshold of 10%. The most important species is *Gammarus fossarum* (scoring in 17 streams), following by *Baetis alpinus*, *Leuctra alpina*, *Isoperla goertzi/rivulorum/silesica*, and *Philopotamus ludificatus*. The remaining 12 streams (especially six largest BF streams and Große Ohe) showed diverse array of (medium) acid sensitive species scoring to the acid class 2. Acid status of streams based on weighted average is shifted more to acidic streams, because the assemblages are mostly composed of individuals of acid classes 3 and 4 (cf. Table 4). This assessment better recognises assemblages under strong acid stress, i.e. those dominated by acid-tolerant or eurytopic species, such as stoneflies *Brachyptera seticornis*, *Nemoura cinerea*, *Nemurella pictetii*, *Protonemura auberti*, *Leuctra nigra*, and caddisflies, *Plectrocnemia conspersa*, *Chaetopteryx villosa*, which are not accompanied by moderately sensitive species. Weak point of this method can be the proportion of unclassified species in each sample, similarly as the definition of threshold in the method based on maximum sensitivity of bioindicators. Importantly, acid status of sites (assessed by all methods) is not related to altitude, stream size or any habitat feature (Table 6). It indicates that macroinvertebrates are influenced by a mosaic of local conditions within the catchment offering local refugia in different parts of the network and different altitude, which is advantageous for biotic recovery.

Comparison with literature data

Our data include about a third of species recorded by Schulte & Weinzierl (1990; Ephemeroptera, Plecoptera, Trichoptera, Coleoptera) and Pitsch (1994; Trichoptera, Odonata, Crustacea) from the entire Bavarian Forest, including the area of the BFNP. Schulte & Weinzierl (1990) found 289 species, 101 of them were found in our study, and Pitsch (1994) found 111 species of Trichoptera, 44 of them were found in our study. Putting aside obvious differences in the sampling methods and more habitat types covered by these two studies, we can conclude that they recorded almost all species found in our study (Table 3) including also Ephemeroptera (*Ecdyonurus venosus*, *Nigrobaetis niger*) and acid sensitive Trichoptera (e.g. *Agapetus fuscipes*, *Glossosoma conformis*) not found in the core zone of the BFNP in the period of strong acidification (Schöll 1987; Kifinger et al. 2004). This indicates that acid sensitive species had some refugia outside the area impacted by acidification in that time, which could later help them to colonise recovering habitats. On the other hand, many acid sensitive or moderately sensitive species, which are very common and abundant in the Bohemian Forest (including the Czech part of the mountains), are recently still missing in the GO catchment and also in many BF streams. They are, for instance, stoneflies *Perla marginata* and *Dinocras cephalotes*, and mayflies *Ephemera danica*, *Centroptilum luteolum*, *Torleya major*, *Paraleptophlebia submarginata* (e.g. Landa & Soldán 1989, Soldán 1996).

Roughly direct comparison is possible in the GO catchment, where Schöll (1987) and Kifinger et al. (2004) studied 14 sites covering the entire catchment in the period of strong acidification in the 1980 and after the forest dieback in 2001–2002. Total number of species recorded by us, 113 species, is comparable with 106 species recorded by these two studies. We found most of species recorded by them, 51 species of 82 species recorded by Schöll (1987) and 54 species of 72 species recorded by Kifinger et al. (2004). Most of the species not recorded by us are not reliably distinguishable in larval stage (*Nemoura cambrica*, *Leuctra handlirschi*, *L. rauscheri*, *L. pseudosignifera*, *Wormaldia triangulifera*), thus, can be included at higher taxonomic levels in our data, or cannot be captured by spring sampling (mainly stoneflies with emergence in summer and autumn, *Leuctra autumnalis*, *L. digitata*, *Protonemura montana*, *P. nitida*, and the mayfly *Ephemerella ignita*) (Table 4). More important difference is that our data do not include numerous crenophilic and crenobiont species, such as *Parachiona picicornis*, *Beraea pullata*, *Psilopteryx psorosa*, *Adicella reducta*, etc., which indicates that we do not cover the whole (relatively high) beta diversity even by 48 sites within the GO catchment. Very small headwaters and springbrooks can harbour unique fauna highly contrasting to the surrounding rhithral streams (Hubáčková et al. 2016) and, thus, they, despite their low alpha diversity, can considerably contribute to biodiversity at the network scale (Meyer et al. 2007, Clarke et al. 2008, Finn et al. 2011).

Importantly, we found distinctly higher species richness of Ephemeroptera, Coleoptera and Diptera (Table 3) which can be interpreted as a sign of colonisation of recovering streams. Moreover, we recorded five species classified as acid sensitive (preferring continuously neutral streams according to Braukmann & Biss 2004) not recorded by the two compared studies, which, however, occur rarely (mayflies *Habroleptoides confusa* and *Ephemerella mucronata*, caddisflies *Agapetus fuscipes* and *Glossosoma conformis*, and the isopod *Asellus aquaticus*). Only two acid sensitive species, the mayfly *Ephemerella ignita* and the caddisfly *Allogamus auricollis*, are known from the GO catchment in the period of strong acidification. Remarkable number of species (12) not recorded by Schöll (1987) and Kifinger et al. (2004) are moderately acid sensitive (preferring predominantly neutral to episodically weakly acidic conditions), e.g. *Habrophlebia lauta*, *Rhithrogena iridina*/*picteti*, *Rhithrogena loyolaea, Anomalopterygella chauviniana*, *Hydraena dentipes*, and *Ibisia marginata*. The most abundant moderately acid sensitive species, the amphipod *Gammarus fossarum*, referred as absent at the higher altitudes by Schöll (1987), is frequent and locally very abundant at our studied sites, but avoiding the highest altitudes. In total, Schöll (1987) and Kifinger et al. (2004) found same number of acid tolerant and resistant species (classes 3–5) as our study (58 and 56 species, respectively), but they found only 13 species of the classes 1 and 2 comparing to 27 species found by us (see Table 3, 4). Moreover, moderately acid sensitive species are recently much more frequent, for example *Gammarus fossarum* and mayflies (except for *B. alpinus*) were found only in 2 of 14 localities in the 1980s (Schöll 1987). Thus, the comparison with literature data suggests that recent macroinvertebrate assemblages are more diversified and dissimilar to those described by Schöll (1987) and Kifinger et al. (2004).

Acknowledgements. Our thanks are due to the Institute of Hydrobiology, Biology Centre CAS, České Budějovice for analyses of water chemistry, and Burkhard Beudert and Jaroslav Vrba for valuable comments on the manuscript. We thank to Ondřej Hájek (Department of Botany and Zoology, Masaryk University, Brno) for the maps of study area. This research and publication were supported by the Cross-border cooperation programme Czech Republic–Bavaria Free State ETC goal 2014–2020, the Interreg V project No. 26 "Silva Gabreta Monitoring – Implementation of Transboundary Monitoring of Biodiversity and Water Regime".

REFERENCES

AQEM Consortium, 2002: *Manual for the application of the AQEM system. A comprehensive method to assess European streams using benthic macroinvertebrates, developed for the purpose of the Water Framework*

Directive. Version 1.0, February 2002, AQEM Consortium, 202 pp.

Alewell C., Armbruster M., Bittersohl J., Evans C.D., Meesenburg H., Moritz K. & Prechtel A., 2001: Are there signs of acidification reversal in freshwaters of the low mountain ranges in Germany? *Hydrology and Earth System Sciences*, 5: 367–378.

Alf A., Braukmann U., Marten M. & Vobis H., 1992: *Biologisch-ökologische Gewässeruntersuchung – Arbeitsanleitung. Handbuch Wasser 2*. Landesanstalt für Umweltschutz Baden-Württemberg, Karlsruhe, 52 pp.

Anonymus, 2005: *Rote Liste der gefährdeten Tiere und Gefäßpflanzen Bayerns. Kurzfassung.* Bayerisches Staatsministerium für Umwelt, Gesundheit und Verbraucherschutz, München, 186 pp.

Baldigo B.P., Lawrence G.B., Bode R.W., Simonin H.A., Roy K.M. & Smith A.J., 2009: Impacts of acidification on macroinvertebrate communities in streams of the western Adirondack Mountains, New York, USA. *Ecological Indicators*, 9: 226–239.

Bässler C., Seifert L. & Müller J., 2015: The BIOCLIM project in the National Park Bavarian Forest: Lessons from a biodiversity survey. *Silva Gabreta*, 21: 81–93.

Beudert B., Bässler C., Thorn S., Noss R., Schröder B., Dieffenbach-Fries H., Foullois N. & Müller J., 2015: Bark beetles increase biodiversity while maintaining drinking water quality. *Conservation Letters*, 8: 272–281.

Beudert B. & Gietl G., 2015: Long-term monitoring in the Große Ohe catchment, Bavarian Forest National Park. *Silva Gabreta*, 21: 5–27.

Binot M., Bless R., Boye P., Gruttke H. & Pretscher P., 1998: *Rote Liste gefährdeter Tiere Deutschlands*. Bundesamt für Naturschutz, 435 pp.

Braukmann U., 2001: Stream acidification in South Germany – chemical and biological assessment methods and trends. *Aquatic Ecology*, 35: 207–232.

Braukmann U. & Biss R., 2004: Conceptual study – An improved method to assess acidification in German streams by using benthic macroinvertebrates. *Limnologica*, 34: 433–450.

Clarke A., Nally R.M., Bond N. & Lake P.S., 2008: Macroinvertebrate diversity in headwater streams: a review. *Freshwater Biology*, 53: 1707–1721.

Dangles O., Malmqvist B. & Laudon H., 2004: Naturally acid freshwater ecosystems are diverse and functional: evidence from boreal streams. *Oikos*, 104: 149–155.

Eisenreich W., 1974: *Der Seebach. Faunistisch-ökologische Untersuchungen an einem Bergbach im Bayerischen Wald*. Ms., diploma thesis, Universität Tübingen.

Finn D.S., Bonada N., Múrria C. & Hughes J.M., 2011: Small but mighty: headwaters are vital to stream network biodiversity at two levels of organization. *Journal of the North American Benthological Society*, 30: 963–980.

Fricová K., Růžičková J. & Hřebík Š., 2007: Benthic macroinvertebrates as indicators of ecological integrity of lotic ecosystems in the Šumava National Park, Czech Republic. *Silva Gabreta*, 13: 39–55.

Goral F. & Schellenberg J., 2017: goeveg: Functions for Community Data and Ordinations. R package version 0.3.3. Available at https://CRAN.R-project.org/package=goeveg

Harrell Jr F.E., 2017: Hmisc: Harrell Miscellaneous. R package version 4.0-3. Available at https://CRAN.R-project.org/package=Hmisc

Hebauer F., 1975: Kleine Mitteilungen – *Hydroporus piccus* Steph. auch im Bayerischen Wald! (Coleoptera, Dytiscidae). *Nachrichtenblatt der Bayerischen Entomologen*, 24: 16.

Hebauer F., 1980: Beitrag zur Faunistik und Ökologie der Elminthidae und Hydraenidae in Ostbayem (Coleoptera). *Mitteilungen der Münchner Entomologischen Gesellschaft*, 69: 29–80.

Hoffmann A., Schaumburg J. & Maetze A., 2011: Germany: Long-term trends in biota at ICP Waters sites. In: *ICP Waters report 106/2011. Trends in precipitation chemistry, surface water chemistry and aquatic biota in acidified areas in Europe and North America from 1990 to 2008*, Skjelkvåle B.L. & De Wit H.A. (eds) ICP Waters Programme Centre, Norwegian Institute for Water Research, Oslo: 67–69.

Horecký J., Rucki J., Krám P., Křeček J., Bitušík P., Špaček J. & Stuchlík E., 2013: Differences in benthic macroinvertebrate structure of headwater streams with extreme hydrochemistry. *Biologia*, 68: 303–313.

Horecký J., Stuchlík E., Chvojka P., Hardekopf D.W., Mihaljevič M. & Špaček J., 2006: Macroinvertebrate community and chemistry of the most atmospherically acidified streams in the Czech Republic. *Water, Air, and Soil Pollution*, 173: 261–272.

Hubáčková L., Rádková V., Bojková J., Syrovátka V., Polášková V., Schenková J. & Horsák M., 2016: Diversity patterns of aquatic specialists and generalists: contrasts among two spring-fen mesohabitats and nearby streams. *Biologia*, 71: 678–687.

Gordon N.D., McMahon T.A. & Finlayson B.L., 1992: *Stream hydrology. An Introduction for Ecologists*. John Wiley & Sons, Chichester, 256 pp.

Graf W., Murphy J., Dahl J., Zamora-Muñoz C. & López-Rodríguez M.J., 2008: *Distribution and Ecological Preferences of European Freshwater Organisms. Volume 1. Trichoptera.* Pensoft Publishers, Sofia-Moscow, 388 pp.

Guerold F., Boudot J.P., Jacquemin G., Vein D., Merlet D. & Rouiller J., 2000: Macroinvertebrate community loss as a result of headwater stream acidification in the Vosges Mountains (N-E France). *Biodiversity and Con-*

servation, 9: 767–783.

Kifinger B., Schaumburg J. & Lehmann R., 2004: *Monitoringprogramm für versauerte Gewässer durch Luftschadstoffe in der Bundesrepublik Deutschland im Rahmen der ECE. Bericht der Jahre 2001–2002*. Bayerisches Landesamt für Wasserwirtschaft, München, 171 pp.

Kopáček J., Brzáková M., Hejzlar J., Nedoma J., Porcal P. & Vrba J., 2004: Nutrient cycling in a strongly acidified mesotrophic lake. *Limnology and Oceanography*, 49: 1202–1213.

Kopáček J., Fluksová H., Hejzlar J., Kaňa J., Porcal P. & Turek J., 2017: Changes in surface water chemistry caused by natural forest dieback in an unmanaged mountain catchment. *Science of the Total Environment*, 584–585: 971–981.

Kopáček J., Hejzlar J. & Mosello R., 2000: Estimation of organic acid anion concentrations and evaluation of charge balance in atmospherically acidified colored waters. *Water Research*, 34: 3598–3606.

Kopáček J., Stuchlík E., Veselý J., Schaumburg J., Anderson I.C., Fott J., Hejzlar J. & Vrba J., 2002: Hysteresis in reversal of central European mountain lakes from atmospheric acidification. *Water Air Soil Pollution Focus*, 2: 91–114.

Kopáček J. & Veselý J., 2005: Sulfur and nitrogen emissions in the Czech Republic and Slovakia from 1850 till 2000. *Atmospheric Environment*, 39: 2179–2188.

Kuhn I., 1984: Limnologische Untersuchungen an Fließwässern im Nationalpark Bayerischer Wald. Ms., diploma thesis, Universität Bonn.

Landa V. & Soldán T., 1989: *Rozšíření jepic (Ephemeroptera) v ČSSR a jeho změny v souvislosti se změnami kvality vody v povodí Labe*. Studie ČSAV 17, Academia, Praha, 170 pp.

LfU, 2015: *25 Jahre Versauerungsmonitoring in Bayern. Trends und Entwicklungen*. Bayerisches Landesamt für Umwelt, Augsburg, 90 pp.

LfW, 1999: Bayerisches Landesamt für Wasserwirtschaft. Versauerung oberirdischer Gewässer in Bayern. Entwicklung 1983 – 1996. *Informationsberichte*, 4/99: 1–343.

Meyer J.L., Strayer D.L., Wallace J.B., Eggert S.L., Helfman G.S. & Leonard N.E., 2007: The Contribution of Headwater Streams to Biodiversity in River Networks. *Journal of the American Water Resources Association*, 43: 86–103.

Moog O. (ed), 2002: *Fauna Aquatica Austriaca. Edition 2002*. Wasserwirtschaftskataster, Bundesministerium für Land- und Forstwirtschaft, Umwelt und Wasserwirtschaft, Vienna, 92 pp.

Neuwirth E., 2014: RColorBrewer: ColorBrewer Palettes. R package version 1.1-2. Available at https://CRAN.R-project.org/package=RColorBrewer

Oksanen J., Blanchet F.G., Friendly M., Kindt R., Legendre P., McGlinn D., Minchin P.R., O'Hara R.B., Simpson G.L., Solymos P., Stevens M.H.H., Szoecs E. & Wagner H., 2017: vegan: Community Ecology Package. R package version 2.4-5. Available at https://CRAN.R-project.org/package=vegan

Pitsch T., 1994: Untersuchungen zur Besiedlung der Fließgewässer im Vorfeld des Nationalparks Bayerischer Wald Trichoptera, Odonata, Amphipoda, Isopoda. *Acta Albertina Ratisbonensia*, 49: 127–174.

R Core Team, 2017: R: A language and environment for statistical computing. R Foundation for Statistical Computing, Vienna, Austria. Available at https://www.R-project.org/

Růžičková J., 1998: Společenstvo vodního hmyzu v šumavských tocích s různým stupněm acidifikace. *Silva Gabreta*, 2: 199–209.

Schaumburg J., Kifinger B., Lehmann R., Maetze A., Coring E., Baltzer S. & Zahn H., 2008: *Monitoringprogramm für versauerte Gewässer durch Luftschadstoffe in der Bundesrepublik Deutschland im Rahmen der ECE. Bericht der Jahre 2005 – 2006*. Bayerisches Landesamt für Umwelt im Auftrag des Umweltbundesamtes, München, 235 pp.

Schaumburg J., Kifinger B., Lehmann R., Maetze A., Coring E., & Baltzer S., 2010: *Monitoringprogramm für versauerte Gewässer durch Luftschadstoffe in der Bundesrepublik Deutschland im Rahmen der ECE. Bericht der Jahre 2007 – 2008*. Bayerisches Landesamt für Umwelt im Auftrag des Umweltbundesamtes, München, 134 pp.

Scheel T., Fischer F., Neumann J., Schaumburg J. 2014. 25 Years of Acidification Monitoring activities in Bavaria: Results, Trends and Perspectives Article. *Hydrologie und Wasserbewirtschaftung*, 58: 286–288.

Schöll F., 1987: Limnofauna des Nationalparks Bayerischer Wald unter besonderer Berücksichtigung der Gewässerversauerung. Dissertation, Rheinische Friedrich-Wilhelms-Universität zu Bonn, 178 pp.

Schöll F., 1989: Zur näheren Kenntnis des Makrozoobenthos der Fließgewässer im Nationalpark Bayerischer Wald. *Entomologische Zeitschrift*, 99: 257–267.

Schulte H. & Weinzierl A., 1990: Beiträge zur Faunistik einiger Wasserinsektenordnungen (Ephemeroptera, Plecoptera, Coleoptera, Trichoptera) in Niederbayern. *Lauterbornia*, 6: 1–83.

Seitz G., 1988: Beitrag zur Kriebelmückenfauna Niederbayerns (Insecta, Diptera, Simuliidae). *Nachrichtenblatt der Bayerischen Entomologen*, 37: 89–94.

Seitz G., 1992: Verbreitung und Ökologie der Kriebelmücken (Diptera: Simuliidae) in Niederbayern. *Lauterbornia*, 11: 1–230.

Skjelkvåle B.L. & De Wit H.A. (eds), 2011: *ICP Waters report 106/2011. Trends in precipitation chemistry, surface water chemistry and aquatic biota in acidified areas in Europe and North America from 1990 to 2008*. ICP Waters Programme Centre, Norwegian Institute for Water Research, Oslo, 128 pp.

Soldán T.,1996: Přehled pošvatek (Plecoptera) Šumavy s poznámkami k jejich současnému výskytu [A review of stoneflies (*Plecoptera*) of the Bohemian Forest with notes to their recent occurence]. *Sborník Jihočeského Musea v Českých Budějovicích, Přírodní Vědy*, 36: 37–47.

Soldán T., Bojková J., Vrba J., Bitušík P., Chvojka P., Papáček M., Peltanová J., Sychra J., & Tátosová J., 2012: Aquatic insects of the Bohemian Forest glacial lakes: Diversity, long-term changes, and influence of acidification. *Silva Gabreta*, 18: 123–283.

Svobodová J., Matěna J., Kopáček J., Poláková S. & Vrba J., 2012: Spatial and temporal changes of benthic macroinvertebrate assemblages in acidified streams in the Bohemian Forest (Czech Republic). *Aquatic Insects*, 34, Suppl. 1: 157–172.

Traister E.M., McDowell W.H., Krám P., Fottová D., Kolaříková K., 2013: Persistent effects of acidification on stream ecosystem structure and function. *Freshwater Science*, 32: 586–596.

Vrba J., Kopáček J., Fott J. & Nedbalová L., 2014: Forest dieback modified plankton recovery from acidic stress. *AMBIO*, 43: 207–217.

Wickham H., 2009: ggplot2: Elegant Graphics for Data Analysis. Springer-Verlag, New York, 216 pp.

Thiem K., 1906: Biogeographische Betrachtung des Rachels. *Abhandlungen der Naturhistorichen Gessellschaft Nürnberg*, 16: 5–58.

Weinzierl A., 1999: Nachweise von *Isoperla albanica*, *Brachyptera starmachi* und *Brachyptera trifasciata* (Plecoptera) aus Niederbayern. *Lauterbornia*, 37: 19–22.

Zahrádková S., Soldán T., Bojková J., Helešic J., Janovská H. & Sroka P., 2009: Distribution and biology of mayflies (Ephemeroptera) of the Czech Republic: present status and perspectives. *Aquatic Insects*, 31 (suppl. 1): 629–652.

Received: 31 May 2018
Accepted: 27 October 2018

Silva Gabreta	vol. 24	p. 213–221	Vimperk, 2018

Floodplain vegetation of the restored Jedlový Potok stream in the Bohemian Forest

Hana Čížková[*] & Markéta Padrtová

Faculty of Agriculture, University of South Bohemia, Studentská 1668, CZ-37005 České Budějovice, Czech Republic

[*] hcizkova@zf.jcu.cz

Abstract

A segment of the Jedlový Potok stream, a tributary of the Teplá Vltava River, was restored in 2015 as part of a large restoration programme aiming to ameliorate the water regime in the Vltavský Luh wetland complex. This paper describes plant communities occurring in the Jedlový Potok floodplain at the time of its restoration and immediately afterwards with the aim to provide baseline information for further monitoring of vegetation development. Four main types of open wetland habitats were distinguished. An extensively mown wet *Cirsium* meadow and a *Phalaris arundinacea* marsh occurred in the riparian zone with a more fluctuating water table while a short-sedge fen and an *Eriophorum vaginatum* mire formed a peatland zone further away from the watercourse. In spite of some degradation caused by previous drainage, the communities have preserved their characteristic physiognomy and species composition and thus represent good examples of wetland plant communities of the Vltavský Luh wetland complex.

Key words: biodiversity, Bohemian Forest, stream restoration, water regime, wetlands, zonation

INTRODUCTION

Numerous watercourses were channelized in the Bohemian Forest (Šumava in Czech) in the past in order to increase the production of the surrounding agricultural land and woodland. These measures have seriously altered the water regime of adjacent wetlands, which in turn changed soil conditions and microclimate and, consequently, also the biota inhabiting these habitats.

Within a large restoration programme of the Bohemian Forest wetlands, near-natural conditions were restored among others in three streams, the Hučina, the Jedlový Potok, and the Žlebský Potok, which feed the wetland complex of Vltavský Luh. Wetland vegetation, physico-chemical parameters of the stream water, communities of benthic invertebrates, and aquatic and wetland vegetation have been monitored on these sites since the restoration (BOJKOVÁ et al. 2015).

The Jedlový Potok stream is a left-hand tributary of the Teplá Vltava stream, to which it discharges near the village Dobrá. The middle course of the Jedlový Potok stream was moved to a new bed in connection with the railway construction at the end of the 19th century. In the 1950s, the stream bed was straightened along most of its course and reinforced with concrete blocks and stones. The artificial bed was 0.5–1.1 m deep and, at some places, up to 5 m wide. The canal drained adjacent meadows and also served as part of the drainage system along the perimeter of the nearby Soumarský Most peatland, from which peat was excavated.

In autumn 2015, the downstream, straightened segment of the Jedlový Potok stream was restored. The restoration included the construction of a new meandering bed, which was 0.2-0.4 m deep and, except for through-flow pools, less than 2 m wide. The former artificial channel was filled up by soil except for several parts which were modified into pools. The 985-m long, formerly channelized section of the Jedlový Potok stream was thus extended to the restored length of 1115 m.

The restoration has initiated the natural development of the stream bed and its floodplain; it is anticipated that the changes in water regime, namely the increased groundwater level, will affect also the local vegetation. This paper describes the plant communities in the Jedlový Potok floodplain at the time of its restoration and immediately afterwards with the aim to provide a baseline information for potential long-term monitoring of the restoration effects.

METHODS

Eight permanent plots (15–25 m^2, see Table 1) were laid in the floodplain of the restored segment of the Jedlový Potok stream. Two quadrats were placed in each of four habitat types, distinguished by their physiognomy, dominant plant species and distance from the stream bed (Fig. 1).

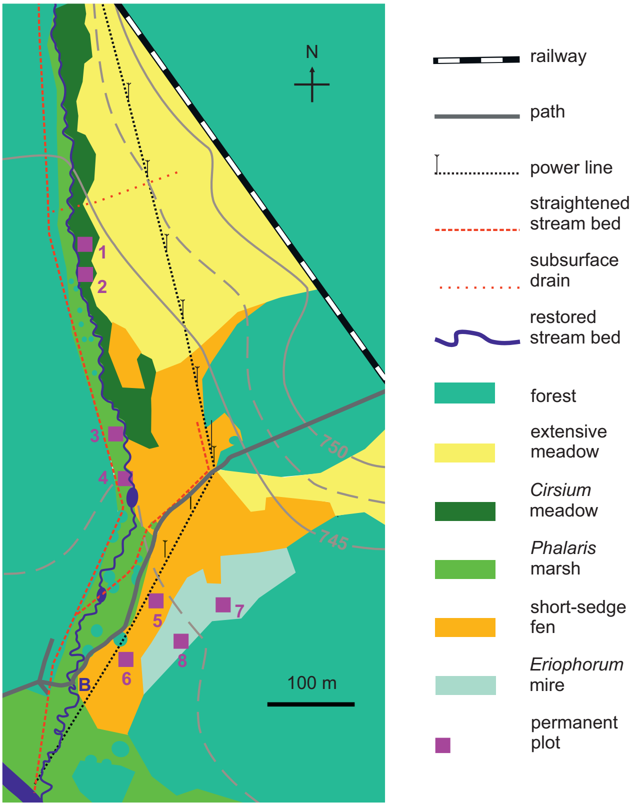

Fig. 1. A schematic map of the restored part of the Jedlový Potok stream and its surroundings. B – bridge.

(i) A wet meadow habitat with a high dominance of dicotyledonous species (called wet *Cirsium* meadow in further text), which formed a several meter wide interface between the stream and an extensively managed meadow. The habitat lies on a gley soil based on quaternary deluvial sediments (ČGS 2018a,b). The soil is mineral, sandy loam by texture.

(ii) A marsh habitat overgrown with *Phalaris arundinacea* (*Phalaris* marsh), which extended along the stream in the unmanaged part of the open floodplain. This habitat also lies on poorly developed soil on sandy sediments.

(iii) A waterlogged peaty habitat with a high dominance of sedges and rushes, situated within 100 m from the stream (short-sedge fen). The soil is gley based on quaternary deluvial sediments. In contrast to the habitats above, it has a surface organic horizon more than 0.3 m deep (ČGS 2018a,b).

(iv) A mire habitat with *Eriophorum vaginatum* and *Molinia caerulea* (*Eriophorum* mire), situated more than 100 m away from the stream and close to the waterlogged spruce forest neighbouring the open floodplain. The soil is histosol based on a thick layer of peat (ČGS 2018a,b).

The plots were marked on 21 August 2015 except for the two plots with *P. arundinacea*, which were selected on 29 June 2017 (this particular part of the floodplain was not accessible in summer 2015 because of the construction works). A perforated PVC tube (0.05 m in diameter) was installed to a depth of 0.5–0.6 m near each plot for measurement of the depth to the groundwater level. The groundwater levels were measured approximately at one-month intervals from June to October 2017 and from April to July 2018.

Lists of phanerogam species were made within each habitat type in August 2015, i.e. at the time the restoration started. Phytosociological relevés of the permanent plots were recorded on three dates of 2017 (1–2 June, 28–29 June and 27–28 July) in order to cover the late spring, early summer and late summer aspects of the vegetation, and repeated in early summer 2018 (12 June). The cover of phanerogam species was recorded using a combined abundance-dominance scale, in which the symbol "r" was used for one or several small individuals and the symbol "+" for one big or many small individuals with a cover smaller than 1%. A species dominance ≥1% was estimated as percentage of total cover.

With some exceptions, the same plant species were found in the habitats in 2015, 2017 and 2018. Also differences in species cover among the dates of 2017 were fairly small and largely corresponded with the species' phenological phases. Therefore, only relevés taken on early summer dates of the two consecutive years (29 June 2017 and 12 June 2018) are presented here.

The names of phanerogams follow Kubát et al. (2002). Bryophytes were classified only to broad taxonomic categories. The habitat classification follows Chytrý et al. (2010). The diagnostic species of syntaxonomical units are based on Chytrý (2007, 2011).

Results and discussion

Groundwater level

The habitats differed in their water regimes. Both habitats occurring close to the watercourse had great ranges of water level fluctuations. The wet *Cirsium* meadow had the lowest minima and medians of the groundwater depth, followed by the *Phalaris* marsh (Fig. 2). On the *Cirsium* meadow, even the maximum groundwater levels remained below the soil surface at all measurement dates; this was the case also at a peak discharge following continuous rain on 13 June 2018, when flood warnings (i.e. the 2nd level of flood activity) were issued by the nearest measurement stations at the Teplá Vltava stream in Lenora and Chlum. In comparison, the habitats occurring at greater distances from the watercourse, i.e. the short sedge fen and the *Eriophorum* mire had a more stable water regime with smaller fluctuations. The mean groundwater level remained within a 0.2-m depth from the soil surface and the habitats were shallowly flooded at times of continuous rain.

Although the ranges of groundwater level fluctuations correspond to the general knowledge of the habitats, the exact values should be interpreted with caution because the number of sampling was fairly small, the sampling dates did not reflect the frequency and duration of wet and dry periods and they did not include early spring. In addition, it should be born in mind that they describe the state after (not before) the restoration.

Characteristics of the plant communities

The wet *Cirsium* meadow had by far the greatest species richness with a total of 47 phanerogams (Table 1). Dicots constituted more than 50% of the species number and 50% total cover (Table 2). The community included diagnostic species of the association *Holcetum lanati* 1934, characterized by soils that are moist in spring but can dry out in the second part of the vegetation season, when the groundwater level can drop to as much as –1 m. Such conditions were probably common before the stream restoration. The rich representation of dicots both in species number and cover together with the respective diagnostic species are features of the association *Polygono bistortae-Cirsietum heterophylli* Balátová-Tuláčková 1975, which typically occur along watercourses on soils that are moist throughout the vegetation season. This habitat corresponded to the *Deschampsia caespitosa-Alopecurus pratensis* community according to Bufková et al. (2005).

The *Phalaris* marsh hosted a species-poor community with one or two strong dominants (*P. arundinacea* in plot 3 and its mixture with *Scirpus sylvaticus* in the wetter plot 4). It corresponded to the association *Phalaridetum arundinaceae* Libbert 1931, which is supported

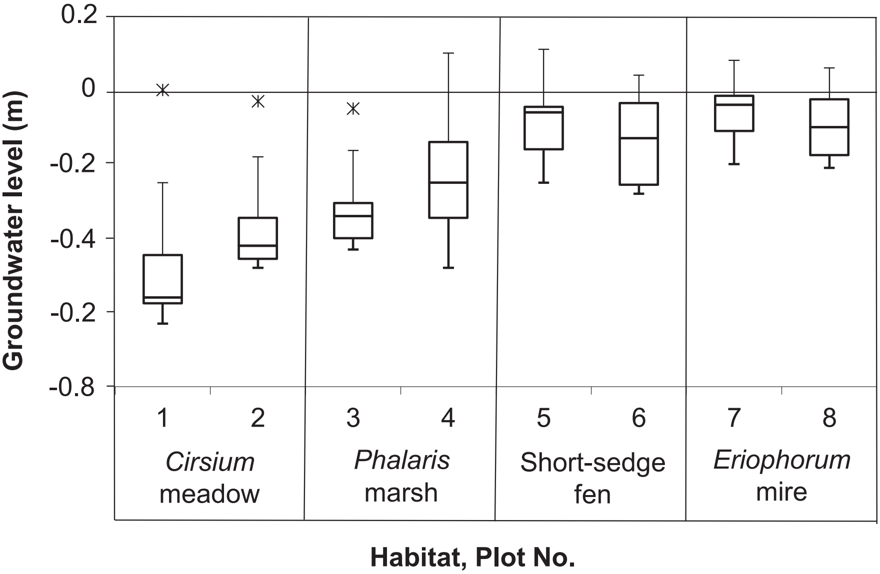

Fig. 2. Ranges of groundwater level fluctuations recorded on permanent plots in the restored part of the Jedlový Potok floodplain in 2017–2018. The graph shows medians (squares), 25 and 75 percentiles (boxes), minima and maxima (bars) of 10 sampling dates; the outliers (asterisks) in plots 1–3 and maxima in other plots were measured during an extremely high discharge on 13 June 2018.

Table 1. Representation of phanerogam species in the phytosociological relevés recorded on permanent plots in the floodplain of Jedlový Potok. Numbers indicate percentage of species cover (in %); r: species present as one or few small individuals; +: species present as one robust or a greater number of small individuals with negligible cover. Even relevés (No. 1, 3, 5, 7, 9, 11, 13, 15) were taken on 28–29 June 2017; odd relevés (No. 2, 4, 6, 8, 10, 12, 14, 16) were taken on 12 June 2018.

Habitat	***Cirsium* meadow**				***Phalaris* marsh**				**Short-sedge fen**				***Eriophorum* mire**			
Plot No.	1		2		3		4		5		6		7		8	
Area (m)	4×4		4×4		2.5×6		2.5×6		5×5		5×5		5×5		5×5	
Relevé No.	1	2	3	4	5	6	7	8	9	10	11	12	14	14	15	16
Number of species	43	41	38	34	16	16	11	14	29	24	23	24	13	12	11	10
Diagnostic species of the class *Molinio-Arrhenatheretea* and ass. *Holcetum lanati*																
Carex brizoides	10	12	10	15	7	8	.	.	+	+	8	1	.	.	.	.
Lathyrus pratensis	+	1	1	1	+	1	.	.	r	+	.	.	.	.	.	.
Rumex acetosa	+	+	1	1	.	r	.	.	.	r	r	r	.	.	.	.
Holcus lanatus	1	+	+	1	.	.	.	.	.	.	+	r	.	.	.	.
Cirsium palustre	r	r	1	+	.	.	.	.	.	.	r	+	.	.	.	.
Lychnis flos-cuculi	+	+	+	r	r	+	.	.	.	.	.	.	.	.	.	.
Alopecurus pratensis	1	1	+	+	.	.	.	.	.	.	.	.	.	.	.	.
Ranunculus acris	+	1	1	+	.	.	.	.	.	.	.	.	.	.	.	.
Achillea ptarmica	.	r	r	.	.	.	.	.	.	.	+	+	.	.	.	.
Galium palustre	.	.	.	.	.	.	r	r	.	.	.	.	.	.	.	.
Diagnostic species of the alliance *Calthion palustris* and ass. *Polygono bistortae-Cirsietum heterophylli*																
Bistorta major	1	6	9	7	2	5	.	+	10	10	8	5	.	.	.	.
Galium uliginosum	4	1	4	1	+	+	r	+	1	1	.	r	.	.	.	.
Cirsium heterophyllum	5	6	4	7	.	.	.	.	2	1	+	+	.	.	.	.
Agrostis capillaris	5	10	5	7	r	.	.	.	.	.	.	.	.	.	.	.
Angelica sylvestris	.	.	.	.	.	.	r	r	1	3	.	r	.	.	.	.
Scirpus sylvaticus	.	.	.	.	+	1	10	25	.	.	.	.	.	.	.	.
Hypericum maculatum	3	6	6	4	.	.	.	.	.	.	.	.	.	.	.	.
Crepis paludosa	+	3	r	+	.	.	.	.	.	.	.	.	.	.	.	.
Caltha palustris	.	.	.	.	.	.	.	r	.	.	.	.	.	.	.	.
Diagnostic species of the ass. *Phalaridetum arundinaceae*																
Lysimachia vulgaris	r	r	.	.	1	1	r	1	.	.	.	r	.	.	.	.
Phalaris arundinacea	r	.	.	.	75	50	85	40	.	.	.	.	.	.	.	.
Scutellaria galericulata	.	.	.	.	+	+	.	r	.	.	.	.	.	.	.	.
Diagnostic species of the class *Scheuchzerio palustris-Caricetea nigrae*																
Potentilla erecta	5	8	1	+	r	r	.	.	1	3	10	8	3	3	2	3
Carex nigra	1	3	.	r	.	.	.	.	15	6	3	+	4	1	+	+
Agrostis canina	.	.	.	.	.	.	.	.	r	3	2	7	2	7	4	6

Table 1. Continued.

Habitat	***Cirsium* meadow**				***Phalaris* marsh**				**Short-sedge fen**				***Eriophorum* mire**			
Plot No.	1		2		3		4		5		6		7		8	
Area (m)	4×4		4×4		2.5×6		2.5×6		5×5		5×5		5×5		5×5	
Relevé No.	1	2	3	4	5	6	7	8	9	10	11	12	14	14	15	16
Number of species	43	41	38	34	16	16	11	14	29	24	23	24	13	12	11	10
Viola palustris	.	.	.	.	.	.	.	.	+	r	+	r	+	r	r	.
Carex rostrata	.	.	.	.	.	.	.	.	20	10	.	.	1	r	.	.
Eriophorum angustifolium	.	.	.	.	.	.	.	.	1	1	+	r	.	.	.	.
Carex panicea	+	r	.	.	.	.	.	.	.	.	r	.	.	.	.	.
Potentilla palustris	.	.	.	.	.	.	.	.	.	.	.	.	2	1	.	.
Diagnostic species of the class *Oxycocco-Sphagnetea*																
Eriophorum vaginatum	.	.	.	.	.	.	.	.	.	.	.	.	30	20	35	13
Other species																
Filipendula ulmaria	9	10	12	15	5	8	r	2	2	3	r	.	.	.	.	.
Festuca rubra	3	3	5	7	.	.	.	.	2	1	5	2	.	r	r	r
Luzula multiflora	+	+	r	r	.	.	.	.	r	.	1	+	+	.	+	+
Sanguisorba officinalis	4	7	3	1	.	.	.	.	3	4	8	7	r	.	.	.
Deschampsia cespitosa	5	5	8	8	.	+	.	.	2	2	2	4	.	.	.	.
Vicia cracca	+	+	+	+	+	.	r	r	r	+	.	.	.	.	.	.
Juncus filiformis	.	.	.	.	.	.	.	.	20	25	15	20	3	6	5	+
Peucedanum palustre	.	.	.	.	.	.	.	.	6	6	8	8	3	8	3	8
Chaerophyllum hirsutum	2	5	3	5	r	+	.	.	r	.	.	.	.	.	.	.
Pimpinella major	1	1	1	4	.	.	.	.	1	2	.	.	.	.	.	.
Veronica chamaedrys	1	1	2	1	.	.	.	.	r	r	.	.	.	.	.	.
Molinia caerulea	.	.	.	.	.	.	.	.	.	.	.	.	13	15	10	10
Aegopodium podagraria	.	.	4	6	r	4	.	.	.	.	.	.	.	.	.	.
Carex pallescens	3	5	+	1	.	.	.	.	.	.	.	.	.	.	.	.
Holcus mollis	1	3	+	1	.	.	.	.	.	.	.	.	.	.	.	.
Juncus effusus	1	1	.	.	1	2	.	.	.	.	.	.	.	.	.	.
Alchemilla sp.	2	1	+	+	.	.	.	.	.	.	.	.	.	.	.	.
Achillea millefolium	r	+	r	r	.	.	.	.	.	.	.	.	.	.	.	.
Anemone nemorosa	.	.	.	.	.	.	.	r	r	.	r	+	.	.	.	.
Avenella flexuosa	.	.	.	.	.	.	.	.	.	.	.	.	r	+	r	r
Cardaminopsis halleri	r	r	+	r	.	.	.	.	.	.	.	.	.	.	.	.
Epilobium palustre	.	.	.	.	.	.	r	r	r	.	.	r	.	.	.	.

Table 1. Continued.

Habitat	*Cirsium* meadow				*Phalaris* marsh				Short-sedge fen				*Eriophorum* mire			
Plot No.	1		2		3		4		5		6		7		8	
Area (m)	4×4		4×4		2.5×6		2.5×6		5×5		5×5		5×5		5×5	
Relevé No.	1	2	3	4	5	6	7	8	9	10	11	12	14	14	15	16
Number of species	43	41	38	34	16	16	11	14	29	24	23	24	13	12	11	10
Poa pratensis	r	+	+	+	.	.	.	.	.	.	.	.	.	.	.	.
Stellaria graminea	r	r	r	r	.	.	.	.	.	.	.	.	.	.	.	.
Cerastium holosteoides subsp. *triviale*	r	r	r	.	.	.	.	.	.	.	.	.	.	.	.	.
Trifolium pratense	.	r	r	r	.	.	.	.	.	.	.	.	.	.	.	.
Poa chaixii	.	.	.	.	.	.	.	.	2	2	.	.	.	.	.	.
Aconitum plicatum	.	.	.	.	.	.	.	.	1	2	.	.	.	.	.	.
Campanula patula	r	.	r	.	.	.	.	.	.	.	.	.	.	.	.	.
Carex ovalis	+	+	.	.	.	.	.	.	.	.	.	.	.	.	.	.
Dactylis glomerata	r	r	.	.	.	.	.	.	.	.	.	.	.	.	.	.
Galeopsis tetrahit	.	.	.	.	.	.	r	r	.	.	.	.	.	.	.	.
Mentha arvensis	r	r	.	.	.	.	.	.	.	.	.	.	.	.	.	.
Succisa pratensis	.	.	.	.	.	.	.	.	.	.	r	r	.	.	.	.
Urtica dioica	.	.	.	.	.	.	r	+	.	.	.	.	.	.	.	.
Viola tricolor	r	.	r	.	.	.	.	.	.	.	.	.	.	.	.	.

Species present in small abundances (as indicated by symbol r) only in one relevé (relevé No. given in brackets): *Trifolium spadiceum* (1), *Ajuga genevensis* (3), *Tanacetum vulgare* (7), *Avenula pubescens* (9), *Briza media* (11).

Table 2. Cover of plant functional groups on permanent plots in the floodplain of Jedlový Potok in early summer 2017 and 2018. Even relevés (No. 1, 3, 5, 7, 9, 11, 13, 15) were taken on 28–29 June 2017; odd relevés (No. 2, 4, 6, 8, 10, 12, 14, 16) were taken on 12 June 2018.

Habitat	***Cirsium* meadow**				***Phalaris* marsh**				**Short-sedge fen**				***Eriophorum* mire**			
Plot No.	**1**		**2**		**3**		**4**		**5**		**6**		**7**		**8**	
Relevé No.	**1**	**2**	**3**	**4**	**5**	**6**	**7**	**8**	**9**	**10**	**11**	**12**	**14**	**14**	**15**	**16**
Moss layer	0	0	0	0	0	0	0	0	0	0	0	5	60	50	75	70
Sphagnales	0	0	0	0	0	0	0	0	0	0	0	5	60	50	75	70
Other mosses	0	0	0	0	0	0	0	0	0	0	0	+	r	r	1	1
Herb layer	70	95	80	90	90	75	95	65	90	80	70	60	60	60	60	40
Poaceae	16	22	18	24	75	50	85	40	6	7	9	13	13	22	14	16
Cyperaceae	14	20	10	16	7	9	10	25	35	16	11	1	5	1	0	0
Other monocots	1	1	0	0	1	2	0	0	21	26	16	20	33	26	40	13
Dicots	37	57	53	53	8	19	0	3	28	34	36	35	8	13	5	11
Total cover	**70**	**95**	**90**	**90**	**90**	**75**	**95**	**65**	**90**	**80**	**70**	**60**	**70**	**60**	**80**	**75**

by the presence of *Lysimachia vulgaris* and *Scutellaria galericulata* and absence of long-term flooding (cf. Fig. 2), which excludes disturbances by water flow. The *Phalaris* marsh is a type of the tall grass marsh communities described by Bufková et al. (2005).

The short-sedge fen had the second greatest species richness with a total of 30 phanerogams, which included 18 dicots forming about 30% total cover (Table 1, 2). The community shared many species with the *Cirsium* meadow including the tall herbs *Cirsium heterophyllum*, *Bistorta major* and *Filipendula ulmaria,* which formed conspicuous seasonal colour aspects. Several phanerogam species were diagnostic of the class *Scheuchzerio palustris-Caricetea nigrae* Tüxen 1937. The presence of short-sedge species and the fragmentary development of the moss layer indicated its closeness to the association *Caricetum nigrae* Braun 1915. The habitat resembled the short-sedge mire of the *Carex rostrata–C. canescens* community as described by Bufková et al. (2005). The high representation of *Juncus filiformis* and *C. brizoides* is considered a sign of degradation caused by the previous drainage and abandonment.

The *Eriophorum* mire hosted the smallest number of species of the four habitats. The community was formed mainly by two strong dominants, *E. vaginatum* and *Molinia caerulea*, and a few additional species in small abundances that occurred also in the neighbouring habitats. It was the only one of the four habitats with a well-developed moss layer, formed mostly by *Sphagnum* species. *Eriophorum vaginatum* might indicate a transition toward an open bog of the association *Eriophoro vaginati-Sphagnetum recurvi* Hueck 1925; another species diagnostic of this association, *Vaccinium uliginosum*, was absent from the permanent plots but occurred closer to the neighbouring waterlogged spruce forest. On the other hand, the high dominance of *M. caerulea* indicated pronounced fluctuations of the groundwater table in the past. The community is probably identical with the tall grass fen dominated by *Molinia caerulea* according to Bufková et al. (2005).

Ideally, the relevés should be taken prior the restoration for at least three years. However, it was not possible in this study. A question therefore remains how much the relevés reflect the state of the vegetation before the restoration. It seems that they do because vegetation changes are usually identifiable after a longer time, in some cases even after decades (Prach 1993, 2008) while inter-annual differences rather reflect meteorological differences. The two years after the restoration were exceptionally dry, which most probably weakened the immediate restoration effect.

CONCLUSION

The vegetation of the Jedlový Potok floodplain includes typical plant communities of the Vltavský Luh wetland complex. The sequence of the unmanaged habitats extending from the stream bank further away, i.e. the *Phalaris* marsh, the short-sedge fen, and the *Eriophorum* mire, represent a good example of the local wetland zonation, encompassing both the regularly-flooded riparian zone and the marginal peatland zone. The wet *Cirsium* meadow, resulting from the joint effects of water regime and extensive mowing, adds both to the species and habitat diversity of the area. Although the communities bear signs of degradation such as fairly high covers of *Carex brizoides*, *Juncus filiformis*, and *Molinia caerulea*, resulting from the previous drainage and abandonment, they have preserved their characteristic physiognomy and species composition, which will hopefully be further supported by the restored natural water regime of the stream.

Acknowledgements. This study was supported by the Grant Agency of the University of South Bohemia (project No. 081/2016/Z). We thank V. Januš and J. Čížek for their help with field work, A. Kučerová for revision of the plant determination, E. Rejmánková and an anonymour reviewer for helpful comments on the manuscript. This research and publication were supported by the Cross-border cooperation programme Czech Republic–Bavaria Free State ETC goal 2014–2020, the Interreg V project No. 26 "Silva Gabreta Monitoring – Implementation of Transboundary Monitoring of Biodiversity and Water Regime".

References

Bojková J., Čížková H., Kučerová A., Rádková V., Soldán T., Svidenský R. & Vrba J., 2015: Monitoring of the restored streams in the Vltavský Luh (Šumava National Park). *Silva Gabreta*, 21: 73–79.

Bufková I., Prach K. & Bastl M., 2005: Relationships between vegetation and environment within the montane floodplain of the Upper Vltava River (Šumava National Park, Czech Republic). *Silva Gabreta*, Supplementum 2: 1–78.

ČGS, 2018a: Geologická mapa 1 : 50 000, List 3212 [Geological map 1: 50 000, Sheet 3212]. Česká Geologická Služba, Praha (in Czech). Online https://mapy.geology.cz/geocr50/ (cit. 5. 10. 2018) (in Czech).

ČGS, 2018b: Půdní mapa 1 : 50 000, List 3212 [Soil map 1 : 50 000, Sheet 3212]. Česká Geologická Služba, Praha (in Czech). Available at https://mapy.geology.cz/pudy/ (cit. 5. 10. 2018) (in Czech).

Chytrý M. (ed.), 2007: *Vegetace České republiky 1. Travinná a keříčková vegetace* [*Vegetation of the Czech Republic 1. Grassland and heathland vegetation*]. Academia, Praha, 526 pp. (in Czech).

Chytrý M. (ed.), 2011: *Vegetace České republiky 3. Vodní a mokřadní vegetace* [*Vegetation of the Czech Republic 3. Aquatic and wetland vegetation*]. Academia, Praha, 827 pp. (in Czech).

Chytrý M., Kučera T., Kočí M., Grulich V. & Lustyk P. (eds), 2010: *Katalog biotopů České republiky. Druhé vydání* [*Habitat catalogue of the Czech Republic. Second edition*]. AOPK, Praha, 445 pp. (in Czech).

Kubát K., Hrouda L., Chrtek J. jun., Kaplan Z., Kirschner J. & Štěpánek J. (eds), 2002: *Klíč ke květeně České republiky* [*Key to the flora of the Czech Republic*]. Academia, Praha, 928 pp. (in Czech).

Prach K., 1993: Vegetational changes in a wet meadow complex, South Bohemia, Czech Republic. *Folia geobotanica & phytotaxonomica*, 28: 1–13.

Prach K., 2008: Vegetation changes in a wet meadow complex during the past half-century. *Folia Geobotanica*, 43: 119–130.

Received: 13 July 2018
Accepted: 10 October 2018

Silva Gabreta	vol. 24	p. 223–243	Vimperk, 2018

Vrba černající (*Salix myrsinifolia*) v jižní části Čech
Salix myrsinifolia in southern Bohemia

Petr Lepší[1,*], Karel Boublík[2], Martin Lepší[3], Petr Koutecký[4], Milan Štech[4], Jana Janáková[1] & David Půbal[5]

[1]*AOPK ČR, Správa CHKO Blanský les, Vyšný 59, CZ-38101 Český Krumlov, Česká republika*
[2]*Fakulta životního prostředí, Česká zemědělská univerzita, Kamýcká 129, CZ-16521 Praha 6–Suchdol, Česká republika*
[3]*Jihočeské muzeum v Českých Budějovicích, Dukelská 1, CZ-37051 České Budějovice, Česká republika*
[4]*Přírodovědecká fakulta, Jihočeská univerzita, Branišovská 1760, CZ-37005, České Budějovice, Česká republika*
[5]*Správa NP Šumava, 1. máje 260, CZ-38501 Vimperk, Česká republika*
[*] plepsi@seznam.cz

Abstract
This paper summarises the distribution of *Salix myrsinifolia* in southern Bohemia (Czech Republic). The species has been found at eight probably natural localities to date, especially in the Bohemian Forest (Šumava Mts.). Recently, we confirmed seven of them. In southern Bohemia, *S. myrsinifolia* mostly grows in poor acidic fens (*Sphagno-Caricion canescentis*) and meadows around springs (*Calthion palustris*). The populations are composed of only one or two individuals; altogether, only nine shrubs of this critically endangered species in the Czech Republic are extant in the study area. There was no generative offspring observed at any locality, whereas vegetative sprouting was recorded around some shrubs. The species has also been planted in this region, mostly the cultivar 'Cotinifolia'.

Key words: Czech Republic, endangered species, *Salicaceae*, willow

ÚVOD

Vrba černající (*Salix myrsinifolia* Salisb.) patří k nejproměnlivějším druhům evropských vrb. Variabilní je především velikost, tvar, odění listů a okraj listové čepele (Rechinger 1964). Jenom ve střední Evropě je uváděno 10 variet rozlišených pouze na základě tvaru čepele (Wagenitz 1981). Tato morfologická proměnlivost vedla k popisu různých morfologických odchylek jako samostaných druhů, popř. domnělých hybridů (Skvortsov 1999). V současnosti jsou v Evropě rozlišovány poddruhy dva (Skvortsov 1999) – subsp. *myrsinifolia* a subsp. *borealis* (Fr.) Hyl. Nominátní poddruh má boreomontánní rozšíření, jehož severní souvislá část zahrnuje Britské ostrovy, Skandinávii, severovýchodní Evropu a západní Sibiř, jihozápadní okraj souvislého výskytu probíhá východní polovinou Polska. Dále tento poddruh roste v celých Alpách a vzácně je udáván i z dalších, především horských oblastí střední Evropy. Izolované výskyty jsou uváděny z Pyrenejí (nejistý údaj) a hor severní části Balkánského poloostrova (Uotila 2011). Vyznačuje se listy na rubu pýřitými až olysalými a nápadně ojíněnými (kromě špičky listu, která je zelená) a jehnědami, které se objevují před vyrašením listů. Poddruh *Salix myrsinifolia* subsp. *borealis* (Fr.) Hyl. je udáván pouze ze severní části Fenoskandinávie a Ruska a od nominátního se odlišuje většími listy, které jsou na rubu více chlupaté, víceméně bez ojínění a jehnědami rašícími zároveň s listy (Rechinger 1964, Skvortsov 1999). V minulosti byl rozlišován na úrovni samostatného druhu, avšak nedostatečná morfologická a geografická diferenciace od nominátního poddruhu takové hodnocení neopravňují (Skvortsov 1999).

Do okruhu vrby černající, tj. do sekce *Nigricantes* Kerner, dále patří endemit rakouských a italských Alp, *Salix mielichhoferi* Saut., který je na rozdíl od *S. myrsinifolia* na rubu listů zcela lysý (Wagenitz 1981, Fischer 2008). Třetím v Evropě v současnosti akceptovaným druhem je *Salix apennina* A. K. Skvortsov rostoucí na Apeninském poloostrově a izolovaně také na Sicílii, Korsice a v jižním Švýcarsku (Uotila 2011). Tento taxon má listy na rubu ojíněné (včetně špičky) a oproti *S. myrsinifolia* má více vyniklé žilky na rubu listů, na větvích větší počet delších lišt pod kůrou a kratší čnělky (Lauber et al. 2018). Z území České republiky je udávána pouze *Salix myrsinifolia* subsp. *myrsinifolia*.

V České republice je vrba černající obvykle považována za prvek alpského migrantu, protože její výskyt byl donedávna znám pouze z jižních a jihozápadních Čech – Český les, Třeboňská pánev, Šumava (Chmelař & Koblížek 1990). V poslední době byla však nalezena také na Liberecku u Machnína (Petřík in Hadinec & Lustyk 2007) a v Krušných horách u Petrovic (Koblížek in Hadinec & Lustyk 2014). Protože se lokality nacházejí často v blízkosti existujících či zaniklých osad, je původnost mnohých z nich zpochybňována. Situaci také komplikuje skutečnost, že druh je vysazován i v současnosti, a to zejména v samičím klonu ‘Cotinifolia‘ s téměř okrouhlými listy (Koblížek in Hadinec & Lustyk 2014); z výsadby podél silnice také zjevně pochází další publikovaná lokalita v Krušných horách u Hory

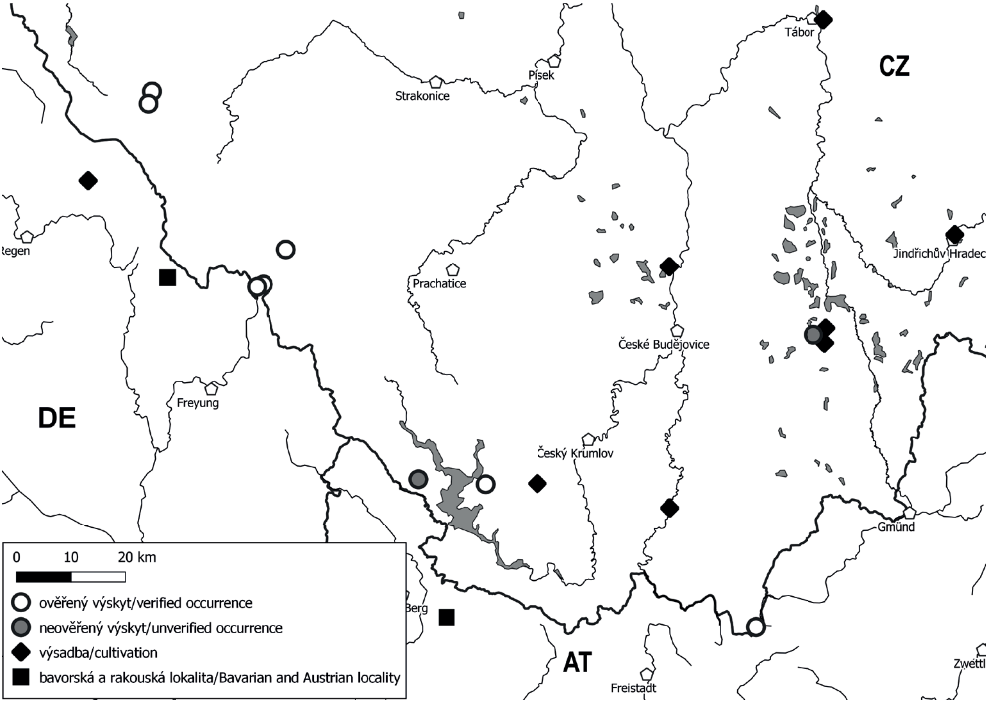

Obr. 1. Mapa známého rozšíření *Salix myrsinifolia* v jižní části Čech a přilehlých oblastech Bavorska a Horního Rakouska.

Fig. 1. Map of known distribution of *Salix myrsinifolia* in southern part of Bohemia (CZ) and adjacent Bavaria (DE) and Upper Austria (AT).

Sv. Šebestiána a možná i u Svatošských skal v průlomovém údolí Ohře u Karlových Varů (obojí Koblížek in Hadinec & Lustyk 2014). Na druhou stranu se řada lokalit nachází v oblastech s výskytem rašelinných a mokřadních biotopů, což odpovídá ekologickým nárokům druhu v oblastech hojnějšího a jasně přirozeného výskytu.

Dosud známý výskyt vrby černající v jižní části Čech shrnul Ekrt (2013). Po roce 2000 se podařilo objevit několik nových lokalit druhu, zároveň ale nebyly známy aktuální a podrobné informace o dříve objevených lokalitách. V této práci uvádíme přehled všech známých lokalit vrby černající v jižní části Čech i výsledky našeho terénního průzkumu dříve uváděných lokalit.

Metodika

V tomto článku uvádíme přehled herbářových položek vrby černající z jižní části Čech uložených v herbářích Jihočeského muzea v Českých Budějovicích (CB), Přírodovědecké fakulty Jihočeské univerzity v Českých Budějovicích (CBFS), Národního muzea v Praze (PR) a Univerzity Karlovy v Praze (PRC). Dále jsme přehled doplnili o nedoložené záznamy z terénních zápisníků Stanislava Kučery (Kučera 1992). Uvedeny jsou všechny herbářové položky *Salix myrsinifolia* ze studovaného území uložené ve výše zmíněných sbírkách a jsou uvedena jejich inventární čísla, pokud existují. Lokality jsou zařazeny do fytochorionů dle práce Skalický (1988) a do mapovacích polí, která odpovídají ¼ základního pole středoevropského síťového mapování (Ehrendorfer & Hamann 1965). Souřadnice lokalit jsou zapsány v systému WGS 84 a byly odečteny z přístroje GNSS (Global Navigation Satellite System) nebo z www.mapy.cz.

Jednotlivé lokality jsou nejdříve uvedeny stručným komentářem, za nímž následuje seznam herbářových sběrů, které se k lokalitě vztahují. U dokladů, u nichž to bylo možné zjistit, je uvedeno pohlaví jedince. Pokud nebylo na herbářové etiketě zapsáno datum nálezu, je použita zkratka „s. d.“. Texty v hranatých závorkách v textu herbářových etiket jsou naše upřesňující informace o lokalitě. Akronymy herbářových sbírek odpovídají databázi Index Herbariorum (Thiers 2018). Nomenklatura syntaxonů je uvedena podle Vegetace České republiky (Chytrý 2007, 2011) a nomenklatura taxonů podle práce Danihelka et al. (2012). Vymezení území „jižní část Čech“ pro účely této práce je totožné s územím, pro které byla zpracována Červená kniha květeny jižní části Čech (Lepší et al. 2013).

Vrba černající se od všech ostatních našich původních druhů vrb liší v počtu chromosomů (Chmelař & Koblížek 1990) – je hexaploidní (2n = 114), zatímco ostatní druhy jsou diploidní (2n = 38) nebo tetraploidní (2n = 76). Díky tomuto rozdílu bylo možné potvrdit určení nově nalezených rostlin měřením velikosti genomu metodou průtokové cytometrie (měřeny čerstvě sebrané listy standardní dvoustupňovou metodikou, viz např. Doležel et al. 2007, s fluorescenčním barvivem DAPI, jako standard byla použita sedmikráska, *Bellis perennis*). Informace o cytometrickém ověření stupně ploidie je uvedena v přehledu lokalit zkratkou „FCM“ (z anglického „flow cytometry“) za citací příslušné herbářové položky.

Přehled lokalit vrby černající v jižní části Čech (obr. 1)

Pravděpodobně původní lokality

Knížecí Pláně a okolí (88b. Šumavské pláně, 7047b), obr. 2–4

Vrbu černající našel u Knížecích Plání J. Chmelař v roce 1961 (Chmelař 1966), poté byla dokladována ještě S. Kučerou v letech 1974 a 1983 ze dvou až tří míst. Nám se podařilo ji ověřit v letech 2015 a 2016 na dvou lokalitách. První leží u bývalé osady Chaloupky západně

HERBARIUM MUSEI REGIONALIS BOHEMIAE MERIDIONALIS
ČESKÉ BUDĚJOVICE

Flora: Southern Bohemia, Šumava Mts

CB/84167

Salix myrsinifolia Salisb.

Knížecí Pláně (distr. Prachatice), ca 1.3 km WSW of restaurant, wet abandoned meadow

Frequence: one old and large ca 7 m high shrub
Note: found by M. Štech

Altitude: 900 m **WGS 84:** 48°57'12,1''N; 13°36'31,4''E
Quadrant: 7047bcd **ID GPS:**
Phytogeographical distr.: Šumavské pláně
Date: 27.6. 2015 **Collected:** Martin Lepší, Petr Lepší

Quadrant according to Ehrendorfer et Hamann 1965, Ber. Deutsch. Bot. Ges.; Phytogeographical distr. - Skalický 1988, Květena ČR 1

Obr. 2. Herbářový doklad *Salix myrsinifolia* z opuštěné vlhké louky cca 1,3 km zjz. od restaurace v Knížecích Pláních na Šumavě z roku 2015.
Fig. 2. *Salix myrsinifolia* specimen from abandoned wet meadow ca. 1.3 km WSW of the restaurant in the Knížecí Pláně settlement (Bohemian Forest) from 2015.

HERBARIUM MUSEI REGIONALIS BOHEMIAE MERIDIONALIS
ČESKÉ BUDĚJOVICE

Flora: Southern Bohemia

CB/84375

Salix myrsinifolia Salisb.

Knížecí Pláně (distr. Prachatice), ca 740 m NNE of former church in village, Sphagno-Caricion canescentis

Frequence: shrub ca 2,5 high
Note:

Altitude: 1010 m **WGS 84:** 48°57'28,87''N; 13°37'13,55''E
Quadrant: 7047bcd **ID GPS:** 248
Phytogeographical distr.: Šumavské pláně
Date: 7.9. 2016 **Collected:** Petr Lepší, et al.

Quadrant according to Ehrendorfer et Hamann 1965, Ber. Deutsch. Bot. Ges.; Phytogeographical distr. - Skalický 1988, Květena ČR 1

Obr. 3. Herbářový doklad *Salix myrsinifolia* z opuštěné a křovinami zarůstající rašelinné louky cca 740 m ssv. od bývalého kostela v Knížecích Pláních na Šumavě z roku 2016.
Fig. 3. *Salix myrsinifolia* specimen from abandoned peaty meadow ca. 740 m NNE of the former church in the Knížecí Pláně settlement (Bohemian Forest) from 2016.

HERBARIUM MUSEI REGIONALIS BOHEMIAE MERIDIONALIS
ČESKÉ BUDĚJOVICE

Flora: Southern Bohemia

CB/84374

Salix myrsinifolia Salisb.

Knížecí Pláně (distr. Prachatice), ca 720 m NNE of former church in village, Sphagno-Caricion canescentis

Frequence: shrub ca 5 m high
Note:

Altitude: 1010 m **WGS 84:** 48°57’28,08’’N; 13°37’13,8’’E
Quadrant: 7047bcd **ID GPS:** 249
Phytogeographical distr.: Šumavské pláně
Date: 7.9. 2016 **Collected:** Petr Lepší, et al.

Quadrant according to Ehrendorfer et Hamann 1965, Ber. Deutsch. Bot. Ges.; Phytogeographical distr. - Skalický 1988, Květena ČR 1

Obr. 4. Herbářový doklad *Salix myrsinifolia* z opuštěné a křovinami zarůstající rašelinné louky cca 720 m ssv. od bývalého kostela v Knížecích Pláních na Šumavě z roku 2016.
Fig. 4. *Salix myrsinifolia* specimen from abandoned peaty meadow ca. 720 m NNE of the former church in the Knížecí Pláně settlement (Bohemian Forest) from 2016.

od bývalého kostela, kde roste jeden mohutný rozlomený starý keř (pravděpodobně spíše dožívající a bez výrazné obnovy koruny) v mozaice mokrých luk, pramenišť a porostů dalších druhů vrb (*Salix aurita*, *S. caprea*). Druhá lokalita je asi 1 km vzdálená a leží asi 720–740 m ssv. od bývalého kostela. Vyskytují se na ní dva keře ve vzdálenosti asi 25 m. Oba rostou na okraji rozsáhlého porostu rákosu obecného, který přerůstá ostřicovo-rašelinnou enklávu. První, víceméně košatý keř je asi 5 m vysoký, druhý je nevelký, vysoký jen asi 2,5 m. Oba keře zčásti prosychají, ale je patrná i obnova pomocí výmladků. Je pravděpodobné, že se jedná o stejné exempláře nalezené S. Kučerou.

Herbářové doklady: Čechy, Šumava, rašeliniště u Knížecích Plání, 1000 m (leg. J. Chmelař 26. 6. 1961 CB 52642). – Knížecí Pláně: rašelinné pastviny v nivě potoka u zaniklé osady Chaloupky, cca 0,5 km Z kostela (leg. S. Kučera 6. 9. 1974 CB 13921, 13922, 13923, 13924). – ♀ Knížecí Pláně, potok na Chaloupkách (leg. S. Kučera 5. 5. 1983 CB 13776, 13777, 13778). – Knížecí Pláně: wet abandoned meadow ca 1.3 km WSW of restaurant, 48°57'12,1''N, 13°36'31,4''E (GNSS), cca 990 m n. m., one old and large ca 7 m high shrub (not. M. Štech a kolektiv Jihočeské pobočky ČBS, leg. M. Lepší & P. Lepší 27. 6. 2015 CB 84167), FCM, obr. 2. – Knížecí Pláně, (rozsáhlé) pramenné mokřiny v pastvinách, cca 0,4 km SSV kostela (leg. S. Kučera 3. 9. 1974 CB 13925, 13926, 13927, 13928, 13929). – ♂ Knížecí Pláně, pram.[prameništní] močál (střelnice) (leg. S. Kučera 5. 5. 1983 CB 13773, 13774, 13775). – Knížecí Pláně: *Sphagno-Caricion canescentis* ca. 740 m NNE of former church in village, 48°57'28.9''N, 13°37'13.6''E (GNSS), 1010 m a.s.l., shrub ca. 2.5 m high (leg. P. Lepší et al. 7. 9. 2016 CB 84375), FCM, obr. 3. – Knížecí Pláně: *Sphagno-Caricion canescentis* ca. 720 m NNE of former church in village, 48°57'28.1''N, 13°37'13.8''E (GNSS), 1010 m a.s.l., shrub ca. 5 m high (leg. P. Lepší et al. 7. 9. 2016 CB 84374), FCM, obr. 4.

Borová Lada (88b. Šumavské pláně, 6947d), obr. 5

U Chalupské slati u Borových Lad sbíral vrbu černající v roce 1983 S. Kučera. V roce 2016 jsme na lokalitě našli jeden mohutný starý keř na západním okraji rašelinného komplexu na okraji prameniště v mokré louce. Keř byl asi 7 m vysoký a v bezprostředním okolí jsme pozorovali kořenové výmladky anebo zahřížené postranní větve (asi 0,5 m vysoké). V podrostu keře roste velký jedinec *Ribes nigrum*.

Herbářové doklady: ♂ Borová Lada, při Chalupské slati (leg. S. Kučera 5. 5. 1983 CB 13783, 13784, 13785, 13786). – Nový Svět: edge of spring in wet meadows, W edge of Novosvětská slať bog, 49°00'31.1''N, 13°39'23.8''E (GNSS), 920 m a.s.l., one large and old shrub (leg. M. Štech et al. 7. 9. 2016 CB 84376), FCM, obr. 5.

Okolí bývalé osady Zhůří (u Hartmanic) (88b. Šumavské pláně, 6845b, 6846a), obr. 6–7

V roce 1999 našli F. Procházka, J. Hadinec a P. Havlíček v prostoru Zhůří u Hartmanic na horním toku Křemelné jeden exemplář (Procházka et al. 2001). Doklady, které by měly být uloženy v PL a PRC, se nám nepodařilo revidovat. V prvém případě doklad nebyl ani po opakované snaze nalezen a je možné, že se do PL nedostal (S. Pecháčková, úst. sděl.). Druhý je zatím zařazen ve veřejně nepřístupných fondech PRC (J. Hadinec, úst. sděl.). Lokalitu naposledy ověřili a dokladovali v roce 2014 M. Štech a T. Štechová. Lokalita se nachází na levém břehu Zhůřského potoka na okraji rašelinného komplexu jižně od silnice v prostoru zaniklé vesnice. Jedná se o jediný malý keř asi 1 m vysoký, poškozený okusem a pastvou. Tentýž rok se podařilo najít další lokalitu na severním úpatí Hadího vrchu v přírodní rezervaci Zhůřská pláň ve vzdálenosti asi 2 km od předešlé lokality. Roste zde poměrně mohutný, zhruba 5 m vysoký vitální exemplář na suchém okraji smrkového lesa pod rašelinnými loukami.

Herbářové doklady: Keply (u Hartmanic): Zhůří, na levém břehu Zhůřského potoka na okraji rašelinného komplexu jižně od silničky v prostoru zaniklé vesnice cca 90 m jz. od soutoku Zhůřského potoka s Křemelnou, 49°10'27,7''N, 13°19'59,4''E (GNSS), cca 880 m n. m., 1 malý keř (cca 1,5 m vysoký) (leg. M. Štech & T. Štechová 11. 10. 2014, CB 85489), obr. 6. – Zhůří, Hadí vrch, okraj nelesní enklávy zaniklé osady v PR Zhůřská pláň, cca 550 m sev. od kóty Hadí vrch (1021 m), 49°11'29,5''N, 13°20'14,6''E (GNSS), cca 980 m n. m., 1 mohutný a vitální keř (leg. M. Štech & T. Štechová 20. 9. 2014 CBFS, CB 85490), FCM, obr. 7.

HERBARIUM MUSEI REGIONALIS BOHEMIAE MERIDIONALIS
ČESKÉ BUDĚJOVICE

Flora: Southern Bohemia

CB/84376

Salix myrsinifolia Salisb.

Nový Svět (distr. Prachatice), W edge of Novosvětská slať bog, edge of spring in wet meadows

Frequence: one large and old shrub
Note:

Altitude: 920 m **WGS 84:** 49°0'31,07''N; 13°39'23,83''E
Quadrant: 6947ddd **ID GPS:** 247
Phytogeographical distr.: Šumavské pláně
Date: 7.9. 2016 **Collected:** Milan Štech, et al.

Quadrant according to Ehrendorfer et Hamann 1965, Ber. Deutsch. Bot. Ges.; Phytogeographical distr. - Skalický 1988, Květena ČR 1

Obr. 5. Herbářový doklad *Salix myrsinifolia* z okraje lučního prameniště na záp. okraji Novosvětské slati u Borových Lad na Šumavě z roku 2016.
Fig. 5. *Salix myrsinifolia* specimen from the edge of meadow spring community in the western margin of the Novosvětská Slať bog close to the Borová Lada village (Bohemian Forest) from 2016.

Keply (u Hartmanic): Zhůří, na levém břehu Zhůřského potoka na okraji rašelinného komplexu jižně od silničky v prostoru zaniklé vesnice ca 90 m jz. od soutoku Zhůřského potoka s Křemelnou (49°10'27.7"N, 13°19'59.4"E (GNSS), 880 m n. m.). Jediný malý keř (ca 1,5 m vysoký), poškozený pastvou.
2014-10-11
leg. M. Štech & T. Štechová

HERBARIUM MUSEI REGIONALIS BOHEMIAE MERIDIONALIS
ČESKÉ BUDĚJOVICE

Oblast: západní Čechy

CB/85489

Salix myrsinifolia Salisb.

Keply (okres Klatovy), Zhůří, na levém břehu Zhůřského potoka na okraji rašelinného komplexu jižně od silničky v prostoru zaniklé vesnice ca 90 m jz. od soutoku Zhůřského potoka s Křemelnou,

Početnost: jeden malý keř (ca 1,5 m vysoký)
Nadm. výška: 880 m **WGS 84:** 49°10'27,7''N; 13°19'59,4''E
Kvadrant: 6845bdb
Fytogeografický okres: Šumavské pláně
Datum: 11.10. 2014 **Sbíral:** Milan Štech, Táňa Štechová

Kvadrant podle Ehrendorfer F. et Hamann U. 1965, Ber. Deutsch. Bot. Ges.; Fytogeografický okres podle Skalický V. 1988, Květena ČR 1.

Obr. 6. Herbářový doklad *Salix myrsinifolia* z okraje rašelinné enklávy na levém břehu Zhůřského potoka v prostoru zaniklé vesnice Zhůří na Šumavě z roku 2014.
Fig. 6. *Salix myrsinifolia* specimen from the edge of peaty area at the left-hand bank of the Zhůřský Potok stream in the former Zhůří village (Bohemian Forest) from 2014.

Zadní Zvonková (88g. Hornovltavská kotlina, 7249d), obr. 8

Vrbu černající našel na rašelinných loukách pod Zadní Zvonkovou S. Kučera v roce 1975 (Procházka 1990). V roce 2016 jsme lokalitu navštívili, ale nepodařilo se nám vrbu najít. Není ovšem vyloučeno, že se na lokalitě nebo v blízkém okolí dosud vyskytuje. Louky pod silnicí jsou sice odvodněny a lokalitou protékající Hamerský potok je částečně napřímen, ale severovýchodním směrem (zhruba 1,2 km sv. od kostela v Zadní Zvonkové, mimo S. Kučerou udávaný výskyt) jsou dobře zachovalé mokřadní biotopy na velkých rozlohách, kde je výskyt vrby černající možný (zde byl průzkum proveden pouze orientačně).
Herbářový doklad: ♀ Zadní Zvonková, rašelinné louky v úvalu malého potoka pod silnicí, cca 0,8 km SV od kostela (leg. S. Kučera 28. 5. 1975 CB 13854, 13855, 13856, 13857), obr. 8.

Slavkovice u Černé v Pošumaví (37l. Českokrumlovské Předšumaví, 7250d), obr. 9

V prostoru mezi Černou v Pošumaví a Slavkovicemi našla vrbu černající v roce 1961 D. Blažková, poté byla lokalita ověřena S. Kučerou v roce 1989. Na exkurzi v roce 2016 jsme našli jeden odumírající asi 6 m vysoký stromový exemplář ve stinném smrkovém lese. Většina spodních větví byla bez listů a pravděpodobně již odumřelá, pouze nejvyšší větve měly listy. Procházka (1990) usuzuje, ovšem bez bližšího komentáře, na výsadbu; domníváme se však, že lokalitu lze podle charakteru výskytu považovat za pravděpodobně přirozenou.


Keply (u Hartmanic): Zhůří, Hadí vrch, okraj nelesní enklávy zaniklé osady v PR Zhůřská pláň, ca 550 m sev. od kóty Hadí vrch (1021 m), 49°11'29,5"N, 13°20'14,6"E (GNSS), ca 980 m n. m., 1 mohutný a vitální keř
2014-09-20
leg. M. Štech & T. Štechová

HERBARIUM MUSEI REGIONALIS BOHEMIAE MERIDIONALIS
ČESKÉ BUDĚJOVICE

Oblast: západní Čechy

CB/85490

Salix myrsinifolia Salisb.

Keply (okres Klatovy), Zhůří, Hadí vrch, okraj nelesní enklávy zaniklé osady v PR Zhůřská pláň, ca 550 m sev. od kóty Hadí vrch (1021 m),

Početnost: 1 mohutný vitální keř
Nadm. výška: 980 m **WGS 84:** 49°11'29,5''N; 13°20'14,6''E
Kvadrant: 6846aaa
Fytogeografický okres: Šumavské pláně
Datum: 20.9. 2014 **Sbíral:** Milan Štech, Táňa Štechová

Kvadrant podle Ehrendorfer F. et Hamann U. 1965, Ber. Deutsch. Bot. Ges.; Fytogeografický okres podle Skalický V. 1988, Květena ČR 1.

Obr. 7. Herbářový doklad *Salix myrsinifolia* z okraje lesa na severním úpatí Hadího vrchu u zaniklé vesnice Zhůří na Šumavě z roku 2014.
Fig. 7. *Salix myrsinifolia* specimen from the edge of forest at northern foot of the Hadí Vrch hill close to the former Zhůří village (Bohemian Forest) from 2014.

Obr. 8. Herbářový doklad *Salix myrsinifolia* z rašelinné louky cca 0,8 km sv. od kostela v Zadní Zvonkové na Šumavě z roku 1975. Výskyt druhu na lokalitě se v roce 2016 nepodařilo ověřit.
Fig. 8. *Salix myrsinifolia* specimen from peaty meadow ca. 0.8 km NE of the church in the Zadní Zvonková village (Bohemian Forest) from 1975. We did not confirm the occurrence of the species at this locality in 2016.

Herbářové doklady: Černá v Pošumaví, východně od obce, záp. pod kótou 726 – smrkový les v široké úžlabině (leg. D. Blažková 22. 8. 1961 CB) [nadmořská výška kóty je uvedena chybně a vztahuje se podle speciální mapy 3. vojenského mapování v měřítku 1 : 75 000, kterou nálezkyně patrně použila, k Černé v Pošumaví]. – Černá v Pošumaví, Slavkovice, niva potoka poblíž osady (leg. S. Kučera 26. 6. 1989 CB 22307), obr. 9. – Černá v Pošumaví: Slavkovice former village, planted spruce forest along Černý potok stream, ca. 660 m SW of house in former village, 1 old and dying tree, ca. 6 m high, 48°44'12''N, 14°07'30''E (GNSS), 740 m a.s.l. (leg. J. Janáková, P. Lepší et M. Štech 27. 9. 2016 CB 103203), FCM.

Pohoří na Šumavě (89. Novohradské hory, 7454a), obr. 10

U Pohoří na Šumavě našel vrbu černající v roce 2003 M. Lepší. Lokalita byla publikována bez podrobnějších údajů v práci Lepší & Lepší (2004), přinášíme tedy přesnou lokalizaci nálezu. Vrba zde roste v lese vzniklém na místě rozvalin samot bývalé obce Pohoří na Šumavě v blízkosti hranic s Rakouskem. Vrba černající se tam vyskytuje ve dvou samičích exemplářích; první je 5–6 m vysoký šestikmenný keř s obrážejícími výmladky, druhý je až 8 m vysoký keř s asi 15 kmeny, které mají 5–10 cm v průměru a časté výmladky. Oba rostou asi 5 m od sebe v silně podmáčené rašelinné světlině (na prameništi), která z části samovolně zarůstá a z části je osázena smrkem a olší lepkavou. Perspektiva obou keřů není veliká, oba jsou poškozovány zvěří a zastiňovány okolními dřevinami (*Salix aurita*, *Picea abies*).
Herbářové doklady: Pohoří na Šumavě (u Pohorské Vsi): cca 1,4 km jv. od kostela, rašelinná louka nedaleko rozvalin, 48°35'41,3''N, 14°42'29,7''E (GNSS), 940 m n. m. (leg. M. Lepší 12. 6. 2003 CB 38786), obr. 10. – ♀ Pohoří na Šumavě (distr. Český Krumlov), forest ca. 1.34 km SE of church in village, *Calthenion* with scrubs and planted trees, 6–8 m high ex., polycormon with 15 trunks up to 10 cm in diameter and with frequent sprout shoots, 48°35'40''N, 14°42'30''E (GNSS), 940 m a.s.l. (leg. P. Lepší 13. 8. 2017 CB), FCM. – ♀ Pohoří na Šumavě (distr. Český Krumlov): forest ca. 1.34 km SE of church in village, *Calthenion* with scrubs and planted trees, 5–6 m high ex., 6 trunks up to 10 cm in diameter with frequent sprout shoots, 48°35'40''N, 14°42'30''E (GNSS), 940 m a.s.l. (leg. P. Lepší 13. 8. 2017 CB), FCM.

Okolí rybníka Svět u Třeboně (39. Třeboňská pánev, 7054a nebo 7054b)

Od rybníka Svět v Třeboňské pánvi uvádí samičího jedince vrby černající Chmelař & Koblížek (1990) s tím, že na lokalitě byl vysazen také pestíkový klon. Podrobnější informace o této lokalitě nám nejsou známy, může se jednat o údaj o pěstovaných rostlinách (srov. níže).

Lokality, na nichž byla vrba černající pěstována nebo zplaněla

Doklady o prokazatelně pěstovaných jedincích vrby černající pocházejí z různých míst jižní části Čech. Jde o zahrady u zámku Ohrada u Hluboké nad Vltavou, v Jindřichově Hradci, botanickou zahradu v Táboře (obr. 14), okraj města Kaplice, okraj vsi Pasovary u Českého Krumlova a Opatovický rybník u Třeboně. Dvě posledně zmíněné lokality by mohly působit dojmem přirozeného výskytu, ale druh byl na nich vysazen. V případě lokality u Pasovar to je zřejmé z poznámky J. Chmelaře (který lokalitu osobně navštívil) na herbářové etiketě sběru V. Chána (viz níže a obr. 11). Vrba černající u Opatovického rybníka byla již samotným nálezcem, A. Weidmannem, považována za pěstovanou (Houfek 1952); její výskyt tam již dávno zanikl (Kurka 1959, Chmelař 1966, obr. 13). Lokalita u Kaplice vznikla zplaněním nebo přímo výsadbou, neboť ještě v roce 2005 rostlo několik keřů této vrby v liniové výsadbě asi 0,5 km proti proudu řeky. Pro adventivní výskyt svědčí i morfologický charakter jedince – jedná se o vysazovaný kultivar ‘Cotinifolia‘ (obr. 12).
Herbářové doklady: 37l. Českokrumlovské Předšumaví, ♀ Pasovary (7251c): při okraji Pasovar, několik keřů (leg. V. Chán 1962 CB 52628; poznámka J. Chmelaře na herbářové etiketě: v terénu jsem si 8. 9. 1964 ověřil, že jde o vysazený materiál), obr. 11. – 37n. Kaplické mezihoří, ♀ Kaplice (7253c): břehové porosty cca 600 m vjv. náměstí, levý břeh řeky Malše na vých. okraji města, 48°44'16,4''N, 14°30'07,3''E (GNSS), 540 m n. m., jeden starý [v roce 2015 poničený keř] (leg. M. Lepší 22. 9. 2005 CB 50825, 29. 7. 2015 CB 83854), cv. ‘Cotinifolia‘, obr. 12. – 38. Budějovická pánev, Hluboká nad Vltavou (6952d): v bývalé zahradě u lovčího zámku Ohrada u Hluboké n. Vlt., 394 m (leg. R. Kurka 8. 1950 CB 38069). – 39. Třeboňská pánev,

Salix myrsinifolia Salisb.
Rev.-det. L. Úradníček 2015

HERBARIUM MUSEI REGIONALIS BOHEMIAE MERIDIONALIS
ČESKÉ BUDĚJOVICE

Flora: Bohemia meridionalis No. 22307

Salix pent-aur nebo nigricans Doklad kód, 5/20

Habitat: Černá v Pošumaví, Slavkovice, niva potoka poblíž osady

Kvadrant: 7250d
Fytochorion: .
Die: 26. 6.1989
Legit: Stanislav Kučera

Obr. 9. Herbářový doklad *Salix myrsinifolia* z nivy potoka nedaleko osady Slavkovice u Černé v Pošumaví v Českokrumlovském Předšumaví z roku 1989. Výskyt druhu se na lokalitě podařilo ověřit v roce 2016.
Fig. 9. *Salix myrsinifolia* specimen from the stream alluvium close to the Slavkovice settlement (Český Krumlov district) from 1989. We confirmed the occurrence of the species at this locality in 2016.

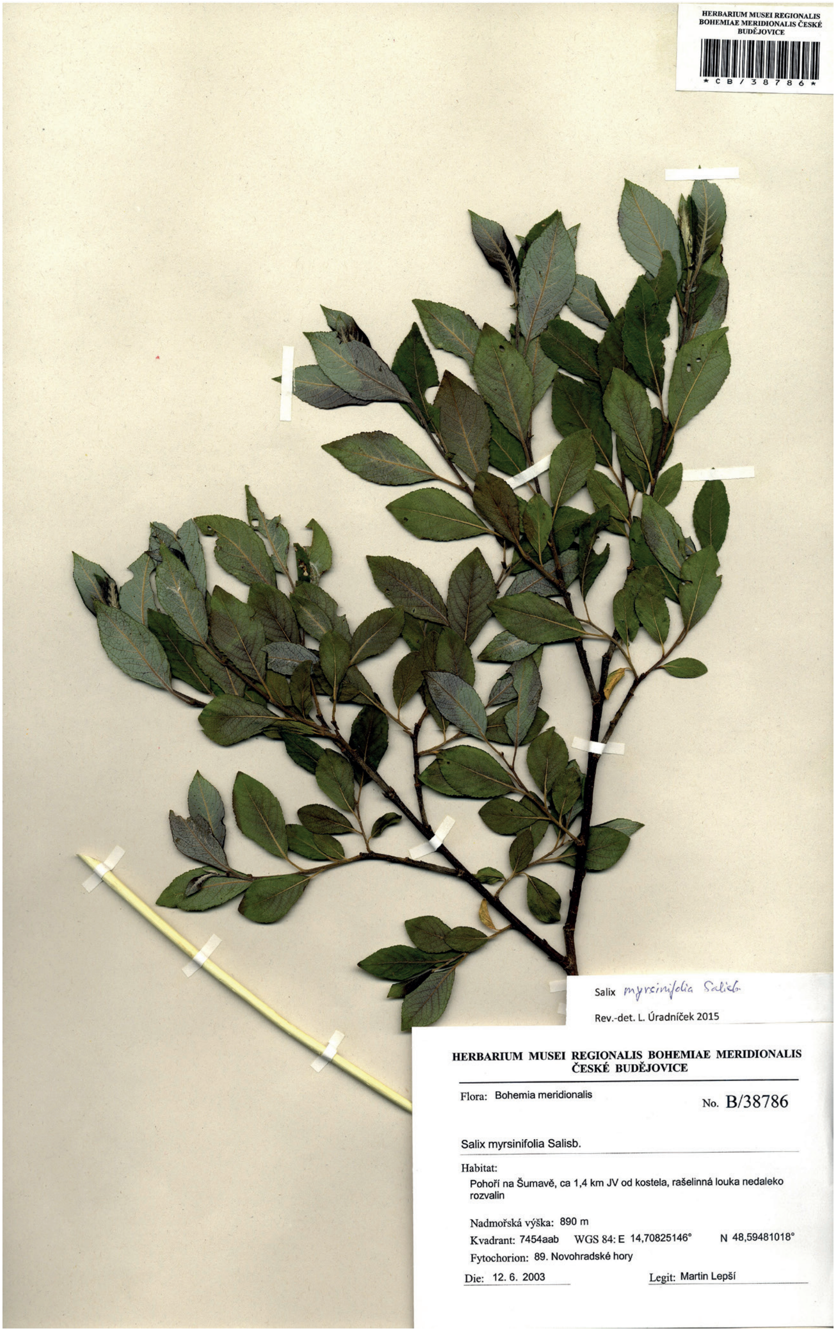

HERBARIUM MUSEI REGIONALIS BOHEMIAE MERIDIONALIS ČESKÉ BUDĚJOVICE
CB/38786

Salix myrsinifolia Salisb.
Rev.-det. L. Úradníček 2015

HERBARIUM MUSEI REGIONALIS BOHEMIAE MERIDIONALIS
ČESKÉ BUDĚJOVICE

Flora: Bohemia meridionalis
No. B/38786

Salix myrsinifolia Salisb.

Habitat:
Pohoří na Šumavě, ca 1,4 km JV od kostela, rašelinná louka nedaleko rozvalin

Nadmořská výška: 890 m
Kvadrant: 7454aab WGS 84: E 14,70825146° N 48,59481018°
Fytochorion: 89. Novohradské hory
Die: 12. 6. 2003
Legit: Martin Lepší

Obr. 10. Herbářový doklad *Salix myrsinifolia* z rašelinné louky cca 1,4 km jv. od kostela v Pohoří na Šumavě v Novohradských horách z roku 2003. Výskyt druhu se na lokalitě podařilo ověřit v roce 2017.
Fig. 10. *Salix myrsinifolia* specimen from peaty meadow ca. 1.4 km SE of the church in the village of Pohoří na Šumavě (Novohradské Hory Mts.). We confirmed the occurrence of the species at this locality in 2017.

♀ Třeboň (7054b): pod hrází Opatovického rybníka (leg. A. Weidmann 15. 5. 1889 CB 38071), obr. 13. – ♀ Třeboň (7054b): pod hrází ryb. Opatovického (leg. A. Weidmann 19. 5. 1888 PR). – ♀ Třeboň (7054b), v parku u sv. Jiljí (leg. A. Weidmann 7. 6. 1884 PRC), cv. ‚Cotinifolia'. – 42b. Táborsko-vlašimská pahorkatina, ♂ Tábor (6554c): bot. z. [botanická zahrada] (leg. Weselý 29. 4. 1954 CB 38065), obr. 14. – Tábor (6554c), botan. [botanická] zahrada (leg. R. Kurka 20. 5. 1993 CB 38066). – 67. Českomoravská vrchovina, Jindřichův Hradec (6855 nebo 6856): pěstov. [pěstovaná] v zahradě p. Albrechta (leg. R. Veselý 20. 9. 1953 CB 38067), cv. 'Cotinifolia'.

Nejasné údaje

V herbáři Jihočeského muzea je uložen doklad vrby černající lokalizovaný k Třeboni a sbíraný Steinerem. Není jasné, zda se vztahuje k lokalitě u Opatovického rybníka, rybníka Svět nebo jde o jinou lokalitu (může se jednat i o sběr rostliny pěstované ve městě, viz výše).
V kartogramu B. Slavíka jsou obsazena také mapovací pole 6854 a 6954 (Slavík 1990), která zaujímají prostor přibližně mezi Veselím nad Lužnicí a Třeboní. Další údaj publikoval J. Dostál od Starého Města pod Landštejnem na Českomoravské vrchovině (Dostál 1989). O původu těchto údajů se nám nepodařilo zjistit žádné informace.
Herbářový doklad: 39. Třeboňská pánev, Třeboň (leg. Steiner s. d. CB).

Mylné údaje

Údaj od Žofínského pralesa (od výpusti bývalého Tisového rybníka) v Novohradských horách diskutovaný v práci Lepší et al. (2007) pochází z terénního zápisníku S. Kučery z roku 1971 (Kučera 1992). V herbáři Jihočeského muzea se podařilo najít herbářový doklad k tomuto údaji, jedná se však o *Salix aurita* (CB 13981).

DISKUZE A ZÁVĚR

Na některých lokalitách přirozeného charakteru se díky neopadaným jehnědám nebo časně sbíraným herbářovým položkám podařilo zjistit pohlaví jednotlivých rostlin. Zaznamenáni byli převážně samičí jedinci (celkem v pěti případech), pouze keře severně od Knížecích Plání jsou samčí (dva jedinci). Samčí jedinec je udáván také z Třeboňské pánve (Chmelař & Koblížek 1990). Obojí pohlaví bylo zaznamenáno i na lokalitách v kultuře, příp. vzniklých výsadbou. Je třeba však mít na paměti, že na rozdíl od většiny vrb může být část jedinců vrby černající oboupohlavná a pohlavnost se může během života jedince měnit (Mirski 2016).

U všech jedinců analyzovaných pomocí průtokové cytometrie bylo potvrzeno, že jde o hexaploidní rostliny. To odpovídá údajům v literatuře a z jiných území (např. Chmelař & Koblížek 1990).

Morfologická variabilita zaznamenaných jihočeských rostlin není vysoká a všichni nalezení jedinci odpovídají nominátnímu poddruhu. Mezi pěstovanými exempláři byli pozorováni kromě cv. 'Cotinifolia' i jedinci odpovídající spíše rostlinám z přirozených lokalit.

V jižní části Čech roste vrba černající (na lokalitách, které považujeme za pravděpodobně původní) zejména na přechodových rašeliništích svazu *Sphagno-Caricion canescentis* a okrajích lučních pramenišť svazu *Calthion palustris*. Na takových místech se může dlouhodobě udržet, zatímco v zástinu (např. ve vysazené smrkové monokultuře na místě bývalých mokrých luk) coby světlomilná dřevina odumírá.

Vrba černající pravděpodobně nebyla v jižní části Čech častým druhem ani v minulosti, pro což svědčí absence herbářových i literárních dokladů a vzácný současný výskyt. Původnost výskytu však zůstává do jisté míry nejasná, protože na lokalitách považovaných za přirozené vrba často roste v blízkosti zaniklých stavení a netvoří větší populace. Na druhou stranu lze předpokládat, že současný stav je jen posledním zbytkem původně hojnějšího výskytu poté, co byly mnohé mokřadní lokality v minulosti razantně odvodněny a intenzivně obhospodařovány.

Obr. 11. Herbářový doklad *Salix myrsinifolia* vysazené u jižního okraje Pasovar v Českokrumlovském Předšumaví z roku 1962. Výskyt druhu se nepodařilo v roce 2016 ověřit.

Fig. 11. Specimen of cultivated *Salix myrsinifolia* at the southern edge of the former Pasovary settlement (Český Krumlov district) from 1962. We did not confirm the occurrence of the species at this locality in 2016.

HERBARIUM MUSEI REGIONALIS BOHEMIAE MERIDIONALIS
ČESKÉ BUDĚJOVICE

Flora: Southern Bohemia

CB/83854

Salix myrsinifolia Salisb.

Kaplice (distr. Český Krumlov), ca 600 m ESE of town square, left hand bank of Malše river at E edge of town, alluvium scrub

Frequence: one old large damaged shrub
Note:

Altitude: 540 m **WGS 84:** 48°44'16,37''N; 14°30'7,34''E
Quadrant: 7253caa **ID GPS:** 9
Phytogeographical distr.: Kaplické mezihoří
Date: 29.7. 2015 **Collected:** Martin Lepší

Quadrant according to Ehrendorfer et Hamann 1965, Ber. Deutsch. Bot. Ges.; Phytogeographical distr. - Skalický 1988, Květena ČR 1

Obr. 12. Herbářový doklad *Salix myrsinifolia* pravděpodobně vysazené nebo zplanělé v údolí Malše na okraji Kaplice v Kaplickém mezihoří z roku 2015.
Fig. 12. Specimen of probably planted or escaped *Salix myrsinifolia* from the Malše River valley near Kaplice town (Český Krumlov district) from 2015.

Obr. 13. Herbářový doklad *Salix myrsinifolia* vysazené pod hrází Opatovického rybníka u Třeboně z roku 1889. Výskyt druhu pominul.
Fig. 13. Specimen of planted *Salix myrsinifolia* from the Opatovický Rybník fishpond near Třeboň (Jindřichův Hradec district) from 1889. The occurrence of the species has already passed.

Obr. 14. Herbářový doklad *Salix myrsinifolia* pěstované v botanické zahradě v Táboře z roku 1954. Výskyt druhu nebyl ověřován.
Fig. 14. Specimen of cultivated *Salix myrsinifolia* from the botanical garden in Tábor from 1954. We did not attempt to confirm the occurrence at this locality.

V posledních několika letech jsme ověřili 9 jedinců z celkového počtu asi 10 jedinců objevených na pravděpodobně původních lokalitách za dobu výzkumu jihočeské květeny. Proto lze vrbu černající řadit mezi druhy přirozeně vzácné a ohrožené a vyžadující pozornost ochrany přírody. Na téměř všech lokalitách, kromě lokality u Zhůří, jsme našli staré, mohutné (v některých případech dožívající) exempláře bez zjevného zmlazení. Je proto pravděpodobné, že některé z ověřených lokalit v blízké budoucnosti zaniknou. Na většině z nich by byl vhodný managementový zásah, spočívající alespoň ve výřezu okolních, vrbu zastiňujících dřevin. Jako vhodné opatření se také nabízí odběr vzorků všech 9 jedinců a jejich zařazení do genofondových sbírek našich domácích dřevin (např. do VÚKOZ, v. v. i., v Průhonicích).

Z bavorského a hornorakouského pohraničí jsou známy dvě lokality navazující na jihočeský výskyt. Na bavorské straně Šumavy je vrba černající udávána z úpatí Roklanu (Procházka et al. 2001), který je vzdálen asi 15 km od lokalit u Knížecích Plání. Z rakouské části Šumavy existuje údaj z mapovacího čtverce 7450b (okolí města Sankt Stefan am Walde; Kraml & Lindbichler 1997), což je území asi 20 km vzdálené od lokalit u Zadní Zvonkové a Černé v Pošumaví. Současný stav obou lokalit neznáme. V bavorské části Šumavy je druh také vysazován jako okrasná dřevina (např. na parkovišti u centra National Park Bayerischer Wald „Haus zur Wildnis“ v obci Ludwigsthal; not. M. Štech). Jihočeské lokality pravděpodobně s blízkými nalezišti na bavorské Šumavě a v hornorakouském Mühlviertelu souvisejí a mohou mít společný původ (obr. 1). Je pravděpodobné, že při podrobném výzkumu vhodných lokalit zejména na Šumavě budou nalezeny další výskyty.

Poděkování. Děkujeme Správě NP Šumava za umožnění výzkumu v I. zónách a kurátorům herbářových sbírek Národního muzea v Praze (PR) a Univerzity Karlovy v Praze (PRC) za umožnění studia herbářových položek. P. K. a M. Š. byli podpořeni projektem GA ČR č. 14-36079G (Centrum excelence PLADIAS). Publikace byla podpořena z Programu přeshraniční spolupráce Česká republika–Svobodný stát Bavorsko Cíl EÚS 2014– 2020, Interreg V projekt č. 26 „Silva Gabreta Monitoring – Realizace přeshraničního monitoringu biodiversity a vodního režimu“.

LITERATURA

Danihelka J., Chrtek J. jr. & Kaplan Z., 2012: Checklist of vascular plants of the Czech Republic. *Preslia*, 84: 647–811.

Doležel J., Greilhuber J. & Suda J., 2007: Estimation of nuclear DNA content in plants using flow cytometry. *Nature Protocols*, 2: 2233–2244.

Dostál J., 1989: *Nová květena ČSSR. 1, 2* [*New Flora of Czechoslovakia. 1, 2*]. Academia, Praha (in Czech).

Ehrendorfer F. & Hamann U., 1965: Vorschläge zu einer floristischen Kartierung von Mitteleuropa. *Berichte der Deutschen Botanischen Gesellschaft*, 78: 35–50.

Ekrt L., 2013: *Salix myrsinifolia* Salisb. – vrba černající. In: *Červená kniha květeny jižní části Čech* [*Red book of the South Bohemian flora*], Lepší P., Lepší M., Boublík K., Štech M. & Hans V. (eds), Jihočeské muzeum v Českých Budějovicích: 371–372 (in Czech).

Fischer M.A., Oswald K. & Adler W. (ed.), 2008: *Exkursionsflora für Österreich, Liechtenstein und Südtirol. Ed. 3.* OÖ Landesmuseen, Linz, 1391 pp.

Hadinec J. & Lustyk P. (eds), 2007: Additamenta ad floram Reipublicae Bohemicae. VI. [Additions to the flora of the Czech Republic. VI]. *Zprávy České botanické společnosti*, 42: 247–337 (in Czech).

Hadinec J. & Lustyk P. (eds), 2014: Additamenta ad floram Reipublicae Bohemicae. XII. [Additions to the flora of the Czech Republic. XII] *Zprávy České botanické společnosti*, 49: 73–206 (in Czech).

Houfek J., 1952: Studie o květeně Jindřichohradecka se zvláštním zřetelem k Třeboňské pánvi a přilehlým územím (příspěvek k fytogeografii jižních Čech) [Study of the flora of the Jindřichův Hradec region with special regard to the Třeboň Basin and the adjacent area (contribution to phytogeography of South Bohemia)]. Ms., dissertation thesis, Faculty of Science, Charles University, Prague, 398 pp. (in Czech). (Library of the Department of Botany, Faculty of Science, Charles University in Prague)

Hultén E. & Fries M., 1986: *Atlas of North European vascular plants (North of the Tropic of Cancer). Vols. 1–3.* Koeltz Scientific Books, Königstein, 1172 pp.

Chmelař J. & Koblížek J., 1990: *Salicaceae* Mirbel. In: *Květena České republiky 2* [*Flora of the Czech Republic 2*] Hejný S. & Slavík B. (eds), Academia, Praha, 458–495 pp. (in Czech).

Chmelař J., 1966: Vrba černající (*Salix nigricans* SM.), nová botanická vzácnost Šumavy [*Salix nigricans* SM., a new botanical rarity of the Bohemian Forest]. *Zpravodaj Chráněné Krajinné Oblasti Šumava, Plzeň et České Budějovice*, 4: 34–35 (in Czech).

Chytrý M. (ed.), 2007: *Vegetace České republiky. 1. Travinná a keříčková vegetace*. [*Vegetation of the Czech Republic 1. Grassland and heathland vegetation*]. Academia, Praha, 528 pp. (in Czech).

Chytrý M. (ed.), 2011: *Vegetace České republiky. 3. Vodní a mokřadní vegetace*. [*Vegetation of the Czech Republic 3. Aquatic and wetland vegetation*]. Academia, Praha, 828 pp. (in Czech).

Kraml P.A. & Lindbichler N., 1997: Kartierungsergebnisse des 7. südböhmisch-oberösterreichischen Botanikertreffens im Böhmerwald, 8.–14. Juli 1996. *Beitrage Naturkunde Oberösterreichs*, 5: 235–304.

Kučera S., 1992: Floristické údaje z terénního průzkumu jižních Čech (exkurzní deníky) [Floristic records from the field research of South Bohemia (field notebooks)]. Ms., Field notebooks no. 1971/4: p. 50; 1974/34: p. 48; 1974/36: p. 7; 1975/8: p. 20; 1977/7: p. 10 and 18; 1983/2 p. 61 and 67 (in Czech). (deposited in the South Bohemian Museum in České Budějovice)

Kurka R., 1959: Příspěvek ke květeně Třeboňské rybniční pánve [Contribution to the flora of the Třeboň Basin]. *Sborník Krajského Vlastivědného Muzea, Přírodní Vědy*, 2: 75–83 (in Czech).

Lauber K., Wagner G. & Gygax A., 2018: *Flora Helvetica – Illustrierte Flora der Schweiz*. Haupt Verlag, Bern, 813 pp.

Lepší M. & Lepší P., 2004: Fytogeograficky významné, ohrožené a vzácné rostliny [Phytogeographical important, endangered and rare plants]. In: *Biota Novohradských hor: modelové taxony, společenstva a biotopy* [*Biota of the Novohradské hory Mountains: model taxa, communities and biotopes*], Papáček M. (ed.), Jihočeská univerzita, České Budějovice: 80–90 (in Czech).

Lepší M., Lepší P. & Boublík K., 2007: Květena národní přírodní rezervace Žofínský prales [Flora of the Žofínský Prales National Nature Reserve]. *Silva Gabreta*, 13: 15–37 (in Czech).

Lepší P., Lepší M., Boublík K., Štech M. & Hans V. (eds), 2013: *Červená kniha květeny jižní části Čech*. [*Red book of South Bohemian flora*]. Jihočeské muzeum v Českých Budějovicích, 503 pp. (in Czech).

Mirski P., 2016: Spatio-temporal dynamics of sex structure in trioecious and dioecious populations of *Salix myrsinifolia*. *Folia Geobotanica*, 51: 39–49.

Procházka F., 1990: *Chráněné a ohrožené rostliny prachatického okresu*. [*Protected and endangered plants of the Prachatice district*]. Okresní muzeum, Prachatice, 70 pp. (in Czech).

Procházka F., Hadinec J. & Havlíček P., 2001: Příspěvek ke květeně české Šumavy a kontaktních území. [Contribution to the flora of the Czech part of the Bohemian Forest and adjacent areas]. *Zprávy České Botanické Společnosti*, 35 (2000): 173–180 (in Czech).

Rechinger K.H., 1964: *Salix* L. In: *Flora Europaea*, Tutin T.G., Heywood V.H., Burges N.A., Valentine D.H., Walters S.M. & Webb D.A. (eds) Cambridge University Press, Cambridge: 43–54.

Skalický V., 1988: Regionálně-fytogeografické členění [Regional phytogeographical division]. In: *Květena České republiky 1* [*Flora of the Czech Republic 1*], Hejný S. & Slavík B. (eds) Academia, Praha: 103–121 pp. (in Czech).

Skvortsov A.K., 1999: *Willows of Russia and adjacent countries. Taxonomic and Geographic Revision*. Joensuu University Press, Joensuu, 307 pp.

Slavík B., 1990: *Fytokartografické syntézy ČR 2*. [*Phytogeographical synthesis of the Czech Republic 2*]. Botanický ústav ČSAV, Průhonice (in Czech).

Thiers B., 2018: Index Herbariorum: a global directory of public herbaria and associated staff. New York Botanical Garden's Virtual Herbarium. http://sciweb.nybg.org/science2/IndexHerbariorum.asp (accessed in January 2018).

Uotila P., 2011: *Salicaceae***.** In: Euro+Med PlantBase – the information resource for Euro-Mediterranean plant diversity. URL: http://ww2.bgbm.org/EuroPlusMed/ (accessed August 2018).

Wagenitz G., 1981: *Salix* L. In: *Gustav Hegi, Illustrierte Flora von Mitteleuropa*, Conert H.J., Hamann U., Schultze-Motel W. & Wagenitz G. (eds) Verlag Paul Parey, Berlin & Hamburg, Ed. 3, Vol. III/2: 44–135.

Received: 16 March 2018
Accepted: 18 September 2018

Silva Gabreta	vol. 24	p. 245–249	Vimperk, 2018

Window gnats (Diptera: Anisopodidae) of the Czech part of the Bohemian Forest

Libor Dvořák

Municipal Museum Mariánské Lázně, Goethovo náměstí 11, CZ-35301 Mariánské Lázně, Czech Republic
lib.dvorak@seznam.cz

Abstract
A three-week survey of window gnats was performed in the Šumava National Park in June 2016 and all records of Anisopodidae from the Czech part of the Bohemian Forest (Šumava) were summarised. Altogether the data to six species in 187 specimens of Anisopodidae were analysed. The record of *Sylvicola fenestralis* (Scopoli, 1763) was the first finding for the Bohemian Forest. The studied area has the highest diversity of Anisopodidae in the Czech Republic.

Key words: distribution, faunistics, new records, Šumava Mountains

INTRODUCTION

Window gnats (Diptera: Anisopodidae) of the Šumava National Park and Protected Landscape Area (NP and PLA) in the Bohemian Forest (Šumava in Czech) have not been systematically studied yet. Ševčík (2004) published the record of the rarest Czech species, *Sylvicola limpidus* (Edwards, 1923). Later on, Dvořák (2014b) reported the presence of *S. cinctus* (Fabricius, 1787), *S. punctatus* (Fabricius, 1787), and *S. zetterstedti* (Edwards, 1923).

In 2016, beer traps were placed on the territory of the Šumava NP and PLA for the purpose of faunistic study of window gnats. The results of this trapping survey are published in this study together with other published and unpublished data.

MATERIAL AND METHODS

Twelve localities were studied in this survey using beer traps. They covered typical habitats (open, semiopen, forested) in the altitudes 785–1305 m a.s.l. in the Bohemian Forest, on the whole area of the Šumava NP, including its current buffer zone (Šumava PLA till 2016, Fig. 1). All the traps were managed by T. Lorenc and these sites are arranged as follows: locality – code of the mapping square, habitat, altitude, GPS coordinates, and dates of installation and recovery.

Vysoké Lávky – 6846, sedge meadow, 835 m, 49°7'48.698" N, 13°22'39.522" E, 9–28 Jun 2016.

Poledník – 6946, forest-free area on the top of Poledník Mt., 1305 m, 49°3'52.561" N, 13°23'42.597" E, 9–28 Jun 2016.

Staré Srní – 6946, wet meadow with willow shrubs, 840 m, 49°5'4.468" N, 13°28'38.687" E, 9–28 Jun 2016.

Filipova Huť – 6947, meadow with bushes, 1110 m, 49°1'51.039" N, 13°31'16.926" E, 7–28 Jun 2016.

Svinná Lada – 6947, Chalupská Slať peat-bog, peat-bog margin, 925 m, 49°0'7.668" N, 13°39'1.655" E, 8–28 Jun 2016.

Březník – 7046, dead spruce forest, 1140 m, 48°58'6.580" N, 13°29'11.399" E, 7–28 Jun 2016.

Bučina – 7047, montane meadow, 1175 m, 48°58'14.218" N, 13°35'53.094" E, 8–28 Jun 2016.

Strážný – 7048, alderwood by a small pond W of the village, 830 m, 48°54'57.431" N, 13°43'12.978" E, 8–28 Jun 2016.

Polka – 7048, wet meadow by a stream, 835 m, 48°56'42.918" N, 13°42'35.940" E, 8–28 Jun 2016.

Volary – 7049, bushes behind a gas station, 785 m, 48°54'36.065" N, 13°52'20.120" E, 8–28 Jun 2016.

České Žleby – 7148, forest margin, 875 m, 48°53'29.563" N, 13°47'52.967" E, 8–28 Jun 2016.

Nová Pec – 7249, Plechý Mt., light gap in montane mixed forest, 1050 m, 48°47'11.936" N, 13°51'43.413" E, 8–28 Jun 2016.

The used beer traps were very simple: a PET bottle of 1.5–2 litres was filled with 0.5 litre of lager beer. The opened traps were hung on a branch of tree or shrub and exposed at the localities studied (Fig. 1). The traps were emptied after ca. three weeks. For more details see Dvořák (2014a,b).

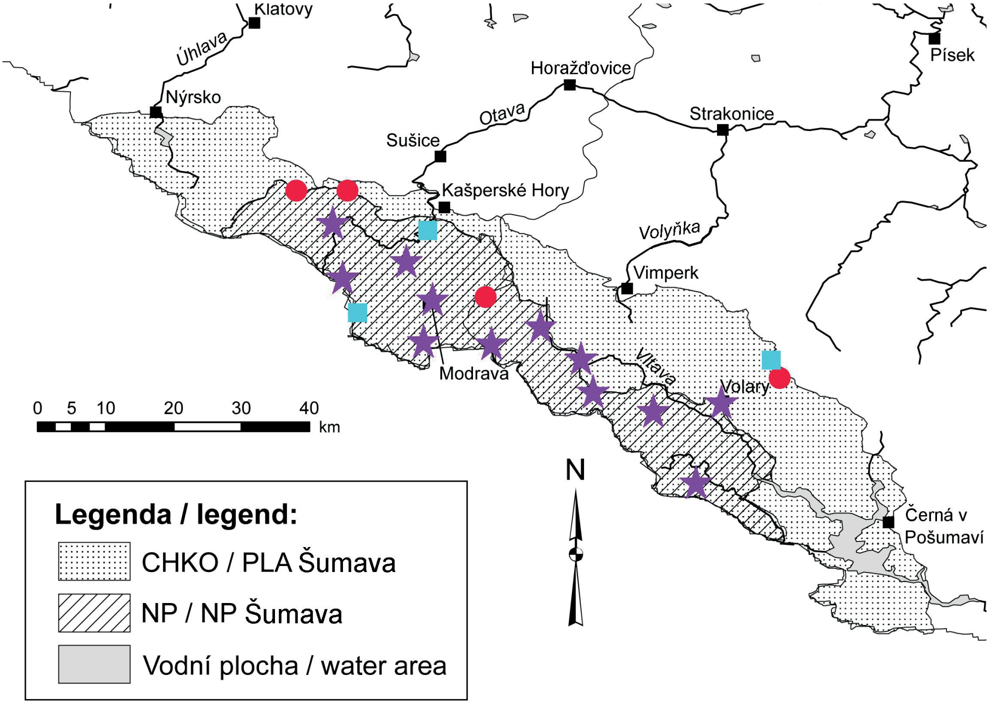

Fig. 1. All localities of Anisopodidae known from the territory of the Šumava NP and PLA in the Bohemian Forest. Violet stars: beer traps in 2016 (present survey); red circles: published records; blue squares: other unpublished records.

The material was identified using Haenni (1997) and Söli & Rindal (2014). The voucher specimens are deposited in the collections of the Municipal Museum Mariánské Lázně, Czech Republic, if not stated otherwise.

Results

Altogether five species and 66 specimens of window gnats were collected during the survey in June 2016 and records of other three specimens from previous studies are presented. Here we present these records along with all available data. All records are arranged as follows: (i) localities of systematic study using beer traps are named according to the list in Material and methods chapter and (ii) randomly received material locality – code of the mapping square, other collecting information provided by the collector, number of ♂♂ and/or ♀♀, collector.

Sylvicola cinctus (Fabricius, 1787)

Published data

Nová Hůrka – 6845; Rovina – 6846 (Dvořák 2014b).

New records

Poledník, 1 ♂, 12 ♀♀. Staré Srní, 1 ♂, 4 ♀. Filipova Huť, 3 ♀♀. Svinná Lada, 2 ♀♀. Březník, 1 ♂, 9 ♀♀. Strážný, 3 ♀♀. Polka, 1 ♀. Volary, 6 ♀♀. České Žleby, 2 ♀♀. Nová Pec, 2 ♀♀.

In the studied area, this species prefers semi-open to forested habitats and was caught in 785–1305 m a.s.l. Dvořák (2014a) considered *S. cinctus* as a eurytopic species and Dvořák (2014b) noted the species to be often found in forests, while it seems rather rare in open stands.

Sylvicola fenestralis (Scopoli, 1763)

New records

Volary, 2 ♂♂, 1 ♀.

This species is such rarely collected in the Czech Republic that no habitat preferences could be stated.

Sylvicola fuscatus (Fabricius, 1775)

New records

Poledník, 1 ♂. Volary, 1 ♀.

Two records from open and semi-open stands confirmed the preference of similar stands, as Dvořák (2014a) has been published.

Sylvicola limpidus (Edwards, 1923)

Published data

Jezerní Slať peat-bog – 6947 (Ševčík 2004).

The only record is known from the very cold mountain peat-bog.

Sylvicola punctatus (Fabricius, 1787)

Published data

Nová Hůrka – 6845; Rovina – 6846; Spálenec – 7049 (Dvořák 2014b).

Table 1. Overview of Anisopodidae specimens from both the published and unpublished sources known from the Bohemian Forest (Šumava NP and PLA).

Species	**Published**	**Unpublished**	**Total**	**%**
S. cinctus	28 ♂♂, 58 ♀♀	3 ♂♂, 44 ♀♀	31 ♂♂, 102 ♀♀	71.1
S. fenestralis	–	2 ♂♂, 1 ♀	2 ♂♂, 1 ♀	1.6
S. fuscatus	–	1 ♂, 1 ♀	1 ♂, 1 ♀	1.1
S. limpidus	1 ♂	–	1 ♂	0.5
S. punctatus	9 ♂♂, 19 ♀♀	5 ♂♂, 11 ♀♀	14 ♂♂, 30 ♀♀	23.5
S. zetterstedti	3 ♂♂	1 ♂	4 ♂♂	2.1
Total	41 ♂♂, 77 ♀♀	12 ♂♂, 57 ♀♀	53 ♂♂, 134 ♀♀	100.0

New records

Vysoké Lávky, 1 ♀. Bučina, 1 ♂, 8 ♀♀. Strážný, 1 ♀. Volary, 2 ♂♂.

Svojše – 6846, Dračí Skály rocks, 14–15 May 2015, light trap, 1 ♂, P. Heřman, leg.

Modrava – 6946, Rokytecká Nádrž dam, 16 Jun 2014, 1 ♀, J. Máca, leg. et coll.

Spálenec – 7049, 800 m, 48°56' N, 13°57' E, 10 Jul 1988, light trap, 1 ♂, M. Barták leg. et coll.

This species was recorded in open to semi-open stands only (as in Dvořák 2014a) in ca. 800–1305 m a.s.l. Dvořák (2014b) noted the species to be predominant in forests and very commonly found (more than 90%) in open stands.

Sylvicola zetterstedti (Edwards, 1923)

Published data

Nová Hůrka – 6845; Rovina – 6846 (Dvořák 2014b).

New records

Poledník, 1 ♂.

This species was first recorded in the Czech Republic by Dvořák (2014a). In the Bohemian Forest, the species was caught on two semi-open wet stands at ca. 900 m a.s.l. and on a deforested top area at 1305 m a.s.l.

Overall results

The data of four species in 118 specimens were published from the Šumava NP and PLA and the data of five species in 69 specimens are newly published in this study. Altogether the data of six species in 187 specimens of Anisopodidae were analysed. Two species were eudominant: *S. cinctus* with 71.1% and *S. punctatus* with 23.5% of all specimens; the other four species were represented by 0.5–2.1% of specimens (Table 1).

From the new material, a single species was recorded on 12 localities and two species on one locality. In three cases, three species were caught on one locality; *S. cinctus* and *S. zetterstedti* were recorded in all three cases (Nová Hůrka, Poledník, Rovina). On the locality Volary, four species were caught: *S. cinctus*, *S. fenestralis*, *S. fuscatus*, and *S. punctatus*. One new locality of *S. zetterstedti* and the first records of *S. fenestralis* and *S. fuscatus* are the most interesting results of this survey.

Conclusions

Six species of the family Anisopodidae have been recorded from the Czech Republic (Ševčík 2009, Dvořák 2014a) and all of them are recently known from the Bohemian Forest, with the new records of *S. fenestralis* and *S. fuscatus* in the present study. Thus this area has the highest biodiversity of Anisopodidae in the Czech Republic. In comparison, five species are known from the high altitudes of the Giant Mts. (Krkonoše Mts.) (Ševčík et al. 2009), from the Jizerské Hory Mts. and Ještědský Hřbet ridge (Dvořák & Vonička 2015).

Acknowledgements. The author wishes to thank T. Lorenc (Šumava NP, Kašperské Hory) for managing the traps in 2016, and M. Barták (Czech University of Life Sciences, Prague) and J. Máca (Veselí nad Lužnicí) for the possibility to study their material. The publication was supported by the Cross-border cooperation programme Czech Republic–Bavaria Free State ETC goal 2014–2020, the Interreg V project No. 26 "Silva Gabreta Monitoring – Implementation of Transboundary Monitoring of Biodiversity and Water Regime".

References

Dvořák L., 2014a: Window gnats (Diptera: Anisopodidae) from beer traps in the vicinity of Mariánské Lázně with the first records of *Sylvicola zetterstedti* (Edwards, 1923) from the Czech Republic. *Mitteilungen der Schweizerischen Entomologischen Gesellschaft*, 87: 41–48.

Dvořák L., 2014b: Window gnats (Diptera: Anisopodidae) from beer traps in various countries across Europe. *Mitteilungen der Schweizerischen Entomologischen Gesellschaft*, 87: 247–254.

Dvořák L. & Vonička P., 2015: Stružilky (Diptera: Anisopodidae) Jizerských hor a Ještědského hřbetu (severní Čechy) [Window gnats (Diptera: Anisopodidae) of the Jizerské hory Mts and Ještědský hřbet Ridge (northern Bohemia)]. *Sborník Severočeského Muzea, Přírodní Vědy*, 33: 199–203 (in Czech, English abstract).

Haenni J.P., 1997: Anisopodidae (Diptera) de la faune de Suisse, avec la description d'une espèce nouvelle. *Mitteilungen der Schweizerischen Entomologischen Gesellschaft*, 70: 177–186.

Söli G. & Rindal E., 2014: The genus *Sylvicola* Harris, 1780 (Diptera, Anisopodidae) in Norway – with a key to the North European species. *Norwegian Journal of Entomology*, 61: 190–200.

Ševčík J., 2004: Faunistic records from the Czech and Slovak Republics: Diptera. Anisopodidae. *Folia Facultatis Scientiarum Naturalium Universitatis Masarykianae Brunensis, Biologia*, 109: 323–324.

Ševčík J., 2009: Anisopodidae Edwards, 1921. In: *Checklist of Diptera of the Czech Republic and Slovakia,* Jedlička L., Stloukalová V. & Kúdela M. (eds) Electronic version 2. http://www.edvis.sk/diptera2009 + CD-ROM: ISBN 978-80-969629-4-5.

Ševčík J., Barták M. & Vaněk J., 2009: Dvoukřídlí (Diptera) čeledí Anisopodidae (stružilkovití), Mycetobiidae a Dixidae (komárcovití) vysokých poloh Krkonoš (Česká republika) [Flies (Diptera) of the families Anisopodidae, Mycetobiidae and Dixidae of high altitudes of the Krkonoše Mts. (Czech Republic)]. *Opera Corcontica*, 46: 159–163 (in Czech, English abstract).

Received: 25 September 2017
Accepted: 1 February 2018

Silva Gabreta	vol. 24	p. 251–256	Vimperk, 2018

The first record of the rare beetle *Phloeostichus denticollis* W. Redtenbacher, 1842 (Coleoptera: Phloeostichidae) from the Bohemian Forest with a note on the biology of the species

Jiří Procházka[1,2,3,*] **& Jiří Schlaghamerský**[2]

[1]*Silva Tarouca Research Institute, Lidická 25/27, CZ-60200 Brno, Czech Republic*
[2]*Faculty of Science, Masaryk University, Kotlářská 2, CZ-61137 Brno, Czech Republic*
[3]*Moravian Museum, Hviezdoslavova 29a, CZ-62700 Brno, Czech Republic*
[*] jiri.prochazka@mail.muni.cz

Abstract

The presence of the endangered beetle *Phloeostichus denticollis* was confirmed at two sites (Liščí Hřbety near Kubova Huť and Zátoňská Hora Nature Reserve) in the Bohemian Forest (Šumava in Czech, Böhmerwald in German), Czechia. In total four individuals were captured by peeling the bark of sycamore maples. These are the first published records of *P. denticollis* from western and southern Bohemia. They confirm the importance of old sycamore maples for this rare species and suggest its possible association with the fungus *Hymenochaete carpatica*.

Key words: Coleoptera, *Phloeostichus denticollis*, faunistics, Šumava Mts., Czech Republic

INTRODUCTION

Phloeostichus denticollis W. Redtenbacher, 1842 is a rare species reported mainly from Europe (KOLIBÁČ 2003, VOGT 1967). It has been recorded in France (ROSE & CALLOT 2007), Germany (REIBNITZ 1987, KLAUSNITZER 2002), Denmark (STOLTZE & PIHL 1998), Poland (KUBISZ et al. 1998), Czechia (KOLIBÁČ 2003), Slovakia (FRANC 2002), Switzerland, Italy, and Romania (HORION 1960). *P. denticollis* is known also from the Caucasus (NIKITSKY 1991) and from the Sikhotealin Range in eastern Siberia (KRIVOLUSHKAYA 1992). From Czechia, *P. denticollis* has been reported from the mountain ranges of the Moravskoslezské Beskydy Mts. (NOHEL 1970, KOLIBÁČ 2003, KULA 2009, WEISS et al. 2016), Slezské Beskydy Mts. (Schlesische Beskiden in German; Wanka 1920), Orlické Hory Mts. (MACKOVČIN et al. 2002), the Broumovsko Protected Landscape Area, including the Čáp mount (Storchberg in German; GERHARDT 1910, HAMET & VANCL 2016), the Hrubý Jeseník Mts. (Altvatergebirge in German), and the Kralický Sněžník Mts. (Glatzer Schneegebirge in German; GERHARDT 1910, HORION 1960). Nearby finds across the border of Czechia have been reported from Wolibórz (Volpersdorf), the Góry Stołowe Mts. (Heuscheuergebirge in German) and the Góry Sowie (Bögenberge in German) near Świdnica in Poland (GERHARDT 1910, HORION 1960), from several sites in the Bavarian Forest National Park in Germany (MÜLLER et al. 2007), and from one site in the Gratzener Bergland Mts. in Austria (MITTER 1998). So far, there were no published records from the Czech part of the Bohemian Forest (Šumava in Czech) or, more generally, from western and southern Bohemia. The bionomy of the species is still unknown. Adults are rarely found under the bark scales of living sycamore maples in well-preserved beech–fir forests (Vávra 2017). *P. denticollis* is classified as endangered in the Czech red list (Vávra 2017).

Material and methods

Study sites

The site of Liščí Hřbety (nearby Kubova Huť village, Kubohütten in German, 1014 m a.s.l., 48°59' N, 13°43' E, Fig. 1) is situated in an old-growth beech-dominated forest interspersed with silver fir (*Abies alba* Mill.), Norway spruce (*Picea abies* L.), and sycamore maple (*Acer pseudoplatanus* L.). The vegetation was classified following Chytrý (2013) as a mesotrophic beech forest (*Galio odorati-Fagetum sylvaticae* Sougnez et Thill 1959).

The Zátoňská Hora Nature Reserve (nearby the village of Zátoň, 976 m a.s.l., 48°57' N, 13°50' E) is situated in an old-growth beech-dominated forest interspersed with Norway spruce (*Picea abies* L.) and sycamore maple (*Acer pseudoplatanus* L.). Vegetation was classified following Chytrý (2013) as a eutrophic beech forest (*Mercuriali perennis-Fagetum sylvaticae* Scamoni 1935). The site was surveyed for the occurrence of selected ground beetle taxa by Linhart et al. (2015), but a thorough inventory of beetle fauna in the nature reserve is lacking.

Sampling methods

Peeling of sycamore (*Acer pseudoplatanus* L.) bark was used in a targeted search for the given species. Five flight interception traps were also placed at each of the two sites to collect saproxylic beetle fauna, but no *P. denticollis* specimen was captured using this method.

Results and discussion

We found four adults of *Phloeostichus denticollis* W. Redtenbacher, 1842 (Fig. 2) – Liščí hřbety: 8 June 2017, 1 specimen; 30 August 2017, 2 specimens; Zátoňská hora: 28 August 2017, 1 individual; leg. et det. J. Procházka. All specimens were collected between one and two metres above ground under the bark scales on trunks of old living trees of *Acer pseudoplatanus* in old-growth forests. Beetles are deposited in the Moravian Museum, Brno. At the Liščí Hřbety site, the fungus *Hymenochaete carpatica* Pilát 1930 from the order Hymenochaetales (leg. et det. J. Běťák) was found under bark scales on the same maple tree as *P. denticollis*.

The present records of *Phloeostichus denticollis* are the first ones from the Czech side of the Bohemian Forest (Šumava), although some entomologic surveys have been conducted in the area (e.g. Heyrovský 1923, Fleischer 1925, Boháč & Matějíček 2004, Máca 2008). However, this rare beetle is known from Bayerischer Eisenstein, Albrechtschachten, Rachel, and Ruckowitzschachten at the Bavarian part of the mountain range (Horion 1960, Müller et al. 2007). There are no published records from the Upper Austrian part of the Bohemian Forest (Böhmerwald in German), but there is one from Rosenhof (Mitter 1998) in the Austrian part (Freiwald) of the Gratzener Bergland Mts. (Novohradské Hory in Czech), adjacent to the southeast. Most of the Austrian records are from the Alps (Horion 1960, Mitter 1998).

The bionomy of *P. denticollis* is unknown (Jelínek 2005). What is known is that it occurs under the bark scales of old living trees of *Acer pseudoplatanus* and rarely under the bark of *Fagus sylvatica* or under mosses covering trunks of these species (Horion 1960, Vogt 1967). Rose & Callot (2007) mentioned a find of *P. denticollis* under the bark of fir in Slovakia,

Fig. 1. Old sycamore maple (*Acer pseudoplatanus*), on which *Phloeostichus denticollis* was found at the site of Liščí Hřbety in August 2017.

Mitter (1998) reported a find under the bark of larch in Austria. In our study, surprisingly, no individual was captured by flight interception traps operated in 2017 at these and several similar sites in the area, even though some individuals of *P. denticollis* have been collected by this trap type elsewhere (e.g. Dodelin 2005, Müller et al. 2007, Rose & Callot 2007, Weiss et al. 2016). It was assumed that the beetle is active in winter or that it lives on sycamore in winter and on beech in summer (J. Vávra – pers. comm.). Our finding of living beetles in the late spring and summer together with the above-mentioned captures using flight interception traps and some of the records presented by Horion (1960) show that the species is active during the vegetation season. Though adult beetles were mostly found overwintering under the sycamore bark scales, a trophic connection with sycamore maple is uncertain (J. Vávra – pers. comm.). Dodelin (2005) speculated about the connection of *P. denticollis* with decaying beech, but maples were also present at the locality. As his only individual was found in a window trap, no direct information about the biology of this species could be obtained (Dodelin 2005).

Our finding of *P. denticollis* under bark scales together with the fungus *Hymenochaete carpatica* suggests a possibility that the beetle might be feeding on its mycelia. However, further research is needed to learn about the feeding biology of *P. denticollis*. The fungus *Hymenochaete carpatica* is an inconspicuous, often overlooked species. It grows only on the bark scales of old live *Acer pseudoplatanus* and has not been found on any other host (Tomšovský 2001). Describing the bionomy of *P. denticollis* might prove difficult, as larvae are extremely rare and hard to identify (J. Kolibáč – pers. comm.). For instance, the larval specimen found by Crowson in Slovenia and used in the interactive key by Lawrence et al. (1999), as well as the two larvae described as *P. denticollis* by Kolibáč (2003), were considered to be misidentified (Leschen et al. 2005). Larvae were described briefly by Weise (1897) from specimens collected from mossy bark of old maple trees. Morphological chara-

Fig. 2. *Phloeostichus denticollis* W. Redtenbacher, 1842, Zátoňská Hora Nature Reserve, August 2017.

cters of the larva, collected by N.B. Nikitsky under the bark of maple, were described and compared with other Phloeostichidae by Leschen et al. (2005).

Acknowledgements. We thank Jan Běťák for the identification of *Hymenochaete carpatica* and Jiří Vávra and Dominik Vondráček for help with gathering some literature records. The Administration of the Šumava National Park and the Forests of the Czech Republic, state enterprise, permitted us to work in the forest and nature reserve under their direction. This paper was partly supported by a grant of the Ministry of Culture of the Czech Republic to the Moravian Museum, Brno (ref. MK000094862) and by Institutional subsidy VUKOZ-IP-00027073. The publication was supported by the Cross-border cooperation programme Czech Republic–Bavaria Free State ETC goal 2014–2020, the Interreg V project No. 26 "Silva Gabreta Monitoring – Implementation of Transboundary Monitoring of Biodiversity and Water Regime".

References

Alexander K.N.A., 2004: Revision of the index of ecological continuity as used of saproxylic beetles. *English Nature Research Reports*, Peterborough, 60 pp.

Boháč J. & Matějíček J., 2004: Beetle assemblages on the monitoring plots of the Boubín massive in the Bohemian Forest and perspectives of long term monitoring of biotopes state. In: *Aktuality šumavského výzkumu II*, Dvořák L. & Šustr P. (eds) Vimperk: 212–217.

Dodelin B., 2005: Nouvelle station française du rare *Phloeostichus denticollis* Redt., coléoptères associé au bois mort en hętraie-érablaie (Phloeostichidae). *Bulletin Romand d'Entomologie*, 23: 49–55.

Fleischer A., 1925: Zajímavé nálezy brouků na Šumavě [Important findings of beetles in the Šumava Mts.]. *Časopis Československé Společnosti Entomologické*, 22: 21.

Franc V., 2002: Beetles (Coleoptera) of the Veľká Fatra Mts. with special reference to bioindicatively significant species. *Matthias Belivs University Proceedings*, Suppl. 2: 165–177.

Gerhardt J., 1910: *Verzeichnis der Käfer Schlesiens preußischen und österreichischen Anteils, geordnet nach dem Catalogus coleopterorum Europae vom Jahre 1906. Dritte, neubearbeitete Auflage*. Julius Springer, Berlin, 431 pp.

Hamet A. & Vancl Z., 2016: Catalogue of the beetles (Coleoptera) of the Broumovsko Protected Landscape Area. Second completed and corrected edition. *Elateridarium* 10 (Supplementum), 137 pp.

Heyrovský L. 1923: Příspěvek k poznání fauny šumavských Coleopter [Contribution to the knowledge of beetle fauna in the Bohemian Forest]. *Časopis Národního Musea, Řada Přírodovědná*, 97: 35–36.

Horion A., 1960: *Faunistik der mitteleuropäischen Käfer. Bd. VII. Clavicornia 1. (Sphaeritidae bis Phalacridae).* A. Feyel, Überlingen-Bodensee, 346 pp.

Chytrý M. (ed.), 2013: *Vegetation of the Czech Republic 4. Forest and scrub vegetation*. Academia, Praha, 551 pp.

Jelínek J., 2005: Phloeostichidae. In: *Red list of threatened species in the Czech Republic. Invertebrates,* Farkač J., Král D. & Škorpík M. (eds) Agentura ochrany přírody a krajiny ČR, Praha: 491.

Klausnitzer B., 2002: *Phloeostichus denticollis* Redtenbacher, 1842 neu für Sachsen (Col., Phloeostichidae). *Entomologische Nachrichten und Berichte*, 46: 195.

Kolibáč J., 2003: Description of a larva of *Phloeostichus denticollis* Redtenbacher, 1842 (Coleoptera, Phloeostichidae). *Entomologica Basiliensia*, 25: 135–140.

Kubisz D., Kuśka A. & Pawlowski J., 1998: *Red list of Upper Silesian beetles (Coleoptera).* Centrum Dziedzictwa Przyrody Górnego Ślaska, Katowice, 62 pp.

Krivolushkaya G.O., 1992: Family Cucujidae. In: *Key to the insects of the Far East of the USSR in six volumes. Volume III. Beetles, Part 2*, Ler P.A. (ed.) Nauka, St. Petersburg, Russia: 233–245 (in Russian).

Kula E., 2009: Možnosti užití zoocenózy bezobratlých k bioindikaci relativně trvalých ekologických podmínek smrkových a bukových ekosystémů Moravskoslezských Beskyd [The use of invertebrate zoocenose for bioindication of relatively persistent ecological conditions of spruce and beech ecosystems in the Moravian-Silesian Beskids]. Ms., unpubl. report, Pilotní projekt pro grantovou agenturu NAZV, 28 pp. (in Czech). (deposited in the library of the Mendel University, Brno)

Lawrence J.F., Hastings A.M., Dallwitz M.A., Paine T.A. & Zurcher E.J., 1999: *Beetles of the World. A key and information system for families and subfamilies*. CD-ROM, Version 1.0 for MS-Windows, CSIRO Publishing, Melbourne, Australia.

Leschen R.A.B., Lawrence, J.F. & Slipiński, S.A., 2005: Classification of basal Cucujoidea (Coleoptera: Polyphaga), with a cladistic analysis, description of new genera and species, and keys to adults and larvae of cucujoid families. *Invertebrate Systematics*, 19: 17–73.

Linhart M., Vonička P., Moravec P. & Veselý P., 2014: Results of survey of the occurrence of selected ground beetle taxa (Coleoptera: Carabidae) in the Bohemian Forest Mts in 2011 and 2012 and summary of the previous knowledge. *Západočeské Entomologické Listy*, 6: 69–135.

Máca J., 2008: Interesting findings of beetles (Coleoptera) and dipterous insects (Diptera) in the southeastern part of the Bohemian Forest and its environs. *Silva Gabreta*, 14: 179–186 (in Czech with English abstract).

Mackovčin P., Sedláček M. & Faltysová H. (eds), 2002: *Chráněná území ČR. Svazek V., Královéhradecko* [*Protected areas of the Czech Republic, volume V, Hradec Králové region*]. Agentura ochrany přírody a krajiny ČR, Praha, 409 pp. (in Czech).

Mitter H., 1998: Bemerkenswerte Käferfunde aus Oberösterreich V (Insecta: Coleoptera). *Die Beiträge zur Naturkunde Oberösterreichs*, 6: 11–29.

Müller J., Bußler H., Goßner M., Gruppe A., Jarzabek-Müller A., Preis M. & Rettelbach T., 2007: Forest edges in the mixed-montane zone of the Bavarian Forest National park – hot spots of biodiversity. *Silva Gabretta*, 13: 1–27.

Nikitsky N.B., 1991: News on the genus *Triphylli*a Reitter, 1898 (Coleoptera, Tetratomidae). *Elytron*, 5: 159–168.

Nohel P., 1970: A contribution to the knowledge of Coleoptera in Czech Silesia. *Acta Rerum Naturalium Musei Nationalis Slovaci Bratislava*, 16: 127–139.

Reibnitz J., 1987: Dorcatoma-Funde (Col., Anobiidae) aus Baden-Württemberg. *Mitteilungen des Entomologischen Vereins Stuttgart*, 22: 99.

Rose O. & Callot H., 2007: Redécouverte de *Phloeostichus denticollis* Redtenbacher, 1842 dans le massif des Vosges (France) (Coleoptera Phloeostichidae). *L'Entomologiste*, 63: 129–133.

Stoltze M. & Pihl S., 1998: *Redliste 1997 over planter og dyr i Danmark*. Miljø- og Energiministeriet, Danmarks Miljøundersøgelser Skov- og Naturstyrelsen, 219 pp.

Tomšovský M., 2001: Remarks on the distribution of *Hymenochaete carpatica* in Central and Eastern Europe. *Czech Mycology*, 53: 141–148.

Vávra J., 2017: Phloeostichidae. In: *Red list of threatened species in the Czech Republic. Invertebrates*, Hejda R., Farkač J., Chobot K. (eds) Edition 36: 397.

Vogt H., 1967: Cucujidae. In: *Die Käfer Mitteleuropas, Band 7: Clavicornia*, Freude H., Harde K.W. & Lohse G.A. (eds) Goecke & Evers, Krefeld: 83–104.

Wanka T., 1920: Dritter Beitrag zur Coleopterenfauna von Österreich-Schlesien. *Entomologische Blätter*, 16: 202–213.

Weise J., 1897: Biologische Mitteilungen. *Deutsche Entomologische Zeitschrift*, 1897: 389–395.

Weiss M., Procházka J., Schlaghamerský J., Čížek L., 2016: Fine-scale vertical stratification and guild composition of saproxylic beetles in lowland and montane forests: similar patterns despite low faunal overlap. *PLoS ONE,* 11(3): e0149506.

Received: 10 March 2018
Accepted: 18 June 2018

Silva Gabreta	vol. 24	p. 257–258	Vimperk, 2018

In memoriam Tomáš Soldán
*9 November 1951 – †13 August 2018

An outstanding entomologist Tomáš Soldán passed away in August 2018 after a short and unexpected illness at the age of 67. Tomáš travelled around the world, yet the Bohemian Forest was his most favourite landscape close to his heart, which he liked to visit and explore. His work significantly contributed to the knowledge of biodiversity of aquatic biotopes in the Bohemian Forest. He even named a new mayfly, considered as endemic species, *Ecdyonurus silvaegabretae*, in honour of these mountains.

Tomáš was born in Prague and, since his childhood, he was fascinated by insects, especially butterflies and beetles. That is why his study of systematic zoology and entomology at the Charles University was predestined. During his studies, he met important personalities of the Czech entomology who significantly influenced his next career. After graduation in 1975, he joined the Entomological Institute of the Czechoslovak Academy of Sciences, where he worked for 43 years of his professional life. Together with his mentor, Vladimír Landa, he studied the mayflies (Ephemeroptera) in the broadest sense, from morphology and taxonomy to ecology and faunistics. He has become a world-renowned and leading researcher of Ephemeroptera, whose work culminated in the opus magnum, The Mayflies of Europe (2012), written together with his friend Ernst Bauernfeind. Tomáš described more than 70 species of mayflies, while nine other species of aquatic insects were described by foreign colleagues in his honour and bear the patronymic name *soldani*. Nevertheless, his scientific scope was much wider. He dealt with the development and ultrastructure of insect gonads, influences of biologically active substances on insect reproduction, or participated in the development of the method of sterilization of male tse-tse flies, which was applied in several African countries. His footprint was also tracked in the field of hydrobiology, as he conducted long-term research of the biodiversity of streams in the Czech Republic and worked in several projects dealing with the assessment of the ecological status of streams.

After moving to České Budějovice in 1979, Tomáš became more intensely engaged in the research of aquatic ecosystems in South Bohemia and the Bohemian Forest. Since 1991, he also was one of the first lecturers at the newly founded Faculty of Science of the University of South Bohemia. His long-term study of aquatic insects in various aquatic habitats in the Bohemian Forest and elsewhere brought the knowledge on biodiversity and species distribution and, in particular, unique data for evaluating long-term changes in biodiversity of streams and lakes. These data have been increasingly valuable over time as they describe aquatic biotopes prior to recent anthropogenic interventions. As one of the first scientists, he participated in long-term research on the recovery of the Bohemian Forest lakes from acidification, which currently benefits from historical data collected by several generations of scientists. In his monographic study (Silva Gabreta, 2012), he summed up all the knowledge on aquatic insects of the Bohemian Forest lakes. He often invited young colleagues and students to participate on the field work in the Bohemian Forest and, thus, a number of studies in the Bohemian Forest began as a field trip with Tomáš. In recent years, he participated in the research of restored streams in the Vltavský Luh.

Tomáš Soldán wrote more than 300 scientific publications, but their list and description can hardly capture their author's personality. Tomáš was a well-educated and friendly man, who travelled over dozens of countries and inspired many followers by his range of knowledge and experience. He was a passionate collector of mayflies, who is remembered first of all as the man in rubber boots with a metal strainer collecting mayflies in the middle of the river. He always amused people around him with his unrepeatable sense of humour, so we will really miss his jokes, "heroic stories", and bon mots.

Jindřiška Bojková